

## Local Organizing Committee

Jose Daniel Figueroa Villar  
IME, Chair  
Sonia Cabral de Menezes  
PETROBRAS, Vice-Chair  
Anita J. Marsaioli  
UNICAMP  
Claudia Jorge do Nascimento  
UNIRIO  
Dorila P. Veloso  
UFMG  
Fábio C.L. Almeida  
UFRJ  
Fernando Hallwass  
UFPE  
Jairton Dupont  
UFRGS  
Jerson Lima da Silva  
UFRJ  
Luiz Alberto Colnago  
EMBRAPA  
Naira M. da Silva Ruiz  
PUC/RJ  
Rosane A. da Silva San Gil  
UFRJ  
Jochen Junker  
FIOCRUZ  
Sandra Mello  
Event Production Coordination

## Welcome to the 18<sup>th</sup> ISMAR 2013/14<sup>th</sup> NMR Users Meeting!

I am very proud of your participation at this event, which is the most important magnetic resonance event in Brazil and Latin America in the last 27 years. The scientific development of the world strongly depends on this topic, and each participant is certainly contributing with science and technology to improve human life condition.

This meeting is organized including ten Plenary Lectures, four Parallel Sessions with more than 150 lectures and oral presentations, three Poster Sessions and exhibit booths of 17 companies. The event is financed by 24 industries and 7 Brazilian foment agencies. The Student Grants were financed by 13 companies, a very important contribution for this event, helping economically 37 students.

Several actions necessary for all participants are financed by the event, for the comfort of participants like the wireless Internet system, freely available in the whole event region and transportation to the meeting, which is free and arranged for all the event participants and accompanying people. The respective information on transportation and internet is part of this book.

In this event we also have two satellite meetings, the V<sup>th</sup> Iberoamerican NMR Meeting (Friday afternoon) and the Biomedical Imaging Symposium (Wednesday afternoon). To see the programs and to participate at the satellite meetings, it is necessary to register for them at the event's secretary desk. We strongly encourage everyone to join!

The social activities will start with a Welcome Reception on Sunday after the opening, honor and prizes lectures. On Thursday evening we will have the Brazilian Night at the Fogo de Chão Brazilian Steak House, including dinner, music shows and dancing. We strongly encourage your participation at this party, which will be a special opportunity for fraternization for all participants. Free transportation will be provided by the Meeting Organization.

Rio de Janeiro is a nice city, with many attractive sites, including mountains, beaches, forests, parks and districts, restaurants, museums, shopping and show centers. Wednesday and Friday afternoon/evening the ISMAR2013/14<sup>th</sup> NMR Users Meeting is also offering some excursions to the major touristic sites.

I hope you will enjoy this event and Rio de Janeiro!



**José Daniel Figueroa-Villar**

Chairman

18<sup>th</sup> ISMAR 2013/14<sup>th</sup> NMR Users Meeting

## Contents

Committees . . . . .	ii	Program . . . . .	1
Honor and Prizes . . . . .	iii	Abstracts of Talks . . . . .	21
General Information . . . . .	iv	Poster Abstracts . . . . .	69
Map of the Event Locations . . . . .	vii	Index of Authors . . . . .	161
Event Sponsors . . . . .	viii	Directory of Participants . . . . .	172
Student Travel Awards . . . . .	ix	Late Participants . . . . .	186

## Committees

### Scientific Committee

**Ad Bax**  
NIH, USA

**Alejandro Vila**  
IRB, Argentina

**Angelo da Cunha Pinto**  
IQ/UFRJ, Brazil

**Antonio José da Costa Filho**  
USP-RP, Brazil

**Bob Griffin**  
MIT, USA

**Carlos Geraldes**  
Univ. of Coimbra, Portugal

**Eduardo Ribeiro Azevêdo**  
USP-SC, Brazil

**Gunnar Jeschke**  
ETH, Switzerland

**Lucio Frydman**  
Weizmann Institute, Israel

**Miquel Pons**  
Univ. of Barcelona, Spain

**Warren Warren**  
Duke Univ., USA

### ISMAR Officers

**President** Hans Wolfgang Spiess  
Germany

**Vice President** Daniella Goldfarb  
Israel

**Past President** Ad Bax  
USA

**Secretary General** Roxanne Deslauriers  
Canada

**Treasurer** David Ailion  
USA

## Honor and Prizes

ISMAR awards Prizes that recognize important accomplishments and developments in Magnetic Resonance and its applications to various fields of science. All awardees will present plenary lectures in the opening session on Sunday, May 19<sup>th</sup>.

The principal Prize of ISMAR is the

### ISMAR Prize

sponsored by Cambridge Isotope Laboratories

for world renowned scientists, who have made outstanding contributions in the field of magnetic resonance. Former Prize winners include Anatole Abragam, Erwin Hahn, Jean Jeener, Charles Slichter and John Waugh to name just a few - see <http://www.ismar.org/ismar-prize>.

This year's Awardee is

Professor **Jack H. Freed**, Cornell University, Ithaca, USA.

Professor Freed is honored for the foundation of modern EPR through an extraordinary range of contributions from mathematics and theory to methodology and instrumentation; and for the application of his ingenious methods of pulsed EPR spectroscopy to fundamental problems in areas from chemistry to biophysics.

In 2011 ISMAR established the

### Anatole Abragam Prize

sponsored by Bruker Biospin



to pay tribute to the outstanding achievements of the late Anatole Abragam who made seminal contributions to both NMR and EPR and was himself a recipient of the ISMAR Prize and a Fellow of ISMAR. In addition to his contributions to science, education through his written books and other works, and the fostering of science and people in science was clearly a valuable component of his sensibility and legacy. With this in mind, ISMAR has established an award bearing his name for young investigators within 5 years of completing their PhD. The award aims to recognize and encourage outstanding young scientists at an important early point of their career.

The first Awardee is

### Vikram S. Bajaj, Ph.D.

University of California & Lawrence Berkeley National Laboratory, Berkeley, USA

He is honored for his achievements in magnetic resonance methodology, including contributions to high field DNP, remote detection of microfluidic flow, optical encoding and detection of magnetic resonance, and new implementations of the Xenon biosensor.

Both Awardees were selected by the ISMAR Prize committee, chaired by Alex Pines, and I thank all members very much, see <http://www.ismar.org/organization>.

### Paul Callaghan Lecture

sponsored by Magritek

ISMAR has a particular responsibility and privilege to celebrate the legacy of the late Paul Callaghan who made singular contributions to science in general and to the function and welfare of ISMAR in particular. Professor Callaghan served as Vice President, President and Past President until his death in March 2012. To honor his memory, a lecture in his name was introduced, the first one to be given by

Professor **Lucio Frydman**,

The Weizmann Institute of Science, Rehovot, Israel.

During the course of his career, Lucio Frydman has made exciting and significant contributions to NMR methodology and instrumentation and to the applications of his techniques to many fields of science. Among them are innovative studies of the flow behavior of complex fluids, an area of research at the center of Paul Callaghan's wide-ranging interests.



### Hans Wolfgang Spiess

ISMAR President

## General Information

Detailed information is available at the conference website: <http://www.ismar2013.net>

### Conference site:

Royal Tulip Rio de Janeiro - Rua Aquarela do Brasil, 75, São Conrado - 22610-010, Rio de Janeiro, Brazil. Tel: +55 21 3323 2200 - Fax: +55 21 3322 5500

### Program:

All lectures and posters abstracts are in this ISMAR 2013 Book. The electronic version of the book, including last submitted abstracts, is available on the conference website.

### Special Activities:

Sunday, May 19th – Pre-conference meetings

8:30 - 15:00	We-NMR Workshop (Room: Água Marinha)
8:30 - 15:10	WW-NMR Workshop (Room: Ágata)
12:00 - 14:40	Bruker Users Meeting (Room: Turmalina/Topázio)
9:00 - 13:00	Agilent Users Meeting (Room: Ônix)

During ISMAR Meeting:

Monday, May 20 <sup>th</sup> , 12:30 - 14:00	MESTRELAB Users Meeting (Room: Água Marinha)
Tuesday, May 21 <sup>st</sup> , 12:30 - 13:30	AUREMN GENERAL ASSEMBLY (Room: Ônix)
Wednesday, May 22 <sup>nd</sup> , 14: 15 - 18:00	Satellite Meeting - Biomedical Imaging Symposium (Room: Ônix)
Friday, May 24 <sup>th</sup> , 14:30 - 18:20	Satellite Meeting - V <sup>th</sup> Iberoamerican NMR Meeting (Room: Turmalina/Topázio)

### ISMAR Activities:

Tuesday, May 21 <sup>st</sup> , 19:30	ISMAR Executive Committee Meeting (Room: Água Marinha)
Wednesday, May 22 <sup>nd</sup> , 19:30	ISMAR Council Meeting (Room: Água Marinha)

### Posters:

Poster Sessions: Room Quartzzo A/B

Poster Set Up: until 10:30 of Monday, May 20<sup>th</sup>.

Poster removal: until 10:30, Friday, May 24<sup>th</sup>.

Posters to be presented on Monday are labeled: MOxxx

Posters to be presented on Tuesday are labeled: TUxxx

Posters to be presented on Thursday are labeled: THxxx

### Talks:

Speakers must arrive 1/2 hour prior to the start of their sessions to set up their laptops or talks in the media available.

### Internet Access:

Free WiFi is provided in all conference area

Select wireless network: ISMAR

Password: ismar2013

### Lunch and Dinner:

There are restaurants available at the conference hotel, further restaurants, cafes and fast foods are at "Fashion Mall", located in walking distance from the conference site. A list of restaurants and locations is provided in the conference bag.

## Social Events:

Sunday, May 19 <sup>th</sup>	Welcome Reception (18:30 at Foyers)
Thursday, May 23 <sup>rd</sup>	Brazilian Night, the Conference Banquet (20:00) Fogo de Chão Brazilian Steak House: Address: Av. Rep. Nestor Moreira, 12, Botafogo, Phone: ++ 55 21 2542 1545 Free transportation will be provided for the conference attendees from the Royal Tulip and back (following the hotels routes). Tickets for the Brazilian Night are required.

## Tours:

Wednesday and Friday afternoon are free for sightseeing. There will be a Travel Agency offering tours to the main tourist attractions in Rio throughout the meeting. If you are interested, please get tickets at the Tour Desk.

## Exhibition and Sponsorship:

Exhibitions will be held during the Conference period. Exhibits of many companies will be available. The map of exhibitors is available on this book.

## Transportation:

The conference attendees can use regular city buses and taxi.

Regular City Buses from Copacabana to São Conrado (conference site):

- Number 522 (São Conrado, R\$2.75) at BRS 2 stops at Barata Ribeiro St.
- Number 557 (Rio das Pedras, R\$2.75) at BRS 3 stops at Barata Ribeiro St.
- Number 318 (Recreio dos Bandeirantes, R\$3.10) at Atlântica Av.

Taxi cabs- Estimated prices to the event location from: Leme R\$ 70, Copacabana: R\$ 50, Ipanema R\$ 35; rates increase by 20% after 9 PM and sundays. Yellow cabs are also available at the Royal Tulip Hotel for your return trip.

Shuttle buses are free provided for the attendees during the conference.

Morning Route and stops:

1. Golden Tulip Continental Hotel, main entrance (Leme)
2. Barata Ribeiro St. (1), Bus stop BRS3 close to #204 Barata Ribeiro St., at the Metro station Cardeal Arco Verde (Copacabana)
3. Barata Ribeiro St. (2), Bus stop BRS2 close to #426 Barata Ribeiro St., at the intersection of Siqueira Campos and Barata Ribeiro, close to Metro station Siqueira Campos (Copacabana)
4. Barata Ribeiro St. (3), Bus stop BRS1 close to #774 Barata Ribeiro St., at the intersection of Bolivar and Barata Ribeiro (Copacabana)
5. Prudente de Moraes St., Bus stop in front of #149 Prudente de Moraes St., at General Osório Square (Ipanema)
6. Bartolomeu Mitre Av., Bus stop close to #246 Bartolomeu Mitre Av., in front of Antero de Quental Square (Leblon)
7. Royal Tulip Hotel (São Conrado), ISMAR 2013 venue

Return Route and stops:

1. Royal Tulip Hotel, main entrance (São Conrado)
2. Delfin Moreira Av., at the intersection with Bartolomeu Mitre Av. (Leblon)
3. Vieira Souto, at the intersection with Teixeira de Mello St. (close to General Osório Square, Ipanema)
4. Atlantica Av. (1), intersection with Miguel Lemos St. (Copacabana)
5. Atlantica Av. (2), intersection with Siqueira Campos St. (Copacabana)
6. Atlantica Av. (3), intersection with Rodolfo Dantas St. (Copacabana)
7. Golden Tulip Continental Hotel (Leme)

**Timetable:**

Sunday - May 19 <sup>th</sup>					
From Golden Tulip Cont. Hotel to Royal Tulip	Afternoon	12:00	13:00	14:00	
From Royal Tulip to Golden Tulip Cont. Hotel	Evening	19:30	20:00	20:30	21:15
Monday - May 20 <sup>th</sup>					
From Golden Tulip Cont. Hotel to Royal Tulip	Morning	7:00	7:20	7:40	
From Royal Tulip to Golden Tulip Cont. Hotel	Evening	18:30	19:00	22:15	
Tuesday - May 21 <sup>st</sup>					
From Golden Tulip Cont. Hotel to Royal Tulip	Morning	7:00	7:20	7:40	
From Royal Tulip to Golden Tulip Cont. Hotel	Evening	19:15	20:30	22:00	
Wednesday - May 22 <sup>nd</sup>					
From Golden Tulip Cont. Hotel to Royal Tulip	Morning	7:00	7:20	7:40	
From Royal Tulip to Golden Tulip Cont. Hotel	Afternoon	12:30			
From Royal Tulip to Golden Tulip Cont. Hotel	Evening	18:15			
Thursday - May 23 <sup>rd</sup>					
From Golden Tulip Cont. Hotel to Royal Tulip	Morning	7:00	7:20	7:40	
From Royal Tulip to Fogo de Chão Hotel	Evening	18:30			
From Fogo de Chão to Hotels	Night	22:30	24:00		
Friday - May 24 <sup>th</sup>					
From Golden Tulip Cont. Hotel to Royal Tulip	Morning	7:00	7:20	7:40	
From Royal Tulip to Golden Tulip Cont. Hotel	Afternoon	12:30			
From Royal Tulip to Golden Tulip Cont. Hotel	Evening	18:40			

Please note that buses will only leave if a minimum occupancy of 30 is reached!

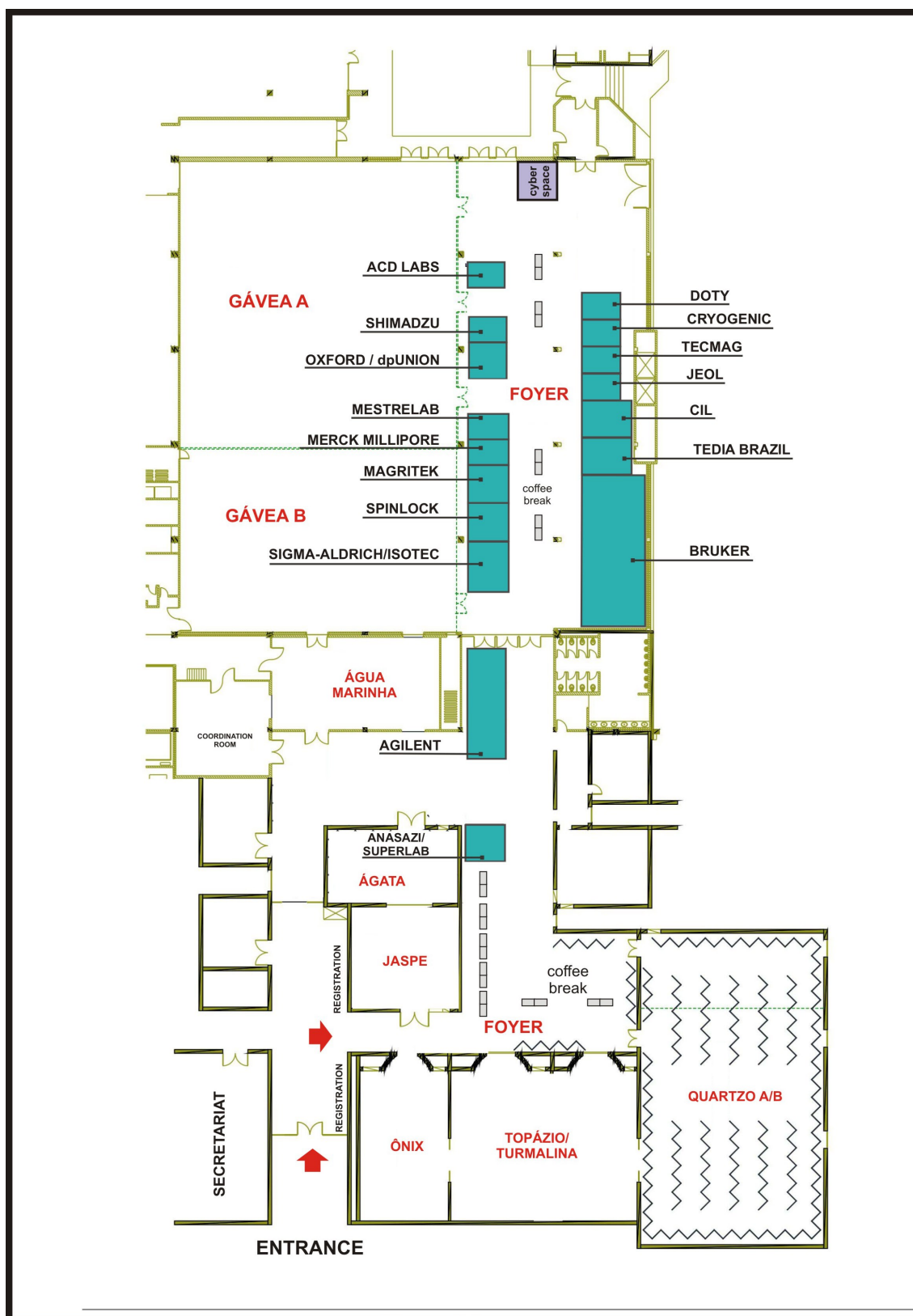
**Other Information:**

Message Board: Available at the poster room (Quartzo A/B).

Regulations:

- Badges are required at all time on event premisses, specially conference sessions, including posters and social events.
- Exhibitor badges are restricted to the exhibition area.
- The whole event site is a smoking free environment. NO SMOKING is permitted.
- Please turn off your cell phones during oral sessions.
- NO photography or recording is permitted in any session, including posters.

## Map of the Event Locations



## Event Sponsors

---

Main Sponsors

---



---

Funding Agencies and Universities

---

CAPES   CNPq   CRQ-RJ   FCC/UFRJ   IQ/UFRJ   PUC-Rio

**Sponsor Category****Company**

---

Diamond

---

Bruker

---

Sapphire

---

Agilent Technologies

---

Platinum

---

Cambridge Isotope Labs  
Schlumberger  
SIGMA-ALDRICH/ISOTEC  
Tedia Brazil

---

Gold

---

Anasazi/Superlab  
Magritek Limited  
Oxford/dpUNION  
Philips  
Spinlock

---

Silver

---

ACD Labs  
Cryogenic  
Doty Scientific, Inc.  
Halliburton  
Jeol  
Merck-Millipore  
Mestrelab Research  
Shimadzu  
Tecmag

---

Bronze

---

Baker Hughes  
Daedalus Innovations  
Euriso-top



## Student Travel Awards



WILEY



Graduate Student Travel Recipients funded by the sponsors above:

**Elias Akoury**  
Max-Planck-Institute for Biophysical  
Chemistry  
**Rohan Alvares**  
University of Toronto  
**Yang Bai**  
Nanyang Technological University,  
School of Biological Sciences  
**Emeline Barbet-Massin**  
Centre de RMN à Très Hauts Champs  
**Otonye Braide**  
University of Florida  
**Paula Burdisso**  
Instituto de Biología Molecular y  
Celular de Rosario  
**Tonci Cvitanic**  
University of Zagreb  
**David M Dias**  
University of Cambridge  
**Yesu Feng**  
Duke University  
**Alexander M Funk**  
Durham University  
**Piotr Garbacz**  
University of Warsaw  
**Eduard M. Gataullin**  
Kazan (Volga Region) Federal  
University

**Mariano M. Gonzalez**  
IBR - CONICET  
**Sheetal Kumar Jain**  
Aarhus University  
**Danielle Kaminski**  
University of Oxford  
**Natalia V Kulminkaya**  
Aarhus University  
**Zhao Li**  
University of California, Los Angeles  
**María Eugenia Llases**  
Institute of Molecular and Cell  
Biology of Rosario; Max-Planck  
Laboratory of Rosario  
**Antonio Marchi Netto**  
Rheinisch-Westfälische Technische  
Hochschule Aachen  
**Irene Marco-Rius**  
University of Cambridge and Cancer  
Research UK  
**Marco C Miotto**  
Institute of Molecular and Cell  
Biology of Rosario; Max-Planck  
Laboratory of Rosario  
**Marcos N Morgada**  
Instituto de Biología Molecular y  
Celular de Rosario

**Damjan Pelc**  
University of Zagreb, Faculty of  
Science  
**Daniel C Pizetta**  
Instituto de Física de São Carlos -  
USP  
**Katherine M Poole**  
University of Florida  
**Matthew P Renshaw**  
University of Cambridge  
**Benjamin Schomburg**  
Max-Planck-Institute for Biophysical  
Chemistry  
**Emilia V. Silletta**  
FAMAF – Universidad Nacional de  
Córdoba, IFEG –CONICET  
**Camila P Silveira**  
UFRJ - UNICAMP  
**Romana Spitzer**  
University of Innsbruck  
**Sebastian Täubert**  
Max-Planck-Institute for Biophysical  
Chemistry  
**Bruno L S Vicentin**  
Universidade Estadual de Londrina  
**Alexandre Zagdoun**  
CRMN ENS Lyon



Undergraduate Student Travel Recipients funded by the sponsor above:

**João Felipe Alves da Cruz**  
Federal University of São Carlos  
**André S. Carvalho**  
Federal University of São Carlos

**William S. Nunes**  
Mato Grosso do Sul University

## Program

<b>Sunday – May 19<sup>th</sup></b> <b>Pre-Conference Meetings</b>
---

8:30-15:00	<b>We-NMR Workshop</b> , Room Água Marinha, coordinated by Roberto Salinas (USP)
8:30-15:10	<b>WW-NMR/COSMOS Meeting</b> , Room Ágata, coordinated by Fábio Almeida (UFRJ) and Ulrich Günther (University of Birmingham)
12:00-14:40	<b>Bruker Users Meeting</b> , Rooms Turmalina/Topázio
9:00-13:00	<b>Agilent Users Meeting</b> , Room Ônix

12:00-15:30	<b>Registration</b>
-------------	---------------------

<b>Sunday – May 19<sup>th</sup></b> <b>Opening Ceremony</b> Room Gávea A
--

15:30-16:00	<b>Welcome</b> José Daniel Figueroa President of AUREMN Chair of the 18 <sup>th</sup> ISMAR 2013/14 <sup>th</sup> NMR Users Meeting
-------------	--

<b>Sunday – May 19<sup>th</sup></b> <b>Honor and Prizes Session</b> Presiding: Hans Spiess Room Gávea A
--

16:00-16:45	<b>Anatole Abragam Prize Lecture</b> Winner 2013: Vikram Bajaj, <i>UCLA &amp; Lawrence Berkeley National Laboratory, USA</i>	page
16:45-17:30	<b>ISMAR Price Lecture</b> Winner 2013: Jack Freed, <i>Cornell University, USA</i>	
17:30-18:15	<b>Paul Callaghan Lecture</b> <b>PL001: Emerging Frontiers in Ultrafast Multidimensional NMR and MRI</b> Rita Schmidt, Eddy Solomon, Avi Leftin, * <b>Lucio Frydman</b> ; <i>Department of Chemical Physics, Weizmann Institute of Science, Israel</i> .....	21
18:30	<b>Welcome Reception (Foyer)</b>	
18:30-21:00	<b>Vendors Exhibit Booths (Foyer)</b>	

## Monday – May 20<sup>th</sup> - Plenary Session

Chair: Daniella Goldfarb  
Room Gávea A

		page
8:30-9:15	<b>PL002: Biomolecular NMR at Very Low Temperatures</b> * <b>Robert Tycko</b> , Kent Thurber, Alexey Potapov, Wai-Ming Yau, Eric Moore; <i>National Institutes of Health</i> .....	21
9:15-10:00	<b>PL003: Sensitivity enhancement in High Field NMR and EPR</b> Vasyl Denysenkov, Petr Neugebauer, Phillip Spindler, Burkhard Endeward, * <b>Thomas F. Prisner</b> ; <i>Institute of Physical and Theoretical Chemistry and Center of Biomolecular Magnetic Resonance, Goethe University Frankfurt, Germany</i> .....	21
10:00-10:30	<b>Coffee Break</b>	

## Monday – May 20<sup>th</sup> - Dynamics and Catalysis

Chair: Jarbas Resende  
Room Gávea A

		page
10:30-10:55	<b>OP004: Control of Periplasmic Interdomain Thiol: Disulfide Exchange in the Transmembrane Oxidoreductase DsbD</b> <sup>1</sup> Despoina A.I. Mavridou, <sup>2</sup> Emmanuel Saridakis, <sup>1</sup> Paraskevi Kritsiligkou, <sup>1</sup> Lukas Stelzl, <sup>1</sup> Erin C. Mozley, <sup>1</sup> Alan D. Goddard, <sup>1</sup> Julie M. Stevens, <sup>1</sup> Stuart J. Ferguson, <sup>1</sup> * <b>Christina Redfield</b> ; <sup>1</sup> <i>Department of Biochemistry, University of Oxford</i> , <sup>2</sup> <i>National Center for Scientific Research Demokritos</i> .....	21
10:55-11:20	<b>OP005: Hydration of yeast Thioredoxin 1 Modulates Slow Dynamics</b> * <b>Fabio C. L. Almeida</b> ; <i>Institute of Medical Biochemistry, National Center of Nuclear Magnetic Resonance, Federal University</i> .....	22
11:20-11:35	<b>UP006: The magnitude of a pre-existing equilibrium tunes adenylate kinase activity</b> <sup>1</sup> Jörgen Åden, <sup>2</sup> Abhinav Verma, <sup>2</sup> Alexander Schug, <sup>1</sup> * <b>Magnus Wolf-Watz</b> ; <sup>1</sup> <i>Umeå University</i> , <sup>2</sup> <i>Karlsruhe Institute of Technology</i> .....	22
11:35-11:50	<b>UP007: Structural and dynamic insights into substrate binding and catalysis in human Lipocalin Prostaglandin D synthase</b> <sup>1</sup> * <b>Konstantin Pervushin</b> , <sup>1,2</sup> Pär Nordlund, <sup>1,2</sup> Sing Mei Lim, <sup>1</sup> Dan Chen, <sup>1</sup> Hsiangling Teo, <sup>2</sup> Annette Roos, <sup>2</sup> Tomas Nyman, <sup>2</sup> Lionel Trésaugues; <sup>1</sup> <i>Nanyang Technological University</i> , <sup>2</sup> <i>Karolinska Institute</i> .....	22
11:50-12:15	<b>OP008: EPR Studies of Radical SAM Enzymes</b> * <b>R. David Britt</b> ; <i>University of California, Davis</i> .....	22

## Monday – May 20<sup>th</sup> - General Solids

Chair: Bernhard Blümich  
Room Gávea B

		page
10:30-10:55	<b>OP009: Structure Determinations of Molecularly Ordered, Non-Crystalline Silicate, Borosilicate, and Aluminosilicate Frameworks by Combined NMR, Scattering, and DFT Analyses</b> <sup>1</sup> *Bradley F. Chmelka, <sup>2</sup> Sylvian Cadars, <sup>3</sup> Darren H. Brouwer, <sup>1</sup> Ming-Feng Hsieh, <sup>1</sup> Robert J. Messinger, <sup>1</sup> Matthew T. Aronson, <sup>2</sup> Mounesha N. Garaga, <sup>2</sup> Zalfa Nour; <sup>1</sup> University of California, Santa Barbara, USA, <sup>2</sup> CNRS, Université d'Orléans, France, <sup>3</sup> Redeemer College, Ancaster, Ontario, Canada.....	22
10:55-11:20	<b>OP010: Zero- and low-field NMR spectroscopy</b> <sup>1,2</sup> *Dmitry Budker; <sup>1</sup> Department of Physics, University of California, Berkeley, <sup>2</sup> Nuclear Science Division, E. O. Lawrence Berkeley National Laboratory, Berkeley.....	23
11:20-11:35	<b>UP011: Use of <sup>1</sup>H Chemical Shifts to Determine Structural Motifs in <math>\pi</math>-Conjugated Polymers</b> *Michael Ryan Hansen; Max Planck Institute for Polymer Research.....	23
11:35-11:50	<b>UP012: NMR Crystallography, from “Pas de deux” to Spin Choreography. Nanoporous Crystal Structures of Powders : Methods and Hardware.</b> <sup>1</sup> *Francis Taulelle, <sup>2</sup> Frank Engelke, <sup>2</sup> Frank Decker, <sup>1</sup> Boris Bouchevreau, <sup>1</sup> Charlotte Matineau; <sup>1</sup> University of Versailles, <sup>2</sup> Bruker-Biopspin GmbH.....	156
11:50-12:15	<b>OP013: High Frequency Dynamic Nuclear Polarization</b> *Robert G. Griffin; Francis Bitter Magnet Laboratory and Department of Chemistry, MIT	24

## Monday – May 20<sup>th</sup> - NMR in Medicinal Chemistry

Chair: Anita Marsaioli  
Rooms Turmalina/Topázio

		page
10:30-10:55	<b>OP014: HTS by NMR of combinatorial libraries: a new approach to peptide and ligand discovery</b> *Maurizio Pellecchia; Chemical Biology, Sanford-Burnham Medical Research Institute, La Jolla, CA.....	24
10:55-11:20	<b>OP015: Enzyme Kinetics and Inhibition by NMR</b> *José Daniel Figueroa-Villar; Military Institute of Engineering.....	24
11:20-11:35	<b>UP016: Integrated structural biology shows how scarce sequence elements control the function of single <math>\beta</math>-thymosin/WH2 domains in actin assembly</b> <sup>1</sup> François-Xavier Cantrelle, <sup>2</sup> Dominique Didry, <sup>1</sup> Célia Deville, <sup>1</sup> Jean-Pierre Placial, <sup>2</sup> Clotilde Husson, <sup>3</sup> Javier Perez, <sup>2</sup> Marie-France Carlier, <sup>2</sup> Louis Renault, <sup>1</sup> Carine van Heijenoort, <sup>1</sup> *Eric Guittet; <sup>1</sup> CNRS-ICSN, <sup>2</sup> CNRS-LEBS, <sup>3</sup> Synchrotron SOLEIL.....	24
11:35-11:50	<b>UP017: Human Macrophage Lectin (CLEC10A) recognition of monosaccharides related to tumor marker Tn-antigen studied by <sup>1</sup>H and <sup>19</sup>F NMR.</b> <sup>1</sup> *Francisco Javier Cañada, <sup>1</sup> Anneloes Oude Vrielink, <sup>1,2</sup> Filipa Marcelo, <sup>1</sup> Ana Manzano, <sup>1</sup> Pilar Blasco, <sup>1</sup> Jesús Jiménez-Barbero, <sup>3</sup> Sabine Andre, <sup>3</sup> Hans-Joachim Gabius; <sup>1</sup> Centro de Investigaciones Biológicas, CIB-CSIC Chemical and Physical Biology Department. Ramiro de, <sup>2</sup> REQUIMTE, CQFB, DQ, FCT-UNL, 2829-516 Caparica, Portugal, <sup>3</sup> Institute of Physiological Chemistry, Faculty of Veterinary Medicine, Ludwig-Maximilians-University, .....	158
11:50-12:15	<b>OP018: High-yield expression and NMR structural studies of Antimicrobial Peptides</b> Ji-Ho Jung, Ji-Sun Kim, *Yongae Kim; Depart of Chemistry and Protein Research Center for Bio-Industry, Hankuk University of Foreign Studies, Korea.....	25

## Monday – May 20<sup>th</sup> - EPR and New Materials

Chair: Eduardo Di Mauro  
Room Ônix

		page
10:30-10:55	<b>OP019: EPR of thermo- and photoswitchable copper-nitroxide based molecular magnets</b> <sup>1</sup> *Matvey Fedin, <sup>1</sup> Sergey Veber, <sup>1</sup> Irina Drozdyuk, <sup>1</sup> Ksenia Maryunina, <sup>1</sup> Evgeny Tretyakov, <sup>2</sup> Hideto Matsuoka, <sup>2</sup> Seigo Yamauchi, <sup>1</sup> Renad Sagdeev, <sup>1</sup> Victor Ovcharenko, <sup>1,3</sup> Elena Bagryanskaya; <sup>1</sup> International Tomography Center SB RAS, Novosibirsk, Russia, <sup>2</sup> Tohoku University, Sendai, Japan, <sup>3</sup> N.N. Vorozhtsov Novosibirsk Institute of Organic Chemistry SB RAS, Novosibirsk, Russia .....	25
10:55-11:20	<b>OP020: Theoretical EPR Spectroscopy of Open-Shell Transition Metal Complexes with Strong Spin Orbit Coupling</b> *Frank Neese, Mihail Atanasov, Michael Römelt, Kantharuban Sivalingam; <i>Max-Planck-Institut für Chemische Energiekonversion</i> .....	26
11:20-11:35	<b>UP021: Multifunctional in vivo EPR-based spectroscopy and imaging of paramagnetic probes</b> *Valery V. Khramtsov; <i>The Ohio State University Medical Center, Columbus, OH, USA</i>	26
11:35-11:50	<b>UP022: New Kind of Mesoscopic EPR In Some Itinerant Undoped Ferromagnets</b> *Vladimir A. Ivashin, Eduard M. Gataullin; <i>Kazan (Volga region) Federal University</i> .	26
11:50-12:15	<b>OP023: Elucidating Smart Polymeric Materials Using Electron Paramagnetic Resonance (EPR) Spectroscopy</b> *Dariush Hinderberger; <i>Max Planck Institute for Polymer Research</i> .....	27
12:15-14:15	<b>Lunch Break</b>	
12:30-13:30	<b>Mestrelab Users Meeting, Room Água Marinha</b>	

## Monday – May 20<sup>th</sup> - Membrane Proteins

Chair: Ana Carolina Zeri  
Room Gávea A

		page
14:15-14:40	<b>OP024: Structural studies of membrane proteins in membrana</b> *Francesca M. Marassi; <i>Sanford-Burnham Medical Research Institute, La Jolla CA, USA</i>	27
14:40-15:05	<b>OP025: Brain Fatty-acid Binding Protein and its Interactions with Membrane Model Systems</b> <sup>1</sup> Fábio H. Dyszy, <sup>1</sup> Ítalo A. Salvini, <sup>1</sup> Daniel F. Silva, <sup>1</sup> Andressa P. A. Pinto, <sup>1</sup> Ana P.U. Araújo, <sup>2</sup> Hans Robert Kalbitzer, <sup>1</sup> Claudia Elisabeth Munte, <sup>1,3</sup> *Antonio José Costa-Filho; <sup>1</sup> Grupo de Biofísica Molecular Sérgio Mascarenhas, Instituto de Física de São Carlos, USP, <sup>2</sup> Department of Biophysics and Physical Biochemistry, University of Regensburg, <sup>3</sup> Laboratório de Biofísica Molecular, Faculdade de Filosofia, Ciências e Letras de Ribeirão Preto, USP .....	27
15:05-15:20	<b>UP026: Defining the Flexible and Fixed Sides of a Protein Channel by EPR</b> *Betty J. Gaffney; <i>Florida State University</i> .....	158
15:20-15:35	<b>UP027: Conformational selection of GPCR ligands upon binding to their receptors as observed by NMR</b> <sup>1</sup> *Laurent Catoire, <sup>2</sup> Marc Baaden, <sup>1</sup> Jean-Luc Popot, <sup>3</sup> Eric Guittet, <sup>4</sup> Jean-Louis Banères; <sup>1</sup> Laboratory of Biology and Physico-Chemistry of Membrane Proteins - UMR 7099 CNRS & University Paris, <sup>2</sup> Laboratory of theoretical Biochemistry - UPR 9080 CNRS, <sup>3</sup> ICSN- UPR 2301 CNRS, <sup>4</sup> IBMM - UMR 5247 CNRS, Université Montpellier 1 & 2.....	28
15:35-16:00	<b>OP028: Structural Biology by DNP MAS NMR and Investigations on the Transport Cycle of an ABC Transporter</b> *Hartmut Oschkinat; <i>Leibniz-Institut für Molekulare Pharmakologie, Berlin, Germany</i> .	28

## Monday – May 20<sup>th</sup> - Dynamics and Recognition

Chair: Robert Kaptein  
Room Gávea B

		page
14:15-14:40	<b>OP029: Dynamic Aspects of Indirect DNA Readout by Nucleoid Associated Proteins</b> <sup>2</sup> Tiago Cordeiro, <sup>2</sup> Jesús García, <sup>3</sup> Oscar Millet, <sup>1*</sup> Miquel Pons; <sup>1</sup> <i>University of Barcelona</i> , <sup>2</sup> <i>Institute for Research in Biomedicine</i> , <sup>3</sup> <i>CIC-bioGUNE</i> .....	28
14:40-15:05	<b>OP030: Protein Kinase A and Conformational Dynamics: ‘Not too fast... not too slow... but just right’</b> <sup>*</sup> Gianluigi Veglia; <i>University of Minnesota</i> .....	29
15:05-15:20	<b>UP031: Sliding and target location of DNA-binding proteins: an NMR view of the lac repressor system</b> <sup>1*</sup> Rolf Boelens, <sup>2</sup> Karine Loth, <sup>4</sup> Manuel Gnida, <sup>5</sup> Julija Romanuka, <sup>1,3</sup> Robert Kaptein; <sup>1</sup> <i>Utrecht University</i> , <sup>2</sup> <i>University of Orleans</i> , <sup>3</sup> <i>Novosibirsk State University</i> , <sup>4</sup> <i>Paderborn University</i> , <sup>5</sup> <i>Shell Research Laboratories</i> .....	29
15:20-15:35	<b>UP032: RNA regulation - A new Twist</b> <sup>*</sup> Harald Schwalbe; <i>Goethe-University Frankfurt</i> .....	29
15:35-16:00	<b>OP033: Protein interactions and function studied by novel NMR methods</b> <sup>*</sup> S. Grzesiek, M. Gentner, J.-r. Huang, S. Morin, L. Nisius, H.-J. Sass, L. Skora, N. Vajpai, M. Wiktor; <i>Biozentrum, University of Basel, Switzerland</i> .....	29

## Monday – May 20<sup>th</sup> - Methods for Inorganic Materials

Chair: Bradley Chmelka  
Rooms Turmalina/Topázio

		page
14:15-14:40	<b>OP034: NMR Non-Crystallography</b> <sup>1*</sup> Philip J. Grandinetti, <sup>1</sup> Kevin Sanders, <sup>1</sup> Eric Keeler, <sup>2</sup> Jay H. Baltisberger; <sup>1</sup> <i>Ohio State University, Columbus, USA</i> , <sup>2</sup> <i>Berea College, Berea, KY, USA</i> .....	30
14:40-15:05	<b>OP035: Hunting for Hydrogen in Wadsleyite: Multinuclear Solid-State NMR and First-Principles Calculations</b> <sup>1*</sup> Sharon E. Ashbrook, <sup>1</sup> John M. Griffin, <sup>2</sup> Andrew J. Berry, <sup>3</sup> Stephen Wimperis; <sup>1</sup> <i>School of Chemistry and EaStCHEM, University of St Andrews, UK</i> , <sup>2</sup> <i>Research School of Earth Sciences, Australia National University, Canberra, Australia</i> , <sup>3</sup> <i>School of Chemistry and WestCHEM, University of Glasgow, UK</i> .....	30
15:05-15:20	<b>UP036: Uniform excitation and inversion of broad NMR spectra in rotating solids using DANTE</b> <sup>1</sup> Veronika Vizthum, <sup>1</sup> Marc Caporini, <sup>1</sup> Diego Carnevale, <sup>1</sup> Simone Ulzega, <sup>2</sup> Julien Trébosc, <sup>2</sup> Olivier Lafon, <sup>1</sup> Geoffrey Bodenhausen, <sup>2*</sup> Jean Paul Amoureux; <sup>1</sup> <i>Ecole Polytechnique Fédérale de Lausanne, Switzerland</i> , <sup>2</sup> <i>Lille University, France</i> .....	30
15:20-15:35	<b>UP037: A homonuclear version of REDOR for recoupling dipolar interactions in multi-spin systems: Applications to inorganic phosphorus clusters and networks</b> <sup>1,2*</sup> Hellmut Eckert, <sup>2</sup> Jinjun Ren; <sup>1</sup> <i>University of Sao Paulo</i> , <sup>2</sup> <i>WWU Münster</i> .....	31
15:35-16:00	<b>OP038: Topologic, Geometric, and Chemical Order in Materials: Insights from Solid-State NMR</b> Dominique Massiot, Sylvian Cadars, Michael Deschamps, Emmanuel Véron, Mounesha N.Garaga, Robert J. Messinger, Mathieu Allix, <sup>*</sup> Pierre Florian, Franck Fayon; <i>CEMHTI UPR3079 CNRS, France</i> .....	31

# Monday – May 20<sup>th</sup> - Hyperpolarization/ Instrumentation

Chair: Dmitry Budker  
Room Onix

		page
14:15-14:40	<b>OP039: Imaging Pulmonary Gas Exchange from Mouse to Human with Hyperpolarized <sup>129</sup>Xe MRI</b> <b>*Bastiaan Driehuys</b> ; <i>Department of Radiology, Duke University Medical Center, Durham</i>	32
14:40-15:05	<b>OP040: Hyperpolarized Carbon-13 MR Pre-Clinical and Human Research Studies</b> <sup>1</sup> <b>*Daniel B. Vigneron</b> , <sup>1</sup> Sarah Nelson, <sup>2</sup> Andrea Harzstark, <sup>3</sup> Marcus Ferrone, <sup>1</sup> Robert Bok, <sup>1</sup> John Kurhanewicz; <sup>1</sup> <i>Department of Radiology &amp; Biomedical Imaging, University of California, San Francisco</i> , <sup>2</sup> <i>Investigational Therapeutics, University of California, San Francisco</i> , <sup>3</sup> <i>Clinical Pharmacy, University of California, San Francisco</i> .....	32
15:05-15:20	<b>UP041: Universal tags to sustain long-lived hyperpolarized signal: Extension of hyperpolarization to broad range of biomarkers</b> <b>Yesu Feng</b> , Thomas Theis, Ryan M. Davis, Kevin Claytor, Qiu Wang, Pei Zhou, *Warren S. Warren; <i>Duke University</i> .....	32
15:20-15:35	<b>UP042: Avalanching Amplification of NMR/MRI Sensitivity by Solvent-Generated Feedback Fields</b> Zhao Li, Susie Y. Huang, Jamie D. Walls, <b>*Yung-Ya Lin</b> ; <i>Department of Chemistry and Biochemistry, UCLA</i> .....	32
15:35-16:00	<b>OP043: An Implantable Wireless Amplified NMR Detector for High Resolution MRI</b> Chunqi Qian, Xin Yu, Der-Yow Chen, Stephen Dodd, Joseph Murphy-Boesch, <b>*Alan P. Koretsky</b> ; <i>Laboratory of Functional and Molecular Imaging, NINDS, NIH, Bethesda, MD</i>	33
16:00-18:30	<b>Poster Session I</b> Rooms Quartzo A/B, Authors with poster numbers starting "MO" present	
all day	<b>Vendors Exhibit Booths (Foyer)</b>	
19:00-22:00	<b>Bruker's Night (Gávea A)</b>	

## Tuesday – May 21<sup>st</sup> - Plenary Session

Chair: Ad Bax  
Room Gávea A

		page
8:30-9:15	<b>PL044: Singlet Nuclear Magnetic Resonance</b> <i>*Malcolm H. Levitt; School of Chemistry, University of Southampton, UK</i> .....	33
9:15-10:00	<b>PL045: Visualizing Transient Structures of DNA and RNA using NMR</b> <i>*Hashim M. Al-Hashimi; Department of Chemistry and Biophysics, University of Michigan</i> .....	33
10:00-10:30	<b>Coffee Break</b>	

## Tuesday – May 21<sup>st</sup> - Dynamics and Recognition

Chair: Jose Pires  
Room Gávea A

		page
10:30-10:55	<b>OP046: Protein dynamics and interaction mediated by local water dynamics at the ps timescale</b> <i>*Songi Han; Departement of Chemistry and Biochemistry, University of California Santa Barbara</i> .....	34
10:55-11:20	<b>OP047: Molecular Recognition and Dynamics: NMR Studies of Defensins and Epitopes</b> <i>*Ana Paula Valente; Federal University of Rio de Janeiro</i> .....	34
11:20-11:35	<b>UP048: Bacterial transmembrane signalling through a heme/hemophore receptor</b> <i><sup>1,2</sup>*Nadia Izadi-Pruneyre; <sup>1</sup>Institut Pasteur, Paris, France, <sup>2</sup>CNRS UMR 3528</i> .....	34
11:35-11:50	<b>UP049: NMR Mapping of PCNA Interaction with Translesion Synthesis DNA Polymerase Rev1 Mediated by Rev1-BRCT Domain</b> <i>Yulia Pustovalova, Mark W. Maciejewski, *Dmitry M. Korzhnev; University of Connecticut Health Center</i> .....	155
11:50-12:15	<b>OP050: Structural basis of epigenetic regulation</b> <i>*Yunyu Shi; School of Life Sciences, University of Science and Technology of China, Hefei, China</i> .....	34



## Tuesday – May 21<sup>st</sup> - IDPs, Folding and Misfolding

Chair: Gianluigi Veglia  
Room Gávea B

		page
10:30-10:55	<b>OP051: New methods based on <sup>13</sup>C direct detection to study intrinsically disordered proteins</b> <i>*Isabella C. Felli; CERM and Department of Chemistry “Ugo Schiff”, University of Florence, Italy.....</i>	35
10:55-11:20	<b>OP052: NMR-based Structural Biology in Brain Diseases</b> <i><sup>1,2</sup>*Claudio O. Fernández; <sup>1</sup>Universidad Nacional de Rosario (UNR), Instituto de Biología Molecular y Celular de Rosario (IBR-CON, <sup>2</sup>Max Planck Laboratory of Structural Biology, Chemistry and Molecular Biophysics of Rosario (MPLbioR).....</i>	35
11:20-11:35	<b>UP053: Caught in Action: Selecting Peptide Aptamers Against Intrinsically Disordered Proteins in Live Cells</b> <i><sup>1</sup>Jacqueline Washington, <sup>1</sup>Sergey Reverdatto, <sup>1</sup>David Burz, <sup>2</sup>Kathleen McDonough, <sup>1</sup>*Alexander Shekhtman; <sup>1</sup>State University of New York at Albany, Albany, NY, USA, <sup>2</sup>Wadsworth Center, NY Department of Health, Albany, NY.....</i>	35
11:35-11:50	<b>UP054: Phosphorylation Of The Intrinsically Disordered Unique Domain Of c-Src Studied By In-Vivo Real-Time NMR</b> <i><sup>1,2</sup>Irene Amata, <sup>2</sup>Mariano Maffei, <sup>1</sup>Ana Igea, <sup>1</sup>Angel R. Nebreda, <sup>2</sup>*Miquel Pons; <sup>1</sup>Signaling and Cell Cycle Laboratory, Institute for Research in Biomedicine, Barcelona, Spain, <sup>2</sup>Biomolecular NMR, Organic Chemistry Department, University of Barcelona, Barcelona, Spain.....</i>	35
11:50-12:15	<b>OP055: NMR of Intrinsically Disordered Proteins: Tools for Increasing Sensitivity and Resolution</b> <i><sup>1</sup>Zsolia Solyom, <sup>1</sup>Melanie Schwarten, <sup>1</sup>Sophie Feuerstein, <sup>2</sup>Dieter Willbold, <sup>3</sup>Michael Plevin, <sup>1</sup>*Bernhard Brutscher; <sup>1</sup>Institut de Biologie Structurale, CEA-CNRS-UJF, Grenoble, France, <sup>2</sup>Institute of complex systems, Structural Biochemistry, FZ Jülich, Germany, <sup>3</sup>Department. of Biology, University of York, UK.....</i>	36

## Tuesday – May 21<sup>st</sup> - Methods for Organic Materials

Chair: Klaus Schmidt-Rohr  
Rooms Turmalina/Topázio

		page
10:30-10:55	<b>OP056: <sup>14</sup>N-<sup>1</sup>H Solid-State NMR Spectroscopy of Organic Solids</b> <i>*Steven P. Brown; Department of Physics, University of Warwick, UK.....</i>	36
10:55-11:20	<b>OP057: Separated Local Field NMR as a tool for probing molecular dynamics in organic solids</b> <i><sup>1</sup>Marcio F. Cobo, <sup>2</sup>Anja Achilles, <sup>1</sup>Gregório C. Faria, <sup>2</sup>Detlef Reichert, <sup>2</sup>Kay Saalwächter, <sup>1</sup>*Eduardo Ribeiro de Azevêdo; <sup>1</sup>Universidade de São Paulo, São Carlos-SP, Brazil, <sup>2</sup>Martin-Luther-University Halle Wittenberg, Halle, Germany.....</i>	36
11:20-11:35	<b>UP058: Low-field <sup>1</sup>H-NMR investigations to reveal local properties of polymer networks</b> <i><sup>1</sup>*Maria Ott, <sup>2</sup>Roberto Pérez-Aparicio, <sup>1</sup>Horst Schneider, <sup>2</sup>Paul Sotta, <sup>1</sup>Kay Saalwächter; <sup>1</sup>Institut für Physik – NMR, Martin-Luther-Universität Halle-Wittenberg, Betty-Heimann-Str. 7, D-0, <sup>2</sup>Laboratoire Polymères et Matériaux Avancés, CNRS/Rhodia, 85 avenue des Frères Perret, F-69192 Sai.....</i>	37
11:35-11:50	<b>UP059: Efficient Heteronuclear Cross Polarization Techniques for Solid State NMR</b> <i>Sheetal Kumar Jain, Morten Bjerring, *Niels Christian Nielsen; Aarhus University.....</i>	37
11:50-12:15	<b>OP060: NMR crystallography of small molecules: from ionic solids to pharmaceuticals</b> <i>*Luís Mafra, Sérgio M. Santos; Department of Chemistry, University of Aveiro, CICECO, Portugal.....</i>	37

## Tuesday – May 21<sup>st</sup> - MRI/In-Vivo

Chair: Michael Garwood  
Room Ônix

		page
10:30-10:55	<b>OP061: Parallel imaging with nonlinear gradient fields</b> * <b>Gigi Galiana</b> , Leo Tam, Dana C. Peters, R. Todd Constable; <i>Yale University</i> .....	37
10:55-11:20	<b>OP062: Relaxivity Optimized Metal Based MRI Molecular Imaging Agents</b> * <b>Carlos F.G.C. Geraldês</b> ; <i>Department of Life Sciences, Center of Neurosciences and Cell Biology and Coimbra Chemistry Center, University of Coimbra</i> .....	38
11:20-11:35	<b>UP063: Magnetic Resonance Microimaging of a Swelling Gel</b> <sup>1</sup> <b>Wilson Barros Jr.</b> , <sup>1</sup> Eduardo N. de Azevedo, <sup>2</sup> *Mario Engelsberg; <sup>1</sup> <i>Universidade Federal de Pernambuco, Recife</i> , <sup>2</sup> <i>Universidade Federal de Pernambuco, Caruaru</i> .....	38
11:35-11:50	<b>UP064: Early Detection of Pancreatic Cancers &amp; Brain Tumors by Active-Feedback Controlled MR</b> <sup>1</sup> <b>Zhao Li</b> , <sup>2</sup> Chaoxiung Hsu, <sup>2</sup> Lian-Pin Hwang, <sup>1</sup> *Yung-Ya Lin; <sup>1</sup> <i>Department of Chemistry and Biochemistry, UCLA</i> , <sup>2</sup> <i>Department of Chemistry, National Taiwan University</i> .....	38
11:50-12:15	<b>OP065: Detecting Tumor Treatment Response using Metabolic Imaging with hyperpolarized <sup>13</sup>C-labeled Cell Substrates</b> *Kevin M. Brindle, Mikko I. Kettunen, <b>Tiago B. Rodrigues</b> , Eva M. Serrao, Brett W.C. Kennedy, De-en Hu; <i>Department of Biochemistry and CRUK Cambridge Institute, University of Cambridge, UK</i> .....	39
12:15-14:15	<b>Lunch Break</b>	
12:30-13:30	<b>AUREMN General Assembly</b> (AUREMN members only, lunch box included), Room Ônix	

## Tuesday – May 21<sup>st</sup> - Plenary Session

Chair: José Figueroa-Villar  
Room Gávea A

		page
14:15-15:00	<b>PL066: Recent contributions for Zero-, Low-, and High-field NMR</b> * <b>Tito J. Bonagamba</b> ; <i>Instituto de Física de São Carlos - Universidade de São Paulo, São Carlos, Brazil</i> .....	39
15:00-15:25	<b>OP067: Magnetic resonance studies of topological materials</b> * <b>Louis Bouchard</b> ; <i>UCLA</i> .....	40
15:25-15:50	<b>OP068: Hyperpolarized Molecular Sensing and Detection</b> <sup>1,2</sup> * <b>Vikram S. Bajaj</b> ; <sup>1</sup> <i>Department of Chemistry and California Institute of Quantitative Biosciences, University of California, Berkeley</i> , <sup>2</sup> <i>Materials Sciences Division, Lawrence Berkeley National Laboratory</i> .....	40
15:50-16:35	<b>PL069: Structures and mechanisms of viral ion channels and fusion peptides from solid-state NMR</b> * <b>Mei Hong</b> ; <i>Iowa State University</i> .....	40
16:35-19:30	<b>Poster Session II</b> Rooms Quartz A/B, Authors with poster numbers starting "TU" present	
all day	<b>Vendors Exhibit Booths (Foyer)</b>	

### Wednesday – May 22<sup>nd</sup> - Amyloids

Chair: Ana Paula Valente  
Room Gávea A

		page
8:30-8:55	<b>OP070: Amyloid aggregates and large soluble protein complexes</b> <sup>1,2,3</sup> Sam Asami, <sup>1,2,3</sup> Juan-Miguel Lopez del Amo, <sup>1,2,3</sup> Andi Mainz, <sup>1,2,3</sup> Muralidhar Dasari, <sup>3</sup> Uwe Fink, <sup>4</sup> Marcus Fändrich, <sup>5</sup> Erich E. Wanker, <sup>5</sup> Jan Bieschke, <sup>6</sup> Tomasz Religa, <sup>6</sup> Lewis E. Kay, <sup>1,2,3</sup> * <b>Bernd Reif</b> ; <sup>1</sup> <i>Technische Universität München (TUM), Department Chemie</i> , <sup>2</sup> <i>Helmholtz-Zentrum München (HMGU)</i> , <sup>3</sup> <i>Leibniz-Institut für Molekulare Pharmakologie (FMP)</i> , <sup>4</sup> <i>Max-Delbrück Centrum für Molekulare Medizin (MDC)</i> , <sup>5</sup> <i>Max-Planck-Forschungsstelle für Enzymologie der Proteinfaltung, Martin-Luther Universität Halle-Wittenberg</i> , <sup>6</sup> <i>University of Toronto, Department of Medical Genetics and Microbiology</i> ....	40
8:55-9:20	<b>OP071: Amyloid Fibrils: Towards a Molecular Level Picture with Solid-State Nuclear</b> * <b>P. K. Madhu</b> ; <i>Tata Institute of Fundamental Research</i> .....	41
9:20-9:35	<b>UP072: Metallobiology of neurodegenerative diseases: Structural and mechanistic basis behind the acceleration of amyloid protein assembly</b> <sup>1,2</sup> <b>M.C. Miotto</b> , <sup>1,2</sup> A.A. Valiente Gabioud, <sup>3</sup> Andres Binolfi, <sup>4</sup> L. Quintanar, <sup>5</sup> Christian Griesinger, <sup>1,2</sup> * <b>Claudio O. Fernández</b> ; <sup>1</sup> <i>Instituto de Biología Molecular y Celular de Rosario (IBR-CONICET)</i> , <i>Universidad Nacional de Rosario</i> , <sup>2</sup> <i>Max Planck Laboratory of Structural Biology, Chemistry and Molecular Biophysics of Rosario (MPLPbioR)</i> , <sup>3</sup> <i>Department of NMR-assisted Structural Biology, In-cell NMR, Leibniz Institute of Molecular Pharmacology</i> , <sup>4</sup> <i>Centro de Investigación y de Estudios Avanzados (Cinvestav)</i> , <sup>5</sup> <i>Department of NMR-based Structural Biology, Max Planck Institute for Biophysical Chemistry</i> .....	155
9:35-10:00	<b>OP073: Structural studies of an engineered mimic of neurotoxic amyloid-<math>\beta</math> protofibrils</b> <sup>1</sup> Christofer Lendel, <sup>2</sup> Morten Bjerring, <sup>3</sup> Andrei Filippov, <sup>3,4</sup> Oleg N. Antzutkin, <sup>2</sup> Niels Christian Nielsen, <sup>1</sup> * <b>Torleif Härd</b> ; <sup>1</sup> <i>Dept. of Molecular Biology, Swedish University of Agricultural Sciences (SLU), Uppsala, Sweden.</i> , <sup>2</sup> <i>Dept. of Chemistry, Aarhus University, Aarhus, Denmark.</i> , <sup>3</sup> <i>Chemistry of Interfaces, Luleå University of Technology, Luleå, Sweden.</i> , <sup>4</sup> <i>Dept. of Physics, Warwick University, Coventry, United Kingdom.</i> .....	41

### Wednesday – May 22<sup>nd</sup> - Dynamics and Recognition

Chair: Rodolfo Rasia  
Room Gávea B

		page
8:30-8:55	<b>OP074: Probing Protein Conformational Flexibility with Pulsed EPR Spectroscopy</b> Xi Huang, I.M.S. de Vera, Manuel Britto, Mandy E. Blackburn, Angelo M. Veloro, Jamie L. Kear, * <b>Gail E Fanucci</b> ; <i>University of Florida</i> .....	42
8:55-9:20	<b>OP075: NMR Spectroscopy reveals alternative Ground States in Copper Proteins</b> * <b>Alejandro J. Vila</b> , Luciano A. Abriata, Andrés Espinoza-Cara, Marcos N. Morgada, María-Eugenia Zaballa; <i>Institute for Molecular and Celular Biology (IBR), University of Rosario, Argentina</i> .....	42
9:20-9:35	<b>UP076: NMR Studies of the Loop Dynamics of the Nitrophorins</b> * <b>F. Ann Walker</b> , Dhanasekaran Muthu, Robert E. Berry, Hongjun Zhang; <i>The University of Arizona</i> .....	42
9:35-10:00	<b>OP077: EPR Method Development for Addressing Protein Structure and Dynamics</b> <sup>1</sup> * <b>Gunnar Jeschke</b> , <sup>1</sup> Yevhen Polyhach, <sup>1</sup> Tona von Hagens, <sup>2</sup> Carsten Dietz, <sup>2</sup> Harald Paulsen; <sup>1</sup> <i>ETH Zurich</i> , <sup>2</sup> <i>University of Mainz</i> .....	43

### Wednesday – May 22<sup>nd</sup> - Workshop: NMR on Porous Media

Chair: Vinicius Machado  
Rooms Turmalina/Topázio

		page
8:30-8:55	<b>OP078: Improved Estimation of Oil and Gas Reserves Using Magnetic Resonance Imaging “MRI” Technology - Applications and Case Histories</b> *Maged Fam; <i>HALLIBURTON, Bogota, Colombia</i> .....	43
8:55-9:20	<b>OP079: Transport and Reaction in Porous Media: New Information Obtained Using Compressed Sensing and Bayesian Methods</b> *Lynn F. Gladden, D. J. Holland, Mick D. Mantle, J. Mitchell, Andrew J. Sederman, A. B. Tayler; <i>University of Cambridge, Department of Chemical Engineering and Biotechnology</i> .	43
9:20-9:35	<b>UP080: Pore Sizes Distribution of Unconsolidated Geomaterials</b> <sup>2,3</sup> *Marcos Montoro, <sup>1,3</sup> Lucas C. Cerioni, <sup>3</sup> Daniel José Pusioli; <sup>1</sup> <i>Spinlock SRL</i> , <sup>2</sup> <i>Universidad Nacional de Córdoba</i> , <sup>3</sup> <i>CONICET</i> .....	160
9:35-10:00	<b>OP081: Diffusion dynamics in porous media</b> *Yi-Qiao Song; <i>Schlumberger</i> .....	44

### Wednesday – May 22<sup>nd</sup> - Small Molecules and Methods

Chair: Jochen Junker  
Room Ônix

		page
8:30-8:55	<b>OP082: Structure Determination Using Anisotropic NMR Parameters</b> *Burkhard Luy; <i>Karlsruhe Institute of Technology</i> .....	44
8:55-9:20	<b>OP083: New NMR strategies for the accurate measurement of small heteronuclear coupling constants</b> *Teodor Parella; <i>Servei de Resonància Magnètica Nuclear, Universitat Autònoma de Barcelona, Catalonia</i> .....	44
9:20-9:35	<b>UP084: Experimental measurement and theoretical assessment of fast lanthanide electronic relaxation in solution with four series of isostructural complexes</b> <sup>1</sup> Alexander M. Funk, <sup>1*</sup> David Parker, <sup>1</sup> Peter Harvey, <sup>1</sup> Alan M. Kenwright, <sup>2</sup> Pascal H. Fries; <sup>1</sup> <i>Durham University</i> , <sup>2</sup> <i>CEA, Grenoble</i> .....	44
9:35-10:00	<b>OP085: Structural Analysis of Small Organic Molecules Assisted by Residual Dipolar Couplings</b> *Roberto R. Gil; <i>Carnegie Mellon University</i> .....	45
10:00-10:30	<b>Coffee Break</b>	

### Wednesday – May 22<sup>nd</sup> - Challenging Systems

Chair: Roberto Salinas  
Room Gávea A

		page
10:30-10:55	<b>OP086: Protein Dynamics: Its Kinetics and Implications for Function</b> <sup>1</sup> David Ban, <sup>1,2</sup> Colin Smith, <sup>1</sup> Michael Sabo, <sup>3</sup> R. Bryn Fenwick, <sup>1</sup> Korvin F. A. Walter, <sup>1</sup> Claudia Schwegk, <sup>1</sup> Stefan Becker, <sup>3</sup> Xavier Salvatella, <sup>1</sup> Berend L. de Groot, <sup>1</sup> Donghan Lee, <sup>1*</sup> <b>Christian Griesinger</b> ; <sup>1</sup> Max Planck Institute for Biophysical Chemistry - NMR based Structural Biology, <sup>2</sup> Max Planck Institute for Biophysical Chemistry - Theoretical and computational biophysics, <sup>3</sup> ICREA and Institute for Research in Biomedicine Barcelona ..	45
10:55-11:20	<b>OP087: Distance measurements in biomolecules using Gd<sup>3+</sup> spin labels</b> <sup>*</sup> Daniella Goldfarb; Weizmann Institute of Science, Rehovot, Israel.....	45
11:20-11:35	<b>UP088: Detection of light induced intermediates of photoreceptor membrane proteins by in-situ photo-irradiated solid-state NMR</b> <sup>1*</sup> Akira Naito, <sup>1</sup> Yuya Tomonaga, <sup>1</sup> Tetsuro Hidaka, <sup>1</sup> Hiroki Yomoda, <sup>1</sup> Teruki Makino, <sup>1</sup> Izuru Kawamura, <sup>2</sup> Yuki Sudo, <sup>3</sup> Akimori Wada, <sup>3</sup> Takashi Okitsu, <sup>4</sup> Naoki Kamo; <sup>1</sup> Yokohama National University, <sup>2</sup> Nagoya University, <sup>3</sup> Kobe Pharmaceutical University, <sup>4</sup> Matsuyama University.....	155
11:35-11:50	<b>UP089: High resolution conformational description of Alpha-synuclein inside neurons using mammalian In-cell NMR</b> Andres Binolfi, Beata Bekei, Francois-Xavier Theillet, Honor M. Rose, <sup>*</sup> Philipp Selenko; Leibniz Institut für Molekulare Pharmakologie (FMP-Berlin).....	158
11:50-12:15	<b>OP090: NMR studies of the structure and dynamics of protein-RNA interactions in gene regulation</b> <sup>1,2*</sup> Michael Sattler; <sup>1</sup> Institute of Structural Biology, Helmholtz Zentrum München, Germany, <sup>2</sup> Munich Center for Integrated Protein Science and Biomolecular NMR, Department Chemie, TUM, Germany.....	46

### Wednesday – May 22<sup>nd</sup> - Metabolomics and Chemometrics

Chair: Ana Gil  
Room Gávea B

		page
10:30-10:55	<b>OP091: Deciphering Cancer Metabolism for Drug Discovery</b> <sup>*</sup> Ulrich L. Günther, Christian Ludwig, Katarzyna Koczula, Farhat Khanim, Chris Bunce; University of Birmingham, UK.....	47
10:55-11:20	<b>OP092: Food NMR applied to typical Brazilian food products</b> <sup>*</sup> Antonio Gilberto Ferreira; Federal University of São Carlos - Chemistry Department.	47
11:20-11:35	<b>UP093: Visualizing metabolic system catalyzed by microbial ecosystem using statistical correlation analysis</b> <sup>1,2,3,4*</sup> Jun Kikuchi; <sup>1</sup> RIKEN Plant Science Center, <sup>2</sup> Biomass Engineering Program, RIKEN, <sup>3</sup> Nagoya University, <sup>4</sup> Yokohama City University.....	47
11:35-11:50	<b>UP094: The Use of Magnetic Resonance in Pollution Assessment: Theory and Applications</b> <sup>*</sup> Oliver A.H. Jones; RMIT University.....	47
11:50-12:15	<b>OP095: Rapid-dissolution <sup>13</sup>C DNP in kinetics of cellular transmembrane exchange</b> <sup>1*</sup> Philip W. Kuchel, <sup>2</sup> Guilhem Pagès, <sup>1</sup> Max Puckeridge; <sup>1</sup> University of Sydney, <sup>2</sup> Singapore Bioimaging Consortium.....	48

### Wednesday – May 22<sup>nd</sup> - Workshop: NMR on Porous Media

Chair: Vinicius Machado  
Rooms Turmalina/Topázio

		page
10:30-10:55	<b>OP096: Earth's-field Surface NMR for Groundwater Characterization</b> <sup>1,2</sup> * <b>Elliot Grunewald</b> , <sup>2</sup> Rosemary Knight, <sup>1</sup> David Walsh, <sup>2</sup> Denys Grombacher, <sup>2</sup> Jan O. Walbrecker, <sup>2</sup> Katherine Dlubac; <sup>1</sup> <i>Vista Clara, Inc.</i> , <sup>2</sup> <i>Stanford University</i> .....	48
10:55-11:20	<b>OP097: Magnetic Resonance Imaging of Fluids in Porous Media</b> * <b>Bruce J. Balcom</b> ; <i>MRI Research Centre, Department of Physics, University of New Brunswick, Canada</i> .....	48
11:20-11:35	<b>UP098: Single-scan T1-T2 relaxation correlation experiment</b> * <b>Susanna Ahola</b> , Ville-Veikko Telkki; <i>University of Oulu</i> .....	48
11:35-11:50	<b>UP099: High Pressure Magic Angle Spinning NMR Capability</b> <sup>1,2</sup> * <b>Flaviu R.V. Turcu</b> , <sup>1</sup> David W. Hoyt, <sup>1</sup> Jesse A. Sears, <sup>1</sup> John S. Loring, <sup>1</sup> Kevin M. Rosso, <sup>1</sup> Jian Z. Hu; <sup>1</sup> <i>Pacific Northwest National Laboratory</i> , <sup>2</sup> <i>"Babes-Bolyai" University, Romania</i> .....	49
11:50-12:15	<b>OP100: Efficient measurement of T1/T2 ratio in porous media</b> * <b>Martin D. Hürlimann</b> ; <i>Schlumberger – Doll Research, USA</i> .....	49

### Wednesday – May 22<sup>nd</sup> - Materials and Applications

Chair: Hellmut Eckert  
Room Ônix

		page
10:30-10:55	<b>OP101: Following Function in Real Time: New In situ NMR Methods for Studying Structure and Dynamics in Batteries and Supercapacitors</b> <sup>1</sup> Lina Zhou, <sup>1</sup> Michal Leskes, <sup>1</sup> Hao Wang, <sup>1</sup> Alex Forse, <sup>1</sup> John Griffin, <sup>2</sup> Nicole M. Trease, <sup>1</sup> Elodie Salager, <sup>1</sup> * <b>Clare. P. Grey</b> ; <sup>1</sup> <i>Chemistry Department, Cambridge University, UK</i> , <sup>2</sup> <i>Chemistry Department, Stony Brook University, USA</i> .....	49
10:55-11:20	<b>OP102: Unique Insights into Carbon Capture and Geosequestration of CO<sub>2</sub> from In Situ High-Pressure, High-Temperature NMR</b> J. Andrew Surface, Jeremy Moore, Mark Conradi, * <b>Sophia E. Hayes</b> ; <i>Washington University in St. Louis</i> .....	50
11:20-11:35	<b>UP103: Direct Alcohol Fuel Cells Investigated In Situ and Ex Situ by NMR Spectroscopy</b> <sup>1,2</sup> * <b>Oc Hee Han</b> ; <sup>1</sup> <i>Korea Basic Science Institute</i> , <sup>2</sup> <i>Chungnam National University</i> .....	50
11:35-11:50	<b>UP104: Local Order and Cation Distribution in Mixed-Alkali Phosphate Glasses</b> <sup>1</sup> * <b>José Fabian Schneider</b> , <sup>1</sup> Jefferson Tsuchida, <sup>2</sup> Hellmut Eckert, <sup>2</sup> Rashmi Deshpande; <sup>1</sup> <i>Instituto de Física de São Carlos, Universidade de São Paulo</i> , <sup>2</sup> <i>Institut für Physikalische Chemie, Westfälische Wilhelms-Universität Münster</i> .....	50
11:50-12:15	<b>OP105: Nanoscale Imaging of Electron and Nuclear Spins</b> * <b>Jörg Wrachtrup</b> ; <i>3rd Institute of Physics, University of Stuttgart, Stuttgart, Germany</i> .	50

12:15 -14:15 | **Lunch Break**

		page
14:15-18:00	Free for Excursions	
14:15-18:00	Satellite Meeting: <b>Biomedical Imaging Symposium</b> , Chair: Fernanda Moll, Room: Ônix. Requires separate registration.	

all day | **Vendors Exhibit Booths (Foyer)**

### Thursday – May 23<sup>rd</sup> - Plenary Session

Chair: Beat Meier  
Room Gávea A

		page
8:30-9:15	<b>PL106: Spectroscopy in the Clinic – from dreams to reality</b> * <b>Jeremy K. Nicholson</b> ; <i>Department of Surgery and Cancer, Faculty of Medicine, Imperial College London</i> .....	51
9:15-10:00	<b>PL107: New contraptions/gadgets/techniques for solid-state NMR</b> * <b>K. Takegoshi</b> ; <i>Department of Chemistry, Graduate School of Science, Kyoto University, Kyoto, Japan</i> .....	51
10:00-10:30	<b>Coffee Break</b>	

### Thursday – May 23<sup>rd</sup> - DNP

Chair: Christian Griesinger  
Room Gávea A

		page
10:30-10:55	<b>OP108: Magnetic resonance is no longer the world's least sensitive form of spectroscopy</b> <sup>1,2</sup> * <b>Geoffrey Bodenhausen</b> ; <sup>1</sup> <i>Ecole Normale Supérieure, Paris</i> , <sup>2</sup> <i>Ecole Polytechnique Fédérale, Lausanne</i> .....	51
10:55-11:20	<b>OP109: Dissolution Dynamic Nuclear Polarization of Large Molecules</b> * <b>Christian Hilty</b> , Mukundan Ragavan, Hsueh-Ying Chen, Youngbok Lee, Haifeng Zeng, Hlaing Min; <i>Texas A&amp;M University, Chemistry Department, USA</i> .....	52
11:20-11:35	<b>UP110: DNP Surface Enhanced NMR (SENS): a Tool for Structural Investigation of Supported Catalysis</b> <sup>1</sup> * <b>Moreno Lelli</b> , <sup>1</sup> Alexandre Zagdoun, <sup>1</sup> David Gajan, <sup>1</sup> Aaron J. Rossini, <sup>4</sup> Olivier Ouari, <sup>4</sup> Paul Tordo, <sup>3</sup> Chloé Thieuleux, <sup>2</sup> Christophe Copéret, <sup>1</sup> Anne Lesage, <sup>1</sup> Lyndon Emsley; <sup>1</sup> <i>Centre de RMN à Très Hauts Champs, Université de Lyon (CNRS/ENS Lyon/UCB Lyon 1)</i> , <sup>2</sup> <i>Department of Chemistry, ETH Zürich, Switzerland</i> , <sup>3</sup> <i>Institut de Chimie de Lyon, Université de Lyon (CNRS-Université Lyon 1-ESCE Lyon)</i> , <sup>4</sup> <i>Aix-Marseille Université, CNRS, Institut de Chimie Radicale (ICR), Marseille</i> .....	159
11:35-11:50	<b>UP111: Sensitivity enhancement in solution NMR through dynamic nuclear polarization of encapsulated proteins</b> <sup>1</sup> Kathleen G. Valentine, <sup>2</sup> Guinevere Mathies, <sup>1</sup> Nathaniel V. Nucci, <sup>1</sup> Igor Dodevski, <sup>1</sup> Sabrina Bédard, <sup>1</sup> Matthew Stetz, <sup>2</sup> Thach V. Can, <sup>2</sup> Robert G. Griffin, <sup>1</sup> * <b>A. Joshua Wand</b> ; <sup>1</sup> <i>University of Pennsylvania</i> , <sup>2</sup> <i>Massachusetts Institute of Technology</i> .....	159
11:50-12:15	<b>OP112: Dissolution DNP: Theoretical Considerations and Experimental Implementation</b> Grzegorz Kwiatkowski, Alexander Karabanov, * <b>Walter Köckenberger</b> ; <i>University of Nottingham</i> .....	53

### Thursday – May 23<sup>rd</sup> - Dynamics and Recognition

Chair: Martin Billeter  
Room Gávea B

		page
10:30-10:55	<b>OP113: Use of Solution NMR for Studies of Proteins and Protein Complexes Involved in Protein and Peptide Synthesis</b> <i>*Gerhard Wagner; Department of Biological Chemistry and Molecular Pharmacology, Harvard Medical School, Boston.....</i>	53
10:55-11:20	<b>OP114: Allosteric Motions in periplasmic binding Proteins characterized by NMR Spectroscopy</b> <i>Gabriel Ortega, Tammo Diercks, *Oscar Millet; CIC bioGUNE, Parque Tecnológico de Vizcaya, Spain.....</i>	53
11:20-11:35	<b>UP115: Atomistic Descriptions of Protein Dynamics on Multiple Timescales From NMR Chemical Shifts</b> <i>*Paul Robustelli; Columbia University.....</i>	157
11:35-11:50	<b>UP116: Viral RNAs and Infection</b> <i>Joseph D. Puglisi, Aaron Coey, *Elisabetta Viani; Department of Structural Biology &amp; Stanford Magnetic Resonance Laboratory, Stanford University.....</i>	54
11:50-12:15	<b>OP117: High-Resolution Protein Structures by Magic-Angle Spinning NMR</b> <i>*Chad M. Rienstra, Marcus D. Tuttle, Gemma Comellas, Andrew J. Nieuwkoop, Ming Tang, Lindsay J. Sperling, Robert B. Gennis, Julia M. George; University of Illinois at Urbana Champaign.....</i>	54

### Thursday – May 23<sup>rd</sup> - New Solution NMR Methods

Chair: Julien Wist  
Rooms Turmalina/Topázio

		page
10:30-10:55	<b>OP118: Broadband Inversion of 1JCC Correlations in 1,n-ADEQUATE Spectra</b> <i><sup>1</sup>*Gary E Martin, <sup>1</sup>Mikhail Reibarkh, <sup>1</sup>R. Thomas Williamson, <sup>2</sup>Wolfgang Bermel; <sup>1</sup>Merck Research Laboratories, <sup>2</sup>Bruker BioSpin.....</i>	54
10:55-11:20	<b>OP119: Highlighting Change</b> <i><sup>1</sup>*Ēriks Kupče, <sup>2</sup>Ray Freeman; <sup>1</sup>Bruker Ltd, Coventry, UK, <sup>2</sup>Jesus College, Cambridge, UK.....</i>	55
11:20-11:35	<b>UP120: Measurements of Nuclear Magnetic Shielding</b> <i>*Karol Jackowski; Faculty of Chemistry, University of Warsaw, Poland.....</i>	55
11:35-11:50	<b>UP121: Optimizing Ionic Liquids for CO<sub>2</sub> Capture: an NMR Approach</b> <i><sup>1</sup>Marta Corvo, <sup>1</sup>João Sardinha, <sup>2</sup>Sonia Maria Cabral de Menezes, <sup>3</sup>Jairton Dupont, <sup>3</sup>Graciane Marin, <sup>4</sup>Sandra Einloft, <sup>4</sup>Marcus Seferin, <sup>1</sup>Teresa Casimiro, <sup>1</sup>*Eurico J. Cabrita; <sup>1</sup>REQUIMTE/CQFB, Dept. Química, Fac. Ciências e Tecnologia, Univ. Nova Lisboa, Portugal, <sup>2</sup>PETROBRAS/CENPES, RJ Brazil, <sup>3</sup>Dept. Química Orgânica, Inst. Química, Univ. Federal do Rio Grande do Sul, Brazil, <sup>4</sup>Fac. Química Pontifícia Univ. Católica Rio Grande do Sul, Brazil.....</i>	156
11:50-12:15	<b>OP122: Old Dog, New Tricks: Methodological NMR Developments to Characterize Solution-State Structure and Dynamics</b> <i>Pieter ES Smith, Gonzalo A Álvarez, Noam Shemesh, Gershon Kurizki, *Lucio Frydman; Department of Chemical Physics, Weizmann Institute of Science, Israel.....</i>	56



### Thursday – May 23<sup>rd</sup> - New BioSolid Methods

Chair: Stanley Opella  
Room Onix

		page
10:30-10:55	<b>OP123: Designing efficient re- and decoupling experiments for biological solid-state NMR using optimal control and effective Hamiltonian methods</b> *Niels Christian Nielsen; Aarhus University, Aarhus, Denmark.....	56
10:55-11:20	<b>OP124: Spectrally Edited 2D NMR of Carbon Materials and Proteins</b> <sup>1</sup> *Klaus Schmidt-Rohr, <sup>1</sup> Robert L. Johnson, <sup>1</sup> Keith J. Fritzsche, <sup>2</sup> Jason Anderson, <sup>2</sup> Brent Shanks, <sup>1</sup> Mei Hong; <sup>1</sup> Department of Chemistry, Iowa State University, <sup>2</sup> Department of Chemical and Biological Engineering, Iowa State University.....	56
11:20-11:35	<b>UP125: Recording Quantitative One- and Two-Dimensional <sup>13</sup>C NMR Spectra of Microcrystalline Proteins with Improved Sensitivity</b> <sup>1,2,3</sup> *Piotr Tekely, <sup>1,3</sup> Rudra Narayan Purusottam, <sup>1,2,3</sup> Geoffrey Bodenhausen; <sup>1</sup> Ecole Normale Supérieure (ENS), <sup>2</sup> Centre National de la Recherche Scientifique (CNRS), <sup>3</sup> Université Pierre et Marie Curie (UPMC).....	57
11:35-11:50	<b>UP126: Molecular interactions with the bacterial cell wall by liquid state, standard and DNP solid state NMR.</b> <sup>1</sup> Catherine Bougault, <sup>1</sup> Lauriane Lecoq, <sup>2</sup> Sabine Hediger, <sup>2</sup> Hiroki Takahashi, <sup>2</sup> Gaël De Paëpe, <sup>3</sup> Michel Arthur, <sup>1</sup> *Jean-Pierre Simorre; <sup>1</sup> Institut de Biologie Structurale CEA-CNRS-UFJ Grenoble, <sup>2</sup> Laboratoire de Chimie Inorganique et Biologique, CEA Grenoble, <sup>3</sup> Centre de Recherche des Cordeliers, INSERM, Paris.....	57
11:50-12:15	<b>OP127: The HIPER project – Very High Sensitivity Pulse EPR</b> <sup>1</sup> *Graham Smith, <sup>1</sup> Hassane El Mkami, <sup>1</sup> Paul Cruickshank, <sup>1</sup> Robert Hunter, <sup>1</sup> David Bolton, <sup>1</sup> Duncan Robertson, <sup>1</sup> Bela Bode, <sup>2</sup> Olav Schiemann, <sup>3</sup> Richard Wylde, <sup>4</sup> David Keeble, <sup>4</sup> David Norman; <sup>1</sup> University of St Andrews, Scotland, <sup>2</sup> University of Bonn, Germany, <sup>3</sup> Thomas Keating Ltd, Billingshurst England, <sup>4</sup> University of Dundee, Scotland.....	57
12:15-14:15	<b>Lunch Break</b>	

### Thursday – May 23<sup>rd</sup> - New BioNMR Methods

Chair: Gisele Amorim  
Room Gávea A

		page
14:15-14:40	<b>OP128: High Sensitivity Pulse Dipolar ESR and Protein Structure</b> *Jack H. Freed; Department of Chemistry and Chemical Biology, Cornell University, Ithaca, New York, USA.....	58
14:40-15:05	<b>OP129: Harnessing the Synergies between NMR and Computation for the Understanding of Protein Function</b> <sup>1,2</sup> Mioara Larion, <sup>1,2,3</sup> Roberto Salinas, <sup>4</sup> Vitali Tugarinov, <sup>1,2</sup> Dawei Li, <sup>1,2</sup> Dong Long, <sup>1,2</sup> Yina Gu, <sup>2</sup> Lei Bruschweiler-Li, <sup>1</sup> Brian Miller, <sup>1,2</sup> *Rafael Brüschweiler; <sup>1</sup> Department of Chemistry and Biochemistry, Florida State University, <sup>2</sup> National High Magnetic Field Laboratory, Tallahassee, FL, <sup>3</sup> Institute of Chemistry, University of São Paulo, <sup>4</sup> Department of Chemistry and Biochemistry, University of Maryland.....	58
15:05-15:20	<b>UP130: A unified conformational selection and induced fit approach to the modelling of protein-peptide interactions.</b> Mikael Trellet, Adrien Melquiond, *Alexandre M. J. J. Bonvin; Utrecht University, Faculty of Science, Bijvoet Center.....	58
15:20-15:35	<b>UP131: Replica Averaging-Replica Exchange (RARE) Molecular dynamics simulations with NMR chemical shifts</b> *Carlo Camilloni, Andrea Cavalli, Michele Vendruscolo; University of Cambridge.....	59
15:35-16:00	<b>OP132: Extending the Empirical Limits of Chemical Shifts</b> Yang Shen, Alex Maltsev, Alexey Mantsyzov, Jinfa Ying, *Ad Bax; Laboratory of Chemical Physics, NIDDK, NIH.....	59

### Thursday – May 23<sup>rd</sup> - Bio-Solids

Chair: Mônica Freitas  
Room Gávea B

		page
14:15-14:40	<b>OP133: Type-III secretion needles studied by solid-state NMR</b> <sup>1</sup> Jean-Philippe Demers, <sup>1</sup> Antoine Loquet, <sup>1</sup> Veniamin Shevelkov, <sup>2</sup> Nikolaos Sgourakis, <sup>3</sup> Rashmi Gupta, <sup>3</sup> Michael Kolbe, <sup>1</sup> Karin Giller, <sup>1</sup> Dietmar Riedel, <sup>1</sup> Christian Griesinger, <sup>2</sup> David Baker, <sup>1</sup> Stefan Becker, <sup>1*</sup> <b>Adam Lange</b> ; <sup>1</sup> Max Planck Institute for Biophysical Chemistry, Göttingen, Germany, <sup>2</sup> Department of Biochemistry, University of Washington, USA, <sup>3</sup> Max Planck Institute for Infection Biology, Berlin, Germany .....	59
14:40-15:05	<b>OP134: Solid-State NMR Structural Studies of Proteins Using Paramagnetic Probes</b> <sup>1</sup> Ishita Sengupta, <sup>1</sup> Philippe S. Nadaud, <sup>1</sup> Min Gao, <sup>1</sup> Rajith J. Arachchige, <sup>2</sup> Charles D. Schwitters, <sup>1*</sup> <b>Christopher P. Jaroniec</b> ; <sup>1</sup> The Ohio State University, Columbus, USA, <sup>2</sup> National Institutes of Health, Bethesda, USA .....	59
15:05-15:20	<b>UP135: 100 kHz Magic-Angle Spinning for Proteins</b> <sup>1*</sup> <b>Beat H. Meier</b> , <sup>2</sup> Ago Samoson, <sup>3</sup> Anja Böckmann, <sup>1</sup> Matthias Ernst, <sup>1</sup> Vipin Agarwal, <sup>2</sup> Marie-Laure Fogeron, <sup>1</sup> Matthias Huber, <sup>1</sup> Susanne Penzel, <sup>1</sup> Francesco Ravotti; <sup>1</sup> ETH Zurich, Physical Chemistry, Switzerland, <sup>2</sup> Tallinn University of Technology, Estonia, <sup>3</sup> IBCP, CNRS, Lyon, France .....	60
15:20-15:35	<b>UP136: Determining supramolecular organisation of ion channels by solid-state NMR and computational methods</b> <sup>1*</sup> <b>Markus Weingarth</b> , <sup>1</sup> Elwin van der Cruysen, <sup>1,2</sup> Alexander Prokofyev, <sup>1</sup> Eline Koers, <sup>1</sup> Alexandre M. J. J. Bonvin, <sup>2</sup> Olaf Pongs, <sup>1</sup> Marc Baldus; <sup>1</sup> Utrecht University, Bijvoet Center for Biomolecular Research, Utrecht, The Netherlands, <sup>2</sup> Saarland University, Faculty of Medicine, Department of Physiology, Homburg, Germany .....	157
15:35-16:00	<b>OP137: Membranes, crystals, sediments: solid-state NMR of large proteins</b> <sup>1*</sup> <b>Anja Böckmann</b> , <sup>2</sup> Beat H. Meier, <sup>1</sup> Britta Kunert, <sup>2</sup> Andreas Hunkeler, <sup>2</sup> Susanne Penzel, <sup>2</sup> Anne Schütz, <sup>1</sup> Laurent Terradot Alexandre Bazin, <sup>1</sup> Pierre Falson, <sup>3</sup> Jean-Michel Jault, <sup>1</sup> Carole Gardiennet; <sup>1</sup> Institut de Biologie et Chimie des Protéines, CNRS-Université de Lyon, France, <sup>2</sup> ETH Zürich, Physical Chemistry, CH-8093 Zürich, Switzerland, <sup>3</sup> IBS, CNRS-CEA-Université de Grenoble, France .....	60

### Thursday – May 23<sup>rd</sup> - Contrast Agents/ Instrumentation

Chair: Carlos Geraldès  
Rooms Turmalina/Topázio

		page
14:15-14:40	<b>OP138: New Directions in Dipolar Imaging to Enhance Endogenous Contrast</b> <sup>*</sup> <b>Warren S. Warren</b> , Thomas Theis, Yi Han, Zijian Zhou; Duke University .....	60
14:40-15:05	<b>OP139: Capturing Signals from Ultrafast Relaxing Spins with SWIFT MRI</b> <sup>*</sup> <b>Michael Garwood</b> ; Center for Magnetic Resonance Research, University of Minnesota, USA .....	61
15:05-15:20	<b>UP140: Molecular imaging of tumors using CEST MRI of 2DG and FDG</b> <sup>1</sup> Michal Rivlin, <sup>2</sup> Galia Tzarfaty, <sup>1</sup> Judith Horev, <sup>1</sup> Ilan Tzarfaty, <sup>1*</sup> <b>Gil Navon</b> ; <sup>1</sup> Tel Aviv University, <sup>2</sup> Chaim Sheba Medical center .....	61
15:20-15:35	<b>UP141: Physiological Model for the Determination of rCMR(O<sub>2</sub>) and rCBF by <sup>17</sup>O MRI in the Human</b> <sup>*</sup> <b>Daniel Fiat</b> ; University of Illinois at Chicago .....	61
15:35-16:00	<b>OP142: Magnetic Susceptibility Contrast in Human Brain</b> <sup>*</sup> <b>Jeff Duyn</b> , Peter van Gelderen, Pascal Sati, Afonso Silva, Daniel Reich, Hellmut Merkle, Jacco de Zwart; Laboratory of Functional and Molecular Imaging, National Institutes of Health, Bethesda .....	62

### Thursday – May 23<sup>rd</sup> - Physics

Chair: Jose Schneider  
Room Ònix

		page
14:15-14:40	<b>OP143: Dynamics and Quantum Information Transport in Nuclear Spin Chains</b> *Paola Cappellaro; <i>Massachusetts Institute of Technology</i> .....	62
14:40-15:05	<b>OP144: Loschmidt Echoes as Quantifiers of Decoherence, Quantum Phase Transitions and Thermalization in Interacting Spin Systems</b> <sup>1,2</sup> *Horacio M. Pastawski, <sup>1,2</sup> Patricia R. Levstein; <sup>1</sup> <i>LaNIS de RMS, Instituto de Física Enrique Gaviol (CONICET-UNC)</i> , <sup>2</sup> <i>Facultad de Matemática Astronomía y Física, Universidad Nacional de Córdoba</i> .....	62
15:05-15:20	<b>UP145: Origin of Long-Lived Signals in Dipolar Coupled Spin Systems</b> <sup>1</sup> *Alexej Jerschow, <sup>1</sup> Jae-Seung Lee, <sup>2</sup> Anatoly Khitrin; <sup>1</sup> <i>New York University</i> , <sup>2</sup> <i>Kent State University</i> .....	62
15:20-15:35	<b>UP146: High Resolution Para-Hydrogen Induced Polarization (PHIP) in Inhomogeneous Magnetic Fields</b> <sup>1,2</sup> *Lisandro Buljubasich, <sup>1,2</sup> Ignacio Prina, <sup>3</sup> María Belén Franzoni, <sup>3</sup> Kerstin Münnemann, <sup>3</sup> Hans Wolfgang Spiess, <sup>1,2</sup> Rodolfo Héctor Acosta; <sup>1</sup> <i>FAMAF – Universidad Nacional de Córdoba</i> , <sup>2</sup> <i>IFEG –CONICET</i> , <sup>3</sup> <i>Max Plank Institut für Polymerforschung</i> .....	157
15:35-16:00	<b>OP147: Using single spins for quantum computing and sensing</b> *Dieter Suter; <i>TU Dortmund</i> .....	63
16:00-18:30	<b>Poster Session III</b> Rooms Quartzo A/B, Authors with poster numbers starting "TH" present	
all day	<b>Vendors Exhibit Booths (Foyer)</b>	
18:30	Shuttle Buses start leaving to hotels and Brazilian Night	
20:00-24:00	<b>Brazilian Night (banquet, show and music) at Fogo de Chão Brazilian Steak House (Av. Repórter Nestor Moreira s/n, Botafogo) – Tickets required.</b>	
22:30-24:00	Shuttle Buses will return to hotels	

### Friday – May 24<sup>th</sup> - Membrane Proteins

Chair: Laurent Catoire  
Room Gávea A

		page
8:30-8:55	<b>OP148: NMR studies on the type IV secretion system of <i>Xanthomonas citri</i></b> Diorge Souza, Luciana Coutinho de Oliveira, Denize C. Favaro, Cristina Alvarez-Martinez, Chuck Farah, * <b>Roberto Salinas</b> ; <i>Department of Biochemistry, Institute of Chemistry, USP</i>	63
8:55-9:20	<b>OP149: Magic Angle Spinning Solid-State NMR Studies of Membrane Proteins</b> * <b>Vladimir Ladizhansky</b> ; <i>University of Guelph</i> .....	63
9:20-9:35	<b>UP150: Comparison of Structure of Cyanobacteria and Spinach PSII Studied by PELDOR</b> <sup>1</sup> * <b>Asako Kawamori</b> , <sup>2</sup> Jiang-Ren Shen, <sup>3</sup> Hiroyuki Mino; <sup>1</sup> <i>AGAPE-Kabutoyama Institute of Medicine</i> , <sup>2</sup> <i>Department of Biology, Okayama University</i> , <sup>3</sup> <i>Department of Physics, Nagoya University</i> .....	158
9:35-10:00	<b>OP151: Structure Determination of Membrane Proteins in their Native Environment of Phospholipid Bilayers</b> * <b>Stanley Opella</b> ; <i>University of California, San Diego</i> .....	64

### Friday – May 24<sup>th</sup> - Instrumentation

Chair: Mario Engelsberg  
Room Gávea B

		page
8:30-8:55	<b>OP152: Robust Multi-Phase Flow Measurements Using Magnetic Resonance</b> <sup>1,2</sup> * <b>Daniel José Pusiol</b> , <sup>1</sup> Lucas C. Cerioni; <sup>1</sup> <i>Instituto de Física Enrique Gaviola IFEG, CONICET, Ciudad Universitaria, Córdoba, Argentina</i> , <sup>2</sup> <i>SPINLOCK SRL &amp; CONICET, Córdoba, Argentina</i> .....	64
8:55-9:20	<b>OP153: Using Time Domain NMR to Study Magneto-electrolysis phenomenon in Situ</b> <sup>1</sup> * <b>Luiz Alberto Colnago</b> , <sup>1</sup> Luis Fernando Cabeça, <sup>2</sup> Luiza Maria da Silva Nunes, <sup>2</sup> Paulo Falco Cobra, <sup>2</sup> Bruna Ferreira Gomes, <sup>1</sup> André de Souza Carvalho; <sup>1</sup> <i>Embrapa Instrumentação, São Carlos/SP - Brazil</i> , <sup>2</sup> <i>Instituto de Química de São Carlos - USP</i> .....	64
9:20-9:35	<b>UP154: In situ MR: Pore condensation at elevated temperature and pressure</b> <sup>1</sup> * <b>Matthew P. Renshaw</b> , <sup>1</sup> S. Tegan Roberts, <sup>2</sup> Belinda S. Akpa, <sup>1</sup> Mick D. Mantle, <sup>1</sup> Andrew J. Sederman, <sup>1</sup> Lynn F. Gladden; <sup>1</sup> <i>University of Cambridge</i> , <sup>2</sup> <i>University of Illinois at Chicago</i>	159
9:35-10:00	<b>OP155: Compact NMR of Materials and Processes</b> * <b>Bernhard Blümich</b> ; <i>RWTH Aachen University</i> .....	65

### Friday – May 24<sup>th</sup> - Innovative NMR/MRI Methods

Chair: Betty Gaffney  
Rooms Turmalina/Topázio

		page
8:30-8:55	<b>OP156: Relaxometry and dynamics</b> * <b>Claudio Luchinat</b> ; <i>Magnetic Resonance Center (CERM), University of Florence</i> .....	65
8:55-9:20	<b>OP157: The Nitrogen-Vacancy Center in Diamond As A Nanoscale Spin Sensor</b> <sup>1</sup> Abdelghani Laraoui, <sup>2</sup> Florian Dolde, <sup>2</sup> Tobias Staudacher, <sup>2</sup> Jörg Wrachtrup, <sup>2</sup> Friedemann Reinhard, <sup>1</sup> * <b>Carlos A. Meriles</b> ; <sup>1</sup> <i>Department of Physics, CUNY - City College of New York, New York</i> , <sup>2</sup> <i>3rd Physics Institute, University of Stuttgart, Germany</i> .....	66
9:20-9:35	<b>UP158: Mitochondrial function in diabetes: Novel methodology and new insight</b> * <b>Liping Yu</b> , Brian Fink, Judith Herlein, William Sivitz; <i>University of Iowa</i> .....	66
9:35-10:00	<b>OP159: Using SABRE as a route to hyperpolarization in NMR and MRI</b> <sup>1</sup> * <b>Simon B Duckett</b> , <sup>1</sup> Kevin D. Atkinson, <sup>1</sup> Alex J. J. Hooper, <sup>1</sup> Lyrelle S. Lloyd, <sup>2</sup> Gary G. R. Green, <sup>1</sup> Marianna Fekete, <sup>1</sup> Richard A. Green, <sup>1</sup> Ryan E. Mewis, <sup>1</sup> Louise A. R. Highton; <sup>1</sup> <i>York Centre for Hyperpolarisation in Magnetic Resonance</i> , <sup>2</sup> <i>York Neuroimaging Centre</i> ..	66

### Friday – May 24<sup>th</sup> - Small Molecules and Bioactive Peptides

Chair: Marta Bruix  
Room Ônix

		page
8:30-8:55	<b>OP160: NMR Studies of the Self-Association and Membrane Binding of Cytoclotides</b> *David J Craik, Conan Wang, K Johan Rosengren, Anne Conibear, Sonia T Henriques; <i>Institute for Molecular Bioscience, The University of Queensland, Australia.....</i>	66
8:55-9:20	<b>OP161: Separative NMR: adapted resolution for complex mixtures of small molecules</b> <sup>1,2</sup> *Stefano Caldarelli; <sup>1</sup> Aix Marseille Université, Marseille, France, <sup>2</sup> CNRS UPR 2301 <i>Ecole Palaiseau France.....</i>	67
9:20-9:35	<b>UP162: Structural Basis for the Interaction of Human <math>\beta</math>-Defensins 1 and 6 and Its Putative Chemokine Receptor CCR2 and Breast Cancer Microvesicles</b> *Viviane Silva de Paula, Robson Q. Monteiro, Fabio C. L. Almeida, Ana Paula Valente; <i>Universidade Federal do Rio de Janeiro.....</i>	155
9:35-10:00	<b>OP163: Breaking the barrier: NMR of membrane-active peptides</b> *Frances Separovic; <i>School of Chemistry, Bio21 Institute, University of Melbourne, Australia.....</i>	67

10:00-10:30 | Coffee Break

### Friday – May 24<sup>th</sup> - Plenary Session

Chair: Sonia Menezes  
Room Gávea A

		page
10:30-11:15	<b>PL164: Nuclear Spins, High Magnetic Fields, and Traveling Waves in Pursuit of Human Brain Function and Connectivity</b> *Kamil Ugurbil; <i>CMRR, University of Minnesota, USA.....</i>	68
11:15-12:00	<b>PL165: Synergy between NMR, cryo-EM and large-scale MD simulations - Novel Findings for HIV Capsid Function</b> *Angela M. Gronenborn; <i>Department of Structural Biology, University of Pittsburgh...</i>	68

### Closing Ceremony

Room Gávea A

12:00-12:30 12:30	Closing Remarks by José Daniel Figueroa-Villar and Hans Spiess Adjourn	page
----------------------	---	------

12:30-14:30 | Lunch Break

14:30-18:20	Free for Excursions	page
14:30-18:20	Satellite Meeting: <b>V<sup>th</sup> Iberoamerican NMR Meeting</b> , Chair: Fabio Almeida (UFRJ, Brazil), Room: Turmalina/Topázio. Requires separate registration.	

## Abstracts of Talks

**Sunday – May 19<sup>th</sup>  
Honor and Prizes Session**

Presiding: Hans Spiess  
Room Gávea A

**PL001: Emerging Frontiers in Ultrafast Multidimensional NMR and MRI**

Rita Schmidt, Eddy Solomon, Avi Leftin, \***Lucio Frydman**  
*Department of Chemical Physics, Weizmann Institute of Science, Israel*

We have developed a scheme enabling the acquisition of arbitrary multidimensional NMR spectra and/or images (MRI), within a single scan. This is by contrast to the hundreds or thousands of scans that are usually needed to collect this kind of data. Provided that the target molecule's signal is sufficiently strong, the acquisition time of NMR/MRI scans can thus be shortened by several orders of magnitude. This new "ultrafast" methodology is compatible with existing multidimensional pulse sequences and can be implemented using conventional hardware. The manner by which the spatiotemporal encoding of the NMR interactions –which is the new principle underlying these new protocols– proceeds in these experiments, will be summarized. The new horizons that are opened by these protocols will also be exemplified with a variety of NMR and MRI projects we are currently involved in in fields of chemistry, biophysics, biology and medicine. The incorporation into these experiments of nuclear hyperpolarization procedures capable of increasing the single-scan sensitivity of single-scan liquid state NMR by factors ranging from 103-106, will also be assessed.

Acknowledgments: : BioNMR EU Grant #261863, EU ERC Advanced Grant # 246754, Kamin-Yeda Grant (Israel), Israel Science Foundation, Fulbright and Natl. Science Foundations (US)

**Monday – May 20<sup>th</sup>  
Plenary Session**

Chair: Daniella Goldfarb  
Room Gávea A

**PL002: Biomolecular NMR at Very Low Temperatures**

\***Robert Tycko**, Kent Thurber, Alexey Potapov, Wai-Ming Yau, Eric Moore

*National Institutes of Health*

Our group pursues research on solid state NMR methods and their application to structural problems in biological systems. This lecture will focus on recent efforts to develop and apply new technology for NMR measurements on biological systems at temperatures below 30 K. These efforts include the design and construction of an apparatus for magic-angle spinning with sample temperatures in the 20-25 K range, in which the sample is cooled with liquid helium while sample rotation is driven with nitrogen gas, and the development of a dynamic nuclear polarization (DNP) system that operates at temperatures as low as 8 K (without MAS) or 20 K (with MAS) and uses relatively low microwave powers at 264 GHz (the electron spin resonance frequency of nitroxides in a 9.4 T magnet). Our latest results from experiments that use very low temperatures will be described, possibly including structural studies of transient intermediate states in a rapid protein folding process (trapped by rapid freeze-quenching), structural studies of intermediate states in the self-assembly of beta-amyloid peptides into amyloid fibrils, or attempts to obtain micron-resolution magnetic resonance images with the assistance of low temperatures and DNP.

**PL003: Sensitivity enhancement in High Field NMR and EPR**

Vasyl Denysenkov, Petr Neugebauer, Phillip Spindler, Burkhard Endeward, \***Thomas F. Prisner**

*Institute of Physical and Theoretical Chemistry and Center of Biomolecular Magnetic Resonance, Goethe University Frankfurt, Germany*

Sensitivity is a major limitation for the application of NMR to samples with low spin concentration or restricted volume. We have explored the use of dynamic nuclear polarization (DNP) to enhance liquid NMR signals at a magnetic field of 9.2 T (400 MHz proton and 260 GHz electron spin resonance frequency) at ambient temperatures. Enhancements of up to -80 have been experimentally observed and rationalized with respect to the electron-nuclear spin coupling efficiency, saturation behavior of the electron spin and viscosity of the solvent. EPR offers increased sensitivity, compared to NMR, because of the at 660 times larger magnetic moment of the electron spin with respect to a proton spin, but is typically performed at lower magnetic fields. At high magnetic fields the EPR line shape becomes typically very broad and thus cannot be efficiently excited by the limited power available above 100 GHz microwave frequency. This severely restricts the efficiency of pulsed EPR and DNP methods. We will show new approaches to improve the sensitivity by the application of new pulse schemes for EPR and the use of high power cw microwave gyrotron sources for DNP and discuss the potential and limitations of these methods for biomolecular applications.

ACKNOWLEDGEMENTS: German Research Society and Center of Excellence Frankfurt Macromolecular Complexes for financial support

**Monday – May 20<sup>th</sup>  
Dynamics and Catalysis**

Chair: Jarbas Resende  
Room Gávea A

**OP004: Control of Periplasmic Interdomain Thiol: Disulfide Exchange in the Transmembrane Oxidoreductase DsbD**

<sup>1</sup>Despoina A.I. Mavridou, <sup>2</sup>Emmanuel Saridakis, <sup>1</sup>Paraskevi Kritsiligkou, <sup>1</sup>Lukas Stelzl, <sup>1</sup>Erin C. Mozley, <sup>1</sup>Alan D. Goddard, <sup>1</sup>Julie M. Stevens, <sup>1</sup>Stuart J. Ferguson, <sup>1</sup>\***Christina Redfield**

<sup>1</sup>*Department of Biochemistry, University of Oxford,*  
<sup>2</sup>*National Center for Scientific Research Demokritos*

Oxidative protein folding is essential for stability and function of numerous proteins. *In vivo*, thiol:disulfide exchange reactions are catalyzed by a range of oxidoreductases which often contain the thioredoxin fold. The protein DsbD transfers electrons from the cytoplasm to the periplasm of Gram-negative bacteria. This reducing power is required in the otherwise oxidizing periplasm for the isomerization of incorrect disulfide bonds (Dsb) and for cytochrome c maturation (Ccm). Reductant transfer occurs via a series of thiol:disulfide exchange reactions between pairs of conserved cysteines in the three domains of DsbD, tmDsbD (the integral membrane domain), nDsbD and cDsbD (the N- and C-terminal periplasmic domains) and their partner proteins on both sides of the inner membrane. The flow of electrons starts from cytoplasmic thioredoxin and proceeds to tmDsbD, then to cDsbD and nDsbD and ends with the periplasmic proteins DsbC and CcmG. NMR spectroscopy has been used to study the reactivity and specificity of these processes. cDsbD has a thioredoxin fold; the N-terminal cysteine, C461, in the characteristic CXXC motif attacks the disulfide bond of nDsbD. Knowledge of cysteine pK<sub>a</sub>s is important in understanding

their reactivity. C461 has an unusually high  $pK_a$ ; this makes C461, in isolated cDsbD, a poor nucleophile and implies relative unreactivity towards the target disulfide in nDsbD. NMR studies of an nDsbD- $^{15}\text{N}$ -cDsbD covalent complex allowed specific changes in active-site  $pK_a$  values due to contact with its physiological partner to be examined. The observed modulation of  $pK_a$  values is critical for the specificity and function of cDsbD. In recent studies the interactions of nDsbD and cDsbD have been shown to be oxidation-state dependent such that the functionally-relevant complex nDsbD<sub>ox</sub>-cDsbD<sub>red</sub>, has a higher affinity than the product complex, nDsbD<sub>red</sub>-cDsbD<sub>ox</sub>. The principles established have wider significance for understanding of processes mediated by thioredoxin-like proteins which are critical in prokaryotes and eukaryotes.

#### OP005: Hydration of yeast Thioredoxin 1 Modulates Slow Dynamics

\***Fabio C. L. Almeida**

*Institute of Medical Biochemistry, National Center of Nuclear Magnetic Resonance, Federal University*

Proteins are dynamic entities that move in a hierarchy of timescales that goes from picoseconds to seconds. Motions that occur in microseconds to seconds define biologically relevant events that are frequently involved in binding, allostery and catalysis. We measured relaxation parameter, relaxation dispersion experiments and molecular dynamic simulation in order to correlate hydration and slow dynamics. We will show how conformational dynamics of yeast thioredoxin 1 is correlated with the hydration equilibrium of a water cavity near the active site. The residue Asp24 that is well-recognized as a proton acceptor in the catalytic mechanism also controls dynamic events of the protein that are important for recognition and catalysis.

ACKNOWLEDGEMENTS: FAPERJ, CAPES, CNPq, INBEB-CNPq, Program Science Without Borders-CNPq

#### UP006: The magnitude of a pre-existing equilibrium tunes adenylate kinase activity

<sup>1</sup>Jörgen Åden, <sup>2</sup>Abhinav Verma, <sup>2</sup>Alexander Schug, <sup>1</sup>\***Magnus Wolf-Watz**

<sup>1</sup>Umeå University, <sup>2</sup>Karlsruhe Institute of Technology

Enzymes are extraordinary biocatalysts that accelerate chemical reactions by performing several complex tasks simultaneously. These tasks include; (1) binding of substrates weakly enough to avoid thermodynamic pits; (2) extremely tight binding to the transition state compound; (3) activation of functional groups on the substrate(s); (4) dehydration of active sites and (5) conformational changes.

The free energy landscape of enzymes is tuned such that functionally important structures are accessed within relevant time-scales. Some enzymes have been found to sample "substrate bound-like" structures in the absence of substrate and *Escherichia coli* adenylate kinase (AK<sub>eco</sub>) belongs to this class. These enzymes display pre-existing conformational equilibria between inactive and active structural states in their substrate free states. Here, we probe the free energy landscape of substrate-free AK<sub>eco</sub> with solution state NMR spectroscopy. Perturbation of the pre-existing equilibrium constant in the forward and reverse directions was accomplished with mutation or addition of the osmolyte TMAO, respectively. Surprisingly, we found that the rate constant for the enzymatic turn-over ( $k_{cat}$ ) of AK<sub>eco</sub> is dependent on the magnitude of the equilibrium constant for exchange between active and inactive structures observed in the substrate-free state. A shift of the equilibrium towards the active structure results in a decrease of  $k_{cat}$ , and conversely a shift towards the inactive structure results in an increase of  $k_{cat}$ . These seemingly counterintuitive relations depend on that AK<sub>eco</sub> catalysis is rate-limited by a conformational change coupled to product release. Thus, for AK<sub>eco</sub> the magnitude of a pre-existing equilibrium is directly mirrored in the catalytic rate-

constant of the enzyme. Our data firmly underscore that understanding enzyme dynamics in substrate-free states is required for a full understanding of enzymatic mechanisms.

Reference: Åden, J. et. al. (2012), JACS, 134, 16562-16570

#### UP007: Structural and dynamic insights into substrate binding and catalysis in human Lipocalin Prostaglandin D synthase

<sup>1</sup>\*Konstantin Pervushin, <sup>1,2</sup>Pär Nordlund, <sup>1,2</sup>Sing Mei Lim, <sup>1</sup>Dan Chen, <sup>1</sup>Hsiangling Teo, <sup>2</sup>Annette Roos, <sup>2</sup>Tomas Nyman, <sup>2</sup>Lionel Trésaugues

<sup>1</sup>Nanyang Technological University, <sup>2</sup>Karolinska Institute

Lipocalin-Prostaglandin D synthase converts Prostaglandin-H<sub>2</sub> (PGH<sub>2</sub>) to Prostaglandin-D<sub>2</sub> (PGD<sub>2</sub>), an important inflammatory and signaling mediator. It also binds biliverdin, all-trans retinoic acid and bilirubin, acting as lipophilic compound carrier. We employed structural, biophysical and biochemical approaches to address the mechanistic aspects of substrate entry, catalysis and product exit. The structure of human L-PGDS was solved in a complex with a substrate analog and in ligand-free-form. Catalytic Cys 65 thiol group is found in two different conformations, each making a distinct hydrogen bond network to neighboring residues, elucidating the mechanism of the cysteine nucleophile activation. Ligand electron density was observed in the active site demarking substrate-binding regions, but did not allow unambiguous fitting of the substrate. To further understand ligand binding, we used NMR spectroscopy to map the ligand binding sites and to show the dynamics of protein-substrate and protein-product interactions. A model for ligand binding at the catalytic site is proposed, showing a second binding site involved in ligand exit and entry. NMR chemical shift perturbations and NMR resonance line-widths alterations (observed as changes of intensity in 2D cross-peaks in [<sup>1</sup>H,<sup>15</sup>N]-TROSY) for residues at  $\omega$  helix, E-F loop and G-H loop besides the catalytic sites indicating involvement of these residues in ligand entry/egress.

#### OP008: EPR Studies of Radical SAM Enzymes

\***R. David Britt**

*University of California, Davis*

We are using multifrequency EPR in conjunction with freeze trapping of intermediates and specific isotope labeling to probe the geometrical and electronic structure of such intermediates formed during catalysis by Radical SAM enzymes. A number of Radical SAM enzymes have one or more secondary FeS clusters in addition to the 4Fe4S cluster that binds the SAM cofactors. Two of the enzymes we are studying are biotin synthase, which inserts a S-atom in the final step of forming the vitamin biotin, and HydG, which is a tyrosine lyase which produces the CO and CN- ligands for the Fe-Fe cluster of [Fe-Fe] hydrogenase.

**Monday – May 20<sup>th</sup>**  
**General Solids**

Chair: Bernhard Blümich  
Room Gávea B

#### OP009: Structure Determinations of Molecularly Ordered, Non-Crystalline Silicate, Borosilicate, and Aluminosilicate Frameworks by Combined NMR, Scattering, and DFT Analyses

<sup>1</sup>\*Bradley F. Chmelka, <sup>2</sup>Sylvian Cadars, <sup>3</sup>Darren H. Brouwer, <sup>1</sup>Ming-Feng Hsieh, <sup>1</sup>Robert J. Messinger, <sup>1</sup>Matthew T. Aronson, <sup>2</sup>Mounesha N. Garaga, <sup>2</sup>Zalfa Nour

<sup>1</sup>University of California, Santa Barbara, USA, <sup>2</sup>CNRS, Université d'Orléans, France, <sup>3</sup>Redeemer College, Ancaster, Ontario, Canada

A general protocol is demonstrated for determining the struc-

tures of molecularly ordered but non-crystalline solids, which combines constraints provided by solid-state NMR, X-ray diffraction, and first-principles calculations. The approach is used to determine the structure(s) of surfactant-directed layered silicates with short-range order in two dimensions, but without long-range 3D atomic periodicity. Structural constraints are obtained from solid-state  $^{29}\text{Si}$  MAS NMR analyses, including the types and relative populations of distinct  $^{29}\text{Si}$  sites, their respective  $^{29}\text{Si}$ -O- $^{29}\text{Si}$  connectivities and dipolar interactions, and combined with unit cell parameters from XRD. A comprehensive search of candidate structures leads to the identification of frameworks that are each compatible with all of the experimental constraints. Subsequent refinements of the candidate structures using density-functional theory allow their evaluation and the identification of "best" framework representations, based on their lattice energies and quantitative comparisons of experimental and calculated isotropic  $^{29}\text{Si}$  chemical shifts and  $^2J(^{29}\text{Si}$ -O- $^{29}\text{Si})$ -scalar couplings.

The incorporation of heteroatoms, such as boron or aluminum, into otherwise identical silicate frameworks often leads to dramatically improved adsorption or catalytic properties of the materials, as notably exemplified by nanoporous zeolites. Such properties, however, have been difficult to correlate to specific framework attributes, due to the increased complexity of local structural order and disorder, especially near the heteroatom sites. Distributions of heteroatom bonding environments, in particular, lead to reduced resolution of 1D  $^{29}\text{Si}$ ,  $^{11}\text{B}$ , or  $^{27}\text{Al}$  MAS NMR spectra. By comparison, 2D Heteronuclear Multiple-Quantum Correlation NMR measurements are sensitive to through-bond ( $J$ ) or through-space (dipole-dipole) interactions that can be used to probe the short-range environments of different framework moieties, including those involving heteroatoms. Intensity correlations associated with  $^{11}\text{B}$ ,  $^{29}\text{Si}$ , or  $^{27}\text{Al}$  atoms provide detailed information on the bonding connectivities and distributions of heteroatom sites in boro- and aluminosilicate frameworks, yielding new understanding of the compositions, structures, and properties of these technologically important materials.

Acknowledgements: U.S. National Science Foundation, Agence National de Recherche de France, Chevron

#### OP010: Zero- and low-field NMR spectroscopy

<sup>1,2\*</sup>Dmitry Budker

<sup>1</sup>Department of Physics, University of California, Berkeley,  
<sup>2</sup>Nuclear Science Division, E. O. Lawrence Berkeley National Laboratory, Berkeley

We will present an overview of the recent work on NMR spectroscopy based on measuring J-couplings at zero and low magnetic fields, including experiments on NMR entirely without magnets (not counting a low-field-pulse coil), where signal detection is accomplished with atomic magnetometers. The experiments have been performed by our group in collaboration with the group of Prof. Alexander Pines at the Department of Chemistry at UC Berkeley and the Materials Science Division of LBNL, and our various American and international collaborators. Up-to-date bibliography of this work can be found at the following web sites:

<http://budker.berkeley.edu/PubList.html>

<http://waugh.cchem.berkeley.edu/publications.php>

ACKNOWLEDGEMENTS: NSF, DOE

#### UP011: Use of $^1\text{H}$ Chemical Shifts to Determine Structural Motifs in $\pi$ -Conjugated Polymers

\*Michael Ryan Hansen

Max Planck Institute for Polymer Research

Polymers with extended  $\pi$ -conjugation and narrow band gaps are of broad technological importance due to their promising applications as semiconductors in organic electronic devices. Examples of such devices include organic-based solar cells,

field-effect transistors, and light-emitting diodes, where the active semiconducting polymer layer is formed via solution processing. This produces a final material that is semi crystalline, preventing the direct access to details about the local molecular organization from a conventional approach. In this contribution I will outline a general strategy for determining structural motifs in  $\pi$ -conjugated systems that combines X-ray diffraction and solid-state NMR experiments with Nucleus Independent Chemical Shift (NICS) maps.[1] This combination provides a useful platform to evaluate specific packing structures and in some cases even allows setting up a crystal structure, if sufficient constraints can be determined from experiments. The potential of the proposed strategy will be exemplified by recent and ongoing work on polythiophenes,[1] donor-acceptor-type polymers,[2,3] and shape-persistent macrocycles, forming empty helical nano channels.[4]

References:

[1] D. Dudenko, A. Kiersnowski, J. Shu, W. Pisula, D. Sebastiani, H. W. Spiess, M. R. Hansen, *Angew. Chem. Int. Ed.* 2012, 51, 11068.

[2] H. N. Tsao, D. M. Cho, I. Park, M. R. Hansen, A. Mavrinskiy, D. Y. Yoon, R. Graf, W. Pisula, H. W. Spiess, K. Müllen, *J. Am. Chem. Soc.*, 2011, 133, 2605.

[3] D. Niedzialek, V. Lemaire, D. Dudenko, J. Shu, M. R. Hansen, J. W. Andreasen, W. Pisula, K. Müllen, J. Cornil, D. Beljonne, *Adv. Mater.*, 2013, (in press, DOI: 10.1002/adma.201201058).

[4] M. Fritzsche, A. Bohle, D. Dudenko, U. Baumeister, D. Sebastiani, H. W. Spiess, M. R. Hansen, S. Höger, *Angew. Chem. Int. Ed.*, 2011, 50, 3030.

#### UP012: NMR Crystallography, from "Pas de deux" to Spin Choreography. Nanoporous Crystal Structures of Powders : Methods and Hardware.

<sup>1\*</sup>Francis Taulelle, <sup>2</sup>Frank Engelke, <sup>2</sup>Frank Decker, <sup>1</sup>Boris Bouchevreau, <sup>1</sup>Charlotte Matineau

<sup>1</sup>University of Versailles, <sup>2</sup>Bruker-Biopspin GmbH

Inorganic-organic hybrid nanoporous solids exhibits many challenges for their structure determination. They contain a framework, that is usually periodic or at least topologically periodic. However, these materials are hard to form single crystals, most of the time one has to resolve their crystal structure from powder. Additionally, they contain either additional templating agents, of the same nature than the organic linkers, making the activation (emptying the nanopores) of the materials difficult, if not impossible, and by and large, partial. Therefore, at synthesis or later when exchanged with gases or molecules, these exchanged crystals exhibit a periodic network and a non-periodic sub-lattice.

It will be shown on an alumina-phosphate lamellar nanoporous crystal [1] that X-ray diffraction has intrinsic limits for structure computability from a powder and this limit can be overcome by using NMR data. With this combined usage of XRD and NMR the average periodic structure can be determined. At a second level of structure determination NMR can resolve the structural non-periodic part of the crystal.

In a second part, it will be shown that the large number of NMR experiments that must be acquired to solve structures can be accelerated by using multiple channels probe (4 and 5 channels) [2] with multiple receivers acquisition. Multi-decoupling enhances the resolution that reaches about five times higher resolution power than the best synchrotron resolution power.

NMR Crystallography encompasses usage of prior data from XRD as cost function for the average structure determination as well as using new NMR hardware and software [3,4] with additional pulse sequences [5] to solve all the structure features of nanoporous crystals.



With this instrumental developments, one can devise for each structure resolution an original combination of pulse sequence manipulating the resonances between spins in a complex choreography of spins, grouped in a variety of motives that would progressively address all the aspects of the crystal complexity.

#### References

- [1] B. Bouchevreau, C. Martineau, C. Mellot-Draznieks, A. Tuel, M. R. Suchomel, O. Lafon, J. Trébosc, J. P. Amoureux, F.; Taulelle, Chem. Eur. J. in press.
- [2] C. Martineau, F. Engelke, F. Taulelle, J. Magn. Reson. 212 (2011) 311-319.
- [3] E. Kupce, R. Freeman, J. Magn. Reson. 206 (2010) 147-153, J. Magn. Reson. 213 (2011) 1-13.
- [4] E. Kupce, L. E. Kay, J. Biomol. NMR 54 (2012) 1-7.
- [5] Herbst, C.; Riedel, K.; Ihle, Y.; Leppert, J.; Ohlen-schlager, O.; Görlach, M.; Ramachandran, R. MAS solid state NMR of RNAs with multiple receivers. J Biomol NMR 2008, 41, 121–125.
- [6] C. Martineau, F. Engelke, F. Decker, F. Taulelle. J. Magn. Reson. Submitted.
- [7] V. Munch, F. Taulelle, T. Loiseau, G. Férey, A. Cheetham, S. Weigel, G.D. Stucky, Magn. Reson. Chem. 1999, 37, S100-S107.

#### OP013: High Frequency Dynamic Nuclear Polarization

\*Robert G. Griffin

Francis Bitter Magnet Laboratory and Department of Chemistry, MIT

Over the last few years we have developed cyclotron resonance maser (a.k.a. gyrotron) microwave sources that operate at frequencies of 140-527 GHz that permit DNP enhanced NMR (DNP/NMR) experiments in magnetic fields of 5-18.8 T ( $^1\text{H}$  NMR frequencies of 211-800 MHz, respectively). We review the instrumentation used for these experiments, which include new NMR probe designs and tunable gyrotron oscillators and amplifiers. In addition, we discuss two mechanisms used for DNP experiments in solids at high fields – the solid effect and cross effect – and the polarizing agents appropriate for each. These include metals, biradicals and mixtures of narrow line radicals that enable increased enhancements at reduced concentrations of the paramagnetic center. In addition, we discuss applications of DNP/NMR that illustrate its utility in enhancing signal-to-noise in MAS NMR spectra of a variety of biological systems including membrane and amyloid proteins whose structures are of considerable scientific interest. Presently, enhancements that are routinely available and range from 40-250 depending on experimental variables such as temperature, magnetic field, microwave  $B_1$ , polarizing agent, etc.

Monday – May 20<sup>th</sup>  
NMR in Medicinal Chemistry

Chair: Anita Marsaioli  
Rooms Turmalina/Topázio

#### OP014: HTS by NMR of combinatorial libraries: a new approach to peptide and ligand discovery

\*Maurizio Pellecchia

Chemical Biology, Sanford-Burnham Medical Research Institute, La Jolla, CA

Recently, fragment based ligand design (FBLD) approaches have become more widely used in drug discovery projects from both academia and industry, and are even often preferred to traditional ultra-high-throughput screening (HTS)

of large collection of compounds (>100,000). A key advantage of FBLD approaches is that these often rely on robust biophysical methods such as NMR spectroscopy for detection of ligand binding, hence are less prone to artifacts that too often plague the results from HTS campaigns. However, the challenge of FBLD approaches is that the evolution of initial weakly interacting fragments into more mature compounds with low micromolar is not trivial. In this presentation I will introduce a new fragment screening strategy, that takes advantage of both, the robustness of protein NMR spectroscopy as the detection method, and the basic principles of combinatorial chemistry to enable the screening of large libraries of fragments pre-assembled on a common backbone (>100,000 compounds). Hence we term the approach HTS by NMR. The approach seems particularly suited to target protein-protein interactions and three examples of such successful implementations will be discussed. Identification of simple peptides or even small molecules with this approach does not require expensive resources or medicinal chemistry expertise, hence we believe the method could become routinely used in NMR based structural biology laboratories that are interested in making a significant contribution to translational research.

Wu et al. Chemistry & Biology, 2013, 20, 19-33.

#### OP015: Enzyme Kinetics and Inhibition by NMR

\*José Daniel Figueroa-Villar

Military Institute of Engineering

Enzyme inhibitors are important bioactive compounds for treatment of diseases. However, some available methods for evaluation of enzyme inhibition display important problems. For example, the Ellman test, applied to inhibition of acetylcholinesterase (AChE) requires the use of thioacetylcholine instead of acetylcholine (ACh), leading to different results. Also, with ultraviolet-visible spectroscopy methods, when the initial enzyme product displays  $I_{\text{max}}$  similar to the substrate, is necessary the use of a second enzyme in order to transform the product to a very different compound. The problem using a second enzyme is that some inhibitors of the first enzyme may also have effects on the second one, leading to unacceptable results. The use of NMR methods for evaluation of enzyme inhibition is a very acceptable procedure because this technique is relatively easy for monitoring substrates and products concentration, without the use of other enzymes and/or different substrates, even allowing the obtention of Lineweaver-Burk graphics to determine the type of inhibition of each tested compound. The problem with NMR is its relatively NMR slowness in comparison with the enzyme properties, a process that was resolved using very low enzyme concentrations on the tests and simple  $^1\text{H}$  NMR procedures. This method was successfully used for inhibition of AChE, nucleoside hydrolase (NH) of *Leishmania infantum*, dihydrofolate reductase (DHFR) of *Plasmodium falciparum*, human tyrosinase and reactivation of phosphorylated AChE.

Interaction of inhibitors with enzymes were monitored by relaxation times ( $T_1$  and  $T_2$ ), modification of chemical shifts and DOSY and kinetics by  $^1\text{H}$  NMR.

ACKNOWLEDGEMENTS: CAPES/Pro-defesa, INBEB, FAPERJ.

#### UP016: Integrated structural biology shows how scarce sequence elements control the function of single $\beta$ -thymosin/WH2 domains in actin assembly

<sup>1</sup>François-Xavier Cantrelle, <sup>2</sup>Dominique Didry, <sup>1</sup>Célia Deville, <sup>1</sup>Jean-Pierre Placal, <sup>2</sup>Clotilde Husson, <sup>3</sup>Javier Perez, <sup>2</sup>Marie-France Carlier, <sup>2</sup>Louis Renault, <sup>1</sup>Carine van Heijenoort, <sup>1\*</sup>Eric Guittet

<sup>1</sup>CNRS-ICSN, <sup>2</sup>CNRS-LEBS, <sup>3</sup>Synchrotron SOLEIL

$\beta$ -thymosin ( $\beta\text{T}$ ) and WH2 domains are found as single or repeated units in a large number of multi-domain actin-binding proteins involved multiple cellular processes. They

are archetypes of small intrinsically disordered actin-binding modules with highly variable sequences of 25-55 residues that fold upon binding. Understanding the structure-function relationship governing the versatile or multiple functions of these domains remains extremely challenging.

Here, we reveal the structural and dynamics determinants, which govern the assembly inhibition (Thymosin- $\beta$ 4) or the motility enhancement by directing polarized filament assembly (Ciboulot  $\beta$ T or WASP/WAVE WH2 domains). To reach this goal, we combined mutational, functional and structural analyses by X-ray crystallography, SAXS and NMR in a typical integrated structural biology approach. We show that functionally different  $\beta$ T/WH2 domains do not target alternative actin binding sites but rather differ by alternative dynamics of their C-terminal half interactions with G-actin pointed face [1-3].

The detailed NMR analysis of the dynamics of the free chimeras using  $^{15}\text{N}$  relaxation, residual dipolar couplings and relaxation dispersion experiments demonstrates specific individual behaviors, which bring insight into the folding upon binding mechanisms of these peptides. Isotope-filtered NOESY experiments allow the precise characterization of the structure of the complexes. The structural plasticity of WH2 domains is partially conserved and functional in the G-actin bound state. The distribution of static and dynamic interactions induces their ability to control the function in an ionic strength dependent manner. A single residue controls the local interaction dynamics by strong electrostatic interactions [3].

The results open perspectives for elucidating, including by NMR, the functions of  $\beta$ T/WH2 domains in other modular proteins and enlighten how intrinsic structural disorder can lead to a novel mode of functional versatility.

[1] Hertzog, M.; van Heijenoort, C.; Didry, D.; Gaudier, M.; Coutant, J.; Gigant, B.; Didelot, G.; Preat, T.; Knossow, M.; Guittet, E.; Carlier, MF Cell 2004, 117, 611-623.

[2] Domanski, M.; Hertzog, M.; Coutant, J.; Gutsche-Perelroizen, I.; Bontems, F.; Carlier, MF.; Guittet, E.; van Heijenoort, C. J Biol Chem 2004, 279, 23637-45.

[3] Didry D, Cantrelle FX, Husson C, Roblin P, Moorthy AM, Perez J, Le Clainche C, Hertzog M, Guittet E, Carlier MF, van Heijenoort C, Renault L. EMBO J. 2011, 31, 1000-13.

#### UP017: Human Macrophage Lectin (CLEC10A) recognition of monosaccharides related to tumor marker Tn-antigen studied by $^1\text{H}$ and $^{19}\text{F}$ NMR.

<sup>1\*</sup>Francisco Javier Cañada, <sup>1</sup>Anneloes Oude Vrielink, <sup>1,2</sup>Filipa Marcelo, <sup>1</sup>Ana Manzano, <sup>1</sup>Pilar Blasco, <sup>1</sup>Jesús Jiménez-Barbero, <sup>3</sup>Sabine Andre, <sup>3</sup>Hans-Joachim Gabius

<sup>1</sup>Centro de Investigaciones Biológicas, CIB-CSIC Chemical and Physical Biology Department. Ramiro de, <sup>2</sup>REQUIMTE, CQFB, DQ, FCT-UNL, 2829-516 Caparica, Portugal, <sup>3</sup>Institute of Physiological Chemistry, Faculty of Veterinary Medicine, Ludwig-Maximilians-University,

In pathological tissues mucins, heavily O-glycosylated proteins of cellular surfaces, present perturbed glycosylation patterns that are being considered as tumor markers and are attracting a growing interest for the design and developing of antitumor vaccines. Interestingly, some of these carbohydrate related tumor markers are known carbohydrate antigens recognized by C-type (calcium dependent) lectins expressed in cells of the immune system envisioning an important role for these interactions in both innate and adaptive immune responses[1]. Human macrophages express in their surface the so call Human Macrophage Lectin (HML-2, c-type lectin from family 10, CLEC10A) that recognizes carbohydrate related to Tn antigen, (O-glycosides of N-Acetyl-Galactosamine with serine or threonine). In the presented work the binding mode of Galactose and Galactosamine and fluorogalactoses monosaccharides will be shown as it has been characterized by

means of  $^1\text{H}$  and  $^{19}\text{F}$  NMR studies applying saturation transfer difference (STD) and  $T_2$  perturbation strategies complemented by molecular modeling and docking studies[2]. The importance of all hydroxyl groups of the galactose-derived monosaccharide ligands and the dependency of calcium for carbohydrate recognition by this c-type lectin has been deduced from those studies.

[1] "Sweet preferences of MGL: carbohydrate specificity and function", van Vliet SJ, Saeland E, van Kooyk Y. Trends Immunol. 2008 29(2):83-90.

[2] "Carbohydrate-protein interactions: a 3D view by NMR", Roldós V, Cañada FJ, Jiménez-Barbero J., Chembiochem. 2011 12(7):990-1005.

Acknowledgments: This work has been carried out with financial aid of the MINECO, Spain (Project number CTQ2009-08536)

#### OP018: High-yield expression and NMR structural studies of Antimicrobial Peptides

Ji-Ho Jung, Ji-Sun Kim, \*Yongae Kim

Depart of Chemistry and Protein Research Center for Bio-Industry, Hankuk University of Foreign Studies, Korea

Lactophorin (LPcin), a cationic amphipathic peptide consists of 23-mer peptide, corresponds to the carboxy terminal 113–135 region of component-3 of proteose-peptone. LPcin is a good candidate as a peptide antibiotic because it has an antibacterial activity but no hemolytic activity. Three different analogs of LPcin, LPcin-yk2 which has mutant amino acids, LPcin-yk1 and LPcin-yk3 that has shorter mutant amino acids are recently developed by using peptide engineering in our laboratory. These three LPcin analogs show better antibiotic activities than wild-type LPcin and no toxicity at all.

In order to understand the structural correlation between LPcin analogs structure and antimicrobial activity under the membrane environments, we tried to express and purify as large as amounts of LPcin and three different LPcin analogs. We finally optimized and succeeded to overexpress in the form of fusion protein in *Escherichia coli* and purified with biophysical techniques like Ni-affinity chromatography, dialysis, centrifuge, chemical cleavage, and reversed-phase semiprep HPLC. In here, we will present the optimizing processes for high-yield expression and purification and solution NMR spectra and solid state NMR spectra for antimicrobial mechanisms.

Reference: 1) Tae-Joon Park, Sung-Sub Choi, Ji-Sun Kim, and Yongae Kim (2008) "Expression, Purification, and NMR structural studies of antibacterial peptide, bovine lactophorin" The 1st Italy-Korea Symposium on Antimicrobial Peptides Proceedings 1, P14 2) Tae-Joon Park, Ji-Sun Kim, Sung-Sub Choi, and Yongae Kim (2009) "Cloning, Expression, Isotope Labeling, Purification, and Characterization of Bovine Antimicrobial Peptide, Lactophorin in *E. coli*" Prot. Exp. Purification 65, 1, 23 3) Tae-Joon Park, Ji-Sun Kim, Hee-Chul Ahn, and Yongae Kim (2011) "Solution and Solid-state NMR Structural Studies of Antimicrobial Peptides, LPcin-I and LPcin-II." Biophys. J. 101, 5, 1193

#### Monday – May 20<sup>th</sup> EPR and New Materials

Chair: Eduardo Di Mauro  
Room Onix

#### OP019: EPR of thermo- and photoswitchable copper-nitroxide based molecular magnets

<sup>1\*</sup>Matvey Fedin, <sup>1</sup>Sergey Veber, <sup>1</sup>Irina Drozdnyuk, <sup>1</sup>Ksenia Maryunina, <sup>1</sup>Evgeny Tretyakov, <sup>2</sup>Hideito Matsuoka, <sup>2</sup>Seigo Yamauchi, <sup>1</sup>Renad Sagdeev, <sup>1</sup>Victor Ovcharenko, <sup>1,3</sup>Elena Bagryanskaya

<sup>1</sup>International Tomography Center SB RAS, Novosibirsk, Russia, <sup>2</sup>Tohoku University, Sendai, Japan, <sup>3</sup>N.N. Vorozhtsov Novosibirsk Institute of Organic Chemistry SB RAS, Novosibirsk, Russia

Copper-nitroxide based molecular magnets Cu(hfac)<sub>2</sub>L<sup>R</sup> ("breathing crystals") represent the new and interesting type of thermo- and photoswitchable materials. The unusual type of reversible magnetic switching between weakly- and strongly exchange-coupled states occurs in spin triads nitroxide-copper(II)-nitroxide and can effectively be studied using EPR. In this report we overview experimental approaches developed for these systems, discuss general trends and focus on the characteristics and mechanism of light-induced spin state switching and following relaxation to the ground state using continuous wave X/Q-band and time-resolved (TR) W-band EPR. We found that the light-induced spin dynamics leading to a formation of metastable state occurs on a nanosecond timescale and can be studied by TR EPR. The first application of TR EPR to switchable molecular magnets has shown its potential for estimation of the switching times and study of the fast electron relaxation rates. After being formed, the light-induced metastable state slowly relaxes back to the ground spin state on a timescale of hours at cryogenic temperatures (T < 20 K). This relaxation shows pronounced self-decelerating character for all studied compounds, which is explained by the broad distribution of activation energies in exchange-coupled clusters. Since light-induced phenomena in "breathing crystals" are promising for spintronics, our recent efforts have been focused on optimization of their optical and relaxation properties by chemical modification of nitroxide ligands. In particular, complexes with tert-butylpyrazolyl nitroxides show superior optical properties and slower relaxation rates, allowing photo-switching at up to 65 K. Another interesting direction on the way to applications is the study of light-induced phenomena in thin polymer films and layers based on "breathing crystals", where the high sensitivity of EPR compared to SQUID-magnetometry is crucial. We discuss recent results and future research in this field.

ACKNOWLEDGEMENTS: RFBR (11-03-00158, 12-03-33010), Russian Ministry for Education and Science (8436, 8456), RF President grants (MK-1662.2012.3, MK-1165.2012.3).

#### OP020: Theoretical EPR Spectroscopy of Open-Shell Transition Metal Complexes with Strong Spin Orbit Coupling

\*Frank Neese, Mihail Atanasov, Michael Römel, Kantharuban Sivalingam

Max-Planck-Institut für Chemische Energiekonversion

The majority of molecules have orbitally nondegenerate ground states. The molecular electric and magnetic properties are well described by standard models of electronic structure theory, e.g. perturbation or linear response theory. These methods have found very widespread use in the community of quantum chemistry users. The ORCA program developed in our group features many such methods for the calculation of optical and magnetic properties of transition metal complexes. There is, however, a significant class of molecules with orbitally (nearly) degenerate ground states where the established methods do not work. Here, a more careful treatment of the leading relativistic effects is necessary in order to correctly predict their spectroscopic properties and obtain molecular level electronic structure insight. This is not possible on the basis of density functional theory (DFT). Recently efficient methods based on multireference wavefunction theory have been implemented into ORCA that allow such calculations on large molecules. Their use will be demonstrated by a recent study that deals with the electronic structure of the only low-molecular weight catalyst known to be capable of reducing dinitrogen to ammonia.

#### UP021: Multifunctional in vivo EPR-based spectroscopy and imaging of paramagnetic probes

\*Valery V. Khramtsov

The Ohio State University Medical Center, Columbus, OH, USA

Biological effects of various drugs and treatments observed *in vitro* are often not reproduced *in vivo*, therefore significantly decreasing their potential for translation to medical practice. In recent years it came to realization that tissue microenvironment (TME) plays a key role in this discrepancy. For two leading causes of mortality in the United States, cancer and ischemic heart disease, tissue hypoxia is well documented and is accompanied by changes in glycolysis resulting in tissue acidosis and tissue redox changes. It makes of primary importance the development of approaches for noninvasive monitoring of these TME parameters *in vivo*. Magnetic resonance techniques have the advantage of *in vivo* applications in animals and humans due to sufficient depth of microwave penetration in living tissues. The unique advantage of EPR over NMR is the functional specificity due to the absence of overlap with endogenous signals. However EPR-based techniques are far from attaining their maximum potential because of a lack of stable *in vivo* paramagnetic probes, and technical limitation of EPR and EPR imaging. Here we discussed the recent advances in chemistry of paramagnetic probes[1, 2] and EPR-based techniques[3-5] which make multifunctional monitoring of TME feasible. The exemplified applications include concurrent monitoring of ischemia-induced myocardial oxygen depletion and acidosis in isolated rat hearts[6], and multifunctional (pH, redox, oxygen and glutathione content) monitoring of tumor TME[3], including pH mapping of living tissues using low-field EPR imaging and functional proton-electron-double-resonance imaging (PEDRI)[4, 7]. Supported by NIH grant EB014542.

[1] Khramtsov VV, 2012. In Nitroxides - Theory, Experiment and Applications, Kokorin AI, Ed. InTech: 317-346.

[2] Bobko et al. 2012. Anal Chem, 84: 6054-6060.

[3] Bobko AA et al. 2012. Magn Reson Med 67, 1827-1836.

[4] Khramtsov VV et al. 2010. J Magn Reson 202: 267-73.

[5] Koda S et al. 2012. Anal Chem 84: 3833-7.

[6] Komarov DA et al. 2012. Magn Reson Med 68: 649-55.

[7] Efimova OV et al. 2011. J Magn Reson 209: 227-232.

#### UP022: New Kind of Mesoscopic EPR In Some Itinerant Undoped Ferromagnets

\*Vladimir A. Ivanshin, Eduard M. Gataullin

Kazan (Volga region) Federal University

New Kind of Mesoscopic EPR In Some Itinerant Undoped Ferromagnets Hybridization between local f or d states and conduction electrons (CE) can lead to a dichotomy of localized/itinerant characters of electrons in some strongly correlated electron systems (SCES). Electron paramagnetic resonance (EPR) probes microscopically both the local moment (LM) spins and CE and could be observed in some dense SCES even without any kind of paramagnetic doping [1, 2]. According to very recent different theories [3-5], the key origin of the unexpected narrow EPR signals observed in some undoped intermetallics can be related to a strong hybridization effects between localized electrons and conduction bands in conjunction with ferromagnetic (FM) correlations. We review the EPR and inelastic neutron scattering experiments in several undoped Yb, Ce, and Eu-based intermetallics [2, 6-8] and discuss the role of chemical composition, Kondo effect, anisotropy, and RKKY interactions for the EPR linewidth. It is shown that an increase of the Kondo interaction and FM correlations leads to a stronger hybridization and an essential EPR line narrowing. Possible hybridization mechanisms and the mesoscopic character of EPR are discussed.

- [1] J. Sichelschmidt, V.A. Ivanshin et al., Phys. Rev. Lett. 91, 156401(2003)
- [2] V.A. Ivanshin et al., Diffusion and Defect Data Part B: Solid State Phenomena 170, 170 (2011)
- [3] P. Wölffe, E. Abrahams, Ann. Phys. (Berlin) 523, 598 (2011)
- [4] P. Schlottmann, Phys. Rev. B 79, 045104 (2009)
- [5] D. Huber, Mod. Phys. Lett. B 26, 1230021 (2012)
- [6] L.M. Holanda et al., Phys. Rev. Lett. 107, 026402 (2011)
- [7] T. Gruner et al., Phys. Rev. B 85, 035119 (2012)
- [8] C. Stock et al., Phys. Rev. Lett. 109, 127201(2012)

### OP023: Elucidating Smart Polymeric Materials Using Electron Paramagnetic Resonance (EPR) Spectroscopy

\***Dariusz Hinderberger**

*Max Planck Institute for Polymer Research*

Magnetic resonance methods such as nuclear magnetic resonance (NMR) or electron paramagnetic resonance (EPR) can give valuable insights into complex systems that show long range disorder and some short range or intermediate range order, e.g. synthetic and biological soft matter. In particular, EPR spectroscopy with its high sensitivity and selectivity is complementary to the well-established methods of soft matter characterization (e.g. light-, X-ray, neutron scattering) and delivers information that is otherwise not accessible. While conventional continuous-wave (CW) EPR allows studying rotational dynamics in the microsecond to picosecond regime, EPR methods that measure the dipolar (through-space) interaction of individual electron spins can be used to gain information on the spatial distribution of paramagnetic probe molecules up to 8 nm.

Here, I will show that methods of EPR spectroscopy on small radicals as probe molecules can help illuminating the molecular scale processes in smart, responsive polymeric materials.

This will be highlighted through examples from my lab that span a broad range of thermoresponsive synthetic and biological macromolecules, such as poly(alkylene oxide)-based copolymers and dendronized polymers or genetically engineered elastin-like polypeptides (ELPs). These polymers are a very interesting class of materials envisioned for a multitude of applications such as molecular transport or sensing. I will show that using simple CW EPR on amphiphilic spin probes, mainly simple TEMPO, - performed in a benchtop EPR spectrometer - it is possible to obtain fundamental insight into molecular scale processes during thermal responses of these polymers. This insight can finally be correlated with their macroscopically observable function on much longer length scales to derive structure-function relationships as they are known from proteins and other biomacromolecules.

**Monday – May 20<sup>th</sup>**  
**Membrane Proteins**

Chair: Ana Carolina Zeri  
Room Gávea A

### OP024: Structural studies of membrane proteins in membrana

\***Francesca M. Marassi**

*Sanford-Burnham Medical Research Institute, La Jolla CA, USA*

The two principal components of biological membranes - the lipid bilayer and the proteins integrated within it - have co-evolved for specific functionalities that mediate all interactions of cells with their environment. Since the physical and chemical properties of lipids and proteins are highly

inter-dependent, structure determination of membrane proteins needs to include the membrane environment. This also eliminates the potential for distorting protein structure, dynamics and function due to crystal contacts or detergent molecules, and enables functional and ligand binding studies to be performed in a natural setting. Solid-state NMR spectroscopy is compatible with structure determination of membrane proteins in membranes at physiological conditions. Advances in sample preparation, instrumentation, NMR experiments and effective computational methods, enable very high-resolution solid-state NMR spectra to be obtained from isotopically labeled membrane proteins in lipid bilayers and high quality structures of membrane proteins to be determined in membranes. Orientation restraints are particularly useful for solid-state NMR structural studies of membrane proteins since they provide not only information about three-dimensional structure, but also information about protein orientation in the membrane. We describe recent results obtained for a family of bacterial outer membrane proteins implicated in cell adhesion and pathogenesis.

ACKNOWLEDGEMENTS: This research was supported by the National Institutes of Health.

### OP025: Brain Fatty-acid Binding Protein and its Interactions with Membrane Model Systems

<sup>1</sup>Fábio H. Dyszy, <sup>1</sup>Ítalo A. Calvini, <sup>1</sup>Daniel F. Silva, <sup>1</sup>Andressa P. A. Pinto, <sup>1</sup>Ana P.U. Araújo, <sup>2</sup>Hans Robert Kalbitzer, <sup>1</sup>Claudia Elisabeth Munte, <sup>1,3</sup>\***Antonio José Costa-Filho**

<sup>1</sup>Grupo de Biofísica Molecular Sérgio Mascarenhas, Instituto de Física de São Carlos, USP, <sup>2</sup>Department of Biophysics and Physical Biochemistry, University of Regensburg, <sup>3</sup>Laboratório de Biofísica Molecular, Faculdade de Filosofia, Ciências e Letras de Ribeirão Preto, USP

Fatty acid-binding proteins (FABP) constitute a family of low molecular weight proteins that share structural homology and the ability to bind fatty acids. The common structural feature is a  $\beta$ -barrel of 10 antiparallel strands forming a large inner cavity that accommodates nonpolar ligands, capped by a portal region, comprising two short  $\alpha$ -helices. Here we used magnetic resonance methods (ESR and NMR) to correlate structure and function of B-FABP in the presence of membrane mimetics. Spin probes selectively placed in the portal region and fatty acid spin labels (n-SASL) allowed us to monitor structural changes both in the protein and in the membrane models. ESR spectra of B-FABP labeled mutants were overall divided in two groups that responded differently to the presence of membranes. Group I residues, whose side chains point outwards from the contact region between the helices, had their mobility decreased upon membrane addition. Group II residues, composed by residues with side chains situated at the interface between the  $\alpha$ -helices, showed ESR spectra associated to an increase in mobility in the presence of the model membranes. These modifications in the ESR spectra of B-FABP mutants are compatible with a less ordered structure of the portal region inner residues (group II) that is likely to facilitate the delivery of FAs to target membranes. On the other hand, residues in group I and probes in the membrane mimetic presented decreased mobilities probably as a result of the formation of a collisional complex. NMR HSQC of isotopically labeled B-FABP in the presence of bicelles was also used to identify residues that participate in the binding/gating and allowed us to find a new series of residues that have not been implicated in those processes before. Our results bring new insights for the understanding of the binding, gating and delivery mechanisms in FABPs.

ACKNOWLEDGEMENTS: FAPESP, CNPq, CAPES.

### UP026: Defining the Flexible and Fixed Sides of a Protein Channel by EPR

\***Betty J. Gaffney**

## Florida State University

Lipoxygenases are ubiquitous proteins that oxidize polyunsaturated chains at different positions, but do so with a highly conserved structural motif of 20 helices. Because mechanistic details have been difficult to obtain by crystallography, EPR spectroscopy approaches have been implemented. Lipoxygenases are naturally paramagnetic due to an iron involved in catalysis. We have made them additionally paramagnetic by adding site-directed spin labels at selected sites. Using several EPR approaches, we have found the entrance to the active site and have examined an  $\alpha$ -helix that must move to allow substrate to enter the deep cavity. The non-heme iron is bound to five protein side chains and water and is located centrally in the structure, 25–35 Å from the surfaces. The polar end of a lipid substrate analog was found on the surface at one end the internal cavity in a lipoxygenase with pH-gating of substrate access (Biophys J 103: 2134 (2012)). A new bacterial lipoxygenase structure, with a lipid bound also seems to have a helical "lid" protecting a similar entrance to the active site. To examine how lipid binding "opens" the way to catalytic iron, we have scanned the gating helix with spin labels and examined, by power saturation, relaxation of the spin at many helix residues when a lysolipid is present. In comparison to substrate insensitive positions, measured in the reference above, the gating helix distances to iron increase in the presence of substrate analog, indicating a shift of the helix backbone. The EPR spectra of ferric lipoxygenases with and without lipids in the active site also confirm remarkable conservation of active site structure in lipoxygenases from bacteria and eukaryotes.

**UP027: Conformational selection of GPCR ligands upon binding to their receptors as observed by NMR**

<sup>1</sup>\*Laurent Catoire, <sup>2</sup>Marc Baaden, <sup>1</sup>Jean-Luc Popot, <sup>3</sup>Eric Guittet, <sup>4</sup>Jean-Louis Banères

<sup>1</sup>Laboratory of Biology and Physico-Chemistry of Membrane Proteins - UMR 7099 CNRS & University Paris,

<sup>2</sup>Laboratory of theoretical Biochemistry - UPR 9080 CNRS, <sup>3</sup>ICSN- UPR 2301 CNRS, <sup>4</sup>IBMM - UMR 5247 CNRS, Université Montpellier 1 & 2

The mechanism of signal transduction mediated by G protein-coupled receptors (GPCRs) is a subject of intense research in pharmacological and structural biology. An increasing amount of high-resolution GPCR crystal structures have been established these past few years, in parallel to a large panel of pharmacological, biophysical and biological studies. In spite of these structures have provided a major breakthrough in the field of structural biology of these receptors, and although these structures reveal several common features between all these receptors, the mechanism of GPCR activation remains to be understood at the molecular level. Beside technical issues, like obtaining a sufficient amount of functional receptor [1-3], this difficulty to clearly propose a mechanism for a given receptor is due to the conformational complexity and variability displayed by these membrane proteins, making GPCR signaling a rather sophisticated and subtle biological process. Ligand association to the receptor constitutes a critical event in the activation process. In this context, NMR, with the support of molecular modeling can provide dynamics pictures of receptor-ligand interactions, and has therefore the potential of becoming a leading technique in the study of the structure-function relationships of GPCRs. This will be illustrated here with two fatty acid molecules in interaction with the leukotriene BLT2 receptor [4,5].

[1] Dahmane et al. (2009) Amphipol-assisted in vitro folding of G protein-coupled receptors. Biochemistry, 48, 6516-6521

[2] Banères et al. (2011) New advances in production and functional folding of G-protein-coupled receptors. Trends Biotechnol, 29, 314-322

[3] Popot et al. (2011) Amphipols from A to Z. Annu Rev Biophys, 40, 379-408

[4] Catoire et al. (2010) Structure of a GPCR ligand in its receptor-bound state: leukotriene B4 adopts a highly constrained conformation when associated to human BLT2. J Am Chem Soc, 132, 9049-9057

[5] Catoire et al. (2011) Electrostatically-driven fast association and perdeuteration allow detection of transferred cross-relaxation for G protein-coupled receptor ligands with equilibrium dissociation constants in the high-to-low nanomolar range. J Biomol NMR, 50, 191-195

**OP028: Structural Biology by DNP MAS NMR and Investigations on the Transport Cycle of an ABC Transporter**

\*Hartmut Oschkinat

Leibniz-Institut für Molekulare Pharmakologie, Berlin, Germany

Solid-state NMR enables the investigation of heterogeneous, complex biological samples at high resolution. A major factor enabling such investigations is dynamic nuclear polarisation (DNP), which was introduced to increase signal-to-noise by one or two orders of magnitude. The application of dynamic nuclear polarisation (DNP) requires further optimization of samples, experimental parameters and concepts. In this context, the possibility of 'high-temperature' DNP in solid-state NMR is discussed. A major application of DNP involves investigations of the nascent chain within and directly after leaving the ribosome. The initial folding events are not yet well understood, and this investigation provides an NMR view onto this process. Of particular interest is the occurrence of secondary structure within the tunnel.

Investigations of membrane proteins may be facilitated by extensive deuteration, and subsequent detection of protons under magic-angle spinning conditions. Various schemes for the usage of proton chemical shifts for achieving sequence-specific assignments will be discussed, including a substitute of it, 2H-double quantum chemical shifts. An ABC transporter reconstituted into native lipid bilayers is investigated in variously labelled forms, and spectra of different functional states will be presented together with initial assignments and functional considerations. In essence, the solid-state NMR data suggest a new transport cycle.

**Monday – May 20<sup>th</sup>  
Dynamics and Recognition**

Chair: Robert Kaptein  
Room Gávea B

**OP029: Dynamic Aspects of Indirect DNA Readout by Nucleoid Associated Proteins**

<sup>2</sup>Tiago Cordeiro, <sup>2</sup>Jesús García, <sup>3</sup>Oscar Millet, <sup>1</sup>\*Miquel Pons

<sup>1</sup>University of Barcelona, <sup>2</sup>Institute for Research in Biomedicine, <sup>3</sup>CIC-bioGUNE

The capacity of Enterobacteriaceae to regulate horizontally transferred genes independently from the core genome is probably relevant for their success as pathogens. Escherichia, Yersinia, and Salmonella are among the best-known genus of pathogenic bacteria of the enteric group.

At least two mechanisms allow the selective recognition of horizontally transferred genes: i) the use of specialized forms of the nucleoid-associated protein H-NS and, ii) the use of a co-regulator of the Hha family that converts standard H-NS into a selectively regulating complex [1]. In the two mechanisms, recognition of DNA takes place through an indirect readout mechanism [2].

We shall present unpublished results on the structure of the complex between Hha and H-NS obtained from NMR, including paramagnetic relaxation enhancement experiments.

Proteins of the Hha family (Hha and YmoA) present intrinsic pervasive dynamics in the millisecond timescale [3]. Using CPMG-relaxation dispersion experiments we have characterized the collective motion of YmoA and the effect of mutations known to change its capacity to bind H-NS. We have identified residues that play a dual role in stabilizing the H-NS complex and in modulating the dynamics of the apo-form. We could also show that a mutation of a highly evolutionarily conserved residue, which had no apparent effect on in-vitro H-NS binding, had a strong effect on the dynamics of the apo-form of YmoA.

These results suggest a model in which core and horizontally acquired DNA forms interact with the same protein (H-NS) alone or in a complex with Hha/YmoA, respectively. Hha/YmoA dynamics plays a key role disconnecting the two pools of H-NS and therefore, enables selective regulation.

**ACKNOWLEDGEMENTS:** MINECO, Spain (BIO2010-15683), Generalitat de Catalunya (2009SGR1352), EC 7<sup>th</sup> FP (BioNMR contract 261863).

**References:**

[1] RC Baños et al. PLoS Genet 5(6): e1000513. doi:10.1371/journal.pgen.1000513 (2009).

[2] T Cordeiro, et al. PLoS Pathog 7(11): e1002380. doi:10.1371/journal.ppat.1002380 (2011).

[3] J García, et al. Biochem. J. 388, 755–762 (2005).

**OP030: Protein Kinase A and Conformational Dynamics: ‘Not too fast... not too slow... but just right’**

**\*Gianluigi Veglia**

*University of Minnesota*

Protein kinases mediate a myriad of cell signaling events. Protein kinase A (PKA) is considered the prototypical kinase, sharing its catalytic core (PKA-C) with many kinases. We have analyzed PKA-C’s conformational dynamics in the slow and fast scale of NMR spectroscopy and found that the slow time scale dynamics are linked with the enzyme turnover. Motions synchronous with the  $k_{cat}$  are initiated upon nucleotide binding and pervade the entire enzyme, defining a *dynamically committed* state. The binding of inhibitors quench the enzyme’s conformational dynamics, creating a *dynamically quenched* state. We also found a mutant of PKA-C that enhances the motions in the fast time scale. However, these enhanced motions reduce the catalytic efficiency of the kinase. We conclude that the conformational dynamics of the enzyme is linked to the overall turnover, and an increase or decrease of these motions has negative effects on the catalytic cycle.

**UP031: Sliding and target location of DNA-binding proteins: an NMR view of the lac repressor system**

<sup>1</sup>\*Rolf Boelens, <sup>2</sup>Karine Loth, <sup>4</sup>Manuel Gnida, <sup>5</sup>Julija Romanuka, <sup>1,3</sup>Robert Kaptein

<sup>1</sup>Utrecht University, <sup>2</sup>University of Orleans, <sup>3</sup>Novosibirsk State University, <sup>4</sup>Paderborn University, <sup>5</sup>Shell Research Laboratories

Gene regulatory proteins exert their function through binding to specific DNA sequences. Much progress has been made in understanding specific protein-DNA interactions, primarily from X-ray or NMR structures of the involved complexes. Another important question is how these proteins can efficiently find their targets in the presence of the abundant non-specific DNA in the nucleus.

We present a new approach based on NMR exchange measurements to analyze 1D diffusion of DNA-binding proteins along DNA sequences. Although this problem has been discussed since the pioneering studies of Berg and von Hippel in the early 80’s, results of recent single molecule fluorescence measurements of lac repressor and other proteins slid-

ing along DNA have caused a revival in this field. Our NMR approach shines new light on this matter and has the advantage that it combines kinetics with the possibility to observe the process involved at an atomic level.

In non-specific lac headpiece-DNA complexes selective NMR line broadening is observed that strongly depends on length and composition of the DNA fragments. This broadening involves amide protons found in the non-specific lac-DNA structure to be interacting with the DNA phosphate backbone, and can be ascribed to DNA sliding of the protein along the DNA. This NMR exchange broadening has been used to estimate the 1D diffusion constant for sliding along non-specific DNA. The observed slow sliding rate indicates that other processes such as hopping and intersegment transfer contribute to facilitate the DNA recognition process.

**UP032: RNA regulation - A new Twist**

**\*Harald Schwalbe**

*Goethe-University Frankfurt*

In the recent past, the importance of RNA-based regulation has become increasingly recognized. Regulation is based on structural transitions of RNA modules located in the 5’ untranslated region of mRNA. The regulation mechanism act on the level of transcription as well as translation. Riboswitches sense changes in the concentration of small molecule metabolites while RNA thermometers respond to temperature changes.

In this contribution, we will describe novel novel NMR methods to monitor such structural transitions at atomic resolution in vitro and in cell. In addition, we have developed a new T-jump probe to monitor temperature-induced regulation events in RNA.

**OP033: Protein interactions and function studied by novel NMR methods**

**\*S. Grzesiek**, M. Gentner, J.-r. Huang, S. Morin, L. Nisius, H.-J. Sass, L. Skora, N. Vajpai, M. Wiktor

*Biozentrum, University of Basel, Switzerland*

We extensively use residual dipolar coupling (RDC), paramagnetic labeling (PRE, PCS), scalar couplings and other NMR parameters to characterize folded and unfolded protein states in a quantitative manner [1-11]. We will discuss several recent examples.

Scalar couplings across hydrogen bonds (H-bonds), which report on the electronic overlap between donor and acceptor orbitals, present a highly sensitive measure of H-bond geometry [1,2]. Using H-bond scalar couplings, we have recently mapped the pressure and temperature dependent deformation of ubiquitin’s H-bond network at unprecedented resolution [3].

We recently also obtained atomic details of the pressure-assisted, cold-denatured state of ubiquitin at 2500 bar and 258 K by high-resolution NMR techniques [4]. This state has structural propensities for a native-like N-terminal  $\beta$ -hairpin and  $\alpha$ -helix and a non-native C-terminal  $\alpha$ -helix, which are very similar to ubiquitin’s alcohol-denatured (A-) state. The close similarity of pressure-assisted, cold-denatured and alcohol-denatured state supports a hierarchical mechanism of folding and the notion that similar to alcohol, pressure and cold reduce the hydrophobic effect. Indeed, at non-denaturing concentrations of methanol, a complete transition from the native to the A-state can be achieved at ambient temperature by varying the pressure from 1 to 2500 bar. This method should allow highly detailed studies of protein folding transitions in a continuous and reversible manner.

Abelson kinase (Abl) is an important drug target in the treatment of chronic myelogenous leukemia. We have recently characterized the solution conformations of the kinase domain in complex with different inhibitors by RDCs and other parameters [5]. The NMR analysis has also helped to locate

the interaction side of a new class of allosteric inhibitors that can overcome resistance to ATP-binding-site inhibitors [6]. Time permitting we will show recent results on these interactions.

- [1] A. J. Dingley, L. Nisius, F. Cordier, and S. Grzesiek, *Nature Protocols* 3, 242 (2008).
- [2] F. Cordier, L. Nisius, A. J. Dingley, and S. Grzesiek, *Nature Protocols* 3, 235 (2008).
- [3] L. Nisius and S. Grzesiek, *Nat Chem* 4, 711 (2012).
- [4] N. Vajpai, L. Nisius, M. Wiktor, and S. Grzesiek, *Proc Natl Acad Sci USA* (2013).
- [5] N. Vajpai, A. Strauss, G. Fendrich, S. W. Cowan-Jacob, P. W. Manley, S. Grzesiek, and W. Jahnke, *J Biol Chem* 283, 18292 (2008).
- [6] J. Zhang, F. J. Adrián, W. Jahnke, S. W. Cowan-Jacob, A. G. Li, R. E. Iacob, T. Sim, J. Powers, C. Dierks, F. Sun, G.-R. Guo, Q. Ding, B. Okram, Y. Choi, A. Wojciechowski, X. Deng, G. Liu, G. Fendrich, A. Strauss, N. Vajpai, S. Grzesiek, T. Tuntland, Y. Liu, B. Bursulaya, M. Azam, P. W. Manley, J. R. Engen, G. Q. Daley, M. Warmuth, and N. S. Gray, *Nature* 463, 501 (2010).
- [7] M. Gentner, M. G. Allan, F. Zaehring, T. Schirmer, and S. Grzesiek, *J Am Chem Soc* 134, 1019 (2012).
- [8] J. Habazettl, M. G. Allan, U. Jenal, and S. Grzesiek, *J Biol Chem* 286, 14304 (2011).
- [9] J.-R. Huang and S. Grzesiek, *J Am Chem Soc* 132, 694 (2010).
- [10] D. Häussinger, J.-R. Huang, and S. Grzesiek, *J Am Chem Soc* 131, 14761 (2009).
- [11] S. Meier, M. Blackledge, and S. Grzesiek, *The Journal of Chemical Physics* 128, 052204 (2008).

**Monday – May 20<sup>th</sup>**

**Methods for Inorganic Materials**

Chair: Bradley Chmelka

Rooms Turmalina/Topázio

#### OP034: NMR Non-Crystallography

<sup>1</sup>\*Philip J. Grandinetti, <sup>1</sup>Kevin Sanders, <sup>1</sup>Eric Keeler, <sup>2</sup>Jay H. Baltisberger

<sup>1</sup>Ohio State University, Columbus, USA, <sup>2</sup>Berea College, Berea, KY, USA

A great advantage of solid-state NMR spectroscopy is its ability to reveal atomic-level structure in materials where diffraction techniques fail. This is generally true in non-crystalline solids, where diffraction methods rarely reveal structural details beyond the first-coordination sphere except in the simplest of compositions. While it also true that the spectra of non-crystalline solids in many spectroscopies are often broad and featureless, magnetic resonance spectroscopy has a unique advantage in that the different NMR frequency contributions leading to these broadenings can be separated and correlated in multi-dimensional experiments. This talk will describe efforts in our laboratory over the last few years developing new and improved multi-dimensional NMR methods for structure determination in non-crystalline solids. This work has focused on silicates and involves nuclei, such as <sup>29</sup>Si and <sup>17</sup>O, where we have found strong relationships between NMR couplings and local structure and used these relationships to convert multi-dimensional NMR spectra into multi-dimensional structural correlations. For example, we have shown that <sup>17</sup>O quadrupole coupling constant and asymmetry parameters can be directly related to Si-O bond lengths, Si-O-Si angles, and the presence of coordinating alkali or alkaline earth cations, and exploit these relationships to follow structural changes in various silica and modified silicate

glasses. We have also found that <sup>29</sup>Si nuclear shielding tensor parameters of SiO<sub>4</sub> tetrahedra not only reveal tetrahedral connectivity but can also be related to the nature and coordination number of network modifier cations. These studies have direct implications for the continuous random network and modified random network structural models of silicate glasses. They can provide insight for researchers needing to refine potentials for MD simulations and to connect structure to viscosity, density, strength, transport properties, and thermodynamic properties, impacting fields such as inorganic geochemistry, waste containment technology, and ionic conductors.

#### OP035: Hunting for Hydrogen in Wadsleyite: Multinuclear Solid-State NMR and First-Principles Calculations

<sup>1</sup>\*Sharon E. Ashbrook, <sup>1</sup>John M. Griffin, <sup>2</sup>Andrew J. Berry, <sup>3</sup>Stephen Wimperis

<sup>1</sup>School of Chemistry and EaStCHEM, University of St Andrews, UK, <sup>2</sup>Research School of Earth Sciences, Australia National University, Canberra, Australia, <sup>3</sup>School of Chemistry and WestCHEM, University of Glasgow, UK

It is thought that the inner Earth contains a vast amount of water in the form of hydrogen bound at defect sites within the nominally anhydrous silicate minerals present in the mantle. Structural studies of silicates, therefore, play an important role in our understanding of the physical and chemical properties of the Earth's interior. However, the high-pressure synthesis conditions typically result in small sample volumes (1-10 mg), compromising sensitivity. Here we present experimental solid-state NMR results and first-principles calculations that provide insight into local structure and disorder in hydrous wadsleyite ( $\beta$ -Mg<sub>2</sub>SiO<sub>4</sub>). This deep-Earth mineral has received widespread attention due to its high capacity for the incorporation of water. <sup>17</sup>O MAS and STMAS spectra recorded at 20.0 T enable the identification of hydroxyl oxygen sites in samples with different hydration levels. This is consistent with a model structure previously proposed in the literature; however, considerable broadening is also observed, indicating that the structure is not fully ordered. <sup>1</sup>H/<sup>2</sup>H MAS and two-dimensional <sup>1</sup>H dipolar correlation spectra reveal multiple proton environments in both samples, including some with chemical shifts that are higher than expected for Mg-OH environments. Indeed, DFT calculations carried out for different model structures derived from disordered supercells suggest that some of the observed resonances correspond to Si-OH protons. This is supported by <sup>29</sup>Si CPMAS and heteronuclear correlation spectra, while <sup>1</sup>H-<sup>17</sup>O CPMAS and two-dimensional spectra also indicate the presence of both Mg-OH and Si-OH groups in the structure. The DFT calculations additionally reveal it is an Mg<sub>3</sub>, not an Mg<sub>2</sub>, vacancy that charge balances the structure. The combination of multinuclear solid-state NMR and DFT calculations enables the most complete study to date of this extremely important mantle mineral, providing new insight into the mechanism of water storage.

#### UP036: Uniform excitation and inversion of broad NMR spectra in rotating solids using DANTE

<sup>1</sup>Veronika Vizthum, <sup>1</sup>Marc Caporini, <sup>1</sup>Diego Carnevale, <sup>1</sup>Simone Ulzega, <sup>2</sup>Julien Trébosc, <sup>2</sup>Olivier Lafon, <sup>1</sup>Geoffrey Bodenhausen, <sup>2</sup>\*Jean Paul Amoureux

<sup>1</sup>Ecole Polytechnique Fédérale de Lausanne, Switzerland, <sup>2</sup>Lille University, France

Many solid-state NMR powder patterns span several MHz. These broad patterns arise from large anisotropic interactions (e.g. quadrupolar interaction or electron-nuclei interactions in paramagnetic solids). These ultra-wide-line NMR spectra can provide detailed information on the structure and dynamics at molecular level but high-power rectangular pulses are usually insufficient to excite uniformly these broad patterns.

Herein, we show how trains of rotor-synchronized short pulses in the manner of Delays Alternating with Nutation for Tailored Excitation (DANTE) can provide uniform excitation, inversion or other coherence manipulation for broad spectra of rotating solids, spanning several MHz. In that case, DANTE overcome many limitations of rectangular pulses. Furthermore, interleaved DANTE trains can achieve shorter excitation and hence are less affected by coherent or incoherent decays, and can facilitate the excitation of different chemical environments.

We first demonstrate the efficiency of DANTE for the  $^{14}\text{N}$  observation.[1-3] We show applications to direct detection of  $^{14}\text{N}$  nuclei subject to large quadrupole interactions, using fast MAS, backed up by simulations that provide insight into the properties of DANTE. When used for indirect detection, we show that DANTE can lead to large boost of efficiency compared to rectangular pulses.

We also demonstrate that DANTE can manipulate in paramagnetic samples a large number of spinning sidebands of spin-1/2 nuclei ( $^{19}\text{F}$ ) that extend over more than 1.3 MHz, with rf-fields as low as 20-30 kHz.[4]

[1] Vitzthum, Caporini, Ulzega, Bodenhausen, J. Magn. Reson. 212 (2011) 234.

[2] Vitzthum, Caporini, Ulzega, Trébosc, Lafon, Amoureux, Bodenhausen, J. Magn. Reson. 223 (2012) 228

[3] Lu, Trébosc, Lafon, Carnevale, Bodenhausen, Amoureux, submitted.

[4] Carnevale, Vitzthum, Lafon, Trébosc, Amoureux, Bodenhausen, Chem. Phys. Lett. 553 (2012) 68.

#### UP037: A homonuclear version of REDOR for recoupling dipolar interactions in multi-spin systems: Applications to inorganic phosphorus clusters and networks

<sup>1,2\*</sup>Hellmut Eckert, <sup>2</sup>Jinjun Ren

<sup>1</sup>University of Sao Paulo, <sup>2</sup>WWU Münster

A new solid state NMR technique is presented to re-couple the homonuclear dipole-dipole interactions within spin pairs, clusters and multi-spin distributions of coupled  $I = 1/2$  systems under MAS conditions. In contrast to the usual double-quantum coherence intensity buildup curves, this method measures the amplitude of  $I_z$ , both in the presence and in the absence of the dipolar coupling. Recoupling is accomplished in the form of an effective double quantum Hamiltonian created by a symmetry-based POST-C7 sequence consisting of two excitation blocks, attenuating the signal (intensity  $S'$ ). For comparison, a reference signal  $S_0$  with the dipolar recoupling absent is generated by shifting the phase of the second block by  $90^\circ$  relative to the first block. As in rotational echo double resonance (REDOR), the homonuclear dipole-dipole coupling constant can then be extracted from a plot of the normalized difference signal  $(S_0 - S')/S_0$  versus dipolar evolution time. Detailed simulations indicate that within the range of  $(S_0 - S')/S_0$  0.5 such "homonuclear REDOR curves" can be approximated by simple parabolas, yielding effective squared dipole-dipole coupling constants summed over all the pairwise interactions present. The method has been successfully validated for  $^{31}\text{P}$  in a large number of inorganic crystalline model compounds and successfully applied to various structural issues in inorganic phosphate glasses. It combines efficiency, facile data analysis, and easy extension to multiple spin systems covering a wide range of dipolar coupling strengths. The method is not affected by dipolar truncation and allows CSA effects to be accounted for by simple calibration. All of these advantages will help to trigger novel structural applications elucidating short-, medium-range and nanoscale ordering phenomena disordered state of matter. While the present contribution focuses on  $^{31}\text{P}$  NMR studies of inorganic materials, the method can be applied analogously to other spin-1/2 nuclei that are either abundant ( $^{19}\text{F}$ ,  $^1\text{H}$ ) or

can be prepared with isotopic enrichment ( $^{13}\text{C}$ ,  $^{15}\text{N}$ ), making it also applicable to biological solids.

ACKNOWLEDGEMENTS: DFG, FAPESP, CNPq

#### OP038: Topologic, Geometric, and Chemical Order in Materials: Insights from Solid-State NMR

Dominique Massiot, Sylvian Cadars, Michael Deschamps, Emmanuel Véron, Mounesha N. Garaga, Robert J. Messinger, Mathieu Allix, \*Pierre Florian, Franck Fayon

CEMHTI UPR3079 CNRS, France

Local order, as opposed to the long-range order of the ideal crystalline structures, can be considered as an intrinsic characteristic of real materials, being often the clue to the tuning of their properties and their final applications. While ordering can be easily assessed in two-dimensional imaging techniques with resolution approaching the atomic level, the diagnostic, description, and qualification of local order in three dimensional systems is much more challenging.

Solid-state nuclear magnetic resonance [NMR] and its panel of constantly developed new instruments and methods enable local, atom selective characterization of structures and assemblies ranging from atomic to nanometer length scales. This opens unique opportunities for characterizing a variety of materials, ranging from crystalline compounds to amorphous or glassy materials, for which we show that it becomes possible to separate topologic, geometric and chemical contributions to the order or disorder, in cooperation with other experimental techniques and in-silico approaches.

As identified by solid state NMR, the local structure of amorphous materials or glasses consists of well-identified structural entities up to at least the nanometer scale. Instead of speaking of disorder, we propose a new paradigm to describe their structures in terms of a continuous assembly of locally defined structures, reminiscent of locally favored structures (LFS). This draws a comprehensive picture of amorphous structures based on fluctuations of chemical composition and structure over different length scales. We hope that these new local or molecular insights could open new possibilities for considering key questions related to nucleation and crystallization, as well as chemically (spinodal decomposition) or density driven (polyamorphism) phase separation, which could enable future applications.

#### References

[1] D.Massiot, S.Cadars, M.Deschamps, V.Montouillout, N.Pellerin, E.Véron, R.J.Messinger, M.Allix, P.Florian, F.Fayon, Topologic, Geometric, and Chemical order in Materials : Insights from Solid-State NMR, Accounts Chem. Res. (submitted)

[2] E.Véron, M.N.Garaga, D.Pelloquin, S.Cadars, M.Suchomel, E.Suard, D.Massiot, V.Montouillout, G.Matzen, M.Allix, Synthesis and structure determination of  $\text{CaSi}_1/3\text{B}_2/3\text{O}_8/3$ , a new calcium borosilicate, Inorg. Chem. ASAP (2013)

[3] F.Fayon, C.Duée, T.Poumeyrol, M.Allix, D.Massiot, Evidence of Nanometric-Sized Phosphate Clusters in Bioactive Glasses as Revealed by Solid-State  $^{31}\text{P}$  NMR, J. Phys. Chem. ASAP (2013)

[4] P.Florian, E.Véron, T.Green, J.R.Yates, D.Massiot, Elucidation of the Al/Si ordering in Gehlenite  $\text{Ca}_2\text{Al}_2\text{SiO}_7$  by combined  $^{29}\text{Si}$  and  $^{27}\text{Al}$  NMR spectroscopy / quantum chemical calculations, Chem. Mater. 24 4068–4079 (2012)

[5] R.N.Kerber, A.Kermagoret, E.Callens, P.Florian, D.Massiot, A.Lesage, C.Copéret, F.Delbecq, X.Rozanska, P.Sautet, Nature and structure of aluminum surface sites grafted on silica from a combination of high field aluminum-27 solidstate NMR spectroscopy and first principle calculations, J. Am. Chem. Soc. 134 6767–6775 (2012)



Monday – May 20<sup>th</sup>

## Hyperpolarization/ Instrumentation

Chair: Dmitry Budker

Room Ònix

**OP039: Imaging Pulmonary Gas Exchange from Mouse to Human with Hyperpolarized <sup>129</sup>Xe MRI**

\*Bastiaan Driehuys

Department of Radiology, Duke University Medical Center, Durham

Among the most interesting properties of hyperpolarized (HP) <sup>129</sup>Xe, are its high solubility and large chemical shift. These have long been prized by NMR spectroscopists, but are only now beginning to be exploited in biomedical imaging. Here we describe progress in using the dissolved phase of HP <sup>129</sup>Xe to image the lung's most fundamental function – gas exchange. When inhaled, HP <sup>129</sup>Xe diffuses into the pulmonary blood and tissues where in most mammals, including humans, it exhibits distinct resonances in each compartment. Here we explain the techniques used to HP <sup>129</sup>Xe as it transfers from airspace to blood. Particularly in healthy human subjects, these <sup>129</sup>Xe gas transfer images exhibit intrinsic heterogeneity and are strongly influenced by gravity. This heterogeneity reveals the extraordinary reserve capacity of the healthy lung, and may explain why lung disease has historically been so difficult to detect early. We will discuss not only the basic lung physiology we are learning from HP <sup>129</sup>Xe MRI, but also introduce new techniques to simultaneously acquire gas- and dissolved phase <sup>129</sup>Xe images by efficient radial acquisition. This approach enables short echo times and improves SNR, but also opens the door to separating the dissolved-phase <sup>129</sup>Xe image into its blood and tissue components. Such separation is critically important as we show in our recent work in patients with interstitial lung disease. To complement these human trials, it is equally important to exploit hyperpolarized <sup>129</sup>Xe MRI to image mouse models of lung disease. We now routinely acquire isotropic images of <sup>129</sup>Xe in the mouse with a resolution of <250µm and demonstrate novel ways to extend gas exchange imaging to the mouse by taking advantage of genetically modified strains. Together, these findings are positioning HP <sup>129</sup>Xe MRI as a powerful platform to enable progress in developing new therapies for chronic lung diseases.

ACKNOWLEDGEMENTS: NIH R01HL105643 and P41 EB015897

**OP040: Hyperpolarized Carbon-13 MR Pre-Clinical and Human Research Studies**<sup>1</sup>\*Daniel B. Vigneron, <sup>1</sup>Sarah Nelson, <sup>2</sup>Andrea Harzstark, <sup>3</sup>Marcus Ferrone, <sup>1</sup>Robert Bok, <sup>1</sup>John Kurhanewicz<sup>1</sup>Department of Radiology & Biomedical Imaging, University of California, San Francisco, <sup>2</sup>Investigational Therapeutics, University of California, San Francisco, <sup>3</sup>Clinical Pharmacy, University of California, San Francisco

Hyperpolarized Carbon-13 MR has the potential to become an important new radiological tool for cancer metabolic imaging by directly investigating key cellular enzymatic pathways *in vivo* as described in a Feb. 2011 "White Paper" in Neoplasia titled "Analysis of Cancer Metabolism by Imaging Hyperpolarized Nuclei: Prospects for Translation to Clinical Research". Hyperpolarized <sup>13</sup>C imaging using the dissolution DNP (dynamic nuclear polarization) method provides a >10,000 fold signal enhancement for detecting <sup>13</sup>C probes of endogenous, nontoxic, nonradioactive substances such as pyruvate to monitor metabolic fluxes through multiple key biochemical pathways (glycolysis, citric acid cycle and alanine transaminase). The hyperpolarization of [1-<sup>13</sup>C]pyruvate has demonstrated the ability to not only detect pyruvate uptake but also the *in vivo* enzymatic conversion to <sup>13</sup>C-lactate through the enzyme lactate dehydrogenase (LDH), <sup>13</sup>C-alanine through the alanine transaminase

(ALT) pathway; and <sup>13</sup>CO<sub>2</sub> & <sup>13</sup>C-bicarbonate through the pyruvate dehydrogenase (PDH) catalyzed metabolic pathway. The value of this powerful metabolic imaging technique for cancer imaging was shown first by Golman *et al* 2006 and we have applied it in a number of preclinical animal studies for detecting cancer presence, progression and response to therapy and in a first-ever human Phase 1 clinical trial in prostate cancer patients. This study demonstrated the feasibility to characterize prostate tumors based on dramatically increased conversion of <sup>13</sup>C-pyruvate to <sup>13</sup>C-lactate through LDH. Recent studies have demonstrated significant correlations of gene expression and enzyme activity with new MR techniques to measure kinetic rates *in vivo*. Also a variety of new HP agents to investigate physiological parameters including perfusion, pH, and membrane transport as well as metabolism have been applied in disease models.

**UP041: Universal tags to sustain long-lived hyperpolarized signal: Extension of hyperpolarization to broad range of biomarkers**

Yesu Feng, Thomas Theis, Ryan M. Davis, Kevin Claytor, Qiu Wang, Pei Zhou, \*Warren S. Warren

Duke University

*In vivo* applications of hyperpolarization are largely hindered due to the short T<sub>1</sub> relaxation times of molecules with metabolic relevance. Up till now, very few molecules have been hyperpolarized that have long enough T<sub>1</sub> to acquire *in vivo* metabolic images. By accessing the singlet state between chemically equivalent or slightly inequivalent spin pairs, lifetime extensions above an order of magnitude have been achieved. However, most of the molecules supporting long-lived singlet states have no direct biological function and using these molecules as a tag to label interesting target molecules is not practical given the molecule's size and symmetry requirements. As a result, universal tags to generalize the implementation of long-lived singlet state are still awaited. Here, we present two tags that sustain a long-lived singlet state between either a pair of <sup>13</sup>C spins in <sup>13</sup>C<sub>2</sub>-diphenylethyne or a pair of <sup>15</sup>N spins in <sup>15</sup>N<sub>2</sub>-diazirine. We will also demonstrate two immediate applications of <sup>13</sup>C<sub>2</sub>-diphenylethyne used as a tag. The first one is a potential antibiotic drug which contains diphenylethyne as a substructure. This molecule has been shown to function as an LpxC inhibitor to suppress the lipid biosynthesis of gram-negative bacteria. The second is to use <sup>13</sup>C<sub>2</sub>-diphenylethyne to label suberoylanilide hydroxamic acid (SAHA), which is an FDA approved anti-cancer drug serving as a histone deacetylases inhibitor. As to <sup>15</sup>N<sub>2</sub>-diazirine, which is widely used as a tag for photoaffinity labeling, it is also one of the smallest tags that can support a long-lived singlet state. Studies using diazirine as a tag cover almost every category of drugs (antibiotics, anti-cancer, anesthetics etc.) and endogenous biomolecules (amino acids and their derivatives, nucleic acids and fatty acids etc.). We will show the very first case of extending the hyperpolarized signal through the singlet state on a <sup>15</sup>N<sub>2</sub>-diazirine compound. This might significantly extend the application of hyperpolarization in metabolic imaging.

**UP042: Avalanching Amplification of NMR/MRI Sensitivity by Solvent-Generated Feedback Fields**

Zhao Li, Susie Y. Huang, Jamie D. Walls, \*Yung-Ya Lin

Department of Chemistry and Biochemistry, UCLA

**Introduction.** Low sensitivity is particularly problematic in biomolecular NMR and heteronuclear MRI, where insensitive and/or dilute spins are detected. A general spin amplification scheme has now been developed to enhance sensitivity in NMR/MRI based on dynamic instability of the solvent magnetization under collective feedback fields. The solute spins are first detected by the solvent spins through various magnetization transfer mechanisms and serve as small "input" signals to perturb the solvent magnetization, which is prepared in an unstable state. The weakly detected signal is

then amplified through subsequent nonlinear evolution of the solvent magnetization. By manipulating bulk solvent spins near the threshold of instability to detect dilute solute spins, sensitivity and signal-to-noise ratios (SNR) can be markedly improved.

**Methods and Results.** This general spin amplification scheme is shown here to amplify indirectly detected heteronuclear solute signals. Low-gyromagnetic ratio nuclei can be detected through the large  $^1\text{H}$  solvent magnetization by the distant dipolar field (DDF) [1,2]. The modulated  $^1\text{H}$  transverse magnetization precesses under the DDF created by the spatially modulated  $^{13}\text{C}$  longitudinal magnetization, generating an echo in the  $^1\text{H}$  solvent magnetization that carries information about the  $^{13}\text{C}$  spins. Recently discovered self-refocusing of dephased solvent magnetization due to the joint action of radiation damping and the DDF [2] is exploited to enhance the indirectly detected echo signal. The extreme sensitivity of the first and largest self-refocused echo's phase and amplitude to the phase and amplitude of the initial triggering magnetization (here, the indirectly detected signal) suggests that the nonlinear spin dynamics can serve as a high-gain spin amplifier to enhance the small initial magnetization transferred to the solvent from the dilute  $^{13}\text{C}$  solute spins. The resulting SNR of the amplified indirectly detected echo signal, e.g., 10%  $2\text{-}^{13}\text{C}$  acetone solution, is improved by 3-4x compared to without amplification. The amplification factor can be further improved by controlling the nonlinear spin evolution under the feedback fields. For example, if the  $^1\text{H}$  pulse flip angle  $q > 90^\circ$ , the instability of the inverted net  $^1\text{H}$  longitudinal magnetization under radiation damping aids in refocusing more  $^1\text{H}$  transverse magnetization. The resulting SNR is enhanced by an additional 4x, as demonstrated on  $\text{U-}^{13}\text{C}$  glucose. Moreover, field inhomogeneity or weak continuous gradients may also be exploited to accelerate the self-refocusing process [3] and increase SNR by more than 10x overall. Application of this approach to  $^{13}\text{C}$  MRI will also be shown.

**Conclusion.** Sensitivity enhancement by the dynamic instability of solvent magnetization represents a new direction for surmounting a long-standing weakness of MR through nonlinear feedback.

Reference. [1] R. Bowtell, J. Magn. Reson. 100, 1 (1992) [2] Warren et al. J. Chem. Phys. 108, 1313 (1998) [3] Y.-Y. Lin et al. Science 290, 118 (2000).

#### OP043: An Implantable Wireless Amplified NMR Detector for High Resolution MRI

Chunqi Qian, Xin Yu, Der-Yow Chen, Stephen Dodd, Joseph Murphy-Boesch, \***Alan P. Koretsky**

*Laboratory of Functional and Molecular Imaging, NINDS, NIH, Bethesda, MD*

Optical microscopy is sensitive enough to observe tissue microstructures at sub-cellular resolution but application to deep lying structures in vivo requires a light path in and out of the sample being imaged. Magnetic Resonance Imaging (MRI) has the unique advantage that radiofrequency signals have a large penetration depth and the "near-field" imaging properties of MRI can, in principle generate very high resolution. Indeed, resolution in deep-lying internal organs *in vivo* is presently limited by sensitivity. Conventional MRI utilizes external detectors to receive signals from inside the body, and thus sensitivity is often limited, especially for regions deep inside the body. In this work, a Wireless Amplified NMR Detector (WAND) is developed to enhance the MRI sensitivity of deep-lying internal tissues. This detector has a small dimension to observe the region of interest in close proximity to the WAND. Unlike the MRI detectors that use a wired connection, the WAND utilizes a wireless power source to amplify the MR signal in situ before transmitting the signal to an external receiver. A parametric amplifier is integrated with the detection coil to enable wireless operation and amplification before transmission to the receiver. As

an initial demonstration of this detection technology, a millimeter scale WAND was chronically implanted on the medial surface of a rat kidney. High resolution images were obtained enabling *in vivo* observation of kidney microstructures, such as individual glomeruli. This wireless detector may find applications for high-resolution imaging of other body parts and hold promise to enable integration with tissue engineered constructs for monitoring after implantation.

#### Tuesday – May 21<sup>st</sup> Plenary Session

Chair: Ad Bax  
Room Gávea A

#### PL044: Singlet Nuclear Magnetic Resonance

\***Malcolm H. Levitt**

*School of Chemistry, University of Southampton, UK*

Singlet nuclear spin states are quantum states of a nuclear spin-1/2 pair that are antisymmetric with respect to spin exchange, and which have total spin zero. They are therefore non-magnetic and protected against many important relaxation mechanisms. These states often exhibit long relaxation times which may exceed the normal relaxation time  $T_1$  by an order of magnitude or even more.

I will discuss the phenomenon of singlet nuclear spin order in a variety of contexts - including gas-phase para-hydrogen, small molecules in solution, and some examples in solids. I will discuss how nuclear singlet spin order may be generated from magnetization, how it is maintained, and how it is converted back into observable magnetization.

Some recent developments in our group include:

- direct generation of hyperpolarized nuclear singlet order using dynamic nuclear polarization
- storage and repeated detection of hyperpolarized  $^{13}\text{C}$  nuclear singlet order in solution, over a total time of 30 minutes
- the use of  $^{18}\text{O}$  substitution to access long-lived nuclear singlet states
- demonstration MRI experiments involving hyperpolarized nuclear singlet order
- detection of hyperpolarized  $^{13}\text{C}$  singlet order in vivo
- modelling of nuclear singlet relaxation in solution using molecular dynamics and quantum chemistry
- NMR detection of singlet-triplet conversion between ortho-water and para-water in the solid state.

#### PL045: Visualizing Transient Structures of DNA and RNA using NMR

\***Hashim M. Al-Hashimi**

*Department of Chemistry and Biophysics, University of Michigan*

We will describe the development and application of relaxation dispersion NMR methods to visualize transient state structures of DNA and RNA that exist in low abundance (<13%) and for small periods of time (lifetimes < 1 milliseconds). We will provide evidence that base-pairs in canonical duplex DNA transiently form Hoogsteen base-pairs, and describe basic aspects of these transitions, their occurrence across a variety of DNA sequence contexts, and possible biological functions. We will also report transient structures for three distinct RNAs and describe their potential roles in HIV replication and ribosome translation. The possibility of targeting these transient state structures with small molecules will also be discussed.

**Tuesday – May 21<sup>st</sup>****Dynamics and Recognition**Chair: Jose Pires  
Room Gávea A**OP046: Protein dynamics and interaction mediated by local water dynamics at the ps timescale****\*Songi Han***Departement of Chemistry and Biochemistry, University of California Santa Barbara*

An emerging NMR-ESR double-resonance technique dubbed Overhauser-effect Dynamic Nuclear Polarization (ODNP) has demonstrated the ability to probe the diffusion dynamics of "soft", fast moving, hydration water, surrounding the protein surface and interfacing bulk water. Specifically, ODNP probes the dynamics within 2-4 water layers (i.e. 5-10 Å) of an ESR-active stable nitroxide radical - i.e. "spin-label" - attached to the surface of a bio-macromolecule. We show that changes to the protein surface induced by folding, binding, or aggregation can cause these local hydration dynamics to vary by factors of up to 30, offering a dramatic dynamic range for probing, and possibly predicting, interactions involving proteins. Studies of monitoring early protein aggregation events and the adsorption and insertion of proteins into lipid membrane bilayers will be presented. Interestingly, we show a very weak, nonlinear, scaling of the surface hydration diffusion with bulk water viscosity that is increased by factors of 10-20 by the addition of various molecular crowding agents. Specifically, both a >10-fold increase in bulk viscosity and the restriction of diffusion by confinement on a multiple-nm length-scale change the local translational diffusion coefficient of the surface water by less than 2.5-fold, which is in contrast to the vast modulation experienced by water dynamics on protein surfaces. We begin to suspect that the surface topology and chemistry at the  $\leq 1.5$  nm scale, rather than the characteristics of the bulk fluid, nearly exclusively determine the surface hydration dynamics of aqueous macromolecular solutes, which presents an opportunity for hydration dynamics-based study of protein interaction.

ACKNOWLEDGEMENTS: U.S. National Science Foundation, National Institute of Health

**OP047: Molecular Recognition and Dynamics: NMR Studies of Defensins and Epitopes****\*Ana Paula Valente***Federal University of Rio de Janeiro*

Conformational dynamics play a key role in protein recognition as well as in many biological processes. In order to interfere with these processes, we must characterize in detail the nature of motion and its time scale. In the talk I will show the importance of protein conformation exchange process both in defensins-membrane and antibody-epitope recognition. We have used chemical shift perturbation and relaxation parameters measurements to evaluate the importance of motions in the ps-ns and  $\mu$ s-ms timescales. In the case of defensins, multiple motions seem to be correlated with the stages of membrane recognition and disruption over a large timescale range. I will also discuss the modulation observed in the antibody-epitope affinity due to changes in dynamic. We observed that the decrease in conformational exchange and no change in the structure of epitope, lead to the higher affinity, inducing higher cross-linking to fcc receptors.

ACKNOWLEDGEMENTS: FAPERJ, CAPES, CNPq, INCT-INBEB.

**UP048: Bacterial transmembrane signalling through a heme/hemophore receptor****1,2\*Nadia Izadi-Pruneyre**<sup>1</sup>*Institut Pasteur, Paris, France*, <sup>2</sup>*CNRS UMR 3528*

Bacteria live in complex and changing environment and must adapt to extracellular medium variations including light, oxidative stress, pressure, temperature and presence of some nutrients. They thus need external probes and signalling systems that enable them to sense these extracellular changes and respond by differential gene expression.

In our model system, the availability of heme, the major iron source in mammals, is detected by some Gram-negative bacteria *via* an outer membrane receptor, HasR. A cascade of molecular interactions between five proteins, located in three subcellular compartments, is then used to send this signal from outside to inside the bacteria.

Using structural and biophysical approaches (NMR, Xray, SAXS, microscopy, SPR and ITC), we have studied the molecular interactions between HasR and its various partners in order to define the structural basis of this signalling pathway. Furthermore, we have recently shown, for the first time, that a partially folded protein is involved in this signalling process. Our current data represent the first detailed characterization of this type of bacterial signalling.

**UP049: NMR Mapping of PCNA Interaction with Translesion Synthesis DNA Polymerase Rev1 Mediated by Rev1-BRCT Domain****Yulia Pustovalova, Mark W. Maciejewski, \*Dmitry M. Korzhnev***University of Connecticut Health Center*

Rev1 is a Y-family translesion synthesis (TLS) DNA polymerase involved in bypass replication across sites of DNA damage and postreplicational gap filling. In the process of TLS high-fidelity replicative DNA polymerases stalled by DNA damage are replaced by error-prone TLS enzymes responsible for the majority of mutagenesis in eukaryotic cells. The polymerase exchange that gains low-fidelity TLS polymerases an access to DNA is mediated by their interactions with proliferating cell nuclear antigen (PCNA). Rev1 stands alone from other Y-family TLS enzymes since it lacks the consensus PCNA-interacting protein box (PIP-box) motif, instead utilizing other modular domains for PCNA binding. Here we report solution NMR structure of an 11 kDa BRCA1 C-terminus (BRCT) domain from *S. cerevisiae* Rev1, and demonstrate with the use of TROSY NMR methods that Rev1-BRCT domain directly interacts with an 87 kDa PCNA in solution. The domain adopts  $\alpha/\beta$  fold ( $\beta$ 1- $\alpha$ 1- $\beta$ 2- $\beta$ 3- $\alpha$ 2- $\beta$ 4- $\alpha$ 3- $\alpha$ 4) typical for BRCT domain superfamily. PCNA-binding interface of the Rev1-BRCT domain comprises conserved residues of the outer surface of the  $\alpha$ 1 helix,  $\alpha$ 1- $\beta$ 1,  $\beta$ 2- $\beta$ 3 and  $\beta$ 3- $\alpha$ 2 loops. On the other hand, Rev1-BRCT binds to the inter-domain region of PCNA that overlaps with the binding site for the PIP-box motif. Furthermore, Rev1-BRCT domain bound to PCNA can be displaced by increasing amounts of the PIP-box peptide from TLS DNA polymerase pol $\eta$ , suggesting that Rev1-BRCT and pol $\eta$  PIP-box interactions with a given PCNA subunit are mutually exclusive. These results provide structural insights into PCNA recognition by TLS DNA polymerases that help better understand TLS regulation in eukaryotes.

**OP050: Structural basis of epigenetic regulation****\*Yunyu Shi***School of Life Sciences, University of Science and Technology of China, Hefei, China*

PHD (plant homeodomain) zinc fingers that specifically recognize different histone modification are structurally conserved modules found in proteins. Acetyltransferase MOZ is important for HOX gene expression as well as embryo and postnatal development. In vivo, it forms a tetrameric complex with other subunits including several chromatin binding modules with regulatory functions. Here we report the solution structure of the first and second PHD fingers in BRPF2, a component of MOZ complex. We also report the solution

structure of tandem PHD finger (PHD12) of human MOZ in free state, and the 1.47 Å crystal structure in complex with H3K14ac peptide which reveals the structural basis for the recognition of unmodified R2 and acetylated K14 on histone H3. Moreover, the results of chromatin immunoprecipitation (ChIP) and RT-PCR assays indicate that PHD12 facilitates the localization of MOZ onto the promoter locus of the HOXA9 gene, thereby promoting the H3 acetylation around the promoter region and further up-regulating the HOXA9 mRNA level. Our findings suggest that the combinatorial readout of the H3R2/K14ac by PHD12 might represent an important epigenetic regulatory mechanism that governs transcription and also provide a clue of cross-talk between the MOZ complex and histone H3 modifications.

#### References

1. Qin Su, et al. *J Biol Chem.*, 2011, 286(42):36944-55.
2. Lei Liu, et al. *J Struct Biol.* 2012, 180, 165-173.
3. Yu Qiu, et al. *Genes & Development.*, 2012, 26(12):1376-91.

#### Tuesday – May 21<sup>st</sup> IDPs, Folding and Misfolding

Chair: Gianluigi Veglia  
Room Gávea B

#### OP051: New methods based on <sup>13</sup>C direct detection to study intrinsically disordered proteins

\*Isabella C. Felli

*CERM and Department of Chemistry "Ugo Schiff", University of Florence, Italy*

Recent progress in NMR instrumentation in parallel to the growing interest in understanding the functional role of protein intrinsic disorder and flexibility have stimulated the development of a variety of new NMR methods to study intrinsically disordered proteins (IDPs)[1]. The high flexibility and largely solvent exposed backbone typical of IDPs influence NMR parameters causing reduced chemical shift dispersion and efficient amide solvent exchange. These constitute general features of IDPs that need to be taken into account in the design of NMR experimental approaches. <sup>13</sup>C detected NMR experiments now offer a valuable tool to address these peculiar features of IDPs. The experimental variants to improve the performance of <sup>13</sup>C detected NMR experiments to study IDPs include the design of multidimensional experiments[2], the exploitation of longitudinal relaxation enhancement[3], the design of experiments to alleviate the problem of extensive cross peaks overlap[4]. The new experiments are demonstrated on a paradigmatic IDP,  $\alpha$ -synuclein.

- [1] Felli I.C., Pierattelli R., *IUBMB Life.* (2012), 64, 473-81
- [2] Bermel W., Bertini I., Felli I.C., Gonnelli L., Koźmiński W., Piai A., Pierattelli R., Stanek J., *J.Biomol.NMR.*, (2012), 53, 293-301
- [3] Bermel W., Bertini I., Felli I.C., Pierattelli R., *J.Am.Chem.Soc.* (2009), 131, 15339-45, Bertini I., Felli I.C., Gonnelli L., Kumar M.V.V., Pierattelli R., *ChemBioChem.* (2011), 12, 2347-52, Bertini I., Felli I.C., Gonnelli L., Kumar M.V.V., Pierattelli R., *Angew Chem Int Ed Engl.* (2011), 50, 2339-41
- [4] Bermel W., Bertini I., Chill, J., Felli I.C., Haba N., Kumar M.V.V., Pierattelli R., *ChemBioChem.* (2012), 13, 2425-2432, Bermel W., Bruix M., Felli I.C., Kumar M.V.V., Pierattelli R., Serrano S., *J. Biomol. NMR* (2013), e-pub

#### OP052: NMR-based Structural Biology in Brain Diseases

1,2\*Claudio O. Fernández

<sup>1</sup>Universidad Nacional de Rosario (UNR), Instituto de Biología Molecular y Celular de Rosario (IBR-CON, <sup>2</sup>Max

*Planck Laboratory of Structural Biology, Chemistry and Molecular Biophysics of Rosario (MPLbioR)*

The misfolding of proteins into a toxic conformation is proposed to be at the molecular foundation of a number of neurodegenerative disorders including Alzheimer and Parkinson's disease. One common and defining feature of protein misfolding diseases is the formation and deposition of amyloid-like fibrils. The aggregation of the protein  $\alpha$ -synuclein (AS) and A $\beta$  peptide are recognized as critical steps in the etiology of Parkinson and Alzheimer diseases, respectively. The study of the structural and toxic mechanisms related to amyloid formation is critical to advance in the design of a therapeutic strategy. The identification of aggregation inhibitors and the investigation of their mechanism of action are fundamental in the quest to mitigate the pathological consequences of amyloid formation. By the combined application of a battery of NMR techniques we have addressed structural and molecular unresolved details related to the mechanistic basis behind the inhibitory effects of anti-amyloid compounds

**ACKNOWLEDGEMENTS:** Financial support from ANPCyT, CONICET, Laboratorios Pfortner, Fundación Bunge y Born, Max Planck Society and Alexander von Humboldt Foundation is acknowledged.

#### UP053: Caught in Action: Selecting Peptide Aptamers Against Intrinsically Disordered Proteins in Live Cells

<sup>1</sup>Jacqueline Washington, <sup>1</sup>Sergey Reverdatto, <sup>1</sup>David Burz, <sup>2</sup>Kathleen McDonough, <sup>1\*</sup>Alexander Shekhtman

<sup>1</sup>State University of New York at Albany, Albany, NY, USA, <sup>2</sup>Wadsworth Center, NY Department of Health, Albany, NY

Intrinsically disordered proteins (IDPs) or unstructured segments within proteins play an important role in cellular physiology and pathology. The low cellular concentration, multiple binding partners, frequent posttranslational modifications and presence of multiple conformations make it difficult to characterize IDP interactions in intact cells. We propose to use a combination of peptide aptamers selected by using the yeast two hybrid scheme and in-cell NMR to identify potent binders to transiently structured IDPs and unstructured segments at atomic resolution. Since both selection and characterization of peptide aptamers take place inside the cell, only physiologically relevant conformations of IDPs are targeted. The method is demonstrated by using peptide aptamers selected against the prokaryotic ubiquitin-like protein, Pup, of the mycobacterium proteasome system. Two peptide aptamers, which bind to opposite sides of a transient helix of Pup, have vastly different effects on the survival rate of mycobacteria. This technology can be applied to study the elusive action of IDPs and unstructured segments within folded proteins under near physiological conditions.

**ACKNOWLEDGEMENTS:** This work is supported by NIH grant R01GM085006 to A.S..

#### UP054: Phosphorylation Of The Intrinsically Disordered Unique Domain Of c-Src Studied By In-Vivo Real-Time NMR

<sup>1,2</sup>Irene Amata, <sup>2</sup>Mariano Maffei, <sup>1</sup>Ana Igea, <sup>1</sup>Angel R. Nebreda, <sup>2\*</sup>Miquel Pons

<sup>1</sup>Signaling and Cell Cycle Laboratory, Institute for Research in Biomedicine, Barcelona, Spain, <sup>2</sup>Biomolecular NMR, Organic Chemistry Department, University of Barcelona, Barcelona, Spain

Complex phosphorylation and dephosphorylation patterns at multiple sites are essential for regulation of protein activity in the cytoplasm of living cells. Intrinsically disordered regions are especially rich in post-translational modification sites. NMR offers the unequalled possibility to study proteins at atomic resolution in real-time and in living cells. The Unique domain of c-Src (USrc) has several Serine and Thre-

online phosphorylation sites. We have used *Xenopus laevis* intact oocytes and oocytes and eggs extracts as a model system to study the phosphorylation of USrc. The Src family members are non-receptor protein kinases composed by three folded domains (SH3, SH2 and kinase) and the intrinsically disordered Unique domain, which links the folded core to membrane surfaces. While the folded domains show a high degree of homology within the family, the disordered region is exclusive to each member and swapping of the Unique domain between some of the family members exchange their functional roles. Previous NMR studies from our group identified structurally singular regions in the USrc; a lipid interaction region has also been discovered within USrc using NMR and biochemical assays. These evidences suggest a direct involvement of USrc in c-Src activity.

In this study, by using fast NMR techniques combined with non uniform sampling, we were able to detect and monitor in real-time the phosphorylation of the intrinsically disordered  $^{15}\text{N}$ -labeled USrc in the heterogeneous cellular environment, at 4 different sites presenting different kinetics. Moreover, the in-extract experiments are also performed in experimentally modified conditions by enriching the system of specific kinases and phosphatases inhibitors. Phosphorylation patterns identified by NMR have been compared with results from Mass Spectrometry experiments. This work represents an example of the creative potential of modern NMR to guide biological research and help to understand the essential role of intrinsically disordered domains in signaling events in Eukaryotes.

#### OP055: NMR of Intrinsically Disordered Proteins: Tools for Increasing Sensitivity and Resolution

<sup>1</sup>Zsófia Solyom, <sup>1</sup>Melanie Schwarten, <sup>1</sup>Sophie Feuerstein, <sup>2</sup>Dieter Willbold, <sup>3</sup>Michael Plevin, <sup>1\*</sup>**Bernhard Brutscher**

<sup>1</sup>*Institut de Biologie Structurale, CEA-CNRS-UJF, Grenoble, France*, <sup>2</sup>*Institute of complex systems, Structural Biochemistry, FZ Jülich, Germany*, <sup>3</sup>*Department of Biology, University of York, UK*

Intrinsically disordered proteins (IDPs) have been shown to play important roles in regulatory and signaling processes where the structural flexibility allows the protein to adapt to and interact with a large number of distinct molecular partners. NMR spectroscopy provides a unique tool to study IDPs in solution at atomic resolution. However, due to their low chemical shift dispersion, such NMR studies remain challenging. In addition, fast solvent exchange results in line broadening of amide proton resonances. Other concerns are often limited sample stability, low sample concentrations to avoid protein aggregation, and substantial peak intensity heterogeneities in the NMR spectra. Therefore, sensitive NMR pulse schemes are required to detect correlation peaks also for the sites with the lowest signal intensity; high dimensional ( $\geq 3\text{D}$ ) NMR experiments with long acquisition times in all dimensions are needed in order to resolve overlapping correlation peaks; and last but not least fast acquisition techniques are mandatory to enable multidimensional data acquisition in a reasonable amount of time. Here we show that BEST-TROSY experiments provide significant advantages in terms of experimental sensitivity and spectral resolution as demonstrated for several IDPs varying in length from about 100 to 270 residues. BEST-TROSY allows recording of high-resolution 3D spectra in only a few hours acquisition time. In addition, we present NMR tools that provide site-specific amino-acid type information (HADAMAC, iHADAMAC, isoHADAMAC, and Pro-HN experiments). These experiments are particularly helpful for sequential resonance assignment of large IDPs, as exemplified for the intrinsically disordered region of non-structural protein 5A (NS5A) of hepatitis C virus.

**Tuesday – May 21<sup>st</sup>**

**Methods for Organic Materials**

Chair: Klaus Schmidt-Rohr  
Rooms Turmalina/Topázio

#### OP056: $^{14}\text{N}$ - $^1\text{H}$ Solid-State NMR Spectroscopy of Organic Solids

**\*Steven P. Brown**

*Department of Physics, University of Warwick, UK*

$^{14}\text{N}$ - $^1\text{H}$  heteronuclear multiple-quantum correlation (HMQC) spectra obtained at high magnetic field (850 MHz) and under fast MAS (up to 60 kHz) are presented. Specifically, a modified version of the pulse sequence presented by Gan et al. [1] that utilizes rotary resonance recoupling ( $\text{R}^3$ ) at the  $n = 2$  condition ( $\nu_1 = 2\nu_R$ ) is employed to recouple the NH dipolar coupling: by using short (100  $\mu\text{s}$ ) or longer (500  $\mu\text{s}$ ) recoupling times, spectra showing one-bond NH connectivities or additionally longer-range NH proximities are obtained [2-6]. Applications to supramolecular self-assembly [2], a dipeptide [3] and pharmaceuticals [4-6] are presented, with the methodology being particularly well suited to probing nitrogen containing intra- and intermolecular hydrogen bonds. Moreover, proof for the molecular level mixing in co-crystals [5,6] and an amorphous dispersion [6] is proven via the observation of specific correlation peaks and changes in the  $^{14}\text{N}$  shift via the marked sensitivity of the isotropic second-order quadrupolar shift.

[1] Z. H. Gan, J. P. Amoureux and J. Trebosc, *Chem. Phys. Lett.* 2007, 435, 163.

[2] A. L. Webber, S. Masiero, S. Pieraccini, J. C. Burley, A. S. Tatton, D. Iuga, T. N. Pham, G. P. Spada and S. P. Brown, *J. Am. Chem. Soc.* 2011, 133, 19777.

[3] A. S. Tatton, J. P. Bradley, D. Iuga and S. P. Brown, *Z. Phys. Chem.* 2012, 226, 1187.

[4] A. S. Tatton, T. N. Pham, F. G. Vogt, D. Iuga, A. J. Edwards and S. P. Brown, *CrystEngComm* 2012, 14, 2654.

[5] K. Maruyoshi, D. Iuga, O. N. Antzutkin, A. Alhalaweh, S. P. Velaga and S. P. Brown, *Chem. Commun.* 2012, 48, 10844.

[6] A. S. Tatton, T. N. Pham, F. G. Vogt, D. Iuga, A. J. Edwards and S. P. Brown, *Mol. Pharm.* 2013, 10.1021/mp300423r

#### OP057: Separated Local Field NMR as a tool for probing molecular dynamics in organic solids

<sup>1</sup>Marcio F. Cobo, <sup>2</sup>Anja Achilles, <sup>1</sup>Gregório C. Faria, <sup>2</sup>Detlef Reichert, <sup>2</sup>Kay Saalwächter, <sup>1\*</sup>**Eduardo Ribeiro de Azevêdo**

<sup>1</sup>*Universidade de São Paulo, São Carlos-SP, Brazil*, <sup>2</sup>*Martin-Luther-University Halle Wittenberg, Halle, Germany*

Developments on  $^1\text{H}$ - $^{13}\text{C}$  separated local field experiments and their recoupled variants are discussed as tools for characterizing molecular motions in organic systems. Experimental results, spin dynamics simulations and analytical treatments based on the average hamiltonian theory and Anderson-Weiss (AW) approximation were used to demonstrate the possibility of using these experiments to extract motion parameters for each chemical site resolved in a MAS spectrum. Effects that compromise the precise quantification of the dynamical parameters, such as, homo and hetero decoupling imperfections, rotational resonance recoupling, rf inhomogeneity, etc., are also discussed together with ways of avoiding them. Furthermore, based on the  $\text{CH}_n$  dipolar pattern decomposition, a multi-gaussian approach that improves the motion description by AW treatment to  $\text{CH}_2$  and  $\text{CH}_3$  groups is proposed, so this analytical treatment can be used to obtain a more precise description of chain motions in complex materials.

The methods are demonstrated in model samples as well as in studies of molecular motions in polymer systems.

ACKNOWLEDGMENTS: FAPESP(2009/18354-8-2008/1675-0) and CAPES-DAAD PROBRAL (330-9)

#### UP058: Low-field $^1\text{H}$ -NMR investigations to reveal local properties of polymer networks

<sup>1</sup>\*Maria Ott, <sup>2</sup>Roberto Pérez-Aparicio, <sup>1</sup>Horst Schneider, <sup>2</sup>Paul Sotta, <sup>1</sup>Kay Saalwächter

<sup>1</sup>*Institut für Physik – NMR, Martin-Luther-Universität Halle-Wittenberg, Betty-Heimann-Str. 7, D-0,* <sup>2</sup>*Laboratoire Polymères et Matériaux Avancés, CNRS/Rhodia, 85 avenue des Frères Perret, F-69192 Sai*

We use solid-state  $^1\text{H}$ -NMR techniques to unravel the molecular level mechanisms of the elastic properties of polymeric networks. This unique property makes the material indispensable in widespread applications, not only in the field of material science but also in biomedical and pharmaceutical engineering.

Multiple-Quantum NMR experiments enable to reveal the absolute values and the distributions of the average inter- and intra-segmental residual dipolar couplings [1,2], which are directly related to the local forces acting at the ends of the polymer chains [3].

We investigate the local deformation of highly homogenous networks of Natural Rubber by testing the local response in respect to macroscopically applied forces and the impact of embedded nano-scaled particles. Such filler particles are well-known to lead to improved mechanical properties and we investigate their effect on the local stresses in the network matrix. We are able to proof the existence of matrix overstrain in filled rubber samples in agreement with simple hydrodynamic models and to monitor strain induced network inhomogeneities and the occurrence of highly stressed chains.

[1] K. Saalwächter, *Progr. Nucl. Magn. Reson.* 51 (2007), 1

[2] W. Chassé, J. L. Valentín, G. D. Genesky, C. Cohen, K. Saalwächter, *J. Chem. Phys.* 134 (2011), 044907

[3] J.-U. Sommer, W. Chassé, J. L. Valentín, K. Saalwächter, *Phys. Rev. E* 78 (2008), 051803

#### UP059: Efficient Heteronuclear Cross Polarization Techniques for Solid State NMR

Sheetal Kumar Jain, Morten Bjerring, \*Niels Christian Nielsen

*Aarhus University*

A new and highly efficient approach for heteronuclear coherence transfer in solid-state NMR spectroscopy under high speed spinning conditions is presented along with its adiabatic derivative. *RESPIRATION*CP[1] has been demonstrated as a very simple experiment with easier experimental set up and significantly more robustness towards imperfections such as rf inhomogeneity, misadjustments and sample induced variations. This rotor synchronized set up exploits both  $\pm 1$  or  $\pm 2$  Fourier components of the dipolar coupling with different orientation dependencies and leads to significantly higher transfer efficiencies than state-of-the-art techniques including ramped and adiabatic cross-polarization experiments with long durations of intense rf irradiation. Furthermore the efficiency of this method can be improved by combining this with an amplitude modulated adiabatic scheme. The results are described analytically, numerically and experimentally for biological solids. We demonstrate sensitivity gains of factors of 1.3 and 1.8 using *RESPIRATION*CP for typical  $^1\text{H} \rightarrow ^{15}\text{N}$  and  $^{15}\text{N} \rightarrow ^{13}\text{C}$  transfers and a combined gain of a factor of 2-4 for a typical NCA experiment for biological solid-state NMR. A comparison of these transfer efficiencies with adiabatic *RESPIRATION*CP will be presented along with its application to quadrupolar nuclei.

[1] Jain, S.; Bjerring, M.; Nielsen, N. C.: Efficient and Robust Heteronuclear Cross-Polarization for High-Speed-Spinning Biological Solid-State NMR Spectroscopy. *The Journal of Physical Chemistry Letters* 2012, 3, 703-708.

#### OP060: NMR crystallography of small molecules: from ionic solids to pharmaceuticals

\*Luís Mafra, Sérgio M. Santos

*Department of Chemistry, University of Aveiro, CICECO, Portugal*

Crystal structure determination from diffraction experiments is one of the most important and complete sources of structural information to a broad range of scientific domains, from chemistry and materials science to geology and physics. Diffraction-based experiments are, however, prone to errors, limited to certain particle sizes and depend on crystal quality. Obtaining the crystal structure solution in powders is far more complicated and using powder diffraction methods alone may lead to geometrical ambiguities and to an apparently well-refined structure with the wrong crystal packing arrangement.

Here, we address these challenges presenting a new hybrid approach for crystal structure solution of powdered solids based on the combination of solid-state NMR/solution NMR, powder XRD and an ensemble of computational-assisted structure solution tools including an genetic algorithm based on evolution-inspired operators repeatedly applied to populations of possible crystal structure solutions that evolve to eventually produce the best new "child" candidates. This algorithm also imposes space group symmetry to narrow the search space, thus forcing the possible solutions to belong to the same crystallographic space group and crystal system previously estimated from XRD powder pattern indexation and validated by the algorithm.  $^1\text{H}$  Chemical shifts are also used in the structure-refinement step as pseudo-forces acting on the models, leading to the lowest-energy structure. This methodology, which avoids the use of time-consuming *ab initio* chemical shift calculations, is successfully applied to challenging cases involving multiple component crystals composed by flexible molecules such as a trihydrate  $\beta$ -lactamic antibiotic and an alkyl-substituted imidazolium-based ionic solid.

ACKNOWLEDGEMENTS: Supported by Fundação para a Ciência e a Tecnologia (FCT) - project PTDC/QUIQUI/100998/2008, Portuguese National NMR Network (RNRMN), CICECO, FEDER, COMPETE, and University of Aveiro. SMS acknowledges FCT for his post-doc grant.

**Tuesday – May 21<sup>st</sup>**  
**MRI/In-Vivo**

Chair: Michael Garwood  
Room Ónix

#### OP061: Parallel imaging with nonlinear gradient fields

\*Gigi Galiana, Leo Tam, Dana C. Peters, R. Todd Constable

*Yale University*

Sequences that encode the spatial information of an object using nonlinear gradient fields are a new frontier in MRI, with potential to provide lower peripheral nerve stimulation, windowed fields of view, spatially-varying resolution, curved slices that mirror physiology, and, most importantly, highly undersampled parallel imaging. O-Space imaging, a method that acquires projections along ring-shaped isocontours centered at different locations in the field of view, has been shown to produce good reconstructions from dramatically undersampled multichannel datasets. The ring-shaped isocontours of the O-Space sequence appear to better complement the az-

imutual spatial encoding provided by typical receiver arrays. However, the details of this complementarity have been more difficult to specify.

We present a simple and intuitive framework that describes image encoding with nonlinear gradients in the language of k-space. Focusing on O-Space imaging, we show how the datapoints relate to k-space, the role of coil encoding, and how the gradient trajectory can be used to predict image quality, as is often done for Fourier encoded images. Parallels between the O-Space strategy and that of compressed sensing will also be discussed. Experimental results, in phantoms, *in vivo*, and with a human head insert, demonstrate high quality reconstruction of highly undersampled datasets.

We also show how the framework described above can be used to design trajectories that address clinical practicalities, such as multiecho acquisition. The analysis suggests that multiecho O-Space should employ a modified acquisition order and timing offsets to smooth  $T_2$  weighting across the dataset. Combined with filtering strategies in the reconstruction, we are able to minimize artifacts while still retaining relaxation contrast in a turbo spin echo type acquisition.

#### OP062: Relaxivity Optimized Metal Based MRI Molecular Imaging Agents

\*Carlos F.G.C. Geraldès

Department of Life Sciences, Center of Neurosciences and Cell Biology and Coimbra Chemistry Center, University of Coimbra

The superb spatial resolution of Magnetic Resonance Imaging (MRI) has made it a fundamental clinical diagnostic tool. However, its relatively low sensitivity may limit its use in Molecular Imaging. High relaxivity and specificity of targeted MRI contrast agents (CAs) are currently the most important objectives in the development of such diagnostic imaging tools. The design and relaxivity optimization procedures of  $Gd^{3+}$ -chelates as CAs will be discussed using a few examples. The effect of various molecular parameters of the  $Gd^{3+}$ -chelates on the  $r_1$  relaxivity optimization, such as the inner-sphere water exchange rate and the rotational correlation dynamics, will be illustrated [1,2]. The *in vivo* evaluation of the  $T_1$ -contrast effect of some of these systems by DCE-MRI in Wistar rats will be illustrated [2].

The use of nanosized platforms is an effective way to enhance the efficacy of such contrast agents, by increasing the number of imaging agents reaching the target ("cargo effect"). Several types of nanoparticles (NPs) have been explored for this objective. Among the inorganic ones, gold NPs decorated with relaxivity optimized  $Gd^{3+}$ -chelates [1] originate high  $r_1$  relaxivities in the MRI imaging frequency range due to the slow rotational dynamics of the NPs and the concentration of many chelates at the NP surface [3]. Other inorganic NPs, with high  $r_2$  relaxivities, originate high negative contrast in  $T_{2w}$  MRI images, especially at high magnetic fields. Examples of this are core-shell  $\gamma-Fe_2O_3@SiO_2$  NPs [4]. Nature inspired platforms, such as yeast-cell wall NPs (YCWP), are very efficient carriers of multimodal imaging probes which can be exploited as positive MRI contrast agents for *in vitro* cell labelling and *in vivo* cell tracking applications [5,6].

ACKNOWLEDGEMENTS: Financial support from FCT (Portugal) and EU COST TD1004 Actions is acknowledged.

#### REFERENCES

- [1] Ferreira, M.F.; Martins, A.F.; Martins, J.A.; Ferreira, P.M.; Tóth, É.; Geraldès, C.F.G.C. Chem. Commun. 2009, 6475-6477.
- [2] Ferreira, M.F.; Martins, A.F.; Martins, C.I.O.; Tóth, É.; Rodrigues, T.B.; Calle, D.; Cerdán, S.; López-Larrubia, P.; Martins, J.A.; Geraldès, C.F.G.C. Contrast Media Mol. Imaging, 2013, 8, 40-49.

- [3] Ferreira, M.F.; Mousavi, B.; Ferreira, P.M.; Martins, C.I.O.; Helm, L.; Martins, J.A.; Geraldès, C.F.G.C., Dalton Trans., 2012, 41, 5472 – 5475.

- [4] Pinho, S.L.C.; Laurent, S.; Rocha, J.; Roch, A.; Delville, M.-H.; Carlos, L.D.; Elst, L.V.; Muller, R.N.; Geraldès, C.F.G.C., J. Phys. Chem. C, 2012, 116, 2285-2291.

- [5] Figueiredo, S.; Moreira, J.N.; Geraldès, C.F.G.C.; Rizzitelli, S.; Aime, S.; Terreno, E.; Chem. Comm., 2011, 47, 10635-10637.

- [6] Figueiredo, S.; Cutrin, J.C.; Rizzitelli, S.; De Luca, E.; Moreira, J.N.; Geraldès, C.F.G.C.; Aime, S.; Terreno, E. Molecular Imaging and Biology, in press.

#### UP063: Magnetic Resonance Microimaging of a Swelling Gel

<sup>1</sup>Wilson Barros Jr., <sup>1</sup>Eduardo N. de Azevedo, <sup>2\*</sup>Mario Engelsberg

<sup>1</sup>Universidade Federal de Pernambuco, Recife,

<sup>2</sup>Universidade Federal de Pernambuco, Caruaru

The formation of contour patterns in the heterogeneous growth of layered structures is of considerable interest for understanding the morphogenesis of many structures, including living organisms. We study the time evolution of surface pattern formation in a swelling spherical gel using magnetic resonance microimaging of water molecules migrating into the gel[1]. Relaxation-weighted images permit to map the local evolution of the swelling ratio, which can be identified with the determinant of the deformation gradient tensor. The breaking of spherical symmetry caused by the growth of an instability produces a surface undulation whose wavelength depends upon the width of the region between the surface and the unswollen core of the gel[1, 2]. By controlling the degree of cross linking within a thin surface layer of the gel it is possible to monitor the transition from an undulating folding pattern to the formation of singular creases.

The swelling kinetics is examined with special emphasis on the time evolution of the solvent distribution. We compare our microimaging experimental results with the predictions of a nonlinear poroelastic theory[3] by numerically solving the nonlinear equations of evolution within a spherically symmetric approximation.

- [1] W. Barros Jr., E. N. de Azevedo, and M. Engelsberg, Soft Matter, 2012, 8, 8511.

- [2] J. Dervaux, Y. Couder, M. A. Guedau-Boudeville, and M. Ben Amar, Phys. Rev. Lett., 2011, 107, 0181103.

- [3] W. Hong, X. Zhao, J. Zhou, and Z. Suo, J. Mech. Phys. Solids, 2008, 56, 1779.

ACKNOWLEDGMENTS: CNPQ, FACEPE

#### UP064: Early Detection of Pancreatic Cancers & Brain Tumors by Active-Feedback Controlled MR

<sup>1</sup>Zhao Li, <sup>2</sup>Chaohsiung Hsu, <sup>2</sup>Lian-Pin Hwang, <sup>1\*</sup>Yung-Ya Lin

<sup>1</sup>Department of Chemistry and Biochemistry, UCLA,

<sup>2</sup>Department of Chemistry, National Taiwan University

**Introduction:** Early detection of high-grade malignancy, such as pancreatic cancers (PC) and glioblastoma multiforme (GBM), using enhanced MRI techniques significantly increases not only the treatment options available, but also the patients' survival rate. For this purpose, a conceptually new approach, termed "Active-Feedback Controlled MR", was developed. An active feedback electronic device was homebuilt to implement active-feedback pulse sequences to generate avalanching spin amplification, which enhances the weak magnetic-field perturbations from magnetic nanoparticles in targeted PC or malignant physiological conditions in GBM.

**Theory and Methods:** The general principles of the "Active-Feedback Controlled MR" can be found in our publications [1-4] (and references therein). Here, its specific applications to early tumor detection were developed and demonstrated. (i) First, an active-feedback electronic device was home-built to generate feedback fields from the received FID current. The device is to filter, phase shift, and amplify the signal from the receiver coils and then retransmit the modified signal into the RF transmission coil, with adjustable and programmable feedback phases and gains. The MR console computer can execute the active-feedback pulse sequences to control the trigger signal, feedback phase/gain, and the duration of the feedback fields, allowing us to utilize the active feedback fields in novel ways. (ii) Next, an active-feedback pulse sequence was developed for early tumor detection and was statistically tested on *in vivo* mice tumor models. In essence, the enhanced tumor contrast arises from "selective self-excitation" and "fixed-point dynamics" generated by the bulk water  $^1\text{H}$  under active feedback fields. Use the sensitive detection of magnetic nanoparticles as an example. A small flip-angle ( $\alpha=5-10^\circ$ ) RF pulse tilts the sample equilibrium magnetization. Since the averaged transverse magnetization is mainly contributed from the bulk water  $^1\text{H}$  spins, the resulting active feedback field possesses a frequency closer to that of the bulk water  $^1\text{H}$  spins which are distant from the dipole center. By "selective self-excitation", the feedback field tilts the bulk water  $^1\text{H}$  spins more effectively towards the stable fixed-point,  $-z$ -axis (assume feedback phase  $180^\circ$ ), while the  $^1\text{H}$  spins near the dipole center are less affected due to resonance mismatch. This "selective self-excitation" process continues and enlarges the contrast between the longitudinal magnetization of the  $^1\text{H}$  spins in bulk water and those near the dipole center. Maximum contrast in the longitudinal magnetization can be achieved and locked when all spin magnetizations evolve to the fixed point: all align along  $-z$  in this case.

**Results (1):** Early Detection of Pancreatic Cancers: Anti-CA 19-9 antibodies were conjugated to NH<sub>2</sub>-PEG-coated magnetic nanoparticles. The antigen binding capacity to CA 19-9 over-expressing cell lines (BxPC3) was confirmed by *in vitro* MR cellular images. *In vivo* images of human pancreatic tumors from nude mouse xenografts show that, while T2-weighted image cannot clearly locate the magnetic nanoparticles, the active-feedback images successfully highlight the magnetic nanoparticles distribution with a close correlation with iron-stained histopathology.

**Results (2):** Early Detection of Glioblastoma Multiforme: Stage-1 orthotopic GBM mouse models infected with human U87 cell line were imaged. While both T2 parameter images and T2-weighted images by spin echo successfully locate the GBM tumor, our active-feedback images and decay constant mapping provide 4-5 times of improvements in GBM tumor contrast through sensitively imaging the susceptibility variations due to irregular water contents and deoxyhemoglobin.

**Discussion and Conclusion:** *In vivo* PC and GBM mouse models validated the superior contrast/sensitivity and robustness of the "Active-Feedback MR" for early tumor detection. Statistical results ( $N>10$ ) for PC and GBM mouse models at various cancer stages, alternative active feedback pulse sequences with further improved performance, and active feedback pulse sequences for enhanced R1/R2-weighted images will also be presented.

Reference:

[1] Science 290, 118 (2001) [2] Magn. Reson. Med. 56, 776 (2006) [3] Magn. Reson. Med. 61, 925 (2009) [4] J. Phys. Chem. B 110, 22071 (2006)

**OP065: Detecting Tumor Treatment Response using Metabolic Imaging with hyperpolarized  $^{13}\text{C}$ -labeled Cell Substrates**

\*Kevin M. Brindle, Mikko I. Kettunen, **Tiago B. Rodrigues**, Eva M. Serrao, Brett W.C. Kennedy, De-en Hu

Department of Biochemistry and CRUK Cambridge Institute, University of Cambridge, UK

Patients with similar tumor types can have markedly different responses to the same therapy. The development of new treatments would benefit, therefore, from the introduction of imaging methods that allow an early assessment of treatment response in individual patients, allowing rapid selection of the most effective treatment.

We have been developing methods for detecting the early responses of tumors to therapy, including magnetic resonance (MR) imaging of tumor cell metabolism using hyperpolarized  $^{13}\text{C}$ -labeled cellular metabolites. We have shown that exchange of hyperpolarized  $^{13}\text{C}$  label between lactate and pyruvate can be imaged in animal models of lymphoma and glioma and that this flux is decreased post-treatment. We showed that hyperpolarized [1,4- $^{13}\text{C}$ ]fumarate can be used to detect tumor cell necrosis post treatment in lymphoma and that both the polarized pyruvate and fumarate experiments can detect early evidence of treatment response in a breast tumor model and also early responses to anti-vascular and anti-angiogenic drugs. Fumarate can also be used to detect necrosis in other tissues, such as the kidney. We have shown that tissue pH can be imaged from the ratio of the signal intensities of hyperpolarized  $\text{H}^{13}\text{CO}_3^-$  and  $^{13}\text{CO}_2$  following intravenous injection of hyperpolarized  $\text{H}^{13}\text{CO}_3^-$  and that tumor redox state can be determined by monitoring the oxidation and reduction of [1- $^{13}\text{C}$ ]ascorbate and [1- $^{13}\text{C}$ ]dehydroascorbate respectively. Recently we have shown that we can monitor tumor glycolysis by measuring the conversion of hyperpolarized [U- $^2\text{H}$ , U- $^{13}\text{C}$ ]glucose to lactate. Labeled lactate production was higher in the tumor than in surrounding normal tissue and was markedly decreased at 24 h after treatment with a chemotherapeutic drug.

**Tuesday – May 21<sup>st</sup>**

**Plenary Session**

Chair: José Figueroa-Villar  
Room Gávea A

**PL066: Recent contributions for Zero-, Low-, and High-field NMR**

**\*Tito J. Bonagamba**

Instituto de Física de São Carlos - Universidade de São Paulo, São Carlos, Brazil

Recently our group decided moving to some specific applications of zero-, low-, and high-field NMR, not only because they could drive us to rich physical problems, but also because we could transfer to them methods applied for high-resolution NMR.

**In the case of zero-field NMR**, employed to study magnetic materials, using only two arbitrary rf pulses, we obtained multiple-quantum (MQ) echoes, which were used to construct the spectra. To understand the data observed, we proposed a method for selecting each MQ echo based on phase-cycling and time-averaging, and a model in which there are two regions along the sample with different inhomogeneous spectral line broadenings. These methods offered complementary physical information about the nuclear spin interactions and the properties of the magnetic materials.

**In the case of low-field NMR**, used to study porous media, we are going to discuss new procedures to perform 1D and 2D  $\text{T}_2 \times \text{T}_2$  exchange experiments, which allow observing only the migrating fluid molecules. *In the 2D method*, which employs two CPMG  $\text{T}_2$  encoding stages separated by a  $z$ -store mixing time, the signals from the molecules that do not migrate are subtracted from the raw NMR data, after processing the 2D Inverse Laplace Transform. This procedure eliminates the intense diagonal ridge, providing an accurate study of the migrating molecules. *In the 1D method*, instead of varying the number of  $\pi$  pulses at the first CPMG stage, it is kept fixed and small enough to act as a short  $\text{T}_2$ -filter.



Thus, varying the mixing time in a wide range provides a set of 1D  $T_2$  distributions, which shows simultaneously the effects of both exchange and full  $T_1$  relaxation.

Finally, **in the case high-field NMR**, we are going to present some NMR tools developed for quantum information studies.

ACKNOWLEDGEMENTS: IFSC, USP, FAPESP, CNPq, and CAPES.

#### OP067: Magnetic resonance studies of topological materials

\***Louis Bouchard**

*UCLA*

In recent years the emergence of gapless topologically protected edge states in the solid state has led to searches for new phases of condensed matter in new and existing materials. The protected edge states in topological insulators are due to the combination of spin-orbit coupling and time-reversal invariance. Examples of exotic phenomena include the quantum anomalous Hall effect, fractional quantum anomalous Hall effect, fractional time-reversal invariance, topological Kondo insulator, topological crystalline insulator and the topological magneto-electric effect. The observation of topological phases requires tools which can probe nanoscale electronic and magnetic phenomena at the surface of the material, or at some interface located deep inside the material. Radioactive ion beam spectroscopy uses low energy ions implanted at specific depths in the material to report on the local properties. I shall discuss ongoing experiments at TRIUMF whereby spin-polarized muon and lithium ion beams have emerged as useful depth-resolved reporters of physical properties in topological materials and heterostructures involving topological insulators. New results from conventional solid state NMR studies will also be discussed.

#### OP068: Hyperpolarized Molecular Sensing and Detection

<sup>1,2</sup>\***Vikram S. Bajaj**

<sup>1</sup>*Department of Chemistry and California Institute of Quantitative Biosciences, University of California, Berkeley,*  
<sup>2</sup>*Materials Sciences Division, Lawrence Berkeley National Laboratory*

I will survey our efforts to develop and employ magnetic resonance contrast agents for molecular recognition that use hyperpolarized xenon as a reporting medium. These agents are based on molecular or supramolecular guest-host complexes that bind xenon in reversible exchange, the prototypical examples being the cryptophanes. Because bound xenon is spectroscopically distinct from xenon in the bulk, we are able to exploit chemical exchange saturation transfer (CEST) for additional signal amplification. Further, we have increased the sensitivity and biocompatibility of these cryptophane-based sensors by covalently attaching them in many copies to macromolecular scaffolds, among them the capsids of bacteriophage and MS2. Next, we have developed new, non-cryptophane supramolecular agents, useful both as sensors and reporters of chemical processes in vivo and in vitro. For chemical sensing in portable devices, we are developing combinatorial methods to produce sensors targeted to specific small molecule analytes. These sensors will be used in platforms that contain microfabricated analogues of high field NMR instrumentation including xenon gas polarizers and optical NMR detectors.

#### PL069: Structures and mechanisms of viral ion channels and fusion peptides from solid-state NMR

\***Mei Hong**

*Iowa State University*

I will present on-going studies of the structure, dynamics and mechanism of action of two viral membrane proteins, the pro-

ton channel formed by the M2 protein of the influenza virus, and the fusion peptide and transmembrane (TM) domain of the paramyxovirus, parainfluenza virus 5 (PIV5). MAS NMR yields a rich panel of structural and dynamic information that give insight into the proton-conduction mechanism of M2 and the basis of membrane curvature generation by the fusion peptide. Distance measurements, exchange spectroscopy and  $^1\text{H}$  chemical shifts revealed the proton exchange kinetics and hydrogen-bonding of the proton-selective histidine in M2. The distances between the histidine and the gating tryptophan indicate cation- $\pi$  interactions at low pH, which shed light on the low proton flux of this channel. Mutation of Ser31 to Asn in the M2 TM domain causes drug resistance and affects proton conductivity. Our measurement of the conformation and proton-exchange dynamics of the S31N mutant in the apo state and when bound to a novel drug sheds light on the mutant properties. Outside the TM domain, the M2 cytoplasmic tail is important for virus assembly and budding. We have investigated the structure of the cytoplasmic domain using 2D and 3D NMR, spectral editing, and computational modeling. Similar curvature generation is the key function of viral fusion peptides such as the PIV5 fusion peptide, which merge the lipid membranes of the virus and the target cell. Our studies of the conformation and lipid-interaction of the PIV5 fusion peptide indicate that the peptide structure depends sensitively on the membrane composition. We suggest a correlation between the FP conformations and various stages of membrane fusion.

ACKNOWLEDGEMENTS: NIH grants GM088204 and GM066976

#### Wednesday – May 22<sup>nd</sup> Amyloids

Chair: Ana Paula Valente  
Room Gávea A

#### OP070: Amyloid aggregates and large soluble protein complexes

<sup>1,2,3</sup>Sam Asami, <sup>1,2,3</sup>Juan-Miguel Lopez del Amo, <sup>1,2,3</sup>Andi Mainz, <sup>1,2,3</sup>Muralidhar Dasari, <sup>3</sup>Uwe Fink, <sup>4</sup>Marcus Fändrich, <sup>5</sup>Erich E. Wanker, <sup>5</sup>Jan Bieschke, <sup>6</sup>Tomasz Religa, <sup>6</sup>Lewis E. Kay, <sup>1,2,3</sup>\***Bernd Reif**

<sup>1</sup>*Technische Universität München (TUM), Department Chemie,* <sup>2</sup>*Helmholtz-Zentrum München (HMGU),* <sup>3</sup>*Leibniz-Institut für Molekulare Pharmakologie (FMP),* <sup>4</sup>*Max-Delbrück Centrum für Molekulare Medizin (MDC),* <sup>5</sup>*Max-Planck-Forschungsstelle für Enzymologie der Proteinfaltung, Martin-Luther Universität Halle-Wittenberg,* <sup>6</sup>*University of Toronto, Department of Medical Genetics and Microbiology*

Perdeuteration and back-substitution of exchangeable protons in microcrystalline proteins in combination with recrystallization from  $\text{D}_2\text{O}$  containing buffers reduces  $^1\text{H}$ ,  $^1\text{H}$  dipolar interactions such that amide proton line widths on the order of 20 Hz are obtained (Chevelkov et al., 2006). Aliphatic protons are either accessible via specifically protonated precursors or by using low amounts of  $\text{H}_2\text{O}$  in the bacterial growth medium (Asami et al., 2010). This labeling scheme is applied to amyloid aggregates like fibrils formed by the Alzheimer's disease  $\beta$ -amyloid peptide ( $\text{A}\beta$ ) (Linser et al., 2011). We present data on solid-state NMR studies of drug induced  $\text{A}\beta$  aggregates focussing in particular on the interactions between  $\text{A}\beta$  and the polyphenolic green tea compound epigallocatechin-gallate (EGCG). We show that MAS solid-state NMR techniques are applicable for the structural characterization of large soluble protein complexes (Mainz et al., 2009), in case the tumbling correlation time exceeds the rotor period. Experimental results are presented for the small heat shock protein  $\alpha\text{B}$  crystallin (600 kDa) as well as for the 20S proteasome core particle in complex with its 11S activator (1.1 MDa).

References

[1] Asami S, Schmieder P & Reif B (2010) High resolution  $^1\text{H}$ -detected solid-state NMR spectroscopy of protein aliphatic resonances: Access to tertiary structure information. *J Am Chem Soc* 132: 15133–15135.

Chevelkov V, Rehbein K, Diehl A & Reif B (2006) Ultra-high resolution in proton solid-state NMR at high levels of deuteration. *Angew Chem Int Ed* 45: 3878–3881.

[2] Linser R, Dasari M, Hiller M, Higman V, Fink U, Lopez del Amo J-M, Handel L, Kessler B, Schmieder P, Oesterhelt D, Oschkinat H & Reif B (2011) Proton detected solid-state NMR of fibrillar and membrane proteins. *Angew Chem Int Ed* 50: 4508–4512.

[3] Mainz A, Jehle S, van Rossum BJ, Oschkinat H, Reif, B. (2009). Large Protein Complexes with Extreme Rotational Correlation Times Investigated in Solution by Magic-Angle-Spinning NMR Spectroscopy. *J Am Chem Soc* 131, 15968–15969.

#### OP071: Amyloid Fibrils: Towards a Molecular Level Picture with Solid-State Nuclear

\*P. K. Madhu

*Tata Institute of Fundamental Research*

$\text{A}\beta$  peptides are interesting models for investigating different aspects of amyloid aggregation. On the basis of amyloid cascade hypothesis, which has dominated amyloid disease research for the past two decades, the main therapeutic strategies have aimed either to prevent the aggregation of  $\text{A}\beta$ , or to remove toxic oligomeric and fibrillar species of  $\text{A}\beta$ . Since  $\text{A}\beta$  is ordinarily produced in the brain, and there is no proof that  $\text{A}\beta$  overproduction underlies sporadic AD, the pursuit of former strategy demands a thorough understanding of all the neurochemical factors that initiate  $\text{A}\beta$  deposition in brain. One such factor is the presence of metal ions, especially  $\text{Zn}^{2+}$ .  $\text{Zn}^{2+}$  plays important roles in normal physiology of brain and is also considered to be a major neurochemical factor associated with  $\text{A}\beta$  aggregation and AD. Observations like high  $\text{Zn}^{2+}$  concentrations in senile plaques found in the brains of Alzheimer's patients and evidences emphasising the role of  $\text{Zn}^{2+}$  in  $\text{A}\beta$ -induced toxicity have triggered interest in understanding the nature of  $\text{Zn}^{2+}$ - $\text{A}\beta$  interaction. Of the two strategies mentioned earlier, the later generally involves usage of external agents/drugs which can make  $\text{A}\beta$  follow such aggregation pathways which yield non-pathological species of  $\text{A}\beta$ . In this regard, curcumin, a small phenolic compound and a common Asian spice, has been found to ameliorate the effects of  $\text{A}\beta$  induced neuro-degeneration in AD models. A structural understanding of how curcumin interacts with  $\text{A}\beta$  can provide a significant impetus to such efforts, and we are exploring this aspect with SSNMR spectroscopy. In this work, we have studied both the properties and the molecular structure of both  $\text{A}\beta_{40}$  and  $\text{A}\beta_{42}$  aggregates co-incubated with curcumin. We will present here key results from both of these studies.

#### UP072: Metallobiology of neurodegenerative diseases: Structural and mechanistic basis behind the acceleration of amyloid protein assembly

<sup>1,2</sup>M.C. Miotto, <sup>1,2</sup>A.A. Valiente Gabioud, <sup>3</sup>Andres Binolfi, <sup>4</sup>L. Quintanar, <sup>5</sup>Christian Griesinger, <sup>1,2\*</sup>Claudio O. Fernández

<sup>1</sup>*Instituto de Biología Molecular y Celular de Rosario (IBR-CONICET)*, *Universidad Nacional de Rosario*, <sup>2</sup>*Max Planck Laboratory of Structural Biology, Chemistry and Molecular Biophysics of Rosario (MPLPbioR)*, <sup>3</sup>*Department of NMR-assisted Structural Biology, In-cell NMR, Leibniz Institute of Molecular Pharmacology*, <sup>4</sup>*Centro de Investigación y de Estudios Avanzados (Cinvestav)*, <sup>5</sup>*Department of NMR-based Structural Biology, Max Planck Institute for Biophysical Chemistry*

Alpha-synuclein (AS) aggregation is associated to neurodegeneration in Parkinson's disease (PD). At the same time,

alterations in metal ion homeostasis may play a pivotal role in the progression of AS amyloid assembly and the onset of PD. Elucidation of the structural basis directing AS-metal interactions and their effect on AS aggregation constitutes a key step towards understanding the role of metal ions in AS amyloid formation and neurodegeneration. The structural properties of the AS-metal complexes were determined by the combined application of nuclear magnetic resonance (NMR) and electron paramagnetic resonance (EPR), circular dichroism (CD) spectroscopy, and matrix-assisted laser desorption/ionization mass spectrometry (MALDI MS). This work provides a comprehensive view of recent advances attained in the metallobiology of AS amyloid diseases. A hierarchy in AS-metal ion interactions has been established: while divalent metal ions interact at a non-specific, low-affinity binding interface at the C-terminus of AS, copper binds with high affinity at the N-terminal region and it is the most effective metal ion in accelerating AS filament assembly.[1-4] The strong link between metal binding specificity and its impact on aggregation is discussed here on a mechanistic basis. A detailed description of the structural features and coordination environments of copper to AS is presented and discussed in the context of oxidative cellular events that might lead to the development of PD. These new findings of the structural and metallobiology of PD are discussed via a comparative analysis with the binding and affinity features of metal ions to the beta amyloid peptide of Alzheimer's disease.[5] Overall, the research findings presented here support the notion that perturbations in the metabolism of metal ions may be a common upstream event in the pathogenesis of neurodegenerative processes.[6]

#### References

- [1] Rasia et al, *Proc. Natl. Acad. Sci. U S A*, 2005, 102, 4294-4299.
- [2] Bertoncini et al, *Proc Natl Acad Sci U S A*, 2005, 102: 1430-1435.
- [3] Binolfi et al, *J. Am. Chem. Soc.*, 2008, 130, 11801-11812.
- [4] Binolfi et al, *J. Am. Chem. Soc.*, 2011, 133, 194-196.
- [5] Valiente-Gabioud et al, *J. Inorg Biochem.*, 2012, 117:334-341.
- [6] Binolfi et al, *Coord. Chem Rev.*, 2012, 256:2188-2201.

#### Acknowledgements

Financial support from ANPCyT, CONICET, Laboratorios Pförtner, Fundación Bunge y Born, Max Planck Society and Alexander von Humboldt Foundation is acknowledged.

#### OP073: Structural studies of an engineered mimic of neurotoxic amyloid- $\beta$ protofibrils

<sup>1</sup>Christofer Lendel, <sup>2</sup>Morten Bjerring, <sup>3</sup>Andrei Filippov, <sup>3,4</sup>Oleg N. Antzutkin, <sup>2</sup>Niels Christian Nielsen, <sup>1\*</sup>Torleif Hård

<sup>1</sup>*Dept. of Molecular Biology, Swedish University of Agricultural Sciences (SLU), Uppsala, Sweden.*, <sup>2</sup>*Dept. of Chemistry, Aarhus University, Aarhus, Denmark.*, <sup>3</sup>*Chemistry of Interfaces, Luleå University of Technology, Luleå, Sweden.*, <sup>4</sup>*Dept. of Physics, Warwick University, Coventry, United Kingdom.*

Structural and biochemical studies of the aggregation of the 42-residue amyloid- $\beta$  peptide ( $\text{A}\beta_{42}$ ) are important to understand the mechanisms of Alzheimer's disease, but research is complicated by aggregate inhomogeneity and instability. We previously engineered a hairpin form of  $\text{A}\beta$ , called  $\text{A}\beta_{\text{cc}}$ , which forms stable protofibrils that do not convert into amyloid fibrils [1]. A large number of biochemical and biophysical experiments indicate that the morphology and structure of  $\text{A}\beta_{42\text{cc}}$  protofibrils are very similar to those of wild type  $\text{A}\beta_{42}$  aggregates. Like  $\text{A}\beta_{42}$  aggregates,  $\text{A}\beta_{42\text{cc}}$  protofibrils also induce apoptosis in neuroblastoma cell lines and attenuate spontaneous synaptic activity.  $\text{A}\beta_{42\text{cc}}$  protofibrils are

therefore a good mimic for wild-type A $\beta$ <sub>42</sub> protofibrils. The molecular structure of A $\beta$ <sub>42cc</sub> protofibrils is studied using solid-state NMR spectroscopy as part of the effort to understand the molecular basis for protofibril neurotoxicity. The <sup>13</sup>C NMR spectrum of A $\beta$ <sub>42cc</sub> is partially well resolved with resonance line widths of less than 1.5 ppm and resonances of residues 16-17 and the C-terminal fragment 31-41 have been assigned. NMR chemical shifts and intramolecular <sup>13</sup>C-<sup>13</sup>C correlations indicate a  $\beta$ -strand containing hairpin structure of the C-terminal of A $\beta$ <sub>42cc</sub> protomers in the fibril. Inter-molecular <sup>13</sup>C-<sup>13</sup>C and <sup>13</sup>C-<sup>15</sup>N correlations then suggest that protomers in the protofibril are packed by interacting C-termini. These data allow us to construct models of the packing of A $\beta$ <sub>42cc</sub> protomers within protofibrils.

[1] A. Sandberg et al. (2010) Stabilization of neurotoxic Alzheimer amyloid- $\beta$  oligomers by protein engineering. *Proc Natl Acad Sci USA* 107, 15595-15600.

**Wednesday – May 22<sup>nd</sup>**  
**Dynamics and Recognition**

Chair: Rodolfo Rasia  
 Room Gávea B

**OP074: Probing Protein Conformational Flexibility with Pulsed EPR Spectroscopy**

Xi Huang, I.M.S. de Vera, Manuel Britto, Mandy E. Blackburn, Angelo M. Veloro, Jamie L. Kear, \*Gail E Fanucci  
*University of Florida*

HIV-1 Protease (HIV-1 PR) is an essential enzyme for generating infectious HIV virus particles and is a target in the fight against HIV infection. Current therapeutic inhibitors, which are designed against HIV-1 PR subtype B found in North America and Europe, are less potent inhibitors against other subtypes. Thus, understanding how the polymorphisms alter protein structure, flexibility and interaction with PIs may provide insights for optimizing drug candidate against highly variable targets.

Results from pulsed EPR studies reveal that drug pressure selected mutations and natural polymorphisms alter the HIV-1 PR conformation ensemble. We are currently assessing correlations among the fractional occupancy of the conformational ensemble of nominally four different conformational states with enzyme activity and drug resistance. Additionally recent NMR relaxation results show that the natural polymorphisms also modify the protein backbone dynamics.

We are also investigating how specific single and double natural polymorphisms induce altered flap conformation sampling as seen in other subtypes, which may impact divergent pathways of drug resistance. An examination and comparison of deposited X-ray structures of HIV-1PR variants implies that altered salt-bridge formation of select substitutions may account for pulsed EPR results of CRF\_01\_A/E, which consistently reveal a novel flap conformer that is more curled compare to subtype B. This curled conformation is observed in many of our pulsed EPR distance profiles, but has not been observed in MD simulations of subtype B. We believe the altered salt bridge provides a structural basis for the EPR observations.

**OP075: NMR Spectroscopy reveals alternative Ground States in Copper Proteins**

\*Alejandro J. Vila, Luciano A. Abriata, Andrés Espinoza-Cara, Marcos N. Morgada, María-Eugenia Zaballa

*Institute for Molecular and Celular Biology (IBR), University of Rosario, Argentina*

NMR of oxidized copper proteins has been hampered by the unfavorable electron relaxation times of the Cu<sup>2+</sup> ion which induce fast relaxation rates in nearby nuclei, rendering them undetectable. However, this limitation applies only to T2 copper sites, while T1, T3 and CuA centers are amenable

to NMR studies due to the availability of low-lying excited electronic states. These features are strongly related to the physiological requirements of these copper centers to perform efficient electron transfer or oxidation chemistry.

The binuclear copper sites CuA and T3 display particularly fast electron relaxation rates which are due to low-lying excited states that can be populated at room temperature and contribute to the reactivity of the metal site. Other magnetic techniques, such as EPR, ENDOR and MCD, normally recorded at cryogenic temperatures, are able to monitor exclusively the ground state. NMR in solution, instead can shed light on the availability of these invisible electronic states. We have carried on detailed studies in the CuA site, involved in long range electron transfer in terminal oxidases.

NMR discloses the fact that the CuA site can exist in two alternate ground states with different orbital symmetry, which are invisible to other techniques. We show that thermal fluctuations may populate two alternative ground-state electronic wave functions optimized for electron entry and exit, respectively, through two different and nearly perpendicular pathways. These findings suggest a unique role for alternative or "invisible" electronic ground states in directional electron transfer. Moreover, we show that this energy gap and, therefore, the equilibrium between ground states can be fine-tuned by minor perturbations, suggesting alternative ways through which protein-protein interactions and membrane potential may optimize and regulate electron-proton energy transduction.

References:

- [1] Abriata et al., *J.Am.Chem.Soc.*, 131, 1939–1946 (2009).
- [2] Zaballa et al., *J.Am.Chem.Soc.*, 132, 11191–11196 (2010).
- [3] K. Lancaster et al., *J.Am.Chem.Soc.*, 134, 8241-53 (2012).
- [4] M.E.Zaballa et al., *Proc.Natl.Acad.Sci USA*, 109, 9254-9 (2012).
- [5] L.A.Abriata et al., *Proc.Natl.Acad.Sci USA*, 109, 17348-53 (2012).

**UP076: NMR Studies of the Loop Dynamics of the Nitrophorins**

\*F. Ann Walker, Dhanasekaran Muthu, Robert E. Berry, Hongjun Zhang

*The University of Arizona*

The nitrophorins (NP) are 8-stranded  $\beta$ -barrel ferriheme proteins (lipocalin fold) from the saliva of the blood-sucking bug, *Rhodnius prolixus*, which bind and sequester NO in the insect salivary gland for up to a month, and release it into the tissues and capillaries of a victim, when found. Lipocalins are generally known to be fairly rigid proteins, yet the ligands they sequester are able to bind and to be released at biologically relevant rates. There are two pairs of NPs with high sequence identity, NP1 and NP4 (90%) and NP2 and NP3 (79%); the overall sequence identity is 39%. All four proteins release NO slowly at the low pH of the salivary glands ( $k_{off} = 0.02-0.03$  s<sup>-1</sup> at pH 5.0, but NP1 and NP4 release NO much more rapidly at the higher pH of human tissues (7.3-7.4) ( $k_{off} = 1.1$  and 1.6 s<sup>-1</sup>, respectively), while NP2 shows a much smaller increase in release rate ( $k_{off} = 0.093$  s<sup>-1</sup>), and NP3 behaves similarly. The dynamics of the A-B and G-H loops of these proteins are believed to be responsible for the differences in the two pairs of proteins, yet the G-H loops are identical in length for all four (7 residues), while the A-B loops of NP1,4 are one amino acid longer than those of NP2,3 (11 vs. 10 residues). We are investigating the picosecond to nanosecond and microsecond to millisecond dynamics of these proteins by NMR techniques. Analysis of the chemical shifts of A-B loop residues of NP2 at pH 5.0 suggests that the A-B loop is partially helical (and closed), while the loop has an extended structure at pH 7.3. Dynamic motions of individual A-B loop residues at pH 7.3 are much greater than at pH 6.5 or 5.0, but in no case are the motions correlated.

Little dynamics are seen for the G-H loop at any pH, and there appears to be no pH-dependent change in that loop's conformation. Thus the behavior of the A-B loop is of most interest as we investigate NP2 in the NO-off form (high-spin Fe(III)) and compare these results to those for NP4.

**ACKNOWLEDGEMENTS:** The support of the U. S. National Institutes of Health grant HL054826 is gratefully acknowledged.

#### **OP077: EPR Method Development for Addressing Protein Structure and Dynamics**

<sup>1</sup>\*Gunnar Jeschke, <sup>1</sup>Yevhen Polyhach, <sup>1</sup>Tona von Hagens, <sup>2</sup>Carsten Dietz, <sup>2</sup>Harald Paulsen

<sup>1</sup>ETH Zurich, <sup>2</sup>University of Mainz

Distance distribution measurements in the nanometer range by pulsed EPR techniques have recently become popular in structural biology, mainly for their applicability to proteins of any size in almost any environment. Furthermore, access to distance distribution rather than only mean distances provides valuable additional information on disordered parts of a structure. Due to the matching of the accessible distance range between about 2 and 8 nm with typical protein dimensions coarse information on structure and structural changes can be obtained from a small number of measured distances. This contribution assesses the potential and limitations of such methodology on the example of the major light harvesting complex LHCII of green plants. In particular, we discuss site-resolved information folding of the protein and self-assembly of the complex with chromophores and structural information on the disordered part of the N-terminal domain. By combining the enhanced sensitivity of our high-power Q-band setup with a double-tag LHCII purification strategy developed by our collaboration partners in Mainz our groups have been able to measure distance distributions in a single protomer of the LHCII trimer. Finally, we address artifacts in distance distributions that may arise from the presence of more than two spin labels in a nanoobject, a situation that is commonly encountered for protein oligomers. We show that simple power scaling of time-domain data can reveal and suppress such artifacts. **ACKNOWLEDGEMENTS:** We thank Christoph Dockter and Andre Mueller (University of Mainz, Germany) for providing further samples of LHCII, Alexander Volkov (MPI for Polymer Research Mainz) for further measurements, Adelheid Godt and Muhammad Sajid (Bielefeld University) for providing model compounds, and Enrica Bordignon and Rene Tschaggelar for contributions to the high-power Q-band setup.

**Wednesday – May 22<sup>nd</sup>**  
**Workshop: NMR on Porous Media**

Chair: Vinicius Machado  
Rooms Turmalina/Topázio

#### **OP078: Improved Estimation of Oil and Gas Reserves Using Magnetic Resonance Imaging “MRI” Technology - Applications and Case Histories**

\*Maged Fam

HALLIBURTON, Bogota, Colombia

With the continuing increase in demand for oil and gas as a vital component of the world's supply of energy, it is important to be able to account for every small quantity of reserve through accurate determination of net pay hydrocarbon volume for each well drilled. The initial estimates of hydrocarbon quantity in a reservoir are usually established through formation evaluation using conventional wireline or LWD logs. Those conventional logs, such as resistivity, density, neutron, and sonic, are traditionally used to estimate important reservoir parameters such as porosity, permeability, water saturation and net hydrocarbon volume (or net pay). Sometimes, however, the use of such conventional logs may provide a high degree of uncertainty in the estimation of

net pay as a result of the high complexities in the rock and fluids properties. Such uncertainty in the net pay estimates can cause huge errors in calculating the oil and gas reserves of a reservoir.

This presentation will discuss the effectiveness of applying the MRI logging technology in measuring and estimating critical petrophysical parameters which helps in better characterizing the oil and gas reservoirs and provide improved net pay hydrocarbon volume and better reserves estimates. It also demonstrates the value of using the MRI technology in determining fluid types, including distinguishing between bound water and free water, as well as differentiating between gas and liquid hydrocarbon and even detecting differences between heavy and light oil. This article also illustrates the latest interpretation techniques and applications of the MRI technology in the oil and gas industry.

#### **OP079: Transport and Reaction in Porous Media: New Information Obtained Using Compressed Sensing and Bayesian Methods**

\*Lynn F. Gladden, D. J. Holland, Mick D. Mantle, J. Mitchell, Andrew J. Sederman, A. B. Taylor

University of Cambridge, Department of Chemical Engineering and Biotechnology

Understanding transport processes in porous media, with and without simultaneous reaction, is central to many areas of the process industries, the pharmaceutical industry and, of course, oil recovery. This presentation will give an overview of the opportunities offered by implementation of compressed sensing and Bayesian magnetic resonance (MR) techniques, with illustrations taken from the fields of gas-liquid flows in porous media (i.e., catalytic reactors), gas-liquid bubbly flows, and the structural characterisation of porous media. Both compressed sensing and Bayesian methods exploit our ability to undersample the data acquisition but still recover the information of interest. This opens up opportunities for acquiring data at much higher spatial and temporal resolutions. It follows that new measurements may now also be implemented on low magnetic field hardware.

A first example shows how compressed sensing MR acquisitions have been implemented to enable gas and liquid velocity maps of the gas-liquid flow fields within packings of particles, such that both flow fields are acquired at the same spatial resolution. These data provide new information which can be incorporated into numerical flow simulation codes used to predict reactor behavior. A second example uses a Bayesian MR methodology to size gas bubbles in gas-liquid bubbly flows. This approach is sensitive to changes in bubble shape and can measure bubble sizes at high gas voidages where optical techniques cannot be used. Compressed sensing combined with spiral imaging has also been used to image 3D vector flow fields, with an acquisition time of 16 ms, capturing essentially 'real time' images of the flow field around bubbles as they rise within stagnant water.

Finally, we demonstrate two low field measurements which employ the Bayesian approach: the sizing of spherical particles using an Earth's Field NMR apparatus, and the determination of grain sizes in rocks at 1T.

**ACKNOWLEDGEMENTS:** EPSRC, ExxonMobil, Johnson Matthey, Microsoft Research Connections

#### **UP080: Pore Sizes Distribution of Unconsolidated Geomaterials**

2,3\*Marcos Montoro, <sup>1,3</sup>Lucas C. Cerioni, <sup>3</sup>Daniel José Pusiol

<sup>1</sup>Spinlock SRL, <sup>2</sup>Universidad Nacional de Córdoba, <sup>3</sup>CONICET

Pore size and pore sizes distribution of soils and rocks control many hydraulic and mechanical properties of natural geomaterials such as hydraulic conductivity and shear resistance.

Pore size and sizes distribution of rocks depend on their mineral composition and the geological processes involved in their formation, while for unconsolidated materials such as soils, depend on grain sizes, grain sizes distribution and overburden pressure. The aim of this project is to correlate transversal relaxation time ( $T_2$ ) with grain size of loose sandy soils in systems of single and double porosity. In this research we applied Time Domain Nuclear Magnetic Resonance (TD-NMR) to measure the magnetization decaying curve of samples composed of selected sizes of sand grains, poor graded sands, silty sands, silt and clay. This was performed by a CPMG pulse sequence using a low field (12 MHz) spectrometer (SLK-100). Obtained results show that transversal relaxation time and its distribution are strongly correlated with grain sizes and their distribution. These results allow improving the knowledge about pore sizes distribution when needed for modeling porous materials using numerical techniques such as pore networks.

ACKNOWLEDGEMENTS: CONICET, SECyT-UNC, FONTAR, FONCYT

#### OP081: Diffusion dynamics in porous media

\*Yi-Qiao Song

Schlumberger

Porous media is known to greatly affect the behavior of NMR properties of the fluids inside. Interactions between the solid surface and the spins have been the key source of enhanced spin relaxation inside the porous media. Diffusion of a molecule is also known to be affected compared either due to interaction with other molecules or the surrounding solid structures. Both effects have been explored to study the porous structure in order to understand the fluid flow. These effects are in general determine the average surface-to-volume ratio (SVR) of porous materials.

In addition to reduced diffusion constant, the diffusion propagator can be significantly different from bulk diffusion such as its Gaussian form. This behavior is reflected in diffusion behavior (such as kurtosis) as well as relaxation. For example, slow diffusion could cause multiple relaxation peaks in NMR relaxation spectrum for a single pore size. However, in real porous materials, pore size distribution also results in multiple or broad relaxation times. As a result, it is often difficult to differentiate the intrinsic complex diffusion behavior from the presence of pore size distributions.

We have studied several two-dimensional NMR methods in order to distinguish the presence of complex diffusion and the pore size distributions. For example, we have found unique features in the  $T_1$ - $T_2$  correlation experiment that unambiguously identify the slow diffusion behavior irrespective of the pore sizes. Also we design a 3-pulse-gradient echo (a version of the Double-Pulsed-Field-Gradient) experiment that could quantify the non-Gaussian diffusion behavior (such as kurtosis). Using analytical and numerical solutions of the diffusion dynamics and numerical simulation we have demonstrated these effects and found them consistent with experimental results. These new methods allow the investigation of porous media to extend beyond the language of average SVR.

Wednesday – May 22<sup>nd</sup>  
Small Molecules and Methods

Chair: Jochen Junker  
Room Ònix

#### OP082: Structure Determination Using Anisotropic NMR Parameters

\*Burkhard Luy

Karlsruhe Institute of Technology

Anisotropic NMR parameters like residual dipolar couplings (RDCs), residual quadrupolar couplings (RQCs), and residual chemical shift anisotropies (RCSAs) are very powerful

structural parameters that allow the conformational, configurational, and constitutional analysis of small molecules [1]. If chiral alignment media are used, even the distinction of enantiomers is possible with the approach.

Novel technical developments, like the introduction of useful alignment media, imaging of alignment, useful pulse sequences, and methods for data interpretation will be presented. A special focus will be the identification of meso compounds compared to a racemic mixture of corresponding enantiomers, that cannot be distinguished by optical means.

[1] for a review see e.g.: G. Kummerl we, B. Luy, *Annu. Rep. NMR Spectrosc.* 68, 193-232 (2009).

#### OP083: New NMR strategies for the accurate measurement of small heteronuclear coupling constants

\*Teodor Parella

Servei de Resson ncia Magn tica Nuclear, Universitat Aut noma de Barcelona, Catalonia

Several pulse schemes will be presented for the measurement of heteronuclear coupling constants in small molecules. Important aspects such as the simplicity and the accuracy of the measurement, its general applicability, the extraction of multiple information in a single NMR experiment or the simultaneous determination of the J sign will be discussed. It will be shown how three different J-editing methods (IPAP, E.COSY and J-resolved) can be implemented in a single NMR experiment to provide spin-state-edited 2D cross-peaks from which simultaneous measurement of different homonuclear and heteronuclear coupling constants can be performed. In addition, the interference of homonuclear J(HH) evolution and its effect on distorted cross-peaks will be evaluated in broadband versions of the HMBC-IPAP and HSQMBC-IPAP experiments. Examples on the application of the proposed methods to other heteronuclei will be also provided.

ACKNOWLEDGEMENTS: Financial support for this research provided by MICINN (project CTQ2009-08328) is gratefully acknowledged. We also thank to the Servei de Resson ncia Magn tica Nuclear, Universitat Aut noma de Barcelona, for allocating instrument time to this project.

#### UP084: Experimental measurement and theoretical assessment of fast lanthanide electronic relaxation in solution with four series of isostructural complexes

<sup>1</sup>Alexander M. Funk, <sup>1\*</sup>David Parker, <sup>1</sup>Peter Harvey,  
<sup>1</sup>Alan M. Kenwright, <sup>2</sup>Pascal H. Fries

<sup>1</sup>Durham University, <sup>2</sup>CEA, Grenoble

The rates of longitudinal relaxation for ligand nuclei in four isostructural series of lanthanide(III) complexes have been measured by solution-state NMR at 295 K at five magnetic fields in the range 4.7 to 16.5 T. The electronic relaxation time  $T_{1e}$  is a function of both the lanthanide ion and the local ligand field. It needs to be considered when devising relaxation probes for magnetic resonance applications since it affects the nuclear relaxation, especially over the field range 0.5 to 4.7 T. Analysis of the data, based on Bloch-Redfield-Wangsness theory describing the paramagnetic enhancement of the nuclear relaxation rate, has allowed reliable estimates of electronic relaxation times,  $T_{1e}$ , to be obtained using iterative minimization methods. Values were found in the range 0.10 to 0.63 ps, consistent with fluctuations in the transient ligand field induced by solvent collision. A refined theoretical model for lanthanide electronic relaxation beyond the Redfield approximation is introduced, that accounts for the magnitude of the ligand field coefficients of order 2, 4, and 6 and their relative contributions to the rate  $1/T_{1e}$ . Despite the considerable variation of these contributions with the nature of the lanthanide ion and its fluctuating ligand field, the theory explains the modest change of measured  $T_{1e}$  values and their remarkable statistical ordering across the lanthanide series. Both experiment and theory indicate that complexes

of terbium and dysprosium should most efficiently promote paramagnetic enhancement of the rate of nuclear relaxation.

#### References:

- [1] Funk, A. M.; Fries, P. H.; Harvey, P.; Kenwright, A. M.; Parker, D., *J. Phys. Chem. A*, 2013. accepted
- [2] Walton, J. W.; Carr, R.; Evans, N. H.; Funk, A. M.; Kenwright, A. M.; Parker, D.; Yufit, D. S.; Botta, M.; De Pinto, S.; Wong, K. L., *Inorg. Chem.* 2012, 51 (15), 8042.
- [3] Harvey, P.; Kuprov, I.; Parker, D., *Eur. J. Inorg. Chem.* 2012, 12, 2015-2022.

#### OP085: Structural Analysis of Small Organic Molecules Assisted by Residual Dipolar Couplings

\*Roberto R. Gil

*Carnegie Mellon University*

The 2D structure of most small molecules can be in principle straightforwardly determined by manual or automatic analysis of a set of experimental data that includes the molecular formula, a series of 1D and 2D NMR experiments providing through-bond connectivity (COSY, TOCSY, HSQC, HMBC and ADEQUATE/INADEQUATE based experiments), and chemical shift predictions. This is the main concept embedded in automatic structure elucidation programs. Once the 2D structure is available, the determination of the relative spatial arrangement (configuration and preferred conformation) of all atoms in the molecule is a more challenging task that it is commonly addressed in NMR by using NOE and  $^3J$  coupling constants analysis, as well as recent developments on the application of DFT calculation of  $^{13}\text{C}$  chemical shifts. However, it is difficult to assess how many samples are sitting on the laboratory's refrigerators waiting for an independent methodology that could lift some of the ambiguities generated by the use of conventional NMR methods. The development of the application of Residual Dipolar Couplings (RDCs) to the configurational and conformational analysis of small molecules has matured enough in the recent years to perform this task is an almost straightforward way, without even the need of using NOE and  $^3J$  coupling analysis, as it will be presented here for the analysis of rigid and semi-rigid small molecules. Most of the results presented here use Poly(methylmethacrylate) (PMMA) based flexible gels, whose degree of alignment can be easily tuned by variable and reversible compression. The application of RDCs to the analysis of flexible molecules is still a field of research plenty of room for development and a generally accepted approach is not available yet.

#### Wednesday – May 22<sup>nd</sup> Challenging Systems

Chair: Roberto Salinas  
Room Gávea A

#### OP086: Protein Dynamics: Its Kinetics and Implications for Function

<sup>1</sup>David Ban, <sup>1,2</sup>Colin Smith, <sup>1</sup>Michael Sabo, <sup>3</sup>R. Bryn Fenwick, <sup>1</sup>Korvin F. A. Walter, <sup>1</sup>Claudia Schwiégk, <sup>1</sup>Stefan Becker, <sup>3</sup>Xavier Salvatella, <sup>1</sup>Berend L. de Groot, <sup>1</sup>Donghan Lee, <sup>1</sup>\*Christian Griesinger

<sup>1</sup>Max Planck Institute for Biophysical Chemistry - NMR based Structural Biology, <sup>2</sup>Max Planck Institute for Biophysical Chemistry - Theoretical and computational biophysics, <sup>3</sup>ICREA and Institute for Research in Biomedicine Barcelona

The possibility to explore dynamics of proteins specifically ubiquitin which promiscuously recognizes many binding partners will be presented based on the accurate measurement of anisotropic parameters such as residual dipolar couplings [1]. This approach allows to characterize at unprecedented detail the ground state ensemble of the protein [2]. Rates of in-

terconversion between ensemble members have been measured by low temperature relaxation dispersion, dielectric relaxation [3] and temperature jump SAXS and compared to MD results [4]. In addition correlated motion [5] across  $\beta$ -strands is characterized by novel optimized cross correlated relaxation experiments. Further, with high-power relaxation dispersion measurements [6] it is possible to characterize motion kinetically to one digit ms time scales. With these measurements motion on the time scale of 10 ms at 35°C is detected uniformly in the backbone (detected on the amides) and side chains (detected on methyl groups) of ubiquitin. The amplitude of the relaxation dispersion can be reproduced assuming a backbone conformation dependent variance in the population of the side chain rotamers. Since the backbone conformational changes occur on the 10 ms time scale, also the side chain rotamer redistribution occurs on this time scale. Finally, progress made towards the fitting of the four state recognition model of Dsk2-UBA with ubiquitin will be discussed.

ACKNOWLEDGEMENTS: Max Planck Society, ERC grant agreement number 233227

- [1] Peti, W., Meiler, J., Brüschweiler, R. and Griesinger, C. (2002) Model free Analysis of Protein Backbone Motion from Residual Dipolar Couplings. *J. Am. Chem. Soc.* 124, 5822-5833
- [2] Lange, O., Lakomek, N. A., Farès, C., Schröder, G., Becker, S., Meiler, J., Grubmüller, H., Griesinger, C., de Groot, B.: Recognition dynamics up to microseconds revealed from an RDC-derived ubiquitin ensemble in solution. *Science*, 2008, 320, 1471-1475
- [3] Ban, D., M.F. Funk, R. Gulich, D. Egger, T. M. Sabo, K.F.A. Walter, R. B. Fenwick, K. Giller, F. Pichierri, B.L. de Groot, O. F. Lange, H. Grubmüller, X. Salvatella, M. Wolf, A. Loidl, R. Kree, S. Becker, N.-A. Lakomek, D. Lee, P. Lunkenheimer, C. Griesinger: Kinetics of Conformational Sampling in Ubiquitin. *Angew. Chem. Int. Ed.* 50, 11437-11440 (2011)
- [4] Shaw, David E.; Maragakis, Paul; Lindorff-Larsen, Kresten; Piana, Stefano; Dror, Ron O.; Eastwood, Michael P.; Bank, Joseph A.; Jumper, John M.; Salmon, John K.; Shan, Yibing; Wriggers, Willy. Atomic-Level Characterization of the Structural Dynamics of Proteins. *Science* 330, 341-346 (2010)
- [5] Fenwick, R.B., Esteban-Martin, S., Richter, B., Lee, D., Walter, K.F.A., Milovanovic, D. Becker, S., Lakomek, N.A., Griesinger, C., Salvatella, X.: Weak Long-Range Correlated Motions in a Surface Patch of Ubiquitin Involved in Molecular Recognition. *Journal of the American Chemical Society* 133, 10336-10339 (2011)
- [6] Ban, David, A. D. Gossert, K. Giller, S. Becker, C. Griesinger and D. Lee: Exceeding the limit of dynamics studies on biomolecules using high spin-lock field strengths with a cryogenically cooled probehead. *Journal of Magnetic Resonance*, 221, 1- 4 (2012)

#### OP087: Distance measurements in biomolecules using $Gd^{3+}$ spin labels

\*Daniella Goldfarb

*Weizmann Institute of Science, Rehovot, Israel*

Methods for measuring nanometer scale distances between specific sites in biomolecules (proteins and nucleic acids) and their complexes are essential for analysis of their structure and function. In the last decade pulse EPR techniques, mainly pulse double-electron-electron resonance (DEER), has been shown to be a very effective for measuring distances between two spin labels attached to a biomolecule. DEER is routine for distances up to 5 nm and with some extra effort and favorable conditions distances as high as 8 nm can be accessed. So far such measurements have been applied mostly to biomolecules labeled with nitroxide stable radicals. Re-

cently we have introduced a new family of spin labels that are based on  $Gd^{3+}$  chelates attached to proteins using site directed spin labeling, similar to the common method of labeling proteins with nitroxide spin labels.  $Gd^{3+}$  spin labels are particularly attractive for high field DEER measurements such as W-band (95 GHz, 3.5 T). The benefits such  $S=7/2$  spin labels in combination with high field offer are the high sensitivity that reduces the amount of the biomolecule needed by more than an order of magnitude and the lack of orientation selection that allows straight forward data analysis. Here we will present  $Gd^{3+}$ -  $Gd^{3+}$  distance measurements in models compounds and their applications to study transmembrane peptides in model membranes. The chemical and spin physics requirement for the ultimate  $Gd^{3+}$  label will be discussed.

**UP088: Detection of light induced intermediates of photoreceptor membrane proteins by in-situ photo-irradiated solid-state NMR**

<sup>1</sup>\*Akira Naito, <sup>1</sup>Yuya Tomonaga, <sup>1</sup>Tetsuro Hidaka, <sup>1</sup>Hiroki Yomoda, <sup>1</sup>Teruki Makino, <sup>1</sup>Izuru Kawamura, <sup>2</sup>Yuki Sudo, <sup>3</sup>Akimori Wada, <sup>3</sup>Takashi Okitsu, <sup>4</sup>Naoki Kamo

<sup>1</sup>Yokohama National University, <sup>2</sup>Nagoya University, <sup>3</sup>Kobe Pharmaceutical University, <sup>4</sup>Matsuyama University

Photoreceptor retinal proteins usually absorb photon to generate photo-isomerization, and consequently change the structure and dynamics of proteins. To generate retinal isomerization, we have developed the photo-irradiation system equipped to the solid-state NMR spectrometer [1].

Pharaonis phoborhodopsin (ppR or sensory rhodopsin II) is a negative phototaxis receptor of *Natronomonas pharaonis* and forms a 2:2 complex with the cognate transducer (pHtrII), which transmits the photosignal into cytoplasm. Light absorption of ppR initiates *trans-cis* photo-isomerization of the retinal chromophore followed by cyclic chemical reaction consisting of several intermediates (K, L, M and O). The M intermediate is thought to be an active state for signal transduction.

We have successfully trapped and observed the M intermediate by using newly developed photo-irradiated solid-state NMR system. <sup>13</sup>C NMR signal from [20-<sup>13</sup>C] retinal-ppR and ppR/pHtrII revealed that multiple M-intermediates (M1, M2 and M3) with 13-*cis*, 15-*anti* retinal configurations coexisted under the continuously photo-irradiated condition [1]. Further, since the life time of M1 state was much longer than those of the other M states, this M1 state could be distinguished from the other M states and assigned as N intermediate.

SrSRI (Salinibacter ruber sensory rhodopsin I) is a eubacterium rhodopsin and acting multiple function as attractant and repellent phototaxis. In the photocycle of SrSRI, M intermediate functions as attractant and P intermediate by absorbing second blue light as a double photon process shows as repelment. <sup>13</sup>C NMR signal of M intermediate in SrSRI was successfully trapped by illuminating 520 nm light, and the configuration of retinal was revealed to be 13-*cis*, 15-*anti*. P intermediate was trapped by illuminating second 365 nm light as a double photon process.

Photo-intermediate in photo-receptor membrane proteins is now possible to trap by using in-situ photo-irradiated solid-state NMR.

[1] Y. Tomonaga et al. Biophys. J. 2011, 101, L50-L52.

**UP089: High resolution conformational description of Alpha-synuclein inside neurons using mammalian In-cell NMR**

Andres Binolfi, Beata Bekei, Francois-Xavier Theillet, Honor M. Rose, \*Philipp Selenko

Leibniz Institut für Molekulare Pharmakologie (FMP-Berlin)

The intrinsically disordered protein alpha-synuclein (AS)

has been involved in the onset of Parkinson's disease (PD) through the conversion of its native monomeric state into beta-sheet rich amyloid fibrils in dopaminergic neurons [1]. So far, most of the structural studies aimed to understand this conversion were conducted on isolated protein samples, under conditions that differ substantially from the crowded *in vivo* environments of intact cells. The question remains whether the features observed for AS *in vitro* correlate with its cellular behaviour. Until recently, there were no means of looking into live cells with high enough resolution to address such important unresolved issues. The development of In-cell NMR spectroscopy techniques changed this notion [2]. Here, we present high-resolution In-cell NMR data on the structural and dynamic properties of AS in five different mammalian cell lines that also include dopaminergic neurons of the *Substantia nigra*. By using a novel approach to efficiently deliver isotopically enriched protein samples into the cytosol of cultured mammalian cells we were able to record highly reproducible In-cell heteronuclear NMR spectra. Moreover, residue specific dynamic information from relaxation experiments was obtained. By directly comparing these in-cell NMR results with AS data from different *in vitro* environments mimicking intracellular viscosity and macromolecular crowding, we are in the process of delineating physical and biological contributions to AS's different *in vivo* behaviours. Results emerging from this work contribute to the understanding of the native conformations of AS and lays the ground to further perform high-resolution *in situ* investigations under conditions that lead to intracellular aggregation and neurodegeneration as observed in Parkinson's disease.

[1] Lashuel, H. A. et al (2012) Nat. Rev. Neurosci. 14, 38-48

[2] Ito, Y., and Selenko, P. (2010) Curr. Opin. Struct. Biol. 20, 640-648.

**OP090: NMR studies of the structure and dynamics of protein-RNA interactions in gene regulation**

<sup>1,2</sup>\*Michael Sattler

<sup>1</sup>Institute of Structural Biology, Helmholtz Zentrum München, Germany, <sup>2</sup>Munich Center for Integrated Protein Science and Biomolecular NMR, Department Chemie, TUM, Germany

We are studying the structures, dynamics and molecular interactions of multi-domain proteins and protein complexes involved in the regulation of splicing, and the modulation of these interactions by posttranslational modifications. Early steps during the assembly of the spliceosome involve the binding of SF1 and the U2AF heterodimer to the 3' region of the pre-mRNA. We have recently shown that recognition of the poly-pyrimidine-tract RNA at the 3' splice site involves a conformational shifts between closed and open arrangements of the tandem RRM domains of U2AF65 (Mackereth *et al*, Nature 2011) Currently, we are exploring the potential contributions of conformational selection and induced fit mechanisms for these interactions. We also investigate the role of tandem serine phosphorylation for the molecular interactions of SF1 and U2AF and present structural analysis of the SF1-U2AF65 complex.

For these studies we employ an efficient protocol for determining the quaternary structure of multi-domain proteins and complexes in solution by combining experimental data derived from solution state NMR as well as Small Angle X-ray and/or Neutron Scattering (SAXS/SANS) experiments. Starting from available structures of individual domains or complex subunits, chemical shift perturbations and NOEs are used to define domain interfaces. Overall domain arrangements are defined by long-range distance restraints obtained from paramagnetic relaxation enhancements (PRE) using spin-labeled proteins and/or RNA or solvent PREs. Small Angle Scattering data provide complementary information to validate the NMR derived structures and provide complementary information about the overall shapes

**Wednesday – May 22<sup>nd</sup>**  
**Metabolomics and Chemometrics**

 Chair: Ana Gil  
 Room Gávea B

**OP091: Deciphering Cancer Metabolism for Drug Discovery**

\*Ulrich L. Günther, Christian Ludwig, Katarzyna Koczula, Farhat Khanim, Chris Bunce

*University of Birmingham, UK*

Metabolomics has gained significant ground in Biomedicine, including the field of cancer research. This is in part because metabolomics observes a phenotypical end point, reflecting small changes in various pathways linked to metabolism. Applications range from typical diagnostics to drug discovery. While the potential diagnostic value is increasingly accepted, the use of metabolomics for understanding the mechanisms of drug actions has been realized only more recently. Such developments are very closely linked to the fact that the aspect of altered metabolism in cancer has been rediscovered. Although known since Otto Warburg's research in the 1920s, metabolism has been neglected for a long time.

Now we find altered metabolism in different places of metabolic processing, and we learn how metabolism is affected by drugs. This has been studied in AML and CML (acute and chronic myeloid leukemia) cells, where we observe unforeseen changes in metabolism following a new drug combination. A pronounced metabolic effect arises from the generation of high levels of reactive oxygen species, which chemically modify several metabolites.

For this metabolic analysis we combined metabolomics with isotopic tracer based metabolic flux analysis, using <sup>13</sup>C-labelled metabolic precursors. In this context NMR has a significant advantage as it can observe site-specific label incorporation, revealing unforeseen effects, in particular in Krebs' cycle metabolites.

**OP092: Food NMR applied to typical Brazilian food products**

\*Antonio Gilberto Ferreira

*Federal University of São Carlos - Chemistry Department*

Brazil is undoubtedly one of the major producers and exporters of primary products such as iron ore, soybeans, coffee, concentrated orange juice and in less extent exotic products such as sugar cane spirit, honey and fruit pulp.

With the purpose to have better knowledge of the chemical constitution in different matrix, NMR was used to identify/characterize the majority chemical compounds and also to draw a chemical profile considering variety, seasonality and regionality in different products analyzed using chemometrics tools. The technique SNIF- NMR (*Site Specific Natural Isotopic Fractionation studied by Nuclear Magnetic Resonance*) has also been used to quantify the <sup>1</sup>H/<sup>2</sup>H isotopic relation.

**Orange Juice** – Although Brazil is the largest exporter of concentrated orange juice, domestically this form of drink is not consumed on a large scale being preferred fresh squish orange juice. With the objective to evaluate the products degradations, five different species/varieties of orange were studied considering the effect of temperature and storage time. Using 1D and 2D NMR spectra was possible to characterize the compounds responsible for the juice modification.

**Honey** – Brazil is not a major honey producer when compared to other countries but there is a way to fake the product sold in local shops which is difficult to detect. It is possible to feeding bees with syrups of different origins. Using honey of *Apis mellifera* collected from orange, eucalyptus, sugar cane plantations and wild trees, in São Paulo state, it was possible to distinguish four types of honey using <sup>1</sup>H NMR and SNIF-NMR.

**Sugar cane spirit** – The most consumed beverage in Brazil after beer is sugar cane spirit, which is produced from the sugar cane juice fermentation. On the other hands there are other spirit products also from sugars fermentation (grape, honey, banana and apple) which have higher values in the market. Using <sup>1</sup>H NMR, SNIF-NMR and chemometrics it was possible to discriminate the five types of spirits sold in Brazil.

ACKNOWLEDGEMENTS: FAPESP, CAPES, FINEP and CNPq

**UP093: Visualizing metabolic system catalyzed by microbial ecosystem using statistical correlation analysis**
<sup>1,2,3,4\*</sup>Jun Kikuchi

<sup>1</sup>RIKEN Plant Science Center, <sup>2</sup>Biomass Engineering Program, RIKEN, <sup>3</sup>Nagoya University, <sup>4</sup>Yokohama City University

Within the field of metabonomics, measurement of system responses over time is usually important to obtain a picture of metabolic dynamics after or during the application of some input to an environment, such as foods in animal guts, because the variations in each metabolite have intrinsic behaviors. We have previously developed an approach that applies metabonomics to monitor metabolic dynamics in microbial-animal, as well as microbial-microbial interactions in the gut system [1-3]. In addition to this, the composition of the gut microbiome is highly variable, and its diversity can be significantly affected by alterations in diet. Here firstly, we report an approach to evaluate the intestinal variation and to predict metabolic pathways of major microbial symbionts affected by the variation of plant polysaccharide intakes. The covariance of structural variation in gut microbiome and host metabolism was visualized based on the correlation with the denaturing gradient gel electrophoresis (DGGE) profiles and the urine/feces NMR profiles [4]. Thus, time-dependent variations and timed responses should be considered and applied in the development of a visualization method when evaluating and characterizing metabolic dynamics in microbial ecosystems. Similar approach can be applied for not only in the gut system, but also in industrial process, such as changes in metabolic dynamics of methane fermentation sludge upon different polysaccharide addition [5]. Our approach provides a foundation for evaluation of systemic effects of inputting nutrients that are of relevance to both health and green innovation for opening up a new window that will clear up metabolic dynamics in the complex microbial communities from the gut to industrial process environments.

**References**

1. Fukuda et al., Nature 469, 543-547 (2011).
2. Fukuda et al., Nature (revised).
3. Nakanish et al., J. Proteome Res. 10, 824-831 (2011).
4. Date, Y. et al., PLoS ONE (submitted).
5. Date, Y. et al., J. Proteome Res. 11, 5602-5610 (2012).

**UP094: The Use of Magnetic Resonance in Pollution Assessment: Theory and Applications**

\*Oliver A.H. Jones

*RMIT University*

Nuclear Magnetic Resonance (NMR) has great potential for use in the both the measurement of toxicants and the assessment of their effects on biological organisms, including humans. In this presentation we discuss the reasons why NMR is useful for this type of research and present a number of applications which use NMR based metabolomics (a newly emerging field of research concerned with the comprehensive characterization of the small molecule metabolites in biological systems) to study the effects of both organic and inorganic pollutants on a range of terrestrial and aquatic species. We



also introduce community metabolomics - the use of the study of biochemical profiles of whole microbial communities living in contaminated soils from various sites with very different physicochemical characteristics (levels of metal contamination, underlying geology and soil type) using NMR. While some of these site differences may also have been caused by additional abiotic factors (such as soil type or pH), pattern recognition analysis of the data showed that both site- and contaminant- specific effects on the metabolic profiles could be discerned and individual sites could be resolved on the basis of their individual metabolic profiles. This is the first time whole microbial communities from environmental samples have been studied as opposed to lab cultures of single isolates. The work is of importance since the identification of biomarkers indicative of a defined response to a pollutant, or pollutants, before major outward changes become apparent, could potentially have applications in a range of a number of areas including soil chemistry, contaminated land assessment and re-mediation, the water industry, agriculture and ecology.

#### OP095: Rapid-dissolution $^{13}\text{C}$ DNP in kinetics of cellular transmembrane exchange

<sup>1</sup>\*Philip W. Kuchel, <sup>2</sup>Guilhem Pagès, <sup>1</sup>Max Puckeridge

<sup>1</sup>University of Sydney, <sup>2</sup>Singapore Bioimaging Consortium

Rapid-dissolution dynamic nuclear polarization (RD-DNP) with  $^{13}\text{C}$  NMR decreases the time in which metabolic events can be studied with  $^{13}\text{C}$ -labelled metabolites[1,2,3]. Emphasis has been given to enzyme catalyzed reactions in pathological states of cells, and in a small number of clinical trials for the detection of neoplasms. The range of rapid biochemical reactions that are amenable to study by RD-DNP is limited. New NMR-receptive isotopes are being sought, as are *in vivo* probe molecules carrying hyperpolarizable nuclei. However, an area unexplored by RD-DNP is membrane transport of solutes. Some solutes undergo transmembrane exchange on the 1-second time scale and potential experimental and clinical perturbations of the rates are "legion". Some molecules yield  $^{13}\text{C}$  NMR chemical shifts that differ inside and outside cells, thus affording an NMR-based means of measuring their transmembrane exchange. One such molecule is  $^{13}\text{C}$ -urea. We studied the kinetics of its exchange in human erythrocytes. *Mathematica* was used to describe the exchange and NMR-relaxation kinetics.

#### References:

- [1] J.H. Ardenkjær-Larsen, B. Fridlund, A. Gram, G. Hansson, L. Hansson, M.H. Lerche, R. Servin, M. Thaning, K. Golman, (2003) *Proc. Nat. Acad. Sci.*, 100, 10158-10163.
- [2] M. R. Clatworthy, M. I. Kettunen, D.-E. Hu, R. J. Mathews, T. H. Witney, B. W. C. Kennedy, S. E. Bohndiek, F. A. Gallagher, L. B. Jarvis, K. G. C. Smith, and K. M. Brindle (2012) *Proc. Nat. Acad. Sci.*, 109 (2012) 13374-13379.
- [3] M. C. D. Tayler, I. Marco-Rius, M. I. Kettunen, K. M. Brindle, M. H. Levitt, and G. Pileio (2012) *J. Am. Chem. Soc.* 134, 7668-7671.
- [4] M. Puckeridge, G. Pagès, P. W. Kuchel (2012) *J. Magn. Reson.* 222, 68-73.

**Wednesday – May 22<sup>nd</sup>**  
**Workshop: NMR on Porous Media**

Chair: Vinicius Machado  
 Rooms Turmalina/Topázio

#### OP096: Earth's-field Surface NMR for Groundwater Characterization

<sup>1,2</sup>\*Elliot Grunewald, <sup>2</sup>Rosemary Knight, <sup>1</sup>David Walsh, <sup>2</sup>Denys Grombacher, <sup>2</sup>Jan O. Walbrecker, <sup>2</sup>Katherine Dlubac

<sup>1</sup>Vista Clara, Inc., <sup>2</sup>Stanford University

Geophysical surface NMR measurements utilize Earth's  $B_0$

field and large  $B_1$  surface loops to obtain non-invasive measurements of groundwater. This technology shares many commonalities with other NMR techniques in porous media, including the valuable potential to determine critical flow and storage parameters. There are also certain unique aspects of the measurement configuration and shallow Earth environment that pose distinct challenges requiring innovative solutions. Two challenges that have been the focus of research and progress in recent years are obtaining accurate resolution of subsurface relaxation times and estimating permeability. Resolving relaxation times in surface NMR is complicated by the fact that  $B_1$  is grossly inhomogeneous within the resonant volume and pulses are relatively long. Previous approaches have preferred simple single-pulse FID measurement schemes, with variable pulse amplitudes, to resolve water content and  $T_2^*$  with depth. Recognizing that the  $T_2^*$  response can be dominated by magnetic mineralogy, we have developed improved acquisition schemes to resolve relaxation parameters more sensitive to permeability:  $T_1$  (using double-pulse sequences),  $T_2$  (using CPMG-based sequences), and  $T_1$ - $T_2^*$  distributions (using two-dimensional sequences). Meanwhile, appreciating the advantage of FID measurements to detect the shortest signal components, we have sought a better understanding of the Earth's field  $T_2^*$  response of porous media, and have outlined novel approaches to transform FID data into quasi- $T_2$  distributions. Provided improved determination of relaxation times, challenges remain to estimate permeability in groundwater investigations, since shallow Earth materials differ significantly from reservoir rocks widely studied in oilfield NMR. We have demonstrated that coarse, unconsolidated aquifer materials can be strongly influenced by slow-diffusion and bulk-fluid relaxation dynamics, and have developed refined models to account for these differences. Further, by complementing surface NMR with newly available shallow logging NMR measurements, we have designed novel workflows for calibrating permeability models and mapping aquifer properties over wide areas.

#### OP097: Magnetic Resonance Imaging of Fluids in Porous Media

\*Bruce J. Balcom

MRI Research Centre, Department of Physics, University of New Brunswick, Canada

Magnetic resonance is well known in the petroleum research and development world through down hole logging and companion laboratory MR measurements of bulk fluid properties. Magnetic Resonance Imaging is less well known, but there is growing recognition that laboratory imaging studies, with core plug samples, will provide valuable new information on fluid properties and fluid behavior in the reservoir. Potential measurements of interest include both core analysis measurements and studies of model flooding procedures, including studies of enhanced oil recovery mechanisms.

This lecture will concentrate on recent MRI technique developments, which permit MRI core analysis and model flooding studies to be undertaken, with an emphasis on techniques appropriate for samples that have short  $T_2$  behaviour. These techniques include the SPRITE and hybrid SE SPI methods for simple fluid density imaging and the SE SPI technique for spatially resolved  $T_2$  mapping. Translation of these methods to a new class of MR compatible metal core holders, for variable temperature and pressure studies, will be a major focus of the discussion.

#### UP098: Single-scan $T_1$ - $T_2$ relaxation correlation experiment

\*Susanna Ahola, Ville-Veikko Telkki

University of Oulu

Power of traditional NMR spectroscopy relies on the versatile chemical information reflected by chemical shifts and couplings. Multidimensional experiments multiply the chemical resolution and information content, but they also multiply

the experimental time, restricting the investigations of fast processes. Frydman *et al* introduced single-scan multidimensional NMR as a solution for this issue [i]. It has been broadly considered as one of the brightest recent innovations in NMR spectroscopy.

Typically, NMR spectrum of fluids absorbed in materials reveals little information; it may even consist of a single broad peak. However, the relaxation time distribution may reveal different environments of the fluid molecules, and consequently provide detailed information about the structure of the material. As in traditional NMR spectroscopy, resolution and information content of the relaxation time experiment can be increased by a multidimensional approach such as  $T_1$ - $T_2$  correlation experiment [ii]. A 2D Laplace inversion is used to extract 2D relaxation time spectrum from the experimental data. Original  $T_1$ - $T_2$  correlation experiment is a 3D experiment, and, like in traditional multidimensional NMR, the long experiment time restricts its applicability in the study of fast processes.

Inspired by Frydman's single scan multidimensional NMR approach, we introduce a novel method for single scan measurement of  $T_1$ - $T_2$  relaxation correlation spectrum. The typical experiment time is a few seconds, depending of the relaxation time range in the sample. In many practical cases, the experiment is fast enough for the study of dynamic systems. We demonstrate that the method works by representing the 2D relaxation correlation spectra and showing that the results are in agreement with the relaxation time distributions measured by conventional methods.

[i] A Tal, L Frydman, Prog. Nucl. Mag. Res. Sp. 57 (2010) 241-292

[ii] Y-Q Song, L Venkataramanan, MD Hürlimann, M Flaum, P Frulla, C Straley, J. Magn. Reson. 154 (2002) 261-268.

#### UP099: High Pressure Magic Angle Spinning NMR Capability

<sup>1,2\*</sup>Flaviu R.V. Turcu, <sup>1</sup>David W. Hoyt, <sup>1</sup>Jesse A. Sears, <sup>1</sup>John S. Loring, <sup>1</sup>Kevin M. Rosso, <sup>1</sup>Jian Z. Hu

<sup>1</sup>Pacific Northwest National Laboratory, <sup>2</sup>"Babes-Bolyai" University, Romania

Over the last decades a large number of NMR methods have been developed for addressing numerous biological, chemical and physical problems across essentially all kinds of scientific disciplines. Magic Angle Spinning (MAS) technique is the most widespread NMR methods and is the only one, which allows high resolution NMR spectrum, acquired on solids, semi-solids, or a mixture thereof [1].

High pressure and medium temperature magic angle spinning (MAS) NMR capability [2], composed of a novel high pressure MAS rotor, a high pressure loading/reaction device for in situ sealing and re-opening of the rotor's valve is presented

This high pressure MAS NMR capability is a powerful tool for in situ structure and dynamic investigations in fields like geological carbon sequestration (GCS), subsurface microbiology (1-4). As an example of application, in situ <sup>13</sup>C MAS NMR studies of the reaction products and intermediates associated with GCS [3] using different kind of minerals, i.e., forsterite (Mg<sub>2</sub>SiO<sub>4</sub>), brucite (Mg(OH)<sub>2</sub>) and antigorite (Mg,Fe<sup>2+</sup>)<sub>3</sub>Si<sub>2</sub>O<sub>5</sub>(OH)<sub>4</sub> reacted with wet scCO<sub>2</sub> at various temperatures (50–80°C) are reported [4].

#### References

[1] D.W. Hoyt, R.V.F.Turcu, J.A. Sears, K.M. Rosso, S.D. Burton, J.H. Kwak, A.R. Felmy, J.Z. Hu, Prep-Am. Chem. Soc., Div. Fuel. Chem. 56 (1), 283, (2011).

[2] D.W. Hoyt, R.V.F.Turcu, J.A. Sears, K.M. Rosso, S.D. Burton, J.H. Kwak, A.R. Felmy, J.Z. Hu, J. Magn. Reson. 212, 378 – 385, (2012)

[3] J.S. Loring, H.T. Schaefer, R.V.F. Turcu, C.J. Thompson, Q.R.S. Miller, P.F. Martin, J.Z. Hu, D.W. Hoyt, O. Qafoku,

E.S. Ilton, A.R. Felmy, and K. M. Rosso, Langmuir, 28 (18), 7125 – 7128, (2012)

[4] R.V.F. Turcu, D.W. Hoyt, K.M. Rosso, J.A. Sears, J.H. Loring, A.R. Felmy, J.Z. Hu, J. Magn. Reson, 20120, <http://dx.doi.org/10.1016/j.jmr.2012.08.009>,

#### Acknowledgement

*This research was supported by the Carbon Sequestration Initiative (CSI) funded by Laboratory Directed Research and Development (LDRD) at Pacific Northwest National Laboratory (PNNL)*

#### OP100: Efficient measurement of T1/T2 ratio in porous media

\*Martin D. Hürlimann

Schlumberger – Doll Research, USA

The measurement of the  $T_2$  relaxation properties of fluid filled porous media has long been used a fast method for the characterization of the geometry of the pore space. The distribution of relaxation times reflects the distribution of pore sizes in the sample. More detailed information can be obtained from the measurement of the  $T_1$ - $T_2$  distribution function. In many cases, it is found that the  $T_1$  and  $T_2$  relaxation times are highly correlated, but interestingly, the ratio  $T_1/T_2$  is often larger than unity, even at low fields. An increased ratio indicates the presence of slow motion. The value of the  $T_1/T_2$  ratio gives insight into the interaction between fluid molecules and the pore surfaces or allows the detection of molecular aggregates in the fluid, e.g. micelles and other multi-molecular clusters. Here we discuss a new technique to determine the  $T_1/T_2$  ratio very efficiently that is applicable even in strongly inhomogeneous field encountered in well logging. The technique is based on a modified CPMG sequence where the refocusing pulses are split into two separate pulses. In a single acquisition, the sequence generates simultaneously a CPMG-like and a steady-state like signal that are easily separable in the time domain. The relative amplitude of the two signals is directly related to the  $T_1/T_2$  ratio. Experimental results confirm the theoretical predictions. The analysis of the new sequence shows an interesting connection to the Hofstadter's butterfly. Both theoretically and experimentally, it is shown that the signal power of the steady-state like signal is sensitive to whether the ratio of the two pulse spacings is a rational or irrational number.

#### Wednesday – May 22<sup>nd</sup> Materials and Applications

Chair: Hellmut Eckert  
Room Ñnix

#### OP101: Following Function in Real Time: New In situ NMR Methods for Studying Structure and Dynamics in Batteries and Supercapacitors

<sup>1</sup>Lina Zhou, <sup>1</sup>Michal Leskes, <sup>1</sup>Hao Wang, <sup>1</sup>Alex Forse, <sup>1</sup>John Griffin, <sup>2</sup>Nicole M. Trease, <sup>1</sup>Elodie Salager, <sup>1\*</sup>Clare. P. Grey

<sup>1</sup>Chemistry Department, Cambridge University, UK, <sup>2</sup>Chemistry Department, Stony Brook University, USA

A full understanding of the operation of a chemical energy storage device such as a battery or supercapacitor requires that we utilize methods that allow devices or materials to be probed while they are operating (i.e., *in-situ*). This allows, for example, the transformations of the various cell components to be followed under realistic conditions without having to disassemble and take apart the cell. To this end, the application of new *in* and *ex-situ* Nuclear Magnetic Resonance (NMR) approaches to correlate structure and dynamics with function in lithium-ion and supercapacitors will be described. The *in-situ* approach allows processes to be captured, which are very difficult to detect directly by *ex-situ* methods. For example, we can detect side reactions

involving the electrolyte and the electrode materials, sorption processes at the electrolyte-electrode interface, and lithium ion dynamics. *Ex-situ* NMR investigations allow more detailed structural studies to be performed to correlate local and long-range structure with performance in these systems.

#### OP102: Unique Insights into Carbon Capture and Geosequestration of CO<sub>2</sub> from In Situ High-Pressure, High-Temperature NMR

J. Andrew Surface, Jeremy Moore, Mark Conradi, \*Sophia E. Hayes

Washington University in St. Louis

We have constructed hardware to conduct in situ high-pressure, elevated-temperature study of heterogeneous mixtures of solids, liquids, gases, and supercritical fluids. The objective is to simulate processes at geologically relevant pressures and temperatures, monitoring the kinetics of CO<sub>2</sub> sorption and the stability of the sequestration within geologic materials. Specifically, our aim is to monitor CO<sub>2</sub> uptake in both ultramafic rocks and in more porous geological materials to understand the mechanisms of physisorption and chemisorption as a function of temperature and pressure. A further aim is to spectroscopically characterize and quantify CO<sub>2</sub> in supercritical, "dissolved" (in salt water), and "mineral" CO<sub>2</sub> (mineral carbonation) phases. Thus, the results will allow NMR to be used for quantitative characterization of the phases and their chemistry. We have already developed CO<sub>2</sub> spectroscopy to analyze the phase of CO<sub>2</sub> (liquid, supercritical, or gas) and its conversion into other forms, such as carbonic acid, bicarbonate, and carbonate species. When CO<sub>2</sub> reacts with the calcium or magnesium in a rock sample, such as peridotite, the <sup>13</sup>C chemical shift, linewidth and lineshape, and relaxation times will change dramatically. This change can be monitored in situ and provide instantaneous and continuous characterization that maps the chemistry that is taking place. On the pathway to MgCO<sub>3</sub> formation, there are a number of phases of Mg(OH)<sub>x</sub>(H<sub>2</sub>O)<sub>y</sub>(CO<sub>3</sub>)<sub>z</sub> that are apparent. The in situ NMR experiments consist of heterogeneous mixtures of rock, salty brine solution, and moderate pressure CO<sub>2</sub> gas at elevated temperatures. Results are compared to those from Raman spectroscopy of aquo- hydro- carbonato-magnesium species.

Reference:

"In Situ Measurement of Magnesium Carbonate Formation from CO<sub>2</sub> Using Static High-Pressure and -Temperature <sup>13</sup>C NMR", J. Andrew Surface, Philip Skemer, Sophia E. Hayes, and Mark S. Conradi, *Environ. Sci. Technol.* 2013, 47, 119–125. DOI: 10.1021/es301287n

#### UP103: Direct Alcohol Fuel Cells Investigated In Situ and Ex Situ by NMR Spectroscopy

1,2\*Oc Hee Han

<sup>1</sup>Korea Basic Science Institute, <sup>2</sup>Chungnam National University

Fuel cells are an ideal primary energy conversion device for remote site locations, automobiles, and mobile electrical devices such as mobile phones and laptops. But direct alcohol fuel cells (DAFCs) are challenged to reduce alcohol crossover and to develop less expensive catalysts and electrolyte membranes. Understanding fundamental aspects of DAFCs such as the mechanisms of alcohol oxidation and crossover would provide the direction to overcome the challenges.

We developed the toroidal cavity detectors for *in situ* observation of DAFC by NMR spectroscopy, and demonstrated that the functional difference of anode catalysts such as Pt and PtRu could be detected. The anode exhaust of DAFC was analyzed by liquid state <sup>13</sup>C NMR spectroscopy for quantitative correlation of the amount of electrical current generated to the quantities of each chemical product. The membrane electrode assembly (MEA) composed of triple-polymer electrolyte membrane layers was designed, thereby facilitating a

convenient sampling for *ex situ* NMR investigation, for the study of methanol crossover and methanol reaction intermediates in a DAFC with high resolution magic angle spinning (MAS) NMR spectroscopy.

If time permits, our work on the identification of electronic, chemical and structural changes of FC components during each FC assembly and operation process will be presented. The work includes the influence of hot pressing on the pore structures of PEM investigated by residual quadrupolar splitting in <sup>2</sup>H NMR spectra of D<sub>2</sub>O in PEM and by freezing-point depression of water in nano-sized pores, and on the effects of Nafion ionomers on the local density of electronic states of surface Pt of Pt particle electrode catalysts explored by <sup>195</sup>Pt NMR techniques.

Present work demonstrates that 1) *in situ* NMR studies on real DAFCs can be done, 2) alcohol oxidation reaction mechanism can be studied by the *in situ* and *ex situ* NMR techniques, and 3) various NMR methods can be successfully applied for the identification of electronic, chemical and structural changes of FC components during each FC assembly and operation process.

#### UP104: Local Order and Cation Distribution in Mixed-Alkali Phosphate Glasses

1\*José Fabian Schneider, <sup>1</sup>Jefferson Tsuchida, <sup>2</sup>Hellmut Eckert, <sup>2</sup>Rashmi Deshpande

<sup>1</sup>Instituto de Física de São Carlos, Universidade de São Paulo, <sup>2</sup>Institut für Physikalische Chemie, Westfälische Wilhelms-Universität Münster

The mixed-ion effect (MIE) is the dramatic non-linear variation in the values of transport properties in glasses due to restriction in ionic mobility resulting from the cation mixing. A satisfactory explanation of this phenomenon has been elusive during decades. Metaphosphate glasses A<sub>x</sub>B<sub>1-x</sub>PO<sub>3</sub> with two mobile monovalent cations A<sup>+</sup> and B<sup>+</sup> are archetypical examples of MIE in d.c. conductivity. The deepest known reduction in conductivity is observed in mixed Rb-Li metaphosphates, attaining 8 orders of magnitude with respect to the single-cation glasses. In contrast, reductions of less than 1 order of magnitude are observed in Ag-Na metaphosphates. A comprehensive analysis of local order and alkali distribution in mixed metaphosphates is presented here, covering similar/dissimilar cation pairs as Na-Li, Na-Ag, Na-K, Na-Rb, Na-Cs, and Li-Rb, Li-Cs, Ag-Cs. The aim of this study is the identification of cation segregation or random mixture, which are configurations critical to determine conductivity, and the possible dependence with size mismatch or differences in ionic potential. A broad set of NMR techniques was applied: <sup>31</sup>P, <sup>23</sup>Na, <sup>7</sup>Li and <sup>133</sup>Cs high-resolution NMR, <sup>109</sup>Ag-NMR, <sup>23</sup>Na Triple-Quantum-MAS, REDOR/SEDOR between <sup>31</sup>P-<sup>23</sup>Na, <sup>7</sup>Li-<sup>6</sup>Li, and <sup>7</sup>Li-<sup>133</sup>Cs, <sup>87</sup>Rb quadrupole Carr-Purcell-Meiboom-Gill, and <sup>23</sup>Na-NMR spin-echo decay. The structural picture emerging from these results reveals that each cation site retains its structural specificities, as in single-cation glasses. However, a common structural adjustment on the cation environment was discovered: the compression of the O environment around the smaller cation of the pair, as its concentration diminishes. The mixture of cations species at atomic scale is generally random, even in glasses having the biggest cation mismatch as Li-Cs, but some deviations indicating short-range like-cation preferences were observed for Na-K, Na-Cs and Na-Rb. These findings support recent modeling procedures pointing to a fundamental relation between the dynamic MIE and structure in phosphates, which might be universal in all type of glasses.

ACKNOWLEDGEMENTS: FAPESP, CNPq, CAPES

#### OP105: Nanoscale Imaging of Electron and Nuclear Spins

\*Jörg Wrachtrup

3rd Institute of Physics, University of Stuttgart, Stuttgart,

## Germany

Increasing the sensitivity of magnetic resonance towards sensing single electron and nuclear spins is a prominent goal in NMR and EPR methodology. In addition it opens the way towards using quantum physics itself to increase sensitivity beyond the standard quantum limit. In the recent past diamond defect centers have proven to be exquisitely sensitive sensors for sample spins and detection of single electron spins or as few as  $10^2$  nuclear spin magnetic moments have become possible [1]. The talk will describe approaches to image such small spin ensembles for example to achieve subcellular resolution in MRI imaging of cells [2] or eventually the detection of single proteins.

[1] T. Staudacher et al. "Nuclear magnetic resonance spectroscopy on a (5nm)<sup>3</sup> volume of liquid and solid samples", *Science* (2013) in press

[2] S. Steinert et al. "Magnetic spin imaging under ambient conditions with sub-cellular resolution" (2012) arXiv1211.3242

**Thursday – May 23<sup>rd</sup>**  
**Plenary Session**

Chair: Beat Meier  
 Room Gávea A

**PL106: Spectroscopy in the Clinic – from dreams to reality**

**\*Jeremy K. Nicholson**

*Department of Surgery and Cancer, Faculty of Medicine, Imperial College London*

Systems biology and advanced spectroscopic tools can be applied at both individual and population levels to understand integrated biochemical function in relation to disease pathogenesis. Metabolic phenotyping offers an important window on systemic activity and both advanced spectroscopic approaches can be used to characterize disease processes and responses to therapy [1]. There is now wide recognition that the extensive cross-talk and signalling between the host and the symbiotic gut microbiome links to both to responses to therapy and disease risk factors and indeed these also modulate drug toxicity [2,3]. Such symbiotic supra-organismal interactions greatly increase the degrees of freedom of the metabolic system that poses a significant challenges to fundamental notions on the nature of the human diseased state, the aetiopathogenesis of common diseases and current systems modelling requirements for personalized medicine. We have developed scalable and translatable strategies for "*phenotyping the hospital patient journey*" [4,5] using top-down systems biology tools that capitalizes on the use of both NMR and MS based metabolic modelling and pharmacometabonomics [6,7] for diagnostic and prognostic biomarker generation to aid clinical decision-making at point-of-care. Such diagnostics (including those for near real-time applications as in surgery and critical-care) can be extremely sensitive for the detection of diagnostic and prognostic biomarkers in a variety conditions and are a powerful adjunct to conventional procedures for disease assessment that are required for future developments in "precision medicine" including understanding of the symbiotic influences on patient state [8]. Many biomarkers also have deeper mechanistic significance and may also generate new therapeutic leads or metrics of efficacy for clinical trial deployment. Furthermore the complex and subtle gene-environment interactions that generate disease risks in the general human population also express themselves in the metabolic phenotype, and as such, the NMR-based "Metabolome Wide Association Study" approach [9] gives us a powerful new tool to generate disease risk biomarkers from epidemiological sample collections and for assessing the health of whole populations. Such population risk models and biomarkers an also feedback to individual patient healthcare models thus closing the personal and public healthcare modelling triangle.

[1] Nicholson J.K. and Lindon, J.C. (2008) *Nature* 455 1054-1056.

[2] Swann, J.R. et al (2011) *PNAS* 108 4523-4530.

[3] Nicholson, J.K. et al (2012) *Science* 336 1262- 1267.

[4] Kinross, J. et al (2011) *Lancet* 377 (9780) 1817-1819.

[5] Nicholson, J.K. et al (2012) *Nature* doi:10.1038/nature11708.

[6] Clayton, T.A. et al (2006) *Nature* 440 1073-1077.

[7] Clayton, T.A. et al (2009) *PNAS* 106 14728-14733.

[8] Mirnezami, R. Nicholson, J.K. and Darzi, A. (2012) *New Eng. J. Med.* 366 (6) 489-491.

[9] Holmes, E. et al (2008) *Nature* 453 396-400.

**PL107: New contraptions/gadgets/techniques for solid-state NMR**

**\*K. Takegoshi**

*Department of Chemistry, Graduate School of Science, Kyoto University, Kyoto, Japan*

When I was Post.Doc., I could only use 4 phases for rf pulses with constant amplitude/phase/frequency. The size of data storage was only a few MB and it took 45 min to process 2D data. . . At present, rf amplitude/phase/frequency can be varied continuously. The storage size is almost infinite and the time for data analysis is too quick to finish a cup of coffee. We should fully enjoy these developments and I shall discuss recent advance of hardware, data treatment, and pulse sequences developed in my group. The topics may be covariance data processing for HETCOR,[1] elemental analysis by NMR,[2] a cryo-coil MAS probe for <sup>1</sup>H-<sup>13</sup>C double resonance experiment,[3] a tear-less way of adjustment of magic angle, air-less MAS, etc. If time allows, I shall also present analytical formalism on the derivatives of the density matrix and the observed signal with respect to the experimental parameters varied.[4]

[1] Takeda, Kusakabe, Noda, Fukuchi, and Takegoshi, *Phys. Chem. Chem. Phys.* 14 (2012) 9715.

[2] Takeda, Ichijyo, and Takegoshi, *J. Magn. Reson.* 224 (2012) 48.

[3] Mizuno, et al. to be published.

[4] Momot and Takegoshi, *J. Magn. Reson.*, 221 (2012) 57.

**Thursday – May 23<sup>rd</sup>**  
**DNP**

Chair: Christian Griesinger  
 Room Gávea A

**OP108: Magnetic resonance is no longer the world's least sensitive form of spectroscopy**

**<sup>1,2</sup>\*Geoffrey Bodenhausen**

*<sup>1</sup>Ecole Normale Supérieure, Paris, <sup>2</sup>Ecole Polytechnique Fédérale, Lausanne*

There seem to be only three obstacles to the relentless expansion of the scope of contemporary magnetic resonance: sensitivity, sensitivity, and sensitivity. Dynamic nuclear polarization, which can enhance NMR signals by two orders of magnitude in solids, and by five orders of magnitude in liquids, appears ideal to lift these hurdles. Our laboratory is the only one in the world that has been working successfully on the development of DNP in both solids and liquids side by side. In solids, we have pioneered the characterization of organic molecules grafted on silica surfaces in view of studying heterogeneous catalysts, using <sup>13</sup>C, <sup>29</sup>Si and <sup>27</sup>Al NMR. The effects of spin diffusion have been investigated in porous silicates. By selective enrichment of a protein that is part of the Ribosome with <sup>13</sup>C and <sup>15</sup>N, we have been able to observe signals of this 80 kDa protein complex. In liquids,

many contributions have been made to improve the so-called "dissolution DNP" process by using cross-polarization at low temperatures and high fields, by scavenging radicals during transport, and by reducing losses due to relaxation in low fields.

#### OP109: Dissolution Dynamic Nuclear Polarization of Large Molecules

\***Christian Hilty**, Mukundan Ragavan, Hsueh-Ying Chen, Youngbok Lee, Haifeng Zeng, Hlaing Min

*Texas A&M University, Chemistry Department, USA*

Solid-to-liquid state dynamic nuclear polarization (DNP) has become a popular way of enhancing the signals in liquid state NMR and MRI by several orders of magnitude. Up to now, the most prominent applications of solid-to-liquid state DNP have been for the observation of small molecules. Using highly polarized spin systems, chemical reactions and other dynamic processes can be studied in one single real-time experiment, even if far from equilibrium. In addition to small molecules, NMR has long been applied to determine the structure and function of macromolecules, including proteins. Challenges in making use of the large signal gain of solid-to-liquid state DNP in these applications, however, include the need for dissolution and injection of such samples, as well as spin relaxation that occurs between polarization and NMR measurement. We present strategies that enable the use of dissolution DNP for direct observation of macromolecules by high-resolution NMR spectroscopy. In a first experiment, we transfer polarization from a hyperpolarized ligand to a protein through the Nuclear Overhauser effect. The resulting spectrum contains signals that are specifically enhanced in the vicinity of the binding site. The efficiency of intermolecular polarization transfer depends on the kinetics of binding, cross-relaxation rates and spin diffusion rates within the protein. In a second experiment, we directly hyperpolarize a model protein, the ribosomal protein L23 from *T. Thermophilus*. Hyperpolarization occurs either in the native state or the chemically denatured form. Biosynthetically produced proteins are readily labeled with stable isotopes including  $^2\text{H}$ , which reduces spin relaxation. Final signal enhancements of  $10^2$ - $10^3$  are obtained in the NMR spectrometer, which permit the observation of the re-folding process of the protein in real-time.

#### UP110: DNP Surface Enhanced NMR (SENS): a Tool for Structural Investigation of Supported Catalysis

<sup>1</sup>\***Moreno Lelli**, <sup>1</sup>Alexandre Zagdoun, <sup>1</sup>David Gajan, <sup>1</sup>Aaron J. Rossini, <sup>4</sup>Olivier Ouari, <sup>4</sup>Paul Tordo, <sup>3</sup>Chloé Thieuleux, <sup>2</sup>Christophe Copéret, <sup>1</sup>Anne Lesage, <sup>1</sup>Lyndon Emsley

<sup>1</sup>Centre de RMN à Très Hauts Champs, Université de Lyon (CNRS/ENS Lyon/UCB Lyon 1), <sup>2</sup>Department of Chemistry, ETH Zürich, Switzerland, <sup>3</sup>Institut de Chimie de Lyon, Université de Lyon (CNRS-Université Lyon 1-ESCP Lyon), <sup>4</sup>Aix-Marseille Université, CNRS, Institut de Chimie Radicale (ICR), Marseille

In recent years, our group has demonstrated that high-field DNP in MAS solid-state NMR at low temperature (100 K) can be applied to investigate the structure of surfaces of materials. In this approach, which we dubbed DNP surface enhanced NMR spectroscopy (SENS), the polarizing agent (for example an organic di-nitroxide radicals such as bCTbK, etc.) is introduced into the sample by incipient wetting impregnation with a radical solution. Upon irradiation with microwaves the DNP effect enhances polarization of the  $^1\text{H}$  nuclei of the solvent and the surface, and this enhanced  $^1\text{H}$  polarization can then be transferred to the surface hetero-nuclei ( $^{13}\text{C}$ ,  $^{15}\text{N}$ ,  $^{29}\text{Si}$  or  $^{27}\text{Al}$ ) by cross-polarization (CP).[1,2] The SENS method can be extended to a large set of solvents, thus extending the nature of the accessible systems to include many modern materials, such

as nanoparticulate silica, metal-organic-frameworks (MOF), catalyst precursors or organometallic systems,... Here we will present the most recent developments in DNP SENS, and in particular show how this allows the acquisition of multidimensional  $^1\text{H}$ - $^{29}\text{Si}$  and or  $^1\text{H}$ - $^{13}\text{C}$  correlation spectra of active surface species. The multi-dimensional spectra yield detailed three-dimensional structural information of tethered surface species.[3] The structural information obtained by DNP SENS opens the way to a more rational design of supported catalysis.

[1] A. Lesage, M. Lelli, D. Gajan, M. A. Caporini, V. Vitzthum, P. Mieville, J. Alauzun, A. Roussey, C. Thieuleux, A. Mehdi, G. Bodenhausen, C. Copéret, L. Emsley, J. Am. Chem. Soc. 2010, 132, 15459-15461;

[2] M. Lelli, D. Gajan, A. Lesage, M. A. Caporini, V. Vitzthum, P. Mieville, F. Heroguel, F. Rascon, A. Roussey, C. Thieuleux, M. Boualleg, L. Veyre, G. Bodenhausen, C. Copéret, L. Emsley, J. Am. Chem. Soc. 2011, 133, 2104-2107;

[3] M. Samantaray, J. Alauzun, D. Gajan, S. Kavita, A. Mehdi, L. Veyre, M. Lelli, A. Lesage, L. Emsley, C. Copéret, C. Thieuleux J. Am. Chem. Soc. 2013 in press

#### UP111: Sensitivity enhancement in solution NMR through dynamic nuclear polarization of encapsulated proteins

<sup>1</sup>Kathleen G. Valentine, <sup>2</sup>Guinevere Mathies, <sup>1</sup>Nathaniel V. Nucci, <sup>1</sup>Igor Dodevski, <sup>1</sup>Sabrina Bédard, <sup>1</sup>Matthew Stetz, <sup>2</sup>Thach V. Can, <sup>2</sup>Robert G. Griffin, <sup>1</sup>\***A. Joshua Wand**

<sup>1</sup>University of Pennsylvania, <sup>2</sup>Massachusetts Institute of Technology

Solution NMR has contributed significantly to studies of the structural and dynamic aspects of proteins and the information inherent in NMR phenomena offers much more. Yet, despite tremendous advances in technology, experimental design and analytical strategies, solution NMR remains fundamentally restricted due to its inherent insensitivity. Thus, it seems important to improve the sensitivity of the solution NMR experiment in order to reduce experiment time, lower the absolute quantities of sample required and open a lower concentration regime where proteins of limited solubility can be accessed. With this in mind there has been a revival of dynamic nuclear polarization (DNP). In solution, it is thought that such DNP transfer will occur primarily through the Overhauser effect. The basic strategy is to saturate the electronic transition of a stable free radical and transfer this non-equilibrium polarization to the hydrogen spins of water, which will in turn transfer polarization to the hydrogens of the dissolved macromolecule. Unfortunately, technical aspects of this approach seem to prove fatal to the idea in its current form. The primary reason is that the frequency of the electron transition of suitable radicals lies in the sub-THz spectrum where water absorbs strongly and results in catastrophic heating of the sample. In addition, the residence time of water on the surface of the protein is too short for efficient transfer of polarization. Here we take advantage of the properties of solutions of encapsulated proteins dissolved in low viscosity solvents. Such samples are largely transparent to the subTHz frequencies required and thereby avoid significant heating during saturation of the electronic transition. Nitroxide radical is introduced into the reverse micelle system in three ways: covalently attached to the protein; covalently attached to a surfactant embedded in the reverse micelle shell; and free in the aqueous core. DNP experiments at the X-band EPR frequency have yielded initial enhancements from the nitroxide embedded in the surfactant to the water on the order of -35. In addition, we find that the hydration properties of encapsulated proteins allow for efficient polarization transfer from water to the amide hydrogens in a protein. Thus the merging of the reverse micelle technology with DNP demonstrates the potential to provide a significant increase in the sensitivity of solution NMR spectroscopy of

proteins and other bio-macromolecules. Supported by the NIH and the NSF.

### OP112: Dissolution DNP: Theoretical Considerations and Experimental Implementation

Grzegorz Kwiatkowski, Alexander Karabanov, \*Walter Köckenberger

University of Nottingham

Recent progress made in the experimental implementation of sensitivity enhancement strategies based on dynamic nuclear polarization has attracted much attention in the NMR community. Theoretical models of the DNP mechanism are useful to provide insight into optimal conditions for such experiments. However the theoretical quantum mechanical description of the complex spin dynamics is limited to calculations using only small representative systems consisting of up to 20 spins [1]. Here we present a new strategy that makes it possible to calculate the spin dynamics of DNP experiments for large spin ensembles consisting of a network of several thousand coupled spins. Building on previous work [2] we demonstrate that it is possible under certain conditions to overcome the exponential scaling of the required equations and to reduce the dimensions for a system of  $N$  nuclear spins from  $4^N$  to  $N$  coupled rate equations that describe the polarization dynamics for each individual spin. The huge reduction of the required equations arises from the use of a quantum mechanical projection technique related to a formalism proposed by Nakajima and Zwanzig [3].

We demonstrate numerically the validity of this approach by comparing results derived from solving the master equation in the full Liouville space to simulations obtained from our novel formalism. We show then how realistic build-up times for the experimentally observable nuclear spin polarization can be obtained from simulations involving  $10^3$   $^{13}\text{C}$  spins arranged in a cubic lattice around a single electron. The use of this model enables us to study the transport of polarization between the electron and the nuclear spins and to distinguish between direct transfer of polarization from the electron to the nuclear spins and an indirect transfer via nuclear spin diffusion.

By varying the parameter of this model we gain further insight into the optimal conditions that need to be fulfilled for the generation of maximal nuclear spin polarization. In this theoretical study we explicitly refer to the problems encountered by experimentalists working with hyperpolarized  $^{13}\text{C}$  and discuss how to design the optimal DNP experiment. We report also on recent progress in the development of a DNP NMR spectrometer based on a unique dual centre magnet that makes it possible to transfer the sample in solid state between a cryogenic environment and a probehead kept at ambient temperature.

[1] Y. Hovav, A. Feintuch and S. Vega, "Theoretical aspects of dynamic nuclear polarization in the solid state – The solid effect", J. Magn. Reson., 207(2), 176–189, 2010

[2] A. Karabanov, A. van der Drift, L. J. Edwards, I. Kuprov and W. Köckenberger, "Quantum mechanical simulation of solid effect dynamic nuclear polarization using Krylov-Bogolyubov time averaging and a restricted state-space", Phys. Chem. Chem. Phys. 14(8), 2658–2668, 2012

[3] H.-P. Breuer and F. Petruccione, The Theory of Open Quantum Systems, Oxford University Press, 2007.

Thursday – May 23<sup>rd</sup>  
Dynamics and Recognition

Chair: Martin Billeter  
Room Gávea B

### OP113: Use of Solution NMR for Studies of Proteins and Protein Complexes Involved in Protein and Peptide Synthesis

\*Gerhard Wagner

Department of Biological Chemistry and Molecular Pharmacology, Harvard Medical School, Boston

Solution NMR spectroscopy is ideally suited for studies of dynamic and weak interactions of proteins. We have focused on several macromolecular complexes involved in protein synthesis. A central interest in my laboratory is to understand the mechanisms by which eukaryotes initiate translation of mRNA. This process is highly regulated by numerous weak and transient protein interactions. We have used NMR and other techniques to characterize these interactions and the effect of inhibitors that prevent such interactions. We found that inhibitors of the interaction between the translation initiation factors eIF4E and eIF4G discovered with high throughput screening bind eIF4E at a site distinct from the eIF4G-binding site and act allosterically causing small but decisive rearrangements of the target protein. In addition, we have characterized the 68 kDa complex between the RNA helicase eIF4A and the scaffold protein eIF4G as well as the interactions between initiation factors eIF1, eIF1A and eIF5. We have shown that these interactions control start-codon recognition. In a related project we are working on assembly-line mega-enzymes that synthesize natural products using a set of four domains. Reprogramming of these systems may enable production of new antibiotics.

To enable structural and functional studies of these large systems we have optimized procedures for spectroscopy with large proteins. This includes more efficient pulse sequences, and optimization of methods for non-uniform sampling (NUS). We have developed new reconstruction methods for NUS data that make reconstruction of sparsely sampled high-resolution 3D and 4D data sets feasible.

### OP114: Allosteric Motions in periplasmic binding Proteins characterized by NMR Spectroscopy

Gabriel Ortega, Tammo Diercks, \*Oscar Millet

CIC bioGUNE, Parque Tecnológico de Vizcaya, Spain

Protein function, structure and dynamics are intricately correlated, but studies on structure-activity relationships are still only rarely complemented by a detailed analysis of dynamics related to function (functional dynamics). We have applied NMR to investigate the functional dynamics in two homologous periplasmic sugar binding proteins with bi-domain composition: *E. coli* glucose/galactose (GGBP) and ribose (RBP) binding proteins. In contrast to their structural and functional similarity, we observe a remarkable difference in functional dynamics: for RBP, the absence of *segmental* motions allows only for isolated structural adaptations upon carbohydrate binding in line with an induced fit mechanism; on the other hand, GGBP shows extensive *segmental* mobility in both *apo* and *holo* states, enabling selection of the most favorable conformation upon carbohydrate binding in line with a *population shift* mechanism. Collective *segmental* motions are controlled by the hinge composition: by swapping two identified key residues between RBP and GGBP we also interchange their *segmental* hinge mobility, and the doubly mutated GGBP\* no longer experiences changes in conformational entropy upon ligand binding while the complementary RBP\* shows the *segmental* dynamics observed in *wt*GGBP. Most importantly, the *segmental* inter-domain dynamics always increase the apparent substrate affinity and thus, are functional, underscoring the allosteric control that the hinge region exerts on ligand binding.

ACKNOWLEDGEMENTS: Support was provided from The Department of Industry, Tourism and Trade of the Government of the Autonomous Community of the Basque Country, from the Innovation Technology Department of the Bizkaia County, from the Ministerio de Economía y Competitividad (CTQ2009-10353/BQU; CTQ2012-32183 and CSD2008-00005). G.O. acknowledges a fellowship from the Ministerio de Ciencia y Tecnología.

**UP115: Atomistic Descriptions of Protein Dynamics on Multiple Timescales From NMR Chemical Shifts****\*Paul Robustelli***Columbia University*

NMR chemical shifts are highly sensitive probes of molecular structure. This work illustrates two approaches for utilizing the structural information contained in chemical shifts to obtain atomistic descriptions of the structural fluctuations of proteins on the ns- $\mu$ s and millisecond timescales.

In the first approach, semi-empirical NMR chemical shift prediction methods are used to evaluate the dynamically averaged values of backbone chemical shifts obtained from unbiased molecular dynamics (MD) simulations of proteins on the ns- $\mu$ s timescale [1]. MD-averaged chemical shift predictions generally improve agreement with experimental values when compared to predictions made from static X-ray structures and a detailed analysis of the structural dynamics and conformational changes associated with the improvements provide support for specific motional processes in proteins. Chemical shifts are sensitive reporters of fluctuations in backbone and side chain torsional angles, aromatic ring positions, and the geometries of hydrogen bonds. Improved chemical shift predictions result from population-weighted sampling of multiple conformational states and from sampling smaller fluctuations within conformational basins.

In the second approach, chemical shifts and anisotropic restraints obtained from relaxation dispersion experiments are used to determine the structure of a sparsely-populated, on-pathway folding intermediate that folds on the millisecond timescale [2]. CPMG measurements are used to measure backbone chemical shifts, RDCs, and RCSAs of the 2% populated folding intermediate of the A39V/N53P/V55L Fyn SH3 domain and the structure of the intermediate is calculated using a recently developed chemical shift restrained molecular dynamics structure calculation protocol [3]. The structure provides a detailed characterization of the non-native interactions stabilizing an aggregation-prone intermediate under native conditions and insight into how such an intermediate can derail the folding pathway and initiate fibrillation.

These results illustrate that NMR chemical shifts can be used to provide atomistic descriptions of protein motions on multiple timescales.

[1] P Robustelli, KA Stafford, AG Palmer III, JACS, 134, 6365-6374 (2012)

[2] P Nuedecker, P Robustelli, A Cavalli, P Walsh, P Lundstrom, A Zarrine-Afsar, S Sharpe, M Vendruscolo, LE Kay, Science, 336, 362-366 (2012)

[3] P Robustelli, KJ Kohlhoff, A Cavalli, M Vendruscolo, Structure, 18, 1-11 (2010)

**UP116: Viral RNAs and Infection****Joseph D. Puglisi**, Aaron Coey, \*Elisabetta Viani*Department of Structural Biology & Stanford Magnetic Resonance Laboratory, Stanford University*

Viruses use RNAs in multiple ways during their infection and replication. Using NMR spectroscopy combined with other biophysical approaches, we have explored two general strategies that RNAs and RNA-protein interactions are harnessed to enhance viral infection. First, we have determined the structural basis for initiation of reverse transcription in HIV, by which the viral genomic RNA is converted to a DNA copy by the viral enzyme reverse transcriptase (RT); this is the first step in viral replication after infection. The process is initiated from a specific RNA-RNA complex formed by the genomic RNA and a host tRNA<sup>Lys</sup><sub>3</sub>. We have monitored the conformation of this 40-70 kDa RNA-RNA complex using heteronuclear NMR spectroscopy. We determined the global fold of this RNA complex, and showed the presence of key RNA contacts that stabilize the conformation. Combined

with biochemical and crystallographic approaches, we are determining how HIV RT recognizes this complex, and how this ternary complex can be targeted by novel therapeutics. Second, viruses express RNAs to circumvent host responses to infection. Using NMR we are determining the structure of a 30 kDa RNA from adenovirus that inhibits the innate immune response protein PKR, and how the RNA binds and inhibits this kinase. Our results show how NMR merged with other techniques can illuminate the complex functions of RNAs in viral infection.

**OP117: High-Resolution Protein Structures by Magic-Angle Spinning NMR****\*Chad M. Rienstra**, Marcus D. Tuttle, Gemma Comellas, Andrew J. Nieuwkoop, Ming Tang, Lindsay J. Sperling, Robert B. Gennis, Julia M. George*University of Illinois at Urbana Champaign*

We present multidimensional solid-state NMR methods for protein structure determination, examining alpha-synuclein fibrils and the membrane protein DsbB.

For alpha-synuclein, resonance assignments of several isoforms demonstrate that the major secondary structure motifs observed in the wild type protein are retained in the A30P and A53T (Parkinson's disease early onset) mutants, and furthermore conserved upon fibril incubation on phospholipid vesicles. Spectra of intermediate states give insights into the sequence of fibril assembly. We propose structural models consistent with the available long-range distance restraints.

For DsbB, we have developed a high-resolution structural model by combining experimental X-ray and solid-state NMR with molecular dynamics (MD) simulations. We embedded the high-resolution DsbB structure, derived from the joint calculation with X-ray reflections and solid-state NMR restraints, into the lipid bilayer and performed MD simulations to provide a mechanistic view of DsbB function in the membrane. Further, we validated the membrane topology of DsbB by selective proton spin diffusion experiments, which directly probe the correlations of DsbB with water and lipid acyl chains. NMR data also support the model of a flexible periplasmic loop and an interhelical hydrogen bond between Glu26 and Tyr153.

This work was supported by NIH grants R01-GM073770 and R01-GM075937.

**Thursday – May 23<sup>rd</sup>  
New Solution NMR Methods**Chair: Julien Wist  
Rooms Turmalina/Topázio**OP118: Broadband Inversion of 1JCC Correlations in 1,n-ADEQUATE Spectra****<sup>1</sup>\*Gary E Martin**, <sup>1</sup>Mikhail Reibarkh, <sup>1</sup>R. Thomas Williamson, <sup>2</sup>Wolfgang Bermel<sup>1</sup>Merck Research Laboratories, <sup>2</sup>Bruker BioSpin

ADEQUATE experiments are a family of "out-and-back" 2D NMR experiments that begin with an initial magnetization transfer via 1JCH followed by either a <sup>1</sup>J<sub>CC</sub> (1,1-ADEQUATE) or <sup>n</sup>J<sub>CC</sub> (1,n-ADEQUATE) magnetization transfer. The magnetization is transferred back along the same pathway and detected via the initial proton-carbon heteronucleide pair. The 1,1-ADEQUATE experiment exclusively gives correlations between adjacent protonated or protonated and non-protonated carbons (via <sup>1</sup>J<sub>CC</sub>) that are equivalent to <sup>2</sup>J<sub>CH</sub> correlations in HMBC spectra. Hence, for protonated adjacent carbons, the experiment is analogous to the <sup>2</sup>J, <sup>3</sup>J-HMBC and H2BC experiments. However, for adjacent non-protonated carbons, <sup>2</sup>J, <sup>3</sup>J-HMBC and H2BC cannot yield any correlations. In comparison, magnetization transfer in the 1,n-ADEQUATE via <sup>n</sup>J<sub>CC</sub> is typically with n=3, very usefully affording the equivalent of <sup>4</sup>J<sub>CH</sub> HMBC

correlations. The down side of the 1,n-ADEQUATE experiment is that  $^1J_{CC}$  correlations unavoidably "leak" into the spectrum and must be identified by some means.

A modified 1,n-ADEQUATE pulse sequence employing asymmetrical delays was first investigated as a means of selectively inverting  $^1J_{CC}$  correlations in 1,n-ADEQUATE spectra. The initial method should probably best be described as "semi-selective" in that while it did invert most  $^1J_{CC}$  correlations, some correlations would still have positive intensity due to the oscillatory nature of the amplitude transfer function. Worse, a mismatch of actual  $^1J_{CC}$  coupling constants and the amplitude transfer function could potentially result in a spectrum where most  $^1J_{CC}$  correlations are not inverted.

A new, dual-optimization, inverted  $^1J_{CC}$  1,n-ADEQUATE experiment will be described that provides uniform inversion of  $^1J_{CC}$  correlations across the range of 29-82 Hz. Even more usefully, relative to the original version of the experiment, the dual-optimization version affords significantly better signal-to-noise for the same acquisition time. Using 1.7 mm cryoprobe technology, the experiment can be successfully applied to samples of 1 mg and smaller.

### OP119: Highlighting Change

<sup>1</sup>\*Eriks Kupče, <sup>2</sup>Ray Freeman

<sup>1</sup>Bruker Ltd, Coventry, UK, <sup>2</sup>Jesus College, Cambridge, UK

Two-dimensional NMR has revolutionized modern NMR methodology, not least because it offers a simple, clear display of correlation information in a format well suited to the spatial imagination of chemists. We demonstrate an entirely new version of this technique, where the "evolution" dimension is derived by the Radon transform, instead of the more familiar Fourier transform. The result is a two-dimensional chart that maps changes in the spectrum induced by molecular interactions or external physical influences. For instance, if a given chemical shift depends on temperature, the corresponding correlation peak is displaced in the vertical dimension by an amount determined by the temperature coefficient.

It is important to note that no sensitivity is sacrificed because the experiment benefits from the multiplex advantage of two-dimensional NMR. The line-shapes have weak skirts with characteristic "butterfly" contours, but these are easily converted into the more familiar four-pointed star by a suitable windowing function. We show a simple example where the temperature dependence of NH and NH<sub>2</sub> resonances are highlighted in the 600 MHz proton spectrum of a neuropeptide, substance P. The reduced temperature coefficient of the G9 H<sub>N</sub> proton is indicative of intramolecular hydrogen-bond formation. We call this *particular* application "Temperature-Induced Projection Spectroscopy (TIPSY)".

The general technique for mapping change is not limited to the study of temperature effects. Pressure, pH, solvent, association, hydrogen-bonding, molecular binding, partial alignment, conformational changes, protein folding, or the effect of added paramagnetic agents can all be addressed under the appropriate experimental conditions. Indeed the scheme is not restricted to NMR; initial experiments suggest that it can be applied to infrared spectra. Because the Radon transform is the essential ingredient of the method, we call it "*projection spectroscopy* (PROSPECT)" a term that implies "*a survey of the landscape*", "*something considered promising*" or even "*to explore for gold*".

### UP120: Measurements of Nuclear Magnetic Shielding

\*Karol Jackowski

Faculty of Chemistry, University of Warsaw, Poland

Recently we have demonstrated the method of  $^1\text{H}$  and  $^{13}\text{C}$  shielding measurements available on a standard NMR spectrometer [1]. It is based on the magnetic shielding of an isolated helium-3 atom ( $\sigma_{\text{He}} = 59.96743$  ppm) [2], its reso-

nance frequency and determined according to Eq. (1):  $\sigma_X = 1 - (\nu_X \gamma_{\text{He}} / \nu_{\text{He}} \gamma_X)(1 - \sigma_{\text{He}})$

where  $\nu$ ,  $\mu$  and  $\gamma$  are the resonance frequencies, the nuclear magnetic moments and the gyromagnetic ratios of helium-3 and another observed nucleus (X), respectively. Eq. (1) can be used for the shielding measurement of any nucleus whenever the gyromagnetic ratio of the given nucleus is accurately known. The isolated helium-3 atom serves as the primary reference standard of shielding and can be applied for all the magnetic nuclei. Moreover the vantage point of the absolute shielding scale can be transferred from helium-3 to another reference standard, such as deuterated lock solvent, and one can conveniently use in practice this procedure as described by Eq. (2):  $\sigma_X = 1 - C_X(\nu_X / \nu_D)(1 - \sigma_D^*)$

where  $\sigma_D^*$  represents the shielding of deuterons in selected liquid solvent [1] and  $C_X$  parameters are known for the majority of light magnetic nuclei:  $^1\text{H}$ ,  $^2\text{H}$ ,  $^{11}\text{B}$ ,  $^{13}\text{C}$ ,  $^{15}\text{N}$ ,  $^{17}\text{O}$ ,  $^{19}\text{F}$ ,  $^{29}\text{Si}$  and  $^{31}\text{P}$ .

As shown the chemical shifts can be entirely replaced by the measurement of shielding parameters and this alternative method of standardization of NMR data has numerous distinct advantages.

(1) It unifies multinuclear methods into one NMR spectroscopy because the values of magnetic shielding have the same molecular meaning independently of observed nuclei.

(2) The experimental shielding values determined this way are ready for direct comparison with the results of quantum-chemical calculations for the same molecular objects.

(3) The precision of such measurements is in every case exactly the same as for the appropriate chemical shifts because it is based on the same reading of resonance frequencies.

(4) The new method allows the measurement of first order isotope effects in shielding as it was shown for hydrogen isotopomers [3].

(5) There is no need to use any additional reference standard if NMR experiment is carried out with deuterated lock solvent.

(6) Shielding measurements performed relatively to any external or internal deuterated solvent give practically the same results.

(7) The measurement of shielding can be easily extended on MAS NMR experiments as it was already shown for  $^{13}\text{C}$  spectra [4].

(8) Experimental shielding parameters can be always converted into chemical shifts if the shielding of reference compound is known.

All the above conclusions are efficiently illustrated with the results of our recent experimental studies.

Support from the National Science Centre (Poland) grant DEC-2011/01/B/ST4/06588 is acknowledged.

[1] Jackowski K., Jaszunski M., Wilczek M., J. Phys. Chem. A 114 (2010) 2471 and references there in.

[2] Rudziński A., Pachulski M., Pachucki A., J. Chem. Phys. 130 (2009) 244102-1.

[3] Garbacz P., Jackowski K., Makulski W., Wasylishen R., J. Phys. Chem. A 116 (2012) 11896.

[4] Jackowski K., Makulski W., Magn. Reson. Chem. 49 (2011) 600.

### UP121: Optimizing Ionic Liquids for CO<sub>2</sub> Capture: an NMR Approach

<sup>1</sup>Marta Corvo, <sup>1</sup>João Sardinha, <sup>2</sup>Sonia Maria Cabral de Menezes, <sup>3</sup>Jairton Dupont, <sup>3</sup>Graciane Marin, <sup>4</sup>Sandra Einloft, <sup>4</sup>Marcus Seferin, <sup>1</sup>Teresa Casimiro, <sup>1</sup>\*Eurico J. Cabrita



<sup>1</sup>REQUIMTE, CQFB, Dept. Química, Fac. Ciências e Tecnologia, Univ. Nova Lisboa, Portugal, <sup>2</sup>PETROBRAS/CENPES, RJ Brazil, <sup>3</sup>Dept. Química Orgânica, Inst. Química, Univ. Federal do Rio Grande do Sul, Brazil, <sup>4</sup>Fac. Química Pontifícia Univ. Católica Rio Grande do Sul, Brazil

Global warming has prompted the scientific community to look for new strategies for CO<sub>2</sub> capture and storage. Recent studies suggest that ionic liquids (ILs) can be alternative materials for CO<sub>2</sub> capture due to their high selectivity for CO<sub>2</sub> absorption. ILs physical and chemical properties can be enhanced and modified by both their cationic and anionic moieties and this is the reason for their broad range of applications. Considering that ILs properties can be designed to satisfy specific application requirements, the optimization of ILs for CO<sub>2</sub> capture is a matter of great interest.[1-3]

Herein we present a detailed NMR study focused on the evaluation of the interactions between ILs and CO<sub>2</sub>. Through careful structural modifications we were able to identify CO<sub>2</sub>-philic features by the analysis of CO<sub>2</sub> solvation in imidazolium ILs. Our High Pressure NMR (HPNMR) methodology allows a direct measurement of CO<sub>2</sub> solubility in ILs and an in-situ assessment of the relationship of all the species involved in the solvation process - cation/anion/CO<sub>2</sub>. HP-NMR experiments based on NOE and multinuclear diffusion NMR experiments using the PGSE technique combined with molecular dynamics simulations enabled a molecular based interpretation for the solvation mechanism. This systematic study allowed the identification of promising candidates for CO<sub>2</sub> capture.

[1] X Zhang, X Zhang, H Dong, Z Zhao, S Zhang and Y Huang Energy Environ. Sci., 2012, 5, 6668- 6681.

[2] M Ramdin, TW Loos and TJH Vlucht Energy Environ. Sci., 2012, 5, 8149-8177.

[3] JL Anderson, JK Dixon and JF Brennecke Acc. Chem. Res. 2007, 40, 1208-1216.

*The authors would like to thank Petróleo Brasileiro SA – PETROBRAS, Fundação para a Ciência e Tecnologia (FCT) and Ministério da Educação (CQFB Strategic Project PEst-C/EQB/LA0006/2011 and Project PTDC/QUI-QUI/098892/2008) for financial support. The NMR spectrometers are part of the National NMR Network (RNRMN) and are funded by FCT.*

#### OP122: Old Dog, New Tricks: Methodological NMR Developments to Characterize Solution-State Structure and Dynamics

Pieter ES Smith, Gonzalo A Álvarez, Noam Shemesh, Ger-shon Kurizki, \***Lucio Frydman**

*Department of Chemical Physics, Weizmann Institute of Science, Israel*

NMR utilizes a broad range of manipulations to probe relaxation effects over a broad range of conditions and scenarios – nanomaterials, rocks under the oceans, proteins, and disease in humans. One of the earliest and most widely used forms among these manipulations is the Carr-Purcell Meiboom-Gill sequence, proposed over a half century ago for removing inhomogeneous broadenings[1]. This sequence has found widespread use in NMR and MRI, thanks to its ability to free the evolution of a spin-1/2 from linear I<sub>z</sub> terms, like chemical shifts and inhomogeneity effects. We have recently introduced a new family of spin-echo sequences based on the *selective dynamical recoupling* (SDR) experiment, which although fulfilling  $\langle I_z \rangle = 0$  can still detect site-specific interactions like chemical shift, thanks to the presence of environmental fluctuations of common occurrence in high-field NMR – such as homonuclear spin-spin couplings, chemical exchange[2], or random diffusion.[3] It is conjectured that these new experiments can be used to characterized functionally relevant "invisible" states in exchanging proteins, and serve as new contrast agent for water in confined media.

#### References:

[1] Carr HY & Purcell EM Phys Rev 94(3):630 (1954); Meiboom S & Gill D Rev Sci Instrum 29(8):688 (1965).

[2] Smith PES, Bensky G, Álvarez GA, Kurizki G, Frydman, L. Proc. Natl. Acad. Sci. USA, 109, 5958 – 5961 (2012).

[3] Alvarez, G. A. ; Shemesh, N.; Frydman L; in preparation

Acknowledgments: BioNMR EU Grant #261863, EU ERC Advanced Grant # 246754, Fulbright Foundation (US)

#### Thursday – May 23<sup>rd</sup> New BioSolid Methods

Chair: Stanley Opella  
Room Ônix

#### OP123: Designing efficient re- and decoupling experiments for biological solid-state NMR using optimal control and effective Hamiltonian methods

\*Niels Christian Nielsen

*Aarhus University, Aarhus, Denmark*

Biological solid-state NMR spectroscopy to an increasing extent relies on a multitude of samples with different isotope-labeling patterns and pulse sequences capable of transferring magnetization between different spin species for assignment and establishment of constraints on structure and dynamics from high-resolution spectra. This calls for advanced re- and decoupling experiments providing optimal performance for the specific mode of operation.

In this presentation, we will describe systematic design of efficient re- and decoupling experiments for biological solid-state NMR designed using combinations of optimal control and effective Hamiltonian methods. Focus will be devoted to heteronuclear dipolar recoupling methods for recoupling of dipolar interactions between spins like <sup>1</sup>H, <sup>2</sup>H, <sup>13</sup>C, <sup>14</sup>N, and <sup>15</sup>N using optimal control pulse sequences[1] as well as optimal controlled inspired analytical sequences such as *RESPIRATION* CP[2] (and refined variants) and spin-state selective recoupling.[3] We will also present novel approaches for efficient heteronuclear decoupling using refocused CW (rCW) irradiation.[4,5]

[1] Wei, D.; Akbey, U.; Paaske, B.; Oschkinat, H.; Reif, B.; Bjerring, M.; Nielsen, N. C. J. Phys. Chem. Lett. 2011, 2, 1289.

[2] Jain, S.; Bjerring, M.; Nielsen, N. C. J. Phys. Chem. Lett. 2012, 3, 2020.

[3] Kehlet, C.; Nielsen, J. T.; Tosner, Z.; Nielsen, N. C. J. Phys. Chem. Lett. 2011, 2, 543.

[4] Vinther, J. M.; Nielsen, A. B.; Bjerring, M.; van Eck, E. R. H.; Kentgens, A. P. M.; Khaneja, N.; Nielsen, N. C. J. Chem. Phys. 2012, 137.

[5] Vinther, J. M.; Khaneja, N.; Nielsen, N. C. J. Magn. Reson. 2013, 226, 88.

#### OP124: Spectrally Edited 2D NMR of Carbon Materials and Proteins

<sup>1</sup>\*Klaus Schmidt-Rohr, <sup>1</sup>Robert L. Johnson, <sup>1</sup>Keith J. Fritzsche, <sup>2</sup>Jason Anderson, <sup>2</sup>Brent Shanks, <sup>1</sup>Mei Hong

<sup>1</sup>Department of Chemistry, Iowa State University,

<sup>2</sup>Department of Chemical and Biological Engineering, Iowa State University

Techniques for spectral editing of two-dimensional <sup>13</sup>C-<sup>13</sup>C correlation spectra of <sup>13</sup>C-enriched carbon materials and proteins will be presented. They remove peak overlap and greatly simplify spectral assignment.

Carbon materials produced from renewable feedstocks at moderate temperatures are attracting interest for various

applications, including catalyst supports and soil amendments/carbon sequestration. The aromatic-carbon region of their  $^{13}\text{C}$  NMR spectra often exhibits strongly overlapping bands from furans, arenes, and phenols. These can be separated by two complementary combinations of spectral editing with 2D  $^{13}\text{C}$ - $^{13}\text{C}$  NMR, applicable to materials made from  $^{13}\text{C}$ -enriched feedstocks such as  $\text{u-}^{13}\text{C}$  glucose. Exchange with protonated and nonprotonated spectral editing (EXPANSE) identifies protonated aromatics, selected by short cross polarization, and their nonprotonated bonding partners, selected by dipolar dephasing, while double-quantum/single-quantum NMR with dipolar dephasing of the double-quantum coherence selects bonded nonprotonated carbons. Both spectra are free of a diagonal ridge, which has many advantages; in particular, cross peaks on the diagonal can be detected. Combined with the chemical-shift information, this double spectral editing defines the local bonding environment.

Spectral editing techniques can also be used to simplify spectral assignment in  $^{13}\text{C}$ - $^{13}\text{C}$  spectra of uniformly  $^{13}\text{C}$ ,  $^{15}\text{N}$ -labeled proteins. CH selection by dipolar DEPT, and CN suppression by asymmetric  $^{15}\text{N}$ - $^{13}\text{C}$  REDOR dephasing have been implemented at sufficiently high MAS frequencies (10 kHz). For complete (<2%) suppression of rigid- $\text{CH}_2$  and CO-N signals, standard  $^1\text{H}$ - $^{13}\text{C}$  (in dipolar DEPT) and  $^{15}\text{N}$ - $^{13}\text{C}$  REDOR dephasing proved insufficient, but a lower and broader minimum in the dephasing curve was achieved by asymmetric REDOR with optimized  $180^\circ$  pulse position. The C=O region of the CN-free 2D spectrum contains only peaks of Asp and Glu, while the CH-selective 2D spectrum retains the signals of Ile, Leu, and Val. The experiments are demonstrated on a 56-residue model protein (GB1).

ACKNOWLEDGMENTS: NSF Engineering Center for Biorenewable Chemicals (CBiRC)

#### UP125: Recording Quantitative One- and Two-Dimensional $^{13}\text{C}$ NMR Spectra of Microcrystalline Proteins with Improved Sensitivity

1,2,3\*Piotr Tekely, <sup>1,3</sup>Rudra Narayan Purusottam, <sup>1,2,3</sup>Geoffrey Bodenhausen

<sup>1</sup>Ecole Normale Supérieure (ENS), <sup>2</sup>Centre National de la Recherche Scientifique (CNRS), <sup>3</sup>Université Pierre et Marie Curie (UPMC)

Recording sensitive and quantitative spectra of low- $\gamma$  nuclei such as  $^{13}\text{C}$  constitutes a long-standing challenge in solid-state NMR spectroscopy. The standard  $^{13}\text{C}$  spectra are inherently non-quantitative, i.e. showing the integrated signal intensities which are not proportional to the number of nuclei, when cross-polarization from protons to carbons is employed, or, if the relaxation rates are not equal, when the delay between successive acquisitions is too short to allow a uniform recovery of the longitudinal  $^{13}\text{C}$  magnetization in single-pulse experiments. The most pronounced distortions of intensities in the cross-polarization spectra are observed between proton-carrying carbons on the one hand, and carbonyl, carboxyl, or quaternary carbons on the other. Additional distortions can also arise because of local variations in internal mobility leading to variations in CP efficiency and/or rotating-frame relaxation rates.

We will show first quantitative  $^{13}\text{C}$  spectra of microcrystalline proteins with improved sensitivity as compared with single-pulse, fully relaxed spectra. The approach exploits the equilibration of  $^{13}\text{C}$  magnetization by low-power PARIS irradiation leading simultaneously to the efficient heteronuclear Overhauser enhancement. We will also show how to record sensitive, fully symmetric 2D homonuclear correlation spectra of microcrystalline proteins even at highest available static fields up to 23.5 T (1 GHz for protons).

#### UP126: Molecular interactions with the bacterial cell wall by liquid state, standard and DNP solid state NMR.

<sup>1</sup>Catherine Bougault, <sup>1</sup>Lauriane Lecoq, <sup>2</sup>Sabine Hediger, <sup>2</sup>Hiroki Takahashi, <sup>2</sup>Gaël De Paëpe, <sup>3</sup>Michel Arthur, <sup>1\*</sup>Jean-Pierre Simorre

<sup>1</sup>Institut de Biologie Structurale CEA-CNRS-UJF Grenoble, <sup>2</sup>Laboratoire de Chimie Inorganique et Biologique, CEA Grenoble, <sup>3</sup>Centre de Recherche des Cordeliers, INSERM, Paris

The cell wall is essential for the survival of bacteria. It gives the bacterial cell its shape and protects it against osmotic pressure, while allowing cell growth and division. It is made up of peptidoglycan (PG), a biopolymer forming a multi-gigadalton bag-like structure, and additionally in Gram-positive bacteria, of covalently linked anionic polymers called wall teichoic acids (WTA). TAs are thought to play important roles in ion trafficking, host-cell adhesion, inflammation and immune activation.

The machinery involved in the synthesis of this envelop is crucial and is one of the main antibiotic target. Different protein as transpeptidase, transpeptidase activator or hydrolase are recruited to maintain the morphogenesis of the peptidoglycan during the bacterial cell cycle. Based on few examples involved in the machinery of synthesis of the peptidoglycan, we will demonstrate that a combination of liquid and solid-state NMR can be a powerful tool to screen for cell-wall interacting proteins *in vitro* and *on cell*.

In particular, structure of the L,D-transpeptidases that results in  $\beta$ -lactam resistance in *M. tuberculosis*, has been studied in presence of the bacterial cell wall and in presence of antibiotic. The NMR study reveals new insights into the inhibition mechanism.

In parallel, we have investigated the potential of Dynamic Nuclear Polarization (DNP) to investigate cell surface directly in intact cells. Our results show that increase in sensitivity can be obtained together with the possibility of enhancing specifically cell-wall signals. It opens new avenues for the use of DNP-enhanced solid-state NMR as an on-cell investigation tool.

#### OP127: The HIPER project – Very High Sensitivity Pulse EPR

<sup>1\*</sup>Graham Smith, <sup>1</sup>Hassane El Mkami, <sup>1</sup>Paul Cruickshank, <sup>1</sup>Robert Hunter, <sup>1</sup>David Bolton, <sup>1</sup>Duncan Robertson, <sup>1</sup>Bela Bode, <sup>2</sup>Olav Schiemann, <sup>3</sup>Richard Wyde, <sup>4</sup>David Keeble, <sup>4</sup>David Norman

<sup>1</sup>University of St Andrews, Scotland, <sup>2</sup>University of Bonn, Germany, <sup>3</sup>Thomas Keating Ltd, Billingshurst England, <sup>4</sup>University of Dundee, Scotland

The HIPER project was originally funded in 2003 under the UK's Basic Technology program with the main technical aim of constructing a very high sensitivity, low dead-time, EPR spectrometer that would significantly improve on current state-of-the-art. This new spectrometer operates at 94 GHz at peak power levels of more than 1 kW with short pulses, high isolation, fast averaging capabilities, low dead-time and a wide instantaneous bandwidth of 1 GHz. Unlike traditional 94 GHz spectrometers that use small resonant cavities, this system uses non-resonant sample-holders with relatively large sample volumes that are comparable to those used in pulsed X-band measurements. This combination of high frequency, high power and relatively high sample volume can lead to a spectacular increase in concentration sensitivity for low dielectric loss samples. Gains approaching two orders of magnitude have been observed, for good glasses, relative to conventional X-band systems. Such gains in sensitivity combined with large instantaneous bandwidths are particularly beneficial for popular pulse EPR measurements such as PELDOR, commonly used to characterize large-scale structure in biomolecules, where it is not uncommon to average for 12-24 hours using standard X-band instrumentation. The new system reduces averaging times and allows samples to be measured with excellent signal to noise: at low sample concentrations, or with extended time windows to access longer

distances, or with selective orientation dependent excitations to quantitatively characterize the relative orientation of spin labels rigidly attached to proteins. In the talk, I will give examples, on a variety of biological systems, which clearly demonstrate these advantages and I will examine how pulse EPR (and DNP) instrumentation might evolve even further in the future.

**Thursday – May 23<sup>rd</sup>  
New BioNMR Methods**

Chair: Gisele Amorim  
Room Gávea A

**OP128: High Sensitivity Pulse Dipolar ESR and Protein Structure**

**\*Jack H. Freed**

*Department of Chemistry and Chemical Biology, Cornell University, Ithaca, New York, USA*

The importance of and requirements for high-sensitivity Pulse Dipolar ESR Spectroscopy (PDS) in measurements of distances in the 1 to 10 nm. range will be discussed. As projects in the determination of complex proteins structures become more challenging, increasing the sensitivity and accuracy is required. The relative virtues of double electron-electron resonance (DEER) and Double Quantum Coherence (DQC)-ESR in meeting these objectives is compared. It is shown how micromolar sensitivity is valuable both for dilute solutions and for accurate data analysis. The need for longer dipolar evolution times to measure longer distances in protein complexes is effectively addressed by the new technique of 5-pulse DEER, which can almost double such times. The application of such developments to protein structure is demonstrated in the cases of an integral membrane protein complex and of locating how a substrate penetrates into the active site of an enzyme. In the former, the sodium and aspartate symporter from *Pyrococcus hokoshii*, GLTPh which forms a trimer, has each protomer transporter function by alternating between outward-facing and inward-facing states. We showed that the conformational ensemble of protomers samples both states with nearly equal probabilities, indicative of comparable energies, and independently of each other. In the latter, we located (to  $2\sigma < 2\text{\AA}$  accuracy) how a lysoecithin spin-labeled on the polar-end, interacts with soybean seed lipooxygenase-1. The general approach we developed could be used to locate other flexible molecules in macromolecular complexes.

ACKNOWLEDGEMENTS: Co-workers: Peter Borbat, Elka Georgieva, Betty Gaffney, and Olga Boudker. Support from NIH/NIGMS Grant P41GM103521 and NIH/NIBIB Grant R01EB003150.

**OP129: Harnessing the Synergies between NMR and Computation for the Understanding of Protein Function**

<sup>1,2</sup>Mioara Larion, <sup>1,2,3</sup>Roberto Salinas, <sup>4</sup>Vitali Tugarinov, <sup>1,2</sup>Dawei Li, <sup>1,2</sup>Dong Long, <sup>1,2</sup>Yina Gu, <sup>2</sup>Lei Bruschweiler-Li, <sup>1</sup>Brian Miller, <sup>1,2\*</sup>**Rafael Brüschweiler**

<sup>1</sup>*Department of Chemistry and Biochemistry, Florida State University*, <sup>2</sup>*National High Magnetic Field Laboratory, Tallahassee, FL*, <sup>3</sup>*Institute of Chemistry, University of São Paulo*, <sup>4</sup>*Department of Chemistry and Biochemistry, University of Maryland*

Glucokinase (GCK) is a 52 kDa monomeric enzyme that catalyzes the rate-limiting step of glucose catabolism in the pancreas. GCK is allosterically regulated by glucose, a feature that allows the enzyme to function as the body's glucose sensor. Over 600 mutations were identified in human *glk* gene, some of which lead to protein activation causing persistent hypoglycemic hyperinsulinemia of infancy (PHHI). Wild-type GCK displays a characteristic sigmoidal response in its enzymatic glucose phosphorylation rate to increasing

glucose concentrations in the blood stream, while activating variants as well as the small molecule therapeutics abolish this kinetic cooperativity and lead to a hyperbolic kinetic profile. Despite nearly a half-century of research, the mechanistic basis for GCK's homotropic allostery remains unresolved. 17 selectively <sup>13</sup>C $\delta$ 1-labeled isoleucine methyl groups and 3 <sup>15</sup>N $\epsilon$ 1-labeled tryptophan side chains were assigned and used as sensitive NMR probes to monitor the spatial and temporal behavior of GCK and its mutants in the absence and presence of glucose. It is found that the small GCK domain is intrinsically disordered, while both small-molecule diabetes therapeutic agents and hyperinsulinemia-associated GCK mutations display a population shift toward a narrow, well-ordered ensemble resembling the glucose-bound conformation. The NMR data suggest that GCK generates its cooperative kinetic response at low glucose concentrations by using a millisecond disorder-order cycle of the small domain as a "time-delay loop", which is bypassed at high glucose concentrations, providing a unique mechanism to allosterically regulate the activity of human glucokinase under physiological conditions. We will also discuss recent progress in the characterization of protein dynamics on fast and slow time scales by the combined interpretation of molecular dynamics computer simulations and NMR chemical shifts with the recent protein chemical shift predictor PPM (<http://spinportal.magnet.fsu.edu/ppm/ppm.html>).

ACKNOWLEDGEMENTS: The National Science Foundation, the National Institutes of Health, and the American Heart Association.

**UP130: A unified conformational selection and induced fit approach to the modelling of protein-peptide interactions.**

Mikael Trellet, Adrien Melquiond, **\*Alexandre M. J. J. Bonvin**

*Utrecht University, Faculty of Science, Bijvoet Center*

Protein-protein interactions are vital for all cellular mechanisms. Among those, peptide-mediated interactions contribute up to 40% of all protein-protein interactions. Due to their important role in regulatory and signalling processes, peptides are in many cases implicated in diseases. They are also known to block protein-protein interactions, which makes them interesting leads for protein drug design.

Despite the large amount of structural data available, it remains very challenging to predict protein-peptide interactions by homology modelling. This leaves biomolecular docking as one of the few amenable computational technique to predict these interactions. Yet, the intrinsic flexibility of peptides is a major obstacle for any modelling technique. Docking methods are sensitive to conformational changes and generally require high-resolution structures and/or knowledge of the bound form to perform well. However, it is possible to narrow down the uncertainty by using information to drive the search, allowing concentrating on further refining the conformation of the peptide at the interface.

We have developed HADDOCK (<http://haddock.science.uu.nl>), a flexible information-driven docking program that distinguishes itself from others by the use of experimental and/or bioinformatics data to drive the modelling process [1]. HADDOCK has been widely applied to model 3D structures of protein-protein and protein-nucleic acids complexes and has also demonstrated strong performance in CAPRI, a blind experiment for the prediction of biomolecular interactions. We will present recent results on the application of HADDOCK to protein-peptide modelling using a benchmark of 103 complexes [2]. In the absence of information on the bound form of the peptide, we achieve near-native predictions for 80% of the benchmark by combining the concepts of conformational selection and induced fit into our flexible docking approach.

References:

[1] de Vries S et al. (2007). Proteins: Struc. Funct. & Bioinformatic, 69, 726-733.

[2] London N et al. (2009). Structure, 18, 188-199.

#### UP131: Replica Averaging-Replica Exchange (RARE) Molecular dynamics simulations with NMR chemical shifts

\*Carlo Camilloni, Andrea Cavalli, Michele Vendruscolo

University of Cambridge

Solving the behaviour of proteins from the point of view of statistical mechanics, involves the calculation of the Boltzmann ensemble. A major goal in the study of complex molecular systems is the generation of ensembles of conformations that represent their Boltzmann distributions. The observable properties of these systems can be then predicted by calculating averages over such ensembles. In principle, given accurate energy functions and efficient sampling methods, the ensembles can be generated. In practice, however, often the energy functions are known only approximately and the sampling can be carried out only in a limited manner. We describe here a method that simultaneously enables to increase both the accuracy of the energy and the extension of the sampling. The method incorporates experimental data as structural restraints in molecular dynamics simulations and exploits the replica exchange approach in the well-tempered ensemble metadynamics framework. We illustrate the method in the case of a peptide and show that it enables its free energy landscape to be generated accurately using only backbone NMR chemical shifts.

#### OP132: Extending the Empirical Limits of Chemical Shifts

Yang Shen, Alex Maltsev, Alexey Mantsyzov, Jinfa Ying, \*Ad Bax

Laboratory of Chemical Physics, NIDDK, NIH

NMR chemical shift assignments are often easily obtained and contain important local information regarding biomolecular structure. Our original approach to take advantage of this approach was based on a simple *ad hoc* database search to find small, 3-residue fragments that best match the secondary chemical shifts and residue types of the query segment, culminating in the TALOS program.[1] This program provided  $\varphi$  and  $\Psi$  torsion angle information for about 70% of the residues, with an error rate  $<3\%$ . A subsequent filtering of the TALOS output, using an artificial neural network (ANN) derived relation between chemical shifts, residue type, and approximate region of Ramachandran space, allowed extension of predictions to ca 85%, culminating in the TALOS+ program.[2] The remaining 15% for which angles could not be identified are all in regions outside of regular secondary structure, and therefore the hardest to identify from regular NMR parameters. By further extending both the size of the fragment and the database, and by converting the search to an almost entirely ANN-based approach, we have reduced the fraction of residues whose backbone angles cannot be determined to 10%, without increasing the error rate. This TALOS-N program also provides  $\chi_1$  angle information for approximately half of the residues, with an error rate smaller than 10%. Application to the study of the structure of an intrinsically disordered protein,  $\alpha$ -synuclein, shows significant residue-by-residue variation, despite very small secondary chemical shifts.

[1] Cornilescu, G.; Delaglio, F.; Bax, A. Protein backbone angle restraints from searching a database for chemical shift and sequence homology J. Biomol. NMR 1999, 13, 289-302.

[2] Shen, Y.; Delaglio, F.; Cornilescu, G.; Bax, A. TALOS+: a hybrid method for predicting protein backbone torsion angles from NMR chemical shifts J. Biomol. NMR 2009, 44, 213-223.

Thursday – May 23<sup>rd</sup>

Bio-Solids

Chair: Mônica Freitas

Room Gávea B

#### OP133: Type-III secretion needles studied by solid-state NMR

<sup>1</sup>Jean-Philippe Demers, <sup>1</sup>Antoine Loquet, <sup>1</sup>Veniamin Shevelkov, <sup>2</sup>Nikolaos Sgourakis, <sup>3</sup>Rashmi Gupta, <sup>3</sup>Michael Kolbe, <sup>1</sup>Karin Giller, <sup>1</sup>Dietmar Riedel, <sup>1</sup>Christian Griesinger, <sup>2</sup>David Baker, <sup>1</sup>Stefan Becker, <sup>1\*</sup>Adam Lange

<sup>1</sup>Max Planck Institute for Biophysical Chemistry, Göttingen, Germany, <sup>2</sup>Department of Biochemistry, University of Washington, USA, <sup>3</sup>Max Planck Institute for Infection Biology, Berlin, Germany

Type-III secretion systems (T3SS) are molecular machines found in Gram-negative bacteria that transfer virulence factors to the cytosol of host cells. Based on 2D solid-state NMR experiments recorded on uniformly, [1-<sup>13</sup>C]-glucose and [2-<sup>13</sup>C]-glucose labeled samples, we have obtained the 95%-complete assignment of <sup>13</sup>C and <sup>15</sup>N chemical shifts for the T3SS needle of *Shigella flexneri*, responsible for bacillary dysentery (Demers et al, PLOS Pathogens, 2013, accepted). Very sharp <sup>13</sup>C line-widths are observed, ranging from 0.3 to 0.6 ppm in the uniformly labeled sample and from 0.1 to 0.4 ppm in sparsely labeled samples. Only the first 3 N-terminal residues are flexible; in contrast to the crystal structure of monomeric needle protein where the first 14 N-terminal residues are disordered (Deane et al, PNAS, 2006). The secondary structure consists of a kinked  $\alpha$ -helix (L12 to A38), a loop (E39 to P44) and a second  $\alpha$ -helix which extends up to the C-terminus (Q45 to R83). Although rigid, the N-terminal segment from S2 to T11 does not adopt any conventional secondary structure. The solid-state NMR data have been compared in detail with a recent state-of-the-art high-resolution cryoEM map of the *Shigella* needle (Fujii et al, PNAS, 2012). The secondary structure elements are highly similar to those identified in the homologous needle protein of *Salmonella typhimurium* for which we have recently determined an atomic model (Loquet et al, Nature, 2012), allowing us to propose a common structural architecture for T3SS needles. Furthermore, we discuss *in vivo* data that show the biological relevance of the solid-state NMR structural data. Finally, we will present proton-detected solid-state NMR experiments on perdeuterated T3SS needles. A set of 2D and 3D experiments on such samples was used for the unambiguous assignment of the backbone resonances.

#### OP134: Solid-State NMR Structural Studies of Proteins Using Paramagnetic Probes

<sup>1</sup>Ishita Sengupta, <sup>1</sup>Philippe S. Nadaud, <sup>1</sup>Min Gao, <sup>1</sup>Rajith J. Arachchige, <sup>2</sup>Charles D. Schwieters, <sup>1\*</sup>Christopher P. Jaroniec

<sup>1</sup>The Ohio State University, Columbus, USA, <sup>2</sup>National Institutes of Health, Bethesda, USA

Structural studies of proteins by magic-angle spinning solid-state NMR are hampered by the relative shortage of dipolar coupling based restraints corresponding to distances significantly exceeding 5 Å that can be reliably determined using conventional techniques. This paucity of long-distance structural data can be circumvented by extending the studies to include structural analogs of the protein of interest, intentionally modified to contain covalently-attached paramagnetic tags at selected sites. In such paramagnetic proteins, the dipolar couplings between the nuclear spins and the unpaired electrons of the tag can manifest themselves in NMR spectra in the form of nuclear dipolar shifts or relaxation enhancements that depend on the electron-nucleus distance and can be considerable for nuclei located up to 20 Å away from the paramagnetic center. I will discuss our recent progress in the studies of proteins using paramagnetic solid-state NMR techniques. The topics will include the rapid backbone fold

refinement for the model protein GB1 using only 4-5 longitudinal  $^{15}\text{N}$  PRE restraints per residue recorded using a set of cysteine EDTA-Cu(II) variants and backbone dihedral angle restraints derived from  $^{13}\text{C}$  and  $^{15}\text{N}$  chemical shifts, and the development of improved Cu(II)-binding tags for this type of structural analysis.

**ACKNOWLEDGMENTS:** This research was supported by US National Science Foundation grants MCB-0745754 (CA-REER Award) and MCB-1243461 to C.P.J.

#### UP135: 100 kHz Magic-Angle Spinning for Proteins

<sup>1</sup>\*Beat H. Meier, <sup>2</sup>Ago Samoson, <sup>3</sup>Anja Böckmann, <sup>1</sup>Matthias Ernst, <sup>1</sup>Vipin Agarwal, <sup>2</sup>Marie-Laure Fogeron, <sup>1</sup>Matthias Huber, <sup>1</sup>Susanne Penzel, <sup>1</sup>Francesco Ravotti

<sup>1</sup>ETH Zurich, Physical Chemistry, Switzerland, <sup>2</sup>Tallinn University of Technology, Estonia, <sup>3</sup>IBCP, CNRS, Lyon, France

We report protein spectra obtained at 100 kHz MAS and describe the hardware requirements as well as spectroscopic techniques adapted to these MAS frequencies that significantly exceed the magnitude of the individual dipolar couplings.

Despite the small sample amounts - less than 500 micrograms of protein- well resolved HSQC spectra with good signal-to-noise ratio can be acquired in 10 minutes from deuterated and fully protonated (at the exchangeable positions) or from fully protonated proteins, using proton detection and exploiting the long proton  $T_2$ 's at 100 kHz MAS. A detailed investigation of proton  $T_2$  and  $T_2'$  values as a function of the MAS frequency is presented.

Even at 100 kHz MAS, homogenous contributions to the linewidth (in the sense of Maricq and Waugh) are present. We characterize them and discuss schemes to average them, e.g. in the context of heteronuclear decoupling. Particularities arising for MAS at 100 kHz and above are discussed. Under these conditions, decoupling is most efficiently implemented as low-power sequences, which allow to further improve the signal-to-noise due the reduced interscan delays, in particular if integrated in experiments where all the different periods of the multidimensional experiments are implemented as low-power versions. We discuss the performance of different schemes and introduce a new decoupling sequence to further reduce the linewidth in the carbon and nitrogen dimensions.

These techniques open the perspective for investigations of structure and dynamics of proteins using submilligram amounts of protein, facilitating sample preparation, e.g. by cell-free expression.

#### UP136: Determining supramolecular organisation of ion channels by solid-state NMR and computational methods

<sup>1</sup>\*Markus Weingarth, <sup>1</sup>Elwin van der Cruysen, <sup>1,2</sup>Alexander Prokofyev, <sup>1</sup>Eline Koers, <sup>1</sup>Alexandre M. J. Bonvin, <sup>2</sup>Olaf Pongs, <sup>1</sup>Marc Baldus

<sup>1</sup>Utrecht University, Bijvoet Center for Biomolecular Research, Utrecht, The Netherlands, <sup>2</sup>Saarland University, Faculty of Medicine, Department of Physiology, Homburg, Germany

Protein supramolecular structure invokes the conformation beyond a single protein. While the protein is held together by intramolecular forces comprising strong interactions like covalent bonds, supramolecular structures are often composed of weaker intermolecular contacts. The latter ones confer great diversity and sensitivity to their environment upon these multi-molecular arrangements.

Membrane protein are exposed to a particularly complex habitat which crucially modulates protein structure and functions, however, the molecular basis of such modulations is

hitherto poorly understood. What is more, its transient character renders the study of membrane protein supramolecular organization experimentally very challenging.

Using the potassium channels KcsA and KcsA-Kv1.3 as examples, we demonstrate how the combination of solid-state NMR and computational approaches, assisted by electrophysiological measurements, allows dissecting various aspects of membrane protein supramolecular structure, including, *inter alia*, annular and non-annular protein – lipid binding, the influence of structural water or protein – protein interactions in membranes.

#### OP137: Membranes, crystals, sediments: solid-state NMR of large proteins

<sup>1</sup>\*Anja Böckmann, <sup>2</sup>Beat H. Meier, <sup>1</sup>Britta Kunert, <sup>2</sup>Andreas Hunkeler, <sup>2</sup>Susanne Penzel, <sup>2</sup>Anne Schütz, <sup>1</sup>Laurent Terradot Alexandre Bazin, <sup>1</sup>Pierre Falson, <sup>3</sup>Jean-Michel Jault, <sup>1</sup>Carole Gardienet

<sup>1</sup>Institut de Biologie et Chimie des Protéines, CNRS-Université de Lyon, France, <sup>2</sup>ETH Zürich, Physical Chemistry, CH-8093 Zürich, Switzerland, <sup>3</sup>IBS, CNRS-CEA-Université de Grenoble, France

Solid-state NMR is an increasingly powerful tool to characterize challenging proteins. Notably, it can analyze an astonishing variety of states, as proteins inserted in membranes, crystals and simple sediments. Combined with other biophysical approaches, NMR thus gives unique insight into protein structure, and ultimately function. We will illustrate this with two examples.

DnaB is a helicase from *Helicobacter pylori*. It is believed to function as a dodecamer, each subunit having a molecular mass of 55.7 kDa (488 residues). While EM has revealed the envelope of the multimer, high-resolution structures could only be obtained for the isolated N-terminal and C-terminal parts. Indeed, the entire protein today only yields poorly diffracting crystals, which however give rise to highly resolved NMR spectra. This allowed us to compare the fingerprints from the isolated domains to the functional protein. Also, DnaB has different interaction partners, which however do not co-crystallize. We recently showed that sedimentation can be used as sample preparation, and illustrate how this approach can be a promising possibility to study such proteins and their partners.

BmrA is a membrane protein of the class of ABC transporters. It functions as a dimer of 2x 64.5 kDa (589 residues). It is a close bacterial homologue of the P-glycoprotein, which is involved in multidrug resistance in humans. In order to obtain stable preparations showing a high protein/lipid ratio of BmrA for solid-state NMR studies, we reconstituted it in its native lipids extracted from *B. subtilis*. The obtained samples yield very good signal/noise ratio and linewidths, which do not correlate with sample homogeneity as analyzed by EM. The possibility to prepare the protein under different conditions in a lipid environment will allow to gain insight in the conformational changes between the open, closed and drug-bound states.

**ACKNOWLEDGEMENTS:** CNRS, ANR, SNF, CEA

**Thursday – May 23<sup>rd</sup>**  
**Contrast Agents/ Instrumentation**

Chair: Carlos Geraldes  
Rooms Turmalina/Topázio

#### OP138: New Directions in Dipolar Imaging to Enhance Endogenous Contrast

\*Warren S. Warren, Thomas Theis, Yi Han, Zijian Zhou  
Duke University

For decades, the classical or mean-field picture describing the distant dipolar field (and the coupled spin picture described

by intermolecular multiple quantum coherences (iMQCs)) has always simplified to an effective internuclear coupling proportional to  $I_{zi}I_{zj}$ , differing only by a scale factor of 1.5 for homomolecular (identical resonance frequency) and heteromolecular interactions. We show both theoretically and experimentally that the mathematical framework needs to be modified for modern applications such as imaging. We demonstrate new pulse sequences which produce unexpected effects; for example, modulating an arbitrarily small fraction of the magnetization can substantially alter the frequency evolution, so matched gradient pulse pairs (a seemingly innocuous module in thousands of existing pulse sequences) can alter the time evolution in highly unexpected ways. We also demonstrate improved multiple echo sequences, optimized for fatty tissue imaging.

This approach provides a novel method for imaging local anisotropy in tissue: we model a slab of brain tissue (for example) as if it were a container of water with an irregular boundary, and then compare observed and predicted iDQC images to measure the "dipolar surprisal". A similar method is valuable for enhance field perturbations due to SPIONS, long-lived hyperpolarized agents, or other contrast mechanisms.

ACKNOWLEDGEMENTS: NSF, NIH NIBIB

### OP139: Capturing Signals from Ultrafast Relaxing Spins with SWIFT MRI

\*Michael Garwood

*Center for Magnetic Resonance Research, University of Minnesota, USA*

This presentation focuses on a radically different approach to MR imaging called SWIFT (sweep imaging with Fourier transformation). SWIFT exploits simultaneous or time-shared excitation and acquisition to preserve signals from spins with extremely short transverse relaxation times,  $T_2$  and  $T_2^*$ . In SWIFT, spins are excited using a frequency sweep to minimize the peak RF power needed to excite a broad and uniform response in the presence of the encoding gradient. With SWIFT, time domain data (k-space) is created from FIDs acquired in a radial manner (i.e., with spokes radiating out from  $k = 0$ ).  $T_1$ -weighting can be produced by appropriately setting the flip angle and repetition time (TR), like in conventional gradient echo (GRE) imaging. However, SWIFT avoids bias from  $T_2$  or  $T_2^*$ -weighting because there is no echo time (TE). The latter feature is being exploited in dynamic contrast-enhanced (DCE) MRI to minimize  $T_2^*$ -bias in the shape of the time-intensity curve and thus to improve estimates of perfusion parameters using pharmacokinetic modeling. Furthermore, SWIFT preserves frequency-shifted signals in the vicinity of magnetic objects. For example, magnetically labeled nanoparticles (e.g., SPIOs), which cause signal voids in GRE images, give rise to positive contrast (bright spots) in SWIFT images. The latter capability is being exploited to track cells, identify therapeutic targets (eg, cancer-specific receptors), and to predict therapeutic efficacy using magnetic fluid hyperthermia for cancer treatment. Finally, rather unexpectedly, with SWIFT small magnetic susceptibility variations in tissues give rise to frequency shifts that manifest as phase contrast, like that seen in GRE images. Phase contrast is obtained with SWIFT despite the lack of echo ( $TE=0$ ) and can be visualized without image post-processing (ie, no need for phase-unwrapping algorithms or high pass filtering). In summary, SWIFT is a new tool with many promising prospects for expanding the capabilities of MRI.

ACKNOWLEDGEMENTS: NIH P41 EB15894, Keck Foundation, Komen Foundation

### UP140: Molecular imaging of tumors using CEST MRI of 2DG and FDG

<sup>1</sup>Michal Rivlin, <sup>2</sup>Galia Tzarfaty, <sup>1</sup>Judith Horev, <sup>1</sup>Ilan Tzarfaty, <sup>1\*</sup>Gil Navon

<sup>1</sup>Tel Aviv University, <sup>2</sup>Chaim Sheba Medical center

The chemical exchange saturation transfer (CEST) NMR method enables to detect low concentrations of metabolites that contain residues with exchangeable protons such as amine, amide or hydroxyl. The enhanced sensitivity allows obtaining images of relatively low concentrations of endogenous cellular components or exogenous agents by MRI. 2-deoxyglucose (2DG) and 2-fluoro deoxyglucose (FDG) are two glucose analogues that are taken up by cells through the glucose transporter, they undergo phosphorylation catalyzed by hexokinase but unlike glucose they and their metabolic products accumulate in the cells. The increased glycolysis characteristic of cancer has led to the use of the positron emitter 18-FDG for the PET imaging of tumors and their metastases.

In the present work we demonstrate that xerograph breast tumors in mice can be imaged with high level of contrast using CEST of either 2DG or FDG. During the first 30 min following 2DG or FDG i.v. injection the CEST at the tumors increased gradually, reaching values of over 25% and then remained constant for more than 2 hours. The 2DG-CEST tumor images were similar to the optical and two photon images of the mCherry/2-NBDG labeled tumor cells.

The accumulation of 2DG6P and FDG6P and their phosphorylated metabolic products in the tumors was quantitatively measured using <sup>31</sup>P NMR spectroscopy of the extracted tumors. The concentration of these metabolites was found to exceed 13mM across the total tumor volume. Thus 2DG/FDG CEST MRI has the potential to replace FDG-PET for the detection of tumors and metastases, distinguishing between malignant and benign tumors and monitoring tumor response to therapy, without the need for radio-labeled isotopes.

### UP141: Physiological Model for the Determination of rCMR(O<sub>2</sub>) and rCBF by <sup>17</sup>O MRI in the Human

\*Daniel Fiat

*University of Illinois at Chicago*

A novel physiological model was developed that allows to replace the previous method which required <sup>17</sup>O NMR measurements of arterial blood. The model provides H<sub>2</sub><sup>17</sup>O concentrations in the body organs, including the brain, the veins and the arteries as a function of rCMR(O<sub>2</sub>) and rCBF. A least square fit of the model as a function of rCMR(O<sub>2</sub>) and rCBF to <sup>17</sup>O MRI data allows the determination of rCMR(O<sub>2</sub>) and rCBF.

Previously determination of Regional cerebral Metabolic Rate of Oxygen (rCMR(O<sub>2</sub>)) and Regional Cerebral Blood Flow (rCBF) was carried out by measurement of <sup>17</sup>O signal intensity by <sup>17</sup>O MRI and the measurement of H<sub>2</sub><sup>17</sup>O concentrations in the arterial blood as a function of <sup>17</sup>O inhalation time during the inhalation and washout periods. H<sub>2</sub><sup>17</sup>O concentration measurements in arterial blood were carried out by <sup>17</sup>O NMR of blood samples withdrawn from the arteries.

For the following reasons it was desired to find alternative methods:

- 1) Withdrawal of blood from the arteries, although considered safe, involves discomfort to the patient and requires skilled physician.
- 2) Ideally the NMR measurements should be carried out during the inhalation study to correspond to the time of measurement of H<sub>2</sub><sup>17</sup>O cerebral concentrations by <sup>17</sup>O MRI as the metabolism of oxygen in the red blood cells continues to some extent in the test tube. This requires the use of MRI and NMR equipment during the inhalation study.

The basic equations utilized for the determinations of rCMR(O<sub>2</sub>) and rCBF using arterial experimental values as well as the model equations and the model algorithm will be described.

The results of the data analysis by means of the model algorithm will be presented.

The results conform with accepted literature values for the whole brain.

#### OP142: Magnetic Susceptibility Contrast in Human Brain

\***Jeff Duyn**, Peter van Gelderen, Pascal Sati, Afonso Silva, Daniel Reich, Hellmut Merkle, Jacco de Zwart

*Laboratory of Functional and Molecular Imaging, National Institutes of Health, Bethesda*

At high magnetic field strength (7T and above), *in vivo* MRI can visualize human brain structure in exquisite detail. An important aspect of high field MRI is the increased magnetic susceptibility contrast, which is originates from the subtle differences in the extent to which brain tissues becomes magnetized by application of an external magnetic field. This type of contrast allows visualization of neuroanatomical structure not otherwise visible by imaging and has catalyzed the development of methods to map magnetic susceptibility distributions *in vivo*. In this presentation, we will review the major contributors to magnetic susceptibility contrast, with a focus on observations in white matter. Specifically, contributions of iron, myelin and deoxyhemoglobin will be discussed. In addition it will be discussed how axonal fiber bundles may introduce orientation-dependent contrast that, under certain conditions, allows the distinction of intra-and extra cellular water.

**Thursday – May 23<sup>rd</sup>**  
**Physics**

Chair: Jose Schneider  
Room Ònix

#### OP143: Dynamics and Quantum Information Transport in Nuclear Spin Chains

\***Paola Cappellaro**

*Massachusetts Institute of Technology*

A promising approach toward a scalable quantum information processor is a distributed architecture, where quantum spin wires connect small computational nodes. Coherent transmission of quantum information over short distances is enabled by internal couplings among spins, ideally aligned in a one-dimensional (1D) chain.

Similarities between the transport properties of pure and mixed-state chains enable protocols for the perfect transfer of quantum information and entanglement in mixed-state chains [1].

Owing to their unique geometry, nuclear spins in apatite crystals provide an ideal test-bed for the experimental study of quantum information transport, as they closely emulate an ensemble of 1D spin chains. In this talk I will describe how NMR techniques can be used to drive the spin chain dynamics and probe the accompanying transport mechanisms.

Recently, we demonstrated initialization and read-out capabilities in these spin chains, even in the absence of single-spin addressability [2]. It thus becomes possible to explore experimentally the effects of discrepancy from the ideal 1D nearest-neighbor coupling model and the perturbation due to the interaction of the chains with the environment [3,4].

#### References

- [1] P. Cappellaro, L. Viola and C. Ramanathan, Phys. Rev. A 83, 032304 (2011).
- [2] G. Kaur and P. Cappellaro, New J. Phys. 14, 083005 (2012).
- [3] W. Zhang, P. Cappellaro, N. Antler, B. Pepper, D. G. Cory, V. V. Dobrovitski, C. Ramanathan and L. Viola, Phys. Rev. A 80, 052323 (2009).
- [4] C. Ramanathan, P. Cappellaro, L. Viola and D. G. Cory, New J. Phys. 13, 103015 (2011).

#### OP144: Loschmidt Echoes as Quantifiers of Decoherence, Quantum Phase Transitions and Thermalization in Interacting Spin Systems

<sup>1,2</sup>\***Horacio M. Pastawski**, <sup>1,2</sup>Patricia R. Levstein

<sup>1</sup>*LaNIS de RMS, Instituto de Física Enrique Gaviol (CONICET-UNC)*, <sup>2</sup>*Facultad de Matemática Astronomía y Física, Universidad Nacional de Córdoba*

The Loschmidt Echo [LE] is the amount of signal recovered from a spreading or decaying excitation after an imperfect time reversal procedure [1]. As such, it recognizes a first NMR antecedent in the Hahn Echo and followed by the Magic Echo, the Polarization Echo and the Multiple Quantum Coherence experiments. In crystals with dipolar interacting spins it has allowed us to quantify the decoherence induced by uncontrolled environment or experimental errors [2]. Notably complex many-body dynamics makes the system particularly sensitive to environmental disturbances beyond a small threshold [3]. In this talk, I will summarize, at a tutorial level, the experimental and theoretical results of our group on the LE that fueled the fields of quantum chaos, quantum optics and classical-quantum correspondence [4]. This also will lead us to discuss situations where swiping the environment strength induces non-analytic changes in the dynamical behavior, i.e. quantum dynamical phase transition [QDPT] [5]. In a spectral analysis a QDPT manifest as the collapse of two spectral lines into a short-lived and long-lived state with the same frequency. We briefly discuss how these long-lived states are now helping to design quantum memories [6]. More recently, we have shown that, by filtering trivial parts in the dynamics [6], the numerical evaluation of the LE can be a useful tool to assess thermalization in interacting many-body systems.

[1] Environment-independent decoherence rate in classically chaotic systems. R. Jalabert and HMP, Phys. Rev. Lett. 86, 2490 (2001)

[2] Attenuation of polarization echoes in NMR: A test for the emergence of Dynamical Irreversibility in Many-Body Quantum Systems. P.R. Levstein, G. Usaj, HMP, J. Chem. Phys. 108, 2718 (1998)

[3] A Nuclear Magnetic Resonance answer to the Boltzmann-Loschmidt controversy? HMP, G. Usaj, P. R. Levstein, J. Raya and J. Hirschinger. Physica A 283 166 (2000)

[4] Loschmidt Echo A. Gousev, R.A. Jalabert, HMP and D.A. Wisniacki. Scholarpedia 7, 11687 (2012) [http://www.scholarpedia.org/article/Loschmidt\\_echo](http://www.scholarpedia.org/article/Loschmidt_echo)

[5] Environmentally induced quantum dynamical phase transition in the spin swap operation, G.A.Álvarez, E.P.Danieli, P.R. Levstein, and HMP, J. Chem.Phys. 124, 1 (2006)

[6] Unforgeable noise-tolerant quantum tokens, F. Pastawski, N. Y. Yao, L. Jiang, M.D. Lukin, and J. I. Cirac, PNAS 109 (40) 16079 (2012)

[6] Loschmidt echo as a robust decoherence quantifier for many-body systems P.R. Zangara, A.D. Dente, P.R. Levstein, and HMP, Phys. Rev. A 86, 012322 (2012)

#### UP145: Origin of Long-Lived Signals in Dipolar Coupled Spin Systems

<sup>1</sup>\***Alexej Jerschow**, <sup>1</sup>Jae-Seung Lee, <sup>2</sup>Anatoly Khitrin

<sup>1</sup>*New York University*, <sup>2</sup>*Kent State University*

One typically assumes that one cannot excite narrow lines in a system with a high degree of dipolar broadening. Nevertheless, several examples of this effect were shown in liquid crystals, polymers, and ordinary solids by applying a long and weak rf irradiation (we call this signal long-lived response – LLR) [1-4]. Most recently, such signals were also excited in samples of cortical and trabecular bone [5]. Such long-lived signals would naturally be of great utility in imaging rigid samples, or rigid tissue components.

In this paper, we describe how these long-lived signals may arise as a consequence of the direct excitation of highly correlated states. In the presence of small chemical shift differences, cancellations between certain spin operators no longer occur (e.g. between terms  $I_{ij}I_{jz}$  and  $I_{iz}I_{jy}$ ), and a narrow signal could be seen. After the end of the LLR irradiation, highly correlated terms of the type  $I_{ij}I_{jz}I_{kz}I_{mz}...$  can be converted into observable magnetization by successive action of the dipolar couplings between spin  $i$  and other spins involved in this correlated term. This approach may also explain why highly-correlated terms lead to long-lived signals, since, e.g. dipolar couplings between any  $j, k, m, ...$  spins leave the term  $I_{ij}I_{jz}I_{kz}I_{mz}$  intact.

These simulations point to the fact that the experimentally observed long-lived signals are most likely due to the generation of these highly correlated spin terms. Experiments highlighting the unusual character of the excited signals will be shown as well.

#### References:

- [1] A.K. Khitrin, J. Magn. Reson. 213 (2011) 22-25.
- [2] A.K. Khitrin, J. Chem. Phys. 134 (2011) 154502-154509.
- [3] A.K. Khitrin, V.L. Ermakov, and B.M. Fung, J. Chem. Phys. 117 (2002) 6903-6906.
- [4] A.K. Khitrin, V.L. Ermakov, and B.M. Fung, Chem. Phys. Lett. 360 (2002) 161-166.
- [5] B. Zhang, J.-S. Lee, A. Khitrin, A. Jerschow, 2012, arXiv:1209.4030 [physics.med-ph], <http://arxiv.org/abs/1209.4030>.

#### UP146: High Resolution Para-Hydrogen Induced Polarization (PHIP) in Inhomogeneous Magnetic Fields

<sup>1,2\*</sup>Lisandro Buljubasich, <sup>1,2</sup>Ignacio Prina, <sup>3</sup>María Belén Franzoni, <sup>3</sup>Kerstin Münnemann, <sup>3</sup>Hans Wolfgang Spiess, <sup>1,2</sup>Rodolfo Héctor Acosta

<sup>1</sup>FAMAF – Universidad Nacional de Córdoba, <sup>2</sup>IFEG – CONICET, <sup>3</sup>Max Plank Institut für Polymerforschung

The application of parahydrogen for the generation of hyperpolarization has increased continuously during the last years. When the chemical reaction that deposits the parahydrogen atoms into the target molecule is carried out at the same field as the NMR experiment (PASADENA protocol [1]) an anti-phase signal is obtained, with a separation of the resonance lines of only a few Hz. This imposes a stringent limit to the required homogeneity of the magnetic field in order to avoid signal cancellation. In this work we show that the spectrum of the PHIP signal acquired with a Carr-Purcell-Meiboom-Gil (CPMG) sequence, referred to as *J*-Spectroscopy [2-4], not only presents an enhanced spectral resolution compared to standard the NMR-spectrum, but also avoids partial peak cancellation.

Experimental and numerical simulations concerning the hydrogenation of Hexene with parahydrogen in PASADENA conditions are presented. Acquisition with a digital filter is used to select a desired multiplet, namely a partial *J*-Spectrum acquisition [3]. The performance of the method is tested on a thermally polarized sample, showing that the corresponding partial *J*-Spectra are unaffected by large inhomogeneities in the polarizing magnetic field. Finally, limitations and applicability of the method to obtain either spectral information of the sample or to monitor chemical reactions of very diluted samples will be discussed.

#### References

- [1] Russell, C. and Weitekamp, D. P., J. Am. Chem. Soc. 109, 5541-5542 (1987)
- [2] Allerhand, A, J. of Chem. Phys. 44 (1966)
- [3] Freeman, R. and Hill H. D. W, J. Chem. Phys. 54 (1971)

- [4] Vold, R. L. and Vold, R. R., J. Magn. Res. 13, 38-44 (1974)

#### OP147: Using single spins for quantum computing and sensing

\*Dieter Suter

TU Dortmund

Information processing on the basis of quantum mechanical systems promises breakthroughs in the processing speed. The realization of this potential depends on the availability of suitable quantum systems that must be controllable with high precision and conserve the stored information for the duration of the computation. Spins are in many respects ideal quantum bits, and most of the demonstration experiments for quantum information processing have been performed with spins as qubits. Unfortunately, the most easily accessible spins, nuclear spins in liquids, cannot be initialized into pure quantum states, which is a requirement for many quantum algorithms. The nitrogen-vacancy center in diamond, however, is a spin that allows optical initialization into a nearly pure state as well as the precise readout of single spins by optical techniques. We use this system for demonstrating basic steps of quantum information processing, such as gate operations or protection of quantum information against environmental noise. In addition, these systems can be used as point-like sensors for different environmental variables, such as electric and magnetic field, temperature or pressure.

#### Friday – May 24<sup>th</sup> Membrane Proteins

Chair: Laurent Catoire  
Room Gávea A

#### OP148: NMR studies on the type IV secretion system of *Xanthomonas citri*

Diorge Souza, Luciana Coutinho de Oliveira, Denize C. Favaro, Cristina Alvarez-Martinez, Chuck Farah, \*Roberto Salinas

Department of Biochemistry, Institute of Chemistry, USP

Gram-negative bacteria use specialized supramolecular complexes to secrete macromolecules across the bacterial cell envelope. One such complex is the Type IV Secretion System (T4SS) [1]. T4SSs are generally composed of 12 proteins, VirB1 to VirB11 and VirD4 [2]. The upper layer of the channel of the T4SS consists of fourteen repetitions of an heterotrimer formed by VirB7 and the C-terminal domains of VirB9 (VirB9<sup>CT</sup>) and VirB10 [1,2]. We showed previously that the VirB7 of the phytopathogen *Xanthomonas citri* (Xac) has an extra C-terminal globular domain (residues 52-133) that is absent in the VirB7 of other organisms [3]. This finding suggests a structural variation in the T4SS of *Xanthomonadaceae*. In order to obtain further high-resolution structural information on Xac's T4SS, we initiated a study of the three-dimensional structure of the complex formed by Xac-VirB9<sup>CT</sup> and Xac-VirB7<sup>NT</sup>.

#### References:

- [1] Chandran, V., Fronzes, R., Duquerroy, S., Cronin, N., Navaza, J., Waksman, G. (2009). Nature 462, 1011–1015.
- [2] Zechner, E.L., Lang, S., and Schildbach, J.F. (2012). Philos. Trans. R. Soc. Lond. B Biol. Sci. 367, 1073–1087.
- [3] Souza, Diorge P., Andrade, Maxuel O., Alvarez-Martinez, Cristina E., Arantes, Guilherme M., Farah, Chuck S., Salinas, Roberto K. (2011). PLoS Pathogens 7, e1002031.

#### OP149: Magic Angle Spinning Solid-State NMR Studies of Membrane Proteins

\*Vladimir Ladizhansky

University of Guelph



Magic angle spinning (MAS) solid-state NMR (SSNMR) shows great potential for studying structure and dynamics of membrane proteins, which are not readily amenable to X-ray crystallography and solution NMR. In this presentation we will describe the latest developments in our group, including advances in sample preparation procedures for obtaining MAS spectra with optimal spectral sensitivity, experimental strategies for obtaining spectroscopic assignments, methods for measuring long-range structural restraints for the determination of high resolution structure and supramolecular organization of membrane proteins in the lipid environment. We will present high-resolution structure of a seven-helical photoreceptor Anabaena Sensory Rhodopsin, and discuss progress towards structural characterization of a eukaryotic membrane water channel human Aquaporin 1.

#### UP150: Comparison of Structure of Cyanobacteria and Spinach PSII Studied by PELDOR

<sup>1</sup>\*Asako Kawamori, <sup>2</sup>Jiang-Ren Shen, <sup>3</sup>Hiroyuki Mino

<sup>1</sup>AGAPE-Kabutoyama Institute of Medicine, <sup>2</sup>Department of Biology, Okayama University, <sup>3</sup>Department of Physics, Nagoya University

The Structure of Cyanobacterium has been determined recently with resolution of 1.9 Å (Umena et al. NATURE (2011) 473 55) We have determined the distances between electron transfer components of PSII in Spinach with PELDOR( Pulsed Electron Double Resonance) with accuracy of 1 Å, 27 Å for Y<sub>D</sub>-Y<sub>Z</sub>, Y<sub>D</sub>-Mn<sub>4</sub> cluster by measurement of dipolar interactions between radicals. Usually Electron Spin is not localized and hyperfine constants reflecting spin distribution are observed. Point dipolar approximation is not correct to determine radical distances. In this report we present the distance estimation by taking account of spin distribution. Typically distances of chlorophylls and carotenoid from YD are reported based on spin distributions, which were derived hyperfine constants of each radical, and crystal structure data.

In a cyanobacterium the distances obtained by PELDOR are not coincident with those in spinachs but different values are obtained. Several radical pairs produced by light illumination will be compared for cyanobacteria and spinaches.

#### OP151: Structure Determination of Membrane Proteins in their Native Environment of Phospholipid Bilayers

\*Stanley Opella

University of California, San Diego

NMR spectroscopy is eminently capable of solving the structures of macromolecules, including proteins, as solids, whether polycrystalline or amorphous, or in aqueous solution. However, biological processes rarely occur in such clear-cut physical states. Membrane proteins function in liquid crystalline phospholipid bilayers. They are "immobilized" on NMR timescales, except for rapid rotational diffusion about the bilayer normal, and some local internal motions, primarily at the N- and C- termini. A recently developed approach, Rotationally Aligned (RA) Solid-State NMR is ideally suited for structure determination of membrane proteins; it merges many aspects of Magic Angle Spinning (MAS) Solid-State NMR and Oriented Sample (OS) Solid-State NMR into a method that measures angles between bonds and the bilayer normal. Supplemented with other angles and distances, this approach enables the structures of membrane proteins to be determined with atomic resolution in proteoliposomes under physiological conditions. Complementary experiments describe the global and local motions of these proteins in the bilayer environment. Examples of proteins that range from single domains with one trans-membrane helix to GPCRs with seven trans-membrane helices will be described.

#### Friday – May 24<sup>th</sup> Instrumentation

Chair: Mario Engelsberg  
Room Gávea B

#### OP152: Robust Multi-Phase Flow Measurements Using Magnetic Resonance

<sup>1,2</sup>\*Daniel José Pusiol, <sup>1</sup>Lucas C. Cerioni

<sup>1</sup>Instituto de Física Enrique Gaviola IFEG, CONICET, Ciudad Universitaria, Córdoba, Argentina, <sup>2</sup>SPINLOCK SRL & CONICET, Córdoba, Argentina

The flow metering of multiphase fluids is an actual technical challenge, especially when flow velocity is in the range of 0.1 – 10 m/sec. The primary complication is the existence of 'phase slip' between fluid components. Without physically separating individual fluid components of multi-phase flow, it is impossible to accurately determine the flow rate of each component from the measurement of physical properties that are related to the average fluid displacement in the pipe. A non-linear system of fluid phase velocity and cross-sectional area occupied by each fluid phase is established during multiphase flow, which cannot be adequately approximated by correlations derived from macroscopic properties such as fluid density or pressure drop.

Magnetic resonance is intrinsically sensitive to flow; however, current applications to flow measurement are limited to very low flow rates that are inapplicable to oil-field and other industrial applications. In this paper we discuss real-time quantification NMR-based methods of high-flow rates in multiphase fluids. In particular, we focalize in a recent development which employs a new principle that enables robust 3-phase flow metering with a broader operating envelope than existing flow meters, has no sensors in the flow stream, no radioactive source, yet could potentially be produced at sufficiently low cost to promote increasing numbers of well head installations.

ACKNOWLEDGMENTS: CONICET, FONTAR, SPINLOCK

#### OP153: Using Time Domain NMR to Study Magnetoelectrolysis phenomenon in Situ

<sup>1</sup>\*Luiz Alberto Colnago, <sup>1</sup>Luis Fernando Cabeça, <sup>2</sup>Luiza Maria da Silva Nunes, <sup>2</sup>Paulo Falco Cobra, <sup>2</sup>Bruna Ferreira Gomes, <sup>1</sup>André de Souza Carvalho

<sup>1</sup>Embrapa Instrumentação, São Carlos/SP - Brazil, <sup>2</sup>Instituto de Química de São Carlos - USP

Recently we demonstrate that time domain NMR (TD-NMR) relaxometry can be a very fast, simple, and efficient technique to monitor the variation in the Cu<sup>2+</sup> concentration during an electrodeposition reaction (Anal. Chem. 84, 6351, 2012). In this talk, the effect of NMR magnetic field in the electrodeposition reaction (magnetoelectrolysis) will be presented. The interest in the process is related to the possibility of controlling the deposit morphology, mass transport and the reaction rate. The effect of the magnetic field on electrodeposition reaction has been related to the magneto-hydrodynamic force ( $\mathbf{F}_B$ ) and the magnetic gradient field force ( $\mathbf{F}_{\nabla B}$ ). The TD-NMR analyses were performed in SLK-100 0.23 T, TD-NMR spectrometer (Spinlock) and 0.35 T homemade unilateral NMR sensor. The electrochemical cell was describe elsewhere. The reactions were performed without the magnetic field (W) and with magnetic field with the cell in the center (C) and top border (T) of the bench top magnet and at the top of unilateral sensor (U). The W, U, T and C reactions removed 37, 47, 53 and 60% of the Cu<sup>2+</sup> in solution during 1-hour reaction, respectively. The W reaction was the slowest one because reaction is dependent only on the convection of the Cu<sup>2+</sup> caused by concentration gradient. The reactions in the magnetic field were faster due to the Cu<sup>2+</sup> convection caused by the magnetoconvection forces. The C reaction was the fastest one due  $\mathbf{F}_B$  that causes a

flux perpendicular to  $B_0$  increasing the mass convection and consequently the electrodeposition. The U and T reactions rate decrease when compared to C, because the magnetic field gradient causes a strong  $\mathbf{F}_{\nabla B}$  toward the bottom of the cell, reducing the copper concentration at the top of the cell, around the working electrode. We conclude that TD-NMR can be a useful tool to study magnetoelectrolysis *in situ*.

ACKNOWLEDGMENTS: FAPESP, CNPq

#### UP154: In situ MR: Pore condensation at elevated temperature and pressure

<sup>1</sup>\*Matthew P. Renshaw, <sup>1</sup>S. Tegan Roberts, <sup>2</sup>Belinda S. Akpa, <sup>1</sup>Mick D. Mantle, <sup>1</sup>Andrew J. Sederman, <sup>1</sup>Lynn F. Gladden

<sup>1</sup>University of Cambridge, <sup>2</sup>University of Illinois at Chicago

Magnetic Resonance (MR) methods, being non-invasive and non-destructive, are ideal for probing heterogeneous catalytic systems under realistic operating conditions [1,2]. However, until recently, the processes studied using MR have been performed under mild conditions (typically < 5 atm and < 200 °C). We have recently commissioned a fixed-bed reactor, compatible with operation inside a superconducting magnet, which can be operated up to a temperature of 350 °C and a pressure of 31 atm while simultaneously performing MR experiments.

To demonstrate its capability we have studied the effect of confinement in mesopores on the vapour-liquid phase change of cyclohexane to elucidate pore filling and emptying mechanisms. The understanding of confinement effects, particularly at realistic reaction conditions, is an important consideration in heterogeneous catalysis.

Isothermal (150 °C and 188 °C) vapour-liquid phase change cycles of cyclohexane in a bed of titania pellets were conducted. <sup>1</sup>H spin density images reveal changes in pore saturation of the pellets as the phase boundary is crossed. Pore confinement effects are exhibited, as liquid remains within the pores after bulk liquid has vaporised. Pore saturation during the evaporation-condensation cycles exhibits hysteresis, demonstrating the differences between the filling and emptying mechanisms in these systems. The data are analogous to N<sub>2</sub> adsorption isotherms that characterise pore diameter and surface area, but are conducted for a relevant species at realistic conditions.

Data from these MR images, in conjunction with <sup>1</sup>H  $T_1$  and  $T_2$  relaxation time measurements and pulsed field gradient diffusion measurements, are used to assess the mechanism of pore filling and emptying in addition to revealing information about the formation of liquid films.

The use of the *in situ* MR reactor is currently being extended to study heterogeneous catalytic reactions.

[1] Gladden et al., *Catalysis Today*, 155 (2010) 157-163.

[2] Lysova and Koptuyug, *Chemical Society Reviews*, 39 (2010) 4585-4601.

#### OP155: Compact NMR of Materials and Processes

\*Bernhard Blümich

RWTH Aachen University

Typical NMR spectrometers use superconducting magnets, which are heavy, expensive and require high maintenance. This is one reason, why the reputation of NMR is perceived to be more demanding than that of many other analytical methods including IR spectroscopy and DSC. Yet NMR is also versatile. It provides spectra for chemical analysis, images that give insight into sample heterogeneity and function of devices, and relaxation parameters, which scale with mechanical material properties [1]. While superconducting magnets are common today in NMR, permanent magnets have been used decades before. They were temperature sensitive, hard to shim, heavy, and produce fields much lower

than modern superconducting magnets. Yet in recent times, compact permanent magnets have been developed for NMR, which are light enough to be carried to the object or the production line for analysis [1]. As NMR relaxation can be measured in the inhomogeneous stray field, a portable stray-field NMR device known as the NMR-MOUSE has been developed for non-destructive materials testing [2,3]. It is particularly well suited for studying rubber materials and the morphology and semi-crystalline polymer products as a function of processing parameters and service time. Current research aims at predicting the residual service time of polymer pipes from such measurement [4]. In another project, the use of a desktop MRI magnet is investigated to acquire images of rubber gaskets within a few seconds, from which the position of the inner surfaces can be extracted for control the production process [5]. Last but not least, small magnets are employed to measure <sup>1</sup>H NMR spectra in real time under the fume hood to follow chemical reactions. These and other applications of compact, state-of-the art NMR magnets will be reported [6].

#### References

[1] B. Blümich, F. Casanova, E. Danieli, J. Perlo, St. Appelt, Sub-Compact NMR, in: C.L. Khetrpal, A. Kumar, K.V. Ramanathan (eds.), *Future Directions of NMR*, Springer (India) 2011, pp. 1-10

[2] B. Blümich, F. Casanova, J. Perlo, Mobile single-sided NMR, *Progress Nucl. Magn. Reson. Spectrosc.* 52 (2008) 197-269

[3] F. Casanova, J. Perlo, B. Blümich, eds., *Single-Sided NMR*, Springer, Berlin, 2011

[4] R. Kwamen, B. Blümich, A. Adams, Estimation of Self-Diffusion Coefficients of Small Penetrants in Semicrystalline Polymers Using Single-Sided NMR, *Macromol.* 33 (2012) 943-947

[5] E. Danieli, K. Berdel, J. Perlo, W. Michaeli, U. Masberg, B. Blümich, F. Casanova, Determining object boundaries from MR images with sub-pixel resolution: Towards inline inspection with a mobile tomography, *J. Magn. Reson.* 207 (2010) 53-58

[6] S. Küster, E. Danieli, B. Blümich, F. Casanova, High resolution NMR spectroscopy under the fume hood, *Phys. Chem. Chem. Phys.* 13 (2011) 13172-13176

**Friday – May 24<sup>th</sup>**  
**Innovative NMR/MRI Methods**

Chair: Betty Gaffney  
Rooms Turmalina/Topázio

#### OP156: Relaxometry and dynamics

\*Claudio Luchinat

Magnetic Resonance Center (CERM), University of Florence

Field-cycling relaxometry experiments provide longitudinal relaxation rates of sample nuclei (usually abundant, high- $\gamma$  nuclei) over a wide field range, so that the whole spectral density is experimentally and directly available. Recent applications of relaxometry comprise the analysis of the spectral density of water protons for the characterization of contrast agents [1], for a better understanding of dynamic nuclear polarization (DNP) experiments [2], and for acquiring information on protein aggregation and dynamics in folded and intrinsically disordered proteins. The analysis of the collective spectral density of protein protons in D<sub>2</sub>O solutions is also feasible [3] to obtain information on protein dynamics in terms of reorientation time and generalized order parameter.

Relaxivity profiles can provide reorientation times of solute molecules up to the microsecond range, so that the tumbling time of proteins as large as hundreds kDa can be accessed. In sedimented proteins [4], they can provide information on the intervening motions.

In the context of the characterization of polarizing agents for solution DNP experiments, relaxation profiles of solvent water protons in the presence of nitroxide radicals or paramagnetic metal complexes have been analyzed to obtain the structural and dynamic parameters needed for determining the coupling factor, on which the solvent DNP enhancement depends.  $^1\text{H}$  relaxometry thus represents an easy way to estimate the DNP enhancement at full electron saturation as a function of the applied magnetic field.

[1] Mastarone, Harrison, Eckermann, Parigi, Luchinat, Meade, J. Am. Chem. Soc. (2011) 133, 5329.

[2] Bennati, Luchinat et al. J. Am. Chem. Soc. (2008) 130, 3254; J. Am. Chem. Soc. (2009) 131, 15086; Phys.Chem.Chem.Phys. (2010) 12, 5902; Phys. Chem. Chem. Phys. (2012) 14, 502

[3] Luchinat, Parigi, J. Am. Chem. Soc. (2007), 129, 1055.

[4] Bertini, Luchinat, Parigi, Ravera, Reif, Turano, Proc. Natl. Acad. Sci. USA (2011) 108, 10396.

#### OP157: The Nitrogen-Vacancy Center In Diamond As A Nanoscale Spin Sensor

<sup>1</sup>Abdelghani Laraoui, <sup>2</sup>Florian Dolde, <sup>2</sup>Tobias Staudacher, <sup>2</sup>Jörg Wrachtrup, <sup>2</sup>Friedemann Reinhard, <sup>1\*</sup>Carlos A. Meriles

<sup>1</sup>Department of Physics, CUNY - City College of New York, New York, <sup>2</sup>3rd Physics Institute, University of Stuttgart, Germany

The Nitrogen-Vacancy (NV) center in diamond – a spin-1 point defect formed by a substitutional nitrogen adjacent to a vacancy site – is presently the focus of intense research in areas spanning physics, chemistry, and biology. Thanks to their long spin coherence times at room temperature, NV centers within diamond nanostructures are being explored as a platform for various technologies, most notably nanoscale resolution MRI. Here, I will present recent results on the use of near-surface NVs for nuclear spin spectroscopy, including the detection of proton spins from an organic film deposited on the diamond crystal surface (the effective sample volume being approximately  $(5\text{ nm})^3$ ). I will also discuss recent experiments with diamond nanocrystals, where we use the NV as a probe to detect other, optically-inactive paramagnetic centers within the particle and on its surface.

ACKNOWLEDGEMENTS: National Science Foundation, Research Corporation, Alexander von Humboldt Foundation.

#### UP158: Mitochondrial function in diabetes: Novel methodology and new insight

\*Liping Yu, Brian Fink, Judith Herlein, William Sivitz  
University of Iowa

Diabetes is a group of metabolic diseases associated with malfunction of mitochondria. Major metrics used to describe mitochondrial function include oxygen consumption (respiration), membrane potential ( $\Delta\Psi$ ), ATP production, and generation of reactive oxygen species (ROS) in the form of superoxide. Interpreting mitochondrial function as affected by comparative physiologic conditions is confounding since these individual functional parameters are inter-dependent. In this study, we investigated the relationships between the parameters of muscle mitochondrial function as affected by insulin deficiency. In particular, we examined ATP production in a unique way that provides new information about the function of mitochondria. To achieve our objectives, we developed a novel, highly sensitive and specific ATP production assay using NMR spectroscopy of mitochondria at clamped levels of  $\Delta\Psi$ . ROS production can also be assayed simultaneously. The NMR techniques reported in this study proved far more sensitive than conventional  $^{31}\text{P}$  NMR and allowed high throughput study of small mitochondrial isolates. Over conditions ranging from state 4 to state 3 respiration, ATP production was found to be lower and ROS per unit ATP

generated was greater in mitochondria isolated from diabetic muscle. Moreover, ROS production began to increase at a lower threshold for inner membrane potential in diabetic mitochondria. In summary, we describe a novel methodology for measuring ATP production and provide new mechanistic insight into the dysregulation of ATP production and ROS in mitochondria of insulin deficient rodents.

#### OP159: Using SABRE as a route to hyperpolarization in NMR and MRI

<sup>1</sup>\*Simon B Duckett, <sup>1</sup>Kevin D. Atkinson, <sup>1</sup>Alex J. J. Hooper, <sup>1</sup>Lyrelle S. Lloyd, <sup>2</sup>Gary G. R. Green, <sup>1</sup>Marianna Fekete, <sup>1</sup>Richard A. Green, <sup>1</sup>Ryan E. Mewis, <sup>1</sup>Louise A. R. Highton

<sup>1</sup>York Centre for Hyperpolarisation In Magnetic Resonance, <sup>2</sup>York Neuroimaging Centre

In medicine MRI plays a role in non-invasive diagnosis and it also plays a significant role in clinical research. However, MRI suffers inherently from the underlying physical basis of the method which limits it to the detection of effectively only 1 in every 200,000 hydrogen atoms present in the sample when working at physiological temperatures and a magnetic field strength of 1.5 T as routinely used in clinical MRI.

Hyperpolarization deals with the generation of non-equilibrium populations of these nuclear spins, and provides enhanced sensitivity to both NMR and MRI experiments. One variant of this is dynamic nuclear polarization (DNP) which dramatically increases the sensitivity of  $^{13}\text{C}$  detection.

An alternative approach to achieve substrate hyperpolarization, as pioneered by Weitekamp, involves the use of parahydrogen, a molecule that exists in a pure magnetic state. However, it is not parahydrogen itself that is detected in these experiments, but rather reaction products that are formed by a metal catalyzed hydrogenation. The newly formed molecules now contain non-equilibrium spin state populations for nuclei that are spin coupled to protons that were originally located in parahydrogen. Consequently they yield MR signals that are substantially larger than normal. Indeed 100% polarization has been generated for a pair of metal hydride protons using this method.

A newer route to substrate hyperpolarization with parahydrogen has been termed signal amplification by reversible exchange (SABRE). This approach yields substantial polarization without the need for chemical modification. It is achieved instead through the temporary binding of a substrate and parahydrogen in a suitable transition metal complex. This process of bringing together two materials, for example nicotine and parahydrogen, into temporary contact enables the sharing of their magnetization and hence the spontaneous enhancement of the MR signals of what correspond to ultimately the free substrate. This talk will illustrate how this approach is developing in York.

Friday – May 24<sup>th</sup>  
Small Molecules and Bioactive Peptides

Chair: Marta Bruix  
Room Ònix

#### OP160: NMR Studies of the Self-Association and Membrane Binding of Cyclotides

\*David J Craik, Conan Wang, K Johan Rosengren, Anne Conibear, Sonia T Henriques

Institute for Molecular Bioscience, The University of Queensland, Australia

NMR is a powerful technique for determining the structures, dynamics and interactions of peptides and proteins. Here we describe the application of NMR to the study of cyclic disulfide-rich peptides. Because of their exceptional stability these peptides make valuable leads in drug design applications and have been used as templates to stabilize bioactive

peptide epitopes. Of particular focus are the cyclotides,[1] which are 30 amino acid peptides from plants that have a broad range of biological activities, including antimicrobial, anticancer, anti-HIV and insecticidal activities. The cyclotides are particularly amenable to NMR studies and give well dispersed spectra. We have used a range of NMR techniques to determine the three-dimensional structures, identify key hydrogen bonding networks, and determine the nature of intermolecular interactions of cyclotides, with a particular focus on membrane binding interactions. NMR studies combined with alanine mutagenesis scanning have provided novel insights into the modes of interactions of cyclotides with membranes.[2]

[1] Craik D J, Swedberg J, Mylne J S, Cemazar M: Cyclotides as a basis for drug design. *Expert Opinion on Drug Discovery* (2012) 7, 179-194.

[2] Wang C K, Wacklin H P, Craik D J: Cyclotides insert into lipid bilayers to form membrane pores and destabilize the membrane through hydrophobic and phosphoethanolamine-specific interactions. *Journal of Biological Chemistry* (2012) 287, 43884-43898.

Work in our laboratory is supported by grants from the Australian Research Council (DP0984390) and the National Health & Medical Research Council (APP1026501).

#### OP161: Separative NMR: adapted resolution for complex mixtures of small molecules

1,2\*Stefano Caldarelli

<sup>1</sup>Aix Marseille Université, Marseille, France, <sup>2</sup>CNRS UPR 2301 Ecole Palaiseau France

In this talk, we shall outline the results of two strategies that have been implemented recently in our laboratory as tools to simplify and ameliorate the analysis of mixtures of small molecules.

The basis of the methods are DOSY and the use of multiple-quantum coherences.

- Chromatographic NMR[1, 2] is a matrix-assisted version of DOSY[3], in which the addition of a chromatographic solid phase can induce larger differences of mobility of the mixture components, thus simplifying the analysis. We shall show that the method is capable of discriminating labile supramolecular species (interchanging chiral ion pairs), which have been elusive to conventional LC.[4]

- Multiple-quantum coherences have interesting properties for the study of mixtures. Firstly, they produce spectra with a number of signals inversely proportional to the coherence order. This property in itself can produce spectra with very high discriminating power (up to tens of molecules overlapping in a couple of ppm).[5] In this talk we shall revisit diffusion using homonuclear multiple-quantum coherences based on J couplings.[6, 7] MQ-DOSY allows to increase the apparent diffusion coefficient, by the square of the MQ order. An interesting side-effect of this is that differences in mobility also appear to be amplified. Combined with the reduced number of resonances produced by MQ-filter, MQ-DOSY outperforms regular DOSY, being capable of distinguishing isomers with very similar diffusion coefficients.

[1] S. Viel, F. Ziarelli, S. Caldarelli, *PANS* 2003, 100, 9696.

[2] G. Pages, C. Delaurent, S. Caldarelli, *Angewandte Chemie-International Edition* 2006, 45, 5950.

[3] K. F. Morris, P. Stilbs, C. S. Johnson, *Analytical Chemistry* 1994, 66, 211.

[4] M. Reddy G. N, R. Ballesteros-Garrido, J. Lacour, S. Caldarelli, *Angewandte Chemie International Edition* 2013

[5] M. G. N. Reddy, S. Caldarelli, *Analytical Chemistry* 2010, 82, 3266.

[6] L. E. Kay, J. H. Prestegard, *Journal of Magnetic Resonance* 1986, 67, 103.

[7] C. Dalvit, J. M. Böhlen, *NMR in Biomedicine* 1997, 10, 285.

#### ACKNOWLEDGEMENT

This work was supported by ANR (ANR-08-BLAN-273) and Region PACA (APO-G 2009).

#### UP162: Structural Basis for the Interaction of Human $\beta$ -Defensins 1 and 6 and Its Putative Chemokine Receptor CCR2 and Breast Cancer Microvesicles

\*Viviane Silva de Paula, Robson Q. Monteiro, Fabio C. L. Almeida, Ana Paula Valente

Universidade Federal do Rio de Janeiro

Human  $\beta$ -defensins (hBD) are believed to function as alarm molecules that stimulate the adaptive immune system when a threat is present. In addition to its antimicrobial activity, defensins present other activities such as chemoattraction of a range of different cell types to the sites of inflammation. We have solved the structure of the human  $\beta$ -defensins 6 (hBD6) by NMR spectroscopy that contains a conserved  $\beta$ -defensin domain followed by an extended C-terminus. We also investigated the interaction of  $\beta$ -defensin 1 and 6 with microvesicles shed by breast cancer cell lines using NMR. Chemical shift mapping of the interaction showed that both defensins interact with microvesicles but in slightly different way, suggesting an inverse correlation with the aggressiveness potential of the cell. Furthermore, molecular docking using restraints derived from the NMR chemical shift data produced a model of the complex between hBD6 and a peptide derived from the extracellular domain of CC chemokine receptor 2 (Nt-CCR2) that reveals a contiguous binding surface on hBD6, which comprises amino acid residues of the  $\alpha$ -helix, loop between  $\beta$ 2- $\beta$ 3 and C-terminal. The microvesicles binding surface partially overlaps with the chemokine receptor interface. These data offer new insights into the structure-function relation of the hBD6-CCR2 interaction and may be helpful for the design of novel anti-cancer agents.

ACKNOWLEDGEMENTS: FAPERJ, CAPES, CNPq

#### OP163: Breaking the barrier: NMR of membrane-active peptides

\*Frances Separovic

School of Chemistry, Bio21 Institute, University of Melbourne, Australia

The interaction of antimicrobial peptides (AMP) and amyloid peptides with cell membranes is contingent on the nature of the constituent lipids. Since eukaryotic and bacterial membranes are comprised of different proportions of a range of lipid species with diverse physical properties, we have studied these membrane-active peptides with membranes of different lipid types.

Maculatin 1.1 is a short AMP secreted from the skin of Australian tree frogs. This peptide has a high activity against Gram-positive bacteria but reduced action against Gram-negative bacteria and red blood cells. We have studied the interactions of maculatin 1.1 with various model membranes mimicking prokaryotic or eukaryotic cells to understand the selectivity and mechanism of action and the role of lipids. The impact of unsaturated versus saturated fatty acids, surface charge, presence of cholesterol and heterogeneous compositions were investigated. The peptide adopted an  $\alpha$ -helical structure in contact with eukaryotic and prokaryotic membrane-mimics and inserted into neutral membranes, even in the presence of cholesterol, but remained on the surface of negatively charged membranes. The dynamic and structural changes of lipid vesicles mimicking *E. coli*, *S. aureus* or eukaryotic plasma membranes were monitored using solid-state NMR. Maculatin 1.1 promoted a strong response in saturated lipid model membranes at lower concentration than with *E. coli* lipid extracts and disrupted membranes according to their lipid composition.

The 42-residue amyloid-beta ( $A\beta_{42}$ ) peptide is a fibrous constituent of amyloid plaques found in the brains of Alzheimer's disease patients. Although the precise involvement in neurodegeneration is unknown, interactions with neuronal cell membranes and copper ions may be involved. Our previous work has shown that aggregation kinetics and fibril morphology of  $A\beta_{42}$  is influenced by the lipid compositions of membranes, and we now probe the role of copper ions. Copper, at and above equimolar ratios, stabilised  $A\beta_{42}$  into non-oligomeric  $\beta$ -sheet structures alone and in the presence of lipids. Solid-state NMR revealed that the peptide, with and without copper, significantly disrupted lipid headgroups in brain lipid extract and phospholipid POPC/cholesterol membrane systems containing 10% (molar) POPS or GM1, as indicated by reductions in  $^{31}\text{P}$  chemical shift anisotropy,  $T_1$  and  $T_2$  relaxation values. Copper alone had a strong paramagnetic effect on  $^{31}\text{P}$  relaxation values, which were enhanced in the presence of  $A\beta_{42}$ , suggesting that the peptide does not scavenge copper from the membrane.  $^2\text{H}$  NMR spectra did not indicate copper penetration into the hydrophobic core region. By contrast,  $A\beta_{42}$  induced small vesicle formation and large changes in the headgroup and core regions of POPC/cholesterol systems containing cardiolipin, a mitochondrial lipid. Our results support a superficial interaction of  $A\beta_{42}$  with the model brain lipid membranes and demonstrate the importance of lipid composition on peptide activity.

**Friday – May 24<sup>th</sup>**  
**Plenary Session**

Chair: Sonia Menezes  
Room Gávea A

**PL164: Nuclear Spins, High Magnetic Fields, and Traveling Waves in Pursuit of Human Brain Function and Connectivity**

\***Kamil Ugurbil**

*CMRR, University of Minnesota, USA*

Ever since Plato and Aristotle, the unique abilities of the human brain has been the subject of many philosophers and scientists throughout history, including Descartes who postulated a dualism between mind and matter, and Helmholtz who pioneered contemporary physiology. Today, tremendous strides are being made towards deciphering human brain function using experimental observations performed non-invasively and directly on the human brain as it executes its functions. This rapid progress has been possible because of neuroimaging, and in particular magnetic resonance (MR) imaging of the brain that has rapidly evolved over the last two decades due to incessant developments in instrumentation, ranging from very high field magnets large enough to accommodate humans to parallel RF transmission and signal reception, approaches to manipulating spins, and novel signal processing schemes. These technological accomplishments have permitted mapping of neuronal activity in the human brain at the scale of elementary computational units and functionally distinct ensembles of such computational clusters, complemented with "functional" and "anatomical" connectivity data obtained also by MR techniques to inform us

on neural circuits and networks. The success of these studies are driven by initiatives like the Human Connectome Project (HCP), an ambitious effort initiated by the 16 National Institutes of Health (NIH) Institutes and Centers that support the NIH Blueprint for Neuroscience Research, to map the neural pathways that underlie human brain function and generate a comprehensive description of the connections among gray matter locations in the human brain at the millimeter scale, using MR methodology. It is a remarkable journey from the first demonstrations by Isidor Rabi of resonant spin flips in an atomic beam experiment in 1933, to the observation of the Nuclear Magnetic Resonance in condensed matter by Ed Purcell and Felix Bloch in 1945.

**PL165: Synergy between NMR, cryo-EM and large-scale MD simulations - Novel Findings for HIV Capsid Function**

\***Angela M. Gronenborn**

*Department of Structural Biology, University of Pittsburgh*

Mature HIV-1 particles contain a conical-shaped capsid that encloses the viral RNA genome and performs essential functions in the virus life cycle. Previous structural analysis of two- and three-dimensional arrays provided a molecular model of the capsid protein (CA) hexamer and revealed three interfaces in the lattice. Using the high-resolution NMR structure of the CA C-terminal domain (CTD) dimer and in particular the unique interface identified, it was possible to reconstruct a model for a tubular assembly of CA protein that fit extremely well into the cryoEM density map. A novel CTD-CTD interface at the local three-fold axis in the cryoEM map was confirmed by mutagenesis to be essential for function. More recently, the cryo-EM structure of the tube was solved at 8Å resolution and this cryo-EM structure allowed unambiguous modeling and refinement by large-scale molecular dynamics (MD) simulation, resulting in all-atom models for the hexamer-of-hexamer and pentamer-of-hexamer elements of spheroidal capsids. Furthermore, the 3D structure of a native HIV-1 core was determined by cryo-electron tomography (Cryo-ET), which in combination with MD simulations permitted the construction of a realistic all-atom model for the entire capsid, based on the 3D authentic core structure.

In addition, interaction with the innate immune defense restriction factor TRIM5 $\alpha$  was studied. TRIM5 $\alpha$  recognizes the lattice of the retrovirus capsid through its B30.2 (PRY/SPRY) domain in a species-specific manner. Upon binding, TRIM5 $\alpha$  induces premature disassembly of the viral capsid and activates the downstream innate immune response. We have determined the crystal structure of the rhesus TRIM5 $\alpha$  PRY/SPRY domain that reveals essential features for capsid binding. Combined cryo-electron microscopy (cryo-EM) and biochemical data show that the monomeric rhesus TRIM5 $\alpha$  PRY/SPRY, but not human TRIM5 $\alpha$  PRY/SPRY, can bind to HIV-1 capsid protein assemblies, without causing disruption of the capsid. Our data suggests a model for how this factor disrupts the virion core and suggests that structural damage of the viral capsid by TRIM5 $\alpha$  is likely one of the important components of the mechanism of HIV-1 restriction.

## Poster Abstracts

## Biomolecular Solution NMR

**MO001: Molecular recognition of complex-type biantennary N-glycans by lectins: epitope selection through NMR**

<sup>1</sup>Ana Ardá, <sup>1</sup>Pilar Blasco, <sup>2</sup>Daniel Varón Silva, <sup>2</sup>Volker Schubert, <sup>3</sup>Sabine André, <sup>4</sup>Marta Bruix, <sup>1</sup>Francisco Javier Cañada, <sup>3</sup>Hans-Joachim Gabius, <sup>2</sup>Carlo Unverzagt, <sup>1\*</sup>Jesús Jiménez-Barbero

<sup>1</sup>Centro de Investigaciones Biológicas, CSIC, Madrid, Spain, <sup>2</sup>Universität Bayreuth, Germany, <sup>3</sup>Ludwig-Maximilians-University Munich, Germany, <sup>4</sup>Instituto de Química-Física Rocasolano, CSIC, Madrid, Spain

The molecular recognition of carbohydrates is at the heart of essential biological events. N-glycans are common modifications of membrane/secreted proteins that confer specific properties to the associated protein. Their structures are widely diverse. However, they share a common structural motif, the pentasaccharide N-glycan core, whose branching can give rise to highly complex large glycans. NMR and X-ray crystallography, which provide key information at atomic resolution on biomolecules, have mainly focused, in the protein-carbohydrate interaction field, on acquiring information of complexes formed by lectins with small/medium-sized fragments of natural glycan chains.

Herein, we would like to show our results in the study of the recognition of two complex-type biantennary Asn conjugated N-glycans, undeca- and nonadecasaccharides, by different plant lectins by NMR. Our results highlight the effect of epitope presentation, and multiple vs single lectin domain, which can affect the outcome of the recognition process, precluding extrapolations and generalizations from simple models (small ligands and single protein domains).1

1 A. Ardá, P. Blasco, D. V. Silva, V. Schubert, S. André, M. Bruix, F. J. Cañada, H.-J. Gabius, C. Unverzagt, J. Jiménez-Barbero. *Manuscript submitted*.

**TU002: NMR study of receptor-chemokine interactions using linked extracellular domains: Mapping RANTES surfaces interacting with CCR5**

<sup>1\*</sup>Jacob Anglister, <sup>1</sup>Einat Schnur, <sup>1</sup>Naama Kessler, <sup>1</sup>Tali Scherf, <sup>2</sup>Fa-Xiang Ding, <sup>2</sup>Boris Arshava, <sup>2</sup>Fred Naider, <sup>3</sup>Victoria Kurbatska, <sup>3</sup>Ainars Leonciks, <sup>4</sup>Alexander Tsimanis

<sup>1</sup>Weizmann Institute, <sup>2</sup>College of Staten Island, City University of New York, <sup>3</sup>Latvian Biomedical Research and Study Centre, <sup>4</sup>Bionia Ltd

Chemokines constitute a large family of small proteins that regulate leukocyte trafficking to the site of inflammation by binding to specific cell-surface receptors which belong to the GPCR superfamily. The N-terminal (Nt) segment of the receptor was found to be a major binding determinant in many chemokine-receptor systems and interactions between Nt-peptides and chemokines have been studied extensively using NMR spectroscopy. Due to the lower affinities of peptides representing the three extracellular loops (ECLs) of chemokine receptors to their respective chemokine ligand, information concerning these interactions is scarce. To overcome the low affinity of ECL peptides to chemokines, we linked two or three CCR5 extracellular domains by either biosynthesis in *E. coli* or by chemical synthesis. This approach enabled the study of CCR5 binding to RANTES using <sup>1</sup>H-<sup>15</sup>N-HSQC titrations. Nt-CCR5 and ECL2 were found to be the major contributors by binding to opposing faces of RANTES, creating almost a closed ring around RANTES. A RANTES positively charged surface involved in Nt-CCR5 binding is reminiscent of a positively charged surface in HIV-

1 gp120 formed by the C4 and the base of the V3, part of which was implicated in Nt-CCR5 binding. An opposing surface consisting mostly of RANTES  $\beta$ 2- $\beta$ 3 hairpin residues and that is involved in ECL2 binding was found to be similar to a surface in the crown of the V3. The chemical and biosynthetic approaches presented in this study for linking GPCR surface regions may be widely applicable to investigation of interactions of the extracellular segments of chemokine receptors with their respective ligands.

**TH003: Improved <sup>13</sup>C-<sup>13</sup>C isotropic mixing experiments for side chain assignment of labeled proteins**

<sup>1</sup>Helena Kovacs, <sup>2\*</sup>Alvar Gossert

<sup>1</sup>Bruker BioSpin Switzerland, <sup>2</sup>Novartis Pharma Switzerland

Progress in cryogenic probe technology makes it now possible to apply <sup>13</sup>C-<sup>13</sup>C-spinlocks at RF field strengths that are sufficient to cover the whole <sup>13</sup>C- frequency bandwidth at medium magnetic field strengths. Wide bandwidth spinlocks on carbon enable the following three experiments that considerably facilitate the assignment of side chain resonances in labeled proteins and, in particular, allow connecting aromatic side chains to the protein backbone.

1. HCCH-TOCSY to connect aromatic ring carbons to aliphatic carbons
2. HCC-TOCSY to detect all carbon frequencies in a single experiment
3. HCCCONH for large proteins

To connect the aromatic ring to the aliphatic C-beta and C-alpha positions is a long-standing problem that can now easily be resolved with the wide carbon bandwidth HCCH-TOCSY. Even more demanding is to connect the aliphatic carbons directly to the backbone carbonyl, because of the large difference between the chemical shifts of C-alpha and carbonyl carbon. The <sup>13</sup>C-detected all-carbon HCC-TOCSY yields all carbon connectivities comprising both the side chains and the backbone.

HCCCONH is an ever so useful experiment while it yields the correlations from the side chain directly to the backbone amides. The experiment suffers, however, of low sensitivity for medium size proteins (>10kDa). By applying a sufficiently strong carbon spinlock to directly transfer carbon magnetization from the side chain resonances to the carbonyl, a shortened experiment that omits the INEPT step between C-alpha and carbonyl, is obtained. This experiment is favorable for larger proteins prone to relaxation losses. An additional consequence of the spinlock that covers all carbon frequencies is that the proposed HCCCONH experiment also connects the aromatic carbons directly to the backbone amides.

Spectra are presented at 600 and 700 MHz magnetic fields on <sup>13</sup>C, <sup>15</sup>N-labeled ubiquitin (7kDa) and kRas (21kDa) and IVL-methyl protonated, <sup>13</sup>C, <sup>15</sup>N, <sup>2</sup>H-labeled MBP (43kDa) to demonstrate the usefulness of the above mentioned experiments. In addition, theoretical calculations of the transfer efficiency were carried out for the aromatics to C-alpha and C-beta transfer in phenylalanine and for methyl to carbonyl transfer in isoleucine, valine and leucine. The theoretical transfer efficiencies were compared to experimental data using 16.7kHz spinlocks at 600MHz and 17.9kHz spinlock at 700MHz and going up to 50ms mixing times. Practical consequences for the optimal setup of the spinlock experiments are discussed.

**MO004: A NMR-based platform for efficient structural characterization of families of small proteins**

<sup>1</sup>Jonas Fredriksson, <sup>2</sup>Viviane Silva de Paula, <sup>2</sup>Ana Paula

Valente, <sup>2</sup>Fabio C. L. Almeida, <sup>1\*</sup>Martin Billeter

<sup>1</sup> University of Gothenburg Sweden, <sup>2</sup> Universidade Federal do Rio de Janeiro Brasil

Defensins form an ancient family of antimicrobial proteins that form an innate immune system in most higher organisms including plants and animals [1]. They are active against both bacteria and fungi. Their strong antimicrobial activity makes them potent drug candidates.

NMR projection techniques combined with analysis based on decompositions offer rapid experiments, high dimensionality, full resolution and a very high degree of automation; they are well suited for systematic studies of entire protein families, which may also include unstable molecules [2-3].

We are developing a platform for complete and fast structural and functional characterization of families of small proteins e.g. defensins. Once fully implemented, this platform will encompass high-throughput expression, fast NMR experiments, automated spectral analysis, and systematic structural and functional characterization. We are combining the locally developed cell free expression protocol [4] with our projection-decomposition approach and with standard structure determination.

As an application, a complete characterization of human beta defensin 6 based on projection experiments analyzed via simultaneous decompositions of all spectra is presented and discussed. NMR measurements consist of five experiments recorded in less than 3 days, two for backbone assignment (5D and 4D), two for side chain assignments (4D, different TOCSY mixing times), and one 4D NOESY. A standard structure determination approach, using secondary structure analysis, sequence comparisons, and 3D structure calculation yields identification of a flexible tail and structures with accuracies of 0.6 Å RMSD (excluding the tail).

[1] H Ulm, M Wilmes, Y Shai, HG Sahl, *Frontiers in Immunology* 3, 1-4 (2012).

[2] J Fredriksson, W Bermel, DK Staykova, M Billeter, J. Biomol. NMR 54, 43-51 (2012).

[3] J Fredriksson, W Bermel, M Billeter, J. Magn. Reson. 217, 48-52 (2012).

[4] A Pedersen, K Hellberg, J Enberg, BG Karlsson, N. Biotechnol. 28, 218–224 (2010).

#### TU005: Mechanistic Basis of Phenothiazine-driven Inhibition of Tau Aggregation

<sup>1,3</sup>Elias Akoury, <sup>1,2\*</sup>Markus Zweckstetter

<sup>1</sup>Max Planck Institute for Biophysical Chemistry, <sup>2</sup>German Center for Neurodegenerative Disease (DZNE), <sup>3</sup>GGNB doctoral program Biomolecules: Structure – Function – Dynamics, University of Göttingen

Alzheimer's disease (AD) is the most widespread dementia syndrome showing progressive presence of abundant deposits of extracellular senile  $\beta$ -amyloid polypeptide (A $\beta$ ) plaques and intracellular neurofibrillary tangles (NFTs) consisting of Tau protein.[1] Tau protein is an intrinsically disordered protein that is abundant in neuronal axons where it promotes and stabilizes microtubule assembly.[2] With progression of AD, Tau aggregates and accumulates into NFTs. As there is still no causative treatment or cure for AD and other tauopathies, Tau-based research aims to reveal the pathological consequences of amyloid formation and to implement new therapeutic strategies. In this effort identification of inhibitors of tau aggregation as potential disease-modifying drugs and investigation of their mode of action play an important role.[3]

Methylene Blue (MB), a tricyclic phenothiazine also known as methylthionine hydrochloride, has been shown to prevent Tau aggregation *in vitro*[4] and to reduce the amount of Tau aggregates in a *C. elegans* model of Tau pathology.[5] Moreover, MB progressed to phase II clinical trial in human

AD patients with promising results [6] and was recently announced to enter a phase III clinical trial [7].

Using an integrated approach combining solution-state NMR spectroscopy and other biophysical techniques, we reveal a distinct mechanism of action of MB and its metabolites azure A and azure B in the inhibition of Tau aggregation.[8] We show that the mechanism of Tau aggregation inhibition is based on the interplay of reduction/oxidation of the native cysteine residues of Tau. This prevents the formation of filaments by retaining Tau in a monomeric disordered conformation. Our data demonstrate that MB and its N-demethylated derivatives azure A and azure B modify the two native cysteines of Tau to sulfenic, sulfinic and sulfonic acid. The modification of protein cysteine residues through reversible oxidation of cysteine sulfhydryl groups and the formation of sulfenic acids are a crucial regulatory event in biological systems.

In summary we provide mechanistic insights into the inhibition of Tau aggregation by the family of phenothiazines. Specific modification of the native cysteine residues retains Tau in a monomeric conformation preventing the formation of filaments and their toxic precursors. Demethylation of methylene blue establishes new interactions with Tau and enables additional means for modulation of Tau aggregation.

[1] J. Hardy, D. J. Selkoe, *Science* 2002, 297, 353-356.

[2] D. G. Drubin, M. W. Kirschner, *J Cell Biol* 1986, 103, 2739-2746.

[3] B. Bulic, M. Pickhardt, B. Schmidt, E. M. Mandelkow, H. Waldmann, E. Mandelkow, *Angew Chem Int Ed Engl* 2009, 48, 1740-1752.

[4] R. H. Schirmer, H. Adler, M. Pickhardt, E. Mandelkow, *Neurobiol Aging* 2011, 32, 2325 e2327-2316.

[5] C. M. Wischik, P. C. Edwards, R. Y. Lai, M. Roth, C. R. Harrington, *Proc Natl Acad Sci U S A* 1996, 93, 11213-11218.

[6] C. Wischik, R. Staff, *J Nutr Health Aging* 2009, 13, 367-369.

[7] C. Wischik, TauRX Therapeutics: Sept 10-th, 2012 Press release announcing the initiation of a global Phase 3 clinical trial in a type of Frontotemporal Dementia (FTD) also known as Pick's Disease.

[8] E. Akoury, M. Pickhardt, M. Gajda, J. Biernat, E. Mandelkow, M. Zweckstetter, *Angew Chem Int Ed Engl* 2013, DOI:10.1002/anie.201208290

#### TH006: Inhibiting the S100B-p53 protein protein interaction

<sup>1,2\*</sup>David J. Weber

<sup>1</sup>University of Maryland School of Medicine, <sup>2</sup>Center for Biomolecular Therapeutics

Inhibiting S100B-target interactions in the p53 tumor suppressor degradation pathway is underway as a possible means for treating malignant melanoma and other human cancers with elevated S100B.

However, specifically inhibiting protein-protein interactions (PPIs) is often not straightforward, and requires a plethora of structural and dynamic data for achieving this goal. In this presentation, methods used for inhibiting protein-protein interactions with small molecule inhibitors will be included with a focus on how NMR and information pertaining to protein dynamics is increasingly becoming a necessity. Likewise, a "PPI final folding model" will be presented as it pertains to blocking the S100B-p53 interaction with small molecule inhibitors of S100B (SBiXs).

#### MO007: Insights into the Intramolecular Coupling between the N- and C-Domains of Troponin C Derived from High-Pressure, Fluorescence, Nuclear

## Magnetic Resonance, and Small-Angle X-ray Scattering Studies

<sup>1</sup>Guilherme A. P. de Oliveira, <sup>2</sup>Cristiane B. Rocha, <sup>1</sup>Mayra de A. Marques, <sup>3</sup>Yraima Cordeiro, <sup>1</sup>Martha M. Sorenson, <sup>1</sup>Débora Foguel, <sup>1</sup>Jerson L. Silva, <sup>1,4\*</sup>Marisa C. Suarez

<sup>1</sup>Programa de Biologia Estrutural, Instituto de Bioquímica Médica, Instituto Nacional de Biologia Es, <sup>2</sup>UNIRIO-Universidade Federal do Estado do Rio de Janeiro, CCBS-Centro de Ciências Biológicas e da Saúde, <sup>3</sup>Faculdade de Farmácia, Universidade Federal do Rio de Janeiro, Rio de Janeiro, Brazil, <sup>4</sup>Programa de Biologia Estrutural, Instituto de Bioquímica Médica-Polo Xerém, Universidade Federal

Troponin C (TnC), the Ca<sup>2+</sup>-binding component of the troponin complex of vertebrate skeletal muscle, consists of two structurally homologous domains, the N- and C-domains; these domains are connected by an exposed  $\alpha$ -helix. Mutants of full-length TnC and of its isolated domains have been constructed using site-directed mutagenesis to replace different Phe residues with Trp. Previous studies utilizing these mutants and high hydrostatic pressure have shown that the apo form of the C-domain is less stable than the N-domain and that the N-domain has no effect on the stability of the C-domain [Rocha, C. B., (2008) *Biochemistry* 47, 5047–5058]. Here, we analyzed the stability of full-length F29W TnC using structural approaches under conditions of added urea and hydrostatic pressure denaturation; F29W TnC is a fluorescent mutant, in which Phe 29, located in the N-domain, was replaced with Trp. High pressure nuclear magnetic resonance was used to monitor TnC unfolding. From these experiments, we calculated the thermodynamic parameters ( $\delta V$  and  $\delta G^\circ_{\text{atm}}$ ) that govern the folding of the intact F29W TnC in the absence or presence of Ca<sup>2+</sup>. We found that the C-domain has only a small effect on the structure of the N-domain in the absence of Ca<sup>2+</sup>. However, using fluorescence spectroscopy, we demonstrated a significant decrease in the stability of the N-domain in the Ca<sup>2+</sup>-bound state (i.e., when Ca<sup>2+</sup> was also bound to sites III and IV of the C-domain). An accompanying decrease in the thermodynamic stability of the N-domain generated a reduction in  $\delta\delta G^\circ_{\text{atm}}$  in absolute terms, and Ca<sup>2+</sup> binding affects the Ca<sup>2+</sup> affinity of the N-domain in full-length TnC. Cross-talk between the C- and N-domains may be mediated by the central helix, which has a smaller volume and likely greater rigidity and stability following binding of Ca<sup>2+</sup> to the EF-hand sites, as determined by our construction of low-resolution three-dimensional models from the small-angle X-ray scattering data.

## TU008: Millisecond Loop Dynamics in Metallo-Beta-Lactamases Gained During Evolution

Mariano M. Gonzalez, Luciano A. Abriata, Pablo E. Tomatis, \*Alejandro J. Vila

*Instituto de Biología Molecular y Celular de Rosario (IBR) - CONICET*

Metallo-Beta-Lactamases (MBLs) represent one of the most relevant bacterial resistance mechanisms.[1]

The broad substrate spectrum of MBLs is attributed to the particular topology of the active site, a shallow groove formed and flanked by several loops (L3, L10 and L12). We have shown that mutations N70S and G262S, which alter the hydrogen-bond network connecting loops L3 and L12, give rise to evolved enzymes with an extended substrate spectrum.[2,3] In order to explore the role of these mutations in the loops flexibility and (within a broader perspective) the role of flexibility in protein evolution, we decided to study the backbone dynamics of wild type BcII (BcII wt) and *in vitro* optimized mutants.

We have measured backbone R<sub>1</sub> and R<sub>2</sub> relaxation rates, and heteronuclear NOEs for BcII wt, N70S, G262S and N70S/G262S optimized mutants, which were analyzed based on the model-free approach.[4] The enzymes exhibit a relatively rigid backbone in the pico-to-nanosecond time scale,

with a similar S<sup>2</sup> profile and a slight increase in flexibility in loop L3.

Conformational exchange processes that occur on micro-to-millisecond time scales, were probed by using CPMG relaxation dispersion methods.[5,6] We observed that in the wt enzyme there is only eight residues in conformational exchange. During the analysis of mutation N70S, which is deleterious in the wild type background, there is no residues with conformational dynamics. Interestingly, the G262S mutation, which is responsible of moving the Zn<sup>2+</sup> ion in a more solvent exposed position through a direct interaction with C221, displays an enhanced relaxation profile for several residues, most of which are located in and near loop L10. In addition, the N70S/G262S double mutant showed residues located in and near both loops L3 and L10 with an enhanced relaxation dispersion profile. This active site's conformational flexibility suggest a possible scenario for MBLs evolution.

## References:

- [1] Crowder, M. W., Spencer, J., and Vila, A. J. *Acc. Chem. Res.* 39, 721-728, 2006
- [2] Tomatis, P. E., et al. *Proc. Natl. Acad. Sci. U. S. A* 102:13761–13766, 2005
- [3] Tomatis, P. E., et al. *Proc. Natl. Acad. Sci. U. S. A* 105, 20605-20610, 2008
- [4] Mandel, A. M., Akke, M. and Palmer, A. G. 3rd *J. Mol. Biol.* 246, 144-163, 1995
- [5] Loria, J. P., Rance, M., Palmer, A. G. 3rd *J. Am. Chem. Soc.* 121, 2331-2332, 1999
- [6] Boehr, D. D., Dyson, H. J., and Wright, P. E. *Chem. Rev.* 106, 3055-3079, 2006

Acknowledgements: ANPCyT, NIH, CONICET

## TH009: Structural Insights into Eosinophil Cationic Protein's Cytotoxicity: Molecular Recognition of Cell Surface Glycosaminoglycans

<sup>1</sup>María Flor García-Mayoral, <sup>2</sup>Ángeles Canales, <sup>3</sup>Javier López-Prados, <sup>3</sup>Pedro N. Nieto, <sup>2</sup>Jesús Jiménez Barbero, <sup>1\*</sup>Marta Bruix

<sup>1</sup>Instituto de Química Física Rocasolano, CSIC, Madrid, Spain, <sup>2</sup>Centro de Investigaciones Biológicas, CSIC, Madrid, Spain, <sup>3</sup>Instituto de Investigaciones Químicas, CSIC-Universidad de Sevilla, Sevilla, Spain

Protein-glycosaminoglycan interactions are essential in many biological processes and human diseases. Eosinophil Cationic Protein (ECP) is a cytotoxic RNase found in large amounts in the secondary granules of eosinophils. The protein is secreted from activated eosinophils during infection and plays a role in the human innate immune defence, with reported toxicity against bacteria, viruses, and parasites. Cationic and aromatic residues have been found to be essential for ECP's interaction with membranes[1] and glycosaminoglycans (GAGs)[2], suggesting that recognition of heparan sulphates exposed at the mammalian cellular surfaces may drive and modulate its cytotoxicity[3]. To get deeper insight into the cytotoxic process, we have explored the interactions of ECP with a GAG mimetic. By using NMR spectroscopy and MD simulations we have determined the 3D structure of ECP in complex with a representative trisaccharide heparin-derivative and dissected the structural requirements for this interaction. Using NMR-monitored titrations we have also estimated its binding affinity, which is in the  $\mu\text{M}$  range.

The structure of the complex shows that the carbohydrate binds at the catalytic site, revealing the mechanism of inhibition of ECP's ribonucleolytic activity. The charged sulphate and carboxylate groups of the carbohydrate cluster with well-defined orientations interacting with charged and polar residues of the protein. The conserved W10 is also involved in the recognition. The pyranose ring of IdoA adopts the skew-boat <sup>2</sup>S<sub>0</sub> conformation as observed in other complexes[4]. We



propose a molecular model for the membrane interaction process in which this recognition event may constitute the first step of the ECP's cytotoxic mechanism of action by facilitating contacts with the membrane that would subsequently trigger membrane destabilization and cell death. This model can be potentially used for the design of inhibitors to block ECP's toxicity in the treatment of eosinophil pathologies.

[1] E. Carreras, E. Boix, HF. Rosenberg, CM. Cuchillo, and MV. Nogués *Biochemistry*, 2003, 42, 6636-6644.

[2] TC. Fan, SL. Fang, CS. Hwang, CY. Hsu, XA. Lu, SC. Hung, SC. Lin and MDT. Chang *J. Biol. Chem.*, 2008, 283, 25468-25474.

[3] MF. García-Mayoral, M. Moussaoui, BG. de la Torre, D. Andreu, E. Boix, MV. Nogués, M. Rico, DV. Laurents, and M. Bruix *Biophys. J.*, 2010, 11, 2702-2711.

[4] L. Nieto, A. Canales, G. Giménez-Gallego, PM. Nieto, and J. Jiménez-Barbero *Chem. Eur. J.*, 2011, 17, 11204-11209.

This work has been carried out with financial aid of the MINECO (Project number CTQ2011-22514).

#### MO010: Gene Regulation by Ligand-Mediated Macromolecular Condensation

<sup>1</sup>Elihu Ihms, <sup>1</sup>Ian R. Kleckner, <sup>1</sup>Craig A. McElroy, <sup>2</sup>Paul Gollnick, <sup>1\*</sup>Mark P. Foster

<sup>1</sup>The Ohio State University, <sup>2</sup>University at Buffalo

Ligand-mediated allostery plays a central role in the regulation of a wide variety of biological processes. Thermodynamic linkage between allosteric ligands and competing conformational states (minimally two: on, off) provides a mechanism for thermodynamically modulating cellular responses. NMR studies will be presented of ligand-mediated regulation of gene transcription by the 91 kDa un-decameric (11-mer) ring-shaped *Bacillus* TRAP protein, and its inhibition by the trimeric (3-mer) protein Anti-TRAP, AT. Trp binding to TRAP leads to altered protein dynamics and promotes high-affinity binding to RNA thereby inhibiting Trp production via transcriptional attenuation and translational repression. However, AT can compete with the Trp-TRAP-RNA interaction despite orders of magnitude weaker binding and low relative molar ratios in the cell. By application of NMR and other complementary biophysical measurements, we show that AT binding leads to condensation of multiple TRAP rings into a high molecular weight complex. This condensation process may explain the *in vivo* observation of effective inhibition in the face of sub-stoichiometric abundance and relatively weak binding. Integration of TROSY NMR data with those from other spectroscopies, hydrodynamic and thermodynamic measurements, mass spectrometry, will be presented. The studies suggest a new mechanism by which small signals can be propagated to produce a robust cellular response.

#### TU011: Insights Into Ubiquitin C-Terminal Hydrolase L1 (UCH-L1) Mutation's Association with the Risk of Parkinson's Disease

<sup>1\*</sup>Kong Hung SZE, <sup>2</sup>Ho Sum Tse, <sup>3</sup>Hong-Yu Hu

<sup>1</sup>Microbiology Department The University of Hong Kong, Pokfulam Road, Hong Kong SAR, China, <sup>2</sup>Chemistry Department The University of Hong Kong, Pokfulam Road, Hong Kong SAR, China, <sup>3</sup>Shanghai Institutes for Biology Sciences, Chinese Academy of Sciences, China

Protein ubiquitination and deubiquitination, play important roles in many aspects of cellular mechanisms. Its defective regulation results in diseases that range from developmental abnormalities to neurodegenerative diseases and cancer. Ubiquitin carboxy-terminal hydrolase L1 (UCH-L1) is a protein of 223 amino acids, which is highly abundant in brain, constituting up to 2% of total brain proteins. Although it was originally characterized as a deubiquitinating enzyme, recent studies indicate that it also functions as a ubiquitin

ligase and a mono-Ub stabilizer. Down-regulation and extensive oxidative modifications of UCH-L1 have been observed in the brains of Alzheimer's disease and Parkinson's disease (PD) patients. Of importance, I93M and S18Y point mutations in the UCH-L1 gene have been reported to be linked to susceptibility to and protection from PD respectively. Hence, the structure of UCH-L1 and the effects of disease associated mutations on the structure and function are of considerable interest.

Our circular dichroism studies suggest that the S18Y point mutation only slightly perturbs the structure while a significant decrease in the  $\alpha$ -helical content is observed in the I93M mutant. We have determined the solution structure of S18Y and mapping its interaction with ubiquitin by chemical shift perturbation approach. The electrostatic surface potential analysis reveals that the interaction between ubiquitin and UCH-L1-S18Y is primarily electrostatic in nature, with negatively charged residues on the surface of UCH-L1-S18Y interacting with the positively charged residues on the basic face of ubiquitin. Although the active site and the L8 loop in UCH-L1-S18Y adopts conformations similar to that observed in the crystal structure of UCH-L1-WT, both the altered hydrogen bond network and surface charge distributions have demonstrated that the S18Y substitution could lead to profound structural changes. In particular, the difference in the dimeric interfaces of the wild-type and the S18Y mutant has shown that mutation can significantly affect the distribution of the surface-exposed residues involved in the dimeric interface. Such observed difference might weaken the stability of the UCH-L1 dimer and hence may explain the reduced dimerization-dependent ligase activity of UCH-L1-S18Y in comparison to UCH-L1-WT.

ACKNOWLEDGEMENTS: Research Grant Council of Hong Kong (GRF 776509M and 765312M)

#### TH012: An irreversible protein rearrangement linked to cellular function

Stefan Frost, Oanh Ho, Frederic Login, Christoph Weise, Hans Wolf-Watz, <sup>\*</sup>Magnus Wolf-Watz

Umeå University

While a firm coupling between equilibrium structural dynamics and protein function has been found for many systems, less is known about irreversible protein rearrangements and their potential coupling to functionality. Here, we provide *in vitro* (NMR) and *in vivo* based evidence for a coupling between the irreversible dissociation of a "hetero-dimeric" protein and functionality at a cellular level. Pathogenicity of *Yersinia pseudotuberculosis* is dependent on secretion of virulence effector proteins into eukaryotic host cells. Secretion is controlled by a multi-protein machinery denoted the type III secretion system (T3SS). The *Yersinia pseudotuberculosis* protein YscU plays a central role in regulation of effector protein secretion. YscU is composed of an N-terminal trans-membrane domain (YscU<sub>N</sub>) and a soluble cytoplasmic domain (YscU<sub>C</sub>). The cytoplasmic domain undergoes auto-proteolysis (self-cleavage) at a conserved NPTH motif and the resulting structure is a hetero-dimer. Dissociation of YscU<sub>C</sub> into its two polypeptides was found to be irreversible and triggered *in vitro* by increased temperature. Surprisingly, we discovered that dissociation of YscU<sub>C</sub> occurs also *in vivo* since the C-terminal YscU<sub>C</sub> polypeptide is secreted from the bacterium by the T3SS machinery. To test if dissociation is functionally relevant we analyzed destabilized gain of function YscU<sub>C</sub> mutations. These point mutants displayed accelerated dissociation kinetics, and whereas the wild-type protein is completely resistant to dissociation at 30 °C mutated variants dissociate at this temperature. The *in vitro* observations were manifested *in vivo*; whereas wild-type strain secrete effector proteins at 37 °C but not at 30 °C, strains with mutated YscU<sub>C</sub> secrete effector proteins efficiently at 30 °C. Thus, dissociation of YscU<sub>C</sub> is coupled to effector secretion and in turn pathogenicity of *Yersinia pseudotuberculosis*. These findings may be general since the T3SS machinery is

utilized by many different pathogenic bacteria. In summary our data provide a strong coupling between an irreversible protein rearrangement and biological function at a cellular level.

Reference: Frost, S. et. al. PLOS ONE, 2012, 7(11):e49349

**MO013: The role of hydrophobic and aromatic interactions on the amyloid assembly of alpha-synuclein: An NMR view.**

<sup>1,2</sup>M. E. Llases, <sup>1,2</sup>M. L. Orcellet, <sup>1,2</sup>G. R. Lamberto, <sup>3</sup>C. W. Bertoncini, <sup>4</sup>Christian Griesinger, <sup>1,2\*</sup>Claudio O. Fernández

<sup>1</sup>*Instituto de Biología Molecular y Celular de Rosario (IBR-CONICET), Universidad Nacional de Rosario,* <sup>2</sup>*Max Planck Laboratory of Structural Biology, Chemistry and Molecular Biophysics of Rosario (MPLPbioR),* <sup>3</sup>*Institute for Research in Biomedicine Barcelona, Barcelona, Spain,* <sup>4</sup>*Department of NMR-based Structural Biology, Max Planck Institute for Biophysical Chemistry*

Protein amyloidosis are considered the main cause of several neurodegenerative disorders with fatal consequences, such as Parkinson's disease (PD) and Alzheimer's disease (AD). Parkinson's disease is the second most common neurodegenerative disorder after AD, and is characterized by loss of dopaminergic neurons in the substantia nigra and formation of filamentous intraneuronal inclusions of the protein alpha-synuclein (AS).

The general objective of our group is to study the structural and toxic mechanisms related to amyloid formation[1] and to understand the structural and molecular basis behind the aggregation inhibitory effects of small molecules[2,3] in order to advance in the design of a therapeutic strategy based on amyloid inhibitors.

By using small compounds as structural probes, we have contributed recently to the development of this area of research. Through a multidisciplinary strategy we elucidated the structural and molecular basis of the interaction between AS and one of the most studied aggregation inhibitors, the cyclic tetrapyrrole Phthalocyanine tetrasulfonate (PcTS). The residue-specific structural characterization of the AS-PcTS complex provided the basis for the rational design of non-amyloidogenic species of AS, highlighting the role of aromatic and hydrophobic interactions in driving AS amyloid assembly.

In this work we studied the impact of conservative and non-conservative mutations on the amyloidogenic potential of human and mouse AS. The information derived from our analysis is key to understand the structural basis behind the amyloid aggregation of AS and to advance in the rational design of more efficient amyloid inhibitors.

References:

[1] Bertoncini et al, Proc Natl Acad Sci U S A, 2005, 102: 1430-1435.

[2] G.R. Lamberto, A. Binolfi, M.L. Orcellet, C.W. Bertoncini, M. Zweckstetter, C. Griesinger and C.O. Fernández, Proc Nat Acad Sci (USA). 106, (2009) 21057-21062.

[3] G.R. Lamberto, V. Torres-Monserrat, C.W. Bertoncini, X. Salvatella, M. Zweckstetter, C. Griesinger and C.O. Fernandez, J Biol Chem.

286 (2011) 32036-32044.

Acknowledgements:

Financial support from ANPCyT, CONICET, Laboratorios Pfortner, Fundación Bunge y Born, Max Planck Society and Alexander von Humboldt Foundation are acknowledged.

**TU014: Preliminary solution NMR studies of a Membrane Protein in Type VII Secretion System of M. tuberculosis**

<sup>1</sup>Yao He, <sup>1</sup>Chenwei Zhang, <sup>2</sup>Fangming Wu, <sup>1,2\*</sup>Changlin Tian

<sup>1</sup>*School of Life sciences, University of Science and Technology of China,* <sup>2</sup>*High Magnetic Field Laboratory, Chinese Academy of Sciences*

Rv3882c has been reported to be a conserved component of the Type VII Secretion System of mycobacteria. It was described as a protein anchored on the inner membrane with two trans-membrane helices. Here the recombinant trans-membrane domain of its homolog protein in *M. smegmatis*, which named MS0082-TMH, is overexpressed in *Escherichia coli*. Then the isotope labeled MS0082-TMH was purified in detergent solution. With the NMR spectroscopy data we finished the backbone assignment and the relaxation analysis ( $T_1$ ,  $T_2$ , NOE). Moreover, with the titration data of  $Mn^{2+}$ EDDA<sup>2-</sup> we confirm the starting point and ending point of this trans-membrane region.

**TH015: Characterization of intermediates states of Sugarcane defensin 5 by relaxation dispersion NMR: thermodynamics and stability**

<sup>1\*</sup>Luciana Elena S. F. Machado, <sup>2</sup>Yulia Pustovalova, <sup>1</sup>Viviane Silva de Paula, <sup>2</sup>Irina Beszonova, <sup>1</sup>Ana Paula Valente, <sup>2</sup>Dmitry M. Korzhnev, <sup>1</sup>Fabio C. L. Almeida

<sup>1</sup>*National Center of NMR, Institute of Medical Biochemistry, Federal University of Rio de Janeiro, Bra,* <sup>2</sup>*Department of Molecular, Microbial and Structural Biology, University of Connecticut Health Center 2*

The sugarcane defensin 5 (Sd5) is a small protein with antifungal activity. Sd5 has a long unfolded C terminal region which is unique within the defensin protein family. Also, all the Sd5 secondary structure elements are in conformational exchange, which are those responsible to bind membranes. Based on these features, we aimed here to identify and to characterize the pre-existing state (invisible state) of Sd5, which would be important for protein function using relaxation dispersion experiments by Nuclear Magnetic Resonance (NMR). The <sup>15</sup>N relaxation dispersion of Sd5 could be fitted using a two site exchange model (native and intermediate). The population of Sd5 intermediate increased as a function of temperature as well as the exchange rate ( $k_{ex}$ ). Interestingly, all these events were mostly enthalpy-driven. In the presence of urea, we observed opposite results, since the population of intermediate decreased as a function of urea concentration while  $k_{ex}$  was kept constant. The urea dependence of  $\delta G$  (m value) is negative, indicating that the excited state of Sd5 is more compact. This suggestion is strengthened by evidence demonstrating that: *i*) the hydrophobic residues of defensins are usually exposed to solvent, and *ii*) four pairs of cysteines are key to maintain defensin fold and two of them that connect the  $\alpha$ -helix to the  $\beta$ -sheet are in conformational exchange. Concluding, we demonstrate that Sd5 has an intermediate conformational state that is enthalpically-driven and disturbance of its structure indicates that the charge residues are in conformational exchange and could favor its contact for guarantee the fold of Sd5 and preservation of its structure.

Acknowledgments: CAPES, FAPERJ, Ciências sem Fronteiras-CNPq, INBEB

**MO016: NMR with Multiple Receivers**

<sup>1\*</sup>Ēriks Kupče, <sup>2</sup>Ray Freeman, <sup>3</sup>Kevin J. Donovan, <sup>3</sup>Lucio Frydman, <sup>4</sup>Lewis E. Kay

<sup>1</sup>*Bruker Ltd, Coventry, United Kingdom,* <sup>2</sup>*Jesus College, Cambridge, United Kingdom,* <sup>3</sup>*Department of Chemical Physics, Weizmann Institute of Science, 76100 Rehovot, Israel,* <sup>4</sup>*Departments of Molecular Genetics, Biochemistry and Chemistry, The University of Toronto, Toronto, O*

The advent of multiple receivers that record several data sets in a single experiment increases the efficiency of spectrometer use. At the same time, development of cryogenically cooled probes has significantly increased the sensitivity of NMR ex-

periments. This opens an exciting possibility of changing the traditional paradigm of experiment design.

We show two main approaches for recording free induction decays (FIDs) in multi-receiver experiments - parallel and sequential acquisition. In both cases the magnetization is typically split into different pathways with the resultant signals from each of the paths recorded using different receivers.

The sequential acquisition method has been exploited in a number of applications to date involving a range of different molecules, from small molecule to bio-molecular applications. Notably, one application, PANACEA has been used for structure determination of small molecules from a single measurement. In labelled bio-molecules, e.g. proteins the weak signal that remains after  $^{13}\text{C}$  detected experiments (the  $^{13}\text{C}$  "afterglow") is measured with high sensitivity by proton detection. This is illustrated by the combined dual-receiver 2D (HA)CACO / 3D (HA)CA(CO)NNH experiment.

The utility of the parallel acquisition is established through the introduction of the  $^1\text{H}$  and  $^{13}\text{C}$  detected 2D HSQC and 3D HNCA experiments in which pairs of 2D and 3D spectra are recorded simultaneously. The potential of combining parallel-receiving, multi-nuclear technologies with ultra-fast spatial encoding methods is demonstrated by the 2D  $^1\text{H}$ - $^1\text{H}$  and  $^1\text{H}$ -X (X =  $^{19}\text{F}$ ,  $^{31}\text{P}$ ) correlation spectra acquired within a single scan. The experiment brings new opportunities for high-throughput analyses, chemical kinetics, and fast experiments on metastable hyperpolarized solutions.

With the anticipated further increases in cryogenic probe sensitivity it is expected that multiple receiver experiments will become an important approach for efficient recording of NMR data.

#### TU017: Lipid binding by the Unique and SH3 domains suggests a new regulation mechanism for c-Src

<sup>1</sup>Mariano Maffei, <sup>1,2</sup>Irene Amata, <sup>3</sup>Yolanda Perez, <sup>2</sup>Ana Igea, <sup>4</sup>Pau Bernadó, <sup>2</sup>Angel R. Nebreda, <sup>1\*</sup>Miquel Pons

<sup>1</sup>Biomolecular NMR laboratory, University of Barcelona, Spain, <sup>2</sup>Signaling and Cell Cycle laboratory, IRB Barcelona, Spain, <sup>3</sup>IQAC-CSIC, NMR facility Barcelona, Spain, <sup>4</sup>Centre de Biochimie Structurale, Montpellier, France

The non-receptor protein kinase c-Src was the first proto-oncogene to be discovered and plays a central role in many signaling pathways that regulate cell growth, differentiation, migration, proliferation and survival. c-Src is constituted by a series of folded domains (SH2, SH3 and kinase) as well as a 85 residue long intrinsically disordered segment that is divided in two distinct regions: the SH4 domain, which is myristoylated and acts as a primary attachment point to the membrane surface, and the Unique domain (USrc) connecting the SH4 and SH3 domains.

In this study, by combining NMR and biochemical techniques, we found that a short peptide motif within the Unique domain (ULBR - Unique Lipid Binding Region) acts as a secondary lipid binding region of c-Src. Moreover, we show, for the first time, that the SH3 domain of c-Src contains also a lipid binding region in the opposite side of its peptide binding site. We have further characterized the intra-molecular interaction between the USrc and SH3 domains and its allosteric modulation by a SH3-binding peptide or by Calcium-loaded calmodulin. These NMR results were integrated with in vivo experiments, in which the functional relevance of this novel lipid binding region of c-Src was confirmed in the *X. laevis* oocytes model system. Together, these results uncover an important functional role for the intrinsically disordered Unique domain and suggest the existence of a novel regulation layer in c-Src.

#### TH018: Can Melatonin Help Prevent Alzheimer's Disease?

Katherine Clausen, Lianna Di Maso, Kalah Bermudez,

Shannon Naughton, \*Sandra Chimon-Peszek

DePaul University

In previous studies, the orthomolecular species melatonin has been found to have a tremendous impact on the  $\beta$ -amyloid peptide that causes Alzheimer's disease. Melatonin has been shown to inhibit oxidative stress and the death of neurons and neuroblastoma cells exposed to the peptide. The purpose of research on an orthomolecular species such as melatonin is to determine how the chemical substance reacts with a disease or abnormality by restoring proper levels of the chemical substance in the brain. The first step in the process of researching the effects of melatonin on the Alzheimer's  $\beta$ -amyloid peptide is to make melatonin water soluble. Studies suggest that melatonin powder can become water soluble when mixed with water at 20 °C or 50 °C. Studies have also shown that melatonin is soluble in ethanol. This study utilized all three techniques to create melatonin solutions. Melatonin in a fine powder was added to water at 20 °C, water at 50 °C, and ethanol at 20 °C. All three of the solutions were centrifuged in order to gather only the water soluble aspects of the melatonin solutions. The melatonin concentration of each solution was determined by using a calibration curve. The calibration curve was created by using a UV/vis machine to measure the absorbances of serially diluted solutions with known concentrations made from pure melatonin. The presence of melatonin in each solution was confirmed using ATR-IR spectroscopy by comparing the spectra of each solution to a melatonin reference spectra. Each solution was then combined with the  $\beta$ -amyloid peptide and Congo red and measured in the UV/vis machine for a week. Each solution was combined with the  $\beta$ -amyloid peptide and measured with ATR-IR for a week. The data was then analyzed and compared to solutions with  $\beta$ -amyloid peptide and no melatonin.

#### MO019: Mapping the residues crucial for protein stability - low-temperature studies of p53 tetramerization domain.

Lukasz Jaremko, Mariusz Jaremko, Stefan Becker, \*Markus Zweckstetter

Department for NMR-based Structural Biology, Max Planck Institute for Biophysical Chemistry

The tumour suppressor protein p53 plays an important role in preventing cancer. Its active conformation is tetrameric and one domain - the tetramerization domain permits the oligomerization of this protein.

Cold denaturation of proteins is a physical phenomenon that can be tracked by NMR spectroscopy to study structural changes induced by temperature at atomic level [1]. Previously several point mutations among nine hydrophobic core residues were reported to be crucial for the p53 tetramerization domain stability [2]. The p53 wild-type (WT) tetramerization domain together with selected mutants were studied in several different temperatures ranging from 298K down to 259K by solution NMR spectroscopy techniques. This allowed us to track the structural stability of the tetramerization domain of p53 and to identify residues affected by temperature changes. Low temperature-induced changes of  $^1\text{H}$ ,  $^{13}\text{C}$  and  $^{15}\text{N}$  chemical shifts occurred among hydrophobic residues, which were previously identified to be the key determinants of the thermodynamic stability of p53 tetramerization domain [2].

[1] Jaremko, M., Jaremko, L., Kim, H.-Y., Cho, M.-K., Schwieters, C. D., Giller, K., Becker, S., Zweckstetter, M. (2013) Cold denaturation of a protein dimer monitored at atomic resolution, Nat. Chem. Biol. Accepted

[2] Mateu, M. G., Fersht, A. R. (1998) Nine hydrophobic side chains are key determinants of the thermodynamic stability and oligomerization status of tumour suppressor p53 tetramerization domain, EMBO J. 17, 2748-2758.

**TU020: A Grid-enabled web portal for NMR structure refinement with AMBER**<sup>1</sup>Lucio Ferella, <sup>1</sup>Andrea Giachetti, <sup>2</sup>David A. Case, <sup>1\*</sup>**Antonio Rosato**<sup>1</sup>*University of Florence*, <sup>2</sup>*Rutgers University*

The typical workflow for NMR structure determination involves collecting thousands of conformational restraints, calculating a bundle of 20–40 conformers in agreement with them and refining the energetics of these conformers. The structure calculation step employs simulated annealing based on molecular dynamics (MD) simulations with very simplified force fields. The value of refining the calculated conformers using restrained MD (rMD) simulations with state-of-art force fields is documented. This refinement however presents various subtleties, from the proper formatting of conformational restraints to the definition of suitable protocols.

Here we describe a web interface to set up and run calculations with the AMBER package, which we called AMPS-NMR (AMBER-based Portal Server for NMR structures). The interface allows the refinement of NMR structures through rMD. Some predefined protocols are provided for this purpose, which can be personalized; it is also possible to create an entirely new protocol. AMPS-NMR can handle various restraint types. Standard rMD refinement in explicit water of the structures of an all-helical and an all-beta protein are shown as examples. AMPS-NMR additionally includes a workspace for the user to store different calculations. As an ancillary service, a web interface to AnteChamber is available, enabling the calculation of force field parameters for organic molecules such as ligands in protein-ligand adducts.

AMPS-NMR is available at <http://py-enmr.cerm.unifi.it/access/index/amps-nmr> ;

Reference: I. Bertini et al., *Bioinformatics*, 2012, 27:2384–2390.

Acknowledgement: This work was supported by the European Commission [contract no. 261572, WeNMR project].

**TH021: The WeNMR e-Infrastructure for Structural Biology****\*Antonio Rosato***University of Florence*

The WeNMR (<http://www.wenmr.eu>) project is a European Union funded international effort to streamline and automate analysis of Nuclear Magnetic Resonance (NMR) and Small Angle X-Ray scattering (SAXS) imaging data for atomic and near-atomic resolution molecular structures of proteins and nucleic acids [1]. Conventional calculation of biomacromolecular structure requires the use of various software packages, considerable user expertise and ample computational resources. To facilitate the use of NMR spectroscopy and SAXS in life sciences the WeNMR consortium has established standard computational workflows and services through easy-to-use web interfaces, while still allowing expert users to tune parameters and protocols to their liking. At present, a number of programs often used in structural biology have been made available through application portals. WeNMR is also committed to fostering the development of automated procedures in the field of biomolecular NMR, mainly through the CASD-NMR initiative [2]. A selection of the most widely used portals is described, addressing, among other things, the use of paramagnetic NMR data in NMR structural biology.

## References

[1] Wassenaar et al. *Journal of Grid Computing* (2012), 10:743–767.

[2] Rosato et al. *Structure* (2012), 20:227–236.

## Acknowledgement

The WeNMR project (European FP7 e-Infrastructure grant, contract no. 261572, [www.wenmr.eu](http://www.wenmr.eu)), supported by the European Grid Initiative (EGI) through the national GRID Initiatives of Belgium, France, Italy, Germany, the Netherlands (via the Dutch BiG Grid project), Portugal, Spain, UK, South Africa, Taiwan and the Latin America GRID infrastructure via the Gisela project is acknowledged for the use of web portals, computing and storage facilities.

**MO022: Structural studies of protein disulfide isomerase P5****Guennadi Kozlov**, Roohi Vinaik, \*Kalle Gehring*McGill University, Montreal, Canada*

Protein disulfide isomerases (PDIs) constitute a class of enzymes that catalyze the oxidative folding of proteins in the endoplasmic reticulum (ER). Human PDI P5, also known as PDI A6, is a 47 kDa protein which contains three thioredoxin-like domains: two active domains possessing catalytic CGHC motifs and a non thiol-reactive C-terminal domain. P5 associates with BiP, an Hsp70 ER homologue. BiP binds to heavy chains of immunoglobulins as they enter the ER and the luminal domains of receptors as part of the unfolded protein response, and prevents the accumulation of misfolded proteins in the ER. We obtained high-resolution structures of all three domains of P5 and are currently using small-angle X-ray scattering to determine the global shape of the full-length protein in solution. The structures provide novel insights into mechanism of P5 regulation. We use pulldown assays, NMR and site-directed mutagenesis in order to characterize the interaction between P5 and BiP and identify domains in both proteins that are required for the binding. These studies will provide novel insights into involvement of these proteins in the ER protein folding.

## ACKNOWLEDGMENTS: NSERC

**TU023: Interaction Studies of Human Laforin with Oligosaccharides by NMR, MST and ITC**<sup>1,2,3</sup>David M. Dias, <sup>4</sup>Joana Furtado, <sup>3</sup>Emeric Wasielewski, <sup>3</sup>Tiago Faria, <sup>1</sup>Alessio Ciulli, <sup>3</sup>Rui M. Brito, <sup>5</sup>Philipp Baaske, <sup>4</sup>Pedro Castanheira, <sup>2,3\*</sup>**Carlos F. G. C. Geraldes**<sup>1</sup>*University of Cambridge*, <sup>2</sup>*University of Coimbra*, <sup>3</sup>*Centre for Neurosciences and Cell Biology of Coimbra*, <sup>4</sup>*Biocant - Association for Technology Transfer*, <sup>5</sup>*Nano Temper Technologies GmbH*

Laforin is a unique human dual-specificity phosphatase as it contains an amino terminal carbohydrate binding module (CBM) and a carboxyl terminal phosphatase domain containing a HCXXGXXR(S/T) catalytic active site motif [1]. Laforin mutations have been associated with Lafora disease, an early onset fatal progressive myoclonus epilepsy with autosomal recessive inheritance [2]. The laforin CBM carbohydrate binding activity has been poorly characterized. We describe here our studies of the interaction of recombinant human Laforin [3] with a series of oligosaccharides using a variety of techniques. The Laforin oligosaccharide binding preferences were first screened by Microscale Thermophoresis (MST) using soluble oligosaccharides of increasing length, which has shown an increased preference of laforin for longer oligosaccharides (both linear and circular), with the highest affinity at pH 7.5. The affinity constant of Laforin to linear oligosaccharides decreased systematically from  $K_d = 2700 \mu\text{M}$  for maltotriose to  $K_d = 173 \mu\text{M}$ , while for the cyclodextrins  $K_d$  varied from  $841 \mu\text{M}$  for  $\alpha$ -CD to  $114 \mu\text{M}$  for  $\gamma$ -CD. The Laforin affinity constants obtained for  $\gamma$ -CD and maltoheptaose by Isothermal Titration Calorimetry (ITC) titrations compare favorably with the above results. The thermodynamic parameters determined by ITC were also consistent with other protein-carbohydrate interactions.

Finally we assessed ligand binding of  $\gamma$ -CD and maltoheptaose using STD [4] and CPMG NMR techniques [5]. Both compounds were detected unambiguously on the two ligand-based

NMR experiments. Although various resonance overlaps are observed for this kind of molecules, a group epitope mapping (GEM) from the STD-NMR experiment discloses the most likely binding profile for these sugars.

#### Acknowledgments

We are grateful for funding from FCT, Portugal (project PTDC/BIA-PRO/11141/2009 and PhD grant SFRH/BD/81735/2011 awarded to D.M.D.)

References [1] Wang, J., Stuckey, J. A., Wishart, M. J., and Dixon, J. E. (2002) *J. Biol. Chem.* 277, 2377-2380

[2] Chan, E. M., Andrade, D. M., Franceschetti, S., and Minassian, B. (2005) *Adv. Neurol.* 95,

[3] Castanheira, P., Moreira, S., Gama M. and Faro C. (2010) *Prot. Expr. Purif.* 71, 195-199.

[4] Mayer, M. and Meyer, B. (1999) *Angewandte Chemie-International Edition* 38, 1784-1788.

[5] Hajduk P, Olejniczak E, Fesik S (1997) *J. Am. Chem. Soc.* 119, 12257-12261

#### TH024: NMR Structural Studies of the LyeTx-II Peptide

<sup>1</sup>Bruno A. de Assunção, <sup>1</sup>Natália G. S. Pinheiro, <sup>2</sup>Rodrigo M. Verly, <sup>1</sup>Daniel M. Santos, <sup>1</sup>Maria E. de Lima, <sup>1</sup>Dorila Piló-Veloso, <sup>1\*</sup>Jarbas M. Resende

<sup>1</sup>Universidade Federal de Minas Gerais, <sup>2</sup>Universidade Federal dos Vales do Jequitinhonha e Mucuri

The peptide LyeTx-II has recently been isolated from the venom of the spider *Lycosa erythrogna*, a species known as wolf spider, which is commonly found in the Brazil South-east Region. Antimicrobial assays indicate that LyeTx-II exhibit activity against different pathogens. This peptide carries three charged lysine residues and is naturally amidated at C-terminus. In order to investigate the structure as well as the interactions of this peptide with mimetic membranes, we have performed CD and NMR experiments.

LyeTx-II was prepared by solid-phase synthesis, by using Fmoc chemistry. The obtained peptide was purified by HPLC and its identity was confirmed by mass spectrometry. CD spectra of the peptide were recorded at different TFE:H<sub>2</sub>O mixtures as well as in the presence of aqueous micellar solutions of DPC and SDS. A sample containing LyeTx-II at 1 mM in TFE-d<sub>2</sub>:H<sub>2</sub>O (50:50, v/v) was prepared for the NMR analyses. TOCSY, NOESY, <sup>1</sup>H-<sup>13</sup>C HSQC and <sup>1</sup>H-<sup>15</sup>N HMQC experiments were acquired at 20 °C on a Bruker Avance-III 800 MHz spectrometer equipped with a triple resonance (<sup>1</sup>H/<sup>13</sup>C/<sup>15</sup>N) 5 mm gradient probe.

The CD spectrum of the LyeTx-II in water shows a profile coherent with spectra of random coil peptides, however for solutions containing significant amounts of TFE and in the presence of either DPC or SDS micelles, the spectra show clear profile of well defined helical structures. This is a quite common feature of several antimicrobial peptides, which are usually unstructured in aqueous media but tend to adopt well defined conformations when in contact with the membrane environment.

The spin systems of all residues have been recognized on the TOCSY spectra. Many of the sequential connections were completed mainly on the basis of the strong dNN connections. The high number of cross peaks  $\alpha\text{N}(i,i+3)$ ,  $\alpha\beta(i,i+3)$ , and  $\alpha\text{N}(i,i+4)$  suggested that the peptide shows a significant helical content, which extends from the third amino acid residue to the C-terminal carboxamide. In spite of showing a high helical content, the distribution between hydrophilic and hydrophobic residues within the helix is not coherent with an amphipathic structure. We have already synthesized this peptide with selective <sup>15</sup>N and <sup>2</sup>H labeling in order to obtain information about the peptide topology through solid state NMR experiments of samples containing LyeTx-II reconstituted into lipid bilayers.

ACKNOWLEDGMENTS: CAPES, FAPEMIG, CNPq, PRPq-UFG, CNRMN

#### MO025: Structural and Thermodynamic Characterization of the Capsid Protein of Hepatitis C Virus and its Interaction with the Tumor Suppressor Protein p53

<sup>1</sup>Fabiana Pestana Albernaz, <sup>1</sup>Vanessa L. Azevedo Braga, <sup>2</sup>Theo L. F. Souza, <sup>1</sup>Thiago Rodrigues Pinto, <sup>1</sup>Luciana Pereira Rangel, <sup>3</sup>David Peobody, <sup>1</sup>Jerson Lima, <sup>1</sup>Andre Marco de Oliveira, <sup>1</sup>Fabio C. L. Almeida, <sup>1\*</sup>Andrea Cheble de Oliveira

<sup>1</sup>Programa de Biologia Estrutural and Centro Nacional de Ressonância Magnética Nuclear de Macromolé, <sup>2</sup>Faculdade de Farmácia - UFRJ, RJ, Brazil, <sup>3</sup>Department of Molecular Genetics and Microbiology and Cancer Research and Treatment Center, Universi

Hepatitis C virus (HCV) acts as a major agent of chronic hepatitis, cirrhosis, and hepatocellular carcinoma. The HCV core protein (HCVcp) is involved with the nucleocapsid assembly and with different cellular processes. The interaction of HCVcp with the tumor suppressor protein p53 has been described in hepatocellular carcinoma but the mechanism of this interaction remains unknown. In this work we use thermodynamic and spectroscopic techniques to achieve the structural characterization of HCVcp and its interaction with p53. Although HCVcp is an intrinsically unstructured protein, our fluorescence spectroscopy results demonstrated a significant decrease in the spectral center of mass of the protein in function of increasing concentrations of chemical denaturants, indicating the presence of structural elements. These data are corroborated by Circular Dichroism (CD) and Nuclear Magnetic Resonance (NMR). HCVcp backbone assignments strategy based on projection spectroscopy, a way of reducing the experiment time when recording high-dimensional NMR experiments and Triple resonance experiments are in course. To evaluate the interaction between HCVcp and p53, <sup>1</sup>H/<sup>15</sup>N HSQC NMR spectra of labeled HCVcp were acquired in the absence and in the presence of unlabeled p53. Changes in the chemical shift of some resonances of the HCVcp were observed, showing changes in the chemical environment of these amino acid residues and suggesting interaction with p53. Fluorescence polarization assays of FITC-labeled p53 in the presence of HCVcp corroborate the interaction *in vitro* between both proteins. Additionally to these studies, we are also investigating the interaction of the HCVcp with the p53 in HepG2 and H1299 cells. We constructed vectors to express both HCVcp and p53 fused to the proteins GFP and DsRed-Monomer, respectively, in order to perform Fluorescence Resonance Energy Transfer analyses and these studies are in progress. Our data reveal a new approach to understand the HCVcp-p53 interaction.

ACKNOWLEDGEMENTS: FAPERJ, CAPES, CNPq and IN-BEB

#### TU026: Effect of an antihistaminic-containing syrup in salivary metabolites

<sup>1</sup>Liana B. Freitas-Fernandes, <sup>1</sup>Tatiana Kelly S. Fidalgo, <sup>1</sup>Ivete R. P. de Souza, <sup>2</sup>Fabio C. L. Almeida, <sup>2\*</sup>Ana Paula Valente

<sup>1</sup>Department of Pediatric Dentistry and Orthodontics, School of Dentistry, <sup>2</sup>National Center Nuclear Magnetic Resonance

The effect of medicines-containing syrup on the tooth surface is largely studied in literature. On the other hand, few studies evaluate salivary metabolites changes.

Objectives: The aim of this study was to evaluate *in vitro* and *in vivo* local effect of an antihistaminic-containing syrup in salivary metabolites using high-resolution <sup>1</sup>H NMR spectroscopy.

Methods: For *in vitro* interaction, unstimulated whole saliva from 10 healthy volunteers was collected and its supernatant was analyzed (G1) and then it was *in vitro* mixture with Claritin® antihistaminic-containing syrup (G2) and antihistaminic pill suspension as a control (G3). For *in vivo* study, after sample collection, the same volunteers were instructed to rinse the mouth with Claritin® for 20 seconds and the content was analyzed (G4). The *in vitro* and *in vivo* mixture were studied in  $^1\text{H}$  NMR spectra were acquired and processed on a Bruker 400 MHz Advance spectrometer. For statistical analysis it was used principal analysis component (PCA) and ANOVA and Tukey test ( $p < 0.05$ ).

Results: PCA demonstrated similarity between the groups G1 and G4 as well as G2 and G3. Products characteristics from microorganism metabolism found in salivary metabolites demonstrated a reduction after antihistaminic containing syrup assay (G2 and G3), such as propionate, acetate and butyrate (Tukey,  $p < 0.05$ ). In the same way, arginine, glutamine, valerate, and proline were statistically higher before antihistaminic-containing syrup *in vitro* and *in vivo* interaction (Tukey,  $p < 0.05$ ). Conclusion: Similarity in salivary metabolites were found both *in vitro* and *in vivo* antihistaminic interaction. In addition, it was demonstrated that *in vitro* assays could be an alternative method for medicines and salivary interaction studies.

ACKNOWLEDGEMENTS: FAPERJ, CAPES, CNPq, UFRJ.

#### TH027: NMR analysis and site specific protonation constants of streptomycin

Gábor Orgován, \*Béla Noszál

Semmelweis University, Budapest, Hungary

Streptomycin is the most widely known member in the aminoglycoside antibiotic class of drugs, and also, the first effective remedy for tuberculosis. The two guanidino and the secondary amino sites make the molecule peculiar: it has long been known to be the most basic antibiotic drug.

$^1\text{H}$  NMR-pH and  $^1\text{H}$ - $^{13}\text{C}$  HSQC-pH titrations were carried out on streptomycin and streptidine, a symmetrical constituent compound of reduced complexity to monitor the proton-binding processes of the basic sites. Accurate, undistorted, electrodeless pH measurement was ensured by a new set of in tube indicators, which made possible the accurate determination of extremely high pH values [1,2].

The microscopic protonation constants of the two guanidino groups of streptomycin were calculated by evaluating the various NMR-pH data and transferring the pair-interactivity parameter from streptidine to streptomycin. Inherent guanidino basicities fall in the range of 13.03 – 13.39 logK units, which drop to 12.48 – 12.85 upon protonation of the other site [3]. The basicity of the secondary amino group is, however, 5 logK units lower.

Our results showed that at 1 M NaOH solution 25 % of the streptomycin molecules are still protonated. At physiological pH (pH = 7.4) the vast majority of streptomycin is triprotonated.

The constants determined also indicate the hydrogen-bonding acceptor propensity of streptomycin at the site-specific level, an important property in the highly selective biochemical processes. The fact, that the molecule exists in every aqueous biological medium in a tricationic form, implies that it presumably enters the central nervous system by means of transporter protein system(s).

[1] Orgován, G.; Noszál, B. Journal of Pharmaceutical and Biomedical Analysis 2011, 54, 958.

[2] Szakács, Z.; Hägele, G.; Tyka, R. Analytica Chimica Acta 2004, 522, 247.

[3] Orgován, G.; Noszál, B. Journal of Pharmaceutical and Biomedical Analysis 2012, 59, 78.

#### MO028: Site-specific acid-base properties of ovothiol, the octafarous antioxidant, determined by $^1\text{H}$ and $^{15}\text{N}$ NMR spectroscopy

Arash Mirzahosseini, Sándor Hosztafi, Gábor Orgován, \*Béla Noszál

Semmelweis University, Faculty of Pharmacy, Department of Pharmaceutical Chemistry, Budapest, Hungary

Thiol-disulfide equilibria in amino acids, peptides and proteins are essential in maintaining the redox balance in living systems, providing thus protection against oxidative stress. Probably the smallest, yet most-faceted thiol-containing biomolecule is ovothiol, a mercaptohistidine derivative in marine invertebrate eggs. It is also assumed to be a highly potent antioxidant, due to its remarkably low thiolate basicity.

Because the four basic moieties of ovothiol are in close vicinity, the microconstants can not be determined by the titration of ovothiol alone. Nevertheless, the fortunate position of the imidazole 2H and  $\alpha\text{H}$  results in the selective sensitivity of these NMR nuclei towards the imidazole nitrogen/thiolate, and amino/carboxylate groups, respectively.

A deductive method was designed to elucidate the entire microspeciation of ovothiol, by examining three derivative compounds (ovothiol amide, *S*-methyl ovothiol, *S*-methyl ovothiol amide) that model the minor microspecies. By conducting  $^1\text{H}$  NMR-pH titrations, the macroscopic protonation constants of the model compounds were determined, and were then involved to calculate the microscopic protonation constants of ovothiol. To ensure accurate logK determination, an internal indicator system was used to measure the *in situ* pH.

Our results include the entire microspeciation of ovothiol (32 site-specific protonation constants for 16 microspecies) determined by the  $^1\text{H}$ -NMR data. Each proton-binding site of ovothiol bears 8 different basicity values depending on the protonation state of the surrounding moieties. The unusually large interaction between the basic centers, especially the one between the thiolate and imidazole nitrogen, causes that basicity extrema of the imidazole differ by more than five orders of magnitude, the largest difference observed in any biomolecule so far. The interactivity parameters between the proton-binding sites, along with the Sudmeier-Reilly protonation shift constants could also be determined. These results were confirmed with UV-pH titration and  $^{15}\text{N}$ -HMBC-pH titration data.

#### TU029: NMR Structure Determination of the Hypothetical Protein Q4DY78 Conserved in Kinetoplastids

\*Everton Dias D'Andréa, Gabriela Pinheiro Heredia, José Ricardo Murari Pires

Universidade Federal do Rio de Janeiro

Chagas Disease, Sleeping Sickness and Leishmaniasis are between the so called Neglected Diseases, endemic in poor countries of South America and Africa, exposing million of economic most disfavoured people at risk. Sequencing of the genome of the kinetoplastids *Trypanosoma cruzi*, *Trypanosoma brucei* and *Leishmania major* open up new perspectives for drug research against these diseases. In each diploid genome ca. 10,000 gene pairs were identified and around 50% code for proteins of unknown function. In the present work using bioinformatic tools available we mined the Trityp Databank to end up with a list of 197 proteins up to 30 kDa, conserved in kinetoplastids, without orthologues in mammals, plant or fungi, without transmembrane regions and without homologous sequences in the PDB that should be suitable for structural studies by solution NMR. From these proteins, the Q4DY78, which is predicted to be an a/b protein, its gene was obtained commercially cloned into the plasmid pUC57 (GenScript Inc.). It was sub-cloned into the expression plasmid pGEX-4T2, followed by expression and purification of the protein. The Q4DY78 protein  $^1\text{H}$  NMR spectrum is compatible to a small monomeric protein. A set

of NMR experiments were obtained: with a unlabeled sample - 2D TOCSY, 2D NOESY (in H<sub>2</sub>O and D<sub>2</sub>O); with a <sup>15</sup>N-labeled sample - <sup>15</sup>N HSQC, <sup>15</sup>N HSQC TOCSY, <sup>15</sup>N HSQC NOESY, <sup>15</sup>N HSQC series with different relaxation delays for measurement of  $T_1$  and  $T_2$ , and <sup>1</sup>H, <sup>15</sup>N-heteronuclear NOE; and with a <sup>13</sup>C, <sup>15</sup>N-double-labeled sample - <sup>13</sup>C HMQC, CBCANH, CBCACONH, HCCH-COSY, HBHACONH, <sup>13</sup>C HSQC NOESY, plus spectra using Fast NMR methodology, bCBCANH, bCBCACONH, and bHNCO bHNCOi. <sup>15</sup>N HSQCs were made at different temperatures to verify hydrogen bonds and the amino acid are in secondary structure. The protein backbone assignment is in progress.

### TH030: Experimental and Simulated Yeast Thioredoxin 1 Dynamics: Exchange Path of a Tightly Bound Water Molecule Essential for Biological Activity

<sup>1</sup>Natália Corrêa Pereira, <sup>2</sup>Francisco Gomes Neto, <sup>1</sup>Luciana Elena M. S. Fraga, <sup>1</sup>Ana Paula Valente, <sup>1\*</sup>Fabio C. L. Almeida

<sup>1</sup>Biomolecular NMR Laboratory, National Center for Nuclear Magnetic Resonance, Institute of Medical Biochemistry, Federal University of Rio de Janeiro, <sup>2</sup>Toxinology Lab., Oswaldo Cruz Institute -FioCruz, Rio de Janeiro, Brazil

Thioredoxins (Trx1) are small ubiquitous proteins with disulfide reductase activity. The active site lies in a loop (Trp29-Cys30-Gly31-Pro32-Cys33) where the disulfide reduction of substrate involves a sequence of two nucleophilic attacks performed by the thiolate of Cys33 and Cys30. yTrx1 activity depends on Asp24, a residue buried in the protein hydrophobic core, positioned near but not adjacent to the active site, working as a proton acceptor in the oxidation of cysteines. The proton transfer from Cys33 to Asp24 is mediated by a tightly bound water molecule, forming a water cavity. The mutation of D24N abolishes protein activity. Our group showed by NMR relaxation experiments that the residues within the water cavity are in conformational exchange, while mutation D24N quenches millisecond motion of these residues.

We studied by MD simulations the influence of the hydration state of Asp24/Asn24. We evaluated the hydrogen bond lifetime involving Asp24/Asn24 and showed that the mutation D24N led to an important decrease of the water residence time in the water cavity and a decrease in the average size of the cavity. These results corroborate the experimental dynamics that shows stabilization of a conformational state. The total amount of water also decreases in the mutant.

Supported by: CAPES, FAPERJ, CNPQ, INCT-INBEB

### MO031: NMR structural characterization of Q4D059, a conserved hypothetical protein from Trypanosoma cruzi

Aracelys López Castilla, \*José Ricardo Murari Pires  
Federal University of Rio de Janeiro

Q4D059 (Uniprot ID) is a hypothetical protein of 86 amino acids from *T. cruzi*. A PSI-BLAST search using Q4D059 sequence as query only identified hypothetical proteins from trypanosomatids (E-value above the threshold), so failed to provide insight into the protein function. Q4D059 is conserved in the kinetoplastid genomes and show low-sequence homology with mammal proteins; therefore it is considered a potential target for drug development against trypanosomatids parasites. Structural studies of this protein could give information about its function and facilitate drug screening. In this work, the gene coding for Q4D059 was cloned into a pGEX expression vector and <sup>13</sup>C- and <sup>15</sup>N- NMR protein samples were overexpressed in *Escherichia coli* as a GST-fusion protein. Purification of Q4D059 was performed by GST-affinity chromatography. GST was removed by thrombin protease digestion and as last step a size-exclusion chro-

matography was carried out. 1D <sup>1</sup>H and <sup>15</sup>N-<sup>1</sup>H HSQC spectra of Q4D059 showed a well-behaved and structured protein in solution. The NMR spectra required for protein structure determination were recorded. Assignment of most atoms in the protein was achieved and structure calculation is in progress.

### TU032: Conformation Changes in Somatostatin Analogue analyzed by NMR

<sup>1,2\*</sup>Luisa Mayumi Ribeiro Arake, <sup>2,3</sup>Diego Arantes Teixeira Pires, <sup>2</sup>Maura Viana Prates, <sup>2</sup>Carlos Bloch Jr.

<sup>1</sup>Instituto de Biologia, Universidade de Brasília, DF, Brasil,

<sup>2</sup>Embrapa Recursos Genéticos e Biotecnologia, DF, Brasil,

<sup>3</sup>Instituto de Química, Universidade de Brasília, DF, Brasil

Small peptides are attracting increasing interest in nuclear oncology to target tumors and thus facilitate cancer therapy. The high level expression of the somatostatin receptors on various tumor cells has provided its successful use as tumor tracer. The use of Technetium (<sup>99m</sup>Tc) as the coupled radioactive element is much explored in this kind of study and it utilizes the 6-Hydrazinonicotinamide (HYNIC) as the bifunctional complexing agent. In this work we analyzed conformational changes in the tridimensional structure of the somatostatin synthetic analogue Tyr<sup>3</sup>-Octreotide. This study is of relevant issue given that changes in the molecule structure might prevent it from binding to the radioactive element. The TYR<sup>3</sup>-octreotide was synthesized, purified and characterized by Mass Spectrometry. During the purification step, two fractions (P1 and P2) were identified which had the same molecular mass and the same fragmentation profile, which implies differences in their conformational structures. To elucidate their structure, P1 and P2 were analyzed by NMR performing H-NMR, TOCSY, ROESY and HSQC experiments, using H<sub>2</sub>O/D<sub>2</sub>O as solvent. The structures in question showed significant differences and P2 was not able to complex to the <sup>99m</sup>Tc even in the presence of HYNIC.

ACKNOWLEDGEMENTS: CAPES/Embrapa (001/2011), CNPq, CNRMN

### TH033: Unraveling thioredoxin-interacting protein (TXNIP) functions through structural studies

Gisele Cardoso de Amorim, Ramon Pinheiro Aguiar, Ana Paula Valente, \*Fabio C. L. Almeida

BioNMR Laboratory, National Center for Nuclear Magnetic Resonance, Federal University of Rio de Janeiro

The thioredoxin-interacting protein (TXNIP), also known as VDUP1 (vitamin D up-regulated protein) for its strong regulation by vitamin D, belongs to the  $\alpha$ -arrestin protein family. TXNIP was shown to function as a cell growth and transcription repressor, metabolic regulator, modulator of inflammatory response, cardiac function and cell signaling and apoptosis. It is also the only member of the  $\alpha$ -arrestin family capable of binding to thioredoxin in a redox-dependent fashion. Redox-dependent and independent regulatory roles were attributed to TXNIP activity. It has been demonstrated to play a crucial role in several pathological conditions such as cancer and cardiovascular diseases, increasing the interest in studying its structure, dynamics and interaction with cellular targets.

Very few structural information is available for this class of proteins, and for their interactions in the cell. One of our goals is determining the 3D solution structure of TXNIP using different constructions for each structural domain, called here D1 (17 kDa) and D2 (15 kDa). The native and cysteine-mutated <sup>15</sup>N and <sup>15</sup>N/<sup>13</sup>C D1 and D2 have been expressed and purified and the NMR spectra are being assigned. We also probed their interaction with both oxidized and reduced human thioredoxin, and we have evidence that mostly D2 interacts with thioredoxin. We have also collected SAXS data with the aim to reconstruct the entire TXNIP structure based on the domain structures determined by solution NMR.

These data might be crucial for understanding the participation of TXNIP in many different cell pathways and the molecular mechanisms involved in the different functions TXNIP can play.

Acknowledgments: FAPERJ, CNPq, INBEB, CNPq-Science w/o Borders, LNLs

#### MO034: Screening for new anticancer agents through the inhibition of the thioredoxin system

<sup>1</sup>Thais Oliveira, <sup>2</sup>Anne Caroline Candido, <sup>2</sup>Ricardo M Kuster, <sup>1</sup>Fabio C. L. Almeida, <sup>1\*</sup>Gisele Cardoso de Amorim

<sup>1</sup>BioNMR Laboratory, National Center for Nuclear Magnetic Resonance, Federal University of Rio de Janeiro, <sup>2</sup>Laboratório de Plantas Mediciniais, Instituto de Pesquisa de Produtos Naturais, Federal University of Rio de Janeiro

Cancer is still one of the primary causes of death in the world. Furthermore, many cancers are becoming resistant to conventional chemotherapeutic approaches. The discover of novel molecular targets and new anticancer agents are therefore of greatest interest.

Thioredoxin (Trx) is a small ubiquitous oxidoreductase conserved from Archebacteria to humans. Trx can interact with a broad range of proteins by a redox-sensitive mechanism that regulates reversible oxidation of two cysteine thiol groups to a disulfide. In addition to its function as a scavenger of reactive oxygen species, thioredoxin has been implicated in a great variety of cellular processes, including transcription factors modulation, cell growth and cell-survival regulation, through interaction with an extensive number of signaling molecules. Trx expression is increased in a variety of human primary cancers, where it is associated with aggressive cell growth and inhibition of apoptosis. Several studies implicate Trx as a contributor to cancer progression and metastasis, representing thus a molecular target for development of new anticancer drugs.

In the search for new agents, flavonoids emerged as cancer chemopreventive molecules because of their antioxidant activity. However, the precise mechanisms of flavonoids action are not totally understood. It has been demonstrated that this class of molecules can bind to and inhibit different proteins of the Trx system, including hTrx1.

With the aim to find new molecules able to inhibit the Trx system, we performed a screening using flavonoids extracted from sugarcane. Using <sup>15</sup>N-HSQC and saturation transfer difference (STD) experiments we were able to identify a glycoflavonoid that binds to the active site of hTrx1. A docking model is being calculated based on the experimental NMR data. Other extracts from sugarcane are being tested and showed a high potential to present inhibitor molecules.

Acknowledgments: FAPERJ, CNPq and INBEB

#### TU035: Interaction studies of Yersinia pestis Plasmin (Bubonic Plague Agent) and Human Plasminogen by Circular Dichroism and NMR

\*Carolina Galvão Sarzedas, Thaís Jerônimo Vidal, Jéssica Resende Barreto, Luzineide Wanderley Tinoco  
Universidade Federal do Rio de Janeiro

*Yersinia pestis* is the agent of bubonic plague classified in category A of bioterrorism agents according with Center for Disease Control and Prevention, USA. Plasmin (Pla) of *Y. pestis* is a membrane protein that cleaves/activates the human plasminogen in the cell invasion process, destabilizing the fibrinolytic cascade causing bleeding. Our goal was to characterize the pH effect in the Pla folding and their interaction with human plasminogen peptide (PK2). The structural characterization of PK2-Pla interaction could be useful to plan mimetic peptides to inhibit such interaction. Gel filtration chromatography showed that Pla is dimeric at pH 6.5 and monomeric at pH 8.0. CD and NMR analyses were

performed to evaluate the pH effect in the Pla folding and in the PK2-Pla interaction. CD studies showed structural changes of PK2 in the presence of Pla at pH 8.0, indicating Pla-PK2 interaction in this condition. NMR spectra of PK2 in the presence of Pla were acquired for the sample at pH 5.0. It was observed an increase in the peaks intensities compared with the PK2 free spectra, suggesting less conformational variability of PK2, probably due PK2-Pla interaction. However, a slight chemical shift change was observed only for Ha of VV residues of PK2 in the presence of Pla, suggesting that Pla-PK2 interaction is affecting specifically the RVV region. In the plasminogen activation process, Pla cleaves the R561-V562 bond in the sequence PGRVVGG. The absence of significant alteration on the NMR spectra suggests that PK2-Pla interaction at pH 5.0 could be weak, probably because Pla in this condition is in the dimeric form. These data show that Pla folding and aggregation state is sensitive to pH changes and interfere in the PK2-Pla interaction.

ACKNOLEDGEMENTS: FAPERJ, CNPq, INBEB

#### TH036: Solution-state NMR structure of a cytomegalovirus nuclear egress complex subunit and identification of the critical interaction surface with its heterodimer partner

Kendra Leigh, My D. Sam, Mayuri Sharma, Ming Lye, Gerhard Wagner, James M. Hogle, Donald M. Coen, \*Haribabu Arthanari

Harvard Medical School, Boston MA

Murine cytomegalovirus (MCMV) makes use of a conserved, essential heterodimeric nuclear egress complex (NEC) consisting of M50, a membrane protein, and M53, a soluble protein. Genetic, electron microscopy, and immunohistochemical studies have revealed the importance of these proteins for viral replication, localization of the complex to the inner nuclear membrane, and specific steps during nuclear egress of the viral nucleocapsid. We present here an NMR-determined solution-state structure of residues 1-168 of M50 (M50-NTD), which exhibits a novel protein fold. We mapped the binding of a highly conserved region of the M53 homologue, HCMV UL53, required for heterodimerization and identified specific residues in a groove on the surface of the M50 NTD that interacts with the UL53 peptide. Single amino acid substitutions of the corresponding residues of the M50 human homologue, UL50, resulted in decreased UL53 binding in vitro as measured by isothermal titration calorimetry, eliminated UL50-UL53 co-localization in immunofluorescence experiments, and caused lethal defects in the context of HCMV infection in human foreskin fibroblasts. These findings combined with essential nature of nuclear egress in CMV infections, and the novelty of the structure make the HCMV NEC an attractive potential drug target.

#### MO037: Looking for participation of an intermediate state on the mechanism of chaperon-like activity of yeast thioredoxin 1

<sup>1</sup>Mariana T. Q. Magalhães, <sup>1</sup>Luciana Elena S. F. Machado, <sup>1</sup>Adolfo H. Moraes, <sup>2</sup>Dmitry M. Korzhnev, <sup>1</sup>Ana Paula Valente, <sup>1\*</sup>Fabio C. L. Almeida

<sup>1</sup>Biomolecular NMR Laboratory, National Center for Nuclear Magnetic Resonance, Institute of Medical Biochemistry, Federal University of Rio de Janeiro, <sup>2</sup>University of Connecticut Health Center

Thioredoxins (Trx) are small ubiquitous proteins with disulfide reductase activity. Trxs are able to reduce buried disulfides more efficiently than small reductants. A chaperon-like activity was postulated to explain this behavior. However there is no accumulated knowledge on this particular activity. We showed the participation of the Asp24 in the modulation of the slow dynamics of residues involved in the formation of the water cavity. Asp24 works as a proton acceptor in the oxidation of Trx. The proton transfer from Cys33 to Asp24 is mediated by a tightly bound water, which forms the con-



served Trxs water cavity. Its dynamics might be linked to water exchange and catalysis. In this work, we are aiming to explore if the excited state conformation is involved in the opening of this water cavity, which might explain chaperon activity. In order to investigate this hypothesis, we use relaxation dispersion NMR over a range of experimental conditions, such as temperature and urea concentration, to identify a low-populated folding intermediate state.

Additionally, we are investigating the monomer-dimer equilibrium, which also plays an important role in Trxs biological activity. Our research group demonstrated that the monomer-dimer equilibrium is in slow exchange regime, while the monomer to intermediate works in fast to intermediate exchange. Significant information on this equilibrium can be obtained performing HSQC and HMQC experiments at different temperatures, concentrations and magnetic fields. Here we will show partial results on complex system characterization by using global fitting of data provided from our experiments.

Acknowledgements: CNPq-Science w/o Borders, CAPES, FAPERJ, INCT-INBEB

#### **TU038: NMR structure of human restriction factor APOBEC3A reveals substrate binding and enzyme specificity**

<sup>1,2</sup>In-Ja L. Byeon, <sup>1,2</sup>Jinwoo Ahn, <sup>3</sup>Mithun Mitra, <sup>1,2</sup>Chang-Hyeock Byeon, <sup>3</sup>Kamil Hercik, <sup>1</sup>Jozef Hritz, <sup>1,2</sup>Lisa M. Charlton, <sup>3</sup>Judith G. Levin, <sup>1,2\*</sup>Angela M. Gronenborn

<sup>1</sup>University of Pittsburgh Medical School, <sup>2</sup>Pittsburgh Center for HIV Protein Interactions, <sup>3</sup>National Institutes of Health

Human APOBEC3A (A3A) is a member of the A3 family of single-stranded DNA (ssDNA) deoxycytidine deaminases that play a role in the innate immune response to viral pathogens. A3A has a broad range of activities: it potently restricts LINE-1 retrotransposition, inhibits replication of retroviruses (e.g., HIV-1 and HTLV-1) and certain DNA viruses, degrades foreign DNA, and can function as a genomic DNA mutator. Here, we report the NMR solution structure of A3A, define the critical interface for interaction with its ssDNA substrates and model complex structures. The overall structure of A3A is very similar to that of the A3G catalytic C-terminal domain, although structural details are different. Oligonucleotides containing the A3A-specific recognition site TTCA bind A3A 10-fold more tightly ( $K_d$  60  $\mu$ M) than dCTP alone and the interaction surface includes residues that extend beyond the catalytic center. A3A also binds with similar affinity (90  $\mu$ M) to oligonucleotides containing the A3G-specific CCCA sequence. Real-time monitoring of the deamination reaction by NMR on A3A- and A3G-specific ssDNA substrates was conducted to determine the catalytic constants for A3A. Based on the structural and biochemical results, we propose a molecular mechanism that provides new insights into A3A functional activities.

#### **TH039: Improving the stability of Cdc25B for NMR measurements**

Raphael Santa Rosa Sayegh, Fabio Kendi Tamaki, Sandro Roberto Marana, Roberto Kopke Salinas, \*Guilherme Menegon Arantes

University of São Paulo

Cdc25B phosphatase plays an essential role on cell cycle checkpoints and is overexpressed in several kinds of tumors. Therefore, it has become a potential target for the development of new anticancer drugs. Computer simulations, bioinformatic analyses and crystallographic data indicate that the C-terminus of this protein is highly flexible and might influence the binding affinity of inhibitors. In order to obtain a better structural representation of Cdc25B in solution, we plan to evaluate different NMR data (e.g., chemical shifts and RDC's). However, Cdc25B is a 25 kDa protein

with low stability at the relatively high concentrations and temperatures typically required for NMR measurements. To overcome these challenges, different buffer conditions were screened in order to obtain samples stable enough to allow NMR data acquisition. The best buffer condition was in MES 50 mM pH 6.5 with 100 mM NaCl and glycerol 1%. In this condition, the protein (300  $\mu$ M) was fairly stable for 3 days at 288 K. Increasing the temperature to 298 K resulted in great protein precipitation. The <sup>1</sup>H-<sup>15</sup>N HSQC spectra of Cdc25B full-length catalytic domain displayed relatively good cross-peak dispersion, 198 peaks were observed out of 188 expected. Clustering of amide cross-peaks in the <sup>1</sup>H chemical shift region of 8 ppm suggest the presence of disordered regions. Several peaks which were absent in the HSQC spectra of a truncated construct, where the C-terminus was removed, were also clustered in the 8 ppm region of <sup>1</sup>H chemical shift, pointing to the flexibility of this region. ACKNOWLEDGEMENTS: FAPESP & CNPq

#### **MO040: NMR Structure Determination of a Meta Domain Conserved in Kinetoplastids**

Rachel Santos de Menezes, \*José Ricardo Murari Pires

Federal University of Rio de Janeiro

Chagas disease, sleeping sickness, and leishmaniasis are among the neglected tropical diseases, which affect the economically most disfavored population. Recently the genome of kinetoplastids etiological agents of these diseases, *Trypanosoma cruzi*, *Trypanosoma brucei* and *Leishmania major* were sequenced, so the perspectives of research for new drugs are being increased. META domain is a small domain family found in proteins of unknown function and occurs in *Leishmania spp* as an essential gene. Over-expression of that domain is related with virulence increase in *Leishmania amazonensis*, and is also implicated in motility in bacteria. The gene codifying META domain, that form part of the Q582E3 (Uniprot ID) hypothetical protein from *Trypanosoma brucei*, was cloned into a pGEX-4T2 expression vector and protein sample was overexpressed in *Escherichia coli* BL21(DE3) as a GST-fusion protein. Purification was performed by GST-affinity chromatography and then GST-tag was removed by cleavage by thrombine. A second step of purification, a size-exclusion chromatography, was carried out. <sup>1</sup>H spectra revealed a well-behaved and structured protein in solution. The NMR spectra required for protein structure determination are being recorded.

#### **TU041: Human beta-defensin 6/Glycosaminoglycan interaction by NMR: a model for extracellular matrix complex**

Jessica Oliveira, Viviane Silva de Paula, Vitor Hugo Pomin, Fabio C. L. Almeida, \*Ana Paula Valente

Centro Nacional de Ressonância Magnética Nuclear, Instituto de Bioquímica Médica, Universidade Federal do Rio de Janeiro

Defensins are small cationic, cysteine-rich, antimicrobial peptides that play a crucial role in host defense against pathogens. Human  $\beta$ -defensins (hBD) plays important roles in the innate and adaptive immune system when a threat is present. Defensins present other activities such as chemoattraction of a range of different cell through specific chemokine receptors and this chemoattraction could be regulated by glycosaminoglycan (GAG). In analogy to hBD2 and chemokine/(GAG) interactions, we decided to characterize the interaction between human  $\beta$ -defensin 6 (hBD6) and GAG. In the present study we use NMR spectroscopy of <sup>15</sup>N hBD6 to map the binding site for a synthetic pentasaccharide fondaparinux (Arixtra<sup>®</sup>), a highly sulfated heparin mimetic. Chemical shift mapping of the interaction reveals a contiguous binding surface on hBD6, which comprises amino acid residues of the  $\alpha$ -helix and loop between  $\beta$ 2- $\beta$ 3. The dissociation constant of the hBD6/GAG complex was determined by NMR spectroscopy to be 4 $\pm$ mM. The formation

of the hBD6/GAG complex was also confirmed by the overall decrease in  $^{15}\text{N}$   $R_1$  concomitant with an increase in  $^{15}\text{N}$   $R_2$  indicating an increase in the overall tumbling time of the protein.

**TH042: Structural and dynamics properties of the glycoprotein E – domain III of dengue virus free and in complex with specific single chain fragments (scFv) analyzed by NMR spectroscopy**

<sup>1</sup>Geovana Vargas, <sup>1</sup>Adolfo H. Moraes, <sup>1</sup>Fabio C. L. Almeida, <sup>2</sup>Luca Varani, <sup>1\*</sup>Ana Paula Valente

<sup>1</sup>Centro Nacional de Ressonância Magnética Nuclear, IBqM-UFRJ, RJ, Brazil, <sup>2</sup>Medical Institute for Research in Biomedicine, Bellinzona, Switzerland

The dengue virus belongs to the family of flavivirus and is responsible for more than 100 million cases annually. The viral envelope glycoprotein E is the major constituent of dengue virus surface and is the main target for antibody response against DENV. The crystal structures of the virus demonstrate that glycoprotein E is a dimer, where each monomer is composed by three domains: DI, DII and DIII. The development of a dengue vaccine has been hampered by the poorly understood process: antibody dependent enhancement (ADE) in which antibodies generated against a dengue serotype facilitate the infection by a different one. This process can lead to dengue hemorrhagic fever, a lethal form of the disease. In this work, we characterized the dynamics and the structural properties of the DIII of serotypes 1 and 4 using NMR spectroscopy. We mapped residues that participate in the interaction with specific scFv using chemical shift perturbation. The molecular dynamics on ps-ns time scale, which is related to thermal flexibility, and movements on ms-ms time scale, which are associated to conformation exchange events, were studied using  $^{15}\text{N}$  relaxation experiments. Quantitative analyses were obtained using relaxation dispersion experiments based on CPMG pulse sequences. We will present the conformational dynamics characterization of DIII in the free state and in complex with scFv. These data can be crucial for a better understanding of epitope-antibody interaction and can help in the development of new dengue vaccine.

ACKNOWLEDGEMENTS: FAPERJ, CNPq, CAPES, INBEB.

**MO043: Solution structure of the VirB9Ct-VirB7Nt complex from the Xanthomonas Type IV Secretion System**

Luciana Coutinho de Oliveira, Diorge Paulo de Souza, Denize Cristina Favaro, Angie Lizeth Davalos, Chuck S. Farah, \*Roberto Kopke Salinas

Department of Biochemistry, Institute of Chemistry, University of São Paulo

Type IV secretion systems (T4SS) are supramolecular complexes used by bacteria to secrete proteins or nucleoprotein complexes to the extracellular environment, or to deliver them inside a host cell [1]. T4SSs are generally composed of 12 proteins, VirB1 to VirB11 and VirD4, as found in the prototype T4SS of *Agrobacterium tumefaciens* [2]. VirB7, VirB9 and VirB10 form the channel used to translocate substrates across the bacterial cell envelope. This channel consists of an inner layer and an outer layer [1]. A high-resolution crystal structure of the outer layer from the T4SS of a conjugative plasmid of *E. coli*, pKM101, shows fourteen repetitions of a complex formed by VirB7 and the C-terminal (CT) domains of VirB9 and VirB10. *Xanthomonas axonopodis* pv. citri (Xac), a phytopathogen that infects citrus, has one T4SS encoded by the chromosome [3]. Previously we showed that a Xac VirB7-VirB9-VirB10 complex assembles *in vivo*. We also showed that Xac VirB7 has a C-terminal globular domain (residues 52-133) that is absent in the VirB7 of other organisms [4]. This observation suggests that there could be a structural variation in the T4SS of *Xanthomonadaceae*. Isolated Xac VirB9<sup>CT</sup> and Xac-VirB7 form a tight complex,

in slow exchange at the NMR time scale. Spectral changes observed in the  $^{15}\text{N}$ -HSQC spectra of Xac VirB9 in the absence and presence of a peptide corresponding to residues 24-46 of Xac VirB7 (VirB7<sup>NT</sup>), suggest that at least part of Xac-VirB9<sup>CT</sup> undergoes a disorder-order transition upon binding [4]. In order to obtain further high-resolution structural information on Xac's T4SS, we initiated a study of the three-dimensional structure of the complex formed by Xac-VirB9<sup>CT</sup> and Xac-VirB7<sup>NT</sup>. As much as 96% of the backbone NMR resonances were assigned. Experiments for backbone and side-chain NMR resonance assignment were recorded and are being analyzed. Preliminary  $^{13}\text{C}$  chemical shift analysis indicates the presence of 8 beta-strands, which is consistent with the available structures for *E. coli* VirB9 C-terminal domain (PDB 3JQO and 2OFQ).

ACKNOWLEDGEMENTS: FAPESP, CNPq

[1] Chandran, V., Fronzes, R., Duquerroy, S., Cronin, N., Navaza, J., Waksman, G. (2009). Structure of the outer membrane complex of a type IV secretion system. *Nature* 462, 1011–1015.

[2] Zechner, E.L., Lang, S., and Schildbach, J.F. (2012). Assembly and mechanisms of bacterial type IV secretion machines. *Philos. Trans. R. Soc. Lond., B, Biol. Sci.* 367, 1073–1087.

[3] Da Silva, A.C.R., Ferro, J.A., Reinach, F.C., Farah, C.S., Furlan, L.R., Quaggio, R.B., Monteiro-Vitorello, C.B., Van Sluys, M.A., Almeida, N.F., Alves, L.M.C., et al. (2002). Comparison of the genomes of two *Xanthomonas* pathogens with differing host specificities. *Nature* 417, 459–463.

[4] Souza, Diorge P., Andrade, Maxuel O., Alvarez-Martinez, Cristina E., Arantes, Guilherme M., Farah, Chuck S., Salinas, Roberto K. (2011). A Component of the Xanthomonadaceae Type IV Secretion System Combines a VirB7 Motif with a N0 Domain Found in Outer Membrane Transport Proteins. *PLoS Pathogens*, v. 7, p. e1002031.

**TU044: Structural studies on Trypanosoma cruzi P21 protein as a strategy for Chagas disease treatment**

Francesco Brugnera Teixeira, Eduardo Horjales, \*Claudia Elisabeth Munte

Physics Institute of São Carlos, University of São Paulo, Brazil

Cell invasion by the different infective forms of *Trypanosoma cruzi*, the causative parasite of Chagas disease, involves several mechanisms which culminate in entry of *T. cruzi* into host cells. Numerous studies have been performed in order to identify surface and secreted proteins related to cell invasion, mostly from metacyclic and tissue culture trypomastigote forms. However, little attention has been given to the extracellular amastigote, also capable to invade mammalian cells in an alternative invasion mechanism. The molecules involved in this alternative process are still poorly known or studied and may be significant to *T. cruzi* survival under high cytotoxic conditions afforded by the host cells. In this context, a new protein named P21 has been recently identified. Its participation in the invasion mechanism cannot yet be explained at molecular level, but experiments suggest that P21 interacts with the CXCR4 chemokine receptor, activating phagocytosis in macrophages and promoting actin polymerization in mammalian cells.

As the first step towards P21 NMR structural studies, we developed a purification/refolding protocol and performed the  $^1\text{H}$ ,  $^{13}\text{C}$  and  $^{15}\text{N}$  sequential assignment using triple resonance NMR spectra (Bruker 600 MHz). The secondary structure prediction, based on chemical shifts (TALOS+), showed five  $\alpha$ -helix regions and an unstructured N-terminal region (residues 1-42). We also identified several regions of the protein with multiple conformations, indicating a large structural flexibility. Future structural and interaction experiments with the N-terminal peptide of CXCR4, essential

for the protein activation, may lead to a new therapy based on peptides, which may change the current worldwide scenario on the Chagas disease treatment.

#### TH045: Excited States of the Alzheimer beta-Amyloid Peptide can be Detected by High Pressure NMR Spectroscopy

<sup>1,2</sup>Claudia Elisabeth Munte, <sup>2</sup>Markus Beck Erlach, <sup>2</sup>Werner Kremer, <sup>2</sup>Joerg Koehler, <sup>2\*</sup>Hans Robert Kalbitzer

<sup>1</sup>Physics Institute of São Carlos, University of São Paulo, 13566-590 São Carlos, SP, Brazil, <sup>2</sup>Institute of Biophysics and physical Biochemistry, University of Regensburg, D-93053 Regensburg, Germany

Amyloid fibrils in the brain consisting of the amyloid peptide ( $A\beta$ ) are a lead marker of Alzheimer's disease. A deeper understanding of the mechanism of fibril formation may help to design drugs for preventing the deposition of amyloid, therefore the existence of specific conformations of monomeric  $A\beta$  is potentially important.  $A\beta$ -monomers in aqueous environment are usually assumed to occur in a disordered state. In contrast, by high pressure NMR spectroscopy we detect two main conformational states at atmospheric pressure, a compactly folded state 1 and a partly unfolded state 2, with relative populations of 0.7 and 0.3, respectively. Pure random coil like structures were not detected. The pressure response indicates an ordered structure between amino acids 16 to 24 and 30 to 37 in state 1.  $A\beta$ -fibrils depolymerise at high pressure, the dissociation constant of monomers from the fibrils increases by two orders of magnitude at 200 MPa and 283 K. The partial molar volume of the monomer unit changes by 101 ml/mol with binding. The thermodynamic data suggests that state 1 is responsible for fibril elongation.

#### MO046: NMR study of the calcium-binding domains of the $Na^+/Ca^{2+}$ exchanger of *Drosophila melanogaster* by solution NMR

<sup>1</sup>Layara A. Abiko, <sup>1</sup>Priscila Hauk, <sup>1</sup>Denize C. Favaro, <sup>1</sup>Luciana Coutinho de Oliveira, <sup>2</sup>Lei Bruschweiler-Li, <sup>2</sup>Rafael Bruschweiler, <sup>1\*</sup>Roberto Kopke Salinas

<sup>1</sup>Institute of Chemistry, University of São Paulo, <sup>2</sup>Department of Chemistry and Biochemistry, Florida State University

*Drosophila melanogaster's*  $Na^+/Ca^{2+}$  exchanger (CALX) catalyzes the co-transport of  $Na^+$  and  $Ca^{2+}$  across the plasma membrane and is essential for the maintenance of  $Ca^{2+}$  homeostasis in *Drosophila's* sensory neuronal cells. The exchanger consists of a transmembrane domain, which is responsible for ion translocation across the membrane, and an intracellular loop that contains two calcium binding domains (CBDs). Besides transporting  $Ca^{2+}$ , the exchanger is also regulated by this ion. There are two CALX isoforms, CALX-1.1 and CALX-1.2, which only differ in a segment of five amino acid residues located in the second calcium-binding domain, CBD2. Binding of four calcium ions to the first intracellular  $Ca^{2+}$ -binding domain, CBD1, of CALX-1.1 inhibits the exchanger. In contrast, the isoform CALX-1.2 is insensitive to the binding of  $Ca^{2+}$  to CBD1. In order to understand how the binding of  $Ca^{2+}$  to CBD1 could be involved in the regulation of CALX, we initiated a study of the structure and dynamics of a covalent construct containing the two CBD domains (CBD12) by high-resolution NMR. <sup>1</sup>H-<sup>15</sup>N-TROSY spectra of CBD12-1.1 and CBD12-1.2 acquired in the absence or presence of  $Ca^{2+}$  are consistent with well-folded domains. The translational diffusion coefficient (Dt) was measured for CBD12-1.1 in the apo and  $Ca^{2+}$ -bound states by Diffusion-Ordered NMR Spectroscopy. The Dt values obtained for CBD12-1.1 ( $7.68 \times 10^{-11}$  and  $7.38 \times 10^{-11} m^2 s^{-1}$ , for the unliganded and  $Ca^{2+}$ -bound forms, respectively) are consistent with predicted data using SOMO ( $8.04 \times 10^{-11} m^2 s^{-1}$ ) or HYDROPRO ( $7.92 \times 10^{-11} m^2 s^{-1}$ ), and indicate that the proteins are monomeric in solution. Further studies

are being carried out in order to characterize the structure and dynamics of CBD12-1.1 in solution.

ACKNOWLEDGEMENTS: FAPESP, CAPES.

#### TU047: Structure and Dynamics of Allergen Gad m 1 free and in complex with single chain variable fragment by NMR Spectroscopy

<sup>1</sup>Adolfo H. Moraes, <sup>2</sup>Daniela Ackerbauer, <sup>2</sup>Maria Kostadinova, <sup>2</sup>Merima Bublin, <sup>3</sup>Fatima Ferreira, <sup>1</sup>Fabio C. L. Almeida, <sup>2</sup>Heimo Breiteneder, <sup>1\*</sup>Ana Paula Valente

<sup>1</sup>Centro Nacional de Ressonância Magnética Nuclear, IBqM-UFRJ, RJ, Brazil, <sup>2</sup>Medical University of Vienna, Vienna, Austria, <sup>3</sup>University of Salzburg, Salzburg, Austria

Allergenic proteins are able to stimulate an inappropriate IgE production in atopic individuals, which results in manifestations of clinical symptoms such as asthma, rhinitis and atopic dermatitis. Gad m 1 is the major allergen from *Atlantic cod* and belongs to  $\beta$ -parvalbumin protein family, which are the most important fish allergens and their high cross-reactivity is the cause of the observed polysensitization in allergic patients. Despite extensive efforts, the complete elucidation of  $\beta$ -parvalbumin-IgE complexes has not been achieved yet. In this work, we solved the solution structure of Gad m 1 using NMR spectroscopy. Concomitantly, scFv interaction studies were performed, using chemical shift perturbation assays. We compared our results with other sites mapped in homologous parvalbumins: Cyp c 1, Sco j 1 and Gad c 1. Residues around positions 30 to 40 matched epitopes mapped for the three allergens. Residues around position 50 to 60 were only observed for Gad m 1 and Gad c 1, while residue around 80 was mapped on Cyp c 1. On the other hand, the N-terminal was only mapped in Gad m 1 and our results did not showed the participation of residues around position 90. The dynamic properties of Gad m 1 in the free state and in the complex with scFv were obtained from relaxation experiments. Residues 31-33 and 75-78 exhibit increased  $R_2/R_1$  ratios. These residues are located in two regions mapped by CSP. The big ratios observed may be due to chemical exchange between bound and free forms. This work will present for the first time the solution structure of a  $\beta$ -parvalbumin as well as the characterization of Gad m 1-scFv interaction as a first and crucial step in the development of hypoallergenic vaccine and to an understanding of the molecular interactions between allergens and IgE's.

ACKNOWLEDGEMENTS: FAPERJ, CNPq, CAPES, and IN-BEB

#### TH048: The Putative Hepatitis C Virus Fusion Peptide Interacts with Model Membranes and Gains Helix Content

<sup>1\*</sup>Nathalia S. Alves, <sup>1</sup>Ygara S. Mendes, <sup>2</sup>Theo L. F. Souza, <sup>1</sup>M. Lucia Bianconi, <sup>3</sup>Cristiane D. AnoBom, <sup>1</sup>Ana Paula Valente, <sup>1</sup>Jerson L. Silva, <sup>1</sup>Andre M. O. Gomes, <sup>1</sup>Andrea Cheble de Oliveira

<sup>1</sup>IBqM, UFRJ, RJ, Brazil, <sup>2</sup>Faculdade de Farmácia, UFRJ, RJ, Brazil, <sup>3</sup>IQ, UFRJ, RJ, Brazil

**Introduction:** The Hepatitis C virus (HCV) is an enveloped RNA virus, and the most common cause of chronic liver disease. Although much information has been gathered in recent years, the exact mechanisms that lead to membrane fusion are poorly understood. The envelope glycoprotein, E1 or E2, directly interacts with biological membranes, throughout the fusion peptide (FP). As the localization of FP remains unknown, we aim to characterize the interaction of a putative HCV FP, corresponding to residues 421-445 (HCV<sub>421-445</sub>), present in E2, with different membrane models. **Methods:** We used spectrophotometry, fluorescence spectroscopy, circular dichroism (CD), isothermal titration calorimetry (ITC), differential scanning calorimetry (DSC), dynamic light scattering (DLS) and nuclear magnetic resonance (NMR) to evaluate peptide-membrane interaction and conformational

changes due to this interaction. **Results:** ITC and fluorescence polarization data showed that HCV<sub>421–445</sub> can interact with large unilamellar vesicles (LUV). However, DSC revealed that the peptide cannot change the phase transition temperature of multilamellar vesicles. Photometry analyses revealed that the peptide can induce LUV aggregation, but DLS data revealed that the peptide can either disrupt or aggregate the same vesicles. Since the interaction of fusion peptides with membranes can lead to an important structural gain, we also aim to solve HCV<sub>421–445</sub> structure. NMR data of the peptide free in solution indicated low structure content but addition of SDS micelles led to a structural gain, confirmed by CD data. The preliminary structure calculation showed that the C-terminal of the peptide in the presence of micelles presents a tendency to form an  $\alpha$ -helix, which could be stabilized by a helix stabilization motif, GXXXG. **Conclusions:** Altogether our results indicate that HCV<sub>421–445</sub> peptide is able to perturb lipid membranes, and becomes structured. These studies are important to better understand the fusion mechanisms of HCV, which could help in the development of new antiviral therapies.

Support: Capes, CNPq, FAPERJ, PRONEX, INBEB

#### MO049: Structure and Dynamics of D24A mutant of yeast thioredoxin reveals a less stable conformation with increased flexibility.

Anwar Iqbal, Luciana Elena S. F. Machado, Catarina A. Miyamoto, Ana Paula Valente, \*Fabio C. L. Almeida

*Biomolecular NMR Laboratory, National Center of Nuclear Magnetic Resonance, Institute of Medical Biochemistry, Federal University of Rio de Janeiro, B*

Thioredoxins are ubiquitous proteins that play a key role in cell regulation. They interact with multiple targets in the cell. Thioredoxin exhibits chaperonin like activity, allowing local unfolding of the target proteins, thereby gaining access to the internal disulfide bonds, making it a very efficient enzyme. Our group determined the structure of *S. cerevisiae* Trx1 and its dynamics in different timescales (pico to seconds). The dynamics is modulated by Asp24 that is buried in the core of the protein, facing a water cavity. We have studied the mutant D24A to examine if the presence of a small hydrophobic residue would stabilize a closed conformational state without a water cavity. The presence of an alanine at position 24 induced conformational exchange in residues facing the water cavity, such as C33. This is an indication of the role of this cavity in the stabilization of the protein. We also compared the temperature coefficients obtained from the chemical shift variation of HN and observed an increased thermal susceptibility for several residues, indicating a decrease in protein stability. Lipari-Szabo order parameters were the same as for the wild type protein. The uniformly <sup>13</sup>C and <sup>15</sup>N labeled sample were used to acquire the experiments to calculate the structure of D24A and methyl order parameters.

Supported by: FAPERJ, CNPq and INBEB.

#### TU050: Structural and Orientational Topology of the Antimicrobial Peptide Hylaseptin P2 from Conjoint Use of Solution and Solid-State NMR

<sup>1,2\*</sup>Victor H. O. Munhoz, <sup>1,3</sup>Rodrigo M. Verly, <sup>1</sup>Jarbas M. Resende, <sup>2</sup>Burkhard Bechinger, <sup>1</sup>Dorila Piló-Veloso

<sup>1</sup>Universidade Federal de Minas Gerais, <sup>2</sup>Université de Strasbourg, <sup>3</sup>Universidade Federal dos Vales do Jequitinhonha e do Mucuri

The Hylaseptin P2 (HSP-2) is an antimicrobial peptide found on the skin secretions of *Hypsiboas punctatus anurans*, an species mainly found at the Amazon rainforest. This peptide has shown considerable activity against pathogens such as bacteria and fungi. Like most of the antimicrobial peptides, it is believed that HSP-2 mechanism of action is guided by its affinity for bacterial membranes. Therefore, understand-

ing of membrane surface interaction process, which is probably followed by cell lysis, is of crucial importance. Although the outlines of the mechanism are well consolidated, its full pathway is not yet completely unveiled, hence the need to perform different studies to elucidate it better.

In this work, solution NMR spectra were acquired with a sample containing the peptide in micellar medium and, through the resulting geometric restraints, a model containing the 20 least energetic structures was determined. The solid-state NMR-derived orientational restraints, calculated from the <sup>15</sup>N chemical shift and <sup>2</sup>H quadrupolar splitting with static samples containing the peptide locally labelled with <sup>15</sup>N and <sup>2</sup>H<sub>3</sub>-Ala and reconstituted in phospholipid bilayers, were then applied to all of the structures that compose the solution-NMR model. With this approach, it was possible to determine the topologies adopted by the peptide during its interaction with membranes and also to cover a broader orientational landscape, by considering a higher number of geometries which are coherent with NMR data.

This work has been carried out with financial aid of CNPq, CAPES, FAPEMIG, PRPq-UFMG and CNRS

#### TH051: Dynamics and Structural Studies of an Internal Fusion Peptide from SARS-CoV Spike Glycoprotein in Lipid Model Membranes

<sup>1</sup>Luis Guilherme M. Basso, <sup>2</sup>Tácio Vinício Amorim Fernandes, <sup>1</sup>José Fernando de Lima, <sup>1</sup>Claudia Elisabeth Munte, <sup>1</sup>Edson Crusca Júnior, <sup>3</sup>Eduardo Festozo Vicente, <sup>3</sup>Eduardo Maffud Cilli, <sup>2</sup>Pedro Geraldo Pascutti, <sup>1\*</sup>Antonio José Costa-Filho

<sup>1</sup>University of Sao Paulo, <sup>2</sup>Federal University of Rio de Janeiro, <sup>3</sup>Sao Paulo State University - UNESP

The S2 domain of the spike glycoprotein from SARS-CoV is responsible for driving viral and host cell membrane fusion. An internal fusion peptide (SARS<sub>IFP</sub>), located near the S2 domain N-terminus, plays a crucial role in the fusion process. Although much information has been obtained in recent years on membrane fusion, many aspects of the molecular mechanism behind virus-host cell membrane fusion are still not totally understood. For instance, major questions regarding the structure and function of fusion peptides still remain to be answered. In this regard, we report here magnetic resonance and computational studies on the structure and dynamics of SARSIFP in different membrane mimetic environments. The observation of strong  $d_{NN-(i,i+1)}$  NOEs along with the presence of many medium-range  $d_{\alpha N(i,i+3)}$  NOEs and upfield  $H_{\alpha}$  shifts from random coil values suggests an  $\alpha$ -helical conformation for the peptide in DPC micelles, which agrees qualitatively well with CD experiments. The absence of HN- $H_{\alpha}$  cross peaks in the 2D TOCSY NMR spectrum from residues pertaining to the peptide central region is likely due to a slow dynamics experienced by this peptide segment in micelles. On the other hand, CW-ESR spectra of both N- and C-terminally attached spin labeled analogues, TOAC-SARS<sub>IFP</sub> and SARS<sub>IFP</sub>-Cys-MTSSL, indicate a great flexibility of the water-exposed peptide ends. GSA and MD simulations were also used to gain insights on the peptide tertiary structure. The minimum-energy conformation obtained from the fully stretched peptide generated by GSA was further refined by long timescale MD simulations in aqueous, DMSO, and TFE/water solutions using different force fields. Cluster analysis reveals that both Amber99SB-ILDN and CHARMM27/CMAP force fields were able to correctly capture an  $\alpha$ -helix structure for the peptide. The distance distribution between the N- and C-termini obtained from MD was well reproduced by the recovered distance histograms from four-pulse DEER experiments on the double-labeled derivative TOAC-SARS<sub>IFP</sub>-Cys-MTSSL. The average nitroxide-nitroxide distances in different membrane mimetic environments are compatible with a partially folded  $\alpha$ -helix. The broad distance distribution encountered might reflect the great flexibility of the N-terminus and/or the different MTSSL rotamers. Taken together, our results suggest

that SARS<sub>IIFP</sub> is located at the interface of the model membranes in an  $\alpha$ -helical conformation with both ends exposed to the water phase. To our knowledge, this is the first report that provides structural and topological information of SARS<sub>IIFP</sub> in model membranes at atomic resolution, which may shed much light on the mechanism by which the peptide fold and insert into lipid bilayers.

ACKNOWLEDGEMENTS: FAPESP, CAPES, CNPq.

#### MO052: <sup>199</sup>Hg NMR Parameters in thymine-Hg-thymine metal mediated base pair

<sup>1</sup>T. Daraku, <sup>2</sup>K. Furuita, <sup>3</sup>J. šebera, <sup>1</sup>D. Yamanaka, <sup>1</sup>Y. Kondo, <sup>4</sup>A. Ono, <sup>2</sup>R. Katahira, <sup>5</sup>F. M. Bickelhaupt, <sup>3</sup>Vladimir Sychrovsky, <sup>2</sup>C. Kojima, <sup>1\*</sup>Yoshiyuki Tanaka

<sup>1</sup>Laboratory of Molecular Transformation, Tohoku University, <sup>2</sup>Institute for Protein Research, Osaka University, <sup>3</sup>Institute of Organic Chemistry and Biochemistry, Academy of Sciences of Czech Republic, <sup>4</sup>Department of Material & Life Chemistry, Faculty of Engineering, Kangawa University, <sup>5</sup>Department of Theoretical Chemistry, VU University Amsterdam

The thymine-Hg-thymine is one of the most thoroughly studied metal-mediated base pairs owing to its possible usability in future nanotechnologies. The base pairing of T-Hg<sup>II</sup>-T was unambiguously determined by <sup>15</sup>N NMR spectroscopy with the <sup>2</sup>J<sub>15N,15N</sub> J-coupling across <sup>15</sup>N-Hg<sup>II</sup>-<sup>15</sup>N linkage.[1] The mercury bonding to imino nitrogen of thymine was recently characterized as covalent with significant ionic character.[2] The mercury atoms in two consecutive T-Hg<sup>II</sup>-T base pairs attract each other owing to the metalophilic attraction despite their cationic nature.[3] Here we report the <sup>199</sup>Hg NMR chemical shift and the <sup>1</sup>J<sub>199Hg,15N</sub> coupling that was both measured and calculated in thymine-Hg<sup>II</sup>-thymine base pair. The theoretical calculations provided detail information on dependence of the NMR parameters on nature and chemical bonding in metal-mediated base pair.

[1] Tanaka, Oda, Yamaguchi, Kondo, Kojima, Ono, J. Am. Chem. Soc. 2007, 129, 244-245.

[2] Uchiyama, Miura, Takeuchi, Dairaku, Komuro, Kawamura, Kondo, Benda, Sychrovsky, Bour, Okamoto, Ono, Tanaka, Nucleic Acids Res. 2012, 40, 5766-5774.

[3] Benda, Straka, Tanaka, Sychrovsky, Physical Chemistry Chemical Physics 2011, 13, 100-103.

Acknowledgement: Grant Agency of the Czech Republic P205/10/0228.

#### TU053: Structural analysis of Citrus sinensis Poly(A)-Binding Protein PABP

<sup>1\*</sup>Mauricio Luis Sforça, <sup>1</sup>Mariane N. Domingues, <sup>3</sup>Tatiana A.C.B. Souza, <sup>2</sup>Tiago A. Souza, <sup>1</sup>Adriana S. Soprano, <sup>1</sup>Ana Carolina de Mattos Zeri, <sup>1</sup>Celso E. Benedetti

<sup>1</sup>Laboratório Nacional de Biociências (LNBio), Centro Nacional de Pesquisas em Energia e Materiais (CNPEM), Campinas-SP - Brasil., <sup>2</sup>Universidade de São Paulo, Instituto de Ciências Biomédicas, Centro de Facilidades de Apoio a Pesquisa (CEFAP-USP), São Paulo, SP - Brasil, <sup>3</sup>Instituto Carlos Chagas- Fiocruz/PR, ICC., Curitiba, PR - Brasil

Citrus canker, which affects most commercial citrus varieties and is a threat to the Brazilian citriculture, is caused by *Xanthomonas citri*, a bacterial pathogen that induces the formation of eruptions and pustule-like lesions on the surface of leaves, stems and fruits. Development of canker lesions depends on the action of PthA, the major transcription activator-like (TAL) effector of *X. citri*. We have shown that to act as a transcriptional activator, PthA interacts with components of the host basal transcriptional machinery. However, in addition to proteins directly involved in transcription regulation, some of the PthA-interacting proteins play roles in mRNA stabilization. Here we present the solution

NMR structure of a sweet orange Poly(A)-Binding Protein (CsPABP) identified as an interacting partner of PthA.

NMR experiments for structure determination were performed at 293 K using an Agilent Inova 600 MHz spectrometer equipped with a cryogenic probe. The following experiments were recorded: <sup>15</sup>N-HSQC, HNCACB, CBCA(CO)NH, HNCO and HN(CA)CO, <sup>15</sup>N-NOESYHSQC; <sup>15</sup>N-TOCSYHSQC; <sup>13</sup>C-HCCH-TOCSY; <sup>13</sup>C-CCH-TOCSY and <sup>13</sup>C-NOESYHSQC.

The structure of CsPABP is composed by flexible residues at the N-terminal region that include a  $\alpha$ -helix portion following to intercalated  $\beta$ -strand and  $\alpha$ -helix leading to two  $\beta$ -sheets at one side and two  $\alpha$ -helix at the other side of the fold.

Titration of CsPABP with Poly(A) results in shifts on a group of cross-peaks in the <sup>15</sup>N-HSQC (heteronuclear single quantum correlation) spectrum. Considerable shifts were observed for the first  $\beta$ -strand, that comprises residues I77, V79, and the loop that links it to the first  $\alpha$ -helix and contains residues N81, Y84 and C86; L105, at the end of second  $\beta$ -strand and K105 and G106 in the beginning of the third  $\beta$ -strand; and also at the C-terminal region including residues R150, T151 and N152. Most of these contacts are close to residues responsible for the dimerization of the protein.

Supported by: FAPESP, CNPq and LNBio.

#### TH054: A Redox 2-Cys Mechanism Regulates the Catalytic Activity of Divergent Cyclophilins

<sup>1\*</sup>Bruna M. C. Ramos, <sup>1</sup>Mauricio Luis Sforça, <sup>1</sup>Andre Luis Berteli Ambrosio, <sup>1</sup>Mariane N. Domingues, <sup>2</sup>Sara B-M. Whittaker, <sup>1</sup>Mario T. Murakami, <sup>1</sup>Ana Carolina de Mattos Zeri, <sup>1</sup>Celso E. Benedetti

<sup>1</sup>Laboratório Nacional de Biociências (LNBio), Centro Nacional de Pesquisa em Energia e Materiais (CNPEM), CP6192, CEP 13083-970, Campinas, SP, Brazil, <sup>2</sup>The Henry Wellcome Building for Biomolecular NMR Spectroscopy, School of Cancer Sciences, University of Birmingham, Birmingham B15 2TT, United Kingdom

The *Citrus sinensis* cyclophilin CsCyp is a target of the *Xanthomonas citri* TAL effector PthA, required to elicit cankers on citrus. CsCyp binds the citrus thioredoxin CsTdx and C-terminal domain of RNA Polymerase II (CTD). CsCyp is a divergent cyclophilin that carries the additional loop KS-GKPLH, invariable cysteines C40 and C168, and conserved glutamate E83. Despite the suggested roles in ATP and metal binding, the function of these unique structural elements remains unknown. Here we show that the conserved cysteines form a disulfide bond that inactivates the enzyme, whereas E83, which belongs to the catalytic loop and is also critical for enzyme activity, is anchored to the divergent loop to maintain the active site open. In addition, we demonstrate that CsCyp binds the citrus CTD YSPSAP repeat. Our data support the model where formation of the C40-C168 disulfide bond induces a conformational change that disrupts the interaction of the divergent and catalytic loops, via E83, causing the active site to close. This suggests a new type of allosteric regulation in divergent cyclophilins, involving a disulfide bond formation and loop displacement mechanism.

ACKNOWLEDGEMENTS: FAPESP, CNPq, CNPEM (LNBio), UNICAMP

#### MO055: Solution structures and interaction studies of two natural inhibitors of bacterial cell division

<sup>1,2</sup>Patricia Castellen, <sup>1</sup>Mauricio Luis Sforça, <sup>1</sup>Ana Carolina de Mattos Zeri, <sup>2\*</sup>Frederico José Gueiros-Filho

<sup>1</sup>Laboratório Nacional de Biociências, CNPEM, <sup>2</sup>Instituto de Química, Universidade de São Paulo

Bacterial cell division is a highly regulated process. This process is initiated by the assembly of the tubulin like FtsZ protein giving rise to a cytokinetic ring called Z-ring. The Z

ring must be placed at the middle of the cell to ensure the production of equally-sized daughter cells.

The Min system is a well-described negative regulatory system involved in the spatial regulation of the Z ring positioning. This system is highly conserved and consists of MinC and MinD proteins that together act to prevent division at the cell poles. In the absence of min genes, division at cell poles produces nucleoid-free minicells and elongated cells that contain two or more nucleoids. Another inhibitor of cell division was discovered in *Bacillus subtilis*, in a two-hybrid screen using FtsZ as bait. This 40 amino-acid peptide was called MciZ (for mother cell inhibitor of FtsZ). Synthetic MciZ interacts with FtsZ inhibiting its GTPase activity and polymerization. MciZ is produced during sporulation. In the absence of MciZ, a Z-ring forms in the sporangium at a time in development when cytokinetic events normally have ceased.

The structure of *B. subtilis* MinC is unknown and previously little was known about the structure of MciZ. Here we present the solution structure of the N-terminal domain of MinC and the structure of the MciZ peptide. In addition, we determined the interaction interface for FtsZ in the MinC N-terminal domain through NHSQC titration experiments and the binding site in MciZ through STD experiments.

Acknowledgements: FAPESP, USP and LNBio.

#### **TU056: Functional diversification of cerato-platanins in *Moniliophthora perniciosa* as seen by differential expression and protein function specialization**

<sup>1</sup>Juliana Ferreira de Oliveira, <sup>1,2</sup>Mario Ramos de Oliveira Barsottini, <sup>3</sup>Douglas Adamoski Meira, <sup>2</sup>Paulo José Pereira Lima Teixeira, <sup>1,2</sup>Paula Favoretti Vital do Prado, <sup>1</sup>Henrique Oliveira Tiezzi, <sup>1</sup>Mauricio Luis Sforça, <sup>1</sup>Paulo Sérgio Lopes de Oliveira, <sup>1</sup>Ana Carolina de Mattos Zeri, <sup>1</sup>Sandra Martha Gomes Dias, <sup>1,2</sup>Gonçalo Amarante Guimarães Pereira, <sup>1\*</sup>Andre Luis Berteli Ambrosio

<sup>1</sup>Laboratório Nacional de Biociências, CNPEM, <sup>2</sup>Departamento de Genética e Evolução, UNICAMP, <sup>3</sup>Departamento de Genética, Universidade Federal do Paraná

Cerato-platanins (CP) are small cysteine-rich fungal-secreted proteins involved in various stages of the host-fungus interaction process, acting as phytotoxins, elicitors and allergens. It has been suggested that this protein family has important physiological functions, including cell wall interaction and manipulation of the host's defense system. However, the precise molecular function remains elusive. Its members have in common low molecular weights, a high percentage of hydrophobic residues and four conserved cysteine residues involved in the formation of two intramolecular disulfide bonds. Genomic-scale studies have identified twelve sequences encoding putative proteins similar to cerato-platanin proteins (termed MpCP1 to 12) in the genome of *Moniliophthora perniciosa*, the causal agent of witches' broom disease in cacao plants. In this work, we show that the twelve MpCP proteins present distinct expression profiles throughout fungus development and infection. We determined the X-ray crystal structures of MpCP1, 2, 3 and 5, representative of different branches of a phylogenetic tree and expressed at different stages of the disease. The X-ray crystal structures guided the investigation of their capacity of binding and hydrolyzing fungus and plant cell wall components and to self-aggregate. NMR analysis showed that MpCP3 and 5 distinctly bind to N-acetylglucosamine tetramers (NAG4), allowing the description of an unforeseen binding interface in MpCP5. MpCP2 and 3 are the most responsive to self-aggregation into amyloidogenic fibrils, which might be important to hyphae growth and development. The structure and information provided in this work will be a useful platform for compound design which can block the protein activity and help to compose a combat approach against the disease.

\*Juliana F. Oliveira and Mario R.O. Barsottini contributed

equally to this work. Acknowledgments: FAPESP for financial support and LNBio for accessibility to all the facilities.

#### **TH057: Evaluation of Sample Processing Protocols for Metabolomic Studies of Coffee Plants**

<sup>1</sup>Daniel de Menezes Darbello, <sup>1\*</sup>Oliveiro Guerreiro Filho, <sup>2</sup>Carolina de Mattos Zeri

<sup>1</sup>Agronomy Institute of Campinas, <sup>2</sup>National Biosciences Laboratory

A powerful tool to the execution of the early selection in plant breeding programs, is the utilization of biomarkers, that can be identified by the metabolomic associated to the Proton nuclear magnetic resonance (<sup>1</sup>H NMR) in seedlings. The object of this study is related to the standardization of the metabolic extraction technique of foliar tissue coffee trees resistant and susceptible to the leaf coffee miner, in order to define and easy execution protocol, less onerous and that allows the separations between these classes. This way, the adult coffee trees were classified in relation to the resistance *Leucoptera coffeella* resistance level, according to the scale established by Ramiro et al (2004). Thirty plants were utilized to the composition of the insect-resistance groups, being 15 resistant plants (R) and 15 susceptible plants (S). Different techniques were tested in relation to the aqueous extract quality, which are: lyophilized (L/AQ), aqueous extraction of fresh leaves (Fr/Aq), microwave dried leaves (Mw/Aq), fresh leaves extraction in perchloric acid (Fr/Pa). The efficiency of the method were evaluated through the obtained separation between the R and S classes, by partial least squares regression (PLS-DA) and chemometric standards, like standard error of calibration (SEC) and correlation coefficient for calibration (rCal). The metabolic extraction technique Fr/Aq performed as the most efficiency protocol to classify the R and S groups to the leaf coffee miner, allowing the separation of the classes and providing satisfactory data rCal and SEC. It is also the technique with the less number of steps and lower execution costs, comparing to the other studied methods.

#### **MO058: Biomarkers of Resistance to the Leaf Miner in Coffee Plants by NMR**

<sup>1</sup>Daniel de Menezes Darbello, <sup>1</sup>Oliveiro Guerreiro Filho, <sup>2\*</sup>Ana Carolina de Mattos Zeri

<sup>1</sup>Agronomy Institute, Campinas, <sup>2</sup>National Biosciences Laboratory

As the coffee a perennial species with a long reproductive cycle, the time and resources applied in the selection of new cultivars are relatively substantial. One of the methods to shorten the selection time and reduce the costs with agronomic trial is to make an earlier selection. In this way, the object of this study was to identify secondary metabolites by proton spectroscopy (<sup>1</sup>H NMR), which characterize resistance plants (R) and susceptible (S) to the leaf miner coffee. For this, the progeny segregating coffee trees H14954-46 belonging to the generation F<sub>2</sub>RC<sub>5</sub>, were classified in relation to the level of resistance to the insect, according the point scale established by Ramiro et al (2004) e subsequently selected to metabolic analysis by <sup>1</sup>H NMR from aqueous extracts obtained by the adapted Gomes-Cadenas et al, 2002, technique. By means of variance analyses performed with the identified metabolites, it was observed that just the myoinositol metabolite, differed significantly among the groups R and S, performing at higher concentration in the susceptible plants, which can be considered a biomarker candidate to the identification of the resistant plants e susceptible non-infested by using the <sup>1</sup>H NMR analysis.

#### **Biomolecular Solid-State NMR**

#### **TU059: Structure and orientation of bovine lactoferrampin in the mimetic bacterial membrane as re-**

**vealed by Solid-State NMR and molecular dynamics simulation**

<sup>1</sup>\*Akira Naito, <sup>1</sup>Atsushi Tsutsumi, <sup>1</sup>Namsrai Javkhantugs, <sup>1</sup>Atsushi Kira, <sup>1</sup>Masako Umeyama, <sup>1</sup>Izuru Kawamura, <sup>2</sup>Katsuyuki Nishimura, <sup>1</sup>Kazuyoshi Ueda

<sup>1</sup>Yokohama National University, <sup>2</sup>Institute for Molecular Science

Bovine lactoferrampin (LFampinB) is a new antimicrobial peptide found in the N1-domain of bovine lactoferrin (268-284), and consists of 17 amino acid residues. It is important to determine the orientation and structure of LFampinB in bacterial membranes to reveal the antimicrobial mechanism. We therefore performed <sup>13</sup>C and <sup>31</sup>P NMR, <sup>13</sup>C-<sup>31</sup>P REDOR, potassium ion selective electrode (ISE) and quartz crystal microbalance (QCM) measurements for LFampinB with mimetic bacterial membrane and molecular dynamics (MD) simulation in the acidic membrane [1]. <sup>31</sup>P NMR results indicated that LFampinB caused defect in mimetic bacterial membranes. ISE measurements showed that ion leakage occurred for the mimetic bacterial membrane containing cardiolipin (CL). QCM measurements revealed that LFampinB had greater affinity to acidic phospholipids than that to neutral phospholipids. <sup>13</sup>C DD-MAS and static NMR spectra showed that LFampinB formed  $\alpha$ -helix in the N-terminus region and tilted 45° to the bilayer normal and center part to C-terminus region takes random coil structure. REDOR dephasing patterns between carbonyl carbon in the helix and phosphate group were measured by <sup>13</sup>C-<sup>31</sup>P REDOR and the results revealed that LFampinB is located in the interfacial region of the membrane. The results of MD simulation showed that the tilt angle was evaluated to be 42° and the rotation angle to be 92.5° for Leu<sup>3</sup> which are in excellent agreement with the experimental values determined by solid state NMR.

[1] A. Tsutsumi et al. Biophys. J. 2012, 103, 1735-1743.

**TH060: Proton-detected solid-state NMR of viral nucleocapsids**

<sup>1</sup>\*Emeline Barbet-Massin, <sup>2</sup>Kristaps Jaudzems, <sup>1</sup>Andrew J. Pell, <sup>1</sup>Michael J. Knight, <sup>3</sup>Kaspars Tars, <sup>1</sup>Anne Lesage, <sup>1</sup>Lyndon Emsley, <sup>1</sup>Guido Pintacuda

<sup>1</sup>Centre de RMN à Très Hauts Champs, University of Lyon (CNRS / ENS Lyon / UCB Lyon1), Villeurbanne, <sup>2</sup>Latvian Institute of Organic Synthesis, Riga, Latvia, <sup>3</sup>Biomedical Research and Study Center, Riga, Latvia

*Acinetobacter* phage 205 (AP205) is a single-stranded RNA coliphage belonging to the family of *Leviviridae* [1]. In AP205, 180 copies of a dimeric coat protein (2x130 residues) assemble into an icosahedral capsid of about 30 nm in diameter. Atomic-level characterization of this system is a challenge since only low-resolution structures from cryo-EM are available, and crystals of the viral particles do not diffract. However, these crystals or hydrated sedimented precipitates are amenable to solid-state NMR, for which the repetitive positioning of the monomers inside the complex superstructures provides a high degree of local order and consequently highly resolved spectra.

Due to the size and complexity of the system, traditional strategies based on <sup>13</sup>C acquisition for assignment and structural determination are extremely inefficient.

We show here that i) high resolution <sup>1</sup>H-detected fingerprints of the capsid protein can be obtained by combining very high field and MAS at ultra-fast rates, on both deuterated/fully back-exchanged and fully-protonated samples, as already observed for less complex assemblies [2]. Moreover, ii) we present a suite of six 3D <sup>1</sup>H-detected experiments, which yield a rapid and robust assignment of protein backbone <sup>1</sup>H, <sup>15</sup>N, <sup>13</sup>CO and <sup>13</sup>CA and side-chain <sup>13</sup>CB resonances. These experiments combine heteronuclear cross-polarization (CP) steps with homonuclear scalar-based CC out-and-back transfer blocks, which allow us to record the chemical shifts

of short-lived coherences (e.g. CA, CB) while evolving on longer-lived spins (e.g. CO) [3]. Overall, we show how this approach provides complete resonance assignment of backbone and sidechains CB resonances. The whole assignment procedure is i) highly sensitive, using only 2 mg of sample, and less than a week of experimental time; and ii) very robust, since sequential assignment results from the alignment of three common carbon (CO, CA and CB) chemical shifts for each pair of <sup>1</sup>H and <sup>15</sup>N nuclei.

[1] Klovins J, Overbeek GP, van den Worm SH, Ackermann HW and van Duin J (2002). Nucleotide sequence of a ssRNA phage from *Acinetobacter*: kinship to coliphages. J. Gen. Virol. 83:1523-1533.

[2] Marchetti A, Jehle S, Felletti M, Knight MJ, Wang Y, Xu ZQ, Park AY, Otting G, Lesage A, Emsley L, Dixon NE and Pintacuda G (2012). Backbone assignment of fully protonated solid proteins by <sup>1</sup>H detection and ultrafast magic-angle-spinning NMR spectroscopy. Angew. Chem. Int. Ed. 51:10756-10759.

[3] Barbet-Massin E, Pell AJ, Jaudzems K, Franks WT, Retel JS, Akopjana I, Tars K, Emsley L, Oschkinat H, Lesage A and Pintacuda G (2013). "Out-and-back <sup>13</sup>C-<sup>13</sup>C scalar transfers for protein resonance assignment by proton-detected solid-state NMR under ultra-fast MAS", *submitted*.

**MO061: Structural Characterization of Ca-ATPase/Phospholamban Complex by Solid-State NMR Spectroscopy**

\*Gianluigi Veglia, Nathaniel J Traaseth, Dan Mullen, Raffaello Verardi, Martin Gustavsson

University of Minnesota

A detailed understanding of protein function requires structural and dynamic analyses of functional complexes rather than that of the isolated binding partners. I will present our latest results on the structural characterization of the sarcoplasmic reticulum Ca<sup>2+</sup>-ATPase (SERCA) and phospholamban (PLN) reconstituted both in synthetic and native lipid membranes using a *hybrid* NMR approach. This method combines distance and angular restraints from magic angle spinning (MAS) NMR with orientational restraints (<sup>1</sup>H-<sup>15</sup>N dipolar couplings and anisotropic <sup>15</sup>N chemical shift) from oriented solid-state NMR (OSSNMR) for the simultaneous determination of structure and topology of membrane protein complexes. In addition, I will demonstrate how paramagnetic relaxation enhancements (PREs) can be used to determine long-range protein-protein interactions. The structure of the SERCA/PLN complex reveals that the membrane detached, unfolded state of PLN (excited state) binds the cytoplasmic domain of SERCA forming a non-inhibitory complex; while the membrane associated helical state of PLN (ground state) is the inhibitory form and interacts with the transmembrane domains of SERCA, inhibiting Ca<sup>2+</sup> flux.

**TU062: Solid-state NMR study of the mechanism of action of novel amphipathic cationic peptides in model membranes**

\*Michele Auger, Matthieu Fillion, Aurelien Lorin, Mathieu Noel, Marie-Eve Provencher, Normand Voyer

Université Laval, Department of Chemistry, PROTEO, CERMA, Quebec, Canada, G1V 0A6

A wide variety of organisms produce antimicrobial peptides as part of their first line of defense. These short cationic peptides are being considered as a new generation of antibiotics and represent great hopes against multiresistant bacteria which are an important clinical problem. Despite their diversity, the main target of antimicrobial peptides is the membrane(s) of pathogens.

We have previously shown that a non-natural peptide composed of 14 residues (10 leucines and 4 phenylalanines modified with a crown ether) is able to disrupt lipid bilayers but

is not selective towards bacterial membranes. To gain specificity against negatively charged membranes, several leucines of this 14-mer have been substituted by positively charged residues (lysine, arginine and histidine). Biological tests indicate that some peptides are active against *E. coli* but ineffective against human erythrocytes. Solid-state NMR experiments performed in model membranes were used to better characterize the mode of action of the charged peptides. The results suggest that the peptides arrange themselves preferentially near the bilayer interface perturbing the membrane by the formation of pores. The structure and orientation of labelled peptides has also been investigated in bilayers oriented between glass plates as well as in biphenyl bicelles. Simulations of pore formation in bilayers oriented between glass plates will also be presented.

#### TH063: Structural Characterization of MTTR Fibrils by Solid-State NMR

<sup>1</sup>Juliana Santos Santana, <sup>1</sup>Ricardo Oliveira Sant'Anna, <sup>1</sup>Flavia Guedes Andrade, <sup>3</sup>Daniel H A Correa, <sup>3</sup>Lisandra Marques Gava, <sup>2</sup>Annette Diehl, <sup>1</sup>Carolina Alvares Braga, <sup>3</sup>Carlos Henrique Ramos, <sup>2</sup>Hartmut Oschkinat, <sup>1</sup>Débora Foguel, <sup>1\*</sup>Monica Santos de Freitas

<sup>1</sup>Universidade Federal do Rio de Janeiro, <sup>2</sup>Leibniz-Institut für Molekulare Pharmakologie, <sup>3</sup>Universidade Estadual de Campinas

Amyloidosis is a clinical dysfunction caused by extracellular accumulation of proteins that are normally soluble in their original structure, but suffered structural modifications generating insoluble and abnormal fibrils that impair the proper functioning of tissues. Although many challenges have been overcoming in the field of amyloidosis many questions are still waiting for answers. In this work we are interested to evaluate the pathway involved in fibril formation, following structural features that could indicate how soluble proteins undergo conformational changes that result in aggregation. The diffraction pattern did not indicate typical value for interstrand distance, suggesting a variation on fibrillar architecture.  $u\text{-}^{13}\text{C}^{15}\text{N}$  MTTR fibrils displayed a well resolved HN-HSQC with linewidth comparable to solution-state NMR, suggesting a high degree of mobility. On the other hand, poor resolution was obtained for experiments probing dipolar-dipolar interactions, such as Proton Driving Spin Diffusion (PDS). In order to have the sequential assignment, a 10% back hydrogen exchanged sample was analyzed to improve spectral resolution by decreasing line broadening. The data indicates a fibrillar core composed of around 30 amino acids. The solid-state data taking together solution-state NMR has been cooperative tools to improve our knowledge concerning the misfolding pathway.

ACKNOWLEDGEMENTS: ALV, CAPES, FAPERJ, INBEB, UFRJ-ALV

#### Solid State NMR

#### MO064: Structure elucidation of azole-based co-crystals using high-resolution solid-state NMR, X-ray diffraction and molecular mechanics

<sup>1\*</sup>Mariana Sardo, <sup>1</sup>Sérgio M. Santos, <sup>2</sup>Concepción López, <sup>3</sup>Ibon Alkorta, <sup>3</sup>José Elguero, <sup>2</sup>Rosa M. Claramunt, <sup>1</sup>Luís Mafrá

<sup>1</sup>CICECO – Chemistry Department, University of Aveiro, P-3810-193 Aveiro, Portugal, <sup>2</sup>Dep. de Química Orgánica y Bio-Orgánica, Facultad de Ciencias - UNED, E-28040 Madrid, Spain, <sup>3</sup>Instituto de Química Médica (CSIC), E-28006 Madrid, Spain

In the last few years, there has been an increasing recognition of the power of NMR Crystallography, a combined multidisciplinary approach integrating powder diffraction, computer-based structure determination and experimental solid-state

(ss) NMR techniques to obtain structural information difficult to gather using any of these techniques separately. [1]

3,5-dimethylpyrazole (DMPZ) was the first reported compound to present a dynamic process in the solid-state that consists in the transfer of several NH...N protons from different DMPZ molecules forming a trimer. When DMPZ is mixed through mechanical grinding with 4,5-dimethylimidazole (DMIM) - in a 1:1 molar proportion - the aforementioned dynamic behavior is suppressed, the DMPZ trimer breaks down and a new co-crystal is formed. [2]

Our approach combines powder X-ray diffraction data (revealing topological details), solid-state  $^{13}\text{C}$ ,  $^{15}\text{N}$  and  $^1\text{H}$  NMR data (yielding atomic connections, internuclear proximities and orientation relations on local and intermediate length scales), molecular modeling and *ab-initio* DFT calculations (to create meaningful structures). Multinuclear high-resolution 2D  $^1\text{H}$ - $^1\text{H}$  double-quantum,  $^1\text{H}$ - $^{13}\text{C}$  (PRESTO and LG-CP) HETCOR and  $^1\text{H}$ - $^{15}\text{N}$  (CP and LG-CP) HETCOR NMR methods combined with CRAMPS (Combining Rotation And Multiple Pulse Sequences) decoupling [3] were performed and the resulting structural information was combined with symmetry restraints derived from powder X-ray diffraction and included in a crystal structure generation evolutionary algorithm to unveil structural features of the co-crystal formed between DMPZ and DMIM molecules.

We acknowledge FCT for financial support to the Portuguese National NMR Network, project PTDC/QUIQUI/100998/2008 and post-doc grants for MS (SFRH/BPD/65978/2009) and SMS (SFRH/BPD/64752/2009). This work was financed by FEDER, via "COMPETE", and by FCT, PEst-C/CTM/LA0011/2011.

[1] NMR crystallography (EMR Books) 2009, R. K. Harris, R. E. Wasylshen and M. J. Duer (editors), Wiley;

[2] C. López et al., Cent. Eur. J. Chem. 2004, 2(4), 660-671;

[3] M. Sardo et al. J. Phys. Chem. A 2012, 116, 6711-6719.

#### TU065: Structure and nucleation mechanisms in aluminum metaphosphate glasses.

<sup>1,2\*</sup>Jefferson Esquina Tsuchida, <sup>2</sup>Edgar Dutra Zanotto, <sup>1</sup>José Fabian Schneider

<sup>1</sup>Instituto de Física, Universidade de São Paulo, São Carlos, <sup>2</sup>Departamento de Engenharia de Materiais, Universidade Federal de São Carlos

Phosphates glasses are materials with great technological potential (optics, bio-materials, glass-metal seals). Study the structure of these systems has basic and technological interest, due to the close correlation with macroscopic properties desired in applications and the structure of the vitreous network. The low chemical stability of phosphate glasses can be solved by Al incorporation. At this writing no study has shown that phosphate glasses exhibit internal homogeneous nucleation when subjected to a devitrification process. However in recent preparation of  $\text{Al}(\text{PO}_3)_3$  glass, was observed a small internal homogeneous nucleation.

In this study will submit the  $\text{Al}(\text{PO}_3)_3$  glass to different thermal treatments with the purpose to promote the internal homogeneous nucleation process. After the glass melting, the samples are analyzed by X-ray diffraction to identify the possible presence of crystals formed during cooling. The characteristics temperature such as glass transition ( $T_g$ ), crystallization ( $T_c$ ) and melting ( $T_m$ ) are determined by differential scanning calorimetry analysis (DSC), in order to plan appropriate thermal treatments purpose to promote the internal homogeneous nucleation process. After the accomplishment of the thermal treatments the samples obtained are characterized by optical microscopy and scanning electron microscopy in order to evaluate the microstructure formed and identify the aspect ratio of the crystals formed. The structural environments of the forming and modifying species of the network were analyzed through of  $^{31}\text{P}$  and  $^{27}\text{Al}$  NMR, quantifying the



distribution of phosphates groups and determining the coordination number of Al.

The challenges in the development of phosphate glasses that have internal homogeneous nucleation can help considerably in understanding the nucleation mechanisms in a general oxide glasses.

ACKNOWLEDGEMENTS: FAPESP, CAPES, CNPq

#### TH066: Time Reversal Dynamics in Scaled Dipolar Interactions by means of Continuous Radiofrequency Irradiation

\*Axel D. Dente, Lisandro Buljubasich, Patricia R. Levstein, Horacio M. Pastawski, **Ana Karina Chattah**

*IFEG, CONICET-Córdoba, Argentina and FAMAF, UN of Córdoba, Argetnina*

The creation of quantum computing devices requires the precise control in the evolution of quantum states [1]. In this sense, the uncontrolled processes in many-body systems perturb coherent dynamics leading to decoherence. Thus, the understanding and the control of these uncontrolled process constitutes a challenge nowadays. In the last decades, the development of NMR techniques, allowed the study of decoherence in liquid and solid state.

In this work, we combine the Loschmidt Echo with the solid state NMR technique, to study the decoherence process in scaled dipolar evolutions using as a specific model system: the polycrystalline Adamantane. In other words, we have made used the Loschmidt Echo to quantify the amount of decoherence produced by the non-controlled internal interactions, the environment and the experimental conditions [2].

In 1970, Rhim et al. , introduced the Magic Echo pulse sequence, which enable the reversion of the secular terms in the dipolar Hamiltonian [3]. This was, somehow, the first pulse sequence to observe the Loschmidt Echo in multi-spin dynamics. Inspired in the Magic Echo pulse sequence, we have designed new experiments having symmetric conditions, in the sense that the backward and forward evolutions require the same time. In this new pulse sequence we have been able to scale the secular terms of the dipolar evolutions in the range between 0 and  $\frac{1}{2}$  (the 0 value coincides with the Lee-Goldburg condition [4]). Our experimental results are supported by detailed numerical simulations in a Hilbert space of 19-coupled spins, achieved with the aid of GPU cards.

- [1] Zurek, Wojciech Hubert, *Rev. Mod. Phys.* 75, 715 (2003).
- [2] Sánchez, C. M. and Levstein, P. R. and Acosta, R. H. and Chattah, A. K., *Phys. Rev. A* 80, 12328 (2009).
- [3] Rhim, W.-K. and Pines, A. and Waugh, J. S., *Phys. Rev. Lett.* 25, 218 (1970).
- [4] Lee, Moses and Goldburg, Walter I., *Phys. Rev.* 140, A1261 (1965).

#### MO067: Solid-state NMR studies of the influence of halide substitution on an extremely shielded hydride proton of iridium complexes

<sup>1</sup>Piotr Garbacz, <sup>1</sup>Mariusz Kędziorek, <sup>2</sup>Victor Tersikh, <sup>3</sup>Guy Bernard, <sup>3\*</sup>Roderick E. Wasylshen

<sup>1</sup>University of Warsaw, Faculty of Chemistry, Warsaw, Poland, <sup>2</sup>University of Ottawa, Ottawa, Canada, <sup>3</sup>University of Alberta, Department of Chemistry, Edmonton, Canada

Hydrogen nuclei in organic compounds typically have chemical shifts in range, 0 to 15 ppm. In contrast, most transition-metal hydrides are characterized by a strongly shielded proton that has a chemical shift in the range, -3 to -20 ppm [1]. Notable exceptions include hydridodichlorobis(trialkylphosphine)irridium(III) complexes [2], the focus of this report, which contain an extremely shielded proton with an isotropic chemical shift of approximately -50

ppm. Specially, we have investigated the hydride proton shielding tensors of three Ir(III) complexes, hydridodichlorobis(tricyclohexylphosphine)irridium(III), HIrX<sub>2</sub>(PCy<sub>3</sub>) (X = Cl, Br, and I).

The principal components of the hydride proton chemical shift tensors of these three complexes were measured by analyzing magic-angle spinning H-1 NMR spectra acquired at several spinning speeds at Canada's National Ultrahigh Field Facility for Solids in Ottawa using a 900 MHz Bruker Avance II spectrometer. The computer program WSOLIDS was used to irrelatively fit the experimental intensities of spinning-sidebands to those calculated as outlined by Herzfeld and Berger [3]. This presentation will also focus on the development of techniques designed to suppress the probe background as well as peaks of protons from non-hydride protons.

Finally, the principal components of our experimental proton shielding tensors will be compared with recent quantum chemistry calculations by Kaupp and co-workers [4] as well as DFT calculations carried out in our laboratory.

- [1]. Kesz H.D., Saillant, R.B., *Chem. Rev.*, 1972, 72, 231-281.
- [2]. Masters C., Shaw B. L., Stainbank R. E., *J. Chem. Soc. Dalton Trans.*, 1972, 664-667.
- [3]. Herzfeld J., Berger A. E., *J. Chem. Phys.*, 1980, 73, 6021-6030.
- [4]. Hrobárik P., Hrobáriková V., Meier F., Repiský M., Komorovský S., and Kaupp M., *J. Phys. Chem. A*, 2011, 115, 5654-5659.

Acknowledgements:

This project was partly co-operated within the Foundation for Polish Science MPD Program co-financed by the European Union (EU) European Regional Development Fund. Access to the 900 MHz NMR spectrometer was provided by the Canadian National Ultrahigh-Field NMR Facility for Solids (<http://nmr900.ca>). REW acknowledges financial support of the Canada Research Chairs program and NSERC.

#### TU068: The NQR of highly abundant arsenic minerals

\*J. A. Lehmann-Horn, T. Bastow, D. G. Miljak

*Commonwealth Scientific and Industrial Research Organisation*

Arsenic-containing minerals of the form M<sub>x</sub>As<sub>y</sub>S<sub>z</sub> occur in certain types of gold, copper and nickel mineral deposits and are the primary source for natural and anthropogenic arsenic contaminations in groundwater aquifers. The detection of arsenic phases on mining sites would be of significant benefit to mitigate the release of arsenic into mine waters. Nuclear quadrupolar resonance (NQR) is a potentially useful method to characterise minerals in bulk volumes. We report new NQR measurements of arsenic-containing minerals, commonly occurring in the earth crust and important intermetallics in their own right. We determined the NQR frequencies from high-field NMR powder patterns and via zero-field frequency sweeps. A brief discussion is given on how NQR techniques may be employed in mining operations.

#### TH069: Improving Delivery Systems through Supramolecular Complexes of Maltodextrin or Cyclodextrin and Furosemide Polymorphs

<sup>1\*</sup>Ana Karina Chattah, <sup>2</sup>Marcela Longhi, <sup>2</sup>Claudia Garnero

<sup>1</sup>Facultad de Matemática, Astronomía y Física and IFEG (CONICET), Universidad Nacional de Córdoba, <sup>2</sup>Departamento de Farmacia, Facultad de Ciencias Químicas, Universidad Nacional de Córdoba

Two critical factors responsible for the poor and highly variable human bioavailability of Furosemide polymorphs (a loop

diuretic agent) are their low permeability and solubility. On the other side, selecting a proper polymorph and to control polymorphic transformations has a great impact in pharmaceutical and regulation issues. With all these facts in mind, we have focused our work on preparing and characterizing new supramolecular systems of Furosemide polymorphs I and II with maltodextrin and cyclodextrins.

Several techniques have been accomplished to study these complexes in the solution and solid state: spectroscopic techniques as solution and solid state NMR, FT-IR and XRPD, and also thermal analysis, and scanning electron microscopy. Relaxation times measurements ( $^1\text{H-T}_1$ ) have been decisive to confirm the formation of the complexes and to assess differences between them. In order to investigate the potential application of the supramolecular complexes as new delivery systems enhancing the bioavailability of the drug, solubility analysis and dissolution tests were used to correlate the performance between the polymorphic forms and the complexes.

ACKNOWLEDGMENTS: CONICET, SECyT-UNC

#### MO070: Solid-state NMR studies on methane activation and conversion over Zn modified ZSM-5 Zeolites

\*Feng Deng

Wuhan Institute of Physics and Mathematics, Chinese Academy of Sciences

Methane, the cheapest and most abundant natural resource, is the least reactive hydrocarbon molecule due to its strong C-H bond strength (104 kcal/mol). Now, the commercial utilization of methane is still largely dependent on the multi-step syn-gas ( $\text{CO} + \text{H}_2$ ) strategy, which incurs energy costs and lacks selectivity. Environmentally benign heterogeneous catalysts in which transition metal (Ga, Zn, Mo etc.) modified zeolites catalyze the co-conversion of methane with alkanes and alcohol to hydrocarbons ( $\text{C}_2$ – $\text{C}_{12}$ ) at relatively low temperatures ( $< 873\text{K}$ ) have attracted significant attention. However, nearly all those catalysts keep silent for conversion of methane to more valuable chemicals when the reaction temperature is below 523 K.

In this contribution, low-temperature activation and conversion of methane over a new Zn modified H-ZSM-5 zeolite catalyst (denoted as ZnZSM-5) was investigated by solid-state NMR spectroscopy in combination with other spectroscopic methods and DFT theoretical calculations. We found for the first time that the activation of methane resulted in preferential formation of surface methoxy intermediates at room temperature, which mediated the formation of methanol and its further conversion to hydrocarbons. Experimental and theoretical calculation results demonstrated that an oxygen-containing dizinc cluster centre in open shell was responsible for homolytic cleavage of the C-H bond of methane at room temperature, leading to formation of methyl radicals. The zeolite matrix readily trapped the methyl radicals by forming the surface methoxy intermediates for further selective conversion. In addition, carbonylation of methane with carbon monoxide to directly produce acetic acid over the ZnZSM-5 catalyst under mild condition (573–623K) was also investigated by in-situ solid-state NMR technique and two different intermediate-dependent reaction pathways were unambiguously identified.

#### TU071: Hybrid organic-inorganic photochromic xerogels analyzed by solid-state NMR and EPR spectroscopy

<sup>1</sup>\*Marcos de Oliveira Junior, <sup>1</sup>José Fabian Schneider, <sup>2</sup>Ubirajara P. Rodrigues Filho, <sup>1</sup>Cláudio José Magon

<sup>1</sup>Instituto de Física de São Carlos - Universidade de São Paulo, São Carlos, SP, Brazil, <sup>2</sup>Instituto de Química de São Carlos - Universidade de São Paulo, São Carlos, SP, Brazil

Hybrid materials based in dodecatungstophosphoric acid (HPW) show reversible photochromic properties in the 200nm–390nm UV range. The photochemical reduction of

the HPW polyanions yields blue-colored species, a property that makes these materials suitable for UV sensors or personal dosimeters. The strength and duration of the photochromic response depend on the nature of the organic groups interacting with the polyanion, and on the hydration level of the sample. The understanding of the physicochemical mechanisms of the photochromic effect and the structure of these materials are fundamental issues to optimize formulations and preparation conditions. Several solid-state NMR techniques were used to get chemical and structural information: high-resolution  $^1\text{H}$ ,  $^{29}\text{Si}$  and  $^{31}\text{P}$ -NMR,  $^1\text{H}$ - $^{29}\text{Si}$  HETCOR and  $^1\text{H}$ - $^{31}\text{P}$  SEDOR. Identification of different proton species, far/near to the polyanion, was attained analyzing the proton spin-lattice relaxation time in the rotating frame ( $T_{1\rho}$ ) with direct and indirect methods ( $^1\text{H}$ - $^{31}\text{P}$  cross-polarization, TORQUE). The model compound HPW·6H<sub>2</sub>O and photochromic xerogels with varying composition and/or preparation atmosphere were studied. The results show four sets of H species in the xerogels: free H<sub>2</sub>O, loosely bound  $\text{H}^+(\text{H}_2\text{O})_n$ , species strongly interacting with HPW:  $\text{H}_2\text{O}/\text{H}_3\text{O}^+/\text{H}_5\text{O}_2^+$  and species from the ormosil ( $\text{SiOH}/\text{CH}$ ). The first two species are critically dependent on the atmosphere control during preparation and on thermal treatments, and their amount is determinant to the P-H environments and the relative mobility hydrogen-polyanion. EPR experiments carried out in irradiated samples showed a thermally activated hopping process of an unpaired electron, possibly transferred from organic functionalities. The EPR spectra also show dynamical differences dependent on the composition of the hybrid material, which could be traced to differences in the photochromic response. The xerogels prepared in low humidity conditions showed weaker EPR intensities than the xerogels prepared in ambient conditions, indicating that the hydration species on the HPW environment have positive influence in the photochromic effect.

#### TH072: In Situ Monitoring of Lithium Ion Conductive Pathways in Lithium-Ion Rechargeable Batteries using Stray Field Imaging (STRAFI)

<sup>1</sup>Joel A. Tang, <sup>1</sup>Sneha Dugar, <sup>2</sup>Guiming Zhong, <sup>2</sup>Yong Yang, <sup>1</sup>\*Riqiang Fu

<sup>1</sup>National High Magnetic Field Laboratory, Florida State University, <sup>2</sup>Xiamen University, China

Electrochemical processes involve ion conductive pathways to achieve inter-conversion between electric energy and chemical energy for energy storage[1-2]. During charge/discharge cycles, many inter-exchangeable structural phases are developed in the electrodes. Some of them become irreversible, leading to capacity decay, energy inefficiency, and a short cycle life. A variety of diagnostic tools, such as Infrared spectroscopy, optical microscope, scanning electron microscope (SEM), electron diffraction and transmission electron microscope (TEM), X-ray diffraction, and nuclear magnetic resonance (NMR), have been used to identify the main causes responsible for capacity degradation and cycle life limitation of the electrodes. However, the electrodes being investigated are typically extracted from preparative electrochemical cells charged at different potentials, i.e., through *ex situ* processes. During such *ex situ* processes, the equilibrium composition of the samples may be altered. It is always desirable to obtain the local structures of the electrodes at the atomic level under *in situ* conditions to understand the electrochemical processes.

Here, we used the stray-field imaging (STRAFI)[3,4] technique to monitor Li-ion transfers in situ. In STRAFI experiments, samples are placed in the strongest static field gradient ( $> 50\text{T/m}$ ) of a magnet. By translating the samples across the static field gradient, spin populations within a thin slice can be detected. Resolutions as low as  $39\mu\text{m}$  are achievable with minimal influence of metal current collectors, making it capable of imaging thin materials in situ such as rechargeable batteries[5]. Here, we assembled half cell batteries with Li foil as the anode and Graphite/LiFePO<sub>4</sub> as

the cathode and observed in situ Li-ion transfers between the electrodes during charge-discharge cycles. We further discuss the structural changes of these electrodes. These images aid in the visualization for the formation of Li microstructures, the primary cause of poor battery performance[6], and will eventually assist in designing better electrode materials to improve battery performance.

- [1] M. Armand and J.-M. Tarascon, *Nature* 451: 652-657 (2008).
- [2] Kang, et.al., *Science* 311: 977 (2006).
- [3] P. J. McDonald, *Prog. Nuclear Magn. Reson. Spectrosc.* 30: 69 (1997).
- [4] Randall, et.al., *Solid State Nucl. Magn. Reson.* 14: 173-179 (1999).
- [5] Tang et. al, *J. Magn. Reson.* 225: 93-101 (2012).
- [6] Chandrashekar, et.al., *Nat. Mater.* 11: 311-315 (2012).

#### MO073: $^{17}\text{O}$ NMR Study of High-Tc Cuprate (CaLa)(BaLa)CuO

<sup>1</sup>\*Tonci Cvitanic, <sup>1</sup>Miroslav Požek, <sup>2</sup>Amit Keren, <sup>2</sup>Eran Amit

<sup>1</sup>Department of Physics, Faculty of Science, University of Zagreb, <sup>2</sup>Department of Physics, Technion-Israel Institute of Technology

We investigate the high temperature superconductor cuprate  $(\text{Ca}_x\text{La}_{1-x})(\text{Ba}_{1.75-x}\text{La}_{0.25+x})\text{Cu}_3\text{O}_y$  (CLBLCO) [1], with  $\text{YBa}_2\text{Cu}_3\text{O}_y$  like structure by  $^{17}\text{O}$  NMR. Measurements were made on underdoped and optimally doped powder samples from two families ( $x = 0.1$  and  $0.4$ ). Maximum  $T_c$  varies by 30% with minimal structural changes between families [1].

The spectrum differentiates two distinctive oxygen sites - planar and apical. Spin-lattice relaxation times on these two sites differ by more than an order of magnitude as oxygen in conductive plane relaxes much faster. NMR lines shift with respect to temperature occurs only on planar site, while the apical site shift is temperature independent. The temperature dependence of the planar oxygen Knight shift of underdoped and doped samples, shows opening of gap at temperatures high above  $T_c$ , (as previously indicated by magnetization measurements [2]). Unlike YBCO, where optimally doped samples show no evidence of pseudogap forming [3], we observe opening of the gap even in optimally doped samples.

- [1] O. Chmaissem, Y. Eckstein, and C. G. Kuper, *Phys. Rev. B* 63, 174510 (2001).
- [2] Y. Lubashevsky and A. Keren, *Phys. Rev. B* 78, 020505 (2008).
- [3] M. Takigawa et al., *Phys. Rev. B* 43, 247 (1991)

#### TU074: Transmembrane Signalling: combining structural biology methods to tackle multi-domain membrane proteins

<sup>1</sup>Benjamin Schomburg, <sup>2</sup>Gottfried Unden, <sup>1</sup>Stefan Becker, <sup>1</sup>Adam Lange, <sup>1</sup>\*Christian Griesinger

<sup>1</sup>Max-Planck-Institute for biophysical chemistry, <sup>2</sup>Institut für Mikrobiologie und Weinforschung, University of Mainz

NMR spectroscopy has become one of the principal methods for investigating the structure and function of proteins. In spite of recent developments in the field, the study of membrane proteins remains challenging, especially with respect to multi-unit complexes and larger proteins.

We therefore employ a combination of liquid-state and solid-state NMR spectroscopy to shed light on the mechanism of bacterial transmembrane signalling through receptor histidine kinases (HKs).

The Citrate Receptor A (CitA) is used as a model system for HKs[1,2]. Free citrate is recognised by a periplasmic

PAS (Per-Arnt-Sim) domain (PASp) and the input signal is then relayed to a second, cytosolic PAS domain (PASc) before leading to auto-phosphorylation in the conserved kinase core. To gain mechanistic insights, individual domains of the dimerising 60 kDa-protein are characterised with liquid-state NMR. The liquid-state assignments are then used to interpret solid-state NMR spectra of CitA constructs incorporated into liposomes.

Although this approach has been used previously for the HK DcuS[3], for which crystal structures[4] and liquid-state NMR data[5,6] are available only for PASp, we hereby present a study of a HK by solid-state NMR spectroscopy that is able to prepare the activated and inactivated state for comparison and relies on experimental structures for the globular domains. By analysing spectral differences between the citrate-free and citrate-bound states, it is possible to gain knowledge on residues involved in signal transduction. So far, we have been able to determine the alteration of the signal-receiving PASp-domain in context of membrane-embedded CitA, showing a significant reduction in plasticity upon citrate binding. In the near future, the role of PASc in signal transduction will be addressed.

Ultimately, the aim of this study is to acquire an atomic model for signal transduction across the plasma membrane through HKs. Strategies to reach this goal will be discussed.

HKs are the most abundant signal receptors in bacteria and crucial for virulence of several pathogenic species. Thus, understanding the function of CitA will have implications not only for research of transmembrane receptors in general, but could potentially also lead to new approaches for treating certain bacterial infections such as *Helicobacter pylori* - or *Staphylococcus aureus* - related diseases.

- [1] Kaspar et al.: *Mol. Microbiol.* 1999, 33(4): 858-72.
- [2] Sevvana et al.: *J. Mol. Biol.* 2008, 377: 512-23.
- [3] Etzkorn et al.: *Nat. Struct. Mol. Biol.* 2008, 15(10): 1031-39.
- [4] Cheung et al.: *J. Biol. Chem.* 2008, 283(44): 30256-65.
- [5] Pappalardo et al.: *J. Biol. Chem.* 2003, 278(40): 39185-88.
- [6] Kneuper et al.: *J. Biol. Chem.* 2005, 280(21): 20596-603.

#### TH075: Multinuclear solid state NMR investigation of structural development upon heat treatment and dissolution mechanism of sol-gel prepared calcium silicate based biomaterials

Zhongjie Lin, \*John V. Hanna

University of Warwick

Glassy sol-gel prepared calcium silicate materials show significant bioactivity depending strongly on composition. A systematic multinuclear solid-state MAS NMR study involving nuclei such as  $^{17}\text{O}$ ,  $^{29}\text{Si}$ ,  $^{31}\text{P}$ ,  $^{43}\text{Ca}$  and  $^1\text{H}$  has been undertaken on a range of sol-gel prepared silicate-based bioglass with three different compositions  $(\text{CaO})_x(\text{SiO}_2)_{1-x}$  ( $x = 0.2, 0.3, 0.5$ ) to investigate the structural effects induced by heat treatment and the reaction with simulated body fluid (SBF) and formation of bone-like hydroxyapatite  $\text{Ca}_{10}(\text{PO}_4)_6(\text{OH})_2$ .  $^{17}\text{O}$  MAS and 3QMAS NMR measurements on enriched samples have attempted to identify and quantify the bridging oxygen (bo) and non-bridging oxygen species (nbo) which are characterised by very different isotropic chemical shift ( $\delta_{iso}$ ) and electric field gradient tensor parameters ( $C_Q$  and  $\eta_Q$ ) parameters; this analysis has been combined with  $^{29}\text{Si}$  MAS NMR measurements in order to quantify the  $Q^n$  Si speciation and thus monitor the structural evolution of these systems upon heat treatment. These solid state  $^{17}\text{O}$  NMR results show that the silicate network is defined by a dominance of bo at lower temperatures ( $120^\circ\text{C}$ ), however a gradual introduction of nbo into the network is observed at higher temperatures ( $350\text{-}600^\circ\text{C}$ )

as more Ca becomes incorporated and assumes a key network modifier role. The intensity of the nbo resonance increases with both increasing CaO molar ratio and annealing temperatures.

These multinuclear NMR results also demonstrate that the bioreactivity with respect to SBF reaction of sol-gel prepared calcium silicates depend strongly on the surface OH and calcium content. The presence of calcium aids hydroxyapatite (HA) formation via the promotion of surface hydration and increasing supersaturation of  $\text{Ca}^{2+}$  ions. The  $^{17}\text{O}$  MAS and 3QMAS NMR results show that the rapid loss of nbo as Ca is leached from the silicate network results in changes in silicate framework connectivity and the formation of apatite. The new insights from  $^{31}\text{P}$  and  $^{17}\text{O}$  MAS NMR of the dissolution mechanism of these materials indicate the importance of achieving the right balance of bo/nbo ratio for optimal biochemical and mechanical properties, and the importance of an atomic scale probe such as solid state NMR for detailed understanding of the structure, bioactivity, dissolution mechanism and their relationships in such materials.

#### MO076: Host-guest interactions by solid state NMR

<sup>1</sup>\*Ljubica Tasic, <sup>1</sup>Camila P. Silveira, <sup>2</sup>Juliana Fattori, <sup>3</sup>Mariangela B. M. de Azevedo, <sup>4</sup>Leonardo Rojas, <sup>4</sup>Mavis L. Monteiro

<sup>1</sup>Organic Chemistry Department, University of Campinas (UNICAMP), Campinas, SP, Brazil, <sup>2</sup>LNBio, CNPEM, Campinas, SP, Brazil, <sup>3</sup>IPEN, Sao Paulo, SP, Brazil, <sup>4</sup>University of Costa Rica (UCR), San Jose, Costa Rica

Inter and intra molecular interactions are crucial for almost all processes in the world of chemistry, biology and biochemistry, and one of the most powerful techniques in monitoring these interactions is NMR spectroscopy. Herein, we present solid-state NMR applied in monitoring the host-guest interactions in the development of new drug formulations using beta-cyclodextrine as host, and in studies of surface modifications of a biomaterial, hydroxyapatite (HAP). Solid-state NMR spectra were recorded with an AVANCE II 400 MHz spectrometer using a probe equipped with a magic angle spinning system having a rotor diameter of 4 mm.  $^{13}\text{C}$  MAS NMR spectra were recorded at 100 MHz with a spinning rate of 10 kHz.  $^{31}\text{P}$  NMR spectra were recorded at 161.9 MHz, the samples were rotated at a frequency of 15 kHz and an angle of  $54.72^\circ$  to the external magnetic field. Inclusion complexes of two natural products: auraptene (AUR) and 4'-geranyloxyferulic acid (GOFA), known as very powerful cancer chemopreventers, with beta-cyclodextrine as host were prepared and their interactions were monitored using  $^{13}\text{C}$  solid-state NMR. Comparison among host, guest and host-guest  $^{13}\text{C}$  MAS NMR spectra enabled us to propose models for host-guest interactions and to calculate complexation-induced chemical shifts (CICS). Hydroxyapatite  $\text{Ca}_{10}(\text{PO}_4)_6(\text{OH})_2$  (HAP) surface contains two active sites: calcium hydroxide groups and phosphate groups, and can adsorb large quantities of ions or molecules present in solution. These properties make it a very attractive material for the synthesis of hybrid materials. Succinamic acid, succinic anhydride, succinimide, 2-aminoethyl dihydrogen phosphate and stearic acid were used as ligands.  $^{13}\text{C}$  and  $^{31}\text{P}$  MAS NMR measurements indicated that the ligands interacted with hydroxyapatite (HAP) surface and a mechanism of surface modification was proposed based on the obtained results.

FAPESP and Spinlab IQ-UNICAMP

#### TU077: Analysis of kafirin conformation by $^{13}\text{C}$ NMR in solid state

<sup>1</sup>\*Tatiana Santana Ribeiro, <sup>3</sup>Manoel Messias P. Miranda, <sup>2</sup>Juliana Scramin, <sup>2</sup>Luiz Alberto Colnago, <sup>2</sup>Lucimara Aparecida Forato

<sup>1</sup>Federal University of São Carlos - Campus Araras, <sup>2</sup>Brazilian Agricultural Research Corporation - Instrumen-

tation, <sup>3</sup>University of São Paulo-Campus São Carlos

Solid state NMR has been a powerful tool for conformation analysis of water insoluble proteins, found in cereal grains. Therefore, the objective of this work was to study the kafirin conformations extracted by different methods from grain sorghum. kafirin is found in the endosperm of the sorghum, corresponding to approximately 70% of its total proteins. kafirin is insolubility in water and its structure is not known. The analyses were performed in Varian Inova 400 spectrometer. The solid-state  $^{13}\text{C}$  NMR spectra were obtained with CPMAS and high-power decoupling,  $\pi/2$  pulse of 4 ms, 1ms contact time, 1024 points, repetition time of 3s, 5mm ZrO rotor, 8 kHz spinning, 1000 transients and  $\text{lb} = 20$ . The content of  $\alpha$ -helix,  $\beta$ -sheet, and disordered structures at 172, 174 and 176 ppm were determined by fitting the carbonyl peaks area with lorentzian function. The  $^{13}\text{C}$  NMR spectrum of kafirin extracted without bisulfite indicated that this protein has 84% of  $\alpha$ -helix, 14% of disordered and 2% of  $\beta$ -sheet structure. The  $^{13}\text{C}$  NMR spectrum of the kafirin extracted with bisulfite indicated that this protein has 89% of  $\alpha$ -helix and 11% of  $\beta$ -sheet and no disordered structure. Therefore, both  $^{13}\text{C}$  NMR spectra showed that this protein these proteins is predominantly  $\alpha$ -helix, but the extraction with bisulfite, that reduced the disulfide bond, increased the proportion  $\beta$ -sheet and reduced the content of disordered structures to a undetected level. In conclusion the solid-state  $^{13}\text{C}$  NMR was the good method to study of conformation of solid proteins. Although, the bisulfite extraction was more efficient it increase the  $\beta$ -sheet content.

ACKNOWLEDGMENTS: FAPESP, FAPERJ, CAPES, PETROBRAS, CNPq

#### TH078: Solid state NMR study of cement hydration to define chemical compositions

<sup>1</sup>\*Abdul-Hamid Emwas, <sup>2</sup>Rae Taylor, <sup>2</sup>Paulo Monteiro

<sup>1</sup>King Abdullah University of Science and Technology, Thuwal, Kingdom of Saudi Arabia., <sup>2</sup>Civil and Environmental Engineering, University of California Berkeley, USA

Calcium Silicate Hydrate (C-S-H) is the main binding phase in all cement based systems, making it the main binding phase of concrete; worldwide the most widely used material. Using NMR to study the different metal complexes in C-S-H and other cement phases helps to determine the correlation between molecular structure and macro properties, such as compressive strength, permeability and ultimately durability of the concrete. Gaining an understanding of how molecular structure correlates with macro properties is most useful when considering cement replacement material, such as ground granulated blast-furnace slag (GGBS) or fly-ash (pfa). Materials which are commonly used alone side cement to either reduce the amount of cement used or to improve selected properties of the cement. Different silicon coordination models can be correlated with the corresponding  $^{29}\text{Si}$  NMR chemical shifts, affording an effective tool to differentiate between different silicon coordinations modles. The  $^{27}\text{Al}$  isotropic chemical shifts can be used to differentiate tetrahedral  $\text{Al}_{(\text{tetra})}$  and octahedral coordination's, where the range of  $\text{Al}_{(\text{tetra})}$  100-50 ppm and  $\text{Al}_{(\text{octa})}$  in the 20 to -10ppm range [1]. In this study we employed  $^{27}\text{Al}$  and  $^{29}\text{Si}$  solid state NMR spectroscopy to investigate the effect of cement replacement materials and variation of water/cement ratios on C-S-H with the aim of gaining further insight in to the formation of C-S-H and the resulting effect on concretes macro structure.

#### References

[1] Skibsted, J., Jakobsen, H.J., and Hall, C., Direct observation of aluminium guest ions in the silicate phases of cement minerals by  $^{27}\text{Al}$  MAS NMR spectroscopy. Journal of the Chemical Society, Faraday Transactions, 1994. 90(14): p. 2095-98.

**MO079: Multinuclear Solid State NMR Investigation into the Speciation and Structure of Aluminium and Gallium Doped Phosphate Bioactive Glasses**

Scott P. King, Steven P. Brown, \*John V. Hanna

*University of Warwick, Department of Physics, England.*

Calcium phosphate glasses exhibit interesting properties and compatibility for use as bioactive materials by providing bone support and by demonstrating tendencies to stimulate bone regeneration. Doping of these glass systems with different cations can induce more favourable properties; Al that can strengthen the structure and thus result in greater control of dissolution rates from the glass network while Ga exhibits distinct antibacterial properties.[1,2] A multinuclear solid state MAS NMR study of two glass series with the nominal stoichiometry  $x(\text{Al}_2\text{O}_3)$  (11- $x$ )( $\text{Na}_2\text{O}$ ) 44.5(CaO) 44.5( $\text{P}_2\text{O}_5$ ) (with  $x = 0, 3, 5, 8$ ) and  $x(\text{Ga}_2\text{O}_3)$  (25- $x$ )( $\text{Na}_2\text{O}$ ) 30(CaO) 45( $\text{P}_2\text{O}_5$ ) (with  $x = 1, 3, 5, 10, 15$ ) has been undertaken in order to construct a picture of the glass networks, and to determine how the structure may influence the bioactive properties.

$^{27}\text{Al}$  MAS and  $^{71}\text{Ga}$  fast MAS NMR measurements demonstrate that for low  $\text{Al}_2\text{O}_3$  and  $\text{Ga}_2\text{O}_3$  contents in their respective glasses, the Al and Ga speciation is found to be dominated by octahedrally coordinated species upon initial entry into their networks. However, both glass systems tend to favour higher proportions of tetrahedrally coordinated Al and Ga structural moieties as the  $\text{Al}_2\text{O}_3$  and  $\text{Ga}_2\text{O}_3$  contents increase, thus showing that Al and Ga play similar structural roles. Information on the phosphorous  $Q_n$  speciation present within each glass is evidenced by  $^{31}\text{P}$  MAS NMR and the  $^{31}\text{P}$  refocused INADEQUATE Spin Echo (REINE) technique that reveals 2D correlations of the  $^2J_{PP}$  couplings with the  $^{31}\text{P}$  chemical shifts of the coupled nuclei.[3,4] These measurements have been performed for the first time on a coherent suite of samples thus enabling the evolving speciation and polymerisation of the phosphate network to be mapped out throughout the entire series. The overall trend of these NMR data suggests that the Al and Ga are playing important similar roles in the glass network, and may help in providing much greater insight to support their development as bioactive materials.[1,2]

[1] Manupriya et al., Phys. Status Solidi A, 2009, 206, 1447–1455.

[2] Valappil, S. P.; Ready, D.; Abou Neel, E. A.; Pickup, D. M.; Chrzanowski, W.; O'Dell, L. A. Newport, R. J.; Smith, M. E.; Wilson, M.; J.C. Knowles, Adv. Funct. Mater. 2008, 18, 732–741.

[3] Cadars et al., Phys. Chem. Chem. Phys., 2007, 9, 92–103.

[4] Guerry et al., J. Am. Chem. Soc., 2009, 131, 11861–11874.

**TU080: Application of Theoretical Calculations to Unequivocal Assignment of Lamivudine  $^{13}\text{C}$  NMR Signals in Solid-State**

<sup>1</sup>\*Vinicius Sousa Ferreira, <sup>1</sup>Diego Alves Rodrigues, <sup>2</sup>Felipe Terra Martins, <sup>1</sup>Luciano Morais Lião, <sup>1</sup>Luiz Henrique Keng Queiroz Júnior

<sup>1</sup>Universidade Federal de Goiás, Instituto de Química, Laboratório de Ressonância Magnética Nuclear, <sup>2</sup>Universidade Federal de Goiás, Instituto de Química, Laboratório de Cristalografia

Cycle of HIV virus replication presents various events, and proteins play an important role on it. Such proteins become targets of pharmacological antiviral agents and one of these is the lamivudine, which has an important role in the treatment of AIDS. As the number of antivirals increase, there is also a growing concern with the quality control, and an important tool to evaluate the quality of drugs is the Solid-State Nuclear Magnetic Resonance (SS-NMR). However, the assignment of the SS-NMR signals is not a trivial task. In

this context, the study presented here aims to investigate the application of theoretical calculations, as an auxiliary tool on the unequivocal assignment of the  $^{13}\text{C}$  SS-NMR signals of the lamivudine drug and the lamivudine salicylate cocrystal.

The SS-NMR experiments of the lamivudine and the respective cocrystal were obtained on a Bruker Avance III 500 MHz spectrometer. Theoretical calculations were performed in Gaussian 09 program using B3LYP/cc-pVTZ model and GIAO method to calculate the NMR shielding tensors.

The SS-NMR data indicated that there is only one lamivudine in the asymmetric unit of the lamivudine salicylate cocrystal, confirming a previous X-ray analysis. A very good corroboration, between experimental and theoretical SS-NMR data, was observed for the lamivudine drug and the value of linear correlation coefficient ( $R$ ) was 0.99. On other hand, comparing the data of the lamivudine salicylate cocrystal, the correlation ( $R = 0.89$ ) was not as good as for the lamivudine. This difference could be justified by the fact that in the cocrystal there are intermolecular hydrogen bonds between the asymmetric units, and these effects were not taken into account by the calculation performed for the cocrystal. Theoretical calculations provided to be a good tool to help the unequivocal assignment of SS-NMR signals. Calculations with specific conditions for mimic solid-state are currently in study.

**TH081:  $^{29}\text{Si}$  and  $^{27}\text{Al}$  MAS NMR ratio calculation in zeolites**

<sup>2,3</sup>\*Edson de Souza Bento, <sup>1</sup>Antônio Euzébio Goulart Sant'Ana, <sup>1</sup>Henrique Fonseca Goulart, <sup>3</sup>Geoffrey Ernest Hawkes, <sup>3</sup>Harold Toms, <sup>4</sup>Ingrid Graça Ramos, <sup>4</sup>Artur José Santos Mascarenhas

<sup>1</sup>Laboratório de Pesquisa em Recursos Naturais, IQB, Universidade Federal de Alagoas, Brasil, <sup>2</sup>Laboratório de Ressonância Magnética Nuclear, IQB, Universidade Federal de Alagoas, Brasil, <sup>3</sup>NMR Laboratory, SBCE, Queen Mary University of London, UK, <sup>4</sup>Instituto de Química, Universidade Federal da Bahia, Brasil

The objective of this work is to encapsulate pheromones in zeolites, using the nanometric cavities in the zeolite porous structure, so that, when the pheromone is used in the field, its release will be made gradually. The idea is to evaluate how different structural properties of various zeolites prepared synthetically, will affect the encapsulated pheromone release. It has been shown that by increasing the Si/Al ratio and the nature of the compensating cations, i.e., the higher the polarizability and the lower the polarity, the slower the release of attractants.[1]  $^{27}\text{Al}$  MAS NMR studies used a Bruker Avance 600 spectrometer at resonance frequency of 156.375 MHz, with a 4 mm MAS rotor and sample spinning rate of 12 kHz, single-pulse excitation (2ms), and repetition time 0.5s. In the  $^{27}\text{Al}$  MAS NMR spectra, signals at ca. 60 ppm are due to tetrahedral aluminum species,  $\text{Al}^{\text{IV}}$ , and the signals at ca. 0 ppm are due to octahedrally coordinated aluminum species,  $\text{Al}^{\text{VI}}$ . From integration of these separated signals, and by knowing the total Si/Al ratio of these sample, the Si/Al ratio of the tetrahedral framework,  $(\text{Si}/\text{Al})_{\text{fr}}$ , could be calculated using the following equation:[2]

$$(\text{Si}/\text{Al})_{\text{fr}} = (\text{Si}/\text{Al})_{\text{total}} (I_{\text{Al}(\text{tet})} + I_{\text{Al}(\text{oct})})/I_{\text{Al}(\text{tet})}$$

**References**

[1] J. Agric. Food Chem., 2001, 49 (10), pp 4801–4807.

[2] High-Resolution Solid-State NMR of Silicates and Zeolites, John Wiley & Sons, 1987, p. 213.

CNPq

**MO082: Structural Characterization of Oxyfluoride Glasses Using Solid State NMR**

<sup>1</sup>Raphaell Moreira, <sup>1</sup>R. G. Fernandes, <sup>2</sup>Jinjun Ren, <sup>1</sup>A. S. S. de Camargo, <sup>1,2</sup>\*Hellmut Eckert

<sup>1</sup>Physics Institute of Sao Carlos, Sao Paulo University – Sao Paulo, Brazil, <sup>2</sup>Institut für Physikalische Chemie, WWU Münster, Corrensstrasse 30 - Münster, Germany

Oxyfluoride glasses combine the favourable optical properties of fluoride glasses with the superior thermal, mechanical and chemical stability of oxide glasses. Such glasses are attractive candidates for many applications, for instance optical fibers, amplifiers, detectors and sensors.[1]

The present contribution is understanding with detailed structural studies of various glass systems based on fluorophosphates and fluoroborate compositions, using solid state nuclear magnetic resonance (NMR) methods.[2,3] Details of the information on the organization of the framework is obtained by <sup>31</sup>P, <sup>19</sup>F, <sup>27</sup>Al, and <sup>11</sup>B single and double resonance NMR techniques under static and magic-angle sample spinning (MAS) conditions. A number of established (HETCOR, REDOR) and new (DQ-DRENAR)[4] spectral editing techniques are used in these systems based on the selective measurement of homo- and heteronuclear magnetic dipole-dipole interactions. Furthermore, new NMR methodology will be introduced for quantifying the omnipresent problem of fluorine losses during melting.

#### References

- [1] Zuo, X.; Itoh, K.; Toratani, H.J. Non-Cryst. Solids 1997, 11, 215.
- [2] Zhang, L.; Araujo, C. C.; Eckert, H. J. Phys. Chem. B 2007, 111, 10402.
- [3] Fernandes, R. G.; Ren, J.; Camargo, A. S. S.; Hernandez, A. C.; Eckert, H. J. Phys. Chem. C 2012, 115, 6434.
- [4] Ren, J.; Eckert, H. Angew. Chem. Int. 2012, 51, 12888.

#### TU083: Study of the thermal processes in molecular crystals of peptides by means of NMR Crystallography

\*Tomasz Pawlak, Piotr Paluch, Katarzyna Trzeciak-Karlikowska, Agata Jeziorna, Marek J. Potrzebowski

Centre of Molecular and Macromolecular Studies, Polish Academy of Sciences

1D and 2D Very Fast Magic Angle Spinning (VF MAS) NMR experiments with sample rotation up to 55 kHz were applied to study both the dihydrate form of Tyr-(D)Ala-Phe-Gly (N-terminal sequence of opioid peptide dermorphin) and the anhydrous form, which was obtained by thermal treatment. Employing both homo-nuclear (<sup>1</sup>H-<sup>1</sup>H BABA, <sup>13</sup>C-<sup>13</sup>C SHANGHAI) and hetero-nuclear 2D correlations (<sup>1</sup>H-<sup>13</sup>C and <sup>1</sup>H-<sup>15</sup>N) with inverse detection, it was shown that removing water from the crystal lattice of this tetrapeptide does not destroy its subtle pseudo-cyclic structure, and its supra-molecular array is preserved. The GIPAW method was employed to compute the geometry of the peptides and calculate the <sup>13</sup>C *s<sub>ii</sub>* principal elements of the NMR shielding tensor parameters and <sup>1</sup>H isotropic NMR shifts. The theoretical values of <sup>13</sup>C *s<sub>ii</sub>* were compared with the experimental <sup>13</sup>C *d<sub>ii</sub>* chemical shift tensor values obtained by a 2D PASS experiment. The correlations <sup>13</sup>C *s<sub>ii</sub>* versus *d<sub>ii</sub>* and <sup>1</sup>H *s<sub>iso</sub>* versus *d<sub>iso</sub>* were used to evaluate the quality of the computational approach. With the new set of coordinates obtained by the GIPAW method, the crystal and molecular structure of the dehydrated Tyr-(D)Ala-Phe-Gly peptide that was obtained by thermal treatment was constructed. Methodology used in this project combining NMR measurements, analysis of X-ray powder diffraction data and advanced quantum mechanical calculations is known as NMR crystallography.

#### TH084: Probing cefadroxil isomorphous desolvate behaviour by <sup>13</sup>C CPMAS NMR and first principles calculations

<sup>1</sup>Daniel Lima Marques de Aguiar, <sup>1,2\*</sup>Rosane Aguiar da Silva San Gil, <sup>2</sup>Ricardo Bicca de Alencastro, <sup>2</sup>Eugênio Furtado de Souza, <sup>3</sup>Viviane da Silva Vaiss, <sup>3</sup>Alexandre Amaral

Leitão

<sup>1</sup>Instituto de Pesquisas de Produtos Naturais, Universidade Federal do Rio de Janeiro, Brasil, <sup>2</sup>Instituto de Química, Universidade Federal do Rio de Janeiro, Brasil, <sup>3</sup>Departamento de Química, Universidade Federal de Juiz de Fora, Brasil

Different hydration schemes of pharmaceutical solids implies also in distinct intermolecular crystal interactions. This affects the total lattice energy and the solubility, and hence the active pharmaceutical ingredient (API) bioavailability. Cephalexin monohydrate and cefadroxil monohydrate are two very similar  $\beta$ -lactam antibiotics which differ by one phenolic hydroxyl group. Cephalexin monohydrate is described in the literature as an isomorphous desolvated solid, but the cefadroxil monohydrate crystal lattice dehydration behaviour has not been reported so far. In this communication, thermal, X-ray, <sup>13</sup>C CPMAS NMR experiments and first principles calculations were combined to describe, at the atomic level the cefadroxil monohydrate dehydration process.

Cefadroxil monohydrate was purchased from Sigma Aldrich Inc. and dried in a Abderhalden's drying apparatus with refluxing toluene (110.6°C) under reduced pressure by 90 min. The reflux solvent was chosen based on cefadroxil monohydrate thermogravimetric (TG) and differential scanning calorimetry (DSC) analyses. Thermogravimetric analysis shows a 25% loss of H<sub>2</sub>O content, i.e., one water molecule per unit cell before the drying treatment, even though the DSC analysis do not shown any signal in the same temperature range. <sup>13</sup>C CPMAS NMR studies and X-ray measurements were performed before and after the drying treatment. In order to provide evidence on the ionization state of the amine and the carboxyl groups (Zwitterionic structure), infrared spectroscopy (FT-IR) was used. First principles calculations were also done using X-ray cell parameters and the heavy atoms positions, combined with FT-IR based protonation states, with pseudopotential and plane waves approach. The <sup>13</sup>C CPMAS NMR spectra shows great changes, especially at the  $\beta$ -lactam carbonyl and aromatic resonances.

#### MO085: Solid-state <sup>27</sup>Al NMR study of the thermal changes occurring in alumina-carbon composites

Thierry R. Lopes, Gustavo R. Gonçalves, Ewerton de Barcellos Jr., Miguel A. Schettino Jr., Alfredo G. Cunha, Francisco G. Emmerich, \*Jair C. C. Freitas

Laboratory of Carbon and Ceramic Materials, Department of Physics, UFES

Solid-state <sup>27</sup>Al nuclear magnetic resonance (NMR) spectroscopy with magic angle spinning (MAS) is long recognized as a powerful tool for the characterization of crystalline or disordered aluminas. Porous carbon materials containing dispersed aluminum oxides are of interest for applications such as the removal of fluoride from water, besides their advantageous use as catalysts supports. In this work we have investigated the structural and chemical transformations occurring in alumina-carbon composites upon heat-treatment, by using solid-state <sup>27</sup>Al MAS NMR spectroscopy in combination with X-ray diffraction (XRD) and thermal analyses. Two different carbon precursors were employed: a commercial activated carbon (denoted as AC) and a char obtained by carbonization of the endocarp of babassu coconut at 700 °C (denoted as BC), with specific surface areas of 1300 and 340 m<sup>2</sup>/g, respectively. The alumina-carbon composites were prepared by aqueous impregnation of AC or BC with aluminum nitrate and, after filtering and drying, were submitted to heat treatments under argon flow at temperatures up to 1500 °C. The aluminum compounds present in the as-synthesized AC\_Al samples were identified by XRD and solid-state <sup>27</sup>Al MAS NMR as nanocrystalline aluminum oxyhydroxides or hydroxides, depending on the detailed synthesis conditions. On the other hand, all aluminum-containing phases were X-ray amorphous in the as-synthesized BC\_Al samples, with the presence of a distribution of AlO<sub>6</sub> (octahedral Al site), AlO<sub>5</sub> and AlO<sub>4</sub> (tetrahedral Al site) units

revealed by solid-state  $^{27}\text{Al}$  NMR. The quadrupole coupling parameters, isotropic chemical shifts and relative fractions of each component were determined by fitting the spectra to a set of second-order quadrupolar lineshapes broadened by a distribution of quadrupole couplings and chemical shifts associated with disorder in the  $^{27}\text{Al}$  environments. The results showed that the nature of the carbon material used to prepare the composite was of great relevance for the definition of the type and crystallinity of the alumina phases formed after heat treatments.

ACKNOWLEDGEMENTS: CAPES, CNPq, FAPES, FINEP, Petrobras, NCQP/UFES.

#### **TU086: Solid-state $^{13}\text{C}$ and $^{31}\text{P}$ NMR studies of biochars prepared by chemical and thermal treatment of peat**

<sup>1</sup>Hercílio D. A. Honorato, <sup>2</sup>Daniel F. Cipriano, <sup>2</sup>Gustavo R. Gonçalves, <sup>2</sup>Miguel A. Schettino Jr., <sup>1,2\*</sup>Jair C. C. Freitas

<sup>1</sup>Centre of Competence on Petroleum Chemistry (NCQP), Department of Chemistry, Federal University of E,  
<sup>2</sup>Laboratory of Carbon and Ceramic Materials (LMC), Department of Physics, UFES

Biochar is a carbonaceous material produced by pyrolysis of biomass, which attracts great interest due to its applications as soil additive and in carbon sequestration. The physical and chemical properties of biochars can be changed by subjecting the material to different types of chemical and/or thermal treatments. This work was devoted to a study of the occurrence of phosphorus in carbon materials obtained by heat treatments of peat impregnated with  $\text{H}_3\text{PO}_4$ . Solid-state nuclear magnetic resonance (NMR) was used as the primary characterization technique. Peat samples were subjected to heat treatments in the presence of  $\text{H}_3\text{PO}_4$ , leading to the incorporation of phosphorus into the structure of the produced biochars and in some cases to an increase in porosity. The resulting material was then analyzed by solid-state  $^{31}\text{P}$  and  $^{13}\text{C}$  NMR under high magnetic field, among other characterization methods, in order to investigate the nature of the phosphorus-containing species in the structure of the biochars. The results showed that phosphorus was generally incorporated into the biochars as phosphate groups, in most cases bonded to aliphatic groups. The formation of polyphosphate chains was observed at relatively low heat-treatment temperatures (ca. 350 °C), but these groups were decomposed with the increase in the heat-treatment temperature. By X-ray diffraction, it was also possible to observe a beneficial effect of the phosphorus presence for the process of structural organization of graphene-like planes within the turbostratic microcrystallites. With increase in the heat-treatment temperature, a general trend of upfield shifting of the main  $^{31}\text{P}$  NMR peaks was observed, which was associated with the increase in the diamagnetic susceptibility of the graphene-like planes.

ACKNOWLEDGEMENTS: CAPES, CNPq, FAPES, FINEP, Petrobras, NCQP/UFES.

#### **TH087: New Zero-field NMR and NQR Experiments for Studying Materials and Quantum Information Processing**

<sup>1</sup>Christian Rivera Ascona, <sup>1</sup>Rodrigo de Oliveira Silva, <sup>1</sup>Roberson Saraiva Polli, <sup>1</sup>Daniel César Braz, <sup>1</sup>Diogo O. Soares Pinto, <sup>2</sup>João Teles de Carvalho, <sup>3</sup>José Roberto Tozoni, <sup>1\*</sup>Tito José Bonagamba

<sup>1</sup>Instituto de Física de São Carlos - Universidade de São Paulo, <sup>2</sup>Departamento de Ciências da Natureza, Matemática e Educação - Universidade Federal de São Carlos, <sup>3</sup>Instituto de Física - Universidade Federal de Uberlândia

Zero-field Nuclear Magnetic Resonance (NMRz) and Nuclear Quadrupole Resonance (NQR) are techniques that offer important information about nuclear environments, having the

advantage of being sensitive to internal magnetic fields and electric field gradients (EFG), without the need of strong static external magnetic fields. In the case of NMRz, used for studying magnetic materials, the spectra result from strong Zeeman coupling interaction perturbed by quadrupolar interaction. Using two arbitrary radio-frequency pulses, it is possible to observe multiple-quantum (MQ) echoes, where each echo spectrum presents a specific spectral line broadening. To explain such behavior, it was proposed a model in which the magnetic sample presents inhomogeneity distributions of Zeeman and quadrupolar coupling. Our experiments show that the magnetic materials have two different regions where: (i) the Zeeman coupling distribution is larger than the quadrupolar one and (ii) the dispersions of both distributions are similar. Under these two conditions, it was possible to observe one echo for each coherence of  $n$ th order. To observe individually each echo and better explore the physical information contained in each of them, MQ coherence selection was performed by applying specific phase cyclings and time-averaging. These methods offered complementary physical information about the nuclear spin interactions and the magnetic materials properties. In the case of NQR, the quadrupolar coupling is the most intense interaction. A weak external static magnetic field is applied just to remove the nuclear quadrupolar states degeneracy. The transition frequencies depend on the relative orientation between the weak external static magnetic field and the EFG main axis. This feature allows performing some new experiments, being our main goal to employ NQR for designing quantum information procedures, *e.g.*, the creation of pseudopure quantum states and logic gates.

ACKNOWLEDGEMENTS: IFSC, USP, FAPESP, CNPq, and CAPES.

#### **MO088: Comparison of Efavirenz Data Obtained by Solid State NMR Spectra and Molecular Modeling**

<sup>1</sup>Eduardo Gomes Rodrigues de Sousa, <sup>1\*</sup>Erika Martins de Carvalho, <sup>1</sup>Osvaldo Andrade Santos-Filho, <sup>2</sup>Rosane Aguiar da Silva San Gil

<sup>1</sup>Instituto de Tecnologia em Fármacos/ FIOCRUZ, Departamento de Síntese, R.J, Brazil, <sup>2</sup>Universidade Federal do Rio de Janeiro, IQ, Lab. RMN de Sólidos, R.J, Brazil

Nowadays, in order to evaluate a drug in the solid state it is very important to ensure its quality. An extremely powerful tool, which has been increasing their importance and applicability for the characterization of pharmaceutical formulations, is the solid state nuclear magnetic resonance spectroscopy (ss-NMR). Many regulators recognize the importance of the technique of NMR in the process of drug development and quality control thereof by the pharmaceutical industry. On the other hand, molecular modeling (M.M.) is an important tool for predicting the chemical shifts expected for each carbon of a particular molecule. The aim of this work was to compare experimental chemical shifts (ppm) data of Efavirenz (EFZ) obtained by ssNMR and the calculated data obtained by M.M. and verify the ability of the empirical method in predicting the experimental chemical shifts.

The structure of monomeric EFZ was fully optimized with density functional theory –DFT– (B3LYP/6-311+G(2d,p)) methodology. A conformational analysis was carried out on the optimized structure using an adaptation of the method described by Mahapatra et al. (2010). Crystallography data showed that EFZ unitary cell contains two different molecules, associated by two hydrogen bonds (Cuffini, 2009), and thus the molecular modeling of dimeric form was also performed. The X-ray geometry of EFZ dimeric form was used as a starting point for calculations. There are no significant differences between the crystal and optimized structure. The results have shown that the dimeric form is much more stable than the monomer. The largest deviations could be observed between the calculated and experimental  $^{13}\text{C}$  NMR chemical shifts data obtained for the two forms in deuterated chloroform ( $\text{CDCl}_3$ ). However when the experimental

data of dimeric form obtained by ssNMR were compared to those obtained by molecular modeling (in vacuum), it could be seen minimum deviations between experimental and calculated data.

#### References

MAHAPATRA, S. et al. New Solid State Forms of the Anti-HIV Drug Efavirenz. Conformational Flexibility and High Z' Issues. *Crystal Growth & Design*. v. 7, n. 10, p. 3191-3202, 2010.

CUFFINI, S. et al. (S)-6-Chloro-4-cyclopropylethynyl-4-trifluoromethyl-1H-3,1-benzoxazin-2(4H)-one. *Acta Crystallographica Section E: Structure Reports Online*, v. 65, p. 3170-3171, 2009.

ACKNOWLEDGEMENTS: INSTITUTO DE TECNOLOGIA EM FÁRMACOS/ FIOCRUZ, UFRJ.

#### TU089: Influence of the Recrystallization Solvent on the Efavirenz Crystalline Structure Probed by Solid State NMR

<sup>1</sup>Eduardo Gomes Rodrigues de Sousa, <sup>1\*</sup>Erika Martins de Carvalho, <sup>2</sup>Tereza Cristina dos Santos, <sup>3</sup>Rosane Aguiar da Silva San Gil

<sup>1</sup>Instituto de Tecnologia em Fármacos/Fiocruz, Departamento de Síntese Orgânica, Núcleo de RMN, RJ, <sup>2</sup>Instituto de Tecnologia em Fármacos/Fiocruz, Coordenação de Desenvolvimento Tecnológico, RJ, Bra, <sup>3</sup>Universidade Federal do Rio de Janeiro, IQ, Lab. RMN de Sólidos, RJ, Brazil.

In recent years, much attention has been focused on the predisposition of pharmaceutical solids to crystallize in several crystalline forms. The different crystalline forms of a drug can exhibit distinct chemical and physical properties, the important ones being stability, dissolution and bioavailability. Some data on literature[1-3] report that efavirenz (EFZ) crystalline structures are obtained, depending upon the factors such as solvent, temperature, additives and preparation methods. The aim of this work was to obtain crystalline EFZ through the use of different solvents (THF and heptane), probed by solid state nuclear resonance magnetic (<sup>13</sup>C CPMAS) spectroscopy and X-ray diffraction.

<sup>13</sup>C NMR solution spectra of the samples thus obtained showed identical chemical shifts, and the <sup>13</sup>C chemical shifts observed for solid samples were assigned on the basis of liquid-state data. Some differences in the chemical shifts  $\delta\delta = \delta_{liquid} - \delta_{solid}$  observed and are indicative of rigid and conformationally flexible fragments in the molecule (the latter are expected to undergo larger changes). They could be used as a probe for ascertain intermolecular interactions as H-bond. Some <sup>13</sup>C presented large differences  $\delta_{liquid} - \delta_{solid}$  and are splitted into a doublet (C<sub>3</sub>, C<sub>6</sub>, C<sub>9</sub>, C<sub>12</sub>, C<sub>13</sub> and C<sub>14</sub>) or triplet (C<sub>10</sub>), indicating a different chemical environments due to the crystallization process.

#### REFERENCES

[1] DESHMUKH, V. et al. Solubility Enhancement of Efavirenz Hydrochloride by Hot Melt Technique. *Current Pharma Research*, v. 1, n. 4, p. 320-336, 2011.

[2] MAHAPATRA, S.; THAKUR, T. S.; JOSEPH, S.; VARUGHESE, S.; DESIRAJU, G. R. New Solid State Forms of the Anti-HIV Drug Efavirenz. Conformational Flexibility and High Z. *Crystal Growth & Design*, v. 7, n. 10, p. 3191-3202, 2010.

[3] CUFFINI, S. et al. (S)-6-Chloro-4-cyclopropylethynyl-4-trifluoromethyl-1H-3,1-benzoxazin-2(4H)-one. *Acta Crystallographica Section E: Structure Reports Online*, v. 65, p. 3170-3171, 2009.

ACKNOWLEDGEMENTS: FARMANGUINHOS/ FIOCRUZ, UFRJ

#### TH090: Combining Solid-State NMR, X-Ray Diffraction and DFT Calculations to Characterize Carvedilol Polymorphs

<sup>1\*</sup>Carlos A. Rezende, <sup>1</sup>Katia Z. Leal, <sup>2</sup>Rosane Aguiar da Silva San Gil, <sup>2</sup>Daniel Lima Marques de Aguiar, <sup>3</sup>Viviane da Silva Vaiss, <sup>1</sup>Jackson A. L. C. Resende, <sup>2</sup>Ricardo Bicca de Alencastro, <sup>3</sup>Alexandre Amaral Leitão

<sup>1</sup>Universidade Federal Fluminense, <sup>2</sup>Universidade Federal do Rio de Janeiro, <sup>3</sup>Universidade Federal de Juiz de Fora

Drugs can exist in different crystal structures, a phenomenon known as polymorphism. Polymorphism can alter drug's physico-chemical properties which are essential to ensure effectiveness, safety and quality of a product. Thus the knowledge of the solid state properties is very important in the pharmaceutical field. Carvedilol belongs to beta-adrenolytics, a large group of cardiovascular drugs used clinically in the treatment of heart failure, hypertension, and certain types of cardiac arrhythmias. Regarding the polymorphism of carvedilol, the crystal structures of three anhydrous modifications were previously reported, including form I, form II (oral dosage form), form IV and hydrate form III. Solid-state NMR has become an essential technique for the solid-state characterization of pharmaceuticals. The technique can not only differentiate between different solid-state forms of a material, but also intimately probe the structural aspects of each solid-state form. This is especially important for solid-state forms that can not be crystallized and studied by single-crystal X-ray techniques. <sup>13</sup>C Cross Polarization Magic Angle Spinning experiments of Carvedilol form II were made and the number of peaks are exactly the number of atoms present in the molecule. To help in resonance assignment, ab initio codes based on periodic boundary conditions have been used regarding the study of small molecules. QUANTUM - Espresso is an integrated suite of computer codes for electronic structure calculations and materials modeling at the nanoscale. It is based on Density Functional Theory, planewaves, and pseudopotentials (both norm-conserving and ultrasoft). A very good agreement was found for the comparison between the global results of experimental and calculated NMR chemical shifts for carvedilol form II ( $R^2 > 0.99$ ). This work aims a comprehensive understanding of carvedilol crystalline forms employing SSNMR and DFT calculations. Other results and discussion will be included in this communication.

Acknowledgements: CAPES, CNPq and FAPERJ.

#### MO091: Multinuclear Solid-State NMR Characterization of Hydrotreating Catalysts and its Precursors

<sup>1,2</sup>L. S. Chinelatto Júnior, <sup>2,3</sup>H.R.X. Pimentel, <sup>2\*</sup>Rosane Aguiar da Silva San Gil, <sup>1</sup>Sonia Maria Cabral de Menezes, <sup>2</sup>Leandro B. Borré, <sup>1</sup>S.S.X. Chiaro

<sup>1</sup>PETROBRAS-CENPES, <sup>2</sup>Universidade Federal do Rio de Janeiro, <sup>3</sup>Universidade Federal Fluminense

The characterization of hydrotreating (HDT) catalysts and its precursors with multifield, multinuclear and multidimensional solid-state Nuclear Magnetic Resonance (NMR) techniques is essential to achieve a detailed understanding of the large differences in the distribution and structure of the species formed upon impregnation, calcination and sulfidation. In this work, commercial and synthesized pseudoboehmites and  $\gamma$ -aluminas prepared from these precursors, HDT catalysts prepared by impregnation of  $\gamma$ -alumina and hydrotalcite with Mo, Co, Ni, P and sulphidation and commercial HDT catalysts were characterized by solid-state NMR (MAS-NMR) of <sup>27</sup>Al, <sup>31</sup>P and <sup>17</sup>O, using Bruker Avance III (9.4 and 11.7T) and Bruker DRX300 (7.05T) NMR equipments. The characterization of  $\gamma$ -aluminas by using <sup>17</sup>O selective solid echo sequence  $(\pi/2)_s - \tau_{1-}(\pi)_s - \tau_{2-}$  acquire was performed through <sup>17</sup>O enrichment of the samples with H<sub>2</sub><sup>17</sup>O-40% before and after impregnation with the metals and sulphidation. The subscript s in the pulse sequence representation refers to a selective  $\pm 1/2$  cen-



tral transition pulse. The  $^{27}\text{Al}$  MAS NMR spectra of those  $\gamma$ -aluminas evidenced that the enrichment did not alter the alumina. The impregnation with the metals and P was done both in steps and by using co-impregnation. It was possible to establish the presence of P-O-Al bonds, by 2D NMR experiments ( $^{27}\text{Al}$  MQMAS NMR and  $^{27}\text{Al}$ - $^{31}\text{P}$  HETCOR), especially in co-impregnated catalysts, unlike shown in the literature.[1] The presence of phases Mo- $^{17}\text{O}$ -Mo were also confirmed by  $^{17}\text{O}$  MAS (selective solid echo). The results showed that the support structure influences the formation of intermediate species during the early stages of impregnation, calcinations and sulfidation. The natural abundance selective solid echo  $^{95}\text{Mo}$  NMR experiments performed on the HDT catalysts reveals a loss of symmetry upon calcination, probably due to polymerization of the surface species to form a  $\text{MoO}_3$ -like species.

#### References

[1] KRAUS, H.; PRINS, R. The Effect do Phosphoroyls on Oxidic  $\text{NiMo}(\text{CoMo})/\gamma\text{-Al}_2\text{O}_3$  Catalysts: A Solid State NMR Investigation J. Cat, 170: 20-28, 1997.

#### TU092: $^{13}\text{C}$ Solid-State and $^1\text{H}$ Time-domain NMR characterization of mobility and secondary structure of wheat gluten based materials

<sup>1</sup>Fabiana Diuk Andrade, <sup>1</sup>Oigres Daniel Bernardinelli, <sup>2</sup>Ramune Kuktaite, <sup>3</sup>Tomás S. Plivelic, <sup>1\*</sup>Eduardo Ribeiro de Azevêdo

<sup>1</sup>Institute of Physics of São Carlos - University of São Paulo, <sup>2</sup>Department of Agriculture - Farming Systems, Technology and Product Quality, The Swedish University of Agricultural Sciences, <sup>3</sup>MAX-lab - Lund University

We report a combined DSC,  $^{13}\text{C}$  Solid-state and  $^1\text{H}$  Time-domain NMR study in films of gliadin and glutenin rich wheat gluten using different amount of glycerol (0%, 10%, 20%, 30% and 40%) as the plasticizer [1]. High field (400 MHz) Magic Angle Solid-state  $^{13}\text{C}$  NMR experiments performed with cross polarization, CP/MAS, and single pulse excitation, SPE/MAS, allowed the identification of at least three distinct components based on their mobility. While the more mobile components were attributed to the lipid and glycerol moieties, the more rigid segments, solid-like, as well as those with intermediate mobility were attributed to the backbone and side-chains of the proteins. These identifications allowed to analyse low field (20 MHz) FIDs acquired after the application of a Magic-Sandwich Echo sequence (MSE-FID) as well as Time-domain signals obtained with a mixed magic-sandwich echo-Carr-Purcell-Meiboom-Gill sequence (MSE-CPMG) in terms of three components, whose relative amounts and the average motion correlation times were obtained for all samples. Besides, the  $^{13}\text{C}$  CP/MAS spectra and DSC thermograms also showed that the relative fractions of protein segments with  $\alpha$ -helix,  $\beta$ -sheets, and random conformations varied according to glycerol content and relative amount of gliadin and glutenin in the films. The results showed that the segmental mobility and relative fraction of segments with  $\alpha$ -helix conformation tend to increase as a function of the glycerol content in gliadin rich samples, which occur together with a reduction in the conformation disorder of the  $\alpha$ -helices. In contrast, for glutenins rich fractions the results pointed to a promotion of  $\beta$ -sheet conformation for increasing glycerol amounts. Since the predominance of segments with  $\alpha$ -helix or  $\beta$ -sheet conformations has strong effects on the viscoelastic properties of wheat gluten based materials, the results points to a way of controlling these viscoelastic properties towards the achievement of tunable biodegradable and sustainable biomaterials based on gluten.

[1] Kuktaite, R. et al. Biomacromolecules, 2011, 12, 1438-1448.

ACKNOWLEDGMENTS: FAPESP, CNPq

#### TH093: Effects of Pretreatment on Morphology, Chemical Composition and Enzymatic Digestibility

#### of Sugarcane Bagasse and Eucalyptus Bark

<sup>1\*</sup>Oigres Daniel Bernardinelli, <sup>1</sup>Marisa Aparecida Lima, <sup>2</sup>Gabriela Bassetti Lavorente, <sup>2</sup>Hana Karina Pereira da Silva, <sup>2</sup>Juliano Bragatto, <sup>1</sup>Camila Alves Rezende, <sup>3</sup>Leonardo D. Gomez, <sup>3</sup>Simon J. McQueen-Mason, <sup>2</sup>Carlos Alberto Labate, <sup>1</sup>Igor Polikarpov, <sup>1</sup>Eduardo Ribeiro de Azevêdo

<sup>1</sup>Instituto de Física de São Carlos, USP, <sup>2</sup>Laboratório Max Feffer de Genética de Plantas, USP, <sup>3</sup>CNAP, Department of Biology, University of York

Characterization of lignocellulosic biomass to produce multi-products such as ethanol and other biomaterial is challenging due to its structural complexity and heterogeneity. However, know the chemical structure of lignocellulosic biomass is essential to understand possible modifications in the morphology and chemical composition of the materials submitted to specific pretreatment. The pretreatment is responsible for the successful use of lignocellulosic biomass feedstock in ethanol production. Solid state nuclear magnetic resonance (ssNMR) is regarded as one of the best tools for elucidating structures of lignocellulosic biomass. The primary solid state ssNMR technique that has been used so far is the routine  $^{13}\text{C}$  cross polarization-magic angle spinning (CP-MAS) technique. Although this technique has markedly advanced our understanding of lignocellulosic biomass, full potential of ssNMR for characterizing these samples has yet to be realized. Technical developments and applications of advanced solid state NMR have revealed the promise deeper insights into structures of lignocellulosic biomass. In this work, we present a ssNMR oriented characterization of the delignification process with increasing sodium hydroxide concentrations, preceded or not by diluted acid, of two eucalyptus barks clones, *Eucalyptus grandis* (EG) and the hybrid, *E. grandis* x *urophylla* (HGU), as well as in sugarcane bagasse. The enzymatic digestibility and total cellulose conversion were measured and correlated with the modification in the composition of the solid and the liquor fractions, as seen by ssNMR and Fourier-transform infrared spectroscopy (FTIR). Besides, a comparison between the crystalline fraction as obtained by ssNMR and X-Ray diffraction was also performed, showing a tendency of removing the amorphous content by the chemical treatment.

ACKNOWLEDGEMENTS: CNPq

#### MO094: Solid State NMR and Low Field Relaxometry Characterization of Brazilian Clay-EVA Nanocomposites

<sup>1</sup>Elisabeth G. van der Linden, <sup>1\*</sup>Rosane Aguiar da Silva San Gil, <sup>1</sup>Leandro B. Borré, <sup>1</sup>Luis G. V. Gelves, <sup>1</sup>Vera L. P. Soares, <sup>1</sup>Simone P. Silva, <sup>2</sup>Maria Inês Bruno Tavares, <sup>2</sup>Roberto P. Cucinelli Neto, <sup>3</sup>Sérgio S. Camargo Jr., <sup>3</sup>Emanuel Santos Jr.

<sup>1</sup>UFRJ, Instituto de Química, <sup>2</sup>UFRJ, Instituto de Macromoléculas, <sup>3</sup>UFRJ, COPPE, Eng.Metalúrgica e Materiais

Polymer nanocomposites have been used to design new materials with improved properties. The lamellar structure present in montmorillonite furnishes the basic structure necessary for the synthesis of clay based nanocomposites. The substitution of exchanging cations by ammonium quaternary salts leads to organically modified montmorillonites. The presence of these hybrid materials in a polymer matrix increases its thermal stability, and also its mechanical properties. Depending on the polymer nature, other properties, as adhesivity could be also improved. During the development of nanostructured advanced recovering materials to be used in petroleum industry distinct organically modified Brazilian montmorillonite-EVA nanocomposites have been prepared by using a Brazilian clay, in the range 0.5 to 10% w/w. In this communication X-ray diffraction (XRD), thermogravimetry analysis (TGA), hydrophobicity degree by using the contact angle, Fourier transform infrared spectroscopy,  $^{27}\text{Al}$  single pulse solid state NMR,  $^{13}\text{C}$  cross-polarization high resolution solid state NMR, and  $^1\text{H}$  low field NMR were used to

address the structure of the EVA-organoclays. The results were compared with those obtained by using modified carbon nanotubes-EVA nanocomposites, and evidenced that depending on the nanostructured component distinct molecular dynamics for EVA moiety was detected.

Acknowledgements: Rede Nano (Petrobras), PIBIC CNPq-UFRJ, CAPES.

#### References

Aranha, I.B. (2007) Preparação, caracterização e propriedades de argilas organofílicas. Tese de Doutorado, Instituto de Química, Universidade Federal do Rio de Janeiro.

Bain, D.C., Smith, B.F.L. (1994), Chemical analysis, In: Clay Mineralogy, Spectroscopic and Chemical Determinative Methods. Edited by M. J. Wilson, Chapman & Hall, London, 312.

Menezes, R.R., Souto, P.M., Santana, L.N.L., Neves, G.A., Kiminami, R.H.G.A., Ferreira, H.C. (2009) Argilas bentonitas de Cubati, Paraíba, Brasil: Caracterização físico-minerológica. *Cerâmica*, 55, 163-169.

#### TU095: Molecular dynamic of modified graphene oxide/poly(butylene succinate) nanocomposite determined by longitudinal relaxation time NMR

Fernando Luis Miranda Filho, \*Emerson Oliveira Da Silva

IMA/ UFRJ

In this work, graphite was treating with oxidizing agents (modified Hummer method) to obtain graphite oxide (GO). Besides that, the GO was treating with an excess of succinic acid to obtain a graphene succinate sample (SG). Nanocomposites were prepared by the following method: Poly(butylene succinate), PBS, was solubilized in chloroform for two hours. At the same time, the nanoparticle was dispersed in the same solvent with appropriate proportion, which was also in ultrasonic apparatus for two hours. Then, both dispersions had been mixed and kept in ultrasonic apparatus for more two hours. The sample obtained was dried to constant mass in a laboratory oven. The nanocomposites were characterized by low field NMR, to analyze the dispersion of nanoparticles at polymer matrix. The results showed that the PBS presented three domains of mobility. The major domain, in high relaxation time, is due the crystalline phase. The other domains are the amorphous phase in and out the crystal structure. The GO/PBS system presented only two domains shifted to shorter times. Furthermore, all the domains showed wider curves. This indicates that the system became more heterogeneous and with higher mobility as a result of interaction with the GO particles. Probably, the GO particles cause the decrease of the crystalline phases of matrix which increase the mobility. The influence of SG in the PBS matrix was different. The SG/PBS system showed three mobility domains. All of them wider than the PBS system and in lower  $T_1$  values. This occurs because the SG has a better interaction with the PBS matrix what results in a good dispersion. This morphology causes a stronger effect on relaxation time of matrix. The PBS presented three domains of mobility. The major domain, in high relaxation time, is due the crystallinity phase.

#### Liquid state NMR

#### TH096: Regulatory Interactions between a Bacterial Tyrosine Kinase and its Cognate Phosphatase

<sup>1,4</sup>Deniz B. Temel, <sup>2</sup>Kaushik Dutta, <sup>1</sup>Sébastien Alphonse, <sup>3</sup>Julian Nourikyan, <sup>3</sup>Christophe Grangeasse, <sup>1,4\*</sup>Rana Jeet Ghose

<sup>1</sup>The City College of New York, <sup>2</sup>New York Structural Biology Center, <sup>3</sup>Institut de Biologie et Chimie des Protéines, CNRS, Université Lyon 1, Université de Lyon, <sup>4</sup>Graduate

Center of the City University of New York

Bacterial tyrosine kinases (BY-kinases), and their cognate tyrosine phosphatases, form counteracting enzyme pairs regulating diverse physiological processes in both Gram-negative and Gram-positive species. In *Escherichia coli* (K12), the BY-kinase Wzc, plays a critical role in production of the exopolysaccharide, colanic acid, and the formation of biofilms. Wzc kinase contains a cluster of tyrosine residues (YC) at its C-terminus that is autophosphorylated and subsequently dephosphorylated by Wzb phosphatase. This Wzb phosphatase mediated phosphorylation/dephosphorylation cycle in Wzc kinase, rather than its quantitative phosphorylation state, is critical for colanic acid production. Despite extensive genetic and biochemical evidence for Wzb-mediated dephosphorylation of the Wzc YC, the nature of the interactions between these two enzymes, and the regulatory mechanisms that govern dephosphorylation, are unknown for this or for any other BY-kinase/phosphatase pair. Here, using solution NMR methodology, we provide the first insight into the regulatory interactions between a BY-kinase and its opposing phosphatase at residue-level resolution. Wzb phosphatase docks onto the catalytic domain of Wzc (Wzc<sub>CD</sub>) utilizing a surface that is distal to the catalytic elements of the latter. Mutations in this region reduce Wzb phosphatase mediated dephosphorylation of the kinase YC. Wzc<sub>CD</sub> binds Wzb phosphatase in a YC-independent manner near the catalytic site of the latter, inducing allosteric changes therein. Wzb phosphatase principally recognizes the phosphate moiety of phosphotyrosine, and derives tyrosine-selectivity through interactions with a conserved tyrosine at its active site. YC-dephosphorylation is proximity-mediated and reliant on the increased phospho-YC concentration near the Wzb phosphatase active site due to docking interactions with Wzc<sub>CD</sub>.

#### MO097: qNMR for Analysis of Methylodopa-Containing Pharmaceutical Formulations: Comparison Between Free and Marketed Drugs

Wilian da Silva Nunes, \*Glaucia Braz Alcantara

Mato Grosso do Sul Federal University

The Brazilian government has provided various free medicines for the population through the national health care system (SUS). However, it can often observe some doubts from people and even health professionals about the effectiveness of these medicines. The effectiveness depends on the amount of the active principle and its availability for organism (for example, polymorphs species can decrease the bioavailability), among other factors.

Considering that qNMR has been established as a successful analytical method, this work proposes to apply <sup>1</sup>H NMR spectra for quantification of methylodopa on several pharmaceutical formulations, as a first step for comparison between free and marketed drugs. We have compared the results according to the official method (titration in non-aqueous media) described in Brazilian Pharmacopeia, as well as with the permitted values by ANVISA (Brazilian agency of sanitary vigilance).

The measurements of <sup>1</sup>H NMR were performed on a Bruker DPX300 (7.05T) spectrometer, equipped with a <sup>1</sup>H/<sup>13</sup>C dual probe, using the ZGPR pulse sequence, NS: 32; d1: 10s; AQ: 7.29s; relaxation delay > 5 T<sub>1</sub>; TD: 128k and SW: 30 ppm. The singlet of TMSP-*d*<sub>4</sub> was integrated and referenced to calculate the methylodopa concentration, through its methylic singlet ( $\delta$  1.53).

The quantification by NMR showed results between 89.76% and 109.96% of the methylodopa amount, according to the package label. The variation is according to values determined by ANVISA in 93.33% of cases. Methylodopa was found in similar contents in both kinds of pharmaceutical formulations, corroborating that the absolute amount of this active principle in free drugs is in concordance to reference drugs.

qNMR has proved a more reliable method for quantification of methylodopa-containing drugs than titration method,

particularly due to the subjectivity in determining the color change of the indicator and the equivalence point in titration.

Acknowledgment: PET/Química.

#### TU098: Frequent applications of NMR in the IPT as a customer demand.

<sup>1</sup>\*Martha González-Pérez, <sup>1</sup>Shoko Ota, <sup>1,2</sup>Eli da Silva Ferreira Júnior

<sup>1</sup>Instituto de Pesquisas Tecnológicas do Estado de São Paulo S.A – IPT, <sup>2</sup>Instituto de Química, Universidade de São Paulo

NMR spectroscopy is a powerful analytical tool for chemical analysis and structural identification. For that reason, the Chemical Analysis Laboratory (LAQ) from Technological Research Institute of the State of São Paulo recently has acquired two VARIAN spectrometers operating at 400 MHz. One spectrometer is used for analyzing liquid samples and the other for solid state. On customers demand, the common applications in our Research Institute are the followings:

Qualitative Analysis:

- 1- Chemical structure identification of organic compounds used for inspection and classification of custom office,
- 2- Monomer identification and degree of polymerization used for evaluating the kind and quality of production processes,
- 3- Determination of average ethoxylate number of polymers for confirming physical and chemical properties.

Quantitative analysis:

- 1- Monomer's quantification of two types of polymers: Acrylonitrile - Butadiene - Styrene (ABS) and Styrene - Butadiene (SBR), necessary for confirming raw matter quality in the automobile industry.
- 2- Chain configuration analysis of polypropylene (evaluation of random copolymerization through Randall method) for custom verification.

This work will show some of results carried out on client's demands, i.e., analysis of very different samples, in order to illustrate the possibilities and versatility of IPT Laboratory.

Acknowledgment: IPT

#### TH099: Singlet NMR of [1,4-<sup>13</sup>C<sub>2</sub>]fumarate

<sup>1,2</sup>\*Irene Marco-Rius, <sup>3</sup>Michael C. D. Tayler, <sup>1,2</sup>Timothy J. Larkin, <sup>1,2</sup>Kevin M. Brindle

<sup>1</sup>University of Cambridge, Department of Biochemistry, UK, <sup>2</sup>Cancer Research UK, UK, <sup>3</sup>Radboud University, Institute for Molecules and Materials, NL

Hyperpolarised NMR, for instance using dissolution DNP, is a non-invasive technique to image tissue metabolism *in vivo*. However, the range of reactions that can be investigated is limited by the fast T<sub>1</sub>-dependent decay of the nuclear spin order. In metabolites with coupled nuclear spin-1/2 pairs, polarization may be maintained for a longer time by exploiting the non-magnetic singlet state of the pair. This may allow preservation of hyperpolarization *in vivo* during transport to tissues of interest, such as tumours, and detection of slow metabolic processes. One of the promising substrates in which to combine DNP with the longer-lived singlet state to study metabolism is fumarate, the precursor of malate, which is a marker of cell necrosis. Hyperpolarised [1,4-<sup>13</sup>C<sub>2</sub>]fumarate has been used previously to monitor response to cancer treatment [1], and its longitudinal relaxation times in a D<sub>2</sub>O buffer were measured to be 15 s for proton and 30 s for carbon at a magnetic field strength of 11T. To test whether the singlet state of the carbon or proton pairs of [1,4-<sup>13</sup>C<sub>2</sub>]fumarate was slower relaxing than their corresponding longitudinal relaxation time, we accessed the singlet state by breaking the symmetry of the pairs. This was done using the J-couplings in a similar way to that described by Feng

*et al* [2]. However, in the case we present here, neither the proton-proton nor the carbon-carbon couplings are negligible, which implies that the two zero quantum subspaces of the Hamiltonian that describe this four-spin system evolve in a different way during the magnetisation-to-singlet (M2S) pulse sequence. We measure the singlet relaxation time to be 20 s for both carbon and proton pairs. This shows that although <sup>1</sup>H-NMR could benefit from the slower relaxing singlet, for <sup>13</sup>C-NMR it would be detrimental.

[1] Gallagher, F. A., Kettunen, M. I., Hu, D.-E., Jensen, P. R., in 't Zandt, R., Karlsson, M., Gisselsson, A., Nelson, S. K., Witney, T. H., Bohndiek, S. E., Hansson, G., Peitersen, T., Lerche, M. H., and Brindle, K. M. (2009) Production of hyperpolarized [1,4-<sup>13</sup>C<sub>2</sub>]malate from [1,4-<sup>13</sup>C<sub>2</sub>]fumarate is a marker of cell necrosis and treatment response in tumors, Proc. Natl. Acad. Sci. USA, 106, 19801-19806.

[2] Feng, Y., Davis, R. M., and Warren, W. S. (2012) Accessing long-lived nuclear singlet states between chemically equivalent spins without breaking symmetry, Nature Physics, 2425.

#### MO100: RNA induced folding of the first double stranded RNA binding domain from A. thaliana DCL1.

<sup>1</sup>Paula Burdisso, <sup>1</sup>Irina Paula Suarez, <sup>1</sup>Guillermo Hails, <sup>2</sup>Matthieu Benoit, <sup>2</sup>Jerome Boisbouvier, <sup>1</sup>\*Rodolfo Maximiliano Rasia

<sup>1</sup>Instituto de Biología Molecular y Celular de Rosario, Facultad de Ciencias Bioquímicas y Farmacé, <sup>2</sup>Institut de Biologie Structurale (IBS) Jean-Pierre Ebel, Commissariat à l'Energie Atomique (CE)

MicroRNAs are essential gene regulators in multicellular organisms. Plant miRNAs are processed in the nucleus by a protein complex formed by DICER-LIKE1 (DCL1), HYL1 and SERRATE. DCL1 has a central role in the recognition and processing of the heterogeneous plant precursors. Little is known about the structural aspects of this protein. In a previous work, we characterized the second dsRBD of DCL1. Here we present a structural characterization of the first DCL1 double stranded RNA binding domain.

In contrast with canonical dsRBDs, this domain binds dsDNA with a similar affinity as dsRNA, the same as DCL1-dsRBD2. We found that both domains cooperate for substrate binding, but not for DNA binding.

Quite unexpectedly we found that dsRBD1 is intrinsically disordered, even in the context of flanking domains, but folds upon binding substrate RNA. We have assigned the backbone resonances corresponding to the free unfolded and bound folded protein. The free protein, though intrinsically disordered, shows a tendency to populate folded conformations that correspond to those expected for a dsRBD. The assignment of the bound form allowed us to calculate the fold of the protein in complex with dsRNA employing CS-Rosetta. This analysis shows that this domain acquires the dsRBD fold when bound to substrate. We further found that the negatively charged surface provided by SDS micelles shifts the protein towards folded conformations, but these are different from that found in the complex with RNA. Experimental comparison with dsRBDs from other Dicer proteins show that the intrinsically disordered nature is exclusive of DCL1-dsRBD1. Sequence analysis and *in vivo* function of the protein suggests that in this domain the instability of the free form and the ability to fold upon binding the substrate have to be essential for the function of the whole DCL1 enzyme in miRNA processing.

#### TU101: NMR analysis of asphaltene extracted from field deposits

<sup>1</sup>Camila P. Silveira, <sup>2</sup>\*Peter R. Seidl, <sup>1</sup>Ljubica Tasic, <sup>2</sup>Fernanda B. da Silva, <sup>2</sup>Maria José C. O. Guimarães

<sup>1</sup>University of Campinas (UNICAMP), <sup>2</sup>Federal University of Rio de Janeiro (UFRJ)

Asphaltenes correspond to the heaviest and most polar fraction of petroleum. They are defined by their solubility properties (soluble in aromatics and insoluble in n-paraffins). The price attributed to a crude oil is related to its asphaltene content: the higher the content, the lower its price when marketed, since asphaltenes tend to aggregate and deposit during production and to form coke on refining. Despite the considerable investment in determination of molecular properties of asphaltenes, their individual structures have not been completely elucidated. In view of the large number of constituents of heavy oils that are soluble in aromatics, we are developing fractionation procedures in order to better understand the relationships of asphaltene structures with their physical and chemical properties.

Asphaltene samples were extracted from field deposits, fractionated by two different methods and compared mainly by NMR analysis. Our objective was to verify if the traditional but time-consuming and relatively costly IP 143 procedure could be substituted by an alternative method, developed in our labs and based in a solvent blend, without losing information on the sample's asphaltene composition.  $^1\text{H}$  Nuclear Magnetic Resonance (NMR),  $^{13}\text{C}$  NMR without NOE,  $^{13}\text{C}$  NMR DEPT, elemental analysis, infrared spectra and X-ray fluorescence data were collected for both types of samples. It was possible to verify that the new extraction method is capable of isolating asphaltenes that contain the same type of organic functions as samples obtained by the IP method, but in different proportions. It was also shown, mainly by NMR analysis, that the alternative method can be applied to fractionation of heavy petroleum as well as vacuum residues.

#### TH102: Cold-denaturation of a protein dimer monitored at atomic resolution.

<sup>1</sup>Mariusz Jaremko, <sup>1</sup>Lukasz Jaremko, <sup>1</sup>Hai-Young Kim, <sup>1</sup>Min-Kyu Cho, <sup>2</sup>Charles D. Schwieters, <sup>1</sup>Karin Giller, <sup>1</sup>Stefan Becker, <sup>1,3</sup>\*Markus Zweckstetter

<sup>1</sup>Department for NMR-based Structural Biology, Max Planck Institute for Biophysical Chemistry, <sup>2</sup>Computational Bioscience, Center for Information Technology, NIH, <sup>3</sup>Center for Neurodegenerative Diseases (DZNE)

Protein folding and unfolding are crucial for a range of biological phenomena and human diseases. Defining the structural properties of the involved transient species is therefore of prime interest. Using a combination of cold-denaturation with nuclear magnetic resonance spectroscopy we reveal detailed insight into the unfolding of the homodimeric repressor protein CylR2. Seven three-dimensional structures of CylR2 at temperatures from 25 °C to -16 °C reveal a progressive dissociation of the dimeric protein into a native-like monomeric intermediate followed by transition into a highly dynamic, partially folded state. The core of the partially folded state appears critical for biological function and misfolding [1].

[1] Jaremko, M., Jaremko, L., Kim, H.-Y., Cho, M.-K., Schwieters, C. D., Giller, K., Becker, S., Zweckstetter, M. (2013) Cold denaturation of a protein dimer monitored at atomic resolution, *Nat. Chem. Biol.* Accepted

#### MO103: Solution Structure of a Lithium Organyl: Dilithiated Aminophosphazenes in Action

María Casimiro, Ignacio Fernández, \*Fernando López Ortiz

University of Almería

As part of an ongoing project on the synthetic applications of phosphorus-bearing lithium organyls, we have developed efficient methodologies for the ortho functionalization of several phosphinic amides and phosphazenes via directed ortho lithiations (DoLi) and subsequent electrophilic trapping [1]. These reactions proceed in some cases with very high diastereoselectivities and provide rapid access to multidentate hemilabile ligands which are being explored in asymmetric catalysis.

We describe herein the study of the aminophosphazenes *ortho* lithiation process through the use of advanced multinuclear magnetic resonance methods. The powerful combination of standard NMR techniques and 2D nOe,  $^7\text{Li}$ ,  $^{31}\text{P}$ - and  $^7\text{Li}$ ,  $^{15}\text{N}$ -HMQC experiments helped us to unravel the structure of the key intermediate lithium species involved in the DoLi reactions of secondary aminophosphazenes.  $^1\text{H}$ ,  $^7\text{Li}$  and  $^{31}\text{P}$  NMR spectra as a function of temperature and concentration will be also showed in order to obtain critical coupling constants and determining the aggregation state of the existing species. In this sense, the signal observed at  $\delta$  208.9 ppm in the  $^{13}\text{C}$  NMR spectrum measured at -100 °C that is assigned to the lithiated ortho carbon defines a specific type of structure. The multiplicity of this carbon signal, a quartet with a  $^{13}\text{C}$ ,  $^7\text{Li}$  coupling constant of 30.2 Hz, establishes the monomeric nature of the lithiated species.

[1] (a) Fernández, I.; Oña-Burgos, P.; Oliva, J. M.; López-Ortiz, F. J. *Am. Chem. Soc.* 2010, 132, 5193. (b) García-López, J.; Morán-Ramallal, A.; González, J.; Oña Burgos, P.; Iglesias, M. J.; Rocas, L.; García-Granda, S.; López-Ortiz, F. J. *Am. Chem. Soc.* 2012, 134, 19504.

ACKNOWLEDGEMENT: We thank the Ministerio de Economía y Competitividad (MINECO) and FEDER program for financial support (project CTQ2011-27705). M.C. thanks MICINN for a predoctoral fellowship.

#### TU104: Experimental and Theoretical Study of Tamiflu NMR Data: a Comparative Analysis

<sup>1</sup>\*Diego Alves Rodrigues, <sup>1</sup>Vinicius Sousa Ferreira, <sup>2</sup>Felipe Terra Martins, <sup>1</sup>Luciano Morais Lião, <sup>1</sup>Luiz Henrique Keng Queiroz Júnior

<sup>1</sup>Universidade Federal de Goiás, Instituto de Química, Laboratório de RMN, <sup>2</sup>Universidade Federal de Goiás, Instituto de Química, Laboratório de Cristalografia

Oseltamivir is an antiviral drug, marketed under the trade name Tamiflu, used in the treatment and prophylaxis of infections by the influenza A and B viruses. It is one of the promising therapeutic agents for the treatment of avian influenza H5N1 infection. The objective of the study is to correlate the theoretical results, with and without the solvent's effect, with the experimental  $^1\text{H}$  and  $^{13}\text{C}$  NMR data for the drug Tamiflu, aiming to confirm the unequivocal assignment of all the NMR signals of this compound.

The NMR experiments of a Tamiflu solution were obtained in a spectrometer Bruker Avance III 11.75 T. The theoretical calculations were performed using the Gaussian 03 program. The lower energy structures were obtained by the optimization at MP2/cc-pVDZ, and the magnetic properties ( $\delta$ ) were calculated with the method GIAO, using the B3LYP/cc-pVTZ model. All the calculations were done with and without solvent's effect ( $\text{H}_2\text{O}$  – PCM model).

Comparing the theoretical and the experimental data of  $^{13}\text{C}$  NMR, we can observe that there was no great variation in coefficient of linear correlation ( $R = 0.99$ ), either with or without the consideration of the solvent's effect. This fact can be justified due these  $^{13}\text{C}$  nuclei are located more internally in the molecule. As for the  $^1\text{H}$  nuclei, the inclusion of the solvent's effect in the calculations provided a better corroboration between the theoretical and experimental data, what can be verified by the value of the linear correlation coefficient ( $R = 0.98$ ) and because the solvent's effect leads to lower values of mean and standard deviations. It was not observed discrepancies between the theoretical and experimental assignments. So, theoretical calculations provided to be an excellent tool for unequivocal assignment of all the  $^1\text{H}$  and  $^{13}\text{C}$  NMR signal of the Tamiflu drug.

#### TH105: $^1\text{H}$ NMR Spectroscopy used as an Analytical Technique for Gasoline

<sup>1</sup>Vinicius S. Pinto, <sup>1</sup>\*Francisco F. Gambarra-Neto, <sup>2</sup>Marcos Roberto Monteiro, <sup>1</sup>Luciano Morais Lião

<sup>1</sup>Universidade Federal de Goiás, Instituto de Química, Laboratório de RMN, <sup>2</sup>Universidade Federal de São Carlos, DEMA, CCDDM, Laboratório de Combustíveis

The development of instrumentation in Nuclear Magnetic Resonance (NMR) has increased the sensitivity of the technique, allowing the analyses of samples in micro and nanogram scales. The new technologies enable the NMR technique to be applied as an analytical tool for the quantification of the substances in different organic matrices. A commercial gasoline is composed by alkanes (paraffin), cycloalkanes (naphthenic), alkenes (olefin), aromatic and may additionally contain oxygenates. These information appears in the <sup>1</sup>H NMR spectrum, which was separated in 0.46 to 3.21, 2.49 to 5.93, and 6.25 to 8.34 ppm regions for the construction of Partial Least Squares (PLS) calibration models. The Brazilian gasoline control quality is based on various physicochemical parameters such as amounts of xylene, toluene, distillation temperature for 50% and 90% (T50 and T90), saturated, olefins and aromatic compounds, ethanol (ETOH), methyl tert-butyl ether (MTBE), compounds of oxygen, tert-amyl methyl ether (TAME) and diisopropyl ether (DIPE) calculated by laboratories accredited by National Petroleum Agency (ANP). In this work these parameters for 11 gasoline samples were calculated through <sup>1</sup>H NMR spectroscopy combined with quantitative chemometrics, and presented an R2 value of 0.98, 0.98, 0.99, 0.99, 0.99, 0.98, 0.98, 0.98, 0.96, 0.97, 0.94, 0.97, respectively, in PLS full cross-validation model. Therefore, these high R2 values demonstrated that <sup>1</sup>H NMR and PLS provided quantitative and alternative tools for gasoline analyses. This is something absolutely new for the quality control of Brazilian gasoline.

ACKNOWLEDGEMENTS: CNPq, CAPES, UFG, FUNAPE, CCDDM/DEMA/UFSCar

#### MO106: Uses of Steady-State Free Precession pulse sequences with phase alternation and phase increment for fast high resolution NMR acquisition

<sup>1,2</sup>Tiago Bueno de Moraes, <sup>2</sup>\*Luiz Alberto Colnago

<sup>1</sup>University of São Paulo, <sup>2</sup>Embrapa Instrumentação

Steady State Free Precession (SSFP) sequences have been used to enhance signal to noise ratio in high resolution NMR spectrum but it introduces severe phase and amplitude anomalies. These distortions are essentially caused by the truncation of the signal and the strong interaction between the free induction decay (FID) and echo component.

Problems involving the use of SSFP in high-resolution applications were observed by Ernest and Anderson, Freeman and Hill and Schwenk. In the 1970s some new methods were proposed to overcome this limitation, like the Scrambled Steady-State (SSS) and Quadriga Fourier Transform (QFT) methods, but none have been able to completely overcome the limitations. Recently new methodologies in Steady State pulse sequences are being proposed for fast acquisition in low resolution and for rapid imaging in MRI. Similarly, we are proposing SSFP sequences with phase alternation and phase increment for fast acquisition in high resolution NMR.

A theoretical treatment of the steady state was already presented in the literature, but for SSFP sequences with phase alternation and phase increment the magnetization behavior is not well described. To understanding the effect of the phase alternation and phase increment in SSFP signals we have been performing numerical simulations using Bloch equations.

The <sup>1</sup>H and <sup>13</sup>C experiments have been performed in an Inova 400 Varian spectrometer (9.4 T). Results show that it is possible to enhance S/N using SSFP with phase alternation, reducing the echo component and signal suppression. These techniques widens the band spacing acquired resulting in better spectra, however still have some modulation in the signal magnitude.

**Acknowledgments**

This work is supported by FAPESP (Proc. 2011/11160-3).

#### TU107: <sup>1</sup>H NMR spectroscopy and SIMCA model for classification of common and premium gasolines

<sup>1</sup>\*Vinícius S. Pinto, <sup>1</sup>Francisco F. Gamarra-Neto, <sup>2</sup>Marcos Roberto Monteiro, <sup>1</sup>Luciano Morais Lião

<sup>1</sup>Universidade Federal de Goiás, <sup>2</sup>Centro de Caracterização e Desenvolvimento de Materiais – CCDDM, DEMA, Universidade Federal de São Carlos

The NMR spectroscopy has been used as a powerful analytical tool for fuel analysis due to its versatility and low time for spectrum acquisition. Several examples of fuel quality control performed by NMR and chemometric treatment are found in literature. In Brazil, automotive gasoline is commercialized as common gasoline (CG), additived gasoline (AG) and premium gasoline (PG), with different prices. The difference between CG and PG lies in the octane number, a parameter for quality control required by National Agency of Petroleum, Natural Gas and Biofuels - ANP. The <sup>1</sup>H NMR spectroscopy associated with Soft Independent Modeling of Class Analogies (SIMCA) was used for classifying samples collected in São Carlos- SP/Brazil region in CG or PG. <sup>1</sup>H NMR spectra of 5 CG and 6 PG samples were analyzed in triplicate. All samples were applied in the development of the prediction model. The SIMCA model identified the regions of paraffinic, aromatic and unsaturated hydrogens as the responsible for distinction between the CG and PG. Individual analysis of each region in SIMCA indicated aromatic hydrogen region as the most important for CG and PG classification. The successful result in SIMCA model was attributed to the difference in octane number of premium and common gasolines. Finally, the results showed the potentiality of <sup>1</sup>H NMR and SIMCA association for gasoline analyses presented in this work.

ACKNOWLEDGEMENTS: CNPq, UFG, FUNAPE and CCDDM/DEMA/UFSCar.

#### TH108: Structural dynamics affect the allergenic potential of Bet v1

<sup>1</sup>Aline Batista, <sup>2</sup>Claudia Asam, <sup>1</sup>Adolfo G. Moraes, <sup>1</sup>Fabio C. L. Almeida, <sup>2</sup>Fatima Ferreira, <sup>2</sup>Michael Wallner, <sup>1</sup>\*Ana Paula Valente

<sup>1</sup>Centro Nacional de Ressonância Magnética Nuclear de Macromoléculas, Instituto de Bioquímica Médica - Universidade Federal do Rio de Janeiro, <sup>2</sup>Christian Doppler Laboratory for Allergy Diagnosis and Therapy, University of Salzburg

Bet v 1 is the major allergen of birch pollen with molecular mass of 17.5 kDa. It is estimated that 100 million people are sensitized to Bet v 1, in Northern American and Western Europe. Bet v 1 secondary structure arrangement is  $\beta$ - $\alpha$ 2- $\beta$ 6- $\alpha$  where seven anti-parallel  $\beta$ -sheet surround a long C-terminal  $\alpha$ -helix. Also, a Y-shaped hydrophobic pocket is present inside the protein. Its biological function is associated with the transport of hydrophobic molecules such as brassinosteroid (plant hormone). In this work we used Na-deoxycholate (Doc) that is structurally similar to plant steroids, in order to analyze the influence of ligand binding on dynamics, conformation and IgE-binding. Recombinant <sup>15</sup>N isotope labeled Bet v 1 was produced in E. coli and purified. We used NMR spectroscopy to probe dynamics aspects using R<sub>1</sub>, R<sub>2</sub> and <sup>1</sup>H-<sup>15</sup>N-NOE for free and bound state. To further understand the free state dynamics we performed <sup>15</sup>N CPMG relaxation dispersion experiments at 800 and 600 MHz. Moreover, we performed experiments to map IgE epitopes in the free and Doc-bound state of Bet v 1 using purified human IgE antibodies from birch pollen allergic patients. Bet v 1 is a dynamic protein with several residues in conformational exchange. The epitopes for three patients were slightly different but several residues are in common. Doc interaction changed slightly the protein conformation and profoundly the dynamics. These changes did not affect the IgE epitope

but there was an increase in antibody affinity. Understanding the structural dynamics of Bet v 1 and its interaction with IgE with or without ligands may help to develop hypoallergic derivatives for immunotherapy and as well as understand the correlation between dynamics of allergens and the forces that drive the allergenicity.

**MO109: Calculation of Average Molecular Descriptions of Heavy Petroleum Hydrocarbons by Combined Analysis by Quantitative  $^{13}\text{C}$  and DEPT-45 NMR Experiments**

<sup>1</sup>\*John C. Edwards, <sup>2</sup>A. Ballard Andrews

<sup>1</sup>Process NMR Associates, Danbury, CT, USA,

<sup>2</sup>Schlumberger-Doll Research, Cambridge, MA, USA

Much debate has centered around the validity and accuracy of NMR measurements to accurately describe the sample chemistry of heavy petroleum materials. Of particular issue has been the calculated size of aromatic ring systems that in general seem to be underestimated in size by NMR methods. This underestimation is principally caused by variance in chemical shift ranges used by researchers to define the aromatic carbon types observed in the  $^{13}\text{C}$  NMR spectrum, in particular the bridgehead aromatic carbons that can be shown to overlap strongly with the protonated aromatic carbons. The ability to discern between bridgehead aromatic carbons and protonated carbons in the 108-129.5 ppm region of the spectrum is key in the derivation of molecular parameters that describe the "molecular average" present in the sample. Utilizing methodologies developed by Pugmire and Solum for the solid-state  $^{13}\text{C}$  NMR analysis of coals and other carbonaceous solids [1], we have developed a new liquid-state  $^{13}\text{C}$  NMR method that allows the relative quantification of overlapping protonated and bridgehead aromatic carbon signals to be determined [2].

The NMR experiments involve the combined analysis of both quantitative  $^{13}\text{C}$  single pulse excitation which observes all carbons quantitatively, and a DEPT45 polarization transfer which observes only the protonated carbons in the sample. Though the DEPT45 results are not quantitative across all carbon types ( $\text{CH}$ ,  $\text{CH}_2$ , and  $\text{CH}_3$ ) due to polarization transfer differences, the technique is well enough understood that simple multiplication factors allow the relative intensities of the different carbons to be determined. The average ring system sizes derived from these NMR experiments tend to be several ring systems larger than has been calculated in previous studies. In heavy petroleum asphaltenes the average aromatic ring system is 5-7 rings in size which is in agreement with FTICR-MS and fluorescence measurements, rather than the 3-4 rings previously reported.

The results obtained by liquid-state NMR are compared to the carbon-type NMR and molecular parameters derived from the solid-state  $^{13}\text{C}$  analysis of the same samples. A chemometric approach to the derivation of the parameters has been developed so that automated output of the analysis results can be routinely provided by technician level personnel.

Finally, a quantitative  $^{13}\text{C}$  NMR method is described that utilizes internal standards to quantify the amount of carbon in the sample observed in the NMR experiment. This  $^{13}\text{C}$  quantitation yields information on the degree of aggregation in the asphaltene components.

[1] Carbon-13 solid-state NMR of Argonne-premium coals, Mark S. Solum, Ronald J. Pugmire, David M. Grant, *Energy Fuels*, 1989, 3 (2), pp 187–193.

[2] "Comparison of Coal-Derived and Petroleum Asphaltenes by  $^{13}\text{C}$  Nuclear Magnetic Resonance, DEPT, and XRS", A. Ballard Andrews, John C. Edwards, Andrew E. Pomerantz, Oliver C. Mullins, Dennis Nordlund, and Koyo Norinaga, *Energy Fuels*, 2011, 25 (7), pp 3068–3076.

**TU110: Identification and Quantification of Meningococcal Serogroups C and W135 Polysaccharides by NMR**

<sup>1</sup>Ana Paula F. Leal, <sup>1</sup>Milton Neto da Silva, <sup>1</sup>Ivna A. F. B. Silveira, <sup>2</sup>\*Erika Martins de Carvalho

<sup>1</sup>Bio-Manguinhos/FIOCRUZ, <sup>2</sup>Instituto de Tecnologia em Fármacos Far-Manguinhos/FIOCRUZ

Bio-Manguinhos has been, in recent years, the only manufacturer of meningococcal vaccines that are used for the meningococcal disease control. To ensure the effectiveness of these vaccines are verified two determining factors in the quality control: the purity and O-acetyl concentration of polysaccharide. The meningococcal C polysaccharide (PSC) consists of sialic acid while meningococcal W135 polysaccharide (PSW135) consists of sialic acid and galactose. The classic method used in the control of these molecules is the UV-Vis spectroscopy, which requires a large number of manipulations in the sample preparation, negatively impacting the final result of analysis. NMR spectroscopy is capable of minimizing such problem, enabling yet, the reduction in the sample amount and analysis duration. This paper aims the use of  $^1\text{H}$ NMR to identify and quantify PSC and PSW135 using the GARP experiment (qNMR) [1,2].

First, spectra were obtained using standard of sialic acid (NANA) and galactose for selecting the signal to be quantified. The analysis of these spectra showed the signals at > 2.06 and 2.15 ppm regarding to methyl groups hydrogen of -NAc and -Oac, respectively in PSC and 2.09 ppm in PSW135, are suitable for the quantification of NANA; while the signal at > 5.07 ppm is the most suitable for the quantification of galactose in PSW135. The parameters have been optimized for the quantification as a function of the signal-to-noise ratio, and the delay was determined using the inversion-recovery method. The qRMN results showed that both polysaccharides have purity above 80%, similar to that one found in the classical method. The qRMN method was able to determine the identity, purity and degree of O-acetylation of polysaccharides in a single experiment with excellent reproducibility and efficacy. These preliminary results suggest that the methodology would be applied in the quality control of meningococcal polysaccharides.

**Reference**

[1] Jones C. & Lemercinier X. J. *Pharm. Biom. Anal.* 2002, 30, 1233-1247.

[2] Jones, C. J. *Pharm. Biom. Anal.*, 2005, 38, 840-850.

ACKNOWLEDGEMENTS: FARMANGUINHOS, BIOMANGUINHOS

**TH111: Monomer-dimer equilibrium of canecystatin-1 studied by high-resolution NMR**

<sup>1</sup>Ítalo Augusto Cavini, <sup>1</sup>Richard Charles Garratt, <sup>2</sup>Hans Robert Kalbitzer, <sup>1</sup>\*Claudia Elisabeth Munte

<sup>1</sup>Physics Institute of São Carlos, University of São Paulo, Brazil, <sup>2</sup>Institute for Biophysics and Physical Biochemistry, University of Regensburg, Germany

Cystatin superfamily comprises tight and reversibly binding inhibitors of cysteine proteases. They are present in a wide variety of organisms including vertebrates, invertebrates and plants. Plant cystatins, which are named phytocystatins, are distinguished by the absence of disulfide bonds. The best studied phytocystatin, oryzacystatin I from rice (*Oryza sativa*), has its three-dimensional structure solved by high-resolution NMR, showing a monomeric tertiary fold consisting of a five-stranded antiparallel  $\beta$ -sheet wrapped around an  $\alpha$ -helix. The inhibition is caused by action of three structural motifs, including L1 loop, region that connects  $\beta$ -2 and  $\beta$ -3 strands. We recently reported the X-ray structure of canecystatin-1 from *Saccharum officinarum*, that presented a domain-swapped dimeric form, similar to the topology found in other non-plant cystatins like human cystatin C, human

stefin A and B. These domain-swapped structures exhibit the hairpin L1 loop in a  $\beta$ -strand conformation, linking  $\beta$ -2 and  $\beta$ -3 strands and forming the contiguous  $\beta$ -2,3 strand. The dimer is not expected to be active due to the accessibility restriction of L1 loop. Complementing the X-ray studies, our NMR spectra showed the presence of two conformations for canecystatin-1: a low populated monomeric state and a high populated domain-swapped form, coexisting in solution in a slow exchange process.

Our present work aims to explore the physiological relevance of the canecystatin-1 domain-swapped structure by studying its equilibrium with the active monomers in solution. For this, uniformly  $^{15}\text{N}$ -labeled canecystatin-1 samples were produced and a set of  $^1\text{H}$ - $^{15}\text{N}$ -HSQC spectra varying pressure (up to 240 MPa, 303 K) and temperature (278 to 318 K, ambient pressure) were recorded on Bruker 800-MHz and 600-MHz spectrometers. Thermodynamic parameters associated with conformations in fast exchange were obtained and a new intermediate conformation was identified. The equilibrium characterization of this cystatin may be helpful to better understand the action mechanism of this inhibitor.

#### MO112: Use of $^1\text{H}$ NMR to analyze *Leishmania* sp. under different conditions

1,2\***Paulo Falco Cobra**, <sup>3</sup>Matheus Pereira Postigo, <sup>3</sup>Otávio Henrique Thiemann, <sup>2</sup>Luiz Alberto Colnago

<sup>1</sup>Instituto de Química de São Carlos, IQSC/USP, <sup>2</sup>Empresa Brasileira de Pesquisa Agropecuária, EMBRAPA-CNPDIA, <sup>3</sup>Instituto de Física de São Carlos, IFSC/USP

Leishmaniasis is a tropical disease caused by protozoa of the genus *Leishmania*, transmitted by a sand-fly of the genus *Phlebotomus*. It affects mainly Africa and the Americas, manifesting different forms and can lead to skin sores (cutaneous leishmaniasis) or to liver and spleen injuries (visceral leishmaniasis), when it's generally fatal. The World Health Organization (WHO) estimates that approximately 350 million people live in areas under constant risk of contamination, while currently near 12 million are infected and 1.6 million new cases are reported each year. There is still not an effective treatment for leishmaniasis, and the use of pentavalent antimonials, amphotericin B or pentamidines, which are toxic, and the combat to the vector of the disease are the only forms of controlling it. Besides, it is not exactly known how these drugs act in the organism of the parasite.

Metabolomics and Metabonomics are tools of modern Biochemistry widely employed nowadays in the study of metabolism for several organisms and are often associated to analytical chemistry techniques.

In an attempt of better understanding these parasites, and in the future to propose a new treatment for leishmaniasis, this work shows the first metabolic analysis applied to *L. donovani* and *L. major* cultures, under different conditions, including the use of new drug candidates. The resulting metabolomic and metabonomic studies by high-resolution Nuclear Magnetic Resonance (NMR) are providing valuable information about the metabolism of the parasites and how it varies in the presence of a biologically active molecule.

The NMR analyses of *Leishmania* cells and extract shows the main metabolites inside the protozoa cell matrix, when these grow in the appropriate medium. Afterwards, these data will be employed as a comparative basis for a metabonomic evaluation of possible variations in the chemical composition of these organisms.

ACKNOWLEDGEMENTS: FAPESP, CNPq, CAPES

#### TU113: Spectroscopic studies of *Hs*DHODH N-terminal domain: an evaluation of the peptide-membrane interaction

<sup>1</sup>Edson Crusca, <sup>3</sup>Eduardo Festozo Vicente, <sup>2</sup>Antonio José Costa-Filho, <sup>1</sup>Claudia Elisabeth Munte, <sup>3</sup>\*Eduardo Maffut Cilli

<sup>1</sup>Grupo de Biofísica Molecular Sérgio Mascarenhas, Instituto de Física de São Carlos, USP, <sup>2</sup>Laboratório de Física Molecular, Faculdade de Filosofia, USP, <sup>3</sup>Instituto de Química de Araraquara, Universidade Estadual Paulista

Human dihydroorotate dehydrogenase (*Hs*DHODH) catalyzes the fourth and only redox step of the de novo pyrimidine biosynthesis. *Hs*DHODHs are monomeric and membrane-bound proteins and their inhibition represents an important strategy for antineoplastic and antiproliferative drugs. Here we report structural studies of the *Hs*DHODH N-terminal peptide, which is responsible for anchoring the enzyme to the inner mitochondrial membrane and then to allow access to ubiquinones, essential for the enzyme catalysis. Fluorescence studies using Tyr7 residue showed that the peptide interacts with micelles and vesicles and that this residue is located inside the membrane. CD studies indicate that the molecule, when in TFE and model membranes, acquired a high amount of  $\alpha$ -helix. A complete sequence-specific proton resonance assignment of the peptide in the presence of  $d_{38}$ -DPC micelles was performed by means of two-dimensional  $^1\text{H}$ - $^1\text{H}$  NOESY, TOCSY and QDF-COSY analyses. Based on the chemical shift index, two helical segments (Gly1-Gln15 and Pro20-Gly34) separated by a turn were predicted. In addition to the backbone  $\text{H}\alpha$ -HN ( $i,i+1$ ) and HN-HN ( $i,i+1$ ) NOEs, a large number of medium-range NOEs  $\text{H}\alpha$ -HN ( $i,i+3$ )/( $i,i+4$ ) between residues 2-15 and 21-33, a typical pattern of a helical structure, were observed. In both cases, proline residues showed only *trans* conformation, confirmed by strong NOEs between Met11C $\alpha$ H-Pro12C $\delta$ H and Asp19 C $\alpha$ H-Pro20C $\delta$ H. The  $d_{38}$ -DPC induced structure of the peptide is a well defined amphipathic helix (Glu3-Gly16 and Ser22-Ser32) connected by a short loop (Leu17-Glu21) with average backbone and heavy atoms r.m.s.d. of 0.71 and 1.1 Å, respectively. Our findings suggest that the peptide adopts a hairpin-like conformation laid on the membrane, with the hydrophobic face in contact with the acyl chains of the membrane mimetic and the hydrophilic face pointing towards the aqueous surface. These results can open new insights regarding the development of antineoplastic and antiproliferative drugs that could bind to this specific region while anchored to the membrane.

Supported by FAPESP, CNPq and CAPES.

#### TH114: Antimicrobial Peptide Triterpticin (TRP3): Conformational Variability and Membrane Interaction evaluated by NMR

<sup>1</sup>Talita LoSan, <sup>2</sup>\*Shirley Schreier, <sup>1</sup>Fabio C. L. Almeida, <sup>1</sup>Ana Paula Valente

<sup>1</sup>IBqM-UFRJ, <sup>2</sup>IQ- USP

Antimicrobial peptides (AMPs) play a major role in the innate immune system of all living organisms and they are generally thought to kill by disrupting lipid membranes. Due to the increase in antibiotic resistant-organisms, AMPs are being considered as an alternative antimicrobial agent. Triterpticin (TRP3) is a 13 residue antimicrobial peptide, from cathelicidin family, with a high proportion of tryptophan residues. TRP3 is highly selective to bacterial membrane and does not act in mammalian cells. TRP3 does not present a unique conformation in solution and conformational exchange occurs in slow exchange regime that is possible to be detected by 1D- $^1\text{H}$  NMR spectra. Since NMR spectroscopy is capable of not only determination of tertiary structure as well as monitoring movements of chain in diverse timescales, we studied structure and dynamics of peptide TRP3, trying to correlate its conformational variability with its mechanism of action and selectivity. TRP3 structural dynamics was studied in four membrane mimetic systems, lyso-phosphocholine (LPC), dodecylphosphocholine (DPC), n-octyl- $\beta$ -D-glucopyranoside (NOG) and N-dodecyl-N,N-(dimethylammonio)butyrate (DDMAB). The stabilized structure in LPC, NOG and DDMAB was analyzed through 2D- $^1\text{H}$  NMR spectra and compared with stabilized structure in DPC (Schibli and co-workers, 2006). Although TRP3 pre-

sented different interaction pathway in each system, the final structure in all mimetic systems was very similar. Our data show that TRP3 interact through conformation selection with the four kinds of micelles and the final structure is achieved through peptide accommodation.

ACKNOWLEDGEMENTS: FAPERJ, CAPES, and CNPq

#### MO115: Quality control of Beer by NMR concerted with Chemometric Analysis

<sup>1</sup>Camilla do Nascimento Bernardo, <sup>1</sup>Raquel Pantoja Barreiros Rodrigues, <sup>2</sup>Paula Fernandes de Aguiar, <sup>1\*</sup>Jochen Junker

<sup>1</sup>Fundação Oswaldo Cruz - CDTS, <sup>2</sup>IQ, UFRJ

Beer is fermented beverage produced from malted grains, hops, yeast, and water. Over 800 compounds constitute beer, and numerous of them give taste. The major groups of compounds are carbohydrates, prenylflavonoids, amino acids, amines among other inorganic and organic compounds. Beer is the main dietary source of xanthohumol and prenylflavonoids. Xanthohumol and other prenylated flavonoids from hops bring positive effects to health: flavonoids are natural antioxidants; weak estrogenic activity was observed in hops and xanthohumol is a potent cancer chemo preventive agent.

Beer composition can be correlated to origin and quality. Compounds related to flavor and aroma usually are identified by sensorial analysis. Identification and quantitative analysis of substances in beers is done by various techniques, such as HPLC/Electrospray mass spectrometry, NMR spectroscopy, MALDI-TOF mass spectrometry and others.

High resolution NMR spectroscopy technique has been developed to aim at a rapid identification of the nature and origin of the beer sample, outside recognition aromatic compounds, carbohydrates, amino acids and others. <sup>1</sup>H NMR spectroscopy is an efficient method used to discriminate orange and grapefruits juices and to prevent of frauds.

Quality control of beers by NMR methods concerted with chemometric analysis has been studied. The combination of spectroscopy and Principal Components Analysis provide information about compositional properties like authenticity, quality and origin. Furthermore, spectroscopic quantification of peaks on spectra gives quantitative information of compounds of sample.

#### TU116: A Metabolomic Assessment of the In Vitro Skin Permeation Method

<sup>2</sup>Ana Paula Azambuja, <sup>2</sup>Julia Menegola, <sup>1</sup>Rafael Renatino Canevarolo, <sup>1\*</sup>Ana Carolina de Mattos Zeri

<sup>1</sup>Brazilian Biosciences National Laboratory, <sup>2</sup>Natura

The *in vitro* skin permeation approach is considered a classical tool in the development and improvement of topically applied pharmaceuticals and cosmetics. Besides its wide employment as predictive of *in vivo* absorption for safety and formulation quality control purposes, skin permeation tests are mainly applied as a barrier test, where no biological activity is assessed. Aiming at the establishment of a model to evaluate the metabolic profile and probe skin conditions during the permeation studies, we optimized the classical method for *in vitro* skin absorption. Here we depict that, either under control conditions or after treatment with a cosmetic formulation, pig ear skin samples mounted on Franz diffusion cells, with Dulbecco's Modified Eagle Medium (DMEM) as receptor fluid, can sustain metabolic activity as described by the identification of biomarkers from the respiratory, amino acid, and nucleic acid metabolism. Metabolomics studies were performed assessing receptor fluid samples from 0, 2, 4, 10 and 24 hours of *in vitro* permeation employing Nuclear Magnetic Resonance spectroscopy (NMR) at 600MHz, and evaluating the data using Chenomx NMR Suite (7.5 version; Chenomx Inc., Edmonton, Canada) for targeted profiling analysis, and

MetaboAnalyst (metaboanalyst.ca) for principal component analysis (PCA). Since NMR allows the direct evaluation of liquid, solid and semi-solid samples without sample destruction or extensive preparation or extraction steps, it can be applied as a strong and practical tool for complex mixtures studies. In our experiments, this technology displayed robust sensibility for the identification and quantification of skin metabolites and formulation compounds over time. Therefore, here we describe that the combination of a skin permeation approach designed for the biological activity maintenance, with a robust detection technique, can be a powerful tool for evaluation of compound absorption associated with skin health and drug metabolism assessment. We also believe that the evolution of similar approaches, employing human skin samples and combined detection systems, can improve efficacy and safety studies for cosmetic and pharmaceutical development.

[1] Xia, J., Mandal, R., Sinelnikov, I., Broadhurst, D., and Wishart, D.S. (2012). Nucl. Acids Res. first published online May 2, 2012.

[2] Xia, J., Psychogios, N., Young, N. and Wishart, D.S. (2009). Nucl. Acids Res. 37, W652-660.)

#### TH117: <sup>51</sup>V NMR in solution of substituted Keggin ion [α-SiV<sub>2</sub>W<sub>10</sub>O<sub>40</sub>]<sup>6-</sup>

\*Rodrigo de Paiva Floro Bonfim, Luiza Cristina de Moura, Jean Guillaume Eon

Universidade Federal do Rio de Janeiro

Heteropolianions are oxides of transition metals which have a high versatility in composition and properties. The heteropolianions substituted Keggin has the general formula [XM'<sub>y</sub>M<sub>12-y</sub>O<sub>40</sub>]<sup>x-</sup> where X = P and Si, M = Mo and W, M' = transition metal and y = 1, 2 and 3. These ions are synthesized from species lacunar [XM<sub>11</sub>O<sub>39</sub>]<sup>n-</sup>, [XM<sub>10</sub>O<sub>36</sub>]<sup>n-</sup> and [XM<sub>9</sub>O<sub>34</sub>]<sup>n-</sup> or [α-SiW<sub>12</sub>O<sub>40</sub>]<sup>4-</sup>. The obtaining of mixed Keggin ions is hampered by the complexity and stability of compounds can be formed. The pH is a determining factor for the formation of these compounds in aqueous solution. In this work the synthesis of Keggin ions [α-SiV<sub>2</sub>W<sub>10</sub>O<sub>40</sub>]<sup>6-</sup> were accompanied by <sup>51</sup>V NMR in solution. We used the Keggin lacunar [α-SiW<sub>11</sub>O<sub>39</sub>]<sup>7-</sup> and [α-SiW<sub>9</sub>O<sub>34</sub>]<sup>10-</sup> as precursors and pH between 5.5 and 8.0. All syntheses were performed following the methodology in which the pH of the reactional medium is kept constant.

The <sup>51</sup>V NMR spectra in solution of the Keggin ion [α-SiV<sub>2</sub>W<sub>10</sub>O<sub>40</sub>]<sup>6-</sup> were obtained from aliquots of the reaction medium and the products crystallized. The spectra of the products obtained from lacunar [α-SiW<sub>11</sub>O<sub>39</sub>]<sup>7-</sup> showed three peaks at -519.9 ppm, -545.8 ppm and -549.6 ppm. The peak at -545.8 ppm is more intense at pH 6.5. The peak at -549.6 ppm can be attributed to the mono-substituted Keggin [α-SiVW<sub>11</sub>O<sub>40</sub>]<sup>5-</sup>. The spectra of the solutions of the crystals obtained in pH 6.5 from lacunar [α-SiW<sub>11</sub>O<sub>39</sub>]<sup>7-</sup> and [α-SiW<sub>9</sub>O<sub>34</sub>]<sup>10-</sup> showed an intense peak at -544.8 ppm indicating the formation of the Keggin ion [α-SiV<sub>2</sub>W<sub>10</sub>O<sub>40</sub>]<sup>6-</sup>. The diffractograms and infrared show the formation of a single product and confirms the results of NMR <sup>51</sup>V.

ACKNOWLEDGEMENTS: CAPES, CNPq

#### NMR of Membrane Proteins

#### MO118: Solid state NMR studies of membrane proteins

<sup>1\*</sup>Vladimir Ladizhansky, <sup>1</sup>Shenlin Wang, <sup>1</sup>Sanaz Emami, <sup>1</sup>Rachel Munro, <sup>2</sup>Lichi Shi, <sup>1</sup>Ying Fan, <sup>3</sup>Izuru Kawamura, <sup>1</sup>Leonid Brown

<sup>1</sup>University of Guelph, <sup>2</sup>University of Toronto, <sup>3</sup>Yokohama National University

Magic angle spinning (MAS) solid-state NMR shows great



potential for studying structure and dynamics of membrane proteins, which are not readily amenable to X-ray crystallography and solution NMR. In this presentation we will describe the latest developments in our group, including advances in sample preparation procedures for obtaining MAS spectra with optimal spectral sensitivity, experimental strategies for obtaining spectroscopic assignments, methods for measuring long-range structural restraints for the determination of high resolution structure and supramolecular organization of membrane proteins in the lipid environment. We will present high-resolution structure of a seven-helical photoreceptor Anabaena Sensory Rhodopsin, and discuss progress towards structural characterization of a eukaryotic membrane protein human Aquaporin 1.

#### TU119: Structural determinants and functional aspects of specific lipid binding to potassium channels as seen by coarse grained MD and solid state NMR

<sup>1</sup>\*Markus Weingarth, <sup>1,2</sup>Alexander Prokofyev, <sup>1</sup>Elwin A. W. van der Cruisen, <sup>1</sup>Deepak Nand, <sup>1</sup>Alexandre M. J. J. Bonvin, <sup>2</sup>Olaf Pongs, <sup>1</sup>Marc Baldus

<sup>1</sup>Bijvoet Center for Biomolecular Research, Utrecht University, <sup>2</sup>Saarland University, Faculty of Medicine, Department of Physiology

CGMD simulations overcome the typical length- and timescale limits of atomistic simulations, which greatly enhances the potential to compare computational observations to powerful experimental techniques like confocal microscopy or solid state NMR.

Here we have investigated specific lipid binding to the pore domain of potassium channels KcsA and KcsA-Kv1.3 on the structural and functional level using coarse-grained and atomistic MD simulations, solid state NMR and single channel conductance measurements. We show that while KcsA activity is critically modulated by the specific and cooperative binding of anionic non-annular lipids close to the channel's selectivity filter, the influence of non-annular lipid binding on KcsA-Kv1.3 is much reduced. These findings provided the basis to deduce a molecular mechanism of lipid modulated activity in KcsA [1].

[1] Markus Weingarth, Alexander Prokofyev, Elwin A. W. van der Cruisen, Deepak Nand, Alexandre M. J. J. Bonvin, Olaf Pongs, and Marc Baldus, *J. Am. Chem. Soc.*, 2013, 135 (10), pp 3983–3988.

#### TH120: NMR Structural Characterization of Membrane Proteins in a Lipid Environment

<sup>1,2</sup>Rasmus Linser, <sup>1</sup>Franz Hagn, <sup>1</sup>Thomas Raschle, <sup>1</sup>\*Gerhard Wagner

<sup>1</sup>Harvard University, Biol. Chem. and Mol. Pharm., <sup>2</sup>University of New South Wales, Sydney

Membrane proteins are naturally constituted into a lipid bilayer environment. This setting is decisive for the function of the majority of such proteins. For most structural biology techniques, however, it poses major hurdles. Besides approaches using, e.g., cubic lipid phases in crystallography, techniques potentially amenable to membrane-integral biopolymers are solid-state and solution-state NMR. A milestone for a native setting of membrane proteins is the nanodisc concept,[1] which we could use successfully for NMR structural characterization recently.[2] We employ this technique to gain a functional understanding of different membrane proteins. One target presented is a membrane anchor domain of a transcriptional activator precursor protein that is immanent for regular cell physiology and has been found to be associated to cancer, a second one is an alpha-helical pore protein.

We will show NMR data for the two proteins in both settings and discuss differences of nanodisc embedding with respect to detergent micelle reconstitution.

[1] Denisov et al. (2004), *J. Am. Chem. Soc.*, 126, p. 3477.

[2] Hagn et al. (2013), *J. Am. Chem. Soc.*, 135, p. 1919.

### NMR of Nucleic Acids

#### MO121: Investigation of RNA-small molecule interactions by NMR spectroscopy

<sup>1</sup>\*Romana Spitzer, <sup>2</sup>Roland Huber, <sup>1</sup>Christoph Wunderlich, <sup>2</sup>Klaus Liedl, <sup>1</sup>Christoph Kreutz

<sup>1</sup>University of Innsbruck, Institute of Organic Chemistry, <sup>2</sup>University of Innsbruck, Institute of Inorganic and Theoretical Chemistry

The starting point of the presented research was a recently published X-ray crystal structure of the cyclic di guanosine monophosphate (c-di-GMP) class I riboswitch aptamer in complex with its cognate ligand c-di-GMP. [1,2]

Riboswitches are RNA sequences that are capable to respond to the concentration level of a metabolite and subsequently regulate gene expression by binding of the metabolite.[3-5]

During this gene regulation process two very interesting properties of RNA sequences are highlighted, namely the ability to recognize binding partners (small molecules up to large proteins) with high affinity and selectivity and secondly, RNAs have the intrinsic propensity to undergo large scale structural rearrangements triggered by a specific event (e.g. binding of a ligand or addition of a complementary sequence partition).

Based on the molecular details of ligand recognition we rationally designed a ligand, cyclic iso-cytidine-guanosine monophosphate (c-iCG), which binds with even higher affinity than the native one and under preservation of specificity. In the first step we confirmed the binding properties of c-iCG by an *in silico* approach using molecular dynamics (MD) simulations. We then set out for the experimental validation by NMR spectroscopy of the results obtained from the computational methods.

[1] N Kulshina, NJ Baird, AR Ferré-D'Amaré, *Nat. Struct. Mol. Biol.* 2009, 16 (12), 1212-7.

[2] KD Smith, SV Lipchok, TD Ames, J Wang, RR Breaker, *Nat. Struct. Mol. Biol.* 2009, 16, 1218 - 1223

[3] RK Montagne, RT Batey, *Annu. Rev. Biophys.* 2008, 37, 117-33.

[4] M Mandal, RR Breaker, *Nat. Rev. Mol. Cell Biol.* 2004, 5, 451-63.

[5] KF Blount, RR Breaker, *Nat. Biotechnol.* 2006, 24 (12), 1558-64.

#### TU122: New Tagging Strategies for DNA-Strands of Modified Nucleobases and Cys-Ph-TAHA tag

Sebastian Täubert, Florian Siepel, Andrei Leonov, \*Christian Griesinger

Max Planck Institute

Paramagnetic tagging of proteins introduces paramagnetic parameters such as residual dipolar couplings, pseudocontact shifts and paramagnetic relaxation into otherwise diamagnetic proteins. From those information on structure and dynamics of domains and within domains can be derived. For proteins several tags are known in literature with a wide range of different properties. However, there are neither convenient tags nor accessible binding sites for oligonucleotides which we address in this contribution.

Here we introduce two modified nucleobases to provide an exposed thiol moiety for tagging reactions via a disulfide formation. These nucleobases are synthesized within six steps and can be introduced into oligonucleotides easily by chemical synthesis. The yields during the DNA synthesis are nearly the same as for unmodified nucleobases. The first version

of the modified nucleobase contains a cyanoethyl protected sulfur-atom. The protection group is removed after the DNA synthesis. The second version provides a terminal acetylene moiety where the sulfur-atom is introduced via a copper catalyzed click-reaction after the DNA synthesis. We used the Cys-Ph-TAHA tag developed in our department to test the new approach. The preloaded tag was incubated with the DNA and subsequent HPLC purification leads to the tagged DNA quantitatively.

Furthermore, we synthesized a new paramagnetic tag based on the Ph-TAHA construct which will be attached to phosphorothioate DNA.

After the tagging protocol was successfully established with the diamagnetic species NMR spectra will be shown for a self-complementary DNA strand of 24 nucleobases and Cys-Ph-TAHA tag with various paramagnetic lanthanides. The prospect of characterizing DNA and RNA dynamics with this approach will be discussed.

### TH123: Conformational capture mechanism of the neomycin B riboswitch

Christoph Wunderlich, \*Christoph Kreutz

University Innsbruck

The goal of the presented project is the characterization of a low populated state of a gene-regulative RNA sequence, namely an artificial riboswitch responsive to neomycin B. For that purpose we apply a multi-disciplinary approach using the chemical synthesis of  $^{13}\text{C}$ -modified building blocks and state-of-the-art solution NMR spectroscopy. In a favourable case we will be able to determine the population of the excited state (i.e. thermodynamic), the exchange rates from the ground to the excited state and for the backward reaction (i.e. kinetics), and also information on the structure of the excited state (i.e. chemical shift) using CPMG (Carr-Purcell-Meiboom-Gill) relaxation dispersion NMR spectroscopy. The excited state of the artificially designed neomycin B riboswitch will be compared to the ligand bound state. Using the proposed approach we will be able to differentiate between various ligand-host recognition modes. This will deepen the understanding of RNA and its way to interact with ligands allowing the design of high-affinity binder with applications in the field of drug development.

## Molecular Dynamics by NMR

### MO124: Conformational Dynamics of the Partially Disordered Yeast Transcription Factor GCN4 from Molecular Dynamics Simulations and NMR

\*Paul Robustelli, Nikola Trbovic, Arthur G. Palmer III

Columbia University

We have employed molecular dynamics (MD) simulations to study the conformational dynamics of the partially disordered yeast transcription factor GCN4. We demonstrate that a detailed analysis of back-calculated NMR chemical shifts and spin-relaxation data provide complementary probes of the structure and dynamics of partially disordered protein states and enable comparisons of the accuracy of multiple MD trajectories. Back-calculated chemical shifts provide a sensitive probe of the populations of residual secondary structure elements while spin-relaxation calculations are sensitive to a combination of structural factors including the stability of local secondary structure elements, the presence of tertiary contacts, and the presence of residual structure in more distal regions of the protein. We demonstrate that an analysis of back calculated chemical shift and spin-relaxation data can be used to evaluate the populations of specific interactions in disordered states and identify regions of the phase space that are inconsistent with experimental measurements. Our analyses suggest that GCN4 recognizes DNA with a pre-

formed helical binding interface via conformational selection and subsequently completes folding upon binding.

### TU125: Study of Brazilian Asphaltene Agregation by Nuclear Magnetic Resonance Spectroscopy

<sup>1</sup>\*Emanuele Catarina da Silva Oliveira, <sup>1</sup>Alvaro Cunha Neto, <sup>1</sup>Valdemar Lacerda Júnior, <sup>1</sup>Eustáquio Vinícius Ribeiro de Castro, <sup>2</sup>Sonia Maria Cabral de Menezes

<sup>1</sup>Universidade Federal do Espírito Santo, <sup>2</sup>Centro de Pesquisas e Desenvolvimento Leopoldo Américo Miguez de Mello (Cenpes – Petrobras/RJ)

Heavy crude oils have attracted a growing interest from oil industries around the world. In this scenario, asphaltenes, which are molecules known for their low reactivity and high molecular weight, have received special attention in recent decades, due to the problems they cause during oil processing. In an effort to minimize these problems, researchers have increasingly looked for a better understanding of aspects such as molecular structure, stability and physicochemical properties of asphaltenes, as well as for the development of methods to prevent their unwanted precipitation. In recent decades, nuclear magnetic resonance (NMR) has been widely used as a tool for the study of petroleum and its derivatives. The analysis of NMR spectra allows the direct determination of a series of structural parameters such as the fractions of aromatic carbons. Diffusion-ordered NMR spectroscopy (DOSY) is a new developed NMR technique highly useful for the elucidation of complex mixtures. This work sought to identify the differences in average parameters of asphaltenes from national crudes and to correlate them with the physicochemical properties of the asphaltene and of the original crude. The aim was also to investigate and to compare the asphaltenes among themselves, using data such as diffusion coefficient, concentration of these compounds in the oil and state of aggregation. Extraction and quantification of the amount of asphaltenes were performed using ASTM 6560-00 standard and the characterization was performed using the following analytical techniques: elemental analysis,  $^1\text{H}$  and  $^{13}\text{C}$  NMR and DOSY. Significant changes were observed in almost all studied parameters. To study the asphaltene aggregation behavior using DOSY, the asphaltenes were diluted in various concentrations of deuterated toluene and the DOSY spectra were correlated with their respective states of aggregation. The diffusion properties were highly dependent on the concentration and type of oil from which the asphaltene was extracted.

### TH126: Novel intramolecular dynamics within the N-Cap-SH3-SH2 regulatory unit of the c-Abl tyrosine kinase reveal targeting to the cellular membrane

<sup>1</sup>Guilherme A. P. de Oliveira, <sup>1</sup>Elen G. Pereira, <sup>1</sup>Giulia D. S. Ferretti, <sup>1</sup>Ana Paula Valente, <sup>2</sup>Yraima Cordeiro, <sup>1</sup>\*Jerson L. Silva

<sup>1</sup>Programa de Biologia Estrutural, Instituto de Bioquímica Médica, Instituto Nacional de Biologia, <sup>2</sup>Faculdade de Farmácia, Universidade Federal do Rio de Janeiro, Rio de Janeiro, Brazil.

c-Abl is a key regulator of cell signaling and is under strict control via intramolecular interactions. In this study, we address changes in the intramolecular dynamics coupling within the c-Abl regulatory unit by presenting its N-terminal segment (N-Cap) with an alternative function in the cell as c-Abl becomes activated. Using small angle X-ray scattering, nuclear spin relaxation experiments and confocal microscopy, we demonstrate that the N-Cap and the Src homology (SH) 3 domains acquire  $\mu\text{s}$ -ms motions upon N-Cap association with the SH2-L domain, revealing a stabilizing synergy between these segments. The N-Cap-myristoyl tether likely triggers the protein to anchor to the membrane because of this flip-flop dynamic, which occurs in the  $\mu\text{s}$ -ms time range. Chemical shift perturbation ( $\delta\delta$ ) analyses of  $^1\text{H}$ - $^{15}\text{N}$  by nuclear magnetic resonance (NMR) HSQC spectra were carried

out to map critical moieties that are affected by intramolecular interactions within the regulatory unit. The N-Cap segment not only presents the myristate during c-Abl inhibition but may also trigger protein localization inside the cell in a functional and stability-dependent mechanism that is lost in Bcr-Abl+ cells, which underlie chronic myeloid leukemia.

#### MO127: Analysis of the Pirouetting Motion in [2]Rotaxanes by Dynamic $^1\text{H}$ NMR

<sup>1</sup>Clarissa Piccinin Frizzo, <sup>1\*</sup>Lilian Buriol, <sup>1</sup>Letícia V. Rodrigues, <sup>1</sup>Marcos A. P. Martins, <sup>2</sup>José Berná, <sup>2</sup>Mateo Alajarín

<sup>1</sup>Federal University of Santa Maria, <sup>2</sup>Universidad de Murcia

Due to their characteristic of controlling motion, mechanically-interlocked molecules like [2]rotaxanes have received much scientific interest over the last decade, especially in the development of biological machines [1,2]. The [2]rotaxanes interlinked by benzylic amide macrocycles have shown chair-chair co-conformational changes, where methylene hydrogens present in the pseudoaxial position change to the pseudoequatorial position and vice versa. The molecular dynamics of this rotation may be accomplished by the coalescence method using  $^1\text{H}$  NMR experiments in solution [3]. Given this context, our aim in this work is to demonstrate the effect that different stoppers, such as *i*-butyl (1) and butyl (2) substituents attached at succinamide template in the pirouetting motion of the benzylic amide macrocycle around a thread, by using a dynamic  $^1\text{H}$  NMR study in solution. Thus, through  $^1\text{H}$  NMR experiments in DCM-*d*2 as part of the coalescence method we measured the energy barriers for the rotation of the macrocycle around the two different threads. The calculated energy barriers for the macrocycle pirouetting process were: 12.90 kcal.mol<sup>-1</sup> at 293 K for [2]rotaxane (1), and 13.39 kcal.mol<sup>-1</sup> at 303 K for [2]rotaxane (2). The different energy barrier values between the two [2]Rotaxanes are attributed to structural changes in the stoppers of the thread. The pirouetting submolecular motion of these interlocked molecules can be correlated with CH••• $\pi$  interactions between the thread stoppers and the benzylic amide macrocycles and other hydrogen-bonded molecules observed in [2]rotaxane (1).

#### References:

- [1] Stoddart, J. F. Chem. Soc. Rev. 2009, 38, 1802.
- [2] Kay, E. R.; Leigh, D. A.; Zerbetto F. Angew. Chem. Int. Ed. 2007, 46, 72.
- [3] Berná, J.; Alajarín, M.; Martínez-Espín, J. S.; Buriol, L.; Martins, M. A. P.; Orenes, R.-A. Chem. Commun. 2012, 48, 5677.

#### Acknowledgements:

This work was supported by the MICINN (Project CTQ2009-12216/BQU) and the Fundación Séneca-CARM (Project 08661/PI/08). José Berná thanks the MICINN for the Ramón y Cajal contract (RYC-2008-02647) which was co-financed by the European Social Fund. Thanks for financial support is also acknowledged by Lilian Buriol and Letícia V. Rodrigues (to CAPES), by Marcos A. P. Martins (to CNPq), and by C.P. Frizzo (to FAPERGS).

#### TU128: GUARDD: User-friendly MATLAB software for rigorous analysis of CPMG RD NMR data

Ian R. Kleckner, \*Mark P. Foster

Ohio State University

For the past fifteen years, the Carr-Purcell Meiboom-Gill relaxation dispersion (CPMG RD) NMR experiment has afforded advanced NMR labs access to kinetic, thermodynamic, and structural details of protein and RNA dynamics in the crucial  $\mu\text{s}$ -ms time window. However, analysis of RD data is challenging because datasets are often large and require many non-linear fitting parameters, thereby confounding as-

essment of accuracy. Moreover, novice CPMG experimentalists face an additional barrier because current software options lack an intuitive user interface and extensive documentation. Hence, we present the open-source software package GUARDD (Graphical User-friendly Analysis of Relaxation Dispersion Data), which is designed to organize, automate, and enhance the analytical procedures which operate on CPMG RD data (<http://code.google.com/p/guardd/>). This MATLAB-based program includes a graphical user interface, permits global fitting to multi-field, multi-temperature, multi-coherence data, and implements  $\chi^2$ -mapping procedures, via grid-search and Monte Carlo methods, to enhance and assess fitting accuracy. The presentation features allow users to seamlessly traverse the large amount of results, and the RD simulator feature can help design future experiments as well as serve as a teaching tool for those unfamiliar with RD phenomena. Based on these innovative features, we expect that GUARDD will fill a well-defined gap in service of the RD NMR community.

#### TH129: Inter-domain motions of calmodulin from NMR chemical shifts and MD simulations

\*Predrag Kukic, Carlo Camilloni, Michele Vendruscolo

Cambridge University, UK

Around 80% of all proteins in eukaryotes consist of multiple domains that are connected by flexible linkers. Although the multi-domain proteins are involved in a range of important biological processes, detailed knowledge of their structure and dynamics requires extensive experimental characterization. Here, we study the possibility of using the informational content encoded in the most readily and accurately measured NMR observables, such as chemical shifts, to characterize inter-domain motions in proteins. For this purpose, we use chemical shifts measured for the flexible linker of calmodulin in its calcium-bound state ( $\text{Ca}^{2+}$ -CaM) and chemical shifts measured for its two domains. Using cross-validation analysis of the reference ensemble, we firstly demonstrate the ability of chemical shifts implemented in replica-exchanged molecular dynamics simulations to reproduce the inter-domain motion of  $\text{Ca}^{2+}$ -CaM by accurately reproducing the dynamics of its flexible linker. We then use the same procedure with experimentally measured chemical shifts of  $\text{Ca}^{2+}$ -CaM and determine an ensemble of conformations that represents the free-energy surface of  $\text{Ca}^{2+}$ -CaM in the solution. The ensemble is validated against the previously obtained ensemble of  $\text{Ca}^{2+}$ -CaM determined from RDC and SAXS measurements. The results confirm the dominance of  $\text{Ca}^{2+}$ -CaM conformations with both hydrophobic patches oriented towards opposite sides with respect to the central helix. In these conformations, hydrophobic patches of N- and C-terminal domains of  $\text{Ca}^{2+}$ -CaM are highly exposed to the solution and fully accessible to their target proteins.

#### MO130: Refinement of protein conformational ensembles using methyl chemical shifts

Arvind Kannan, Carlo Camilloni, Aleksandr Sahakyan, Andrea Cavalli, Juuso Lehtivarjo, \*Michele Vendruscolo

Cambridge University

The last decade has sparked considerable interest in the development of methods for protein structure determination using only the information encoded in NMR chemical shifts. Chemical shifts are the NMR observables that can be measured under the widest range of conditions and with the greatest accuracy. These parameters are often the only structural data that can be obtained for large protein complexes, making them an invaluable experimental tool for probing the structure and dynamics of these systems. Recent work has resulted in methods for predicting the dihedral angles and secondary structure populations of amino acids from their chemical shifts. Moreover, it is now known that the accuracy of structure-based chemical shift predictions improves dramatically when the calculations are averaged over ensembles

of protein conformations, suggesting that chemical shift data can be used to generate accurate structural ensembles that reflect the true dynamics of proteins in solution. We have recently established the feasibility of this approach by implementing chemical shifts for backbone atoms as structural restraints in replica-averaged molecular dynamics simulations, in analogy to previous work with other NMR observables. In this study we demonstrate that the same methodology can also be applied to methyl proton shifts, leading to further refinement of the resulting structural ensembles and improved agreement with the experimental data. In order to validate this approach, we have run a series of simulations of four model proteins - the autophagy related protein Atg8, a BMP receptor, the DNA-bending HU dimer, and the GPCR regulator RGS10 - involving (1) no restraints, (2) restraints using only the backbone shifts, (3) restraints using only the methyl shifts, and (4) both sets of restraints. Our results indicate that methyl chemical shifts can provide complementary structural information to that obtained from backbone data, and that this complementarity induces global improvements in the accuracy of free energy landscapes computed from ensembles 3 and 4.

#### TU131: NMR Analyses of the Keto-Enol Equilibrium of Avobenzene Type UVA Photoabsorbers

<sup>1</sup>Patrícia Coelho Nascimento, <sup>2,3</sup>Vinícius Soares da Paixão Correia, <sup>2,3</sup>Luiz Antônio Soares Romeiro, <sup>1\*</sup>Edilberto Rocha Silveira

<sup>1</sup>Universidade Federal do Ceará, <sup>2</sup>Universidade Católica de Brasília, <sup>3</sup>Universidade de Brasília

Avobezone [1-(4-methoxyphenyl)-3-(4'-tert-butylphenyl)-propane-1,3-dione] is a photoabsorber of UVA type radiation (320-400 nm). It is present in almost all commercially available sunblockers, where it also works to prevent skin age development. However, avobenzene has low photostability. This has motivated the syntheses of avobenzene analogs as a lead to more stable UVA absorbers. The keto-enol tautomerization of dibenzoylmethanones seems to be associated with their activity, thus NMR raised as a suitable method to analyse this behavior. Either a 300 MHz DPX or a 500 MHz DRX Bruker spectrometer was used in this task. The uni and bidimensional NMR spectra of compound **1** [1-(2-hydroxyphenyl)-3-phenyl-propane-1,3-dione] and of its derivatives **2** [1-(2-hydroxyphenyl)-3-(4'-methylphenyl)-propane-1,3-dione], **3** [1-(2-hydroxyphenyl)-3-(4'-methoxyphenyl)-propane-1,3-dione] and **4** [1-(2-hydroxyphenyl)-3-(4'-fluorophenyl)-propane-1,3-dione], in CDCl<sub>3</sub> solution, showed the presence of only one enol moiety preserving the carbonyl "ortho" to the hydroxyl substituent of ring **A** and enolising just the carbonyl "para" to the substituent of ring **B**. The HMBC spectra allowed the assignment of the phenol hydrogen at about 12.0 ppm, while the hydrogen of the enol hydroxyl appeared about 15.0 ppm, as expected. Compounds **5** [1-(2-hydroxyphenyl)-3-(4'-nitrophenyl)-propane-1,3-dione] and **6** [1-(2-hydroxyphenyl)-3-(4'-cyanophenyl)-propane-1,3-dione], in Pyr-*d*<sub>5</sub>, showed an almost 1:1 keto-enol equilibration what has been characterized through the AB quartet of the  $\beta$ -diketone methylene around 3.4 ppm and HSQC correlation with the carbon about 50 ppm and the vinyl hydrogen of the enol form at 7.5 ppm correlating with the carbon at 97.0 ppm. The compounds **1** and **7** [1-(2-hydroxyphenyl)-3-(4'-dimethylaminophenyl)-propane-1,3-dione], in Pyr-*d*<sub>5</sub>, showed the same behavior of only one enol form predominance. As a conclusion it seems that "meta" orientating deactivating substituents in ring **B** favor the 1:1 equilibrium while "ortho"/"para" orientating substituents in ring **B** favor the enolization of the carbonyl conjugated to ring **B**, preserving the carbonyl of ring **A** hydrogen bonded to the "peri" hydroxyl.

ACKNOWLEDGEMENTS: CNPq, PRONEX, CAPES, FUNCAP

#### New Methods in solution NMR

#### TH132: Padé via Moments: Squeezing the FID and going beyond the limits of the FFT in NMR

\*Carlos Cobas, Santiago L. Ponte

MESTRELAB RESEARCH S.L.

Since the Fourier Transform (FT) was first applied in NMR by R. Ernst and W. Anderson almost 50 years ago,[1] it has become a de facto mathematical procedure for converting the encoded time signal (FID) into its spectral representation in the frequency domain. There are a number of reasons that justify why it has been so widely used for NMR data processing, even to date, ranging from the fact that it is computationally very efficient and robust to its steady convergence with increasing acquisition time.

However, the FT presents several limitations. In one hand, it can be considered as a *low-resolution* estimator as its resolution is pre-determined exclusively by the total acquisition time. Attempts to increase resolution by acquiring the signal for a longer period of time will lead to worsened SNR. Moreover, the FT yields an envelope spectrum with no quantification on its own, and some additional processing or analysis procedures such as peak picking, integration or line fitting (deconvolution) must be applied should any quantitative information is required.

Considering the quantum-mechanical origin of the interesting, genuine signals, an alternative approach is proposed in this work that circumvents the fundamental limits of the FT. It is based on a new mathematical procedure aimed at building stable and accurate rational Padé approximants[2] from which all the spectral parameters, including all elementary frequencies, the corresponding amplitudes and the true number of physical resonances from the time domain signal can be derived. We will show how this new method can resolve and quantify tightly overlapped signals and discriminate between genuine and spurious signals.

[1] R.R. Ernst and W.A. Anderson, Rev. Sci. Instrum. 37, 93 (1966)

[2] Dž. Belkic, Quantum Mechanical Signal Processing and Spectral Analysis (Taylor & Francis Publishers, London, 2005)

#### MO133: Quantitative study chemical exchange of dilute sample by inversion transfer

Qing Luo, Weiping Jiang, Haidong Li, Qianni Guo, Ji Zhang, Zhao Li, Shizhen Chen, Chaohui Ye, \*Xin Zhou

Wuhan Institute of Physics and Mathematics

The remarkable advantage of NMR over other spectroscopy methods, e.g. IR or MS, is the comprehensive ability for the kinetic studies. In addition to tracing the time dependence of chemical reaction, NMR is able to provide the detailed kinetic information, such as chemical exchange, under conditions of the dynamic equilibrium. Exchange-correlated spectroscopy (EXSY) [1] is a regular method for the chemical exchange studies, which can provide both qualitative and quantitative information. However, the usage of such method is unable to study the dilute samples due to the low detection sensitivity, the intrinsic weakness of NMR. Chemical exchange saturation transfer (CEST) [2, 3, 4] is an indirect detection method with a remarkable sensitivity for the species of low concentrations or short lifetimes, and it is typically applied for MR molecular imaging of proteins/peptides which participate in the proton chemical exchange with surrounding water. Some environmental properties, such as pH and temperature, which strongly associate with the chemical exchange, can also be imaged. With these advantages, the CEST becomes a powerful tool for MR molecular imaging.

Theoretically, the CEST effect contains the information of chemical exchange rates. However, the mechanism of magnetization during the CEST experiment can be described by a series of Bloch equations are difficult to be analytically solved. Zhou et al. solved these equations with several simplified assumptions and approximations, which were not very close to the experimental conditions. Sherry et al. gave the numerical solutions of these equations, with several fixed parameters including the concentrations of the chemical exchange sites. But the concentrations are practically difficult to measure for the dilute samples, especially for the in vivo experiments.

Recently, we developed a novel method, called Chemical exchange Inversion Transfer (CEIT), based on the similar signal enhancement strategy to the CEST, but with an extremely improved spin control manner. By removing the radio frequency (RF) during the chemical exchange duration, the Bloch equations of the magnetization processes of the new method are greatly simplified. Thus, the analytical solutions are readily achieved. We applied this method to study the Xe-Xe chemical exchange, i.e., exchange between Xe dissolved in water and Xe trapped inside the functionally modified Cryptophane-A molecular cage, a  $^{129}\text{Xe}$  based MRI biosensor [5, 6]. The chemical exchange rate calculated by CEIT method, without any pre-information of concentrations, is in agreement with that measured by 1D EXSY experiment. Furthermore, such novel method achieved the same sensitivity of the CEST with a much low duty cycle, which hints a great potential with a higher sensitivity in biomedical applications.

#### References:

- [1] J. TAMMY et al, Chem. Rev. 90:935 (1990)
- [2] K. M. Ward et al, JMR 143, 79 – 87 (2000)
- [3] J. Y. Zhou et al, MRM 51:945 (2004)
- [4] D.E. Woessner et al, MRM 53:790–799 (2005)
- [5] Schroder L, et al., Science, 314:446, (2006)
- [6] Meldrum T, et al, JMR, 213:14 (2011).

#### **TU134: Implementation of the Filter Diagonalization Method (FDM) in Matlab® for signal analysis in nuclear magnetic resonance.**

<sup>1,3</sup>Joao Felipe Alves da Cruz, <sup>2,3\*</sup>Tiago Bueno de Moraes, <sup>2</sup>Cláudio José Magon, <sup>3</sup>Luiz Alberto Colnago

<sup>1</sup>Universidade Federal de São Carlos - UFSCar, <sup>2</sup>Instituto de Física de São Carlos - IFSC-USP, <sup>3</sup>Empresa Brasileira de Pesquisa Agropecuária - Embrapa Instrumentação

In 1990, Neuhauser introduced a numerical method for extraction of eigenvalues and eigenvectors in a given energy range of a large quantum system, named "Filter Diagonalization". It apply a Fourier filter for remove the correlation between distant eigenstates, and then, diagonalizing the Hamiltonian matrix in the subspace to calculate the eigenstates of a short range of energy. In 1997 Mandelstam using a rectangular filter, achieved convergence, velocity and reliability and the name "Filter Diagonalization Method" (FDM) was introduced. The FDM was explored in several areas of Physics where the harmonic inversion is necessary. Particularly, one of the most interesting applications of the FDM is Nuclear Magnetic Resonance (NMR). We recently showed that with the use of FDM it is possible to quickly obtain spectra with excellent signal/noise ratio. With these techniques we can suppress the echo component SSFP signal allowing the suppression of signals anomalies in the frequency domain spectrum or to suppress intense solvent signals in biological samples or broad signal in heterogeneous materials.

Our current software developed runs on Origin®, with routines in C/C++ and Fortran. Initially was developed for signal analysis in EPR (Electronic Magnetic Resonance) and subsequently modified to resolve NMR signals. This imple-

mentation in Origin® unfeasible a friendly interface construction, rendering complex software for users not experts.

The main goal of this project is to implement the FDM algorithm on the Matlab® platform, inserting facilities to the users and make the code simpler to new applications. Until now we have finished the implementation of the KBDM method; two regularization method: SVD and Tikhonov; and many simple functions at the interface. The FDM software implemented in Matlab has been tested with several known spectra and compared with Fourier Transform.

#### **TH135: Thermodynamic, Volumetric and Hydrophobic Characterization of Micelles by NMR to Understand Detergent Stabilization of Membrane Proteins**

Rohan Alvares, Shaan Gupta, Peter M. Macdonald, \*Scott Prosser

Department of Chemistry, University of Toronto

Membrane proteins are involved in functions such as catalysis, transport and ion conductance. Furthermore, thirty percent of genes code for membrane proteins and seventy percent of drugs target them. Consequently, determination of structure and dynamics of membrane proteins is of considerable importance. One of the main techniques used to study membrane proteins, NMR, requires solubilization of these hydrophobic proteins in detergents. The choice of detergent, which is imperative to maintaining proper protein structure, is still an empirical process. We have developed a high-throughput NMR methodology to determine detergent thermodynamic and volumetric properties upon micellization in hopes of elucidating the characteristics of detergents that dictate their ability to solubilize membrane proteins. Thermodynamic and volumetric properties were indirectly obtained by observing subtle differences in chemical shifts between micelle and monomeric states of the detergent which yielded the critical micelle concentration (CMCs) and subsequently the Gibbs free energy of micellization. Temperature dependencies of the free energy yielded enthalpic, entropic and heat capacity changes upon micellization, whereas, high pressure studies provide changes in the isothermal compressibility and partial molar volume. We compare differences in these properties between four common detergents: anionic (sodium dodecyl sulfate, SDS), zwitterionic (dodecylphosphocholine, DPC and cyclofos, CyF) and neutral (dodecyl maltoside, DDM) detergents to understand why some are better mimetics of the membrane than others. Furthermore, these measurements are complemented by using a paramagnetic oxygen molecule to probe the hydrophobicity of the micelle interior. This technique can, in theory, provide methylene specific estimates of hydrophobicity along the detergent chain. The results indicate increasing hydrophobicity across the series SDS < DPC < DDM which is generally consistent with tendencies of these detergents to stabilize membrane proteins.

#### **MO136: Real-time mechanistic monitoring of an acetal hydrolysis by ultrafast 2D NMR**

<sup>1,2\*</sup>Luiz Henrique Keng Queiroz Júnior, <sup>3</sup>Patrick Giraudeau, <sup>1</sup>Fabiane Aparecida Batalha dos Santos, <sup>1</sup>Kleber Thiago de Oliveira, <sup>1</sup>Antonio Gilberto Ferreira

<sup>1</sup>Universidade Federal de São Carlos, Departamento de Química, Laboratório de RMN, <sup>2</sup>Universidade Federal de Goiás, Instituto de Química, Laboratório de RMN, <sup>3</sup>cUniversité de Nantes, CNRS, Chimie et Interdisciplinarité: Synthèse, Analyse, Modélisation (CEISAM)

Ultrafast (UF) 2D NMR makes it possible to obtain a 2D NMR spectrum in less than a second.[1] UF-NMR is emerging as a potential technique to study mechanisms in organic reactions at natural abundance. Acetals are a very important class of organic compounds and are normally hydrolyzed using water and an acid catalyst. However, identifying the intermediates of these hydrolysis reactions is problematical

since the lifetime of these species are very short. This work presents the real-time monitoring of an acid catalyzed acetal hydrolysis reaction by UF-HSQC experiments, with no need for  $^{13}\text{C}$ -labeling.[2] It was monitored the hydrolysis of the 2-(4-nitrophenyl)-1,3-dioxolane acetal reacting with trifluoroacetic acid (TFA) in the presence of residual water from the solvent (deuterated chloroform). This reaction was carried out in a 5 mm NMR tube placed in a 400 MHz spectrometer equipped with a 5 mm BBI probe. UF-HSQC experiments were used for the real-time mechanistic study of this acetal hydrolysis at  $^{13}\text{C}$  natural abundance, and it was possible to characterize the presence of the hemiacetal, an intermediate with a well-known short lifetime. This monitoring result in the characterization of a hemiacetal intermediate, which we could not observe by 1D NMR, in spite of numerous attempts, probably due to the very short lifetime of this intermediate. These assignments were confirmed and rationalized by quantum calculations of  $^1\text{H}$  and  $^{13}\text{C}$  NMR chemical shifts and NBO (Natural Bonding Orbital) analysis. While this work showed the potentialities of UF-NMR for real-time mechanistic studies, it also allowed the characterization of the short lifetime hemiacetal intermediate.

[1] Frydman, L.; Scherf, T.; Lupulescu, A.; Proc. Natl. Acad. Sci. USA 2002, 99(25), 15858-15862.

[2] Queiroz Jr., L. H. K.; Giraudeau, P.; Santos, F. A. B.; Oliveira, K. T.; Ferreira, A. G.; Magn. Res. Chem. 2012, 50(7), 496-501.

Acknowledgements: CNPq, CAPES and FAPESP.

#### TU137: Ultrafast High-Resolution J-resolved Spectroscopy in Inhomogeneous Magnetic Fields

\*Shuhui Cai, Hao Chen, Zhiyong Zhang, Zhong Chen

Department of Electronic Science, Xiamen University, Xiamen 361005, China

Ultrafast 2D NMR accelerates the acquisition of 2D NMR spectrum by orders of magnitude. However, like conventional methods, ultrafast methods suffer from line broadening and loss of spectral features in inhomogeneous fields. To circumvent the influence of field inhomogeneity, various approaches based on intramolecular or intermolecular multiple-quantum coherences have been proposed. The protocol based on coherence transfer can obtain high-resolution spectrum in arbitrary inhomogeneous field, but it has difficulty in spectral assignment [1]. The spatially encoded technique combined with homonuclear intermolecular zero-quantum coherence (iZQC) can obtain a high-resolution 2D J-resolved spectrum with two scans [2], but it undergoes difficulty in implementing when the chemical shifts of solvent and solutes are close to each other. Here we propose a new scheme to ultrafast achieve 2D J-resolved spectroscopy in inhomogeneous fields via heteronuclear iZQC. To evaluate the efficiency of the new scheme, experiments were performed. The results show that accurate chemical shifts and J-coupling information can be retrieved in the 2D J-resolved spectrum. As the solvent and solutes are excited through different channels, selective pulses required in homonuclear iMQC methods are no longer necessary. Moreover, the loss of signal-to-noise ratio caused by solvent suppression can be got rid of. All these greatly improve the spectral quality.

[1] Pelulessy, P.; Rennella, E.; Bodenhausen, G. Science, 2009, 60, 429-448.

[2] Lin, Y. L.; Zhang, Z. Y.; Cai, S. H.; Chen, Z. J. Am. Chem. Soc., 2011, 20, 7632-7635.

ACKNOWLEDGEMENTS: This work was supported by the NNSF of China under Grant 11275161.

#### TH138: An Approach for High-Resolution Spatially Encoded Intermolecular Multiple-Quantum Coherence NMR Spectroscopy in Inhomogeneous Fields

Yulan Lin, \*Zhong Chen, Shuhui Cai, Zhiyong Zhang

Department of Electronic Science, Xiamen University, Xiamen, Fujian 361005, China

High-resolution NMR spectroscopy has been a powerful tool for the study of molecular structures and chemical dynamics of a vast range of compounds, materials and reaction processes, from the metabolites of an organism to the compositions of promising new materials. However, there are many circumstances where the magnetic field homogeneity is degraded or the testing object is subject to intrinsic variation in magnetic susceptibility so that the spectral lines are broadened and the spectrum becomes devoid of any chemical information. This precludes NMR spectral analyses based upon the interpretation of the familiar NMR parameters, such as chemical shifts and scalar coupling constants. In this study, we put forward an approach to remove the influence of magnetic field inhomogeneity on NMR spectroscopy via intermolecular multiple-quantum coherence technique [1]. The 2D NMR acquisition is accelerated by spatially encoded technique proposed by Frydman and co-workers [2] and improved by Pelulessy [3]. To increase the signal-to-noise ratio, only the solvent spin is excited to evolve during the spatially encoded period. The area of the decoding gradients is small and the solutes do not experience the diffusion decay from the spatial encoding gradients. The principles and advantages of this new approach are presented, and its application is exemplified with a sample packed with pig brain tissue.

This work was supported by the NNSF of China under Grant 11204256.

[1] Huang, Y. Q.; Cai, S. H.; Chen, X.; Chen, Z. J. Magn. Reson., 2010, 203, 100- 107.

[2] Frydman, L.; Scherf, T.; Lupulescu, A. Proc. Natl. Acad. Sci. U. S. A., 2002, 99, 15858- 15862.

[3] Pelulessy, P. J. Am. Chem. Soc., 2003, 125, 12345- 12350.

#### New Methods in solid-state NMR

#### MO139: Fast and ultra-fast MAS $^{13}\text{C}$ - $^{13}\text{C}$ correlations applied to biological systems

<sup>4</sup>Guangjin Hou, <sup>4</sup>Si Yan, <sup>1</sup>Julien Trébosc, <sup>1</sup>Olivier Lafon, <sup>2</sup>Bingwen Hu, <sup>3</sup>Bernd Reif, <sup>2</sup>Qun Chen, <sup>3,4</sup>Sam Asami, <sup>4</sup>Tatyana Polenova, <sup>1\*</sup>Jean Paul Amoureux

<sup>1</sup>Lille University, France, <sup>2</sup>East China Normal University, Shanghai, China, <sup>3</sup>Munich University, Germany, <sup>4</sup>University of Delaware, Newark, USA

Proteins benefit from high-field spectrometers for the resolution. However, sidebands may obscure the  $^{13}\text{C}$ - $^{13}\text{C}$  spectra and spinning speeds faster than 30 kHz are thus required.

The assignment of the resonances must first be done with 1st-order methods. DQ-SQ experiments present the advantages of: (i) allowing the observation of only one-bond correlations, (ii) short recoupling times, and (iii) no uninformative diagonal peaks, which simplify the assignment of resonances with close frequencies. In a second step, SQ-SQ experiments are useful to observe two-bond cross-peaks. We have developed two such methods, H-BR2 (DQ-SQ)[1] and RFDR-xy8-4<sup>1</sup> (SQ-SQ),[2] which (i) require low rf-power, (ii) are robust to CSA and offset, (iii) are very simple to use with only the recoupling time to optimize, (iv) work at ultra-fast MAS, and (v) do not require  $^1\text{H}$  decoupling.

Once the assignment achieved, long range correlations provide constraints to get the protein structure and folding. This requires sequences less sensitive to dipolar truncation. The most used sequence, DARR, does not work at fast MAS, and PARIS<sub>xy</sub> is currently the most broadband sequence.[3] We present several new sequences, SHANGHAI,[4] SHANGHAI+, [5] and CORD,[6] which are more robust and efficient than previous methods. They even allow observing contacts up to 1000 pm.[5]

To decrease the experimental time, covariance can be used along the indirect dimension. However, this treatment introduces uninformative diagonal peaks that can be avoided with new covariance treatments.[7] Another way is using non-uniform sampling with maximum-entropy interpolation (NUS-MINT).[8]

All the sequences and data treatments have been demonstrated on YajG, SH3 and LC8 proteins, and also compared with PAR and DREAM.[1,6] Moreover, the proteins were either fully or only 15% protonated.

[1] Lafon, Trébosc, Hu, DePaëpe, Amoureux, Chem. Comm. 47 (2011) 6930.

[2] Shen, Hu, Lafon, Trébosc, Chen, Amoureux, JMR. 223 (2012) 107.

[3] Weingarth, Demco, Bodenhausen, Tekely, CPL. 469 (2009) 342; Weingarth, Bodenhausen, Tekely, JACS. 131 (2009) 13937. Weingarth, Bodenhausen, Tekely, CPL. 488 (2010) 10

[4] Hu, Lafon, Trébosc, Chen, Amoureux, JMR. 212 (2011) 320.

[5] Hu, Trébosc, Lafon, Chen, Masuda, Takegoshi, Amoureux, ChemPhysChem. 13 (2012) 3585

[6] Hou, Yan, Trébosc, Amoureux, Polenova, submitted.

[7] Lafon, Hu, Amoureux, Lesot, Chem. Eur. J. 17 (2011) 6716.

[8] Paramasivam, Suiter, Hou, Sun, Palmer, Hoch, Rovnyak, Polenova, JPC-B. 116 (2012) 7416.

#### **TU140: Satellite Saturation HMQC for quadrupolar to spin 1/2 nuclei correlations: transfer faster than the interaction**

<sup>1</sup>Julien Trebosc, <sup>2\*</sup>Qiang Wang, <sup>3</sup>Yixuan Li, <sup>1</sup>Olivier Lafon, <sup>2</sup>Jun Xu, <sup>1</sup>Jean Paul Amoureux, <sup>3</sup>Qun Chen, <sup>3</sup>Bingwen Hu, <sup>2</sup>Feng Deng

<sup>1</sup>Unit of Catalysis and Chemistry of Solids, CNRS-8181, Lille North of France University, 59652 Villen, <sup>2</sup>State Key Laboratory of Magnetic Resonance and Atomic and Molecular Physics, Wuhan Center for Magnet, <sup>3</sup>Physics Department & Shanghai Key Laboratory of Magnetic Resonance, East China Normal University, Sh

When quadrupolar nuclei are involved in HMQC correlation experiments, one usually applies CT selective pulses to manipulate only the central transition. If the quadrupolar nucleus is detected in the indirect dimension using CT selective pulses then approximation of fictitious spin-1/2 applies and the buildup curve of J-HMQC transfert follows the case of 1/2 spin with an optimum mixing time equal to 1/2J. However, the HMQC mixing mechanism can also populate energy levels other than +1/2 or -1/2. Actually, the energy level n/2 is populated with an optimum mixing time of 1/2nJ. At this point, SS-HMQC saturates the n/2 energy levels by irradiating the satellite transition in a manner similar to Double Frequency Sweep (DFS) or other techniques used to enhance signal of the central transition.

We show that Satellite Saturation (SS) HMQC can reduce by a factor S+1/2 the required mixing time in a HMQC sequence. Significant gain is thus achieved in sensitivity due to lower attenuation resulting of transverse relaxation.

Consequences of such results are of first importance as it opens the technique to a much broader set of materials for which transverse ( $T_2'$ ) relaxation and weakness of J coupling make the experiment very insensitive or impossible. We show that this method extends to dipolar based D-HMQC.

We study the robustness of the method to quadrupolar interaction by simulation and show experimental results of <sup>31</sup>P-<sup>27</sup>Al J-HMQC, D-HMQC using the satellite saturation technique with gains over 50% in sensitivity even in favorable

cases (long  $T_2'$ ). We also demonstrate the gain in quad-quad <sup>17</sup>O-<sup>27</sup>Al SS-J-HMQC correlations.

#### **TH141: Probing the proximities and connectivities between close Larmor frequencies nuclei**

<sup>1</sup>Julien Trebosc, <sup>1\*</sup>Frédérique Pourpoint, <sup>1</sup>Régis Gauvin, <sup>2</sup>Qiang Wang, <sup>1</sup>Olivier Lafon, <sup>2</sup>Feng Deng, <sup>1</sup>Jean Paul Amoureux

<sup>1</sup>UCCS – ENSCL - University Lille North of France, Villeneuve d'Ascq 59652 France, <sup>2</sup>State Key Laboratory of Magnetic Resonance and Atomic and Molecular Physics Wuahn Center for Magnet

The usual NMR probe design prevents the observation of connectivities and proximities between numerous pairs of isotopes (<sup>1</sup>H-<sup>19</sup>F; <sup>31</sup>P-<sup>7</sup>Li; <sup>13</sup>C-<sup>27</sup>Al; <sup>13</sup>C-<sup>51</sup>V ...) exhibiting close Larmor frequencies. The absence of such information is a limitation for numerous important systems, including polymers, biomolecules, energy materials or catalysts.

Through the case study of <sup>13</sup>C-<sup>27</sup>Al isotopes, we introduce efficient methods to probe proximities and connectivities between nuclei exhibiting close Larmor frequencies. Over-coupled resonators allow the tuning and matching of a single channel at the close <sup>27</sup>Al and <sup>13</sup>C Larmor frequencies. This commercial device permits the successive irradiation of <sup>27</sup>Al and <sup>13</sup>C isotopes in a pulse sequence and accurate Al-C distances are measured using the S-RESPDOR sequence.[1] We show that in <sup>13</sup>C natural abundance, this approach allows measuring distances of 216 pm between covalently bonded Al-C atoms in lithium tetra-alkyl-aluminate, a commonly used co-catalyst in olefin polymerization processes, and distances ranging from 274 to 381 pm for non-bonded Al-C atoms in aluminum lactate.

We also report the first two-dimensional heteronuclear correlation experiments between <sup>27</sup>Al and <sup>13</sup>C nuclei. HMQC scheme using J coupling allows detecting the <sup>13</sup>C-<sup>27</sup>Al covalent bonds, while HMQC using dipolar coupling reveals multiple proximities between the different <sup>13</sup>C and <sup>27</sup>Al sites proximities.

These methods are expected to be useful for the characterization of supported heterogeneous catalysts, which lack long-range order or to gain insight into the structure of metal organic frameworks. It will help to bring further understanding in the nature of the Al-C bond in terms of distances and proximities and hence, of reactivity.

Other pairs of nuclei available for distance measurement and correlation with our over-coupled resonator include <sup>13</sup>C-<sup>51</sup>V. We demonstrate such methods on oxovanadium complexes. There are potential application for metallo-proteins like van-abins.

We also managed much closer frequency nuclei pair by getting correlations in between <sup>23</sup>Na, <sup>27</sup>Al and <sup>31</sup>P in a 3D experiment of a sodium alumino phosphate glass. Indeed we managed to turn a triple resonance probe into quadruple resonance one. That can be useful to discriminate such phases in complex mixture of recrystallized glasses.

[1] F. Pourpoint et al. Chem. Phys. Chem, 2012 (13), 3605-3615

#### **MO142: Structural Elucidation from Prednisone applying Residual Dipolar Coupling**

<sup>1,2\*</sup>José Adonias Alves de França, <sup>1</sup>Rubens Rodrigues Teles, <sup>1</sup>Fernando Hallwass

<sup>1</sup>Universidade Federal de Pernambuco, <sup>2</sup>Instituto Federal de Alagoas

Structural elucidation of new organic compounds and natural products is a challenge for chemists. In some cases, even very elaborated NMR experiments are not sufficient to find the correct molecular structure. Because of this, different approaches have been carried out in order to provide additional

information to overcome this limitation as, for instance, the realization of experiments in oriented media, where molecular orientation is restrained in the NMR tube, recovering the anisotropic parameter, such as Residual Dipolar Coupling (RDC) and Residual Chemical Shift Anisotropy (RCSA).

In this work we have investigated the molecular structure of the steroid Prednisone (17,21-dihydroxypregna-1,4-diene-3,11,20-trione). It is a synthetic corticosteroid drug that is particularly effective as an immunosuppressant drug, used to treat certain inflammatory diseases and some types of cancer.

An examination of the structure of Prednisone makes it possible to propose 64 different diastereomers. All 64 structures were optimized by molecular mechanic calculations at the DFT level of theory, using Gaussian03. The B3LYP functional along with the 6-311++G(d,p) basis set was used. We carried out NMR experiments, such as  $^1\text{H}$ ,  $^{13}\text{C}$ , gHSQC, gHMBC, NOESY, gCOSY, using a commercial Prednisone sample in DMSO- $d_6$  solution. In order to obtain the  $^1\text{H}$ ,  $^{13}\text{C}$  RDC values we performed coupled gHSQC experiments with PAN Gel, as the alignment media.

We have compared the experimental RDC values with back-calculated ones (obtained by NMRDev software) for the 64 proposed diastereomers. The smallest Q factor was observed for the molecular structure of the correct stereoisomer. The same result would be not possible to obtain if only isotropic parameters had been used. Therefore, RDCs can be seen as a powerful tool to solve assignment ambiguity and to elucidate chemical structures.

In conclusion, we have shown that measurement by RDCs is fundamental to define the correct molecular structure of Prednisone.

ACKNOWLEDGEMENTS: PRONEX/FACEPE/CNPq e UFPE

#### **TU143: Simple and accurate determination of X-H distances under ultra-fast MAS NMR**

<sup>1</sup>\*Piotr Paluch, <sup>1</sup>Tomasz Pawlak, <sup>2</sup>Jean Paul Amoureux, <sup>1</sup>Marek J. Potrzebowski

<sup>1</sup>Polish Academy of Sciences, Centre of Molecular and Macromolecular Studies, <sup>2</sup>Unit of Catalysis and Chemistry of Solids (UCCS), CNRS-8181, University Lille North of France

We demonstrate that a very simple experiment, Cross-Polarization with Variable Contact-time (CP-

VC), is very efficient at ultra-fast MAS ( $\nu_R \geq 60$  kHz) to measure accurately the C-H and N-H distances, and to analyze the dynamics of bio-molecules. This experiment can be performed with samples that are either  $^{13}\text{C}$  or  $^{15}\text{N}$  labeled or without any labeling. The method is very robust experimentally with respect to imperfect Hartman-Hahn setting, and presents a large scaling factor allowing a better dipolar determination, especially for long C-H or N-H distances. At ultra-fast MAS, it can be used quantitatively in a 2D way, because its scaling factor is then little dependent on the offsets. This robustness with respect to offset is related to the ultra-fast spinning speed, and hence to the related small rotor diameter. Indeed, these two specifications lead to efficient  $n = \pm 1$  zero-quantum Hartman-Hahn CP-transfers with large rf-fields on proton and carbon or nitrogen channels, and large dipolar scaling factor.

#### **Exotica**

#### **TH144: New findings with NMR of stretched hydrogels: peculiar urea resonance splittings and fitting z-spectra**

\*Philip W. Kuchel, Christoph Naumann, Max Puckeridge, Bogdan E. Chapman

School of Molecular Bioscience, University of Sydney, Australia

$^1\text{H}$  NMR spectra of high concentrations (several M) of urea in high-concentration gelatin (denatured collagen) gels have two well-separated resonances from the amide  $^1\text{H}$ -atoms and residual water (HDO); this implies slow exchange of urea protons with aqueous solvent, on the NMR timescale. Holding the gel stretched [1-3] generates residual dipolar splittings in urea resonances (and other incorporated guest molecules) and residual quadrupolar splitting in HDO. Association of urea with collagen reduces, but does not completely quench, the anisotropic behavior of stretched and compressed gelatin gels, potentially allowing the structure determination of peptides under denaturing conditions.

We describe the anisotropic  $^1\text{H}$  NMR splitting pattern of urea under these anisotropic conditions with varying degrees of deuteration as well as with  $^{15}\text{N}$ -urea labelling.

We have also refined the method of estimating the values of relaxation time constants of spin states of all ranks and orders of selected quadrupolar ions in stretched gels [4]. This has been done for  $^7\text{Li}^+$  and  $^{23}\text{Na}^+$  [5], and work is in progress on others, using a Markov chain Monte Carlo algorithm.

#### **References:**

- [1] Kuchel, P. W., Chapman, B. E., Mueller, N., Bubb, W. A., Philp, D. J., and Torres, A. M. (2006) *J. Magn. Reson.* 180, 256-265.
- [2] Naumann, C., Bubb, W. A., Chapman, B. E., and Kuchel, P. W. (2007) *J. Am. Chem. Soc.* 129, 5340-5341
- [3] Naumann, C., and Kuchel, P. W. (2008) *J. Phys. Chem. A.* 112, 8659-8664.
- [4] Philp, D. J., Naumann, C., and Kuchel, P. W. (2012) *Concepts Magn. Reson. A* 40, 90-99.
- [5] Puckeridge, M., Chapman, and Kuchel, P. W. (2012) *Magn. Reson. Chem.* 50, S17-S21.

#### **MO145: New Model of Electron Spin Polarization in GaAs and AlGaAs/GaAs Arising from Optical Pumping and Detection by Optically-Pumped NMR**

<sup>1</sup>Dustin Wheeler, <sup>1</sup>Erika Sesti, <sup>2</sup>Dipta Saha, <sup>2</sup>Christopher J. Stanton, <sup>1</sup>\*Sophia E. Hayes

<sup>1</sup>Washington University in St. Louis, <sup>2</sup>University of Florida, Gainesville

Optically-pumped nuclear magnetic resonance (OPNMR) is a radio-frequency detection method to study the coupling of nuclei with both bulk conduction electrons and two-dimensionally confined electrons in quantum wells. OPNMR takes advantage of the hyperpolarization of the nuclei through the Fermi-contact interaction with electrons that have been excited by laser light. Our experiments focus on both bulk GaAs and multiple-quantum well samples of GaAs, and we study the effects of photon energy on  $^{69}\text{Ga}$  OPNMR signal intensities.

An ongoing line of inquiry involves the fundamental physical interactions between optical selection rules, steady-state electron polarization, and transfer of that polarization to nuclei in the impacted sample area. We have made progress on a model for predicting OPNMR signal intensity as a function of input photon energy, including insights into electron spin polarization.

Electron polarization is calculated at a range of photon energies. This photon-energy dependent and variable quantity is informative because it allows us to more accurately model the dependence of the OPNMR signal on optical pumping wavelength.

#### **TU146: Measuring Bipartite Quantum Correlations in NMR Systems**



<sup>1</sup>Isabela Almeida Silva, <sup>3</sup>Davide Girolami, <sup>2</sup>Ruben Auc-  
caise, <sup>2</sup>Roberto Silva Sarthour Júnior, <sup>2</sup>Ivan dos Santos  
Oliveira, <sup>1</sup>Tito José Bonagamba, <sup>1\*</sup>Eduardo Ribeiro de  
Azevêdo, <sup>3</sup>Gerardo Adesso, <sup>1</sup>Diogo O. Soares Pinto

<sup>1</sup> Universidade de São Paulo, Instituto de Física de São Car-  
los, São Carlos-SP, Brazil, <sup>2</sup> Centro Brasileiro de Pesquisas  
Físicas, Rio de Janeiro-RJ, Brazil, <sup>3</sup> University of Notting-  
ham, School of Mathematical Sciences, Nottingham, United  
Kindom

How quantum states differ from classical states? For a long time, entanglement was considered the only responsible for that difference. When it was demonstrated that it is not possible to produce entanglement in conventional room temperature liquid state NMR, the use of the technique as a test bench for quantum information processing (QIP) was severely criticized. This last until it was shown that separable states, as found in most of the NMR implementations, may present other types of non-classical correlations, for instance, the quantum discord proposed by Ollivier and Zurek. Besides a time costly quantum state tomography process, the experimental evaluation of the quantum discord involves large number of mathematical manipulations. Because of that, other alternative discord measures have been proposed. For a two qubit system, Girolami and Adesso proposed the quantity  $Q(\rho)$ , which allow the calculation of the so called geometric quantum discord  $D_G$ , and Nakano *et al.* defined another discord measurement, named the negativity of quantumness  $Q_N^A$ . We demonstrate that in NMR systems both quantifiers are calculated from spin correlations, which are measured directly from the magnetization of one nucleus (qubit) after applying a specific pulse sequence. The equivalency between direct and tomography based measurements of  $D_G$  and  $Q_N^A$  is then demonstrated using a two-qubit NMR system implemented by J-coupled <sup>1</sup>H and <sup>13</sup>C nuclei. Thereafter, we apply these quantities to determine the relative amount of quantum correlations present in two-qubit pseudo-pure states typically used in NMR QIP. At last, NMR is used to experimentally observe that, for some selected states and finite time period, the amount of discord is preserved even under the presence of relaxation (freezing of quantum correlations). We further observe the phenomenon of sudden change in the relaxation behavior of quantum correlations as measured by  $D_G$  and  $Q_N^A$ .

ACKNOWLEDGMENTS: FAPESP, FAPERJ, CAPES

#### TH147: Observation of classical bifurcation in a <sup>133</sup>Cs quadrupolar NMR system

<sup>1</sup>Arthur Gustavo de Araújo Ferreira, <sup>2</sup>Ruben Auc-  
caise, <sup>3</sup>Roberto Silva Sarthour Júnior, <sup>3</sup>Ivan dos Santos  
Oliveira Júnior, <sup>1\*</sup>Tito José Bonagamba, <sup>3</sup>Itzhak Roditi

<sup>1</sup>Instituto de Física de São Carlos - Universidade de  
São Paulo, <sup>2</sup>EMBRAPA Solos - Rio de Janeiro, <sup>3</sup>Centro  
Brasileiro de Pesquisas Físicas

The investigation of classical bifurcation on quantum systems has been the focus of many theoretical and experimental studies. This behavior is typically addressed in the context of Bose-Einstein condensates (BEC) systems. Bifurcation is a signature of phase transition between different regimes, thus the interest in such phenomena. In this work, we use a quadrupolar NMR system based on <sup>133</sup>Cs nuclei with spin  $I=7/2$  to study the bifurcation behavior in analogy to what happens in BEC systems. A two-mode BEC can be described via the Schwinger pseudo-spin representation and entirely mapped onto a quadrupolar NMR Hamiltonian, enabling us to study this type of dynamics using NMR quantum information processing tools. For observing the classical bifurcation we used a lyotropic liquid crystal sample composed of cesium-pentadecafluorooctanoate. The <sup>133</sup>Cs NMR experiments were performed using specially designed radio-frequency pulses in order to implement spin coherent states as initial states. Next, appropriate evolutions were implemented to achieve the desired linear or non-linear regime. Finally, the read out of the quantum state was done using

the quantum state tomography procedure. The experiments were performed on a Varian 500 MHz (11.7 T) spectrometer at 25 °C. We observed the dynamics transition of the system between a linear to a nonlinear regime. This evolution is interpreted using the Josephson Junction model, which is commonly applied in superconductivity. We achieved that behavior when we varied one of the quadrupolar Hamiltonian parameters. The change in the system dynamics lead to a supercritical pitchfork bifurcation that we were able to evaluate and to show the quantum control in the NMR spin scenario.

ACKNOWLEDGEMENTS: IFSC/USP, FAPESP, FAPERJ, CNPq, and CAPES.

#### Instrumentation

#### MO148: Multi-Band Automatically Tunable High-Sensitive Nuclear Quadrupole Resonance Spectrometer

<sup>1,2,\*</sup>Lucas Matías Cerioni, <sup>1,2,3</sup>Daniel José Pusiol

<sup>1</sup>SPINLOCK SRL, Córdoba, Argentina, <sup>2</sup>Argentinian Na-  
tional Research Council, <sup>3</sup>Instituto de Física Enrique Gavi-  
ola, CONICET, Ciudad Universitaria, Córdoba, Argentina

Nuclear quadrupole resonance (NQR) is a nondestructive, highly specific, noninvasive spectroscopic technique. NQR can be used to detect signals from solids and its parameters are highly sensitive to local environment changes. These features make NQR a powerful technique for identifying and study the properties of different polymorphs as well different hydrates forms in pharmaceutical agents, providing effective assistance at the main steps of drug development, manufacturing process and quality control.

In this work we present the development and implementation of a high sensitive pulse NQR spectrometer, capable of measuring in different frequency bands, allowing the scan of new NQR signals in a fast, automatic and unattended way.

The spectrometer was developed for measuring in two different ranges: 1.9-4.1 MHz (<sup>14</sup>N) and 34-36 MHz (<sup>35</sup>Cl). In order to make the spectrometer capable of measuring in both bands, a two capacitively coupled high-Q coils probe-head was built. To cover the whole bandwidth, the high-Q tuning and matching capacitors are mechanically adjustable. The spectrometer also includes a full bandwidth Q-damper system; a switchable transmitter filters; and a sample temperature control. The performance of the two-coil circuit was evaluated and compared with the standard single coil configuration.

The tuning and matching capacitors are adjusted by a fast auto-tuning algorithm, feedbacked by reflected power. Q-damper frequency band and power amplifier filters are also fast and automatically adjusted. This allows making a full frequency sweep, performing measurements on the whole range of interest in a complete automatic way.

The spectrometer sensibility was tested using the standard samples hexamethylenetetramine (hmt) for <sup>14</sup>N, and *p*-diclorobenzene (pdb) for <sup>35</sup>Cl. The spectrometer allows detecting 19 mg of hmt in 30 minutes and 7 mg of pdb in 1 minute.

The spectrometer was tested reconstructing the previously reported spectra of pharmaceutical samples including carbamazepine, furosemide and hydrochloro-thiazide. Unreported lines were found in diclofenac sodium, aripiprazole and clopidigrel bisulfate. No NQR signal of these last two samples had been reported before.

ACKNOWLEDGEMENTS: CONICET, FONTAR, SPIN-LOCK

**TU149: A Cryogen-Free 300 MHz Desk-Top NMR Magnet for Industrial Applications**

\*Jonathan Cole, Steven J. Green, Eugeny Kryukov, Jeremy A. Good

*Cryogenic Ltd.*

Since the 1990s, Cryogenic Ltd. have been developing versatile experimental platforms based on cryogen-free magnets and variable temperature inserts for measurements at high magnetic field (< 20 Tesla) and low temperature (> 30 mK) for research in condensed matter physics.

More recently, this proprietary technology is being adapted to magnetic resonance. In the mid-2000s, Cryogenic built several cryogen-free EPR magnets at 9 to 14 tesla, thereby helping to launch the field of mm-wave EPR spectroscopy [1, 2, 3]. Then, the first cryogen-free 600 MHz wide bore magnet was developed for NMR studies involving quadrupolar-broadened lines up to tens of MHz wide [4, 5]. Last year, the company installed the most compact cryogen-free 1.5 tesla pre-clinical MRI magnet of its type in the world [6].

Here, we describe a cryogen-free 300 MHz narrow bore NMR system that may be operated on an office desk or laboratory bench. The magnet is suspended in vacuum inside a radiation shield held at 40 K and is kept at 3.5 K by a pulse tube cryocooler rated to deliver 0.5 W of cooling at low temperature. The cooler consumes no helium and works on a closed cycle driven by a 3.5 kW compressor connected to 3-phase mains electricity. Little cryogenic experience is required to operate the magnet which may be safely sited in limited space without quench ducting. Following on-site installation, the magnet is left to cool overnight; it may also be left switched off when experiments are not being run. The cryocooler cold-heads have proven to be very reliable, requiring infrequent maintenance at low cost.

Our compact cryogen-free desk-top system offers industrial researchers a practical solution for high field NMR spectroscopy with low overall cost of ownership.

[1] T.I. Smirnova et al., in *ESR Spectroscopy in Membrane Phys.*, 2005

[2] A.I. Smirnov et al., *Rev. Sci. Instrum.*, 2006

[3] E.J. Reijerse et al., *JACS*, 2010

[4] J.W. Harter et al., *Phys. Rev. B*, 2007

[5] L.K. Alexander et al., *Phys. Rev. B*, 2010

[6] J.A. Good et al., *ENC* 2012

**TH150: Selective Imaging of Fluorescent Nanodiamonds and Study of Ion Irradiation Effect on Nanodiamonds**

<sup>1</sup>Shingo Sotoma, <sup>1</sup>Ruji Igarashi, <sup>2</sup>Yosuke Yoshinari, <sup>2</sup>Hiroaki Yokota, <sup>1</sup>Hidehito Tochio, <sup>2</sup>Yoshie Harada, <sup>1,2\*</sup>Masahiro Shirakawa

<sup>1</sup>Graduate School of Engineering, Kyoto University, <sup>2</sup>Institute for Integrated Cell-Material Science (WPI-iCeMS)

Fluorescent imaging is a powerful tool for visualizing intracellular event. Recent development of this technique has enabled us to investigate the localization and dynamics of bio-molecule in real time at a single molecule level. However, such sensitive detection is often hampered by intrinsic fluorescence arising from endogenous molecules. Techniques which reduce intrinsic fluorescence have been investigated but there are no ways to shut that out perfectly. Here, we describe a method for the selective imaging of nitrogen-vacancy center (NVCs) in nanodiamonds. This method relies on the property of NVCs that the fluorescence intensity sensitively depends on the ground state spin configuration which can be regulated by inducing electron spin magnetic resonance. Here, we present a technique for selectively imaging NVCs of diamonds in real-time. We also studied the ion irradiation

effect on nanodiamonds for the sake of improving NVCs concentration in nanodiamonds. Nanodiamonds generally contain sub-ppm nitrogen atoms as impurity and annealing with vacancies results in NVCs. However, because only few vacancies exist in commercially available nanodiamonds, it is necessary to create more vacancies by ion irradiation process to increase NVC concentration in nanodiamonds. We explored various irradiation conditions with H<sup>+</sup>, He<sup>+</sup>, Li<sup>+</sup> and N<sup>+</sup> ions and tested the effect on the NVC concentration in nanodiamonds.

**MO151: Development of an Ultra-High-Power H/C/N NMR Probe for Membrane Proteins**

\*F David Doty, John Staab, George Entzminger, JB Spitzmesser, Daniel Arcos, Laura Holte, Paul Ellis

*Doty Scientific Inc*

Available methods for molecular structure determination have had limited success on the insoluble proteins that are critical to biological function, though various recent developments have enhanced the effectiveness of solids NMR methods incorporating Magic Angle sample Spinning (MAS). However, static (non-MAS) high-power methods, such as PISEMA, have been equally fruitful thus far in yielding structures of large, complex, helical membrane proteins. Preliminary work from several leading research groups has demonstrated the value of advanced 3D methods that could not be carried out at high fields using commercially available probes because large samples are needed with very high rf field strengths at <sup>1</sup>H, <sup>13</sup>C, and <sup>15</sup>N simultaneously. A novel <sup>1</sup>H resonator and novel circuits were developed and demonstrated in a 900 MHz narrow-bore probe that provided order-of-magnitude reduction in RF sample heating compared to single-coil circuits, along with substantial improvements in each of the remaining three most important and technically demanding specifications simultaneously: RF field strength, spectral resolution, and S/N. The probe also included a gradient coil to permit novel methods in static NMR experiments, including solvent and background suppression, coherence selection, and diffusion experiments. The gradient coil was tested to 157 G/cm in the 21.1 T magnet and demonstrated excellent linearity, efficiency, and recovery time. The tests in the 900 MHz magnet at the NRMFL in Tallahassee included CP experiments for <sup>1</sup>H/<sup>13</sup>C, <sup>1</sup>H/<sup>15</sup>N, double CP, and gradient-based coherence selection. The maximum power levels available were 320 W <sup>1</sup>H, 700 W for <sup>13</sup>C, and 1100 W for <sup>15</sup>N. The probe demonstrated superior efficiency and had no difficulty handling these powers under CP conditions, as the <sup>1</sup>H is on an outer resonator while the <sup>13</sup>C and <sup>15</sup>N are on a doubly balanced inner solenoid. The probe is expected to be able to handle at least 40% higher power on all channels.

Acknowledgements: 5R44 GM079888-03

**Medicinal Chemistry**
**TU152: NMR-Based screening exposes new fragment detection possibilities at the pVHL:HIF-1 $\alpha$  protein-protein interface**

<sup>1</sup>David M. Dias, <sup>1</sup>Inge Van Molle, <sup>1</sup>Matthias Baud, <sup>1</sup>Carles Galdeano, <sup>2</sup>Carlos F. G. C. Galdes, <sup>1\*</sup>Alessio Ciulli

<sup>1</sup>Chemistry Department, University of Cambridge, Cambridge, United Kingdom, <sup>2</sup>Department of Life Sciences, Faculty of Science and Technology, Centre for Neurosciences and Cell Bi

The growing interest in Protein-Protein interactions and Interfaces (PPIs) has been hampered by a lack of lucid methods capable of exploring its ligandability. Modulation of large multiprotein complexes has remained incredibly challenging and the relative low hit rates have encouraged other approaches e.g. peptidomimetics to assist lead discovery against

PPIs. However, is the classical fragment-based biophysical screening set-up able to prime and command this challenge?

Here, we investigate the ability of NMR-based screening techniques to guide a hit-to-lead optimization campaign at von Hippel-Lindau protein/hypoxia inducible factor 1 $\alpha$  interface (pVHL:HIF-1 $\alpha$ ). The recently disclosed first lead-like small molecules disrupting this interaction were de-fragmented to assess the minimal pharmacophore for the interaction since pivotal components of the inhibitor's binding affinity had been mostly elusive to binding detection by standard screening procedures.

Isothermal Titration Calorimetry (ITC) experiments further defined the range of detection for the fragments. Fascinatingly Ligand-based NMR techniques (STD, CPMG and WaterLOGSY) accommodate the entire range of affinity contrasting with ineffective X-ray screening efforts.

We postulate that NMR is an invaluable tool to detect binders with such affinity and ligand efficiencies as found between protein surfaces and small molecules, contributing to higher hit rates at PPIs.

#### TH153: Interaction study of Bovine Serum Albumin (BSA) with guanyldrazones by Nuclear Magnetic Resonance

**Denise Cristian Ferreira Neto**, \*José Daniel Figueroa-Villar, Sirlene O. F. Azeredo, Elaine da C. Petronilho

*Military Institute of Engineering, Brazil.*

The interaction between biomolecules and ligands has aroused interest, being fundamental for design and evaluation of new potential drugs. In the last decades many researches have been involved on developed of procedures, including on NMR, to study how these interactions occurs. Albumin is a important protein, and its main function is transport and binding different substances, including drugs, in the blood. Substances that interact strongly with albumin present difficulty in their pharmacological function. However, molecules that do not interact with the albumin are likely to be destroyed by other proteins present in blood. Therefore, to display appropriate action, the drug must provide a medium interaction with albumin, a process that have been used by NMR with many molecules. Our research group developed inedited guanyldrazones as new potent antibiotics, which are effective against different bacteria. These compounds display good potential for treatment of intoxication with antibiotic resistant Gram negative bacteria, especially against *E. coli* ST131. In this work we study the interaction of bovine serum albumin (BSA) with guanyldrazones, via nuclear magnetic resonance (NMR), using as experimental measurements methods the effect on relaxation times ( $T_1$  and  $T_2$ ), saturation transfer difference (STD), nuclear Overhauser effect (NOE), and diffusion coefficients by diffusion ordered spectroscopy (DOSY). Preliminary results by NMR using the techniques described, showed appropriate changes on  $T_1$  and  $T_2$  of guanyldrazones interacting with albumin. These results are confirmed by diffusion coefficient variations and STD, indicating the interaction ligand-BSA. The preliminary results indicate that tested guanyldrazones are potentially stable and transported drugs bacterial infections and cancer.

Acknowledgments: CAPES, IMBEB and Brazilian Army.

#### MO154: Conformational Analysis of 9,10-Phenanthrenequinone Guanyldrazone by Nuclear Magnetic Resonance (NMR) and Molecular Modelling.

**Clara Simões**, \*José Daniel Figueroa-Villar, Sirlene O. F. Azeredo

*Military Institute of Engineering, Brazil.*

In this work we studied the conformational changes as a temperature function in 9,10-phenanthrenequinone guanyldrazone, a novel compound with potential antibiotic and

anticancer activity. This information is important to understand the form of interaction of this compound with DNA and with enzymes of microorganisms.

The molecule 9,10-phenanthrenequinone guanyldrazone has a C(NH<sub>2</sub>)<sub>2</sub> terminal group allowing the rotation of the amines. The structure was studied by NMR under different temperatures and the results confirmed that the amines rotation angle is achieved when the compound is submitted to a temperature above 33 °C. This result was confirmed by molecular modeling.

The interaction of this compound with oligonucleotides was studied by NMR using relaxation time ( $T_1$  and  $T_2$ ), diffusion coefficients (D) and chemical shifts, indicating that it is a DNA ligand.

ACKNOWLEDGEMENTS: CAPES, INBEB and Military Institute of Engineering.

### Natural Products and Small Molecules

#### TU155: The Keto-Enol-Equilibrium of Tetra-Acetones

<sup>3</sup>Queli Aparecida Rodrigues de Almeida, <sup>2</sup>Raphaella Teresa Sant'Anna, <sup>1</sup>Raquel Pantoja Barreiros Rodrigues, <sup>1</sup>Marcela Christina Oliveira Nogueira, <sup>2</sup>Sérgio de Paula Machado, <sup>2</sup>Roberto de Barros Faria, <sup>1</sup>\***Jochen Junker**

<sup>1</sup>Fundação Oswaldo Cruz - CDTS, <sup>2</sup>UFRJ - IQ, <sup>3</sup>IFRJ - IQ

The dimerization of di-acetones to tetra-acetones is a key step for the synthesis of highly substituted pyrroles. The tetra-acetones like 3,4-diacetyl-hexane-2,5-dione are not only very symmetrical, they also feature two highly acidic protons, which could form six membered rings if in the enol-form of the molecule. Further reactivity suggests that that tetra-acetone is mainly in enol-form, but this contradicts the literature.

Different from older literature, we could observe from <sup>1</sup>H NMR that in most solvents the enol-form is actually favored over the keto-form. This also has been confirmed by DFT calculations considering different solvents.

#### TH156: NMR Crystallography: Chemical Shift Driven Crystal Structure Determination of the Antibiotic Amoxicillin Trihydrate

\*Sérgio M. Santos, João Rocha, **Luís Mafra**

*Department of Chemistry, CICECO, University of Aveiro, Portugal*

The recent developments in the field of solid-state NMR spectroscopy (ssNMR) has lead to the emergence of NMR crystallography in which ssNMR data is used to derive the 3-dimensional crystal packing of powdered samples. In this communication, we report a new strategy for NMR crystallography of a molecular solid, in which ssNMR data, in the form of <sup>1</sup>H chemical shifts, enter directly in a structure generation step, and are further used in a refinement step as pseudo-forces acting on the models, driving them towards the final structure. This procedure was successfully applied to powdered amoxicillin trihydrate, a widely used  $\beta$ -lactamic antibiotic.

The methodology takes, as input, unit cell parameters, space group information and solid-state <sup>1</sup>H chemical shifts, and yields a final refined structure compatible with the input data. Processing of the data proceeds in 3 steps: (i) generation of an ensemble of structures; (ii) refinement of the generated structures; (iii) energy minimization of the refined structures. Step (i) employs a genetic algorithm where the fitness of each structure is given by  $E_{total} = E_{lattice} + E_{\delta}$ , where  $E_{lattice}$  is given by the General Amber Force Field (GAFF) force field and  $E_{\delta}$  is a term accounting for the deviation of the on-the-fly-calculated from the experimental chemical shifts.

The genetic algorithm yields, in step (i), a set of generated structures, which moderately obey the input data. In step (ii), these are refined by means of MD simulated annealing, governed by forces  $F_i = -\partial E_{total}/\partial r_i$ . Finally, in (iii) the structures are energy minimized using tight-binding density functional theory. In the whole process, Elattice is responsible for the physical and chemical validity of the generated structures, whereas  $E_\delta$  is responsible for imposing the experimental ssNMR restraints.

#### Acknowledgements

We thank FCT for financial support to project PTDC/QUIQUI/100998/2008 and for the post-doc grant SFRH/BPD/64752/2009. This work was financed by FEDER, via "Programa Operacional Factores de Competitividade – COMPETE", and by FCT (Portugal), PEst-C/CTM/LA0011/2011.

#### MO157: Integrated NMR-MS Approaches for Discovering New Metabolites and Metabotyping

\*Huiru Tang, Yulan Wang

Chinese Academy of Sciences, Wuhan

Metabolism represents all biochemical changes in biological processes and is the basic feature of living systems. Analysis of the metabolite composition (metabonome) is therefore an essential aspect of molecular phenotyping. The integrated NMR-MS techniques have shown great potential for new metabolite discovery and metabolic phenotyping (metabotyping). In this presentation, we will report some recent progresses in developments of the combined NMR/LC-MS metabonomic analytical methods for understanding the metabotypic alterations induced by various exosomic stresses. We will report some discoveries of various new plant secondary metabolites with novel skeletons and the combined NMR-MS approaches in conjunction with DFT calculations will be discussed for *de novo* absolute structure determination for these newly discovered natural products. We will further discuss current bottleneck of metabonomic analysis techniques and possible future developments in the NMR-based metabotyping methods with the effectiveness of integrated metabonomic analysis particularly reflected.

#### References:

- [1] Y. Tian, L.M. Zhang, Y.L. Wang, H.R. Tang, "Age-related topographical metabolic signatures for the rat gastrointestinal contents", *J. Proteome Res.* 11:1397-1411, 2012.
- [2] H.B. Liu, A.M. Zheng, H.L. Liu, H.Y. Yu, X.Y. Wu, C.N. Xiao, H. Dai, F.H. Hao, L.M. Zhang, Y.L. Wang, H.R. Tang, "Identification of three novel polyphenolic compounds, origanine A-C, with unique skeleton from *Origanum vulgare* L. using the hyphenated LC-DAD-SPE-NMR/MS methods", *J. Agric. Food Chem.*, 60:129-135, 2012.
- [3] H. Dai, C.N. Xiao, H.B. Liu, H.R. Tang, "Combined NMR and LC-MS analysis reveals the metabonomic changes in *Salvia Miltiorrhiza* Bunge induced by water depletion", *J. Proteome Res.*, 9:1460-1475, 2010.
- [4] H. Dai, C. Xiao, H. Liu, F. Hao, H.R. Tang, "Combined NMR and LC-DAD-MS analysis reveals comprehensive metabonomic variations for three phenotypic cultivars of *Salvia Miltiorrhiza*", *J. Proteome Res.* 9:1565-78, 2010.
- [5] H.R. Tang, C.N. Xiao, Y.L. Wang, "Important roles of the hyphenated HPLC-DAD-MS-SPE-NMR technique in metabonomics", *Magn Reson Chem*, 47:S157-S162, 2009.
- [6] C. Xiao, H. Liu, H. Dai, L. Tseng, M. Spraul, Y. Wang, H.R. Tang, "Rapid and efficient identification of some rosemary metabolites using HPLC-DAD-SPE-CryoNMR-MS method", *Chin. J. Magn. Reson.*, 26:1-16, 2009.
- [7] M. Li, B. Wang, M. Zhang, M. Rantalainen, S. Wang, H. Zhou, Y. Zhang, J. Shen, X. Pang, M. Zhang, H. Wei, Y. Chen, H. Lu, J. Zou, M. Su, Y. Qiu, W. Jia, C. Xiao, L.

Smith, S. Yang, E. Holmes, H.R. Tang, G. Zhao, J. Nicholson, L. Li, L. Zhao, "Human symbiotic gut microbes specifically modulate metabolic phenotypes" *PNAS*, 105:2117-2122, 2008.

[8] C. N. Xiao, H. Dai, H. B. Liu, Y.L. Wang, H. R. Tang, "Revealing the metabonomic variation of rosemary extracts using  $^1\text{H}$  NMR spectroscopy and multivariate data analysis. *Agric. Food Chem.*, 56:10142-10153, 2008.

[9] E. Holmes, R. Loo, O. Cloarec, M. Coen, H.R. Tang, E. Maibaum, S. Bruce, Q. Chan, P. Elliottm, J. Stamler, I. Wilson, J. Lindon, J. Nicholson, "Detection of urinary drug metabolite (Xenometabolome) signatures in molecular epidemiology studies via statistical total correlation (NMR) spectroscopy", *Anal. Chem.*, 78:2629-2640, 2007.

[10] E. Holmes, H.R. Tang, Y.L. Wang, C. Seger, "The assessment of plant metabolite profiles by NMR- based methodologies", *Plant. Med.* 72:771-785, 2006.

#### TU158: Studying the gem-diol generation in imidazole and pyridine aldehydes derivatives using NMR and X-ray crystallography

<sup>1,2</sup>Juan Manuel Lázaro Martínez, <sup>3</sup>Daniel Vega, <sup>1,4</sup>Gustavo Alberto Monti, <sup>1,4</sup>Ana Karina Chattah, <sup>2\*</sup>Graciela Yolanda Buldain

<sup>1</sup>IFEG-CONICET, <sup>2</sup>Universidad de Buenos Aires, <sup>3</sup>Comisión Nacional de Energía Atómica, <sup>4</sup>Universidad Nacional de Córdoba

The adduct formed upon addition of water to an aldehyde or ketone is called a hydrate or geminal diol (gem-diol). These compounds are rarely stable (and only in aqueous solution), i.e., the equilibrium is greatly dependent on the structure of the hydrate. Thus, formaldehyde in water at 20°C exists 99.99% in the hydrated form, while for acetaldehyde this figure is 58%, and for acetone the hydrate concentration is negligible. For that reason, the few stable crystalline hydrates known (such as polychlorinated aldehydes) are those that have a strongly electronegative group associated with the carbonyl group since, in general, the hydrates can seldom be isolated because they readily revert to the parent aldehyde.

The aim of the present work was to study the existence and stability of the aldehyde-hydrate form of some pyridine or imidazole carboxaldehyde derivatives commonly employed as reagents in the synthesis of active compounds (formylimidazoles and formylpyridines), using solution- and solid-state NMR experiments ( $^{13}\text{C}$  CP-MAS and  $^1\text{H}$ - $^{13}\text{C}$  HETCOR). In addition, some of the derivatives presented here were studied through single-crystal X-ray crystallography.

In particular, the 2-formylimidazole hydrate is a stable crystalline substance because, in order to revert to the aldehyde form, a water molecule must be left out, and this is difficult by the electron-withdrawing character of the imidazolium cation. That was probed since the 2-formylimidazole in  $\text{D}_2\text{O}$ -TFA solution evolved completely to its hydrated form (100%), however, the 4-formylimidazole and 4-methyl-5-formylimidazole existed 40% and 10% in the hydrated form, respectively.

Interestingly, single crystal for the hemiacetal derivative was obtained from *N*-methyl-2-formylimidazole in TFA solution and confirmed by X-ray diffraction techniques. In addition, the hydrate and hemiacetal form coexisted in the solid, after the completely removal of the TFA, according with the  $^{13}\text{C}$  CP-MAS results.

#### TH159: Complete $^1\text{H}$ and $^{13}\text{C}$ NMR Spectral Data Assignment of a new Nemorosinic Acid from *Clusia Nemorosa* (Clusiaceae)

<sup>1\*</sup>Mário Geraldo de Carvalho, <sup>1</sup>Rafaela Oliveira Ferreira, <sup>2</sup>Tania Maria S. da Silva

<sup>1</sup>Universidade Federal Rural do Rio de Janeiro,

<sup>2</sup> Universidade Federal Rural de Pernambuco

*Clusia nemorosa* Mey. is a tree widespread in the northeast region of Brazil, where it is popularly known as 'pororoca'. The previous studies of this species described some polyisoprenylated benzophenones and alkylarylketones, known as nemorosinic acids.[1] The phytochemical investigation of the dichloromethane extract from fruits of *C. nemorosa* allowed the isolation of a yellow gum identified as a new polyisoprenylated ketone, named as nemorosinic acid C (1). The complete proton and carbon NMR assignment of 1 was accomplished by 1D and 2D NMR spectra analysis, including COSY, HSQC and HMBC sequences. 30 mg of 1 were dissolved in MeOD<sub>4</sub>, placed in a 5mm NMR tube, and the spectra were obtained with a Bruker Avance III 500 spectrometer [500.13 MHz for <sup>1</sup>H and 125.77 for <sup>13</sup>C]. NMR spectra analysis of 1 and comparison of the data with those of nemorosinic acid B1 suggests a similar structure with a hydroxyl-isopropyl-furan group. The molecular formula was deduced as C<sub>31</sub>H<sub>44</sub>O<sub>7</sub> from its [M-H] at m/z 527 in the MS spectrum. Characteristic <sup>13</sup>C NMR resonances for a six-member ring consisting of two carbonyl groups [δ 205.5 (C-6) and 191.8 (C-2)], and three sp<sup>2</sup> carbons [δ 109.6 (C-3), 170.3 (C-4) and 103.4 (C-5)] besides one quaternary carbon [δ 60.8 (C-1)]. The <sup>1</sup>H NMR spectrum exhibits signals at δ 4.79 (H-23) of double bond, two vinylic methyl groups [δ 1.55 (H-25) and 1.48 (H-26)] and two allylic protons [δ 2.52 (H-22)], indicating the presence of one isopent-2-enyl group. Additionally, NMR analysis shows signals for one carboxyl function [δ 172.2 (C-21)], four vinyl carbons [δ 145.7 (C-14), 114.1 (C-15), 142.5 (C-18) and 127.5 (C-19)], two vinylic methyl group [δ 17.3 (C-16) and 12.3 (C-20)], two allylic methylene carbons [δ 40.4 (C-12) and 33.2 (C-17)] and one methine carbon [δ 44.2 (C-13)], which correspond to the presence of an oxidized lavandulyl chain. The cross peaks, observed in the HMBC spectrum, between methylene protons at C-22 (δ 2.52) and at C-12 (δ 2.24 + 2.11) with C-1 (δ 60.8) indicated that the isopentenyl and oxidized lavandulyl chain are attached to quaternary carbon C-1. The COSY, HMQC and HMBC data indicated the involvement of H<sub>3</sub>C-10,11 with C-9 (d 71,8) and CH-8(d 92,7) in a 2-(2-hydroxypropyl)-dihydrofuran ring. The cross peaks between methylene protons at C-7 (δ 2.91) and C-3 (δ 109.5) and C-4 (δ 170.3) indicated that the dihydrofuran ring is formed with C-3 and C-4. The additional signals at 196.5 (C), 40.7(CH), 26.6(CH<sub>2</sub>) and 11.9, 17.2 of two CH<sub>3</sub> justify the 1-hydroxy-1-iso isopentylene group (C-27–C-31). Thus, this analysis allowed to make the complete <sup>1</sup>H and <sup>13</sup>C NMR chemical shift assignment of 1, identified as a new compound named nemorosinic acid C.

#### REFERENCE

[1] Monache, F. D.; Monache, G. D.; Gács-Baitz, E. *Phytochemistry*, 1991, 30 (2), 703-705.

CNPq/CAPES/FAPERJ.

#### MO160: Complete <sup>1</sup>H and <sup>13</sup>C NMR Spectral Data Assignment of New Dammarane Saponin Isolated from *Siolmatra brasiliensis* (Cogn.) Baill (CUCURBITACEAE)

<sup>1</sup>\*Mário Geraldo de Carvalho, <sup>1</sup>Carlos Henrique Corrêa dos Santos, <sup>2</sup>Virginia Cláudia da Silva, <sup>2</sup>Paulo Teixeira de Sousa Júnior

<sup>1</sup> Universidade Federal Rural do Rio de Janeiro,  
<sup>2</sup> Universidade Federal de Minas Gerais

*Siolmatra brasiliensis* (Cogn.) Baill is popularly known as "tauiua" or "cipó taua" and often occurs in the central region of Brazil. The plant material was collected in Jangada, Mato Grosso State, Brazil. A voucher specimen is deposited at the herbarium of the Federal University of Mato Grosso do Sul, MS, Brazil, under the number CGMS: 31.643. The fractionation by solvent partition of the hydroalcoholic extract from the stem of this plant yielded the chloroform (SBCMC), ethyl acetate (SBCMA), and methanol (SBCMM) fractions. The fractionation of SBCMA on a silica gel column

(CC) yielded eight groups of the fractions after TLC analysis. The A<sub>7</sub> group was subjected to CC with flash silica gel and the fractions were analyzed by TLC and reunited in 4 groups. The fraction A<sub>73</sub> furnished a white solid that was analyzed by <sup>1</sup>H and <sup>13</sup>C NMR spectral data to define the structure which molecular formula was confirmed by ESI-MS. The dammarane triterpene skeleton was proposed by analysis of 1D and 2D NMR experiments, including <sup>1</sup>H and <sup>13</sup>C NMR (DEPTQ and DEPT-135 and DEPT-90), COSY, HSQC and HMBC pulse sequences, besides comparison with literature data of different part of the structure.[1,2,3] 30 mg of the saponin were dissolved in pyridine-d<sub>5</sub>, placed in a 5 mm NMR tube to obtain the spectra with a Bruker Avance III 500 spectrometer (500.13 MHz for <sup>1</sup>H and 125.77 for <sup>13</sup>C). In the analysis of these spectra, besides the number of CH<sub>3</sub>, CH<sub>2</sub>, CH and C carbon, the chemical shift values detected in the <sup>1</sup>H and <sup>13</sup>C NMR spectra, the corresponding <sup>1</sup>J<sub>HC</sub> in the HSQC, and the connection by <sup>2,3</sup>J<sub>HC</sub> of methyl group with CH-3, -5, -9, -13, -17 (δ<sub>CH</sub> 88.7, 56.2, 50.3, 42.3, 50.8, respectively) and C-10, -8, -14, -20 and -25 (δ<sub>C</sub> 36.8, 40.4, 50.5, 73.8, 131.9, respectively) allowed to define the dammarane skeleton. Besides the δ<sub>CH<sub>2</sub></sub> 75.06, three β-D-glucopyranoside were in agreement with other oxygenated carbons chemical shift values. The <sup>2,3</sup>J<sub>HC</sub> of H-1', with CH-3 (δ<sub>CH</sub> 88.7), H-1" with CH<sub>2</sub>-6' (δ<sub>CH<sub>2</sub></sub> 69.7), and H-1''' with CH<sub>2</sub>-26 (δ<sub>CH<sub>2</sub></sub> 75.06). All of these data, and the m/z 969.5384 (M + Na<sup>+</sup>) and 945.5463 (M - H), are in agreement with the molecular formula C<sub>48</sub>H<sub>82</sub>O<sub>18</sub>, of this new dammarane saponin, identified as 20-hydroxydammar-24-ene-3-O-β-D-gentiobiosyl-26-O-β-D-glucopyranoside, and allowed to make the complete proton and carbon-13 chemical shift assignment.

References: [1] Hu L., Chen Z., and Xie Y. *J. Nat. Prod.* 1996, 59, 1143-1145. [2] Orihara Y. and Furuya T. *Phytochemistry*, 1993, 34[4] 1045-1048. [3] Ky P. T., at all *Phytochemis try* 2010, 71, 994-1001.

Acknowledgment: FAPERJ / CNPq / CAPES / CPP and INAU-MT.

#### TU161: How useful is Inclusion of <sup>13</sup>C NMR Data into an Automated Structure Verification Algorithm?

<sup>1</sup>\*Sergey Golotvin, <sup>1</sup>Rostislav Pol, <sup>2</sup>Patrick Wheeler

<sup>1</sup>ACD Moscow, Moscow, Russia, <sup>2</sup>ACD/Labs, Toronto, ON

Automated Structure Verification (ASV) using the combination of 1D <sup>1</sup>H and 2D <sup>1</sup>H-<sup>13</sup>C single-bond correlation spectrum such as HSQC or HMQC is continuing to gain interest as a routine application for qualitative evaluation of large compound libraries produced by synthetic chemistry [1].

However this method is not always well suited for heterocycles or condensed aromatic structures; they offer a very limited number of correlations in HSQC spectra, and much spectral information is concentrated in unprotonated carbon positions. Ongoing progress in cryoprobe development and deployment has considerably shortened the time necessary to acquire directly detected 1D <sup>13</sup>C spectra. The progress makes it possible to acquire <sup>13</sup>C data in semi-routine fashion and thus expand the NMR dataset used for ASV.

This study highlights the advantages and disadvantages of addition of 1D <sup>13</sup>C data to the combination of 1D <sup>1</sup>H and 2D HSQC spectra for ASV activity. The overall performance of expanded NMR datasets (<sup>13</sup>C, <sup>1</sup>H and 2D HSQC) is evaluated against "standard" (1D <sup>1</sup>H and 2D HSQC) combined datasets using commercially available compounds. For comparison of accuracy of verification, false structures of spectroscopically similar isomers are generated by human and by software [2]. Of special interest are such performance metrics as the False Negative rate, in which correct structures are improperly rejected, and the False Positive rate, in which improper structures are passed through spectroscopic filters.

[1] "Automated structure verification based on a combination of 1D <sup>1</sup>H NMR and 2D <sup>1</sup>H<sup>13</sup>C HSQC spectra", MAG-

NETIC RESONANCE IN CHEMISTRY; Volume 45, Issue 10, October 2007, Pages: 803–813, Sergey S. Golotvin, Eugene Vodopianov, Rostislav Pol, Brent A. Lefebvre, Antony J. Williams, Randy D. Rutkowske and Timothy D. Spitzer

[2] "Concurrent combined verification: reducing false positives in automated NMR structure verification through the evaluation of multiple challenge control structures", MAGNETIC RESONANCE IN CHEMISTRY; Volume 50, Issue 6, June 2012, Pages: 429–435, Sergey S. Golotvin, Rostislav Pol, Ryan R. Sasaki, Asya Nikitina and Philip Keyes

#### TH162: Progressive Structuring of a Branched Antimicrobial Peptide on the Path to the Inner Membrane Target

<sup>1,2</sup>Bai Yang, <sup>2</sup>Roger W. Beuerman, <sup>1\*</sup>Konstantin Pervushin

<sup>1</sup>School of Biological Sciences, Nanyang Technological University, <sup>2</sup>Singapore Eye Research Institute

In recent years, interest has grown in the antimicrobial properties of certain natural and non-natural peptides. The strategy of inserting a covalent branch point in a peptide can improve its antimicrobial properties while retaining host biocompatibility. However, little is known regarding possible structural transitions as the peptide moves on the access path to the presumed target, the inner membrane. Establishing the nature of the interactions with the complex bacterial outer and inner membranes is important for effective peptide design. Structure-activity relationships of an amphiphilic, branched antimicrobial peptide (B2088) are examined using environment-sensitive fluorescent probes, electron microscopy, molecular dynamics simulations, and high resolution NMR in solution and in condensed states. The peptide is reconstituted in bacterial outer membrane lipopolysaccharide extract as well as in a variety of lipid media mimicking the inner membrane of Gram-negative pathogens. Progressive structure accretion is observed for the peptide in water, LPS, and lipid environments. Despite inducing rapid aggregation of bacteria-derived lipopolysaccharides, the peptide remains highly mobile in the aggregated lattice. At the inner membranes, the peptide undergoes further structural compaction mediated by interactions with negatively charged lipids, probably causing redistribution of membrane lipids, which in turn results in increased membrane permeability and bacterial lysis. These findings suggest that peptides possessing both enhanced mobility in the bacterial outer membrane and spatial structure facilitating its interactions with the membrane-water interface may provide excellent structural motifs to develop new antimicrobials that can overcome antibiotic-resistant Gram-negative pathogens.

#### References:

1. Bai, Y.; Liu, S.; Jiang, P.; Zhou, L.; Li, J.; Tang, C.; Verma, C.; Mu, Y.; Beuerman, R. W.; Pervushin, K., Structure-dependent charge density as a determinant of antimicrobial activity of peptide analogues of defensin. *Biochemistry* 2009, 48 (30), 7229–39.
2. Bai, Y.; Liu, S.; Li, J.; Lakshminarayanan, R.; Sarawathi, P.; Tang, C.; Ho, D.; Verma, C.; Beuerman, R. W.; Pervushin, K., Progressive structuring of a branched antimicrobial peptide on the path to the inner membrane target. *J Biol Chem* 2012, 287 (32), 26606–17.

#### MO163: Seneca 2.0: an open source, open data tool for Computer Assisted Structure Elucidation of small molecules.

Kalai Vanii Jayaseelan, Luis de Figueiredo, \*Christoph Steinbeck

*Chemoinformatics and Metabolism, European Bioinformatics Institute (EBI), Cambridge, UK*

Nuclear Magnetic Resonance (NMR) spectroscopy is the most informative analytical tool in natural product chemistry

and increasingly in metabolomics studies, to characterise the structural features of known and unknown metabolites in samples. Here we present Seneca 2.0, an enhanced version of Seneca 1.0 [1], a fully open-source java based cross-platform desktop application to perform stochastic CASE. The CASE engine uses the Chemistry Development Kit (CDK) [2], an open source java library, for the chemical structure representation and manipulation. We have implemented a new evolutionary algorithm scheme within Seneca 2.0, that performs successful CASE in a fully automated fashion. We will also present the evaluation of applying Natural product likeness [3] - a score for a given molecular structure based on a statistical model relying on the differences in occurrence of circular fingerprint of atoms in compound collections - in performing CASE.

#### References

[1] Steinbeck C, SENECA: A platform-independent, distributed, and parallel system for computer-assisted structure elucidation in organic chemistry. *J Chem Inf Comput Sci*. 2001

Nov-Dec;41(6):1500-7

[2] Steinbeck, C., Han, Y. Q., Kuhn, S., Horlacher, O., Luttmann, E., & Willighagen, E.

(2003). The Chemistry Development Kit (CDK): An open-source Java library for

chemo- and bioinformatics. *Journal of Chemical Information & Computer Sciences*,

43(2), 493–500.

[3] Jayaseelan, K.V., Moreno, P., Truszkowski, A., Ertl, P., & Steinbeck, C.(2011). Natural product-likeness score revisited: an open-source, open-data implementation. *BMC Bioinformatics*. 13:106.

#### TU164: Quantitative <sup>1</sup>H NMR Applied to Bioethanol Production

<sup>1</sup>Thiago I. B. Lopes, <sup>2</sup>Antônio M. Júnior, <sup>2</sup>Maria I. Berto, <sup>2</sup>Glauciane R.D. Silva, <sup>3</sup>Daniel I.P. Atala, <sup>1\*</sup>Anita J. Marsaioli

<sup>1</sup>State University of Campinas – UNICAMP, <sup>2</sup>Institute of Food Technology. Laboratory for Applied Microwave-LMA/GEPC, <sup>3</sup>British Petroleum

Greenhouse gas emissions and fossil fuel reservoir depletion increase the biofuel production appeal. Fermentation processes using yeasts to convert sugars to ethanol yield a mixture of ethanol, saccharides, yeast cells and unwanted byproducts (as lactate and acetate). Typically these processes are monitored by HPLC, here quantitative <sup>1</sup>H NMR was applied as an alternative method. The comparison between quantitative NMR and the reference method (HPLC) was performed using two sets of fermentation samples representing 8 hours of process monitoring. All samples were analyzed in triplicate. The test showed that <sup>1</sup>H NMR data are in good agreement with HPLC results and the comparison by linear regression and ethanol showed the best correlation ( $R = 0.9929$ ;  $LOQ = 4.248 \text{ g}\cdot\text{L}^{-1}$ ), followed by glucose ( $R = 0.9831$ ;  $LOQ = 7.055 \text{ g}\cdot\text{L}^{-1}$ ) and sucrose ( $R = 0.9791$ ;  $LOQ = 3.207 \text{ g}\cdot\text{L}^{-1}$ ). Additionally lactate, acetate and pyruvate were detected only by NMR method and these have quantification limits equal to 0.766; 2.316 and 0.291  $\text{g}\cdot\text{L}^{-1}$ , respectively. The results demonstrated that <sup>1</sup>H NMR can be used to monitor: i) amount of produced ethanol, ii) amount of remaining sugars (sucrose and glucose) in the fermentation broth and iii) concentration of byproducts and intermediates (lactate, acetate and pyruvate). Present method was fully validated (regarding accuracy, precision, selectivity, linearity and robustness) and presented many advantages compared to reference method: faster and larger number of monitored compounds.

ACKNOWLEDGEMENTS: FAPESP, CAPES, e CNPq

**TH165: Condensed Symmetry Structure: an approach for automatic assignment of NMR spectra**<sup>1</sup>Andrés Bernal, <sup>2</sup>Andrés M. Castillo, <sup>3</sup>Luc Patiny, <sup>4\*</sup>Julien Wist<sup>1</sup>Grupo de Química Teórica, Universidad Nacional de Colombia, Colombia, <sup>2</sup>Facultad de Ingeniería, Universidad Nacional de Colombia, Colombia, <sup>3</sup>Institute of Chemical Sciences and Engineering, Ecole Polytechnique Fédérale de Lausanne, <sup>4</sup>Chemistry Department, Universidad del Valle, Colombia

Full-search NMR assignment methods aim to score all possible assignments of a structure to an observed spectrum in order to choose the best. The main challenge of this methods consists in dealing with combinatorial explosion on the size of the solution space. We noticed that the suitability of an assignment on the light of any given property should remain invariant under permutations of nuclei/peaks with the same property value. As a consequence, assignments differing only by permutations of homotopic and enantiotopic nuclei are always equally adequate, since such nuclei have identical magnetic properties. Thus, rather than assigning the full chemical structure of the candidate molecule, we can assign a Condensed Symmetry Structure representation of the molecule (CSS) in which each vertex corresponds to a complete family of magnetically equivalent nuclei. This CSS contains the most relevant structural information that corresponds to the NMR spectra of the candidate molecule (some information related to multiplicity and chemical shift is lost).

A second consequence is that the less discriminant a property is, the faster it rejects suboptimal assignments, thereby motivating a strategy where lowly-discriminant properties are used first for quickly pruning the solution tree, whereas highly-discriminant properties are introduced latter to narrow it down to a few solutions. As a proof of concept, we have been evaluating a procedure that uses proton integrals for the early filter and 2D connectivities. We find that it is possible to efficiently discard most suboptimal solutions to the assignment problem, even in presence of peak overlap and artifacts, without any input other than the candidate structure, <sup>1</sup>H integrals, and COSY, HSQC and HMBC connectivities. Remarkably, in several cases a unique solution could be obtained without considering chemical shifts.

**MO166: Residual Dipolar Coupling as an additional NMR tool for defining the configuration of  $\alpha$ -Santonin**<sup>1\*</sup>Rubens Rodrigues Teles, <sup>1</sup>Fernando Hallwass, <sup>1,2</sup>José Adonias Alves de França<sup>1</sup>Universidade Federal de Pernambuco, <sup>2</sup>Instituto Federal de Alagoas

Recently, there have been developed a complementary methodology to the traditional NMR experiments applied to determine tridimensional structure or to solve assignment questions of small molecules, namely RDC (Residual Dipolar Coupling). This methodology is based on measuring anisotropic parameters, produced by partial molecular alignment. Consequently, all geometrical dependent parameters of the NMR Hamiltonian are partially recovered, providing useful additional structural information, when the experiments in isotropic media are not sufficient.

The aim of this work is to show how <sup>1</sup>H,<sup>13</sup>C RDC measurement, associated to the traditional NMR analysis, is fundamental to determine the correct stereochemistry of  $\alpha$ -Santonin -(3S,3aS,5aS,9bS)-3,5a,9-trimethyl-3a,5,5a,9b-tetrahydronaphtho[1,2-b]furan-2,8(3H,4H)-dione. The natural compound  $\alpha$ -Santonin belongs to the class of sesquiterpene lactone, with anti-helminthic and antipyretic activity. The literature reports that the  $\beta$ -isomer has pronounced antipyretic activity, compared to the  $\alpha$ -isomer. Moreover, this class of compounds has wide application as a precursor agent in photochemical synthesis for the production of new products with biological activity.

$\alpha$ -Santonin has 4 chiral centers, making it possible to draw sixteen diastereomers. The structures of these 16 diastereomers were optimized by molecular mechanic calculations at the DFT level of theory, using Gaussian03. The B3LYP functional along with the 6-311++G(d,p) basis set was used. One-dimensional and two-dimensional NMR experiments were performed (<sup>1</sup>H, <sup>13</sup>C, gCOSY, gHSQC, gHMBC, J-Resolved and NOESY). Moreover, coupled gHSQC experiments in isotropic and anisotropic media were carried out. PH gel was used as the alignment media.

Analyzing *J*-coupling and NOE data made it possible to select four suitable structures among the 16 diastereomers. Afterwards, the RDC values in the assay were included. Comparing the Q values of these four structures made it possible to select the correct structure.

In conclusion, RDC values are fundamental to achieve the correct tridimensional structure of  $\alpha$ -Santonin.

ACKNOWLEDGEMENTS: PRONEM/FACEPE/CNPq, PRONEX/FACEPE/CNPq, UFPE

**TU167: Candidate Structures Generated from Molecular Fragments that Match NMR Information**<sup>\*</sup>A.K. Velez-Jurado, I. Tischer, Julien Wist

Universidad del Valle

At present, the process of structural elucidation using nuclear magnetic resonance spectra (NMR) is a tedious task. There is a variety of work done in this field based on different approaches, e.g MS-Molgen, NMRShiftDB and SPECINFO make use of databases of NMR spectra, LSD performs a heuristic algorithm using logical rules and CASA validate the structure suggested by LSD. GENIUS predicts all possible molecular structures given a chemical formula, while StrucEluc accelerates the process using CASE "Computer-Aided Structure Elucidation" technique. This technique consists in taking as initial data any information available from the spectra obtained by NMR, IR and MS as multiplicity and chemical shifts to generate a set of chemical fragments. Structures that satisfy these restrictions are generated and ranked by the system exhaustively, simulating the spectra to compare with the initial spectrum.

Here, we developed an approach for the automatic structural elucidation using artificial intelligence methods, that build candidate structures compatible with NMR experimental data. Therefore, we created a database of 2032 molecular fragments obtained by taking apart 300 known molecules, to ensures that only "chemically" appropriate candidate are formed. As a first step, the structural information is extracted from <sup>1</sup>H, <sup>13</sup>C, TOCSY and HSQC spectra. This information is processed and randomized by a *Las Vegas* algorithm that searches the database for fragments compatible with these experimental data, connectivities and chemical shifts. These are represented as a covariance matrix that match the molecular formula. Candidates are then submitted to an algorithm of optimization randomly generates new feasible solutions from the initial candidates with selected fragments and a weight function that is updated with the simulation of the spectra. Finally, the proton spectra are simulated for the more promising candidates to rank them according on their degree of similarity with the experimental data.

**TH168: Structure elucidation by NMR of a furanocoumarin from the extract of *Simaba maiana* Casar. (Simaroubaceae)**<sup>1,2\*</sup>Edson de Souza Bento, <sup>1</sup>Isis Torres Souza, <sup>1</sup>Carla Karine Barbosa Pereira, <sup>1</sup>Erika Verena Figueiredo Cambui, <sup>1</sup>Antônio Euzébio Goulart Sant'Ana, <sup>2</sup>Geoffrey Ernest Hawkes<sup>1</sup>Universidade Federal de Alagoas, <sup>2</sup>Queen Mary University of London

*Simaba maiana* belongs to the family *Simaroubaceae* and is commonly used to treat stomach ulcer, cancer, malaria and gastrointestinal disorders. Previous studies with an ethanolic extract of *Simaba maiana* have indicated a molluscicidal activity against *Biomphalaria glabrata*. The compounds of the chloroform sub-fraction were isolated by a semi preparative HPLC system consisting of a C18 column (10 x 25 cm), gradient 60-100%B (30 min), 100-100%B (40 min) (A – ultrapure water, B – methanol), with a injection volume of 2 mL and a flow of 20 mL\*min<sup>-1</sup>. One of these compounds, here called SMC2, showed to be active in a molluscicidal test, and, analysis of 1D and 2D NMR spectroscopic data (<sup>1</sup>H, <sup>13</sup>C, COSY, HSQC, HMBC and NOESY) and comparison with literature data, gave evidence for the presence of a furanocoumarin with structure, corresponding to 4-[(3-Methylbut-2-en-1-yl)oxy]-7H-furo[3,2-g]chromen-7-one, and with molecular formulae C<sub>16</sub>H<sub>14</sub>O<sub>4</sub>. The NMR spectra were measured in CDCl<sub>3</sub>, at 300K, on a Bruker Avance NMR spectrometer, operating at frequency of 400,13 MHz, for hydrogen, using Bruker's standard pulse programs, in a direct observe probehead. The acquired NMR data were processed with the top-spin Bruker program and the chemical shifts were reported in δ (ppm) downfield to TMS. The structure here proposed was also confirmed by X-ray diffraction data.

CAPES, CNPq

#### MO169: NMR Analysis of intermolecular interactions of catechins in green tea (*Camellia sinensis*)

<sup>1,2</sup>Gloria Castañeda-Valencia, <sup>1,2\*</sup>Luzineide Wanderley Tinoco

<sup>1</sup>Universidade Federal do Rio de Janeiro, <sup>2</sup>Núcleo de Pesquisas de Produtos Naturais

Catechins are phenolic compounds extracted from plants and found in foods and beverages such as green tea. Several biological activities have been described for catechins as anti-cancer, antioxidants, etc. Although the aggregation of phenolic compounds has already been described, there is a lack of detailed information about the processes of catechins aggregation in samples of green tea. Intermolecular interactions could be identified as changes in chemical shifts, in the times of relaxation and translational diffusion coefficients. Our goal was to use NMR to follow the catechin aggregation process in green tea (*Camellia sinensis*). Lyophilized green tea infusion was prepared at concentrations of 0.5, 1, 2 and 5 mg/ml in D<sub>2</sub>O. <sup>1</sup>H NMR spectra and the relaxation times T<sub>1</sub> and T<sub>2</sub> measurements were carried out on Agilent VNMR-500 at 25 °C. Representative signals for catechins components: epigallocatechin gallate (EGCG), epicatechin (EC), epigallocatechin (EGC) and catechin (CATE) were identified in the <sup>1</sup>H NMR of green tea. It was observed a chemical shifts decrease with the concentration increase, mainly for H-3, H-2 and H-2' of EGCG; H-2, H-6 and H-2' of EGC, H-2' of EC and H-8, H-4α and H-2' of CATE. In the most concentrated sample (5 mg / mL) the broadening line and signals overlapping prevent the recognition of some hydrogens, which were clearly identified in the samples of 0.1 and 1 mg/mL. The relaxation times T<sub>1</sub> and T<sub>2</sub> for the representative hydrogens of EC, EGC and EGCG decrease with the concentration increase. The hydrogens of CATE showed an irregular behavior of the relaxation time according to concentration. These data indicate that catechins, even in the presence of other components present in green tea, undergo a process of aggregation, which should be taken into consideration in assessing the biological activity assays with green tea.

#### TU170: NMR Investigation of Keto-Enol Tautomerism of an Isobenzofuran-1(3H)-one Derivative

<sup>1\*</sup>Diego Arantes Teixeira Pires, <sup>2</sup>Wagner Luiz Pereira, <sup>1,3</sup>Claudia Jorge do Nascimento, <sup>4</sup>José Daniel Figueroa-Villar, <sup>2</sup>Róbson Ricardo Teixeira

<sup>1</sup>Instituto de Química, Universidade de Brasília, Brasil, <sup>2</sup>Departamento de Química, Universidade Federal de Viçosa,

Brasil, <sup>3</sup>Departamento de Ciências Naturais, Universidade Federal do Estado do Rio de Janeiro, <sup>4</sup>Departamento de Química, Instituto Militar de Engenharia, Brasil.

Keto-enol tautomerism is important in many fields of chemistry and biochemistry to better understand the structure of a compound, and it has been investigated for several research groups for a long time. Different studies applied to different systems have been shown that intra and intermolecular interactions, solvents, temperature, concentration and solvent dielectric constant have a strong influence on this equilibrium. In this work we studied the influence of different solvents (DMSO-*d*<sub>6</sub>, CDCl<sub>3</sub>, CD<sub>3</sub>OD and acetone-*d*<sub>6</sub>) and temperatures (ranging from 20-80 °C) on the NMR spectra of the 3-(2-hydroxy-4,4-dimethyl-6-oxocyclohex-1-enyl)isobenzofuran-1(3H)-one. This synthetic compound can inhibit both cancer cell proliferation (lymphoma and myeloid leukemia) and the photosynthesis process. The influence of an intramolecular hydrogen bond formation and the dynamic characteristics of this equilibrium (proton and carbon-13) were analyzed under different conditions.

ACKNOWLEDGEMENTS: CAPES/Embrapa (001/2011), CTEX, FAPEMIG, CNPq.

#### TH171: Discussing structural proposals by theoretical and experimental NMR

<sup>1</sup>Quêzia da Silva Sant'Anna, <sup>2</sup>Marcela Christina Oliveira Nogueira, <sup>1\*</sup>Jochen Junker

<sup>1</sup>Fundação Oswaldo Cruz - CDTS, <sup>2</sup>UFRRJ - IQ

The structure determination of natural products by NMR remains one of the biggest challenges in chemistry. Although NMR correlation data is relatively accessible, the interpretation can still be very hard. But, the use of NMR in this process is not only limited by the experimental part. Frequently molecules are found that are very similar in their constitution, and actually could not have been distinguished by NMR. In these cases complimentary methods are needed, that might be chosen based on the structural proposals.

The identification of such cases is a challenge on its own, and can only be achieved using computer software to interpret the experimental (or better theoretical) data. Over the past years we have found several of these molecules in the literature that deserve more attention. Some of the most challenging will be shown, together with suggested complimentary methods, as far as possible.

#### MO172: Antinociceptive and anti-inflammatory activity of the Oleanane-type triterpenoid

<sup>1\*</sup>Cláudia Quintino da Rocha, <sup>3</sup>Fabiana Cardoso Vilela, <sup>2</sup>Fabiana Cardoso Vilela, <sup>2</sup>Gustavo Prione Cavalcante, <sup>1,3</sup>Vinícius Ferreira Guimarães, <sup>2</sup>Marcelo Henrique dos Santos, <sup>2</sup>Alexandre Giusti-Paiva, <sup>1</sup>Wagner Vilegas

<sup>1</sup>Department of Organic Chemistry, Chemical Institute, Araraquara, Brazil., <sup>2</sup>Department of Pharmacy, Federal University of Alfenas-MG, Brazil, <sup>3</sup>Department of Biomedical Science, Federal University of Alfenas-MG, Brazil

Abe-01 was evaluated the analgesic and anti-inflammatory effects using two animal models. Carrageenan-induced paw edema and peritonitis were used to investigate the anti-inflammatory activity of Abe-01. The acetic acid-induced writhing, formalin and hot-plate tests were used to investigate its antinociceptive activity. At test doses of 5, 10 and 15 mg/kg p.o., Abe-01 had an anti-inflammatory effect as demonstrated by the reduction of paw edema induced by carrageenan and the inhibition of leukocyte recruitment. Abe-01 inhibited nociception induced by an intraperitoneal injection of acetic acid, observed by the decrease in the number of writhing episodes. Additionally, Abe-01 decreased licking time caused by a subplantar injection of formalin. Moreover, the hot plate test produced a increase in latency reaction, demonstrating an antinociceptive effect. The structure of



Abe-01 was identified by NMR  $^{13}\text{C}$ ,  $^1\text{H}$ , HMQC, HMBC, COSY, DEPT, IV and Ms

ACKNOWLEDGEMENTS: FAPESP, CNPq, UNESP E UNIFAL

#### TU173: Structure Elucidation of epimeric Acylphloroglucinols by NMR

<sup>1</sup>\*Renata Mendonça Araújo, <sup>2</sup>Edilberto Rocha Silveira, <sup>3</sup>Raimundo Braz Filho

<sup>1</sup>Instituto de Química, Universidade Federal do Rio Grande do Norte., <sup>2</sup>Centro Nordestino de Aplicação e Uso da RMN, Departamento de Química Orgânica e Inorgânica, Universidade Federal do Ceará., <sup>3</sup>Laboratório de Ciências Químicas, UENF - Departamento de Química, UFRRJ

Phytochemical study of *Harpalyce brasiliensis* revealed that this species is a promising source of geranyl phoroglucinol derivatives. Flash chromatography and HPLC analysis of the  $\text{CHCl}_3$  fraction from the ethanol extract of *H. brasiliensis*, permitted the isolation of two new epimers compounds **1** and **2** ( $\text{MF}: \text{C}_{22}\text{H}_{32}\text{O}_6$ ), named as *rel*-(2'*R*,3'*S*,6'*S*)-1-hexanoyl-2',4,6-tri-hydroxy-3'-methyl-3'-[3-hydroxy-4-methyl-pent-4-enyl]-benzo-dihydropyran and *rel*-(2'*R*,3'*S*,6'*R*)-1-hexanoyl-2',4,6-tri-hydroxy-3'-methyl-3'-[3-hydroxy-4-methyl-pent-4-enyl]-benzo-dihydropyran. Structural elucidation was established through spectroscopic techniques, including 1D and 2D NMR, acquired on a Bruker Avance DRX500 spectrometer, equipped with an inverse detection probe head with Z-gradient accessory working at 500.13 ( $^1\text{H}$ ) and at 125.77 MHz ( $^{13}\text{C}$ ).

The  $^1\text{H}$  and  $^{13}\text{C}$  NMR spectra of **1** displayed typical signals [106.2, 157.7, 101.1, 164.5, 96.1 ( $\text{CH}/\delta_H$  6.52), 166.7, 206.4, 27.2 ( $\text{CH}_2/\delta_H$  3.47 and 3.14), 66.8 ( $\text{CH}/\delta_H$  4.33), 82.0 (C-O)] of a 4,6-dihydroxy-benzo-dihydropyran system, with a carbonyl at C-1. The carbonyl exhibited correlations with both hydrogens at  $\delta_H$  3.33 (CH, dd,  $J = 16.4$ , 7.5 Hz) and 3.25 (CH, dd,  $J = 16.4$ , 8.0 Hz), in the HMBC spectrum. In addition, were observed successive correlations in the gs-COSY spectrum between this hydrogen at  $\delta_H$  3.33 with three methylenes at  $\delta_H$  1.84 (qt, 7.4 Hz), 1.45 (m) and 1.36 (qt, 7.5 Hz) and one methyl at  $\delta_H$  0.90 (t, 7.5 Hz), characterizing the hexanoyl moiety. The gs-COSY spectrum also showed correlations of the oximethine hydrogen at  $\delta_H$  4.44 (t, 6.0 Hz) with the methyl at  $\delta_H$  1.94 (sl), and the vinylidene hydrogens at  $\delta_H$  5.26 and 4.97, and with the methylene at  $\delta_H$  2.20 (m), identifying the 3-hydroxy-4-methylpent-4-enyl moiety, supported by the HMBC data. The compounds were distinguished by small differences in the chemical shifts and gs-NOESY analysis, due to the important NOE for the pentenyl moiety. A peracetyl derivative **3** was synthesized and its NMR was compatible with the proposed structure, also confirming the presence of four hydroxyl groups in both compounds.

#### TH174: Configurational and conformational preferences of an enaminone studied by NMR and theoretical calculation

\*Gil V. J. da Silva, Viviani Nardini

Departamento de Química, FFCLRP, Universidade de São Paulo

$\beta$ -Enaminones are important organic intermediates that present as characteristic structural feature a group  $\text{N}=\text{C}-\text{C}=\text{O}$ . Due to the tautomeric forms of  $\beta$ -enaminones as enol-imines, keto-imines and keto-enamines, these compounds may appear as two geometric isomers and their conformers *s-E* and *s-Z*.

In the development of a synthetic work, we prepared (5*Z*)-6-amino-1-(1,3-dioxan-2-yl)-3-hydroxy-3-methyloct-5-en-4-one. This  $\beta$ -enaminone has additional polar groups that may play a role in the configurational and conformational preferences of this compound.

Experimental and calculated NMR chemical shifts as well as experimental NOE and theoretical distance calculations were used for the stereochemical characterization of the compound as *Z s-E*.

ACKNOWLEDGEMENTS: FAPESP, CAPES, CNPq

#### MO175: Characterization by NMR of Triterpenes from Leaves *Inga Marginata*

\*Nerilson Marques Lima, Dulce Helena Siqueira Silva, Nivaldo Boralle

Universidade Estadual Paulista "Júlio de Mesquita Filho"

The investigation of *Inga marginata* leaves evidenced the presence of triterpenoids in its EtOH extract by  $^1\text{H}$  and  $^{13}\text{C}$  NMR data analysis.

NMR spectra were obtained in Varian-INOVA 500 instrument and the experiments were performed at 28 °C, using  $\text{CDCl}_3$  as solvent and internal standard. Pulse sequence s2pul, 45.0 degrees, relaxation delay of 1.000 seconds, acquisition time of 2.049 s, line broadening of 0.2 Hz and 16 repetitions were used for  $^1\text{H}$  NMR data acquisition, where as pulse sequence s2pul, 45.0 degrees, relaxation delay of 1.000 seconds, acquisition time of 1.300 seconds, line broadening of 0.5 Hz and 1088 repetitions were used for  $^{13}\text{C}$  NMR data acquisition.

The crude EtOH extract from *I. marginata* leaves was submitted to liquid-liquid partition and the Hexane fraction was analysed by NMR, which disclosed the presence of lupeol,  $\alpha$ -amyrin and olean-18-ene esters, in addition to fridelin. Characteristic signals were observed at 0.8 to 1.2 ppm in the  $^1\text{H}$  NMR spectrum for methyl groups in a triterpene skeleton. Additional signals at 4.68 ppm (bd,  $J = 2.1$  Hz) and at 4.56 ppm (dd,  $J = 2.1$  and 1.5 Hz) for the geminal protons of a terminal olefin evidenced the presence of lupeol. The presence of  $\alpha$ -amyrin was determined from  $^{13}\text{C}$  NMR data analysis, which showed signals at 124.3 and 139.4 ppm, associated to sp<sup>2</sup> carbons C12 and C13, respectively. Furthermore, fridelin was confirmed from the  $^{13}\text{C}$  NMR data analysis which showed a signal at 210.0 ppm for a carbonyl group and a signal at 6.80 ppm for a methyl group, typical of the triterpene fridelin. Additionally, signals at 142.4 ppm (C-18), 129.4 ppm (C-19), as well as the signals of methyl groups indicated the presence of an ester derivative of olean-18-ene in the hexane fraction of *I. marginata* leaves extract, and established its major constituents as triterpenes.

#### TU176: DOSY NMR of Flavonoids

\*Gabriel R. Martins, Mauro B. de Amorim, Antonio Jorge Ribeiro da Silva

Núcleo de Pesquisas de Produtos Naturais, UFRJ

Pulse Gradient Spin Echo experiments has been introduced as versatile tools for the study of compound mixtures without the recourse to chromatographic methods. Politi *et al*[1] applied Diffusion-edited  $^1\text{H}$  NMR (1D DOSY) for metabolic fingerprint analysis of crude commercial herbal tinctures. The 2D DOSY version allows the study of random translational motion of molecules in solution, arising from the thermal energy under conditions of thermodynamic equilibrium. The application of 2D DOSY sequences provides spatial labeling of spins and displacement monitoring generating information on self-diffusion of molecules in solution. Because of the relationship between diffusion rates and molecular radii the diffusion dimension reveals the distribution of molecular sizes and allows identification of different molecules in a mixture.[2] The term "NMR chromatography" is applied to regular application of 2D DOSY in the analysis of mixtures where the spectra displays chemical shifts in one dimension and diffusion rates in the other dimension.[3] Rodrigues *et al* took advantage of 2D DOSY to get preliminary identification of the components of the ethyl acetate fraction of ethanol extract from the aerial parts of *Bidens sulphurea*. [4]

As part of our continuing work on the analysis of polyphenols, we undertook a systematic study of DOSY of flavonoids. The chosen flavonoids were rutin, isoquercitrin, quercetin, morin and chrysin. In the present study we intended to verify the effect of rotational diffusion of the B ring in the DOSY of the flavonoids. Initial molecular modeling calculations indicated very low barriers to the rotation of ring B for chrysin, while for rutin, the volume of C-3 substituent would increase the barrier to rotation. We observed that the aspect of the signals relative to protons at C2', C3', C5' and C6' were affected by the rotation of ring B and that the rotation itself is dependent on temperature and steric effects.

Acknowledgements: CAPES, CNPq and FAPERJ

References:

- [1] Politti, M.; Zioh, M.; Pintado, M.E.; Castro, P.M.L.; Heinrich M. and Prieto, J.M. *Phytochemical Analysis* 20:328-334 (2009)
- [2] Parella, T, *Magnetic Resonance in Chemistry* 36:467-495 (1998)
- [3] Pemberton, C.; Hoffman, R.E., Aserin, A. and Garti, N. *Langmuir* 27:4497-4504 (2011)
- [4] Rodrigues, E.D.; da Silva, D.B.; Oliveira, D.C.R and da Silva, G.V.J, *Magnetic Resonance in Chemistry* 47:1095-1100 (2009).

### Chemometrics and metabolomics

#### TH177: NMR studies of infection: bacterial, sub-clinical in open heart surgeries and liver diseases

\*C.L. Khetrpal

*Centre of Biomedical Magnetic Resonance*

Continuous and rapid growth of NMR methodology and technology has been responsible for the exponential growth in the applications of the technique as a noninvasive tool for studying anatomy, structure and *in vivo* metabolism. However, developments of innovative techniques for understanding human diseases at molecular level are still in infancy and hence promise a bright future for research. Variations in metabolic profile resulting from disorders and clinical intervention at molecular level are more sensitive in identifying diseases in early stages and assessing the efficacy of the interventions.

NMR results on bacterial infections and those arising from open heart surgeries and liver diseases will be presented. For such studies results obtained from bio-fluids such as urine, serum, bile acids, and pericardial fluid which have very complex metabolic profiles with numerous structurally similar metabolites will be depicted. Specific metabolic signatures for different diseases from such investigations will be illustrated.

#### MO178: Potentials of metabonomics in Nano-drug screening

<sup>1</sup>\*Yulan Wang, <sup>1</sup>Limin Zhang, <sup>2</sup>Chunying Chen, <sup>1</sup>Huiru Tang

<sup>1</sup>Key Laboratory of Magnetic Resonance in Biological Systems and State Key Laboratory of Magnetic Resonance, <sup>2</sup>CAS Key Laboratory for Biomedical Effects of Nanomaterials and Nanosafety, National Center for Nanosafety

Metabonomics is the science that studies dynamic alterations of metabolites in a cell, organ or entire organism[1]. The definition of the metabonomics was first given in 1999 as "the quantitative measurement of the time-related multiparametric metabolic response of living systems to pathophysiological stimuli or genetic modification"[2]. Technically, metabonomics investigations usually consist of the collection of metabolic profiles using nuclear magnetic resonance spectroscopy or mass spectrometry techniques and analysis

of the collected data using appropriate multivariate statistical techniques. <sup>1</sup>H NMR spectroscopy facilitates the detection of a wide range of low molecular weight metabolites commonly found in tissues and biofluids including urine and blood plasma. It typically generates thousands of resonance signals that can be related to the response of biological systems to perturbation of the system via pathological events. Due to the high density of the spectroscopic data, it is desirable to characterize these modulations by application of multivariate statistical data analysis so as to reduce the complexity of these data and to facilitate visualization of inherent patterns in the data. Various multivariate statistical data analyze, including projection methods such as principal components analysis (PCA) and projection to latent structures (PLS) based methods[3]. Since the birth of metabonomics, it has been proven to be an extremely powerful analytical tool and hence found successful applications in many research areas including molecular toxicology[4,5], pathology, physiology, functional genomics and environmental sciences. In this presentation, examples of metabonomics application in toxicity will be given and some potentials of this technique in the area of nano-sciences will be outlined.

[1] Tang, H. R., et al., *Metabonomics: a revolution in progress*. *Prog Biochem Biophys* 2006, 33 (5), 401-417.

[2] Nicholson, J. K., et al., 'Metabonomics': understanding the metabolic responses of living systems to pathophysiological stimuli via multivariate statistical analysis of biological NMR spectroscopic data. *Xenobiotica* 1999, 29 (11), 1181-1189.

[3] Trygg, J., Wold, S., *Orthogonal projections to latent structures (O-PLS)*. *J. Chemometr.* 2002, 16, 119-128.

[4] Zhao, X. J., et al., *Dynamic Metabolic Response of Mice to Acute Mequindox Exposure*. *J Proteome Res* 2011, 10 (11), 5183-5190.

[5] Zhang, L. M., et al., *Systems Responses of Rats to Aflatoxin B1 Exposure Revealed with Metabonomic Changes in Multiple Biological Matrices*. *J Proteome Res* 2011, 10 (2), 614-623.

#### ACKNOWLEDGEMENTS:

We acknowledge financial supports from National Basic Research Program of China (2012CB934004, 2011CB933401, 2009CB118804) and the National Natural Science Foundation of China (20825520, 21221064, 31070854).

#### TU179: Structure-dependence for the Molecular Dynamics of Metabolites

Jing Huang, Pingping Ren, Limin Zhang, \*Huiru Tang

*Chinese Academy of Sciences, Wuhan*

Molecular dynamics of metabolites are important for their interactions and biological functions in both biology and for their potential applications as natural materials. To understand the relationship between metabolite structure and dynamics, we comprehensively investigated the molecular motions of three sets of structurally related metabolites (sarcosine, N,N-dimethylglycine, betaine,  $\beta$ -alanine,  $\gamma$ -aminobutyrate, 5-aminovaleate, 6-aminocaproate,  $\alpha$ -aminobutyrate, methylamine, dimethylamine, trimethylamine and trimethylamine oxide) by measuring their <sup>13</sup>C CPMAS NMR spectra, the <sup>13</sup>C and <sup>1</sup>H spin-lattice relaxation times ( $T_1$ ,  $T_{1\rho}$ ), CSA and DIPSHIFT properties as a function of temperature.

We found that three-fold reorientations of CH<sub>3</sub> and NH<sub>3</sub> groups were dominant molecular motions in most of these molecules. The re-orientation of whole trimethylamine groups was detectable in betaine and its hydrochloride salt. Whilst similar rotational properties were observable for two methyl groups in N,N-dimethylglycine and for three methyl groups in betaine anhydrous, three methyl groups in betaine hydrochloride had completely different motional properties. The proton  $T_1$  measurements detected a polymorphic phase

transition for DMG at 348.5 K. The DIPSHIFT experiments showed that CH<sub>3</sub> and CH<sub>2</sub> moieties in the N-methylated glycines had dipolar dephasing properties similar to these moieties in alanine and glycine, respectively. The activation energies for CH<sub>3</sub> rotations increased with the increase of the number of substituted methyl groups. The amino groups and backbone reorientations were major motions for  $\omega$ -amino acids except for  $\beta$ -alanine. The activation energies for amino group were positively correlated with the strength of hydrogen-bonds involving these groups in the crystals and the carbon-chain lengths whereas such energies for the backbone motions were inversely correlated with the carbon-chain lengths. Molecular dynamics is associated with two polymorphic transitions in  $\alpha$ -amino-n-butyric acid (ABA). Both proton and <sup>13</sup>C relaxations showed that, apart from two motions corresponding to the reorientations of methyl and amino groups, ethyl motion ( $E_a$ , 16–21.5 kJ/mol) was also present in ABA. DIPSHIFT results further revealed the molecular dynamics of different polymorphs and associations between motions and polymorphic transitions. These findings provided essential information for molecular dynamics of these metabolites and for understanding the structural dependence of molecular dynamics.

## References:

- [1] J. Huang, L. Jiang, P. Ren, L. Zhang, H.R. Tang, *J Phys Chem B*, 116:136–146, 2012.
- [2] J. Huang, L.M. Zhang, H.R. Tang, *J Phys Chem B*, 116:2096–2103, 2012.
- [3] P. Ren, D. Reichert, Q. He, L. Zhang, H. Tang, *J Phys Chem B*, 115:2814–2823, 2011.
- [4] D. Reichert, M. Koverman, N. Hunter, D. Hughes, O. Pascui, P. Belton, *PCCP*, 10:542, 2008.
- [5] H.R. Tang, Y.L. Wang, P. Belton, *Phys Chem Chem Phys*, 3694–3701, 2004.
- [6] Y. L. Wang, H.R. Tang, P. S. Belton, *J Phys Chem B*, 106:12834–12840, 2002.
- [7] H. R. Tang, P. S. Belton, *Solid State NMR.*, 21:117–133, 2002.
- [8] Tang, H. R.; Belton, P. S. *Solid State NMR*. 1998, 12:21
- [9] M. Hong, J. D. Gross and R. G. Griffin. *J Phys Chem B*, 101:5869–5874, 1997; C. A. McDowell, P. Raghunathan, D. S. Williams, *J Chem Phys*, 66:3240–3245, 1977.

#### TH180: Application of MRI and MRS in obesity research with mice

<sup>1,2\*</sup>Luciana Caminha Afonso, <sup>1,2</sup>S Neschen, <sup>1,2</sup>Helmuth Fuchs, <sup>1,2</sup>Valérie Gailus-Durner, <sup>1,2,3</sup>Martin Hrabě de Angelis

<sup>1</sup>Helmholtz Zentrum München, <sup>2</sup>German Center for Diabetes Research, <sup>3</sup>Technical University Munich

Characteristics of a diet can directly affect health, playing an important role in preventing or inducing of the development of diseases. Chronic consumption of high amounts of fat results in obesity. This excess of body fat increases the risk of cardiovascular diseases, type 2 diabetes and some cancers.[1,2,3]

Since decades research on mice is helping to understand several human biological processes, such as hematopoiesis, immunity, infectious diseases, cancers, etc.[4]

This work is was carried out in the facilities of the German Mouse Clinic.[5] Two groups of mice were fed with different diets. One diet has been enriched with safflower oil (composed mainly by polyunsaturated fatty acids), whereas the other has been enriched with lard (composed mainly by monounsaturated and saturated fatty acids).

The mice were analyzed using a multipurpose research system, Bruker Biospec 94/20 (Bruker Biospin), equipped with

a 9.4T horizontal magnet, 20 cm bore. All mice livers were analyzed before starting the high fat diet; then, 3 weeks, 6 weeks and 12 weeks after starting the high fat diet.

The measurements consisted of: a Turbo-RARE sequence (TE= 19.5 ms, TR= 743.9 ms) to image the whole liver for estimating the liver size and a STEAM sequence (TE= 3 ms, TR= 1500 ms) for the spectroscopic investigation of the liver fat deposition.

The preliminary results show a progressive increase in the liver lipid levels for all mice and a liver augmentation due to fat deposition. Further results are under analysis.

## References

1. Wahrburg, U. (2004) What are the health effects of fat? *Eur. J. Nutr.* 43(I), pp. 6
2. Key, T.J., Schatzkin, A., Willett, W.C., Allen, N.E., Spencer, E.A., Travis, R.C. (2004) Diet, nutrition and the prevention of cancer. *Public Health Nutr.* 7(1A), pp. 187
3. Lunati, E., Farace, P., Nicolato, E., Righetti, C., Marzola, P., Sbarbati, A., Osculati, F. (2001) Polyunsaturated fatty acids mapping by <sup>1</sup>H MR-Chemical Shift Imaging. *Mag. Res. in Med.* 46, pp.879
4. Schultz, L.D., Ishikawa, F., Greiner, D.L. (2007) Humanized mice in translational biomedical research. *Nat. Rev. Immunol.* 7, pp. 118
5. Gailus-Durner, V., Fuchs, H. et al (2005) Introducing the German Mouse Clinic: open access platform for standardized phenotyping. *Nat. Meth.* 2(6), pp. 403

#### MO181: <sup>13</sup>C-biomass characterization by data mining of solid/solution NMR

<sup>1,2,3,4\*</sup>Jun Kikuchi, <sup>1,4</sup>Eisuke Chikayama

<sup>1</sup>RIKEN Plant Science Center, <sup>2</sup>Biomass Engineering Program, RIKEN, <sup>3</sup>Nagoya University, <sup>4</sup>Yokohama City University

Plant biomass is now highlighted by view points both basic and applied science such as biorefinery materials [1,2]. It consists polysaccharides and lignin, both are so difficult biomacromolecules in terms of tackling by NMR. Major difficulties are attributed to their low solubility, mixture complexity and low spectral dispersion. In order to "escape" the problem for mixture complexity, firstly we tried NMR experiments using <sup>13</sup>C labeled cellulose. Several solid-state NMR measurements (VPCP, 2D-INADEQUATE and DARR), as well as solution-NMR (2D-HSQC and HSQC-NOESY) were employed for ionic-liquids solubilized and regenerated samples, then statistical multivariate analysis were useful approach to monitor structural variations [3–5]. Next target should be tackling to the mixture complexity, therefore we applied <sup>13</sup>C-labeling techniques developed for plant systems [6–10]. High level of <sup>13</sup>C-incorporation enabled both 2D and 3D-NMR experiments, therefore we have been succeeded several new signal assignments that have not been reported previously (Komatsu et al. to be submitted). Our current limitations both <sup>13</sup>C-labeling as well as solid/solution NMR measurements will be discussed in the conference.

## References

1. Kikuchi et al. (2011) *J. Ecosys. Ecogr.* S2, e001.
2. Ogata et al. (2012) *PLoS ONE* 7, e30262.
3. Okushita et al., (2012) *Biomacromolecules* 13, 1323–1330.
4. Mori et al. (2012) *Carbohydr. Polymers* 90, 1197–1203.
5. Okushita et al. (2012) *Polymer J.* 44, 895–900.
6. Kikuchi et al., (2004) *Plant Cell Physiol.*, 45, 1099–1104.
7. Kikuchi et al., (2007) *Method Mol. Biol.* 358, 273–286.
8. Tian et al., (2007) *J. Biol. Chem.* 282, 18532–18541
9. Sekiyama et al. (2010) *Anal. Chem.* 82, 1643–1652.

10. Sekiyama et al. (2011) Anal. Chem. 83, 719-726.

### TU182: Deciphering Cancer Metabolism by NMR

\*Ulrich L. Günther, John Carrigan, Christian Ludwig, Farhat Khanim, Chris Bunce

*University of Birmingham*

Metabolism and cancer have been associated for a long time, starting with Otto Warburg who discovered that cancer cells metabolise glucose in a manner distinct from normal tissues, forming lactate, even in the presence of sufficient oxygen. While Warburg saw this as a cause of cancer, developments in cancer biology painted a different picture, linking cancer to altered signaling and cell cycle control. During this development the aspects of metabolism were almost completely disregarded, if not rejected. Recent research supports a pronounced role of altered metabolism in cancers, often induced by hypoxic conditions, which can considerably alter oxidative phosphorylation and other mechanisms.

We have analyzed acute myeloid leukemia cell (AML) lines using NMR metabolomics and tracer based metabolic flux analysis. In our analysis we looked at the effect of a drug combination (Bezalip and medroxyprogesterone acetate) [1] which drive AML cells either into re-differentiation or into apoptosis, showing that this treatment acts by generating large levels of reactive oxygen species (ROS). Using  $^{13}\text{C}$ -labeled glucose and glutamate as metabolic tracers we can decipher the effect of ROS, which leads to the formation of new metabolites, specifically malonate, which is in itself potent inhibitor of succinate dehydrogenase.

This analysis also shows how NMR can be used to decipher metabolism, by observing site specific label incorporation, using either signal intensities or  $^{13}\text{C}$ - $^{13}\text{C}$ -couplings.

[1] S Tiziani, A Lodi, M Viant, C Bunce, U Günther. Metabolomic profiling of drug responses in acute myeloid leukaemia cell lines. PloS ONE, 4(1), 4251 (2008).

### TH183: MetaboLights: Towards a new COSMOS of metabolomics data management and dissemination

<sup>1,2\*</sup>Reza Salek, <sup>1</sup>Kenneth Haug, <sup>1</sup>Pablo Conesa, <sup>1</sup>Mark Williams, <sup>1</sup>Tejasvi Mahendrakar, <sup>3</sup>Eamonn Maguire, <sup>3</sup>Alejandra González-Beltrán, <sup>3</sup>Philippe Rocca-Serra, <sup>3</sup>Susanna-Assunta Sansone, <sup>2</sup>Jules Griffin, <sup>1</sup>Christoph Steinbeck

<sup>1</sup>European Bioinformatics Institute, Wellcome Trust Genome Campus, Hinxton, Cambridgeshire, <sup>2</sup>University of Cambridge, Department of Biochemistry and Cambridge Systems Biology Centre, Cambridge, <sup>3</sup>University of Oxford e-Research Centre, Oxford, UK

MetaboLights is a general-purpose, open-access curated repository for metabolomic experiments. Metabolomics is investigation of the small molecular or metabolites response in a cell, tissue or biofluid to an environmental stress, the result of cellular processes or response to disease. Metabolomics studies are growing rapidly and there is a great need to share and disseminate data, making data accessible to public as is increasingly being required by funding organisations and journals. MetaboLights would be the medium to capture the NMR and Mass spectrometry metabolomics experiments including raw experimental data, processed and transformed data and associated metadata. There are wide varieties of proprietary file formats by different instrument vendors in use, hence there is a need for open source file formats and standardization of data. Having a standardized way of exchanging data is of immense importance to making vendor neutral metabolomics portals to automatically visualize and analyse metabolomics-data in web applications (i.e. as planned for MetaboLights). Therefore an EU coordination action initiative for developing metabolomics standards in the EU and worldwide, called COordination of Standards in MetabOmicS - COSMOS (<http://cosmos-fp7.eu>), based on Metabolomics standard

initiative (MSI, [1]) was formed. The MetaboLights ([2], <https://www.ebi.ac.uk/metabolights/>) team is coordinating this consortium of 14 European partners, with MetaboLights playing a central role for the proposed work. A key aspect of this effort aims to develop efficient policies ensuring that metabolomics data is encoded in open standards, tagged with a community-agreed and complete set of meta-data, supported by a communally developed set of open source data management and capturing tools, disseminated in open-access databases adhering to these standards, supported by vendors and publishers, who require deposition upon publication, and properly interfaced with data in other biomedical and life science e-infrastructures. Our aim is to deliver the exchange formats and terminological artifacts needed to describe, exchange and query metabolomics experiments, using the ISA-Tab [3] as core for the description of experiments and building additional 'layers' for the data matrices. We wish to ensure that the proposed standards are widely accepted by involving major global players in the development process. We will also develop and maintain exchange formats for raw data and processed information (identification, quantification), building on experience from standards development within the Proteomics Standards Initiative ([4], PSI). Additionally we are planning to collaborate on developing the missing open standard NMR Markup Language (nmrML) for capturing and disseminating Nuclear Magnetic Resonance spectroscopy data in metabolomics. We aim to explore semantic web standards that facilitate linked open data (LOD) throughout the biomedical and life science realms, and demonstrate their use for metabolomics data.

Database URL: <http://www.ebi.ac.uk/metabolights>

[1] Goodacre, R., et al., Proposed minimum reporting standards for data analysis in metabolomics. Metabolomics : Official journal of the Metabolomic Society, 2007. 3(3): p. 231-241

[2] Haug, K., et al., MetaboLights—an open-access general-purpose repository for metabolomics studies and associated meta-data. Nucleic Acids Research, 2012.

[3] Rocca-Serra, P., et al., ISA software suite: supporting standards-compliant experimental annotation and enabling curation at the community level. Bioinformatics, 2010. 26(18): p. 2354-6.

[4] Taylor, C.F., et al., The work of the Human Proteome Organisation's Proteomics Standards Initiative (HUPO PSI). Omics : a journal of integrative biology, 2006. 10(2): p. 145-51

### MO184: $^1\text{H}$ -MAS NMR metabolomics investigation of human breast cancer; enhancing the results using data fusion approaches with GC and LC mass spectrometry data

<sup>1,7\*</sup>Reza Salek, <sup>2</sup>Michael Eiden, <sup>1</sup>Cecilia Castro, <sup>3</sup>Carsten Denkert, <sup>4</sup>Sibylle Loibl, <sup>5</sup>Matej Oresic, <sup>6</sup>Oliver Fiehn, <sup>1,2</sup>Jules Griffin

<sup>1</sup>Department of Biochemistry and Cambridge Systems Biology Centre, University of Cambridge, UK, <sup>2</sup>Elsie Widowsdon Laboratory, Cambridge, UK, <sup>3</sup>Institute of Pathology, Charité – Universitätsmedizin Berlin, Germany, <sup>4</sup>GBG Forschungs GmbH - Neu-Isenburg, Germany, <sup>5</sup>VTT Technical Research Centre of Finland, Finland, <sup>6</sup>Genome Center, University of California Davis, CA, USA, <sup>7</sup>European Bioinformatics Institute, Wellcome Trust Genome Campus, Hinxton, Cambridgeshire

Breast cancer is the most common malignant tumor in women worldwide, while the disease is curable in the early stages, about 50% of the patients with stage II or III tumours require potential systemic therapy and are in need of better biomarkers for diagnosis. METAcancer project ([www.metacancer-fp7.eu](http://www.metacancer-fp7.eu)), an EU Framework 7 funded project, was setup to determine new metabolic biomarkers of breast cancer to predict grade and hormonal status of breast tumours using  $^1\text{H}$ -

MAS NMR spectroscopy, gas chromatography (GC)-MS and liquid chromatography (LC)-MS, in addition to histological characterisation of the tumours. Our work package task was to acquire data from tumour tissue using HRMAS  $^1\text{H}$  NMR spectroscopy using a 11.7 Tesla Superconducting magnet. Tissue samples were cut, if required, and packed inside 4 mm Zirconium oxide rotors with Teflon caps and kelf CRAMP inserts (total sample volume of 50  $\mu\text{L}$ ) and the remaining volume was filled with phosphate buffered  $\text{D}_2\text{O}$ . The rotor was spun at 5 kHz at  $27^\circ\text{C}$ . The dataset was acquired using a Bruker Avance III spectrometer, equipped with a  $^1\text{H}/^{13}\text{C}$  high-resolution magic angle-spinning (HRMAS) probe. Two different NMR pulse programs, a one-dimensional NOESY presaturation pulse sequence and  $T_2$  filter Carr-Purcell-Meiboom-Gill (CPMG) experiments (to minimize spectral broadening due to lipids) with solvent presaturation, were carried out for each sample. Both experiments were acquired with 128 scans into 64K data-points across spectral width of 16.00 ppm, using a relaxation delay 1.5s and acquisition time of 4.09 s at a proton frequency of 500.3 MHz. For the acquisition of CPMG spectra a total spin echo delay of 400 ms was used. Multivariate pattern recognition techniques were used for NMR data analysis using SIMCA-P+ 12.0 (Umetrics AB, Umeå, Sweden) with the data mean centred and Pareto scaled prior to analysis. Data analysis results proved to be highly discriminatory between tumours, healthy breast tissue and healthy duct tissue. In addition we were able to discriminate between different tumour grades (specifically grade 2 from grade 3) as well as different tumour types (Type 2 from Type 4 demonstrated the best discrimination). In addition we have used several different data fusion approaches to elucidate the combined potential of the multiple profiling techniques for the diagnosis and classification of breast cancer. We systematically tested correlation based approaches, orthogonal projections multivariate data analysis and multi-block principal component analysis data fusion approaches [1] on a combined dataset of  $^1\text{H}$  HR-MAS NMR, GC-MS and LC-MS measured on a cohort of 300 breast cancer patients with regard to various data pre-processing schemes and compared the outcomes. On the level of individual platforms it became obvious, that the differentiation between healthy and diseased samples is often hampered by the heterogeneity of the tissue sample (specifically due to the fat content), with individual platforms being affected to different extents. In comparison, it showed that Multi-Block PCA, as an unsupervised technique aiming to find the common structure inherent across the platforms, was able to differentiate between healthy and diseased subjects. Inspecting the individual block loadings, revealed that choline and phosphocholine metabolites measured by NMR spectroscopy demonstrated similar trends to PC 16:0-18:1 by LC-MS. Both metabolites contributed most to the observed separation of cancer from normal tissue, which is in accordance with current findings in the literature [2, 3]

[1] Bro, R., F. van den Berg, et al. (2002). "Multivariate data analysis as a tool in advanced quality monitoring in the food production chain." *Trends in Food Science & Technology* 13(6-7): 235-244.

[2] Katz-Brull, R., R. Margalit, et al. (1998). "Choline metabolism in breast cancer:  $2\text{H}$ -,  $^{13}\text{C}$ - and  $^{31}\text{P}$ -NMR studies of cells and tumors." *MAGMA* 6(1): 44-52.

[3] M. Hilvo, et. al, "Novel theranostic opportunities offered by characterization of altered membrane lipid metabolism in breast cancer progression", *Cancer Res.* (2011). doi: 10.1158/0008-5472.CAN-10-389

#### **TU185: Impact of nutrient solution recycling on the metabolic content of tomato fruit: a HRMAS NMR study**

\*Maria José Iglesias Valdés-Solis, Jesús García López, Juan Fernando Collados Luján, Fernando López Ortiz

Almería University

Hydroponic production permits good control of plant growth and development even where no suitable soil exists and/or there is limitation of water resources. Classical soilless culture causes environmental problems that can be reduced by partial recycling of the drainage solutions. However, this can produce nutrient imbalances affecting crop yield. This problem is minimized by using the *New Growing System* NGS<sup>®</sup>, a pure hydroponic production system based on the recirculation of nutrient solution through multilayer polyethylene troughs on a close system. Compared to traditional intensive farming, it has many advantages in relation to costs, profitability, quality of production and environment. The better guarantee for product quality and sustainable production requires characterization of biochemical composition. This aspect of NGS<sup>®</sup> utilization has been, however, scarcely studied.

This work is aimed at examining the effect of the hydroponic system NGS<sup>®</sup> on the metabolic content of tomato fruit using HRMAS NMR methods. Two commercial flavor varieties (marmande type) "Tigre" and "Raf", the reference cv. for the investigations in the line of tomato taste in Almería (Spain), were chosen. Tomatoes were harvest under commercial culture conditions in green-house and the fruits were hand-picked at the stage commonly marketed during the months of January, February, March and May. "Tigre" variety was grown in both sand-covered soil traditionally in the area (TS) and in hydroponic NGS<sup>®</sup> (TN) whereas "Raf" tomatoes only in soil (RS).

$^1\text{H}$  HRMAS NMR spectra were measured on tomato purée samples from fresh tomatoes. The data were analyzed by a combination of PLS and integration of selected signals (Assigned Signal Analysis, ASA). Compositional differences between the two varieties grown in soil can be associated to genetic variations that are also reflected in differences in shape and taste. Hydroponic culture affects significantly the metabolic content of the fruits and compositional differences between TN and RS samples decrease in some extension. The results obtained also point that malic acid may be a good marker in order to differentiate "Tigre" tomatoes.

#### **TH186: Metabolomic approach in mapping Huanglongbing markers**

<sup>1</sup>William Ohashi, <sup>1</sup>Ana Paula Espindola, <sup>2</sup>Helvecio Della Colletta Filho, <sup>1\*</sup>Ljubica Tasic

<sup>1</sup>DQO, IQ, UNICAMP, Campinas, SP, Brazil, <sup>2</sup>IAC, SP, Brazil

Key words: metabolomics, oranges, huanglongbing, biomarkers

Brazil is the major orange producer and exporter in the world. Unfortunately, Brazilian production suffers millions of dollars in damage annually due to phytopathogenic microorganisms. One of the major diseases to affect Brazilian orchard is Huanglongbing. This disease caused trough infection with the bacterium *Candidatus Liberibacter asiaticus* was first detected in Sao Paulo in 2004 and is transmitted by insects. Herein, we are looking for biomarkers of the early disease onset. At this stage of our research, we are comparing young and adult leaves of healthy, symptomatic and asymptomatic plants. The leaves extracts were obtained using different solvents: (i) phosphate saline buffer, (ii) methanol, (iii)  $\text{CHCl}_3/\text{Methanol}$  (1:1 v v-1), and (iv)  $\text{CHCl}_3$ .  $^1\text{H}$  NMR spectra were obtained using 600 MHz Bruker spectrometer at equal samples conditions, such as, concentration, acquisition parameters and the same spectra processing. NMR data were then analyzed with chemometrics tools (Pirouette). Principal component analysis (PCA) and hierarchical cluster analysis (HCA) were employed to reduce dimensionality and investigate which variables should be more effective for classifying three different samples classes. Generated PCA and HCA results show that healthy, symptomatic and asymptomatic plants could be divided in three groups with clear influence

of sugars, amino acids and aromatics compounds concentrations.

FAPESP and CNPq

#### MO187: Distinction of Tropical Brazilian Wines by Chemical Profile Through Association of $^1\text{H}$ NMR with Principal Component Analysis

<sup>1,2</sup>R. H. S. Andrade, <sup>2</sup>L. S. Nascimento, <sup>3</sup>G. E. Pereira, <sup>1</sup>A. P. S. Paim, <sup>1\*</sup>Fernando Hallwass

<sup>1</sup>Universidade Federal de Pernambuco, <sup>2</sup>Instituto Federal de Educação, Ciência e Tecnologia de Pernambuco, <sup>3</sup>Embrapa Uva e Vinho/Semiárido

It is essential to take great care with grape growth and the maturation process for winemaking. Thus, particular attention must be paid to the rootstock, preventing pest damage, in order to guarantee the healthy development of the fruit. The selection of the type of rootstock suitable for wine cultivation, however, depends heavily on the environmental conditions of the vineyard. The means of transplantation can intervene with the chemical composition of the fruit, thus affecting the chemical composition and sensory characteristics of the wine. Towards understanding this better, we conducted a study of tropical wines made from grapes growing in the São Francisco Valley (SFV) in the Northeast of Brazil. Two different rootstocks were used: *1103 P* and *IAC 313*.  $^1\text{H}$  NMR spectroscopy associated with the chemometric method of Principal Component Analysis (PCA) was used to study the influence of the rootstocks on the composition of the wine.

Thirty-three samples from SFV bottled wine were rotavaporated, lyophilized, dissolved in a  $\text{D}_2\text{O}$ /TMSP (Sodium 3-Trimethylsilylpropionate) solution, and underwent  $^1\text{H}$  NMR spectra analysis. For statistical analysis we selected the spectral range of interest and generated a matrix of *chemical shift (in ppm) X signal intensity*. The data were mean-centered and exported to the software *Unscrambler 9.7*, with which the PCA study was conducted.

Our results showed an efficient characterization of the samples by the type of rootstock. Samples of the rootstock *1103 P* had higher levels of lactic acid, proline and fructose. Samples of the rootstock *IAC 313* presented higher levels of succinic acid and glycerol.

ACKNOWLEDGEMENTS: FACEPE, CAPES, CNPq, IFPE, UFPE, EMBAPA,

#### TU188: $^1\text{H}$ NMR spectroscopy and chemometrics for comparative study of metabolic changes in *Citrus* sp. caused by different stages of citrus canker

<sup>1</sup>Caroline Silva de Oliveira, <sup>1</sup>Rafael do Prado Aparecido, <sup>2</sup>Eduardo Fermino Carlos, <sup>3</sup>Luciano Moraes Lião, <sup>1\*</sup>Glaucia Braz Alcantara

<sup>1</sup>Universidade Federal de Mato Grosso do Sul, <sup>2</sup>Instituto Agrônomo do Paraná, <sup>3</sup>Universidade Federal de Goiás

Brazil is the highest worldwide citrus producer. Nevertheless, citrus canker, disease caused by *Xanthomonas axonopodis* pv. *citri* bacterium (Xac), is potentially considered a devastate threat to many producer regions of citrus in our country. Although recent studies have indicated metabolic differences in *Citrus* sp. attacked by citrus canker, the knowledge about the variations in different periods of Xac infection was not obtained.

In this context, NMR associated to chemometric analyses was employed to comparative study of metabolomics of *Citrus* sp. for inoculated with Xac bacterium and non-inoculated leaves (control) in different periods of citrus canker evolution (0, 4, 12 and 20 days). Extracts from leaves was obtained using buffered  $\text{D}_2\text{O}$ /TMSP-*d*4. The measurements of  $^1\text{H}$  NMR were performed on a Bruker Avance III 500 spectrometer, equipped with a 5 mm TBI probe. The  $^1\text{H}$  NMR spectra were acquired using the CPMR pulse sequence, NS: 64; d1:

2s; AQ: 4.7s; TD: 64k and SW: 25 ppm. The  $^1\text{H}$  NMR spectra were treated by chemometrics, using principal component analysis (PCA).

The PCA showed the differentiation in PC1 (83.71%) between inoculated and control samples already in the period of 4 days after inoculation due to changes in production of primary metabolites. According to disease progression, we have observed that the greatest change in the metabolites production occurred in the beginning of the disease, without visible symptoms. Throughout the development of disease we have observed the reduction of metabolic changes, leading to the separation of groups of samples in PC2 axis (13.53 %) after 20 days. The detection of citrus canker before the manifestation of disease is the principal advantage of this preliminary study using NMR and chemometric methods.

Acknowledgment: CAPES, UFMS, IAPAR.

#### TH189: HLB in Citrus leaves: evaluation of the metabolic changes by NMR and chemometrics

<sup>1</sup>Deisy dos Santos Freitas, <sup>2</sup>Eduardo Fermino Carlos, <sup>1\*</sup>Glaucia Braz Alcantara

<sup>1</sup>Universidade Federal de Mato Grosso do Sul, <sup>2</sup>Instituto Agrônomo do Paraná

HLB (*Huanglongbing*) is a disease that affects the citriculture in several countries and has been responsible for large losses in the production. Typical symptoms include the presence of yellowish spots on leaves, defoliation, sharp drop in production and fruit dropping.

HLB is associated with *Candidatus Liberibacter* sp. bacterium and its transmission occurs through contaminated plant material and by action of psyllid insects. There is not cure for HLB and the only way to control the disease is the elimination of the contaminated plants. In this context, we have evaluated the metabolic changes caused by HLB in aqueous extracts of leaves of *Citrus* sp. by  $^1\text{H}$  NMR spectroscopy and chemometric analysis.

The NMR measurements were obtained on a Bruker DPX 300 spectrometer (7.05 T). The spectra were acquired with 128 scans (NS), 64k points (TD), 3.64s acquisition (AQ) and relaxation delay of 2s (d1).  $^1\text{H}$  NMR spectra was processing using 64k points (SI), exponential multiplication 0.30 Hz (LB) and manual phase and baseline corrections. Data treatment was performed using the Principal Component Analysis (PCA).

In PCA, there was a clear distinction between HLB symptomatic and asymptomatic leaves from branches containing fruits. The loadings responsible for grouping of asymptomatic leaves in positive values of PC1 were the signals at 3.10 and 3.30 ppm, corresponding to proline-betaine singlets. The signals at 3.66, 3.82 and 5.42 ppm were responsible for grouping of symptomatic leaves in negative values of PC1, corresponding to the region of sugars.

On the other hand, asymptomatic leaves in plants with HLB showed a similar metabolic composition with healthy leaves. The results indicate that these metabolites may be related to the defense mechanism of *Citrus* when affected by HLB, which are detected by NMR in the specific site where the *Candidatus Liberibacter* sp. bacteria are acting.

Acknowledgments: CAPES, IAPAR.

#### MO190: Salivary metabolite signatures of children with and without dental caries lesions.

<sup>1</sup>Tatiana Kelly S. Fidalgo, <sup>1</sup>Liana B. Freitas-Fernandes, <sup>2</sup>Renata Angeli, <sup>3</sup>Adriane M. S. Muniz, <sup>4</sup>Elicardo Gonsalves, <sup>1</sup>Raquel Santos, <sup>3</sup>Jurandir Nadal, <sup>2</sup>Fabio C. L. Almeida, <sup>2\*</sup>Ana Paula Valente, <sup>1</sup>Ivete P. R. de Souza

<sup>1</sup>School of Dentistry, Federal University of Rio de Janeiro, <sup>2</sup>National Center for Nuclear Magnetic Resonance, Federal University of Rio de Janeiro, <sup>3</sup>Biomedical Engineering

Program, Federal University of Rio de Janeiro, <sup>4</sup>School of Physics, Federal University of Rio de Janeiro

A metabolomic approach was used to analyze endogenous metabolites and to correlate with a specific biological state. The analysis of salivary metabolites is a growing area of investigation with potential for basic and clinical applications. Analyses of children's saliva in different dentitions and with or without caries could potentially reveal a specific profile related to oral disease risk. Nuclear Magnetic Resonance (NMR) is well suited for mixture analysis followed by Principal Component Analysis combined with Linear Regression (PCA-LR) statistics and was used to identify differences in the salivary metabolites. The classificatory analysis was performed using PCA-LR based on 1,000 cross-validation bootstrap runs from both classifiers in order to increase the data information from a small sample size. The PCA-LR presented a statistically good classificatory performance for children with and without caries with an accuracy of 90.11 % ( $P < 0.001$ ), 89.61 % sensitivity ( $P < 0.001$ ), and 90.82 % specificity ( $P < 0.001$ ). Children with caries lesions presented higher levels of several metabolites, including lactate, fatty acid, acetate and n-butyrate. Saliva from subjects with different dentition stages was also analyzed. Although the salivary samples were poorly classified, permanent dentition presented increased levels of acetate, saccharides and propionate. The NMR data and PCA-LR were able to classify saliva from children with or without caries, with performance indexes comparable to the partial least-squares regression discriminant analysis (PLS-DA) results also performed. Our data also showed similar salivary metabolite profiles for healthy subjects despite the differences in their oral hygiene habits, socioeconomic status and food intake.

ACKNOWLEDGEMENTS: FAPERJ, CNPq, CAPES, UFRJ.

#### TU191: Metabolic profile of murine melanoma studied by Nuclear Magnetic Resonance

<sup>1</sup>Pedro Bacchi, <sup>1</sup>Roger Chammas, <sup>1</sup>Silvina O. Bustos, <sup>2</sup>Claudia M. G. de Souza, <sup>3</sup>Antonio C. Bloise, <sup>3\*</sup>Said R. Rabbani

<sup>1</sup>Faculdade de Medicina, Universidade de São Paulo, Brazil,

<sup>2</sup>Instituto de Pesquisas Tecnológicas, São Paulo, Brazil,

<sup>3</sup>Instituto de Física da Universidade de São Paulo, Brazil

Using murine melanocytes, a new model of murine melanoma, called *Tm-1*, was produced by repeated cycles of cell disadhesion. In this strain, galectin-3 (*gal-3*), a multifunctional endogenous lectin which seems to act by modulating the mitochondrial response to different types of stress and conditioning the cell death, is silenced. Through transfection of original *Tm-1*, we produced two new strains of melanomas, one expressing *gal-3*, and the other not. In order to evaluate the changes in glucose metabolism induced by *gal-3*, these cells were cultivated in different conditions of oxygen tension and glucose level. Approximately  $10^7$  cells were collected from each culture. These were sonicated 5 times for 1 minute with intervals of 10 seconds between sonication, centrifuged at 4000 rpm for 20 minutes, the supernatant were collected and lyophilized. The lyophilized extracts were diluted in D<sub>2</sub>O and finally their NMR spectra were obtained. These spectra were sectioned in small intervals and the integrals of these sections, representing the concentration of different metabolites present in the liquid, were analyzed by multivariate methods. The modifications in concentration of certain metabolites were attributed to the impact of *gal-3* in the mitochondrial homeostasis process. Among all metabolites pointed out by multivariate analyses, the most relevant were lactate, alanine, free choline, GPC, PC, acetate, 3-hydroxybutyrate and taurine. The results suggest that *gal-3* gene seems to act in the mitochondrial homeostasis only in the specific case where tumorigenic cell are exposed to stress, such as hypoxia. In addition, when the homeostasis is triggered by hypoxia it is only carried out if there is an excess in glucose levels. A possible explanation for the homeostasis relies on the fact that cells expressing the *gal-3* gene are able to remove from

cellular environment those mitochondrias that do not properly metabolize pyruvate received from the glycolytic pathway ("deficient" mitochondria).

#### TH192: Identification of urinary metabolites to discriminate between HCV patients and healthy volunteers using metabolomics

<sup>1\*</sup>Carlos Jonnatan Pimentel Barros, <sup>1</sup>Ronaldo Dionísio da Silva, <sup>2</sup>Michele Maria Gonçalves de Godoy, <sup>2</sup>Edmundo Pessoa de Almeida Lopes, <sup>3</sup>Paulo Renato Alves Firmino, <sup>1</sup>Ricardo Oliveira da Silva

<sup>1</sup>Departamento de Química Fundamental, Universidade Federal de Pernambuco, Recife, Brazil, <sup>2</sup>Departamento de Medicina Clínica, Hospital das Clínicas, Universidade Federal de Pernambuco, <sup>3</sup>Departamento de Estatística e Informática, Universidade Federal Rural de Pernambuco, Brazil

Hepatitis C is an infectious disease that may evolve into cirrhosis or cancer. Since the liver is the main organ of metabolic control in mammals, an HCV infection may change the profile of endogenous metabolites, which can be observed through metabolomics. Recently, our group has demonstrated that it is possible to classify urine samples supplied for healthy or infected HCV volunteers, using <sup>1</sup>H NMR and metabolomics strategy[1]. In the present report, we indicate the possible metabolites and metabolic pathways that are responsible for this classification. We used 61 samples, 30 from patients with hepatitis C and 32 from healthy volunteers. Different forms of preprocessing of the data were used and for each one, multiple hypothesis tests were used to identify the features that differ significantly between the two groups. From the metabolomic study, we identified 12 spectral regions associated with endogenous metabolites, which are responsible for the classification. These metabolites are: L-valine, L-isoleucine, L-leucine, glycine, 2-hydroxy-isovalerate, 3-aminoisobutanoic, dimethylglycine, argininosuccinate and citrate, found in higher concentrations in samples from patients with hepatitis C, and trigonelline, carnosine and creatinine, found in higher concentrations in samples from healthy volunteers. Based on a pathway enrichment analysis software (<http://metpa.metabolomics.ca>),[2] we obtained the most significant metabolic pathways are involved in the discrimination found. They are: (1) Valine, Leucine and Isoleucine biosynthesis; (2) Valine, Leucine and Isoleucine degradation; and (3) Aminoacyl-tRNA biosynthesis.

Acknowledgments: CNPQ, CAPES, FACEPE and PRONEX.

References:

[1] Godoy, M. M. G.; Lopes, E. P. A.; Silva, R. O.; Hallwass, F.; Koury, L. C. A.; Moura, I. M.; Gonçalves, S. M. C.; Simas, A. M.. J. Viral Hepat., 2010, 17, 854-858.

[2] Xia, J.; Mandal, R.; Sinelnikov, I.; Broadhurst, D.; Wishart, D. S.. Nucl. Acids Res., 2012, 1-7.

#### MO193: Hepatitis C and B discrimination using urinary metabolomics

<sup>1\*</sup>Carlos Jonnatan Pimentel Barros, <sup>1</sup>Érika de Almeida Leite, <sup>2</sup>Michele Maria Gonçalves de Godoy, <sup>2</sup>Edmundo Pessoa de Almeida Lopes, <sup>3</sup>Paulo Renato Alves Firmino, <sup>1</sup>Ricardo Oliveira da Silva

<sup>1</sup>Departamento de Química Fundamental, Universidade Federal de Pernambuco, Brazil, <sup>2</sup>Departamento de Medicina Clínica, Hospital das Clínicas, Universidade Federal de Pernambuco, Brazil, <sup>3</sup>Departamento de Estatística e Informática, Universidade Federal Rural de Pernambuco, Brazil

The aim of this preliminary study was to build a metabolomics model for distinguishing urine samples supplied from patients infected with hepatitis B virus (HBV) and from patients infected with hepatitis C virus (HCV). We collected urine samples from 31 patients who were classified into two groups: 13 patients with HBV infection and 18 patients in-

fectured with HCV.  $^1\text{H}$  NMR spectra were obtained using 400  $\mu\text{L}$  of urine *in natura* added to 200  $\mu\text{L}$  of a buffer solution ( $\text{Na}_2\text{HPO}_4/\text{NaH}_2\text{PO}_4$  - 0.2 mol/L). We used the follows experimental parameters: RF pulse of  $45^\circ$ , acquisition time equal to 3.1 s, delay 1.0 s, 16 repetitions and presat pulse sequence. All the spectra were binned into 154 regions of 0.05 ppm, excluding the region between  $\delta$  4.2 and 6.4 ppm. The cases were normalized by sum in row and auto-scaled in column. Statistical analyses were performed by PCA, LDA and PLS-DA. The PCA was unable to separate the two groups, while the PLS-DA and LDA both showed adequate separation between the groups, but the validation of models were not satisfactory. We decided to perform the LDA with the matrix of PC's score and, after a variables selection, a better model was obtained. In the cross-validation, 85% and 83% of the HBV and HCV samples, respectively, were classified correctly. The chemical shifts responsible for discrimination are  $\delta$  3.32 and 3.17 ppm, which are assigned to trimethylamine N-oxide (TMAO), which was found in higher concentrations in samples from patients with hepatitis B.

Acknowledgments: CNPQ, CAPES, FACEPE and PRONEX.

#### References:

Godoy, M. M. G.; Lopes, E. P. A.; Silva, R. O.; Hallwass, F.; Koury, L. C. A.; Moura, I. M.; Gonçalves, S. M. C.; Simas, A. M.. J. Viral Hepat., 2010, 17, 854-858.

#### TU194: NMR analysis of salivary metabolites of lactating women with chronic hypertension

<sup>1</sup>\*Carla Martins, <sup>1</sup>Livia Roberta P. de Oliveira, <sup>1</sup>Luciana Pereira, <sup>1</sup>Tatiana Kelly S. Fidalgo, <sup>2</sup>Luciana Pomarico, <sup>1</sup>Valéria Abreu, <sup>3</sup>Romeu Ricardo da Silva, <sup>1</sup>Liana B. Freitas-Fernandes, <sup>4</sup>Fabio C. L. Almeida, <sup>4</sup>Ana Paula Valente, <sup>1</sup>Ivete P. R. de Souza

<sup>1</sup>Departamento de Odontopediatria e Ortodontia, Universidade Federal do Rio de Janeiro., <sup>2</sup>Departamento de Odontopediatria Universidade Federal Fluminense. (Nova Friburgo), <sup>3</sup>COPPE, Universidade Federal do Rio de Janeiro., <sup>4</sup>CNRMN, Universidade Federal do Rio de Janeiro.

Chronic hypertension during the pregnancy is appointed as one of the most dangerous intercurrent diseases which can lead to women's death and contributes significantly to neonatal morbidity and mortality. This indicates the importance of prevention and early diagnosis of chronic hypertension. The aim of this study was to identify, by  $^1\text{H}$  NMR, salivary metabolites in lactating women with chronic hypertension and compare with lactating healthy women. The Chronic Hypertension Group (CHG) was composed by 12 lactating women with diagnostic of chronic hypertension and the Healthy Group (HG) by 9 clinically healthy lactating women with no history of chronic illness - in particular, no history of chronic hypertension. Unstimulated whole saliva was collected and the salivary samples were centrifuged at  $4^\circ\text{C}$  and 10,000g for 60 minutes. The NMR spectra acquisition was performed by a Bruker 400MHz Advance spectrometer equipped with a 5 mm high-resolution probe and operating at a frequency of 400.13 ( $^1\text{H}$ ) MHz. Statistical analyses were carried out applying MATLAB software for the analysis of metabolites data. The PCA and *k*-means methods were applied. The PCA showed that at PC1 samples from CHG and HG were positioned separately, revealing a tendency of different profiles of salivary metabolites between the groups. However, the sample of three subjects from HG were found along the CHG. The application of *k*-means method (which is based on grouping data searching for similarities between these) revealed that from the three samples from HG found between the samples from CHG, two samples were considered (by similarities) as belonging to CHG. This means that, although these women are considered as healthy ones, maybe they present a tendency to develop chronic hypertension. These results motivate further longitudinal following up

study to identify in saliva changes of those individuals that may indicate the dynamic process of healthy or unhealthy state.

#### TH195: Metabolic profile of murine melanoma studied by Nuclear Magnetic Resonance

<sup>3</sup>Pedro Bacchi, <sup>3</sup>Roger Chammas, <sup>3</sup>Silvina O. Bustos, <sup>2</sup>Claudia M. G. de Souza, <sup>1</sup>Antonio C. Bloise, <sup>1</sup>\*Said R. Rabbani

<sup>1</sup>São Paulo University/Physics Institute, <sup>2</sup>Instituto de Pesquisas Tecnológicas, <sup>3</sup>São Paulo University/ Faculty of Medicine

Using murine melanocytes, a new model of murine melanoma, called *Tm-1*, was produced by repeated cycles of cell disadhesion. In this strain, galectin-3 (*gal-3*), a multifunctional endogenous lectin which seems to act by modulating the mitochondrial response to different types of stress and conditioning the cell death, is silenced. Through transfection of original *Tm-1*, we produced two new strains of melanomas, one expressing *gal-3*, and the other not. In order to evaluate the changes in glucose metabolism induced by *gal-3*, these cells were cultivated in different conditions of oxygen tension and glucose level. Approximately  $10^7$  cells were collected from each culture. These were sonicated 5 times for 1 minute with intervals of 10 seconds between sonication, centrifuged at 4000 rpm for 20 minutes, the supernatant were collected and lyophilized. The lyophilized extracts were diluted in  $\text{D}_2\text{O}$  and finally their NMR spectra were obtained. These spectra were sectioned in small intervals and the integrals of these sections, representing the concentration of different metabolites present in the liquid, were analyzed by multivariate methods. The modifications in concentration of certain metabolites were attributed to the impact of *gal-3* in the mitochondrial homeostasis process. Among all metabolites pointed out by multivariate analyses, the most relevant were *lactate*, *alanine*, *free choline*, GPC, PC, *acetate*, *3-hydroxybutyrate* and *taurine*. The results suggest that *gal-3* gene seems to act in the mitochondrial homeostasis only in the specific case where tumorigenic cell are exposed to stress, such as hypoxia. In addition, when the homeostasis is triggered by hypoxia it is only carried out if there is an excess in glucose levels. A possible explanation for the homeostasis relies on the fact that cells expressing the *gal-3* gene are able to remove from cellular environment those mitochondria that do not properly metabolize *pyruvate* received from the glycolytic pathway ("deficient" mitochondria).

ACKNOWLEDGMENTS: FAPESP, São Paulo University, CNPq

#### MO196: $^1\text{H}$ -NMR-Based Metabolomics of Methotrexate Resistance in Acute Lymphoblastic Leukemia Cell Lines

<sup>1,2</sup>Rafael Renatino Canevarolo, <sup>1,2</sup>Carolina Pereira de Souza Melo, <sup>1</sup>José Andrés Yunes, <sup>2</sup>\*Ana Carolina de Mattos Zeri

<sup>1</sup>Centro Infantil Boldrini, <sup>2</sup>Laboratório Nacional de Biotecnologias

Methotrexate (MTX), a folic acid antagonist used against acute lymphoblastic leukemia (ALL), prevents cell division by inhibiting nucleotide synthesis, therefore causing cell death. In this work, intracellular metabolic concentrations were associated with MTX-resistance in a series of ALL cell lines. MTX-resistance (or susceptibility) was determined by the MTT method in six B- and eight T-derived cell lines. Five cell lines were classified as MTX-resistant and the remaining cell lines, as MTX-sensitive. The intracellular metabolic content was assessed by proton nuclear magnetic resonance ( $^1\text{H}$ -NMR) of cells after 24h culture with MTX or control. In total, 84 metabolites were quantified, 72 of which were also identified. Multivariate analysis by partial least square discriminant analysis (PLS-DA) highlighted the main metabolites that were most associated with MTX-resistance



or -susceptibility, from which the receiver operating characteristic (ROC) curves evidenced carnitine, CB-MTX (unknown compound), cholate, glycocholate, malate and succinate as good metabolic biomarkers of MTX-susceptibility, whereas phosphocholine and sarcosine have proved to be good biomarkers of the MTX-resistant phenotype. The combination of carnitine, sarcosine and succinate showed a 100% sensitivity (15 out of 15 samples) and 92.3% specificity (24 out of 26) in classifying untreated cell lines. In MTX-treated cells, glycocholate, CB-MTX, sarcosine and succinate exhibited 100% sensitivity (15 out of 15) and 85.2% specificity (23 out of 27). Despite the necessity of validation in patients' samples, these results pointed to a promising tool for the early detection of MTX-resistance in ALL.

#### TU197: NMR-based metabolomics profiling to develop prognostic and diagnostic models for an autoimmune disease

<sup>1</sup>Marcos Rodrigo Alborghetti, <sup>2</sup>Maria Elvira Pizzigatti Correa, <sup>1</sup>Mauricio Luis Sforça, <sup>1\*</sup>Ana Carolina de Mattos Zeri

<sup>1</sup>Brazilian Biosciences National Laboratory, Brazilian Center for Research in Energy and Materials, <sup>2</sup>Hematology and Hemotherapy Center, State University of Campinas.

**Background:** we are studying, in patients from Hemocentro, an autoimmune disease that causes high morbidity and mortality. Many tissue injuries due to immune response affects skin, salivary glands, eyes, GI tract, lung and liver. **Objective:** the aim of this work is to develop prognostic and diagnostic models for this disease based on the metabolomics profile of the serum blood of this patients. **Methodology:** time series serum blood collection was performed in periods during the patient's hospitalization and after discharge. The samples were filtrated at 3kDa filter, buffered with phosphate buffer, referenced with D<sub>2</sub>O and DSS. The acquisition of 1D spectra was performed on a Agilent/Varian INOVA spectrometer operating at <sup>1</sup>H resonance frequency of 600MHz. The spectra processing, identification and quantification of metabolites were performed by using the application package Chenomx NMR Suite and the target profiling approach (Chenomx, Inc). The PCA and PLS-DA statistical analyses were performed at Pirouette 4.0 (Infometrix, Inc) and MetaboAnalyst 2.0. Results: we were able to develop preliminary prognostic models at T1, T3 and T4 times comparing patients that will develop the disease (T4, n=9) with patients that will not develop the disease (T4, n=8) and a diagnostic model comparing T5 (with the disease, n=10) with T4 (without the disease, n=17). Here we show the model for the time T4 (figure 2-IV). The PLS-DA statistical model with 7 metabolites shows accuracy = 1.0, Rcal (R2) 0.86529 and Rval (Q) 0.68104. The permutation test shows p=0.017. **Conclusions:** this pilot study suggests that use of time-series models based on metabolic profile could be useful in the medical routine and stimulate a populational study.

ACKNOWLEDGEMENTS: FAPESP

#### In-vivo and in-cell NMR

#### TH198: In-cell fate of Prokaryotic ubiquitin-like protein, Pup, inside the Mycobacterium proteasome.

\*Alexander Shekhtman, Andres Maldonado, David Burz, Sergey Reverdatto

State University of New York at Albany, Albany, NY, USA

Inside a cell, macromolecular complexes are assembled along specific pathways necessary to carry out biological functions in the presence of a crowded cytosol. Often, during assembly, effector molecules such as ligands or substrates are also present. The presence of these molecules prior to or following the expression of components of the complex can play a regulatory role in the assembly of that complex. Further-

more, the binding of these effector molecules may alter the pathway through which proper, biologically active conformations are achieved. It is not clear *a priori* that the final conformation and commensurate activity of the complex will be different due to this temporal control. The *Mycobacterium tuberculosis* proteasome is required for maximum virulence and to resist killing by the host immune system. The prokaryotic Ubiquitin-like protein, Pup-GGE, targets proteins for proteasome-mediated degradation. We demonstrate that Pup-GGQ, a precursor of Pup-GGE, is not a substrate for proteasomal degradation. Using STINT-NMR, an in-cell NMR technique, we studied the interactions between Pup-GGQ, mycobacterial proteasomal ATPase, Mpa, and 1.2 megadalton *Mtb* proteasome core particle (CP) inside a living cell at atomic resolution. We showed that under *in-cell* conditions, contrary to *in vitro* results, in the absence of the proteasome CP, Pup-GGQ interacts with Mpa only weakly, primarily through its C-terminal region. When Mpa and non-stoichiometric amounts of proteasome CP are present, both the N-terminal and C-terminal regions of Pup-GGQ bind strongly to Mpa, committing a pupylated substrate for degradation. This suggests a mechanism by which transient binding of Mpa to the proteasome CP controls the fate of Pup.

ACKNOWLEDGEMENTS: This work is supported by NIH grant R01GM085006 to A.S..

#### MO199: Ex vivo NMR during human cell cycle control

\*Jochen Balbach

Institute of Physics, Biophysics, Martin-Luther-University Halle-Wittenberg, Germany

Cyclins and cyclin-dependent kinases (CDKs) are key regulators of the human cell cycle. CDK4/6 assemble with D-type cyclins for progression from the G1 to S-phase and are negatively controlled by CDK inhibitors of the INK4 family. p19<sup>INK4d</sup> belongs to this inhibitor family, which gets posttranslationally phosphorylated. In earlier studies [1-3] we could show *in vitro* by glutamate substitutions, mimicking phosphorylation, local unfolding of 2 of the 5 ankyrin repeats of p19<sup>INK4d</sup>. This prevents CDK4/6 inhibition. Now, we succeeded to follow this regulation in much more detail and very close to the *in vivo* situation by simply adding crude cell extracts from various cell lines (HeLa, HEK-293, MDA-MB-231 etc.) to the isotope labeled p19<sup>INK4d</sup> NMR samples. The NMR read out directly allows to reveal, which serine residues get phosphorylated and consequently which ankyrin repeats locally unfold. By synchronizing the cells and by employing CDK inhibitors, the so far unknown kinases of p19<sup>INK4d</sup> could be identified. Dephosphorylation by subsequent addition of a phosphatase confirms the integrity of p19<sup>INK4d</sup> in the cell extracts by fully native NMR spectra. These high resolution data furthermore revealed, which serine has to become phosphorylated to induce ubiquitination and subsequent proteasomal degradation of CDK inhibitor p19<sup>INK4d</sup> and thus progression of the cell cycle to the next phase. These *ex vivo* NMR methods correlate cell biology methods with structural biology.

#### REFERENCES:

1. Löw C, Homeyer N, Weininger U, Sticht H, Balbach J. (2009), ACS Chem. Biol. 4, 53-63.
2. Löw C, Weininger U, Neumann P, Klepsch M, Lilie H, Stubbs MT, Balbach J. (2008), PNAS 105, 3779-3784.
3. Löw C, Weininger U, Zeeb M, Zhang W, Laue ED, Schmid FX, Balbach J. (2007), J. Mol. Biol. 373, 219-231.

#### TU200: In-vivo NMR- Acetate Metabolism in C. reinhardtii

Himanshu Singh, \*K. V. R. Chary

TIFR

In recent times, *Chlamydomonas reinhardtii* a unicellular algae has been a model organism for studying metabolic changes associated with biofuel production. Besides, *C. reinhardtii* offers duality of metabolism being both phototrophic and heterotrophic in nature. The major metabolic flux it follows in various conditions is not yet clearly understood. On the other hand, live cell NMR, a non invasive technique, has been extensively used in the past to detect metabolites in the cells. Against this backdrop, we set out to monitor live metabolic changes in *C. reinhardtii* cells during light (mixotrophic) and dark (heterotrophic) phases of growth as well as following the UV/nutritionally stressed stationary phase cultures. The *in-cell* metabolic changes in *C. reinhardtii* cells were followed by monitoring [1, 2-  $^{13}\text{C}$ ]-labelled acetate assimilation over a period of 8 days. For the initial 24 hours of detailed kinetic measurements, the assimilation in dark phase of growth was faster than light phase of growth, reflecting higher heterotrophic metabolic efficiency in dark over mixotrophic metabolism in light. While bicarbonate was the predominant metabolite observed both in light and dark phases of growth, Carbon dioxide was observed only during the dark phase of growth, reflecting a differential metabolic flux in growth. UV stress decelerated acetate assimilation and metabolite formation in cells. The UV effect also resulted in an increased bicarbonate accumulation perhaps due to reduced efficiency of carbon concentrating mechanisms operating in the cell. When the cells were incubated in light or dark for up to eight days and monitored at intervals of about 48 hours, further remodeling in metabolism took place where in bicarbonate and Carbon dioxide were routed towards lipogenic pathway leading to lipid body production containing triacyl glycerol (TAG). We explain this metabolic flow by a model for acetate assimilation in the cell.

ACKNOWLEDGEMENTS: TIFR NMR facility-Mumbai, India

#### TH201: Baseplate protein organization of chlorosome mutant from green-sulfur bacteria *Chlorobium Tepidum*, observed with atomic resolution in vivo

<sup>1</sup>Natalia Kulminkaya, <sup>1\*</sup>Niels Christian Nielsen, <sup>1</sup>Jakob Nielsen, <sup>1</sup>Morten Bjerring, <sup>1</sup>Karen Thompson, <sup>2</sup>Martin Lindahl

<sup>1</sup>Aarhus University, <sup>2</sup>Lund University

In order to obtain high resolution structure information for proteins in native heterogeneous environment, one should choose either cryo-electron microscopy[1] or solid-state NMR spectroscopy[2]. However, combinations of these two techniques provide even more powerful instrumentation for protein research. In this work we present organization of the baseplate in the photoreceptor from *Chlorobium Tepidum* with atomic resolution. Even though the baseplate was earlier observed with freeze-fracture electron microscopy technique, high resolution of the baseplate has been never achieved. We compare solid-state NMR protein structure with the 3-dimensional cryo-EM reconstruction of the protein baseplate and also demonstrate abundance of new information in the supramolecular organization of the protein-pigment composition.

[1] a) G. Zanetti, J. A. Briggs, K. Grunewald, Q. J. Satten-tau, S. D. Fuller, PLoS pathog. 2006, 2, e83; b) F. Brandt, L. A. Carlson, F. U. Hartl, W. Baumeister, K. Grunewald, Mol. Cell 2010, 39, 560-569.

[2] a) A. C. Sivertsen, M. J. Bayro, M. Belenky, R. G. Griffin, J. Herzfeld, J. Mol. Biol. 2009, 387, 1032-1039; b) A. Goldbourt, B. J. Gross, L. A. Day, A. E. McDermott, J. Am. Chem. Soc. 2007, 129, 2338-2344; c) R. Fu, X. Wang, C. Li, A. N. Santiago-Miranda, G. J. Pielak, F. Tian, J. Am. Chem. Soc. 2011, 133, 12370-12373.

#### MO202: Ultrafast Localized Two-Dimensional Correlated Spectroscopy

\*Zhong Chen, Yanqin Lin, Shuhui Cai

Department of Electronics Science, Xiamen University, Xiamen, China

Localized magnetic resonance spectroscopy (MRS) allows noninvasive in vivo analysis of metabolites. Due to the narrow chemical shift range and complexity caused by the resonances of metabolites with coupled spin systems, the spectral resolution of one-dimensional MRS is often low. Therefore two-dimensional (2D) MRS was introduced to alleviate the spectral overlap in one-dimensional MRS [1]. Unfortunately, numerous indirect dimension increments have to be collected for a conventional 2D spectrum with good resolution, which leads the scan fairly time-consuming. This greatly hinders in vivo application of localized 2D MRS. In this work, a new scheme for ultrafast 2D spatially-encoded localized COSY is designed based on spatially encoded technique [2]. In this sequence, the usual indirect dimension encoding is replaced by a spatial encoding, which is decoded by an echo planar imaging like detection scheme during the detection period. It can be executed for a 2D localized COSY spectrum in the order of sub-second. This enables the study of short timescale phenomena via 2D MRS and may greatly reduce the motion effects. Theoretical analysis and experiments are performed to show the performances of the new sequence. The method opens important perspectives for fast in vivo analysis of metabolites in living organisms and may promote the wide in vivo application of 2D localized MRS for more information which is not available in one-dimensional MRS.

ACKNOWLEDGMENTS: This work was supported by the NNSF of China under Grant 11174239.

[1] Lin, Y. Q.; Gu, T. L.; Chen, Z.; Kennedy, S.; Jacob, M.; Zhong, J. H. Magn. Reson. Med., 2010, 63, 303-311.

[2] Tal, A.; Frydman, L. Prog. Nucl. Magn. Reson. Spectrosc., 2010, 57, 241-292.

#### TU203: Analysis of proteins inside human cultured cells using $^{19}\text{F}$ -NMR

<sup>1</sup>Syuei Murayama, <sup>2</sup>Kohsuke Inomata, <sup>3</sup>Ayako Ohno, <sup>4</sup>Kenichi Aakagi, <sup>1\*</sup>Hidehito Tochio, <sup>1</sup>Masahiro Shirakawa

<sup>1</sup>Department of Molecular Engineering, Graduate School of Engineering, Kyoto University, <sup>2</sup>Quantitative Biology Center, RIKEN, <sup>3</sup>Division of Nutritional physiology, Institute of Health Biosciences, The University of Tokushima Graduate School, <sup>4</sup>National Institute of Biomedical Innovation, Japan

*In-cell* NMR is an isotope-aided NMR technique that enables observations of structure of proteins in living cells. In mammalian *in-cell* NMR, the method has mostly relied on 2D  $^1\text{H}$ - $^{15}\text{N}$  correlation spectra of uniformly  $^{15}\text{N}$ -labeled proteins. However, by employing amino acids specific labeling, *in-cell* NMR spectroscopy of proteins can be substantially simplified and thus facilitated. In this study, *in-cell*  $^{19}\text{F}$  NMR spectroscopy of  $^{19}\text{F}$ -labeled proteins in HeLa cells was examined.

FKBP12, a target protein of immunosuppressants, was employed as a model system. The *p*-fluoro-*L*-phenylalanine-incorporated FKBP12 was prepared and delivered into HeLa cells using the CPP (Cell Penetrating Peptide) -mediated protein transduction method.  $^{19}\text{F}$  NMR spectra of the cells were acquired in the presence or absence of FK506 in the cell culture. The obtained  $^{19}\text{F}$  NMR spectra showed that the specific complexes between the protein and FK506 was formed in the cells. Our data demonstrates that *in-cell*  $^{19}\text{F}$  NMR provides an efficient way to monitor proteins functioning in living HeLa cell.

#### TH204: $^1\text{H}$ -NMR metabolic profiling of breast cancer cell lines as a tool for understanding the process of tumor metabolism adaptation.

\*Melissa Quintero Escobar, Rafael Renatino Canevarolo, Kaliandra Gonçalves, Sandra Martha Gomes Dias, Ana Carolina de Mattos Zeri

Laboratorio Nacional de Biociencias, LNBIO.

The analysis of metabolites by nuclear magnetic resonance can be used to define the metabolic phenotype of cells, tissues or organisms. The metabolic phenotype of a cell is not static, but emerges from the coordinated and dynamic network of interactions between genes, proteins and metabolites. Given the complexity of these relationships, the application of metabolomics has the potential to contribute to the understanding of biological mechanisms of tumors. The 'Metabolomic' approach provides important information about tumorigenesis, with the potential of revealing new therapeutic targets and identifying pathways that are perturbed in cancer. Apart from that, Metabolomic has been also broadly employed as a mean of finding diagnostic and prognostic metabolic markers. Tumor cells have altered metabolism compared to quiescent cells, needing constant supplements of macromolecular precursors for their growth and proliferation. The glutaminolytic and glycolytic pathways are the main generators of these metabolic precursors, which will contribute to the synthesis of proteins, nucleic acids and lipids. The goal of this project was use  $^1\text{H}$  NMR to analyze the metabolic profiles of triple negative breast cancer cell lines along with other breast cancer cells lines displaying variable phenotypes regarding to the presence of progesterone (PR), estrogen (ER) and the membrane receptors Her2. The triple-negative phenotype is well known as a difficult to treat type of breast cancer due to its resistance to the hormonal therapies. We identified and quantified in the triple-negative cell line MDA-MB231 several compounds related to the glycolytic pathway, such as lactate and ATP, as well as compounds such as glutamate, glutamine and glutathione, all precursors / products of the breakdown of glutamine. Finally, we found high levels of O-phosphocholine, proline and taurine, previously known biomarkers already described in the literature, validating our methodology. Our perspectives are to extend the approach to other cell lines to look for specific triple-negative biomarkers.

Supported by: São Paulo Research Foundation (Fapesp).

### Magnetic Resonance Imaging

#### MO205: Measuring Optical and Refractive Properties of the Human Eye with In Vivo MRI

<sup>1,2</sup>\*James M. Pope, <sup>2</sup>Catherine E. Jones, <sup>1</sup>Sanjeev Kasthurirangan, <sup>1</sup>David A. Atchison

<sup>1</sup>*Institute of Health & Biomedical Innovation, Queensland University of Technology, Brisbane, Australia*, <sup>2</sup>*Faculty of Science & Technology, Queensland University of Technology, Brisbane, Australia*

We have employed MRI to study optical properties of the human eye that are not measurable by standard techniques of optometry. Unlike a conventional glass or plastic lens, where refraction of light takes place only at the surfaces, the eye lens exhibits a refractive index distribution (RID), so that refraction occurs continuously through the lens. To date it has not been possible to measure the refractive index distribution non-invasively by optical techniques, without making assumptions about its shape and form.

We have developed an MRI technique that for the first time allows the refractive index distribution of human eye lenses to be measured and mapped non-invasively both in vitro and in vivo. We have used it to investigate changes in the distribution with age and the state of accommodation of the eye. The method relies on the fact that the refractive index of the lens is determined by the concentration of proteins (crystallins) in the lens tissue. This in turn determines the NMR transverse relaxation time ( $T_2$ ) of water protons. Consequently there is a direct correlation between  $T_2$  and refractive index ( $n$ ) that can be exploited to map the refractive index distribution using MRI. The results demonstrate that existing models of the human eye lens are inadequate to describe changes that occur with aging of the lens. They also provide new insights into

the origins of presbyopia - the loss of the ability to focus on near objects (i.e. to "accommodate") with age.

#### TU206: Spatial Resolution Enhancement in MRI

\*Daniel Fiat

*University of Illinois at Chicago*

We report here the development of a novel method for enhancement of the spatial resolution in MRI.

Subpixel-shifted MR images were taken at several fields of view to reconstruct the high-resolution image. The experimental method, theory and method of data analysis will be described.

Experimental results that demonstrate significant enhancement of the spatial resolution for  $^1\text{H}$  MRI studies of a phantom, carried out with GE clinical scanner, will be presented.

#### TH207: Intra-aneurysmal flow determination by 3D velocity maps using low field NMR tomography

<sup>1</sup>\*Josefina Perlo, <sup>2</sup>Emilia V. Silletta, <sup>1</sup>Ernesto Danieli, <sup>2</sup>Rodolfo Héctor Acosta, <sup>1</sup>Bernhard Blümich, <sup>1</sup>Federico Casanova

<sup>1</sup>*Institute of Technical and Macromolecular Chemistry, ITMC, RWTH Aachen, Germany*, <sup>2</sup>*Instituto de Física Enrique Gaviola, CONICET - Córdoba, Argentina*

Dynamic NMR imaging is the only method capable of measuring velocity patterns within flowing systems in a complete non-invasive way. This makes MRI velocimetry an attractive technique to study flow phenomena in many areas of research, in particular medical systems. Aneurysms, for instance, are originated by a weakness of the vessel walls, locally increasing the normal size of the artery or vein. The two events that dominate the evolution of an intracranial aneurysm are growth and rupture, being both dependent on intra-aneurysmal flow. Decrease of intra-aneurysmal flow is considered an alternative for treating intracranial aneurysms. Such modification can be achieved by inserting stents or flow diverters. The determination of velocity patterns in such systems promises to be a powerful tool to prevent abnormal behaviors which can have severe health consequences.

In this work we present low field NMR imaging for the study of intra-aneurysmal velocity patterns under steady flow conditions before and after the insertion of a stent. A spin-echo pulse sequence was implemented for velocity map measurements in a portable low-field tomograph (0.22T) to study the flow behavior in phantom systems resembling arteries with an aneurism. 3D velocity maps were measured in liquids with similar rheological properties as blood. It was possible to determine the influence of the local geometry of the artery in the internal flow of the aneurism. In absence of flow diverters, a rotational vortex in the flow pattern could be observed. The flow effects due to the insertion of the stent provoked a complete alteration of the flow patterns and a reduction of velocity magnitudes.

#### MO208: High throughput screen of mouse cardiovascular functions with MRI and Echocardiography

<sup>1</sup>\*Luciana Caminha Afonso, <sup>1</sup>Kristin Moreth, <sup>1</sup>Valérie Gailus-Durner, <sup>1</sup>Helmut Fuchs, <sup>1,2</sup>Martin Hrabě de Angelis

<sup>1</sup>*Institute of Experimental Genetics*, <sup>2</sup>*Technical University Munich*

The rapid increase in the development of mouse models is resulting in a growing demand for non-invasive physiological monitoring of large quantities of mice. Accordingly, we have implemented an experimental set up, which enables us to perform high throughput non-invasive transthoracic echocardiography and electrocardiography on mice. For functional testing of the vascular system and detection of cardiac pathologies in mice, innovative techniques and miniaturized classical

physiological procedures are applied by us to achieve non-invasive analysis of cardiovascular structure and function.

An electrocardiogram (ECG) is a recording of the electrical activity of the heart with surface electrodes. We recorded ECG's to analyze cardiac rhythms, conduction and repolarization patterns within control wildtypes and mice suffering from cardiomyopathy.

Echocardiography is a non-invasive method to assess left ventricular systolic, diastolic, regional and vascular function. Transthoracic echocardiography was performed in awake control wildtypes and mice suffering from cardiomyopathy to systematically evaluate heart rate, respiration rate, stroke volume, left ventricular mass, left ventricular contraction and performance, systolic- and diastolic left ventricular interior diameter, systolic- and diastolic thickness of the interventricular septum and left ventricular posterior wall.

Cardiac magnetic resonance imaging is an important method to diagnose cardiomyopathy. Besides being able to assess dimensions of the left ventricle (at systole and diastole), cardiac MRI allows the analysis of the right ventricle, which is not achievable with echocardiography.

Black-blood short-axis images were acquired with a fast low-angle shot (FLASH) multi-slice sequence employing a self-gated protocol that incorporates a navigator echo to generate cardiac triggering and respiratory gating signals retrospectively (IntraGate™). The application of this technique reduces considerably the time for preparation of the animal, as the use of ECG leads and calibration of ECG signal for gating are unnecessary.

With the combination of these techniques we found significant differences between control mice and mice developing a cardiomyopathy. Further on, this simple and fast protocol with its high sensitivity and specificity permits us to perform primary screening of the murine cardiovascular system in a high throughput setting.

#### **TU209: Developing an API and an IDE to Creating and Managing Pulse Sequences for Nuclear Magnetic Resonance**

**Daniel C. Pizetta**, Danilo M.D. Delfino da Silva, Gustavo V. Lourenço, Guilherme M. Freire, Felipe B. Coelho, Mateus Martins, Edson Luiz Gea Vidoto, \*Alberto Tannús

*University of São Paulo*

Due to the logistic importance of the Magnetic Resonance Imaging (MRI) technology, the CIERMag - through the ToRM-15 Project - is continually developing projects to complete the domain of the technology of Nuclear Magnetic Resonance. This paper will discuss the new tools adopted for building a fully Digital Spectrometer in its more complex form, an MRI scanner. The effort is in particular on the development of the Application Programming Interface (API) and Integrated Development Environment (IDE) to create and manage pulse sequences and ancillary procedures as well as the configuration of the spectrometer as a functional, friendly and free of commercial dependency of software and hardware. Preliminary trials were performed in the spectrometer with digital technology entirely developed by the group, in order to validate the project, and some results have already shown its ability to generate complex MRI sequences.

**Keywords:** resonance magnetic imaging, free software, graphical pulse sequence editor, application programming interface, integrated development environment.

**Acknowledgements:** FAPESP: 2005/5.6663-1 e CNPQ: 565.047/2010-8, CAPES, FINEP, FNS.

#### **TH210: Using fast MRI techniques to study acid-treated rock cores**

<sup>1</sup>Roberson Saraiva Polli, <sup>2</sup>Manuel Krebs, <sup>2</sup>Andre Souza, <sup>2</sup>Bernhard Lungwitz, <sup>2</sup>Alexandre Pepin, <sup>2</sup>Austin Boyd, <sup>1</sup>Edson Luiz Gea Vidoto, <sup>1</sup>Fernando Fernandes Paiva,

<sup>1</sup>Alberto Tannús, <sup>1\*</sup>Tito José Bonagamba

<sup>1</sup>*Instituto de Física de São Carlos, Universidade de São Paulo*, <sup>2</sup>*Schlumberger Brazil Research and Geoengineering Center*

NMR relaxation and MRI are currently used as tools to study both the structure of porous media and the fluid dynamics occurring within, allowing the determination of characteristics such as porosity and permeability. Carbonate rock cores are highly soluble in some acids, so reservoir matrix acid stimulation provides a cost-effective means to enhance well productivity, where acid action forms special paths called wormholes. These matrix acidizing experiments combined with visualization techniques as MRI and X-ray tomography are commonly used to study wormhole networks.

In this work, NMR relaxation and MRI were employed to characterize these materials and follow the wormhole formation. NMR relaxation experiments were performed using a TECMAG Redstone console with a 0.05 T permanent magnet (2.64 MHz for <sup>1</sup>H). Fast MRI sequences based on gradient echo, such as FLASH and UTE were used to characterize a 1" diameter and 3" length cylinder sample of Indiana limestone, before and after the acidizing treatment. MRI experiments were performed using a wide-bore (30 cm diameter) 2 T superconducting magnet (85 MHz for <sup>1</sup>H), interfaced with a Bruker Avance AVIII console. In order to perform the experiments, a crossed saddle radiofrequency coil together with a gradient coil system was used, which was able to provide a maximum gradient of about 15 G/cm.

Before the acid treatment of the Indiana samples, the UTE images showed that even pores with diameters of about 100 mm can be visualized. Using FLASH technique, the images showed pores with diameters higher than 300 μm. Despite this lack of resolution for the micro- and meso-porosity sizes fraction, compared to the low-field NMR relaxation results, it is enough to check for fractures and any related effect that could influence the acidizing experiment results. The cores studied did not show any problem that could influence the wormhole pathway formation. After the acid treatment, wormholes were easily observed using the FLASH MRI technique, allowing the estimation of their diameters (around 1 mm). This information, associated with the acid preferred pathway visualization, could be used to characterize and optimize the porosity and permeability gain observed after the acidizing treatment.

The next step is to apply and develop new techniques to imaging this media, especially those based on single point images as SPRITE, which permits fast images, free of artifacts due to magnetic field inhomogeneities and magnetic susceptibility contrast effects.

**Acknowledgments:** IFSC/USP, FAPESP, CNPq, CAPES

#### **MO211: In-vivo Controlled Deposition of Superparamagnetic Nanoparticles**

<sup>2</sup>Mayara Klimuk Uchiyama, <sup>2</sup>Sergio Hiroshi Toma, <sup>2</sup>Koiti Araki, <sup>3</sup>Stephen Fernandes de Paula Rodrigues, <sup>3</sup>Rodrigo Azevedo Loiola, <sup>1</sup>Hernán Joel Cervantes, <sup>1\*</sup>Said R. Rabani

<sup>1</sup>*Instituto de Física da Universidade de São Paulo*, <sup>2</sup>*Instituto de Química da Universidade de São Paulo*, <sup>3</sup>*Faculdade de Ciências Farmacêuticas da Universidade de São Paulo*

Superparamagnetic iron oxide nanoparticles (SPION) offers many applications in biomedicine, such as the magnetic separation of target cells, hyperthermia, magnetic resonance imaging (MRI) contrast enhancement and controlled deposition of stem cells or drugs.

The superparamagnetic nanoparticles generate a spatial variation of the magnetic susceptibility of the medium and, therefore, the effect of the presence of SPIONs in the volume being scanned is mainly decrease the spin-spin relaxation time (T<sub>2</sub>) and the decay time of the FID (T<sub>2</sub>\*). As a consequence, the affected region becomes hypointense, i.e. there is a decrease

in the pixels intensity in the T2-weighted images. The pixel reduction level depends on the nanoparticles quantity allowing, thus, the determination of local concentration.

One wistar male rat was cannulated in the left femoral vein and a 1 ml suspension of SPIONs 10mg/mL with 5 nm of diameter was injected directly into the vein. In the same paw, 300  $\mu$ L of the same solution was injected in the muscle. At the opposite paw, one magnet was placed subcutaneously in the thigh of the animal. The magnet stayed during 12 hours, and 2 hours later, the rat was scanned. At the paw where it was affixed, due to the presence of the magnet, it was possible to see an accumulation of nanoparticles, as the image of the right thigh became black.

The rat was followed-up for more than 138 days and the clearance of deposited SPIONs was studied. The agglomeration of the nanoparticles remained visible in the image with slow reduction over time. At the opposite paw, where the SPIONs were injected directly into the muscle, the reduction was slower when compared with the first paw. Other organs (liver, kidneys) were also observed.

#### **TU212: Exploring microscopic iDQC MR imaging technique for iron-labeled single cell detection**

<sup>1</sup>Jee-Hyun Cho, <sup>1</sup>Kwan Soo Hong, <sup>1,2</sup>Janggeun Cho, <sup>1</sup>Cheajoon Cheong, <sup>2</sup>Sangdo Ahn, <sup>1\*</sup>Chulhyun Lee

<sup>1</sup>Division of Magnetic Resonance Research, Korea Basic Science Institute, Ochang, Republic of Korea, <sup>2</sup>Department of Chemistry, Chung-Ang University, Seoul, Republic of Korea

Recently, to create magnetic resonance contrasts different from those in conventional techniques, new magnetic resonance imaging methods based on intermolecular double quantum coherences (iDQC) have attracted considerable attention. Owing to its intrinsic sensitivity to changes in the susceptibility structures, iDQC imaging has the potential to provide a fundamentally different contrast from that in conventional MRI.

In this study, we compared iDQC MR images with conventional ones (e.g. GE, Spinecho EPI) acquired in various experimental conditions to evaluate the contributions of excitation and readout methods in image contrasts for detecting iron-labeled single cells.

#### **TH213: Uridine-based Paramagnetic Amphiphilic T1 MRI Contrast Agents and Nano-assembled Bimodal Contrast Agent**

<sup>1</sup>Hyunseung Lee, <sup>1,2</sup>Hyeyoung Moon, <sup>1</sup>Sankarprasad Bhuniya, <sup>3</sup>Junwon Park, <sup>3</sup>Sumin Lee, <sup>3</sup>Jong Seung Kim, <sup>1,2\*</sup>Kwan Soo Hong

<sup>1</sup>Division of MR Research, Korea Basic Science Institute, <sup>2</sup>Department of Bio-analytical Science, University of Science and, <sup>3</sup>Department of Chemistry, Korea University

The chelated Gd<sup>3+</sup> metal ion improves imaging contrast by increasing the longitudinal relaxation time ( $T_1$ ) of proximal water protons, which appear brighter in the  $T_1$ -weighted image. The current Gd<sup>3+</sup>-based contrast agents (CAs) ligated with polyamino carboxylate are incapable of meeting requirements as they do not have optimal relaxivity profiles at high magnetic fields. This requirement drives the research for smart contrast agents with high relaxivities ( $r_1$ ) for better tissue contrast at high magnetic fields. We have chosen a nucleoside as a molecular platform with Gd-DTPA to generate a MRI contrast agent. The relaxation efficiency of these newly synthesized amphiphilic MR CAs was determined by measuring longitudinal relaxivity ( $r_1$ ) and transverse relaxivity ( $r_2$ ) at 20 (0.47 T) and 60 MHz (1.41 T) in phosphate buffered saline (PBS) at 36°C. The highest relaxivities achieved were 30.3 and 23.4 mM<sup>-1</sup> s<sup>-1</sup> in PBS (pH 7.4) at 0.47 and 1.41 T, respectively, for LGd3 (chain length = 10).

Uridine-based paramagnetic molecule (6-Gd<sup>3+</sup>) coated quantum dots (QDs) for multimodal imaging were synthesized

and have been characterized their T1 magnetic resonance imaging (MRI) properties and fluorescent signatures. Comparing with commercial contrast agent such as Omniscan®, 6-Gd<sup>3+</sup>-QD showed high relaxivities of  $11.7 \pm 0.1$  mM<sup>-1</sup> s<sup>-1</sup> and  $10.2 \pm 0.1$  mM<sup>-1</sup> s<sup>-1</sup> per Gd at 36°C in phosphate buffered saline (PBS) at 60 MHz and 200 MHz, respectively. Also, in the cell uptake investigation, 6-Gd<sup>3+</sup> QD was successfully taken to the RAW264.7 cells. This nanoparticle type of contrast agent can easily label cells for MR imaging-tracking and have dozens of Gd<sup>3+</sup> per particle which increases efficacy of labeling cells. In summary, a bimodal fluorescent MR contrast agent, 6-Gd<sup>3+</sup>-QD, has been developed by conjugation of CdSe/ZnS QDs with a uridine-based paramagnetic complex (6-Gd<sup>3+</sup>).

#### **MO214: Real-time visualization of myocardial inflammatory evolution using magnetic nanoparticle-combined cardiac MRI**

<sup>1,2</sup>Hyeyoung Moon, <sup>1,3</sup>Jongseun Kang, <sup>4</sup>Hyo Eun Park, <sup>4</sup>Kiyuk Chang, <sup>1,2,3\*</sup>Kwan Soo Hong

<sup>1</sup>Division of MR Research, Korea Basic Science Institute, Cheongwon, Korea, <sup>2</sup>University of Science and Technology, Daejeon, Korea, <sup>3</sup>Graduate School of Analytical Science and Technology, Chungnam National University, Daejeon, Korea, <sup>4</sup>Department of Internal Medicine, Catholic University, Seoul, Korea

Clinically, myocardial inflammation, a critical pathogenic factor in myocarditis, cannot be directly visualized by conventional CMR. In our study, we investigated whether PEGylated fluorescent magnetic nanoparticles (MNP) could detect the inflammatory areas in experimentally induced autoimmune myocarditis (EAM) rats, and compared the detectability of focal inflammation area between MNP-enhanced CMR and conventional CMR. MNP-CMR was also employed to track the evolution of inflammation in myocarditis.

We performed *in vivo* CMR in EAM and control rats using a 4.7 T MRI system. At first, T2W, and pre-MNP MRI were performed, and then early gadolinium enhancement and late gadolinium enhancement MRI were performed after tail vein injection of Gd-DTPA (Magnevist®, 0.1 mmol/kg). Then, after 24 hrs of tail vein injection of home-made MNPs (10 mg Fe/kg), post-MNP MRI was performed. To observe the inflammatory evolution, we acquired the pre-MNP CMR images at 15 day (15D) post-immunization (PI), and then 5 mg Fe/kg of MNP-FITC was intravenously injected. Post-MNP CMRs were acquired at 16D and 20D PI. After acquiring post-MNP CMR at 20D PI, same dose of MNP-RITC was injected in the same rats. Then, post-MNP CMR imaging was performed at 21D PI.

Relatively large area of myocardial inflammation in EAM rats were detected by conventional T2W-, EGE-, and LGE-MRI, while small-sized inflammation regions consistently failed to be detected. The superiority of MNP-CMR to conventional MRI was clearly shown for focal inflammation. Also, MNP-CMR with two times' MNP injection could visualize the inflammatory evolution.

From our study, we could verify that MNP-CMR could effectively visualize myocardial inflammatory cellular infiltrates, and monitoring the dynamic evolution of myocardial inflammation in a preclinical model of EAM. We showed that MNP-CMR could be a highly efficient tool for visualizing myocardial inflammation in the early course of the disease with a potential for quantifying the response to specific therapies for myocarditis.

#### **TU215: High Performance of Magneto-fluorescent Nanogels for Visualizing Migration of Dendritic Cells by both Magnetic Resonance and Optical Imaging**

<sup>1</sup>Hyun Min Kim, <sup>1</sup>Hyunseung Lee, <sup>2</sup>Young-Woock Noh, <sup>2</sup>Yong Taik Lim, <sup>1,2\*</sup>Kwan Soo Hong

<sup>1</sup>Division of MR Research, Korea Basic Science Institute,

Cheongwon, Republic of Korea, <sup>2</sup>Graduate School of Analytical Science and Technology, Chungnam National University, Daejeon, Republic of Korea

Cell-based therapies have been focused on attention in regenerative medicine and cancer trials. Magneto-fluorescent nanoparticles have a great potential for cell tracking that can possibly monitor labeled cells by MR/optical dual mode imaging. Such probes incorporate fluorescent quantum dots or organic fluorophores into iron oxide nanoparticles or gadolinium chelates. However, fluorescent compounds incorporated to the magnetic nanoparticles could change intrinsic properties such as size and surface charge of nanoparticles. The ideal nanoprobe should be self-fluorescent without the need for conjugation of external fluorophores. We described synthesis of a self-fluorescent high-relaxivity  $T_2$ -weighted MRI contrast agent as a novel type of MR/optical multimodal imaging nanoprobe via electrostatic assembly and crosslinking of biocompatible polyelectrolytes and  $\text{MnFe}_2\text{O}_4$  nanoparticles without fluorescent nanocrystals or organic fluorophores. Multi-core property of ionic assembled magnetic nanogels showed high relaxivity, which  $r_2$  value of the self-fluorescent nanogels was  $382.6 (\text{Fe}^+\text{Mn}) \text{ mM}^{-1}\text{s}^{-1}$ , and fluorescence maximum peak at  $\lambda_{em} = 553 \text{ nm}$  and smooth shoulder peak at  $\lambda_{em} = 510 \text{ nm}$ . The MR/optical multimodal imaging modalities of the  $\gamma$ -PGA/ $\text{MnFe}_2\text{O}_4$ /PLL(PEG) nanogels used for molecular imaging of dendritic cells, which are commonly used in clinical trials to induce tumor-specific immunity. We confirmed that a bright fluorescence signal (in optical) and darkening effects (due to the shortening of  $T_2$  in MRI) in cellular level with a small amount of nanogels. The novel type of MR/optical dual-modality nanoprobe also showed high performance in the labeling and monitoring of dendritic cells migrated to lymphnode *in vivo*. Crosslinking of the ionic assembled polyelectrolyte magnetic nanogels with glutaraldehyde not only stabilized the nanogels but also generated a strong magnetic and self-fluorescence signals. The novel multimodal imaging nanoprobe based on  $\text{MnFe}_2\text{O}_4$  nanoparticles/polyelectrolyte nanocomposites were used to label and monitor therapeutic cell both *in vitro* and *in vivo*.

### Paramagnetic NMR

#### TH216: NMR characterization of an eukaryotic-like paramagnetic $\text{Cu}_A$ center

Marcos N. Morgada, Luciano A. Abriata, \*Alejandro J. Vila

Instituto de Biología Molecular y Celular de Rosario (IBR-CONICET), Facultad de Ciencias Bioquímicas

The dinuclear copper center  $\text{Cu}_A$  is the electron entry point of cytochrome c oxidase (COX).  $\text{Cu}_A$  funnels the electrons from reduced cytochrome c to the  $\text{Cu}_B$  center at subunit I of COX where  $\text{O}_2$  is reduced to water molecules. These electron transfer reactions are highly efficient and this efficiency is given by the characteristic coordination chemistry of this center.

Two alternative electronic ground levels, with different orbital symmetries, have been established for the  $\text{Cu}_A$  center in its oxidized form ( $\text{Cu}^{+1.5}\text{-Cu}^{+1.5}$ )  $\sigma_\mu^*$  and  $\pi_\mu$ . NMR studies of COXII from *Thermus thermophilus* (TtCuA) revealed the presence of signals with Non-Curie temperature dependence behaviour, indicating that these levels are very close in energy[1]. We have shown previously that the energy gap between these levels can be tuned by mutations of residues of the first coordination sphere of the  $\text{Cu}_A$  center in TtCuA[2,3].

Now we have replaced three loops in TtCuA by the ones present in the human homologue. This substitution preserves both  $\text{Cu}_A$  center ligand identity and the loops length present in the native protein, introducing only second sphere perturbations. Using NMR we have found that these mutations

tune the electronic structure of the center reducing by the energy gap between  $\sigma_\mu^*$  and  $\pi_\mu$  electronic levels.

[1] Bertini, I.; Bren, K. L.; Clemente, A.; Fee, J. A.; Gray, H. B.; Luchinat, C.; Malmström, B. G.; Richards, J. H.; Sanders, D.; Slutter, C. E. J.Am.Chem.Soc. 1996, 118, 11658.

[2] Abriata, L. A.; Ledesma, G. N.; Pierattelli, R.; Vila, A. J. J Am Chem Soc 2009, 131, 1939.

[3] Abriata, L. A.; Alvarez-Paggi, D.; Ledesma, G. N.; Blackburn, N. J.; Vila, A. J.; Murgida, D. H. Proc Natl Acad Sci U S A 2012, 109, 17348.

#### MO217: Tuning the Electronic Structure of Electron Transfer Copper Proteins Through Loop Engineering

Andrés Espinoza Cara, Luciano A. Abriata, \*Alejandro J. Vila

Instituto de Biología Molecular de Rosario (IBR-CONICET)

Nature employs metal ions for a wide variety of biological functions. Copper proteins play an important role in electron transfer processes. There are two types of copper electron transfer sites in nature: (a) mononuclear type I centers (T1), also known as blue sites, and (b) the dinuclear  $\text{Cu}_A$  center<sup>1</sup>. Proteins with T1 and  $\text{Cu}_A$  centers share a conserved fold (cupredoxin fold) despite being from different organisms, revealing a common evolutionary origin<sup>2</sup>. The functional properties of these redox sites cannot be compared directly because of being in different protein matrixes. The T1 and  $\text{Cu}_A$  centers presents and ideal situation for loop changing as they share the same protein fold and most of the metal ligands are present in loops. There are few examples using this strategy, but all of them suggest that the ligand-containing loops gather most of the structural information that regulates the function of the redox site<sup>3,4</sup>. In this project we employ loop directed mutagenesis in order to introduce different T1 loops in the soluble fragment of the subunit II of the cytochrome *ba3* oxidase from *Thermus thermophilus*, naturally harboring a  $\text{Cu}_A$  site (TtCuA). Two T1 variants were constructed, employing the loops from amicyanin (Ami-TtCuA) and azurin (Az-TtCuA). These proteins have distinct characteristics from the native sites. Using distinct biophysical approaches such as optical spectroscopy, EPR and NMR we determined that both proteins have properties that vary along those of rhombic T1 sites. Both proteins can also bind exogenous imidazole in a reversible way giving rise to a copper site similar spectral features as those found in nitrosocyanin<sup>5</sup>. Taken together, these observations discard the "loop defines everything" hypothesis and show how reversible binding of small molecules can be elicited in an otherwise occluded metal site.

#### References:

1. Solomon, E. I.; Szilagyi, R. K.; DeBeer, G. S.; Basumallick, L. Chem.Rev. 2004, 104, 419-458.
2. Randall, D. W.; Gamelin, D. R.; LaCroix, L. B.; Solomon, E. I. J.Biol.Inorg.Chem. 2000, 5, 16-29.
3. Hay, M.; Richards, J. H.; Y Lu, Y. PNAS, 1996, 93, 461-464
4. Li, C.; Banfield, M. J.; Dennison, C. J.Am.Chem.Soc., 2007, 129, 3, 709-718
5. Basumallick, L. Sarangi, R.; DeBeer George, S.; Elmore, B.; Hooper, A. B.; Hedman, B.; Hodgson, K. O.; Solomon, E. I. J.Am.Chem.Soc., 2005, 127, 10, 3531-3544.

### EPR/ENDOR

#### TU218: EPR and ED ESE study of the nitroxide radicals confined in breathing MIL-53(Al) nanochannel system

<sup>1,2\*</sup>Elena Bagryanskaya, <sup>2</sup>Alena Nishchenko, <sup>2</sup>Matvey Fedin, <sup>3</sup>Alexander Stepanov, <sup>3</sup>Daniil Kolokolov, <sup>3</sup>Anton Gabrienko, <sup>4</sup>Sergey Gromilov, <sup>1</sup>Inna Shundrina

<sup>1</sup>N.N. Vorozhtsov Novosibirsk Institute of Organic Chemistry, Novosibirsk, Russia, <sup>2</sup>International Tomography Center, Institutskaya, Novosibirsk, Russia, <sup>3</sup>Borshkov Institute of Catalysis, Novosibirsk, Russia, <sup>4</sup>Nikolaev Institute of Inorganic Chemistry, Novosibirsk, Russia

Metal-organic frameworks (MOFs), a novel class of micro and meso-porous materials, have attracted much attention due to their high practical importance in industry and medicine. Adsorption of radical molecules in MOFs could provide novel materials with new catalytic or magnetic properties. The MIL-53 type (MIL: Materials of Institute Lavoisier) has a remarkable feature. Transition from large pore (LP) to narrow pore (NP) in MIL-53(Al) can occur both by influence of guest and by changing the temperature. Moreover, this material is stable at up to 500°C. <sup>2</sup>H nuclear magnetic resonance (NMR)[1-2] as well as continuous wave (CW) and echo detected (ED) electron paramagnetic resonance (EPR) spectroscopy [3] are reliable tools to extract information about the dynamics of molecules confined in porous media. Since EPR is only sensitive to the paramagnetic guest it provides the tool of choice to study the guest properties under modified host conditions. We performed first EPR study of nitroxide radicals (TEMPO and di-tert-butyl nitroxide) adsorbed inside MIL-53(Al). The temperature dependence of CW and ED X-band (9 GHz) and Q-band (34 GHz) EPR spectra has been measured for polycrystalline MIL-53(Al) containing probe radicals with various ratios per MIL-53(Al) unit cell. CW and ED EPR for samples with 1/1000 ratio of TEMPO demonstrated a temperature driven phase transition from paramagnetic to diamagnetic state of adsorbed molecules with pronounced structural hysteresis, in agreement with neutron diffraction and scattering experiments [4]. It was shown observed that the EPR line shape is sensitive to the temperature prehistory. Moreover, it has been demonstrated that the reversible phase transition of MIL-53 from LP crystalline state to the NP crystalline state is accompanied by the reversible changes in the second integral of the CW EPR spectra by a factor of three. This fact was explained by partial complexation of TEMPO molecules with OH groups of MIL-53(Al). The motion of the probe molecules revealed by EPR reflected structural changes of MIL-53(Al). Temperature dependent CW EPR and ED ESE spectra were obtained and simulated using Easy Spin program. The X-ray and FTIR data confirmed the H-bonding between TEMPO and  $\mu$ 2-OH bridging hydroxyl group for the sample with 1/1 ratio of radical per unit cell.

This work was supported by the Russian Foundation for Basic Research, grant no.12-03-33010, 12-03-31329; RF Ministry for Education and Science no.8456

[1] A.M. Nishchenko, et al. J.Phys. Chem., 2011. 115(26): p. 7428-7436.

[2] A.M. Nishchenko et al. , Journal of Physical Chemistry C, 2012.116(16): p. 8956-8963.

[3] E.G. Bagryanskaya et al., Phys. Chem. Chem. Phys., 2009. 11(31): p. 6700-6707.

[4] Y. Liu, et al J.Amer.Chem. Soc. 2008. 130(35): p. 11813-11818.

#### TH219: New spin probes for spin-site labeling and EPR imagine

<sup>1,2\*</sup>Elena Bagryanskaya, <sup>1</sup>Igor Kirilyuk, <sup>2</sup>Olesya Khrumkacheva, <sup>2</sup>Rodion Strizhakov, <sup>2</sup>Matvey Fedin, <sup>1</sup>Igor Grigor'ev, <sup>1</sup>Denis Morozov, <sup>1</sup>Yuliya Polienko, <sup>2</sup>Elena Fursova, <sup>2</sup>Evgeny Tretyakov

<sup>1</sup>N.N. Vorozhtsov Novosibirsk Institute of Organic Chemistry of the SB RAS, Novosibirsk, Russia, <sup>2</sup>International Tomography Center, SB RAS, Novosibirsk, Russia

In this presentation we report the CW and pulse X-band and Q-band EPR study of newly synthesized imidazoline, imidazolidine and fluorine substituted imino-nitroxide nitroxides [1,2], in particular nitronyl nitroxides radical as spin probes

for nitric oxide [1] and spirocyclic substituted pyrroline nitroxides as spin labels to study structure and functions of proteins [2]. The series of new spirocyclohexane substituted nitroxides were synthesized including thiol-specific methane thiosulfonated spin label for site-directed spin labelling [2]. CW and pulse EPR was used to study the effect of spirocyclohexane moieties on nitroxide's chemical and spectral properties. The obtained temperature dependencies of electron relaxation times demonstrate that the new nitroxides may be suitable for PELDOR distance measurements at 80-120 K. Moreover, the new nitroxides demonstrate much higher stability towards reduction by ascorbic acid than spirocyclohexane-substituted nitroxides of piperidine series and showed 3-5 times lower reduction rates compared to corresponding 2,2,5,5,-tetramethyl substituted nitroxides. The first examples of application of new nitroxides to measure distances in real biological systems will be shown.

Nitronyl nitroxides specifically react with NO to form imino nitroxides (IN), with comparatively high reaction constants of about  $10^4 \text{ M}^{-1} \text{ s}^{-1}$ . This reaction has been used for NO detection in a number of biological applications, based on significant differences in the electron paramagnetic resonance (EPR) spectra of NN and IN. New water soluble non-toxic nitronyl nitroxides (NN) as well as their fluorine substituted analogs were used as spin probes for nitric oxide detection *in vitro* and *in vivo*. Stability of these nitroxides was investigated and possibility of their application as NO probes in EPR imaging was studied. Experiments *in vivo* using EPR imaging revealed that entire radical injected in a mouse intravenously accumulates in urinary bladder. Injection of the nitronyl nitroxide while NO expression in mouse' vessels induced by nitroglycerin and observed subsequent slow down of the nitronyl nitroxide accumulating in bladder and no EPR signal of imino nitroxide was detected.

[1] R. Strizhakov, E.Fursova, N.Kolosova, L.Shundrin, V.Ovcharenko, E.Bagryanskaya, Free Rad. In Biol.and Med. 2013, (to be submitted).

[2] I.A. Kirilyuk, Y.F. Polienko, O.A. Khrumkacheva, R. K. Strizhakov, Y.V. Gatilov, I.A. Grigor'ev, and E.G. Bagryanskaya, J. Org. Chem., 2012, 77 (18), pp 8016-8027

Acknowledgment: This work was supported by the Ministry of education and science of Russian Federation, projects 8456 and 8456 and Russian Science Foundation, project 12-04-01435.

#### MO220: Magnetic Transition of the Mineral Goethite by Electron Paramagnetic Resonance

\*Daniel Farinha Valezi, Eduardo Di Mauro

Universidade Estadual de Londrina

Synthetic and natural samples of the mineral goethite were characterized by EPR, with the main objective of studying the magnetic transition from the antiferromagnetic state to the paramagnetic state, that this mineral undergoes upon reaching a certain critical temperature (Néel temperature). EPR experiments were performed at microwave frequency of X-band (9.3 GHz) on a JEOL spectrometer (JES-PE-3X) in LAFLURPE Laboratory at the State University of Londrina. Experiments with temperature variation were performed with variable temperature controller (JES-VT-3A) in a range of 300 to 444K. Synthetic samples were measured in powder form and natural samples were measured in powder and flakes form in quartz tubes of 4mm in diameter in case of room temperature measures, and in tubes of 3mm in diameter in case of variable temperature. Although it will be not expected EPR signal in samples of goethite, due to its antiferromagnetic arrangement, the resonance lines were observed at room temperature, and this behavior was attributed to the existence of a weak ferromagnetism. When increasing of the temperature is above 348K for the natural sample, and 351K for the synthetic sample, goethite spectrum started to present a new line of EPR, which grows in intensity until it stabilizes at 440K. The appearance of this resonance line

was attributed to the magnetic transition that the mineral goethite suffered with the increase in temperature above the Néel temperature. The magnetic transition did not occur at a certain temperature, this fact was attributed to non-uniformity of the samples in both particle size and vacancy concentration. For the first time were performed the simulation of the EPR line of the mineral goethite due to the paramagnetic state, above the Néel temperature, as well as, the variation of signal intensity with increasing temperature.

#### TU221: Polymerization Process Interpretation of Dental Resins via Electron Paramagnetic Resonance (EPR) in X, Q and W Bands.

<sup>1</sup>Adriana Da Silva Fontes, <sup>3</sup>Bruno Luiz Santana Vicentin, <sup>2</sup>Walter Sano, <sup>3\*</sup>Eduardo Di Mauro

<sup>1</sup>Federal Technological University of Paraná, Campo Mourão, <sup>2</sup>Physics Institute, University of São Paulo, São Carlos, <sup>3</sup>LAFURPE, CCE, State University of Londrina, Londrina

Many studies have been done on photopolymerizable dental resins, used on tooth restoration, because its properties, like color, hardness and resistance, shows that they are the best substitutes for the lost part of tooth. The most part of those studies have been done by Electron Paramagnetic Resonance (EPR) experiments, which analysis in X band reveals a nine lines spectrum, due to free radical formation on the polymerization process, initiated by radiating the sample with blue visible light. However, many authors still disagree about the formation of EPR spectrum. Some authors state that the spectrum is formed by a sum of three or more radicals, others says it is a superposition of two radicals, one with five lines and the other one with four lines. In this work, we utilized commercial resins Z100 (3M) to obtain EPR spectrum in X, Q and W bands in order to identify the free radicals involved on the polymerization process, and also theoretically simulated the spectrums with computation resources. These resins are composed essentially by a mixture of dimethacrylate monomers (Bis-GMA and TEGDMA), initiating agents (Camphorquinone and Amine) and inorganic charge particles, zirconia and silica (ZrO<sub>2</sub>/SiO<sub>2</sub>). As blue visible light source we used a LED (ULTRA BLUE-DABI ATLANTE) with intensity of 492 mW/cm<sup>2</sup>. The EPR experiments in X-band were performed on the JEOL spectrometer (JES-PE-3X) at room temperature, at LAFURPE, in University of Londrina (UEL). A g marker of MgO:Mn<sup>2+</sup> (g=1.981 in the fourth line of the spectrum) was maintained in the cavity of the spectrometer, so that the data were obtained simultaneously with the samples spectra. The samples were prepared in silica molds of 2x2mm, irradiated for 40 seconds and immediately analyzed. EPR spectrum in Q-band were obtained in Biophysics Laboratory, at Physics Institute in University of São Paulo (USP) at São Carlos, using a VARIAN (E-109) spectrometer, having chrome as standard. Spectrum in W-band was obtained by a BRUKER (Elexsys E 680) spectrometer, with a TerraFlex probe, in Bruker Laboratory at Rheinstetten, Germany, using samples with 1x1mm. We simulated experimental results considering the spectrum been formed by the sum of three different radicals (named radicals I, II, and III) with distinct life-time. The radical II was considered having a very short life-time. The simulation showed that the spectrum is formed by a superposition of a weak nine lines spectrum of radical I with a strong five lines spectrum of radical III, in perfect agreement with experimental results. The EPR spectrum of the composite resin has been interpreted throughout the analysis performed in X-, Q- and W-band, with their simulations, concluding that for EPR are proposed two methacrylate radical species: (-CH<sub>2</sub>-C·-CH<sub>3</sub>-) and (-CH<sub>2</sub>-C·-CH<sub>2</sub>-), called in this work of RI and RIII, respectively, which are present in concentrations very close. These species are responsible for the continuity of the resin polymerization process after photopolymerization.

#### TH222: Antiferromagnetic ordering in quasi-low dimensional polymeric magnets: a CW-ESR study

<sup>1\*</sup>D. Kaminski, <sup>1</sup>A. L. Webber, <sup>1</sup>J. Liu, <sup>1</sup>P.A. Goddard, <sup>2</sup>J. L. Manson, <sup>1</sup>A. Ardavan

<sup>1</sup>Centre for Advanced Electron Spin Resonance, Clarendon Laboratory, Department of Physics, University, <sup>2</sup>Department of Chemistry and Biochemistry, Eastern Washington University, Cheney, WA, USA

In both 1D and 2D systems, the formation of long-range magnetic order is impossible at temperature  $T > 0$  K. However, attempts experimentally to realise such systems are imperfect, resulting in 'quasi' 1D (Q-1D) and 2D (Q-2D) systems. These have a small but finite coupling across the remaining dimensions, meaning magnetic ordering at  $T > 0$  K is a possibility.

Polymeric magnets are quasi-low dimensional and consist of magnetic ions linked by organic groups, forming chains and layers. With the ability we have to fine-tune their magnetic parameters, they provide a fertile test ground for aspects of the quantum theory of magnetism [1, 2].

We here explore, via X- and D-band CW-EPR at variable temperature, a group of coordination polymers which form antiferromagnetic states at  $T < T_N$  where  $T_N$  is on the order of a few Kelvin. Through careful extraction of linewidth and principle  $g$ -tensor components, we are successful in probing the temperature region above  $T_N$ . We therefore propose use of this method across a wider range of compounds to gain insight into the ordering process itself.

[1] P. A. Goddard et al., *New J. Phys.* **2008** (10) 083025.

[2] P. A. Goddard et al., *Phys. Rev. Lett.* **2012** (108) 0077208.

#### MO223: Chemical Tuning of Molecular Magnets for Quantum Information Processing

<sup>1\*</sup>D. Kaminski, <sup>1</sup>A. L. Webber, <sup>1</sup>C. J. Wedge, <sup>2</sup>E. T. Spielberg, <sup>2</sup>G. A. Timco, <sup>2</sup>F. Tuna, <sup>2</sup>E. J. L. McInnes, <sup>2</sup>R. E. P. Winpenny, <sup>1</sup>S. J. Blundell, <sup>1</sup>A. Ardavan

<sup>1</sup>Centre for Advanced Electron Spin Resonance, Clarendon Laboratory, Department of Physics, University, <sup>2</sup>School of Chemistry and Photon Science Institute, University of Manchester, United Kingdom.

As classical computational devices head towards the atomic scale, they approach their technological limit. Quantum mechanical effects are coming into play and the world is seeking a new way forward: the 'quantum computer'. A quantum computer stores data as 'qubits'. These are two level systems that, as well as either state, can occupy a superposition of the two. A system of  $n$  coherent qubits would allow us to form a superposition of  $2^n$  states and perform certain operations in fewer computational steps than is necessary with a classical machine.

When in 2001 the theoretical possibility of using EPR on high spin molecular magnets to implement elementary quantum algorithms was shown, research in the area exploded [1]. In order to be useful in a quantum computer, the coherence time of a qubit must exceed substantially the time required for single-qubit manipulations. At low enough temperature, this is true of a Cr<sub>7</sub>Ni molecular nanomagnet, whose exchange coupled magnetic core can be treated as an effective electron spin-1/2 system [2]. By varying key structural components, Wedge et al. have studied the dominant mechanisms of decoherence in the Cr<sub>7</sub>Ni nanomagnet family [3]. In particular, a comparison of electron spin coherence times observed for protonated (<sup>1</sup>H,  $I = 1/2$ ) and deuterated (<sup>2</sup>H,  $I = 1$ ) Cr<sub>7</sub>Ni molecules has suggested that the nuclear magnetic moments in the extensive network of protons are key in limiting the spin coherence times in these systems.

The present work aims to further isolate the sources of electron spin decoherence in molecular magnets, initially by chemical substitution of the proton network with halogen elements [e.g. <sup>35</sup>Cl and <sup>19</sup>F]. Coherence lifetimes are presented for dilute, frozen solutions measured using a 2-pulse Hahn-



echo EPR sequence at X-band. In addition, the electron spin properties of Cr<sub>7</sub>Ni dimers are investigated as potential two-qubit systems capable of more complex quantum algorithms.

- [1] M. Leuenberger and D. Loss, *Nature* **2001** (410) 789.
- [2] A. Ardavan et al., *Phys. Rev. Lett.* **2007** (98) 057201.
- [3] C. J. Wedge et al., *Phys. Rev. Lett.* **2012** (108) 107204.

#### TU224: ESR Study of Hybridization Effects in Some New Dense Posphides

Eduard M. Gataullin, \*Vladimir A. Ivanshin

Kazan Federal University

The explanation of transformation of localized electrons at high temperatures into itinerant quasi-particles with an enhanced mass at lower temperatures belongs to the most important challenges in the physics of the solid state. The mechanism of this evolution depends on the Kondo interactions between the CE and the localized *d* or *f* electrons. ESR probes microscopically both the local moment (LM) spins and CE in different strongly correlated electron systems (SCES) such as high-temperature superconductors, pnictides, heavy fermion systems. As a rule, LM ESR is studied in compounds with doped paramagnetic ions and localized electrons. ESR from CE can be detected in metallic systems with an enhanced Pauli susceptibility. Surprisingly, ESR could be also observed in some dense SCES without any kind of paramagnetic doping (s. [1] and references therein). According to several theories, a measurable ESR signals in these experiments are caused by an effective hybridization between localized *f* electrons and conduction bands in conjunction with ferromagnetic (FM) correlations which reduce usually a very fast spin-lattice relaxation [1, 2]. In the present contribution, we report the temperature-dependent ESR spectra in two ternary recently synthesized phosphides YbRh<sub>6</sub>P<sub>4</sub> and CeIr<sub>2</sub>P<sub>2</sub>. A relatively weak ESR signals in both compounds reflect the extremely weak *f-p* hybridization effects in contrast to the case of silicides YbRh<sub>2</sub>Si<sub>2</sub> and YbIr<sub>2</sub>Si<sub>2</sub>. Our results in YbRh<sub>6</sub>P<sub>4</sub> reveal temperature dependences of the ESR g-factor and peak-to-peak linewidth for an Orbach-like ESR relaxation of the Yb<sup>3+</sup> LM which can be related to the first excited crystal-field state at 82.1 K [3].

- [1] P. Schlottmann, *Phys. Rev. B* **86**, 075135 (2012)
- [2] D. Huber, *Mod. Phys. Lett. B* **26**, 1230021 (2012)
- [3] V.A. Ivanshin et al., *Journal of Phys.: Confer. Ser.* **391**, 012024 (2012)

#### TH225: The g-tensor for ESR in single crystals: a new approach for non-perpendicular faces

<sup>1</sup>\*Cesar José Calderon Filho, <sup>2</sup>David Vaknin, <sup>1</sup>Gaston Barberis

<sup>1</sup>IFGW, Unicamp, Campinas (SP) Brasil, <sup>2</sup>Ames Lab, IO, USA

The electron paramagnetic resonance (EPR) spectra of magnetic ions in anisotropic single crystals are characterized by a g-tensor (and hyperfine tensor, if exists) that cannot be obtained directly by a few measurements, except in the case that directions of principal axes of the crystal respect to the macroscopic directions in the sample are known. To obtain the parameters in the general case, Schonland proposed a method for obtaining the g-tensor but only for certain particular cases. This excludes single crystals without growing faces related to the principal axes of the unit cell. This work proposes a general method to obtain the principal values of the g- (and A) tensors, that can be used in any single crystal, where it is known the orientation of three independent planes respect to the crystal axes. Using the fact that the g- (and A) values in a plane can be written as  $g^2 = A + B \cos(2\beta) + C \sin(2\beta)$ , where  $\beta$  is the rotation angle and the parameters A, B and C are functions of the elements of the g-tensor, the measurements of the spectra in the three

linearly independent planes gives us a linear set of equations. The solution of this linear system are principal values and directions of the g(A)-tensor. Our method contains the Schonland method as a particular case. We present here the application of our method to LiMnPO<sub>4</sub> single crystals. In this case, three planes were polished in the sample, and the orientation of them respect to the crystal axes obtained from X-ray diffraction experiments.

#### MO226: Light-Induced Synthesis and Paramagnetic Properties of Phenothiazine Nanoparticles in the Presence of Polyethyleneglycol

<sup>4</sup>Carolina G. dos Santos, <sup>1</sup>André L. Silva, <sup>2</sup>Alexandre J. C. Lanfredi, <sup>3</sup>Otacíro R. Nascimento, <sup>1</sup>\*Iseli L. Nantes

<sup>1</sup>CCNH - Universidade Federal do ABC, <sup>2</sup>CECS - Universidade Federal do ABC, <sup>3</sup>Universidade de São Paulo, São Carlos, <sup>4</sup>Universidade de Mogi das Cruzes

Literature data report that phenothiazines can be converted to cation radical by enzymatic, chemical and photochemical reactions. Previously, our research group had characterized the photochemical behavior of the antipsychotic drugs thioridazine (TR), trifluoperazine (TFP), and fluphenazine (FP) influenced by the aggregation state of the molecules. These compounds are converted to stable cation radicals in high concentration in mild conditions, i.e., aqueous buffered solutions, pH 5.0. The stability of phenothiazine cation radicals in the phenothiazine aggregates at room temperature has been assigned to the stacking of the thiazine phenyl moieties. Therefore, stable cation radicals of phenothiazines have been described for aggregates of the drugs and for dimeric and oligomeric derivatives produced by chemical synthesis. However, water-dependent dimerization of phenothiazines from chemically produced cation radicals was also described but the magnetic properties of these dimers as well as possible formation of nanostructures with these compounds remained to be investigated. In the present study, the synthesis of polyethyleneglycol (PEG)/phenothiazine nucleus (PHT) nanoparticles (NP) using the photochemical properties of PHT is characterized by electronic absorption (EA), electronic paramagnetic resonance (EPR), infrared spectroscopy (ATR/FTIR), atomic force microscopy (AFM) and scanning electronic microscopy (SEM). In the studied system, the UV light-induced formation of NPs is dependent of the formation of PHT cation radical, the presence of water and acetate as the counterion. In the presence of PEG, the formation of NPs was modulated by the PHT/PEG ratio that influences PHT aggregation and oligomerization. The aggregation of PHT molecules stabilizes the cation radical and the photo-oligomerization is dependent of the access to bulk water modulated by the microenvironment provided by PEG. In PEG/PHT NPs, the photochemically produced cation radicals are stable but the distance between the radical center prevents they are coupled in a triplet state.

ACKNOWLEDGEMENTS: FAPESP, CAPES and CNPq

#### TU227: Effects of KL4 on Lipid Bilayer Dynamics and Fluidity Properties

Otonye Braide, \*Joanna Long, Gail E Fanucci

University of Florida

KL4, a 21 residue mimetic of surfactant protein B, is effective in the treatment of infant respiratory distress syndrome (RDS) and functions by lowering aveolar surface tension and promoting oxygen exchange. We utilized a pyrene phospholipid analog to investigate the effect of KL4 on lipid organization and acyl chain dynamics by monitoring changes in excimer-to-monomer (I<sub>e</sub>/I<sub>m</sub>) ratio. This experiment probes the environment of the hydrophobic core of DPPC/POPG and POPC/POPG liposomes. An average decrease of 27-40% and 0-10% in I<sub>e</sub>/I<sub>m</sub> was observed in the DPPC/POPG and POPC/POPG LUVs, respectively, with increasing peptide concentration (0.5 to 5 mol%). This decrease is directly proportional to a lowered probability of excimer formation,

which is highly dependent on proximal interactions of an excited monomer with a pyrene moiety at ground state. The ability of the peptide to modify membrane fluidity properties was studied via anisotropy measurements of a rhodamine-labeled phospholipid. A steady increase in the order was observed in the DPPC/POPG liposomes with relatively constant fluorescence intensity, while collisional quenching was observed in the POPC/POPG liposomes. These observations agree with NMR and EPR observations, and proposed mechanisms of peptide-mediated lipid trafficking.

#### TH228: Topological Games and Spin Gymnastics: a Systematic Approach to ENDOR Pulse Sequences

Daniel Finkelstein-Shapiro, \*Vladimiro Mujica

Arizona State University

Pulsed electron-nuclear double resonance (ENDOR) techniques reveal the nuclei coupled to an electron spin. The two fundamental sequences, Mims and Davies, come in several flavors: hyperfine selective ENDOR, sequences independent of spectrometer deadtime, optimized polarization transfer just to name a few. An understanding of these sequences via the product operator formalism reveals which coherences contribute to the final electron magnetization carrying the electron-nuclear coupling information.

In this work, we propose a classification of ENDOR experiments based on the structure of the pulse sequence itself. We decompose the pulse sequence in the basis of superoperators, where a pulse sequence is naturally represented by a path of vectors whose lengths correspond to the pulse duration or the time during which the system evolves. By restricting our analysis to pulses along the x-axis, the pulse sequence is fully described in the basis ( $S_x$ ,  $I_x$ ,  $H$ ), and as a consequence admits an intuitive representation in  $R^3$ . Using this geometrical representation and a few constraints on starting and ending points, we can generate candidate sequences for ENDOR in a systematic way. We discuss new possible sequences, and begin to explore the properties of this space including its analogy with moduli spaces. We believe that this new representation, which has applicability beyond ENDOR, will provide a more transparent intuition and a systematic way to explore new sequences.

#### MO229: EPR study of copper ethylenediamine intercalated in bentonite clay

<sup>1</sup>\*Cláudio José Magon, <sup>1</sup>J. P. Donoso, <sup>1</sup>I. D. A. Silva, <sup>1</sup>Otacíro R. Nascimento, <sup>1</sup>J. F. Lima, <sup>2</sup>M. Moreno, <sup>2</sup>E. Benavente, <sup>3</sup>G. Gonzalez

<sup>1</sup>Universidade de São Paulo, Brasil, <sup>2</sup>Universidad Tecnológica Metropolitana, Santiago, Chile, <sup>3</sup>Universidad de Chile, Santiago, Chile

Bentonites are rocks dominated by smectites layer clay minerals, which has attracted great interest in environmental pollution treatment due to its remarkable properties [1-3]. Layered clays offer a rich inclusion chemistry, which allows to modify and functionalize materials at nanoscale level, exhibiting new physical and chemical properties [4,5]. In this work we report results from electron paramagnetic resonance (EPR) spectroscopy of Cu(II) exchanged in bentonite and Cu(II) bis(ethylenediamine), Cu(en)<sub>2</sub>, exchanged in bentonite. The observed X-band EPR spectra consist of a hyperfine structure arising from the isolated Cu(II) ions superposed on a broad resonance line, which is attributed to spin-spin exchange interactions between neighbouring Cu(II) ions. The observation of a single Cu(II) isolated species with well resolved hyperfine structure in the EPR spectra of the Cu(II) exchanged bentonite suggests that copper ions preferentially occupy the interlayer regions. The analysis of the spin Hamiltonian parameters suggests that paramagnetic Cu(II) ions are in axially distorted sites. The analysis of the spin Hamiltonian parameters indicates the presence of the Cu(en)<sub>2</sub> complex in the interlayer region of the bentonite, with the copper coordinated to four nitrogen in the equatorial plane and to oxygen

in the the z axis. The evaluation of the Cu(II) bonding parameters indicates that the in-plane sigma-bonding between ethylenediamine and the copper becomes slightly more covalent when the Cu(en)<sub>2</sub> complex is introduced in the bentonite clay. Partial support of Capes, CNPq and Fapesp (Brasil) and of Chilean agencies FONDECYT (1090282), CONICYT, FB0807 (CEDENNA), and ICM and Innovation Fund for Competitiveness, Ministry of Economy, Development and Tourism Project (FP10-061-F-FIC), are gratefully acknowledged.

[1] A. Kaya, A.H. Oren, J. Hazardous Mat. B125 (2005) 183.

[2] L. Chen et al., J. Radioanal. Nucl. Chem. 292 (2012) 1181.

[3] L.F. Gonzalez Bahamon et al., Chemosphere 82 (2011) 1185.

[4] M. Lezhnina et al., Chem. Mater. 19 (2007) 1098.

[5] S. Celedon et al., Materials Research Bulletin 44 (2009) 1191.

[6] C.J. Magon et al., J. Magnetic Resonance 184, 176 (2007).

#### TU230: Deconvolution of the EPR spectra of vanadium oxide nanostructures

<sup>1</sup>\*Cláudio José Magon, <sup>1</sup>J. F. Lima, <sup>1</sup>J. P. Donoso, <sup>2</sup>V. Lavayen, <sup>3</sup>E. Benavente, <sup>4</sup>D. Navas, <sup>4</sup>G. Gonzalez

<sup>1</sup>Universidade de São Paulo, São Carlos, Brazil, <sup>2</sup>Universidad Técnica Federico Santa María, Valparaíso, Chile, <sup>3</sup>Universidad Tecnológica Metropolitana, Santiago, Chile, <sup>4</sup>Universidad de Chile, Santiago, Chile

Vanadium oxide (VO<sub>x</sub>) nanostructures have attracted considerable attention in the last years because of their potential importance for catalysis and electrochemical applications [1-3]. This work reports an electron paramagnetic resonance (EPR) study of two VO<sub>x</sub> nanostructures: nanotubes and nano-urchins. Nanotubes consist of vanadium oxide sheets with alternating layers of long-chain alkyl amines, which bend to form one-dimensional tubular products [4,5]. The urchin-like nanostructure consists of high-density spherical radial arrays of nanotubes [6]. The layers of the nanotubes are constituted by vanadium ions in two different oxidation states, magnetic V<sup>4+</sup> with spin  $S = 1/2$  and non-magnetic V<sup>5+</sup> with  $S = 0$ . The observed X-band EPR spectra of VO<sub>x</sub> nanotubes consist of a hyperfine structure arising from the isolated V<sup>4+</sup> ions superposed on a broad resonance line, which is attributed to spin-spin exchange interactions between neighbouring V<sup>4+</sup> sites [7,8]. In this work we applied the deconvolution approach based on the Krylov basis diagonalization method (KBDM) to separate the contributions of isolated ions (sharper lines) and clusters (broader lines) in the experimental EPR spectra of the VO<sub>x</sub> nanotubes and nano-urchins. The objective is to correlate the spin Hamiltonian parameters and simulation data with the physical structures of different VO<sub>x</sub> nanostructures. Acknowledgments: Partial support of Capes, CNPq and Fapesp (Brasil) and of Chilean agencies FONDECYT (P. 1090282), CONICYT, FB0807 (CEDENNA), and ICM and Innovation Fund for Competitiveness, Ministry of Economy, Development and Tourism Project (FP10-061-F-FIC), are gratefully acknowledged

[1] W. Jin, et al. Applied Surface Science 257 (2011) 7071.

[2] S.D. Perera et al., Advanced Energy Materials 1 (2011) 936.

[3] C. Wu, Y. Xie, Energy and Environment Science 3 (2010) 1191.

[4] C. O'Dwyer et al., J. Electrochemical Society, 154 (2007) K29.

[5] J. Livage, Materials 3 (2010) 4175.

[6] C.O'Dwyer et al. Chemistry of Materials 18 (2006) 3016.

[7] M.E. Saleta et al., J. Applied Physics 109, 093914 (2011).

[8] C.J. Magon et al., J. Magnetic Resonance 222 (2012) 26.

### TH231: Biophysical studies on the orientation of coiled-coils of septin peptides

<sup>1</sup>\*Edson Crusca, <sup>1</sup>Patricia S. Kumagaia, <sup>1</sup>Claudia Elisabeth Munte, <sup>2</sup>Antonio José Costa-Filho, <sup>1</sup>Richard Charles Garratt

<sup>1</sup>Grupo de Biofísica Molecular “Sérgio Mascarenhas”, Instituto de Física de São Carlos, Universidade de São Paulo, <sup>2</sup>Laboratório de Biofísica Molecular, Departamento de Física, Faculdade de Filosofia, Universidade de São Paulo

Mammalian septins form a subfamily of GTP-binding proteins conserved from eukaryotic protists to mammals that are involved in various cellular processes as well as in diverse neuropathological conditions. Specific combinations of septins form hetero-oligomeric complexes that polymerize *in vivo* and *in vitro* into non-polar filaments. Septins share a conserved GTP-binding domain and a predicted coiled-coil domain at their C-terminus. Although the crystal structure of the complex formed by human septins SEPT2, SEPT6 and SEPT7 has been determined by Sirajuddin et al. (2007), no electron density was observed for the C-terminal domains. Therefore, the structure provided no information about how these domains associate to assemble the hetero-oligomeric complexes. A model for the formation of septin complexes was postulated by Kinoshita et al. (2003): SEPTX/6/7, where X could be SEPT1, 2, 4 or 5 (members of the SEPT2 group). Here we present biophysical studies on a series of peptides derived from SEPT2 group proteins, which correspond to the central region of the septin C-terminal domain. The four peptides have been manually synthesized by Fmoc-SPPS strategy with an additional cysteine residue at the C-terminus region in order to allow for the selectively labeling with the spin-label 1-oxyl-2,2,5,5-tetramethylpyrroline-3-methyl-sulfonate (MTSSL). Samples were purified by HPLC-RP (>95% of purity). The peptides have been analyzed by 2D-NMR and showed a helical conformation. CD measurements indicated a high helical content and a typical coiled-coil signal for temperatures below 10°C. For each peptide the coiled-coil orientation was determined by CW-EPR experiments, where the interaction of the MTSSL spin label yielded large dipolar broadening in the cases where the peptides adopted a parallel orientation. Our results show that peptides SEPT1CC, SEPT4CC and SEPT5CC are antiparallel, whereas SEPT2CC is parallel. Thus, despite belonging to the same group, the peptides can form coiled-coils with distinct orientations, which may have crucial implications in the formation of septin complexes.

Supported by FAPESP, CNPq and CAPES.

### MO232: High-Frequency and -Field EPR (HFEPR) Studies of New Magnetic Materials with Unusual Optical Properties that Contain High-spin Mn(III) and Fe(III)

<sup>1</sup>\*Joshua Telser, <sup>2</sup>J. Krzystek, <sup>2</sup>Andrew Ozarowski, <sup>3</sup>Peng Jiang, <sup>3</sup>M. A. Subramanian

<sup>1</sup>Roosevelt University, <sup>2</sup>NHMFL Florida State University, <sup>3</sup>Oregon State University

The Subramanian group at Oregon State University has recently prepared a variety of new oxide-based materials based on YInO<sub>3</sub> [1-2]. In these materials, the In(III) ions are substituted by either Mn(III) or Fe(III), which each find themselves in a trigonal-bipyramidal (tbp) environment. While YInO<sub>3</sub> is white, and YMnO<sub>3</sub> and YFeO<sub>3</sub> are black, systems such as YIn<sub>1-x</sub>Mn<sub>x</sub>O<sub>3</sub> and YIn<sub>1-x</sub>Fe<sub>x</sub>O<sub>3</sub> where 0 < x < 1 display intense colors; in the case of Mn(III) the color is bright blue for 0.02 < x < 0.25. Since both Mn(III) and Fe(III) ions are magnetic (respectively, S = 2 and S = 5/2), and are in an uncommon coordination environment, we initiated a High-Frequency and -Field Electron Paramagnetic Resonance (HFEPR, using frequencies above 90 GHz, B<sub>0</sub> up to 25 T) study of these materials. The aim of this project has

been to correlate the magnetic and optical properties of the materials in question, and elucidate the electronic structure responsible for the unusual colors. This may result in practical industrial applications since historically and currently used blue pigments all show certain deficiencies (e.g., in terms of toxicity and/or stability). Both Mn(III) and Fe(III) compounds gave high-quality HFEPR spectra from low to room temperature showing a variety of spin concentration- and temperature-dependent phenomena that will be discussed during the presentation.

#### References

[1] Smith, A.E., et al., J. Am. Chem. Soc., 2009, 131, 17084-17086.

[2] Mizoguchi, H., et al., Inorg. Chem., 2011, 50, 10-12.

### TU233: EPR and ENDOR Studies of Two-Iron Ferredoxins, [2Fe-2S]<sup>+</sup>, Isolated from the Hyperthermophile Aquifex aeolicus

<sup>1</sup>\*Joshua Telser, <sup>2</sup>George Cutsail III, <sup>2</sup>Peter E. Doan, <sup>2</sup>Brian M. Hoffman, <sup>3</sup>Jacques Meyer

<sup>1</sup>Roosevelt University, <sup>2</sup>Northwestern University, <sup>3</sup>BMC/DRDC CEA

We have employed EPR and a set of recently developed Electron Nuclear Double Resonance (ENDOR) spectroscopies to characterize a suite of [2Fe-2S] ferredoxin clusters from *Aquifex aeolicus* (Aae Fd1, Fd4, and Fd5), which were grown on <sup>57</sup>Fe-enriched media.[1] Antiferromagnetic coupling between the Fe<sup>II</sup>, S = 2, and Fe<sup>III</sup>, S = 5/2, sites of the [2Fe-2S]<sup>+</sup> cluster in these proteins creates a total spin, S = 1/2 ground state. Complete <sup>57</sup>Fe hyperfine coupling (hfc) tensors for both iron sites, with respective orientations relative to the g matrix have been determined by the use of "stochastic" continuous wave and/or "random hopped" pulsed ENDOR, with the relative utility of the two approaches being emphasized. The reported hyperfine tensors include absolute signs determined by a modified Pulsed ENDOR Saturation and Recovery (PESTRE) technique.[2] RD-PESTRE, a post-processing protocol of the 'Raw Data' that comprises an ENDOR spectrum. The <sup>57</sup>Fe hyperfine tensor components found by ENDOR are nicely consistent with those previously found by Mössbauer spectroscopy, while accurate tensor orientations are unique to the ENDOR approach. These measurements demonstrate the capabilities of the newly developed methods. The high precision hfc tensors serve as a benchmark for this class of FeS proteins, while the variation in the <sup>57</sup>Fe hfc tensors as a function of symmetry in these small FeS clusters provides a reference for higher nuclearity FeS clusters, such as those found in nitrogenase. <sup>1</sup>H and <sup>2</sup>H (of protein in D<sub>2</sub>O buffer) ENDOR studies of these systems will also be described.

#### References

[1] Mitou, G, et al., Biochemistry, 2003, 42, 1354-1364.

[2] Doan, P. E., J. Magn. Reson., 2011, 208, 76-86.

### Dynamic Nuclear Polarization

### TH234: Designing Radicals and Surfaces for Efficient Dynamic Nuclear Polarization Surface Enhanced NMR Spectroscopy.

<sup>1</sup>\*Alexandre Zagdoun, <sup>2</sup>Olivier Ouari, <sup>2</sup>Gilles Casano, <sup>1</sup>Aaron J. Rossini, <sup>3</sup>Maxim Yulikov, <sup>3</sup>Gunnar Jeschke, <sup>3</sup>Christophe Copéret, <sup>1</sup>Anne Lesage, <sup>2</sup>Paul Tordo, <sup>1</sup>Lyndon Emsley

<sup>1</sup>Centre de RMN à Très Hauts Champs, Université de Lyon, Villeurb, <sup>2</sup>Aix-Marseille Université, Institut de Chimie Radicale, Marseilles, <sup>3</sup>ETH Zürich, Department of Chemistry, Zürich, Switzerland.

Dynamic nuclear polarization (DNP) is attracting more and

more interest as a method to increase the sensitivity of NMR experiments. In 2010 our research group described the application of DNP enhanced solid-state NMR spectroscopy for the characterization of surfaces, a method dubbed DNP SENS. However the enhancements routinely obtained at 9.4 T and 100 K are still far from the theoretical maximum (70 vs 660), and sensitivity remains an issue for challenging surface experiments. Here we show how enhancements up to 200 can be obtained through controlled design of radicals and the surface.

Biradicals have been demonstrated to be the most efficient polarizing agents at high magnetic fields. The efficiency of these polarizing agents has been shown to depend on many parameters, such as the relative orientation of the electron  $g$  tensors and the strength of the electron-electron dipolar coupling. We show that the electron longitudinal relaxation times are also an important factor for obtaining high  $\epsilon$ . [1] A new series of bTbK derivatives is developed and investigated with the aim of producing radicals with very long electron relaxation times, and the observed dependence of  $\epsilon$  on electronic relaxation properties is discussed. In the best case,  $\epsilon$  of 200 are obtained, unprecedented at this field and temperature.

We also discuss the impact of nuclear relaxation properties and the spin density of the surface groups on both the enhancement and the strength of the paramagnetic effects induced by the radicals at the surface. [2] Here we show that when a substrate possesses methyl groups that have short  $T_1$ 's, these protons act as relaxation sinks and dramatically reduce DNP enhancements. We then illustrate how the DNP enhancement can be restored by replacing these fast relaxing protons with deuterons, or with functionalities containing slowly relaxing protons. [2]

[1] A. Zagdoun et al., J. Am. Chem. Soc., 2012, 134, 2284.

[2] A. Zagdoun et al., Angew. Chem. Int. Ed., 2013, in press, DOI:10.1002/anie.201208699

#### MO235: Pedri-Based Functional Measurements – Concept, Probes, and Instrumentation

<sup>1,2\*</sup>Alexandre Samouilov

<sup>1</sup>The Ohio State University, USA, <sup>2</sup>Wexner Medical Center

Overhauser enhancement is used for numerous biomedical and clinical applications but capacity to map chemical environment (pH, O<sub>2</sub>, redox status, etc.) is still limited. EPR of exogenous paramagnetic probes has the unique advantage of functional specificity due to the absence of overlap with endogenous EPR signals. However EPR-based techniques are far from attaining their maximum potential due technical limitations of low field EPR imaging (EPRI) resulting in longer acquisition times and lower functional and spatial resolution. Proton-electron double-resonance imaging (PEDRI) represents an alternative NMR-based approach for imaging of paramagnetic probes based on the Overhauser enhancement of the proton MRI after EPR irradiation. It inherently offers high resolution, plane selectivity and rapid image data collection. Concepts of functional PEDRI, namely Variable Field (VF) and Variable Radio Frequency (VRF) PEDRI are proposed for functional mapping (e.g. pH mapping) using specially designed paramagnetic probes.

PEDRI oriented paramagnetic probes are required to have functionally-dependent ratiometric spectral parameters (e.g. ratio of intensities measured at two pre-selected fields). With these probes, spectral parameters at each pixel can be extracted from a limited number of PEDRI acquisitions acquired at pre-selected EPR excitation fields or frequencies. Number of probes has been developed and under the development for PEDRI studies of biologically relevant parameters of the medium such as pH, redox state, concentrations of oxygen or glutathione.

Home-made imager/spectrometer based on iron core Resonex 5000/Paradigm resistive magnet has been used for functional

PEDRI experiments. EPR transmit system, surrounding NMR resonator, based on a modified Alderman-Grant design. Also, specially design loop-gap double frequency resonator with coaxial B<sub>1</sub> fields was successfully tested for PEDRI. Studies performed with phantoms and mammary tumor bearing living mice at fields of about 200 G (EPR frequencies 560 MHz, MRI - 784.9 kHz). pH-sensitive nitroxide with enhanced stability towards reduction, narrow linewidth and extracellular targeting was used for in vivo studies. pH map was extracted using only two PEDRI images acquired at pre-selected 8 sec EPR excitations providing pH resolution of 0.1 pH unit and a spatial resolution of 0.5 mm. Acidosis of tumor tissue was observed.

ACKNOWLEDGEMENT: This work was supported by NIH Grant R01EB014542

#### TU236: Quantum Rotor induced Polarization

\*Ulrich L. Günther, Christian Ludwig

University of Birmingham

Among the currently known NMR polarization methods, quantum rotor polarization (QRP) represents the most recent addition. QRP utilizes highly non-linear changes that take place in the populations of the energy levels of tunnelling methyl groups when subject to rapid changes in temperature. In fact the latter exploits effects associated with spin angular momentum, through the influence of the Exclusion Principle on the space-spin symmetry of the molecular states. Analogous polarisation effects occur in PHIP (para-hydrogen induced polarization), in fact QRP can be seen as a C3 symmetry analogue of PHIP.

While QRP has been known for many years, it has been thought to be limited to few molecules, primarily  $\gamma$ -picoline. This effect is often been called the Haupt effect [1,2]. We have recently observed QRP for a series of molecules at temperatures below 1.5K [3]. The polarization generated by this mechanism is efficiently transferred via protons. We observe such effects for a much broader range of substances with very different polarization rates at low temperatures. Moreover, transfer of quantum rotor polarization across a chain of protons is possible. The observed effect not only influences the polarization in low-temperature DNP experiments but also opens a new independent avenue to generate enhanced sensitivity for NMR.

[1] Haupt J. A new effect of dynamic polarization in a solid obtained by rapid change of temperature. Phys Lett 38A:389–90 (1972).

[2] Horsewill A. Quantum tunnelling aspects of methyl group rotation studied by NMR. Prog Nucl Mag Res Sp 35:359–389 (1999).

[3] Ludwig C, Saunders M, Marin-Montesinos I, Günther UL. Quantum Rotor Induced Heteronuclear Hyperpolarization. Proc Nat Acad Sci USA, 107(24), 10799-10803 (2010).

#### Porous Media

#### TH237: <sup>1</sup>H NMR transverse relaxation as a probe to investigate water accessibility in cellulose in pre-treated sugarcane bagasse

<sup>1\*</sup>Jefferson Esquina Tsuchida, <sup>2,3</sup>Camila Alves Rezende, <sup>1</sup>Rodrigo de Oliveira-Silva, <sup>1</sup>Marisa Aparecida Lima, <sup>1</sup>Marcel N. D'Eurydice, <sup>1</sup>Igor Polikarpov, <sup>1</sup>Tito José Bonagamba

<sup>1</sup>Instituto de Física, Universidade de São Paulo, São Carlos, <sup>2</sup>Instituto de Química, Universidade Estadual de Campinas

Biorefining of the lignocellulosic biomass for the production of bioethanol has become a promising research area. Enzymatic hydrolysis is a determining step to the biomass conversion into biofuels and different pretreatment strategies have been

proposed to improve efficiency of this process. Among the different factors affecting hydrolysis yields of the biomass samples, porosity is highlighted due to its intimate relation with enzyme accessibility to cellulose fraction of the biomass. Another important factor is related to the surface area available for hydrolysis also related with biomass porosity. In this way the use of Nuclear Magnetic Resonance (NMR) techniques is necessary because information regarding of the pore size distribution and chemical characteristics of the pore surface can be obtained. In this work, sugarcane bagasse samples treated by acid and alkaline pretreatments were prepared. The changes due to the pretreatments in the total surface area, hydrophilicity and water accessibility in cellulose were investigated by nitrogen adsorption, Scanning Electron Microscopy (SEM), and NMR techniques (relaxometry in low magnetic field and spectroscopy in high magnetic field). With the use of SEM images the transversal relaxation rates,  $T_2$ -distributions, were associated to three different water affinity sites along the sample, corresponding to long and intermediate as well as short  $T_{2M}$ 's, which were assigned to wide and narrow vessels in addition to cell wall surfaces, respectively.

NMR relaxometry revealed that with application of pretreatment, the removal of lignin promotes increase of the water accessibility in cellulose, ie there is an increase in the interaction between water and cellulose. NMR spectroscopy showed the presence of water with different mobilities (free, restricted and rendered) which can be respectively associated with amorphous, semi-crystalline and crystalline cellulose. From the standpoint of NMR, the pretreatment with 1% NaOH showed the better results of the water accessibility in cellulose and therefore more efficiency for hydrolysis. This result is in agreement with the study by Rezende (Rezende, CA et al. *Biotechnol. Biofuels.* 2010, 4, 1-18).

ACKNOWLEDGEMENTS: FAPESP, CAPES, CNPq

#### MO238: Self-diffusion in nanopores studied by the NMR pulse gradient

<sup>1,3\*</sup>Janez Stepišnik, <sup>2</sup>Bernd Fritzing, <sup>2</sup>Ulrich Scheler, <sup>1</sup>Aleš Mohorič

<sup>1</sup>University of Ljubljana, FMF, Ljubljana, Slovenia, EU, <sup>2</sup>Leibniz-Institut für Polymerforschung, Dresden, Germany, EU, <sup>3</sup>Institute Jozef Stefan, Ljubljana, Slovenia, EU

With the proper interpretation of experimental data, the method of NMR pulse gradient spin echo provides information about the molecular self-diffusion in nanopores. We demonstrate it by the analysis of restricted self-diffusion measurement of water molecules trapped in a porous poly(amide)-6 (PA-6) membrane. The PGSE sequence with fixed gradient pulse width, but variable interval between pulses and by changing the magnetic field gradient from zero to 11.6T/m at temperature of 22 °C we observed the spin echo dependences on the gradient that decay with small undulations. These "diffraction" patterns prevent the use of the inverse-Laplace transform method for the extraction of pore size distribution. However, the shape of the diffusion propagator obtained by q-space cosine Fourier transform of experimental data can be perfectly fitted the multi-normal distributions. Their second moments remain fixed as the interval between gradient pulses changes. This is a clear indication of a motional narrowing regime, in which the second moments of propagators are proportional to the fourth power of pore size. Results are presented on the 3-D plot of the spin-relaxation distribution and the pore radius distribution, which shows the prevailing share of spins in the pores with the radius  $r = (100 \pm 10)$  nm (70%) and pores with the radius  $(175 \pm 30)$  nm (20%). Water in these two types of pores has almost identical spin relaxation  $T_2 = (10 \pm 2)$  ms, while water in the pores with the radius of  $r = (282 \pm 7)$  nm (5%) have a broader distribution of relaxation times,  $T_2 = (14 \pm 5)$  ms. These experiments provide information on the nanopore structure in the polyamide membrane not observed in the previous investigation by the method of stimulated gradient spin echo. The results confirm the potential of NMR PGSE

for the characterization of nanoporous systems, and as such also a useful tool in bio-nanotechnology.

#### TU239: Evaporation kinetics in macroporous polymeric supports evaluated by relaxation measurements

<sup>1</sup>Emilia V. Silletta, <sup>2</sup>C.G. Gomez, <sup>2</sup>M.C. Strumia, <sup>1</sup>Gustavo Alberto Monti, <sup>1\*</sup>Rodolfo Héctor Acosta

<sup>1</sup>Universidad Nacional de Córdoba, CONICET, Córdoba, Argentina, <sup>2</sup>Departamento de Química Inorgánica, Universidad Nacional de Córdoba,

Macroporous polymer beads present a permanent well-developed porous structure in the dry state, and have a wide range of applications such as support for catalysts, immobilization of enzymes, HPLC columns, liberation of active substances, or adsorbents (1). Their porous structure improves the diffusion of different solutes through the network. These networks have particular properties as high degree of crosslinking and rigid structure both in swollen and dry state, turning the study of their synthesis conditions of considerable interest. The properties of the polymer mesh change radically due to swelling, a process that strongly depends on the mesh structure; therefore, changes in the content of a selected cross-linker (ethylene glycol dimethacrylate-EGDMA) percentage are studied (3). Evaporation kinetics of swelling liquid molecules (L) distributed in the network show a different interaction with itself (L-L) compared to those liquid molecules adsorbed to the polymer chain (L-P). In the first case the evaporation kinetics present a linear decay; while in the second an exponential decay is present (2). Therefore, monitoring the kinetics of evaporation renders direct information of the swelling process (4). We use <sup>1</sup>H-CPMG sequences to measure the distribution of transverse relaxation times of polar and non-polar solvents contained in the matrices. As non-polar solvents do not interact with the network, information of the unperturbed porous system is obtained. On the other hand, polar solvents present the L-P interactions that compared to L-L provide information on the swelling process.

Kristensen TE, Vestli K, Fredriksen KS, Hansen T, Org. Lett. 2009, 11: 2968-2971.

Errede L., Kueker MJ, J Polym Chem Ed 1988; 26:3375-3380.

C.G. Gomez, M. Strumia; Journal of Polymer Science: Part A: Polymer Chemistry 46, 2557-2566(2008).

C.G. Gomez, G. Pastrana, D. Serrano, E. Zuzek, M.A. Villar, M.C. Strumia, Polymer 2012, 53, 2949-2955.

#### TH240: NMR Relaxation Study of Ionic Liquids Under Confinement in Porous Media

\*Carlos Mattea, Amin Ordikhani Seyedlar, Siegfried Stapf  
Department of Technical Physics II / Polymer Physics, Institute of Physics, Ilmenau University

The investigation of low melting organic salts commonly referred to as ionic liquids, constitutes one of the most fascinating and rapidly developing areas in physical chemistry and engineering. Ionic liquids have been discovered in the last decades and since then received much attention as "green" replacement of common solvents in chemical technology [1].

They are liquid below 100 °C, and are composed of an organic cation and organic or inorganic anion presenting normally negligible vapor pressure. They are benign alternatives to the usual organic solvents for synthesis, liquid/liquid extractions and heterogeneous catalysis. They reveal different properties from the common molecular liquids mainly due to their ionic character. There is much interest in the study of their molecular motions that control transport properties in these materials [1] both in bulk and under confinement. Reorientation and translational dynamics can be suitably studied by Nuclear Magnetic Resonance (NMR) [2].

From both, the fundamental research and for applications, it is important to know the dynamical properties of ionic liquids in porous media, where the transport properties are predominantly affected by the geometrical restrictions and wall interactions.

In this contribution, the spin-lattice relaxation ( $T_1$ ) of two ionic liquids, emim(+)-Tf2N(-) and bmim(+)-Tf2N(-), bulk and confined in porous media are presented. The confinement is done in porous silica glasses with mean nominal pore sizes of 4 nm and porosity of 28%.  $T_1$  relaxation times were measured at different magnetic fields and temperatures, covering a range from 0.24 mT to 0.5 T and from 210K to 300K. The different ions can be independently assessed by NMR selecting either  $^1\text{H}$ -NMR (for the cations), or  $^{19}\text{F}$ -NMR (for the anions).

The relaxation experiments reveal strong changes in the dynamics when the ionic liquids are under confinement. The results show however, that different ions exhibit similar relaxation mechanisms. This is attributed to a strong cooperative dynamics in these kinds of complex liquids. Further studies in order to discriminate whether this influence is a consequence of the physical confinement and/or interaction with the walls are discussed. Furthermore, at low temperatures, evidence of decoupling of translational diffusion from structural relaxation has been found in agreement with recent light scattering experiments [3].

#### References

- [1] P. Wasserscheid, T. Welton (Eds.), *Ionic Liquids in Synthesis*, VCH-Wiley, Weinheim, 2003.
- [2] R. Kimmich, *NMR Tomography, Diffusometry and Relaxometry*, Springer, 1997.
- [3] P. Griffin et al., *J. Chem. Phys.*, 135, 114509 (2011)

#### MO241: Characterization of Compacted Silty Soils by Means of Nuclear Magnetic Resonance

<sup>2,3\*</sup>Marcos Montoro, <sup>1,3</sup>Lucas Matías Cerioni, <sup>3</sup>Daniel José Pusiol

<sup>1</sup>Spinlock SRL, <sup>2</sup>Universidad Nacional de Córdoba, <sup>3</sup>CONICET

Compacted soils are widely employed as construction material for different facilities such as highways, dams and landfills. The aim of soil compaction procedure consists in obtaining the maximum dry unit weight of a particular soil. Resulting dry unit weight depends on the compaction energy and the water content. Maximum dry density can be reached only at the optimum water content, in consequence it can be possible to have compacted soils with the same dry unit weight (same porosity) compacted with different moisture. Soils compacted dry from optimum use to present flocculated fabric characterized by open and big pores, while soils compacted wet from optimum use to present dispersed fabric characterized by small pores. In this work we present a study of soil compaction using Time Domain Nuclear Magnetic Resonance (TD-NMR). We measured samples of compacted silty soils with different molding water content using a low field (12 MHz) spectrometer (SLK-100). We measured the transversal relaxation times ( $T_2$ ) using a CPMG pulse sequence (inter-echo spacing time 400  $\mu\text{s}$ , 1200 echoes and 160 repetitions) in samples with moisture content between 10 and 22%. The amplitude of the obtained signal was correlated with the sample moisture content and comparing cross correlations between the different signals with the one registered for the sample compacted at the optimum moisture content assessed the compaction degree. A high linear correlation between the signal amplitude and moisture content was determined ( $r^2 = 0.9537$ ). The relation between the cross-correlations of the signals and the dry unit weight of the samples presented a non-linear behavior.  $T_2$  distribution curves allowed to identify different pore sizes distribution in sample with the same porosity but compacted either dry or wet from optimum.

ACKNOWLEDGEMENTS: CONICET, SECyT-UNC, FON-CYT, FONTAR

#### TU242: Chromatographic NMR, complement and prediction of LC?

<sup>1</sup>Caroline Carrara, <sup>1</sup>Claire Lopez, <sup>1,2</sup>Manjunatha Reddy G.N., <sup>3</sup>Rafael R. Ballesteros, <sup>3</sup>Jérôme Lacour, <sup>1,2\*</sup>Stefano Caldarelli

<sup>1</sup>Aix Marseille Université, Marseille, France, <sup>2</sup>CNRS UPR 2301 ICSN, Antenne Ecole Polytechnique, Palaiseau, France, <sup>3</sup>Department of Organic Chemistry, University of Geneva, Geneva, Suisse

Chromatographic NMR, introduced in 2003, [1] is a variant of DOSY (diffusion ordered spectroscopy). [2,3] This method allows you to create charts NMR spectra of molecules ordered in relation to their average molecular mobility. The addition of a stationary phase in a mixture analyzed by DOSY can induce changes in the distribution of components which can be correlated to their affinity for the solid. [1,4] In this work, we first show how differences observed between the NMR and LC Chromatography [5] can be explained on the basis of a strong impact of solution-to-solid phase ratio, possibly due to slow exchange between intra- and interparticle porosity. [6] A correct choice of this parameter provides excellent modeling tests for shape selectivity.[7] A further aspect that must be included in comparisons between NMR and LC chromatographic is their different timescale. This will be illustrated by an example of separation of labile diastereoisomers consisting of chiral ion pair. [8]

ACKNOWLEDGEMENTS The stationary phases were kindly provided by Dionex. Funding from ANR (ANR-08-BLAN-273) and Region PACA (APO-G 2009) are gratefully acknowledged.

- [1] C. S. Johnson Jr, *Progr. NMR Spectr.* 34, 203-256 (1999)
- [2] K. F. Morris, P. Stilbs, C. S. Johnson, *Anal. Chem.* 66, 211-215 (1994)
- [3] S. Viel, F. Ziarelli, S. Caldarelli, *PNAS* 100, 9696-9698 (2003)
- [4] G. Pages, C. Delaurent, S. Caldarelli, *Anal. Chem.* 78, 561-566 (2006)
- [5] G. Pages, C. Delaurent, S. Caldarelli, *Angew. Chem. Int. Ed.* 45, 5950-5953 (2006)
- [6] C. Carrara, S. Caldarelli, *J. Phys. Chem. C*, 116, 20030-20034 (2012)
- [7] C. Carrara, C. Lopez, S. Caldarelli, *J. Chromatogr. A* 1257, 204-207 (2012)
- [8] Manjunatha Reddy G.N., R. Ballesteros, J. Lacour and S. Caldarelli *Angew. Chem. Int. Ed.* 52, 3255-3258 (2013)

#### TH243: Artificial ceramic porous media preparation and their characterization by NMR

<sup>1</sup>Elton Tadeu Montrazi, <sup>1</sup>Roberson Saraiva Polli, <sup>1</sup>Edson Luiz Gea Vidoto, <sup>2</sup>Sérgio Rodrigues Fontes, <sup>2</sup>Carlos Alberto Fortulan, <sup>1\*</sup>Tito José Bonagamba

<sup>1</sup>Instituto de Física de São Carlos - Universidade de São Paulo, <sup>2</sup>Departamento de Engenharia Mecânica - Escola de Engenharia de São Carlos - Universidade de São Paulo

In this work we present a method for preparing ceramic materials with controlled porosity and their characterization by NMR relaxation, MRI FLASH, mercury intrusion porosimetry (MIP), and scanning electron microscope (SEM).

Artificial alumina ceramics porous medium was manufactured by a sintering process, which preserves its intrinsic porosity. Additionally, it was added to the manufacturing process a porogenic agent in order to induce bigger pores under a controlled way. Sucrose crystals were chosen as poro-

genic agents and their sizes were carefully selected by using sieves.

During the sintering process, these crystals are burned off, creating along the ceramic material induced pores interconnected by the intrinsic pores.

Three groups of samples were prepared, presenting intrinsic pore sizes of about  $0.5\ \mu\text{m}$  and induced pores sizes in the range of  $10 - 100\ \mu\text{m}$  (sample S),  $30$  to  $300\ \mu\text{m}$  (sample M), and  $300$  to  $1800\ \mu\text{m}$  (sample B), which were estimated by MIP, SEM and MRI.

By the use of CPMG, the following average  $T_2$  values  $0.05$ ,  $1.2$ ,  $1.7$ , and  $1.9$  s were observed for water within the intrinsic and induced pores in samples S, M, and B, respectively. From the point of view of  $T_2$  distributions, the results observed are very consistent with sample preparation, being the average  $T_2$  values directly proportional to the size of the intrinsic and induced pores.

Due to the bigger pore sizes observed for samples M and B, only these samples allowed getting more precise pore size information by using MRI FLASH technique, with a minimum resolution of about  $250\ \mu\text{m}$ . However, due to this resolution the smaller pores in sample M were not properly observed.

The obtained results validate the manufacturing process and the prepared artificial porous media are excellent samples to be used as model for testing traditional and under development NMR pulse sequences. New manufacturing procedures are being developed in order to introduce well distributed paramagnetic impurities along the porous ceramic material.

ACKNOWLEDGEMENTS: IFSC/USP, FAPESP, CNPq, CAPES.

#### MO244: Simulation of Transverse Relaxation in Realistic Porous Media Based on Random Walk and Monte Carlo Methods

Everton Lucas de Oliveira, Mariane Barsi Andreeta, Arthur Gustavo de Araujo Ferreira, Marcel Nogueira D'Eurydice, \*Tito José Bonagamba

*Instituto de Física de São Carlos - Universidade de São Paulo*

NMR transverse relaxation time ( $T_2$ ) distribution of fluids in porous media, such as rock cores, ceramics, bones and cements, is considered one of the most important information to characterize these materials, allowing understanding, for example, permeability, wettability and porosity distribution. Great efforts have been made to simulate these properties and associate them with  $T_2$  distributions obtained from CPMG (Carr-Purcell-Meiboom-Gill) decays in a more detailed way. Usually, it is possible to track and classify the interaction of spins with porous media surfaces based on Monte Carlo and random walk methods, in order to reproduce the liquid Brownian motion. The purpose of this work is to combine two random walk approaches, over the space and phase-space, in order to simulate the relaxation behavior of fluids within porous media, taking into account the dephasing due to the interactions of the nuclei with the pore walls and among themselves. The relationship between  $T_2$  distributions and pore properties, e.g. morphology and S/V ratio distribution, is well-established and can be analyzed under slow and fast translational diffusion regimes. Considering these properties, computer simulations were developed in order to describe the fluid dynamics inside such materials. The pore morphology is computationally represented by a 3D voxel-based description, in which both real (obtained by x-ray microtomography) and virtual idealized models can be used as boundary conditions. The simulated decays obtained by the developed method can be compared to the CPMG experimental results, where the correlation between collision rates and  $T_2$  values can be analyzed. The next step is to apply the proposed computational method to study these materials with well-known porosities and compositions, including computationally constructed and artificial porous media.

ACKNOWLEDGEMENTS: IFSC/USP, FAPESP, CNPq, and CAPES.

#### TU245: Direct Evidence of the Nanopore Inner-Sphere Enhancement (NISE) Effect by NMR and EPR Spectroscopy

<sup>1</sup>\*Daniel R. Ferreira, <sup>2</sup>Marcus V. Giotto, <sup>3</sup>Nadine J. Kabengi, <sup>4</sup>James E. Amonette, <sup>4</sup>Eric D. Walter, <sup>2</sup>Cristian P. Schulthes

<sup>1</sup>*Southern Polytechnic State University*, <sup>2</sup>*University of Connecticut*, <sup>3</sup>*University of Kentucky*, <sup>4</sup>*Pacific Northwest National Laboratory*

The adsorption mechanisms of mono- and divalent cations in zeolite nanopore channels can vary as a function of their pore dimensions. The nanopore inner-sphere enhancement (NISE) theory predicts that ions may dehydrate inside small nanopore channels  $\leq 0.5$  nm in order to adsorb more closely to the mineral surface if the nanopore channel is sufficiently small. Both sets of results from <sup>23</sup>Na MAS Nuclear Magnetic Resonance (NMR) spectroscopy and Electron Paramagnetic Resonance (EPR) spectroscopy of Mn and Cu adsorption on the zeolite minerals zeolite Y (large nanopores), ZSM-5 (intermediate nanopores), and mordenite (small nanopores) support the NISE model. The Na cation adsorbs via an outer-sphere mechanism on zeolite Y, via an inner-sphere mechanism on ZSM-5, and via a mixture of the two mechanisms on mordenite. The Cu and Mn cations both adsorbed via an outer-sphere mechanism on zeolite Y based on the similarity between the adsorbed spectra and the aqueous spectra. Conversely, Mn and Cu adsorbed via an inner-sphere mechanism on mordenite based on spectrum asymmetry and peak broadening of the adsorbed spectra. However, Mn adsorbed via an outer-sphere mechanism on ZSM-5, whereas Cu adsorbed on ZSM-5 shows a high degree of surface interaction that indicates that it is adsorbed close to the mineral surface. Evidence of dehydration and immobility was more readily evident in the spectrum of mordenite than ZSM-5, indicating that Cu was not as close to the surface on ZSM-5 as it was when adsorbed on mordenite. Divalent Mn cations are strongly hydrated and are held strongly only in zeolites with small nanopore channels. Divalent Cu cations are also strongly hydrated, but can dehydrate more easily, presumably due to the Jahn-Teller effect, and are held strongly in zeolites with medium sized nanopore channels or smaller.

ACKNOWLEDGEMENTS: United States Department of Agriculture (USDA-Hatch No. CONS00864) and United States Department of Energy's (DOE) Office of Biological and Environmental Research.

#### TH246: NMR Study of Diffusion and Relaxation in Micro-porous Glass Beads

<sup>1</sup>\*Giovanna F. Carneiro, <sup>2</sup>Lawrence Schwartz, <sup>2</sup>Yi-Qiao Song, <sup>3</sup>Bernardo Coutinho, <sup>3</sup>Edmilson Rio, <sup>3</sup>Willian Andrighetto Trevizan

<sup>1</sup>*Schlumberger Brazil Research and Geengineering Center*, <sup>2</sup>*Schlumberger-Doll Research*, <sup>3</sup>*Centro de Pesquisas e Desenvolvimento Leopoldo Américo Miguez de Mello*

In this study, micro-porous borosilicate glass beads[1] were evaluated since they are a good representation of bimodal porosity systems. They consist of spherical grains with a mean diameter of  $150\ \mu\text{m}$  and each of these grains is, itself, porous with an average micro-pore diameter of  $0.3\ \mu\text{m}$ . The system's total porosity is 80% and is divided equally between the micro- and macro-pores.

Pulsed-field gradient stimulated echo techniques were used to measure the time (t) dependent diffusion coefficient,  $D(t)$ , in a Magritek 2 MHz Rock Core Analyzer. For long diffusion times, the limiting value of  $D(t)$  is directly related to electrical transport.[2] Our experiments are supported by numerical simulations in which we compare two geometrical models for the structure of the micro-pores. We looked first at a model in

which grains of diameter  $150\ \mu\text{m}$  are arranged on an ordered lattice. Each of these grains is comprised of an array of much smaller spherical grains.[2] In the second model, the same ordered packing of  $150\ \mu\text{m}$  grains defines the macro-pores but their micro-structure is represented by a *Swiss cheese* arrangement of (slightly) overlapping spherical pores. For both models the micro-pore diameter is  $30\ \mu\text{m}$  and the net micro-porosity is 40%. Indeed, we saw that only the Swiss cheese model properly described the long time behavior of  $D(t)$ . The lower values of  $D(t)$  reflect the fact that, at a given porosity, diffusion through an array of overlapping spherical pores is considerably more difficult than diffusion through a network of spherical grains. At short times the two models yield results that are quite similar since both have the same total surface area. Unfortunately, the short time regime is difficult to probe experimentally because of limitations on the speed with which gradient pulses can be switched on and off.

[1] <http://www.millipore.com/techpublications/tech1/ds1007en00>

[2] Zhang Z., Johnson D, and Schwartz L, Phys. Rev. E84, 031129 (2011).

[3] Sen P., Schwartz L., Mitra P., and Halperin B., Phys. Rev. B49, 215 (1994).

[4] Feng S., Sen P., and Halperin B., Phys. Rev. B35, 197–214 (1987)

#### MO247: Connectivity and permeability in complex carbonate rocks, through diffusivity measurements.

<sup>1</sup>\*Bernardo Coutinho Camilo dos Santos, <sup>1</sup>Willian Andrighetto Trevizan, <sup>1</sup>Vinicius de França Machado, <sup>3</sup>Andre Souza, <sup>2</sup>Giovanna F. Carneiro, <sup>2</sup>Austin Boyd, <sup>3</sup>Edmilson Helton Rios, <sup>4</sup>Rodrigo Bagueira de Vasconcellos Azeredo

<sup>1</sup>PETROBRAS-CENPES, <sup>2</sup>Schlumberger - BRGC, <sup>3</sup>Observatorio Nacional, <sup>4</sup>Universidade Federal Fluminense - Instituto de Química

In this study we explored techniques uni-dimensional and two-dimensional Nuclear Magnetic Resonance (NMR) measurements of diffusion coefficient ( $D$ ), and its relationship to properties such as connectivity, tortuosity and permeability of porous media. The information is usually extracted from measurements of low field NMR  $T_2$  spectra, which are associated with a pore size distribution. However, when a fluid (hydrocarbon or water) is placed in a porous medium the relaxation time changes pore to pore. The restriction imposed by the rock causes to the diffusion coefficient changes depending on the pore structure. Thus, smaller pores and more tortuous paths decreases the diffusion coefficient, whereas larger pores or less tortuous paths do not restrict dramatically the diffusion. The ability to measure both  $D$  and  $T_2$  allows us to construct two-dimensional maps ( $D$  vs.  $T_2$ ) and estimate besides the pore size distribution the value of  $D$  in each pore size. Measurements over 15 complex carbonate samples from well cores showed the possibility of inferences about the connectivity of the porous medium, and quantify the interaction of water with the rock matrix. Through the two-dimensional maps  $D$ - $T_2$  were obtained the values of surface relaxivities of each samples and compared with the mercury injection method. These values, when incorporated into the Ksdr permeability model, improves by almost 30% of permeability estimates compared with standard petrophysical measurements. There was also a good correlation between the values of  $D$  (obtained by NMR) and the permeabilities  $k$ , obtained from standard petrophysical assays, for specific diffusion times. Therefore, there is an optimum measuring time in which the molecules of fluid diffusing through the porous medium are obtained by NMR and provide information about the connectivity of the pores.

#### TU248: Magnetic Susceptibility Effects on NMR Relaxation of Sedimentary Rock Cores

<sup>1,2</sup>\*Andre Souza, <sup>1</sup>Marcel N. D'Eurydice, <sup>2</sup>Austin Boyd,

<sup>3</sup>Martin D. Hurlimann, <sup>1</sup>Tito José Bonagamba

<sup>1</sup>Instituto de Física de São Carlos, Universidade de São Paulo, São Carlos, Brazil, <sup>2</sup>Schlumberger Brazil Research and Geoengineering Center, Rio de Janeiro, Brazil, <sup>3</sup>Schlumberger-Doll Research Center, Cambridge, USA

Magnetic susceptibility contrast ( $\delta\chi$ ) between the rock and the saturating fluid can cause distortions in the local magnetic fields of the pores in a Nuclear Magnetic Resonance (NMR) experiment. This effect is described as an internal magnetic field gradient, and scales with the pore size distribution, matrix composition and pore geometry. Hurlimann[1] studied in great detail the effect of translational diffusion through those internal gradients on  $T_2$  relaxation time, a mechanism that can influence and even dominate the  $T_2$  distribution of porous media. He was able to obtain a distribution of internal gradients using a variable echo time CPMG methodology. Sun et al.[2] studied the  $\delta\chi$  effect in  $T_2$  relaxation spectra for two sandstone rocks, showing that the pronounced effect for the small pores. Mitchell et al.[3] performed an extensive NMR study on a sandstone rock core at several magnetic field strengths, showing that the internal gradients are nonuniform across an individual pore.

In this work, the contribution of such effects in transversal ( $T_2$ ) and longitudinal ( $T_1$ ) relaxation times was studied in a set of 4 sandstone and 7 carbonate samples. Magnetic fields ranging from 0.047 - 9.4 T were used to characterize the  $\delta\chi$  effects. Also, thin section images, mercury intrusion, magnetic susceptibility measurements and electron paramagnetic resonance experiments were performed, in order to correlate them with NMR results.

The relaxation spectra of carbonates have a low contribution of paramagnetic elements, and so the main magnetic effect arise from the pore shape heterogeneity. In contrast, the sandstones have shown higher magnetic effects due mainly to the presence of paramagnetic species (e.g.  $\text{Fe}_3\text{O}_4$  and  $\text{FeSO}_4$ ). In sequence, two-dimensional NMR  $T_1$ - $T_2$  experiments, capable of investigating molecular dynamics details of the confined saturating fluid and differences in the physico-chemistry properties of pore sites, were performed and correlated with the magnetic susceptibility findings.

[1] Hurlimann M.D., Journal of Magnetic Resonance, Volume 131 (1998), 232-240.

[2] Sun B., Dunn K., Physical Review E, 051309 (2002).

[3] Mitchell, J., Chandrasekera, T.C., Johns, M.L., Gladden, L.F., Fordham, E.J, Physical Review E, 026101 (2010).

ACKNOWLEDGEMENTS: FAPESP, CAPES, CNPq, Schlumberger.

#### TH249: Evaluation of uncertainty in petrophysical properties derived from the profile NMR due to acquisition noise

\*Eduardo Barreto Oliveira, Marcelo Torrez Canaviri

Petrobras

Signal / noise ratio noise in NMR logging is significantly lower than most other logging tools. In the case of Schlumberger CMR tool, each echo has Gaussian noise of zero mean and standard deviation of approximately 3.5 pu. During logging, a moving average of 3 levels is performed to reduce the standard deviation for close to 2 pu, resulting in a decrease of resolution (Freedman & Morriss, 1995). Obtaining the  $T_2$  distribution from the decay is an ill-posed problem, since it allows many solutions and small changes in input data produce significant changes in the solution. Thus, the presence of noise influences the solution of the inversion process and consequently the petrophysical properties estimated from NMR interpretation, especially the irreducible fluid volume. In order to assess the impact of noise in the measurements of NMR tool, it was generated multiple realizations of Gaussian noise with standard deviation equal to the real data, which resulted in multiple  $T_2$  distributions which were subsequently



subjected to the traditional NMR interpretation, being obtained total porosity, free fluid, irreducible fluid and permeability estimated by Timur-Coates model. The main result of this work was to obtain distributions of petrophysical properties rather than a single value. The curves generated showed higher resolution compared to that provided by the logging company, indicating a likely application of a moving average procedure in order to increase the signal / noise ratio.

#### MO250: MRI spatial CPMG in the study of rock heterogeneity and capillary pressure curves

<sup>1,2\*</sup>Edmilson Helton Rios, <sup>1</sup>Irineu Figueredo, <sup>2</sup>Bernardo Coutinho Camilo dos Santos, <sup>2</sup>Willian Andrighetto Trevizan, <sup>2</sup>Vinicius de França Machado

<sup>1</sup>National Observatory, <sup>2</sup>Cenpes, Petrobras

In special core analysis (SCAL) programs, it is very important to consider sample heterogeneity since many petrophysical measurement techniques are based upon models homogeneity assumptions. We present some results of 2MHz MRI phase encoding spatial CPMG measurements along the length of totally and also partially brine saturated core plugs (1.5' diameter per 2' long). With a single fully saturating fluid, the inverse Laplace transform obtained for each core slice represents the core variation in its pore size distribution. This 'heterogeneity probe' can be promising for many applications such as: representativeness verification of core end pieces for MICP analysis and posterior comparison with NMR bulk core measurements; selection of homogeneous samples for relative capillary pressure analysis; monitoring of perm porosity changes after acid injection experiments, etc. For partial saturation samples we applied spatial CPMG along air-water centrifuged cores and it was verified a gradual decreasing in  $T_2$  values and in its computed total area from outer to inner centrifuge radius as result of a saturation gradient. Despite its practicality, traditional centrifuge capillary pressure curve (CCPC) experiments have some drawbacks once they just consider average bulk saturation per rotation speed. We plotted the cumulative pore volume (total area) for each slice against sample length resulting in a one dimension saturation profile. With it, different capillary pressure per saturation slice was quantified in a single speed rotation not only overcoming the simplified average consideration but also decreasing tremendously conventional CCPC acquisition time. In many other SCAL's it is important to use centrifuged cores at the irreducible water saturation. In this sense spatial CPMG was also used to monitor the fluid spontaneous redistribution along the sample (higher the permeability, faster it was) and also to check for eventually trapped water in one of the core sides. All experiments performed here indicate that MRI spatial CPMG is a useful technique to support SCAL programs.

ACKNOWLEDGEMENTS: CNPQ, PETROBRAS, GIT

#### Polymers & Materials

#### TU251: Segmental dynamics in molten polymers studied by modulated gradient spin echo

<sup>1,3\*</sup>Janez Stepišnik, <sup>2</sup>Carlos Mateo, <sup>2</sup>Siegfried Stapf, <sup>1</sup>Aleš Mohorič

<sup>1</sup>University of Ljubljana, FMF, Ljubljana, Slovenia, EU,

<sup>2</sup>Technical University Ilmenau, Ilmenau, Germany, EU,

<sup>3</sup>Institut "Jozef Stefan", Ljubljana, Slovenia, EU

Although, the polymer has a long-standing records of experimental and simulation investigations, the theoretical models of polymer dynamics still remain questionable. We present the investigation of molten polymers by the NMR technique of modulated gradient spin echo (MGSE), which provides a new insight into details of polymer dynamic by direct measurement of the segmental velocity autocorrelation spectrum (VAS). With regard to other experimental methods, the in-

quiry of molecular translational motion by the NMR gradient spin echo is unique, because its signal is the characteristic functional of stochastic process, if the molecular displacements are treated as a random motion. Thus, the theory of random processes provides the relation of spin echo attenuation to VAS. New MGSE technique, which permits the VAS measurement in the frequency range of 100 Hz-100kHz, was used to study the motion in the mono-disperse poly(isoprene-14) using the NMR mouse. Although, the obtained frequency dependence of VAS for the molten polymers with the molecular weights:  $M_n=704$ , 1610 and 3920 at  $M_w/M_n$  1.05, were expected to reflect the segmental tube/reptation motion, they fit well to the spectrum of the Rouse model current for diluted solutions. However, the extracted parameters do not completely agree with this model. The deduced coil diffusion coefficient scales with the molecular weight as  $N^{-2}$  as predicted with the tube/reptation model, the mode amplitude as  $N$  according to the Rouse model, but the relaxation time independence on  $N$  disagrees with both models. Preliminary studies give a polymer like VAS for some hydrogen-bonded liquids (water, glycerol) as well.

#### TH252: Structural characterization and molecular dynamics in the solid-state in Poly(ethyleneimine) polymers

<sup>1,2</sup>Juan Manuel Lázaro Martínez, <sup>2,3</sup>Gustavo Alberto Monti, <sup>2,3\*</sup>Ana Karina Chattah

<sup>1</sup>IFEG-CONICET, <sup>2</sup>FaMAF-Universidad Nacional de Córdoba, <sup>3</sup>FaMAF-Universidad Nacional de Córdoba

The linear polymer *poly*(ethyleneimine) (PEI) has a wide field of applications. It has been used as a cosmetic ingredient to adjust viscosity, as chelating metal ions to inhibit corrosion, and as copolymer to develop energy storage devices. Interestingly, taking into account the biocompatibility of the PEI, it has been used in biotechnology as non-viral vector to carry out gene transfection processes. However, no physical characterization in the solid state has been done. Therefore, the objective of this work is to study the structural and dynamic homogeneity in three synthetic variants of PEI with different molecular weights (22, 87 and 217 kDa) through Nuclear Magnetic Resonance techniques in the solid state (SSNMR). In addition, changes will be explored after the uptake of copper ion (II) by these polymeric matrices, given the importance of the heterogeneous catalysts of Cu(II) for the activation of hydrogen peroxide and degradation of pollutants with high environmental impact.

The SSNMR proved to be a valuable tool for studying the dynamics and homogeneity of the different samples of PEI. Although the results of X-ray powder crystallography do not show significant differences between different samples. SSNMR through  $^{13}\text{C}$  CP-MAS spectra using different spin time dynamics enabled to demonstrate the heterogeneity in each case, as well as  $^{15}\text{N}$  CP-MAS spectra. These results were confirmed by measuring  $^{13}\text{C}$  relaxation time in the rotating frame,  $^1\text{H}$ - $^{13}\text{C}$  2D-WISE and  $^1\text{H}$ - $^{13}\text{C}$  2D-HETCOR.

Finally, the formation of complexes with copper ions (II) produced a significant reduction in the molecular mobility as a result of crosslinking between the different polymer chains to coordinate the metal ion, based on the results of  $^{13}\text{C}$  relaxation time in the rotating frame and  $^1\text{H}$ - $^{13}\text{C}$  2D-WISE.

#### MO253: Proton spin-spin relaxation correlations in glass-forming glycerol

<sup>\*</sup>Damjan Pelc, Miroslav Požek

University of Zagreb, Faculty of Science, Department of Physics

We present the results of stimulated-echo  $T_2$  correlation experiments on protons in glycerol, as the liquid approaches the glass transition at 190 K. The stimulated echo sequence has been used on other systems (and nuclei) to quantify dynamical heterogeneity [1,2], the sequence acting as a filter

for slowly moving molecules. However, our results on protons in glycerol show some unexpected features and a peculiar temperature dependence. In addition to the conventional spin-lattice relaxation contribution (in agreement with previous work [3]), we observe an anomalous signal decay, and a crossover temperature  $T^* > T_g$  at which the decay saturates. We believe this to be a combined effect of several factors, and the influences of glassy slowing-down (modifying motional narrowing contributions), dynamical correlations and spin diffusion are discussed.

#### References:

- [1] A. Heuer et al., Phys. Rev. Lett. 75, 2851 (1995)
- [2] D. Pelc et al., Phys. Rev. Lett. 109, 095902 (2012)
- [3] E. Koivula et al., Phys. Rev. B 32, 4556 (1985)

#### TU254: Synthesis, structural, and physical characterization of new mixed-valent Mn7 clusters containing 2-hydroxymethylpyridine

<sup>1</sup>Katye M. Poole, <sup>1\*</sup>Khalil A. Abboud, <sup>2</sup>Christopher C. Beedle, <sup>2,3</sup>Stephen Hill, <sup>1</sup>George Christou

<sup>1</sup>University of Florida, <sup>2</sup>National High Magnetic Field Laboratory, <sup>3</sup>Florida State University

One of the main research interests in our group for a number of years has been the synthesis and characterization of transition metal compounds such as iron and manganese clusters, which usually contain chelating ligands to prevent polymerization. These complexes are of general interest for a number of reasons, including bioinorganic chemistry, magnetic materials, and oxidation of organic compounds. Manganese (Mn) is found at the active sites of many metalloproteins, with one of the most important being the water oxidation center (WOC) of plants and cyanobacteria, which contains a tetranuclear Mn cluster. Manganese clusters are also of interest due to interesting magnetic properties, and some Mn clusters have been found to be single-molecule magnets (SMM). SMMs are molecules that can function as nanoscale magnets at low temperatures. This behavior results from a large ground state spin (S) due to unpaired electrons and a large and negative (easy axis type) magnetic anisotropy, D, which together give a significant barrier for magnetization reversal, which is characteristic of magnets. This presentation will describe the use of halides (bromide, chloride, and iodide) and pseudo-halides ( $N_3^-$ ,  $NCO^-$ , etc) in a previously known reaction, and the characterization of the resulting five Mn7 wheel compounds. The Mn7 wheel topology can be described as a hexagon with another Mn ion in the center, and is with precedent in the literature, but this work has uncovered examples with a new intermediate spin ground state, S, for this topology.

#### TH255: Synthesis and Electrochemical Characterization of TiO<sub>2</sub> Materials

<sup>1,2\*</sup>Ivan Erick Castañeda Robles, <sup>1</sup>Jorge Uruchurtu Chavarín, <sup>1</sup>E. C. Menchaca Campos, <sup>2</sup>Roberto Rodríguez Muñoz

<sup>1</sup>Universidad Autónoma del Estado de Morelos,

<sup>2</sup>Universidad Tecnológica del Estado de Zacatecas

The anodization of titanium is an electrochemical process that changes the chemical surface of the metal, via oxidation, to produce an oxide layer. During this self organized process, highly ordered arrays of cylindrical shaped pores can be produced with controllable pore diameters and density distribution. This enables titanium applications, such chemical sensors, without the need for expensive lithographical techniques. A oxide (TiO<sub>2</sub>) to be used in a wide range of nanotechnological applications or incorporate it into specific simple method was used, electrochemical techniques from low potential in acidic and basic solutions. Cylindrical pores arrangements of TiO<sub>2</sub> were constructed by anodizing the titanium surface in an aqueous electrolyte of hydrofluoric acid

(0.5% HF) to subsequently evaluate it in hydrogen peroxide (H<sub>2</sub>O<sub>2</sub>).

#### MO256: <sup>1</sup>H NMR Relaxation Time Distributions Study of Styrenic Polymers

<sup>1\*</sup>Naira Machado da Silva Ruiz, <sup>2</sup>Luiz S. C. Junior, <sup>2</sup>Fábio L. L. Farias, <sup>2</sup>Grazielle. V. Tiziano, <sup>2</sup>Eduardo P. Casus, <sup>2</sup>Augusto C. C. Peres, <sup>2</sup>Sonia Maria Cabral de Menezes, <sup>3</sup>Edmilson Helton Rios, <sup>3</sup>João M. Costa

<sup>1</sup>Pontifícia Universidade Católica do Rio de Janeiro, <sup>2</sup>CENPES-PETROBRAS, <sup>3</sup>Fundação Gorceix

The impact resistance of high impact polystyrene (HIPS) is achieved by incorporating a rubber phase into the styrenic rigid phase. The HIPS usually is produced by polymerization of styrene in the presence of varying amounts of polybutadiene (usually 5-12 in weight %), resulting in a material that can be structurally described as a multiphase system. This structure gives multiphase improvement of optical and mechanical properties when compared to polystyrene (GPPS-General Purpose Polystyrene resin) without modification. In this work the microstructure of different commercial rubber-modified polystyrene samples were analysed by time-domain low resolution nuclear magnetic resonance commonly reported as one of the most efficient methods for an independent determination of the complex polymers interfaces.  $T_1$ ,  $T_2$  relaxation time measurements were conducted on a Bruker Minispec mq20 (0,47T) low field NMR equipped with a variable-temperature air-flow probe head. NMR experiments were run at a temperature of 40°C. Typical pulse length was 3.2  $\mu$ s for the 90° pulse. The NMR sequences used were inversion recovery (IR) for  $T_1$  and Carr-Purcell-Meiboom-Gill (CPMG TE=100  $\mu$ s) for  $T_2$  and the relaxation time distributions were obtained by an inverse Laplace transformation (ILT) of IR and CPMG data. For all samples  $T_1$  and  $T_2$  exhibit the typical structure for rubber-modified styrenics and reveal that the rubber phase are poorly described by only a single exponential component. In order to separate the signal contributions from individual phases we combine the ILT data fitted in a Gaussian model with  $T_1/T_2$  ratio. A quantitative evaluation of individual phases revealed the presence of at least two phases in the HIPS sample suggesting the presence of large PS domains segregated from the soft phase which is clearly related to the material properties.

ACKNOWLEDGEMENTS: PETROBRAS, PUC-Rio

#### TU257: Spectroscopic Characterization of meningococcal serogroup C Polysaccharide produced by a new purification process based on chromatographic extraction, 1D and 2D-NMR Spectroscopy

<sup>1,2</sup>Milton Neto da Silva, <sup>1,2\*</sup>Elza C.S. Figueira

<sup>1</sup>Instituto de Tecnologia em Imunobiológicos-Bio-Manguinhos/FIOCRUZ, <sup>2</sup>Instituto de Tecnologia em Fármacos Far-Manguinhos/FIOCRUZ

Neisseria meningitidis is one of the most important pathogens as causes of meningitis and other clinical manifestations. Meningococcal disease is primarily caused by only five meningococcal groups (A, B, C, Y and W135) among 13 groups described. Meningococcal serogroup C polysaccharide (MenCPS) is a homopolymer consisting of  $\alpha$ -(2→9)-linked sialic acid and has been widely used as antigen in polysaccharide and conjugate vaccines. The MenCPS production and purification processes, acquired from Merieux Institut in 1976, has been used up to date. This old process includes different steps. Two of them have some problems for large scale production. The first one is related to use of phenol for protein removal which is a very corrosive and toxic reagent and the other is the ultracentrifugation step used for LPS elimination be very expensive, since many cycles are needed. The new process proposed in the present study is an alternative to substitute the old one, in order to have a convenient purification for scale the MenCPS production up and also increase the process yields.

NMR spectroscopy has been one of most important tool for control the identity of bacterial polysaccharides used in vaccine manufacture. This technique is powerful and useful to release polysaccharide batches. The identity of native MenCPS produced using the new purification process was evaluated by different techniques based on NMR spectroscopy, including 1D and 2D-NMR analyses. NMR spectra were acquired on a BRUCKER AVANCE (400 and 500MHz) using TSP-d4 and DMSO with DSS as internal standard. The compound carbon and proton spectra contain all the important species whose resonances have been assigned to individual atoms in the repeating unit and are consistent with the published structure. These results confirm the molecule identity and suggest the new purification process would be used to produce native MenCPS as vaccine component.

### Low field NMR

#### TH258: Flow Regime Analyzer Based on Low-Field Nuclear Magnetic Resonance and Field-Cycling Scheme for Fluid Contrast

<sup>1,2\*</sup>Lucas Matías Cerioni, <sup>1</sup>Cristian Sebastián Moré, <sup>1</sup>Julia Inés García, <sup>1,2,3</sup>Daniel José Pusiol

<sup>1</sup>SPINLOCK SRL, Córdoba, Argentina, <sup>2</sup>Argentinian National Research Council, <sup>3</sup>Instituto de Física Enrique Gaviola, Ciudad Universitaria, Córdoba, Argentina

The real-time determination of the flow regime and the composition of the complex fluid being extracted through the production line is today one of the main challenges in the oil industry. In this work we present a system, based on a Halbach magnet type, designed for determining in real-time, mean velocity and fraction of components of complex fluids directly in the production vein by means of low-field Nuclear Magnetic Resonance. This constitutes an extension and improvement of a previous work.

The apparatus includes a main Halbach magnet of 35 cm in length, with a cylindrical region of interest (ROI) of 5 cm in diameter and 10 cm in length, allowing to measure in a 5 cm (2 inch) pipe. By means of a method based on the analysis of the early behavior of the echo amplitudes of a CPMG sequence and without applying any static or pulsed gradients, the cuts and mean velocity of oil and water mixtures were measured for flow-rates between 0.2 and 4 m<sup>3</sup>/h. Density contrast between oil and water phases with different longitudinal relaxation times  $T_1$  was accomplished varying the pre-polarization field. Unlike a previous work where the pre-polarization field of variable effective length was achieved by means of Halbach stacks with rotation capabilities, the prepolarization stage of 200 cm in length remains fixed, and an electromagnet of 30 cm in length before the main magnet provides the fluid contrast. A better contrast is achieved using a field-cycling type scheme on the pre-polarizing magnetic field, taking advantage of the greater difference in oil and water relaxation times at Larmor frequencies ranging in low-field values (kHz range). A theoretical modeling using adiabatic processes for the changes in the magnetic field experienced by the sample while flowing allows optimizing the contrast between the two phases. The experimental results are in agreement with the theoretical framework.

ACKNOWLEDGMENTS: CONICET, FONTAR, SPINLOCK

#### MO259: The NMR-MOUSE® as a tool to study depth photo-curing reaction.

<sup>1\*</sup>Antonio Marchi Netto, <sup>2,3</sup>Johannes Steinhaus, <sup>3</sup>Bernhard Moeginger, <sup>2</sup>Berenika Hausnerova, <sup>1</sup>Bernhard Blümich

<sup>1</sup>RWTH Aachen University, <sup>2</sup>Tomas Bata University in Zlín, <sup>3</sup>Bonn-Rhein-Sieg University of Applied Sciences

A current technique in tooth restoration fills shallow cavities

with resins, which are photo-polymerized by visible light (450 nm). In this work, the photo-polymerization of two dental resins was studied quantitatively by NMR relaxometry with the help of a single-sided NMR tool, the NMR-MOUSE as a function of time and depth. With increasing curing time, the transverse relaxation time initially increases due to sample heating from the exothermic reaction and then decreases as the liquid polymerized into a solid.

The curing reaction of a flat sample was initiated by continuous irradiation with the light of a blue LED lamp. The sample was placed on an NMR-MOUSE with 5 mm depth access and 18.1 MHz proton frequency. The curing reaction was studied at depths from 1 to 4 mm in terms of the sum of the firsts 64 echoes of a CPMG train.

The curing curves were modeled with the original Kohlrausch function and modified according to Weibull to account for the initial sample heating effect and for the subsequent signal decay from curing. The use of the Kohlrausch function is justified from the first-order polymerization kinetics of the initiation, propagation and termination steps of the reaction. The depth dependence of the reaction kinetics is accounted for by the law of Lambert and Beer.

By fitting the model to the experimental curing curves at different depths, the kinetic constants of the reaction and the optical extinction coefficient could be determined. The absorption coefficient obtained from the NMR analysis is similar to the one determined by optical transmission experiments. Given the kinetic parameters of the curing reaction, the curing conditions can be optimized.

ACKNOWLEDGEMENTS: Antonio Marchi Netto thanks the Brazilian National Council for Scientific and Technological Development for his PhD fellowship.

#### TU260: Mobile Low-Field <sup>1</sup>H NMR Spectroscopy for on-line monitoring transesterification reactions and biodiesel analysis.

<sup>1</sup>Yamila Garro Linck, <sup>1,2</sup>Mario Henrique Montazzolli Killner, <sup>1</sup>Ernesto Danieli, <sup>2</sup>Jarbas José Rodrigues Rohwedder, <sup>1\*</sup>Bernhard Blümich

<sup>1</sup>Institut für Technische Chemie und Makromolekulare Chemie, Aachen University, Aachen, Germany., <sup>2</sup>Instituto de Química, Universidade Estadual de Campinas, Brazil, Campinas, Brazil

Biodiesel has gained importance in recent decades because of its favorable properties. It is defined as alkyl esters of vegetable oils or animal fats, by means of transesterification with an alcohol. The quality control of biodiesel is important to the successful commercialization of this fuel and its blends[1].

We show the use of a new mobile low-field <sup>1</sup>H NMR device, based on permanent magnets arranged in a modified Halbach geometry[2], for the real time study of transesterification reactions. Low-field <sup>1</sup>H NMR spectra of the compounds co-existing in a typical transesterification reaction are first discussed. Then, the online monitoring of the reaction through NMR spectroscopy is presented, which allows the determination of the conversion rate of the product. This was determined by a partial least squares (PLS) calibration model, validated with high field experiments. Additionally, the relative concentration values of hydroxyl protons were also analyzed, giving a quantitative idea of the alcohols partitioning between the two phases during the reaction. These results are useful to understand the reaction mechanism of biodiesel production. A strong shift in the spectral position of the hydroxyl protons was observed, which shows good correlation with the conversion ratio of the reaction. Moreover, the degree of saturation of different biofuel samples was estimated by low-field NMR spectroscopy measurements[3], which is of great importance because of its direct relation with biodiesel properties such as viscosity, density and higher heating values.

[1] G. Knothe, J. Van Gerpen, J. Krah (eds.), The biodiesel handbook (AOCS Press, Champaign, 2005).

[2] E. Danieli et al. *Angew. Chem. Int. Ed.* 49, 4133 (2010).

[3] Y. Garro Linck, M. H. Killner, E. Danieli and B. Blümich. *Appl. Magn. Reson.* 44, 41 (2013).

#### TH261: Prediction of Sweetness of Papaya, in Intact Green Fruits, Using Online Time Domain NMR Spectrometer Based on Widebore Halbach Magnet.

<sup>1</sup>André de Souza Carvalho, <sup>2</sup>Fernando Henrique Vieira, <sup>3</sup>Luiz Alberto Colnago

<sup>1</sup>Universidade Federal de São Carlos, <sup>2</sup>UNICEP, <sup>3</sup>Empresa Brasileira de Pesquisa Agropecuária

Brazil is the major papaya's producer and exporter with an estimated production about 1,5 million tons/year. The need to export high quality fruits is increasing and aim of this work is to predict papaya sweetness using online time domain NMR spectroscopy. Low field time domain NMR has been evaluated as an industrial sensor for intact measurement of internal fruit quality. Here we are showing that this technique can be used to predict the papaya sweetness, expressed in total content of soluble solids (°BRIX). The analyses can be performed just after harvesting, approximately 10 days before it is read to human consumption. This procedure can be used to discard low sugar papayas in the farms before the exportation. The unripe papayas analyzed were purchased in São Carlos - SP, Brazil and were measured in a SLK CA02.12 spectrometer Spinlock, Cordoba, Argentina, based on  $B_0 = 0.21$  T Halbach magnet with 10 cm free bore. The fruits were analyzed with the CPMG pulse sequence and the Brix value of the ripe papayas with a portable refractometer RT-30ATC. The monoexponential  $T_2$  values obtained from the CPMG decays varied from 0.9 to 1.1 s in the green papaya and show small increased after ripening. The  $T_2$  values of both green and ripe papayas show high and negative correlation (-0.9) with Brix. Therefore, these results indicate that  $T_2$  can be used to predict, even in unripe fruit, if the papaya will be sweet or not. The method is now been tested in large scale and can be a useful tool to help farmers and the consumers with high quality fruits.

ACKNOWLEDGEMENTS: FAPESP and CNPq

#### MO262: Application of a Mobile Low-Field $^1\text{H}$ NMR Device for Quality Control of Diesel Fuel

<sup>1</sup>\*Mario Henrique Montazzolli Killner, <sup>2</sup>Ernesto Danieli, <sup>1</sup>Jarbas José Rodrigues Rohwedder, <sup>2</sup>Bernhard Blümich

<sup>1</sup>Universidade Estadual de Campinas, <sup>2</sup>ITMC-RWTH Aachen University

In 2011, 2.3% of 91,022 diesel samples policed in Brazilian gas stations by ANP (Brazilian National Agency of Petroleum) were nonconforming with the ANP specifications. This finding is mainly attributed to fuel adulteration by diesel providers to increase its profitability. This fact brings forth onus to the country specially because of tax evasion. The most important properties to certify diesel quality are: density, cetane index, sulfur content, flash point, biodiesel content and distillation temperature with 10, 50, 85 and 90% recovered. Although the determination of these properties is inevitable for ensuring diesel quality, it is time-consuming and laborious, which makes an embracing and efficient control more difficult.

In view of this, the present work shows an application of a mobile low-field  $^1\text{H}$  NMR device, built from permanent magnets which generates a magnetic field of 1T (42 MHz  $^1\text{H}$  Larmor frequency, with homogeneity better than 0.04 ppm for the sample region) to diesel fuel quality control. For that, different PLS calibration models applying low-field  $^1\text{H}$  NMR spectra of 40 diesel fuel samples, collected in different Brazil-

ian gas stations, were built. All the samples were previously analyzed by standard methods.

The developed models were validated with 20 external samples that were not used for development of the calibration models. For the properties density, distillation temperature with 10 and 50% recovered, cetane index and flash point the PLS models showed a high correlation coefficient ( $R^2 > 0.9$ ) and determination errors similar to the standard methods. The biodiesel content was directly determined by the integration of the methoxy peak of the fatty acid methyl esters versus an internal standard.

It is important to highlight that the mobile low-field  $^1\text{H}$  NMR device needs only 10 seconds for acquisition of  $^1\text{H}$  NMR spectrum, and applying the developed PLS models the process of diesel fuel quality control can easily work fast (less than 1 minute for each sample) and continuous in automated mode.

ACKNOWLEDGEMENTS: DAAD, CAPES

#### TU263: Prediction of Brazilian crude oils fractional composition by low-field NMR relaxometry

Asif Muhammad, Felipe Silva Semaan, Fabio da Silva Miranda, \*Rodrigo Bagueira de Vasconcellos Azeredo

Universidade Federal Fluminense

Crude oil fractional composition plays an important role in several aspects of the petroleum industry from oil exploration and extraction, to its refining processes, transport, and petroleum derivative marketing. Unlike petrochemicals, which have a well-defined chemical composition, petroleum is a complex multicomponent system, whose individual component characterization is a virtually impossible task. Facing this difficulty, group type classification methods based on solubility (SARA fractionation) and thermogravimetric behavior are frequently used by petroleum industry. However, these methods not always meet the requirements normally demanded for *in situ* applications, like robustness and speed. In this sense, low-field NMR relaxometry can be an interesting alternative to these techniques for oil characterization by well logging, in which measurements are performed downhole into the oil well. Therefore, in the present work we evaluated the application of low-field NMR relaxometry, assisted by multivariate data analysis (MVA), to predict the crude oils fractional composition obtained by Thermogravimetric Analysis (TGA). Fifteen samples of Brazilian crude oils, ranging from light (38.1 °API) to extra-heavy (9.9 °API), were assessed for such purpose. From their respective  $^1\text{H}$   $T_2$  distributions, Partial Least Squares Regression (PLSR) models were developed to predict the composition according to main four groups. All developed PLSR models showed good predictive performances, as follows: group 1 (light compounds,  $<100^\circ\text{C}$ ),  $R^2 = 0.93$  and RMSEP = 0.92; group 2 (heavy compounds,  $100 - 300^\circ\text{C}$ ),  $R^2 = 0.94$  and RMSEP = 2.31; group 2 (resin,  $300 - 450^\circ\text{C}$ ),  $R^2 = 0.90$  and RMSEP = 0.20; and group 4 (asphaltene  $450 - 500^\circ\text{C}$ ),  $R^2 = 0.90$  and RMSEP = 1.27.

TWAS, CNPq, PETROBRAS and ANP (Compromisso com Investimentos em Pesquisa e Desenvolvimento)

#### TH264: Through-package fat determination of commercial mayonnaises with time-domain nuclear magnetic resonance spectroscopy and chemometrics

\*Fabiola Manhas Verbi Pereira, Luiz Alberto Colnago

Embrapa Instrumentação, São Carlos, Brazil

Although fat is an important nutrient in human diet, the high fat content food has been the major cause of one of the serious human healthy problems of modern world, the obesity. Therefore, the precise determination of fat content in raw and processed foods has been an important analytical issue. Here, time domain NMR spectroscopy (TD-NMR) based on wide bore Halbach magnet can be used as fast through-package method in quality control and quality assurance of

fat content in commercial mayonnaises in sealed flasks. The analyses were performed using a CPMG sequence in a Spin-lock (Cordoba, Argentine) TD-NMR spectrometer based on 0.23T Halbach magnet with 10 cm free bore. The comparisons between univariate model using the discrete values of transverse relaxation time ( $T_2$ ) obtained by fitting the sequence of pulses Carr-Purcell-Meiboom-Gill (CPMG) decays to mono-exponential function and multivariate models performed with partial least squares (PLS) were evaluated. The predictability of the PLS model was tested with 10 external samples from another lot. The high linear coefficients ( $>0.9$ ) and low root means square errors (RMSE) for cross validation and validation proved the applicability of the PLS model. The finding about this study is the TD-NMR CPMG relaxation decays successfully predict total fat on sealed packing of commercial mayonnaises varying in fat content up 10.0 to 55.8 g 100 g<sup>-1</sup>. The PLS models combined to these signals shown the best results. The main advantage verified is the no-invasive measurement of fat content performed for intact packing of food products. The high linear correlation coefficients between the reference values from Bligh and Byer lipids extraction and those predicted by PLS model evidences the accuracy of multivariate model against the univariate fitting with the discrete  $T_2$  values.

ACKNOWLEDGEMENTS: CNPq for the fellowship awarded to F.M.V. Pereira, FAPESP and Finep.

#### MO265: Applying NMR relaxometry procedures to characterize and classify soil samples

<sup>1</sup>\*Ruben Aucase Estrada, <sup>2</sup>Rodrigo de Oliveira Silva, <sup>2</sup>Tito José Bonagamba, <sup>1</sup>Fabiano de Carvalho Balieiro, <sup>1</sup>Etelvino Henrique Novotny

<sup>1</sup>Empresa Brasileira de Pesquisa Agropecuária, <sup>2</sup>Instituto de Física de São Carlos, Universidade de São Paulo

The characterization of unsaturated hydraulic properties of soils by using Richard's chamber and van Genuchten phenomenology of water retention are very time consuming methods[1]. By this procedure, many researcher groups treat to describe the dynamics of water molecules in the soils samples. In this description, they take advantage about the dependence of moisture content on different soil water potential, which in some kinds of soils samples takes approximately of some days to many weeks[2].

An alternative and faster procedure is to apply NMR relaxometry protocols and principal component analysis (PCA) technique to perform the classification and characterization in different kinds of soils. The main purpose of this new procedure is to diminish the time of extracting information about characterization and classification of soils samples. To put in practice this idea, we used three different soils with different concentrations of clay, sand and silt[3]. This choice allows us to test the sensibility of this procedure. We compare our results with other well established technique which is the inverse Laplace transform[4].

References:

- [1] M. Th. van Genuchten, Soil Sci. Soc. Am. J., 44, 892-898,(1980).
- [2] B. Minasny et al., Geoderma, 93, 225-253,(1999).
- [3] F. de C. Balieiro et al., Arvore, Viçosa-MG, 32, 153-162, (2008).
- [4] Marcel Nogueira D'Eurycide, PhD Thesis, IFSC-USP, São Paulo Brasil (2011).

ACKNOWLEDGEMENTS: FAPERJ, CAPES, CNPq, FAPESP.

#### TU266: Physical and chemical characterization of products petroleum.

\*Lúcio Leonel Barbosa, Flávio Vinicius Crizóstomo Kock, Vinicius Mansur Dose Lage de Almeida, Valdemar Lacerda

Júnior, Eustáquio Vinicius Ribeiro de Castro

Federal University of Espirito Santo

In this work was investigated the application of low field NMR (LF-NMR) to predict physical and chemical properties of petroleum products.

For the tests two Brazilian crude oil were distilled: the crude oil 1 presented TAN = 1.15 mg KOH/g, density of 0.9749 g cm<sup>-3</sup> and kinematic viscosity 5800 mm<sup>2</sup> s<sup>-1</sup> at 40 °C, and the crude oil 2 with TAN = 1.42 mg KOH/g, density of 0.9164 g cm<sup>-3</sup> and kinematic viscosity 58.115 mm<sup>2</sup> s<sup>-1</sup> at 40 °C.

The NMR experiments were performed using a Maran 2 Ultra NMR spectrometer at 2.2 MHz for <sup>1</sup>H. The  $T_2$  values was measured using the Carr-Purcell-Meiboom-Gill (CPMG) pulse sequence at 27.5 °C. The CPMG pulse sequence was applied employing  $\pi/2$  and  $\pi$  pulses with durations of 8.15  $\mu$ s and 16  $\mu$ s, respectively. In the CPMG experiments were recorded 32 transient with 8192 echoes in each transient, one point per echo, echo spacing of 0.2 ms and recycle time of 3s.

The physical and chemical properties as refractive index, kinematic viscosity, total acid number, boiling point, specific gravity were determined directly by standard methodologies ASTM D-1218, D 445-06, D-664-04, D-2892 and D 4052, respectively. The results showed good correlation with the mean values of the transversal relaxation time ( $T_2$ ).

It can be concluded of this work, that the proposed method for distilled analysis, LF-NMR, presented several advantages as non-destructiveness and not require solvents or dilution. This allows the assessment of several properties simultaneously, based on the output of only one NMR experiment, leading to large economy in terms of energy, time and costs. Thus, it is suggested that the LF-NMR technique can be applied for routine analysis as a guide in the quality control of the distilled products.

ACKNOWLEDGEMENTS: CNPq, FAPES, PETROBRAS, LABPETRO DQUI/UFES.

#### TH267: Influence of the incorporation of fibers in biscuit dough. Characterization by time domain NMR and rheology.

<sup>1</sup>M.R. Serial, <sup>2</sup>M.S. Blanco Canalis, <sup>1</sup>M. Carpinella, <sup>2,3</sup>A.E. León, <sup>2,4</sup>P.D. Ribotta, <sup>1\*</sup>Rodolfo Héctor Acosta

<sup>1</sup>Universidad Nacional de Córdoba, CONICET, <sup>2</sup>Instituto de Ciencia y Tecnología de Alimentos Córdoba, CONICET, <sup>3</sup>Facultad de Ciencias Agropecuarias, Universidad Nacional de Córdoba, <sup>4</sup>Facultad de Ciencias Exactas, Universidad Nacional de Córdoba

Several epidemiological and experimental studies show that consumption of determined food products can act either as protective or as risk factors on non-transmissible diseases. Recommendations have emerged that aim to reducing the ingestion of sugars and fats, or to increase the fiber content (particularly soluble) in the diet. Biscuit or cookie dough is a complex system containing abundant components in different states, such as starch, gluten, lipids (flour constituents), sugars, fats and water. In biscuits, both, the incorporation of fibers or the reduction of sugar and fat, create a number of technological problems in processing and in some cases a loss of acceptability [1]. For this reason, the effects on the physico-chemical, rheological and structural characteristics of biscuit dough upon incorporation or reduction of determined ingredients is of great interest in food industry. It is generally known that the distribution of water can affect the rheology of the dough machinability [2]. Low resolution NMR is an important tool as it allows the study of water mobility by means of relaxation time measurements ( $T_2$ ) in the sample, in a non-invasively, fast and accessible way. In this work we study the proton water mobility in standard biscuit dough through relaxation profiles obtained from a CPMG sequence at 0.5 Tesla. Different populations are assigned to different ingredients [3]. The dependence of mobility as a function

of the dough temperature in a cooking process is correlated to rheological experiments. We analyzed the quality of the final product upon variation of different parameters in the biscuit formula, such as reduction of fat, reduction of sugar and incorporation of fiber with flour reduction.

[1] Maache-Rezzoug et al. Journal of food engineering 35, 23-42 (1998).

[2] Ruan et al. Cereal Chemistry, 76, 231–235 (1999).

[3] Assifaoui et al. Carbohydrate Polymers 64, 197–204 (2006).

#### MO268: On-Line Monitoring by NMR in Time Domain of Chitosan in Marine Environment Contaminated by Oils

\*Flávio Vinicius Crizóstomo Kock, Lúcio Leonel Barbosa, Valdemar Lacerda Júnior, Eustáquio Vinicius Ribeiro de Castro, Eloi Alves da Silva Filho

Federal University of Espírito Santo

Petrochemical accidents have attracted great notoriety in the scientific community due to damage caused in offshore and onshore environments. The present study carried out spread oil in seawater and monitored the action of the biosorbent *on line* inside a NMR spectrometer of 2.2 MHz for  $^1\text{H}$  nucleus.

The biomaterial chosen was chitosan, because of this material has special features, for example, biodegradability, facility for realizes complexation with metals and flocculation ability that makes possible to study their action as bioremediation agent.

The *on line* results indicated that this biomaterial acts increasing the viscosity and reducing by more than 30% of the  $T_2$  values. From of study with dehydrated oils was possible infer that this biomaterial can interact with structure more denser, leading to destabilization complexes compounds, for example, asphaltenes. Moreover, studies only with aqueous phase of emulsion, lead to infer that this biomaterial acts forming strong interaction with molecule of water and consequently increasing the viscosity of the medium.

Finally, this unpublished results showed displacement of  $T_2$  from 63.4ms to 108.3ms without and with application of chitosan, respectively. So, it can be conclude that this biosorbent have power of flocculation, coalescence and sedimentation, provoking so destabilization of water droplet in emulsions water/oil, and this ability can be studied by nuclear magnetic resonance in time domain (TD-NMR).

ACKNOWLEDGEMENTS: UFES, CAPES, PETROBRAS, LABPETRO.

#### TU269: Determination of Droplet Size in oil emulsion by low-field NMR

\*Vinicius Gomes Morgan, Lúcio Leonel Barbosa, Valdemar Lacerda Júnior, Eustáquio Vinicius Ribeiro de Castro

Universidade Federal do Espírito Santo

Emulsions appear commonly in oil industry, formed by presence of water in the reservoir and secondary recovery process. Emulsion is a dispersion of water droplets in the oil, stabilized by natural emulsifiers presents in oil phase as asphaltenes, naphthenic acids and others. The most common type of emulsion is water in oil (W/O). An important property of this system is the droplet size distribution (DSD). The DSD alter significantly some physicochemical properties as viscosity and stability, indicates the best treatment process for separating water from oil, allows to monitor the production according the required specifications and serves as the basis for dimensioning the production equipment and treatment. Several techniques can provide the DSD, including low-field NMR, which was used together with optical microscopy (O.M). Two W/O emulsions was produced from oil 1 ( $^\circ\text{API}$  29.6 and viscosity of  $44.83 \text{ mm}^2/\text{s}$  at  $20^\circ\text{C}$ ) and 2 ( $^\circ\text{API}$  29.4 and viscosity of  $44.15 \text{ mm}^2/\text{s}$  at  $20^\circ\text{C}$ ), adding

10% (w/w) NaCl 50 g/L solution and applying shear rate of 6500 and 3000 rpm, respectively for 3 minutes. Preliminary analysis showed unimodal distributions in the two emulsions. The first emulsion, NMR provided  $3.66 \mu\text{m}$  as the diameter of the largest occurrence frequency of the drops and O.M about 4.20 micrometers. In the second, NMR showed drops with  $4.40 \mu\text{m}$  in diameters, while O.M presented  $5.10 \mu\text{m}$ . It was concluded that there was good agreement between the techniques, demonstrating the potential of low-field NMR to determine droplet size and type of emulsions, i. e, highly stable.

ACKNOWLEDGEMENTS: CNPQ, FAPES, CAPES, LABPETRO-DQUI/UFES

#### TH270: Studies of Magneto-electrodeposition of Copper using time domain NMR.

<sup>1,2</sup>\*Bruna Ferreira Gomes, <sup>2</sup>Luiz Alberto Colnago, <sup>1</sup>Luiza Maria da Silva Nunes, <sup>2</sup>Luís Fernando Cabeça

<sup>1</sup>Universidade de São Paulo, <sup>2</sup>Embrapa Instrumentação

NMR has been used to monitor electrochemical reaction in situ for many years. Although the effect of magnetic field in the electrochemical reaction is known for a long time, no in situ NMR study has considered it. The effect of NMR magnetic field ( $B_0$ ) in presence of electric field has been studied only as a pumping and mixing procedures in microfluidics devices. Therefore we are investigating the influence of NMR magnetic field during copper electrodeposition reaction. The experiments were performed in *Spin Lock* (0.23T) time domain spectrometer. BV Palm Instruments potentiostat were used in the electrochemical measurements. The electrochemical cell was composed of a silver plate ( $100 \text{ mm}^2$ ), a counter electrode of spiral silver and a silver wire as a pseudo reference electrode. Calibration curves were made for copper ion concentration considering  $T_2[1]$ . The copper electrodeposition reaction was higher when the reaction was performed in the NMR magnet (M) than without it (W). In one-hour reaction, the  $\text{Cu}^{2+}$  concentration in solution decayed to 55% and 30% in M and W experiments, respectively. The fast reaction in presence of  $B_0$  is related magneto-convective force (FB) that acts on the species  $\text{Cu}^{2+}$ , where  $\text{FB} = i \times B$  ( $i$  is the current density and  $B_0$  is the magnetic induction vector). Therefore, we demonstrate that the strong effect of  $B_0$  in electrochemical reactions must be considered.

[1] NUNES, L. M., et al. (2012). In situ quantification of Cu(II) during an electrodeposition reaction using time-domain NMR relaxometry. Analytical Chemistry, 84, 6351-6354.

ACKNOWLEDGEMENTS: FAPESP, CNPq

#### MO271: The use of TD-NMR as non-destructive method to analyze mechanical injuries in apple

<sup>1</sup>Lucinéia Vizzotto Marconcini, <sup>2</sup>Douglas William Menezes Flores, <sup>2</sup>Marcos Davi Ferreira, <sup>2</sup>\*Luiz Alberto Colnago

<sup>1</sup>Chemical Institute of Paulista State University, Araraquara., <sup>2</sup>Brazilian Agricultural Research Corporation, Instrumentation Research Center, São Carlos.

Harvesting and post-harvesting systems and managements have a direct effect on incidence and severity of mechanical injuries on fruits, resulting in tissue browning, accelerating water loss and induce  $\text{CO}_2$  and ethylene production. Here time domain NMR (TD-NMR)  $T_2$  relaxometry was used to analyze the effect of mechanical injury in apple quality. The CPMG measurements were carried on Spinlock SLK CA02.12 NMR spectrometer based on wide bore Halbach magnet, 0.21 T, with a  $10 \times 10 \text{ cm}^2$  of detection area. The CPMG decays were analyzed using inverse Laplace transform program. The  $T_2$  distributions spectrum shows three peaks that have been associated to water in the vacuole (1.2s), cytoplasm (0.3s) and cell wall (0.01s). Thirty-six apples were subject to different mechanical damage (ie, 3 to 12 falls

from 40 cm height). The samples were analyzed before and just after the impact, every hour up to 8h, and after 48 hours. All mechanical injuries caused almost instantaneous increases in  $T_2$  values, reaching a peak at about 5h, and then slowly returning to initial value in 48 hours. The increase of  $T_2$  value after the injury is related to reduction of internal oxygen in the fruits, and is direct related to the  $\text{CO}_2$  production. When the injured apples were maintained in nitrogen atmosphere, the  $T_2$  values increased more than three times when compared to storage in air. The ratio between the  $T_2$  area of vacuolar and cytoplasmatic water decreased with the severity of injury and it was able to distinguish between apples with moderate and severe injuries from non-injured ones. Therefore, TD-NMR protocols has the potential to classify apples according to mechanical injuries incidence and severity.

#### **TU272: Use of TD-NMR to Measure Water Imbibition by Seeds Directly in the Soil**

<sup>1</sup>\*Maria Gabriela Aparecida Carosio, <sup>2</sup>Luiz Alberto Colnago

<sup>1</sup>Institute of Chemistry of São Carlos, <sup>2</sup>EMBRAPA Instrumentation

NMR and MRI have been used to measure water content and water transport in soils as well as the water content and distribution in plant roots. Most of these studies are performed in synthetic soil (mixture of sand/silt) or real soils with very low content of magnetic particles. The NMR studies are not well succeeded when the soil has high content of magnetic particles due to the distortion in B0 and the presence of large amount of paramagnetic ions that reduces the relaxation time to the same order of receiver dead time. Here we are showing that the time domain NMR (TD-NMR) can be used to measure the water uptake by seed in moist soil with very high content of magnetic particles. This process is very important because the seed germination begins with water uptake and triggers a series of metabolic changes that culminate in the emergence of the primary root. The CPMG pulse sequence were carried out in a SLK-100 Spinlock spectrometer (model SLIM.01). The spectrometer uses a 0.23T permanent magnet. It was used soybean (*Glycine max*) and garbanzo bean (*Cicerarietinum*) seeds. The soil used was a typical Brazilian soil and it was moistened to field capacity. In this soil, the water signal was not observed by NMR. Therefore, when seeds were placed in this soil the NMR signals was proportional to the water absorbed by the seed (imbibition process). The seeds in the soil absorb water in lower rate than the seeds in pure water, indicating the influence of the soil ionic force in this process. Therefore TD-NMR can be used to follow the imbibition process in intact seed direct in soil which is not possible with current technologies.

ACKNOWLEDGEMENTS: FAPESP (2009/09734-1), EMBRAPA Instrumentation

#### **TH273: Use of Unilateral NMR sensor to Measure Temperature in Intact Seeds and Seeds Inside Soils**

<sup>1</sup>\*Maria Gabriela Aparecida Carosio, <sup>2</sup>André de Souza Carvalho, <sup>3</sup>Luis Fernando Cabeça, <sup>4</sup>Luiz Alberto Colnago

<sup>1</sup>Institute of Chemistry of São Carlos, <sup>2</sup>Federal University of São Carlos, <sup>3</sup>Federal Technological University of Parana, <sup>4</sup>EMBRAPA Instrumentation

Time domain Nuclear Magnetic Resonance (NMR) has been used as non-contact, non-destructive, no reagent chemical analytical method. In this paper we are showing that we can use time domain Unilateral NMR (UNMR) sensor to measure the temperature of intact oilseeds and oilseed in the soil. The measurement is based on the  $T_2$  dependence of either oil viscosity or temperature. As oil viscosity decreases exponentially with temperature the  $T_2$  value is used to measure temperature in intact oilseeds using a UNMR sensor. Some seeds may survive in high temperature environment for days, but the seedling may die in few hours. Therefore,

the seed temperature is an important parameter to agriculture research. The  $T_2$  measurements were carried out in a homemade UNMR. The spectrometer uses a 0.6T (24MHz) home made UNMR sensor and a Tecmag console.

#### **MO274: Estimation of available Water in Soils by NMR Relaxometry**

<sup>1</sup>Rodrigo de Oliveira-Silva, <sup>2</sup>Ruben Aucasse Estrada, <sup>2</sup>Fabiano de Carvalho Balieiro, <sup>2</sup>Etelvino Henrique Novotny, <sup>1</sup>\*Tito José Bonagamba

<sup>1</sup>Instituto de Física de São Carlos - Universidade de São Paulo, <sup>2</sup>Embrapa Solos - Rio de Janeiro

In soil science it is essential to understand water/soil physico-chemical interactions. Traditional procedures to understand these interactions are the measurement of water retention curves and the construction of pedotransfer functions. Both methods give accurate information about soil moisture, but they can be very time consuming depending on the components of soil to be analyzed, including clay, silt and organic matter. Also, normally these measurements offer only bulk data. Soil moisture curves can also be measured by NMR relaxometry, following wetting and dewetting procedures. In this case, the curves can be obtained in a faster way and the physicochemical interactions between water and the various soil components normally result in different average  $T_2$  values, allowing obtaining water retention curves for each specific soil component, being more informative when compared with bulk measurements. In order to measure water retention curves by NMR, we used three different soils: top soil layer of Abruptic Arenic Ochraqult, as well as top and deeper layers of Abruptic Aquic Arenic Hapludult, that differ in terms of composition and particle size distribution. The samples were drained in a controlled way using the moisture pressure plate extractor (Richards chamber), which dries the soil by increasing the internal chamber pressure. NMR experiments were performed at room temperature using a TEOMAG LapNMR console, a 620-Gauss permanent magnet, and a homemade NMR probe.  $T_2$  relaxation times were obtained from CPMG experiments as a function of drained water for all the samples, using draining pressures of 1, 3, 5, 9, 13, 20, 40, 60, and 80 psi. From the  $T_2$  curves obtained versus draining pressures for each soil, different water retention behaviors were observed. These results reflect the different interactions of water with the various soil components, showing the applicability of this method to differentiate soils by their specific water retention capability and composition. This work indicates how NMR relaxometry can be used as an alternative method to obtain water retention curves.

ACKNOWLEDGEMENTS: IFSC/USP, FAPESP, CNPq, and CAPES.

#### **TU275: Compact, Cryogen-Free, High-Resolution 60 MHz Permanent Magnet NMR Systems for Reaction Monitoring and On-Line/At-Line Process Control Observing $^1\text{H}$ , $^{19}\text{F}$ , $^{31}\text{P}$**

<sup>1</sup>\*John C. Edwards, <sup>2</sup>David A. Foley, <sup>2</sup>Mark T. Zell, <sup>2</sup>Brian L. Marquez, <sup>3</sup>Tal Cohen, <sup>1</sup>Paul J. Giammatteo

<sup>1</sup>Process NMR Associates, Danbury, CT, USA, <sup>2</sup>Pfizer Inc, Groton, CT, USA, <sup>3</sup>Aspect AI, Shoham, Israel

A compact high resolution NMR system will be described that can be situated on the bench-top or in the fume hood to be used as a continuous or stop-flow detector and/or an "in-situ" reaction monitoring system. The same system can be fully integrated into on-line shelters for on-line process control or utilized by engineers and technicians in an "at-line" environment. The system uses a unique 1.5 Tesla permanent magnet that can accommodate sample tube diameters of 3-10 mm with half-height spectral resolution (water resonance) approaching 1-3 Hz depending on the sample volume size and with excellent single pulse sensitivity. These systems can be utilized in a traditional NMR methodology approach or combined with chemometric approaches that allow NMR

data to predict chemical and physical properties of materials via regression analyses that establish correlations between observed spectral variability and sample-to-sample property variance [1]. The systems utilized since the early 1990's are capable of single channel operation on higher sensitivity nuclei ( $^1\text{H}$ ,  $^{19}\text{F}$ ,  $^{31}\text{P}$ ,  $^{23}\text{Na}$ ,  $^7\text{Li}$ ,  $^{11}\text{B}$ ). A new generation of NMR systems are now being manufactured featuring multi-channel operation giving the possibility to monitor two nuclei at once or to perform  $^1\text{H}$ - $^{13}\text{C}$ -DEPT and higher sensitivity approaches to  $^{13}\text{C}$  observation. In pharmaceutical applications the Aspect-AI 60 MHz system was utilized in a reaction monitoring scenario where a reaction was monitored simultaneously on a split sample loop by the 60 MHz NMR and a 400 MHz Bruker Avance III superconducting NMR spectrometer [2]. The results obtained on the two systems were virtually identical indicating that the 60 MHz NMR system can be used to transfer PAT knowledge generated on pharmaceutical reactions in the research lab to the manufacturing areas for production monitoring.

[1] "Process NMR Spectroscopy: Technology and On-line Applications", John C. Edwards, and Paul J. Giammatteo, in Process Analytical Technology: Spectroscopic Tools and Implementation Strategies for the Chemical and Pharmaceutical Industries, 2nd Ed., Editor Katherine Bakeev, Blackwell-Wiley, 2010.

[2] "Application of a 60 MHz Permanent Magnet NMR System to Online NMR Reaction Development in the Pharmaceutical Industry", David A. Foley, Mark T. Zell, Brian L. Marquez, John C. Edwards, and Paul J. Giammatteo, Presented at PittCon 2013, Philadelphia, PA, March 21, 2013. Poster PDF available at [www.process-nmr.com](http://www.process-nmr.com).

#### TH276: Effects of Biodiesel/Diesel on Vulcanized Natural Rubber as Revealed by Relaxometry and Double Quantum Time-Domain NMR

<sup>1</sup>Lorena M. A. Silva, <sup>2</sup>Fabiana Diuk, <sup>2</sup>Eduardo Ribeiro de Azevêdo, <sup>1</sup>Elenilson G. A. Filho, <sup>3</sup>Marcos Roberto Monteiro, <sup>1\*</sup>Tiago Venâncio

<sup>1</sup>Departamento de Química, Universidade Federal de São Carlos, <sup>2</sup>Instituto de Física de São Carlos, Universidade de São Paulo, <sup>3</sup>Centro de Caracterização e Desenvolvimento de Materiais, Universidade Federal de São Carlos

Biodiesel is a promising alternative fuel to meet the energy demand. However, its compatibility with the rubber materials employed in automobile engines is a growing concern. Thus, we address the effect of biodiesel and diesel in the network structure of commercial carbon black filled vulcanized natural rubber (VNR). For this purpose, we conducted static immersions of VNR in blends of fuels containing different amounts of biodiesel:diesel (0:100, 5:95, 20:80, 100:0) at 70 °C. These samples were studied using CPMG and DQ (double-quantum) time domain NMR experiments performed in an Bruker mq20 TD-NMR. The Laplace inversion of the CPMG data revealed that for VNR without contact with fuel the decay is comprised by three main components associated to rigidified chains at the filler vicinity ( $T_2 = 0.4$  ms), cross-linked chains ( $T_2 = 2.0$  ms), and less restricted chains in the polymer network ( $T_2 = 13.1$  ms). Immediately after exposure to fuel, the average  $T_2$  increases for all components due to swelling, but stabilizes after few minutes. Over time periods of days and for higher amounts of biodiesel, the average  $T_2$  values rise up. The changes were more pronounced for the shorter component (0.4 ms) and also for immersion periods of 30 to 90 days. This suggests an exudation process, where the removing of the filler is facilitated in biodiesel rich oil mixtures. DQ-NMR measurements indicate a progressive reduction in the averaged  $^1\text{H}$ - $^1\text{H}$  residual dipolar coupling for increasing amounts of biodiesel. These experiments also revealed that the amount of defects (not coupled chains) does not change significantly with the addition of biodiesel, suggesting that the reduction in the  $^1\text{H}$ - $^1\text{H}$  residual dipolar coupling is not due to swelling. Taken together, this behavior allowed inferring a decrease in the molecular mass between

cross-links with biodiesel addition, which would also be in accordance with the increase of exudation in the biodiesel rich oil mixtures. Therefore, our results suggest that the main responsible by the deterioration of the mechanical properties commercial VNR when exposed to biodiesel, as compared to diesel, is an exudation effect.

ACKNOWLEDGMENTS: Schlumberger-Doll for the Laplace inversion program; K.Saalwachter and W.Chassé for the fitreg2.0 program for analyzing DQ NMR data, FAPESP, CNPQ, CAPES.

#### MO277: Applying Data Mining Techniques on NMR Data to Predict Carbonate Rocks Permeability

Eduardo Corrêa Gonçalves, Pablo Nascimento da Silva, Alexandre Plastino de Carvalho, \*Rodrigo Bagueira de Vasconcellos Azeredo

Universidade Federal Fluminense

Data Mining can be defined as a process that applies efficient algorithms to discover valuable knowledge hidden in databases. Over the last years, an increasing number of enterprises have been incorporating this technology into their major processes in order to gain competitive advantage. Different kinds of data repositories can be analyzed by data mining algorithms, such as transactional databases, data warehouses, text files, and image data. This work addresses the application of data mining analysis on an  $^1\text{H}$  NMR relaxation dataset of carbonate reservoir rocks with the goal of accurately predict their class of permeability. The petroleum industry uses NMR as a noninvasive and nondestructive tool to study reservoir fluids (gas or liquid hydrocarbons and aqueous solutions) and rock properties, yet offering the advantage of measurements being performed downhole into the well. Among the important NMR deliverables for reservoir evaluation we may cite porosity, pore size distribution, fluids saturations, wettability, and, specially, permeability, which corresponds to the ability a rock has to allow a fluid to pass through it. The dataset studied in this work consists of a matrix  $X_{78,101}$  formed by  $T_2$  distributions (with 100  $T_2$  bins each) and the respective porosities from 78 fully brine saturated core samples ( $3.8 \times 4.5$  cm plugs). We evaluated the effectiveness of five different data mining algorithms (SVM, Multilayer Perceptron, k-NN, Decision Tree, and Naive Bayes) to predict the absolute rock permeability class according to the following ranges: low ( $<1\text{mD}$ ), fair ( $1\text{--}10\text{mD}$ ), good ( $10\text{--}100\text{mD}$ ) and excellent ( $>100\text{mD}$ ). These data mining algorithms were able to significantly outperform two methods widely adopted by the petroleum industry to estimate permeability (Timur-Coates and Kenyon models). The SVM classifier achieved the overall best result (predictive accuracy of 84.6%), followed by Multilayer Perceptron (83.3%) and k-NN (74.4%), against 57.7 % and 55.1% from Timur-Coates and Kenyon models, respectively.

ACKNOWLEDGEMENTS: BG Brasil, ANP (Compromisso com Investimentos em Pesquisa e Desenvolvimento)

#### TU278: Field Cycling NMR Relaxometry of Starch-PLA Blends with Montmorillonite Clay

<sup>2</sup>Luciana M. Brito, <sup>1\*</sup>Pedro José Sebastião, <sup>2</sup>Maria Inês Bruno Tavares

<sup>1</sup>Instituto Superior Técnico - Lisboa, <sup>2</sup>Universidade Federal do Rio de Janeiro

Low-field NMR spectroscopy has been shown to be a useful method to determine proton relaxation times. Its spectroscopy determines the values of proton spin-lattice relaxation time, which has a time constant  $T_1$ , and proton spin-spin relaxation time, with time constant  $T_2$ . Both relaxation times allow evaluating the sample behavior at the molecular level, because they are sensitive to molecular motions at the MHz scale. Hence, changes in molecular mobility are normally detected and can be accompanied by  $T_1$  and  $T_2$  measurements. The main application fields of field-cycling



NMR relaxometry to be considered in the following are: surface related relaxation processes of fluids in porous materials; polymer dynamics, biopolymers and biological tissue, liquid crystals and lipid bilayers.

The field-cycling technique has been applied to melts, solutions and networks of numerous polymer species. The parameters varied in the experiments were the temperature, the molecular weight, the concentration and the cross-link density.

Starch and PLA hybrids were obtained using clay MMT solution and PVA. All nanocomposites were obtained by the solution intercalation method using chloroform and water as a solvent. The frequency dependence of spin lattice relaxation times measured by means of Fast Field Cycling (FFC). NMR techniques were used to study the molecular dynamics of systems. The renormalized Rouse formalism were applied to describe the polymer behavior in the studied samples. The results of the FFC showed that the starch has only one relaxation time  $T_{11}$ , related to amorphous region. PLA hybrids presented two distinct spin-lattice relaxation times,  $T_{11}$  e  $T_{12}$ . The mixture of the two polymers showed two relaxation times. By adding clay or PVA we can observe differences in relaxation time  $T_{12}$ , observing that adding clay and PVA, the effect that each has on the dynamics of the mixture is canceled when added separately at the same time in the polymer blend.

#### TH279: PLSR-based permeability estimations in carbonates: a combined NMR-Resistivity approach

<sup>1,2\*</sup>Edmilson Helton Rios, <sup>1</sup>Irineu Figueredo, <sup>3</sup>Asif Muhammad, <sup>2</sup>Vinicius de França Machado, <sup>4</sup>André Alves de Souza, <sup>3</sup>Rodrigo Bagueira de Vasconcellos Azeredo

<sup>1</sup>National Observatory, <sup>2</sup>Petrobras Research Center, <sup>3</sup>Fluminense Federal University, <sup>4</sup>Schlumberger Brazil Research and Geoenvironment Center

Empirical models used in nuclear magnetic resonance (NMR) well logging capitalize on the correlation between pore-body and pore-throat-size to estimate permeability from relaxation time distributions. However, one of the drawbacks of these models is that they summarize all the information contained in the distributions to just one variable ignoring that each relaxation bin may have a complex and singular relationship with pore-throat-size. Recently we demonstrated that linear partial least square regression (PLSR) applied in relaxation data can deliver more robust and accurate permeability estimations than the classical models which are based on the relaxation time geometric mean or on the free/bound fluid ratio quantity (function of a relaxation cut-off). The NMR PLSR-based permeability models were originally applied to brine saturated sandstones and here we generalized these models for a set of carbonate samples. Although the acquired performance was still better than classical models, a poor prediction capability was found compared with siliciclastics. Most probably this is due to the inherent complexity and heterogeneity of carbonate pore systems that can present low relaxivity which strengthens bulk relaxation signal especially in large pores (vugs). Furthermore diffusion coupling between different pore sites can also contribute to reduce sensitiveness of relaxation times to pore sizes. Once electrical resistivity response, such as formation factor, cementation coefficient and tortuosity, depends on rock permeability properties, we measured and integrated this extra petrophysical information to the previous NMR PLSR-based permeability models. The proposed novel approach delivered an overall best performance, improving a lot the correlation between predicted and measured permeability and reducing expressively the standard error of prediction. These results highlighted the potentiality of combined NMR-resistivity models, which are also applicable in well logging data, to improve permeability estimation in complex carbonate reservoirs.

ACKNOWLEDGEMENTS: CNPQ, TWAS and PETROBRAS

#### NMR Theory

#### MO280: Coherent and squeezed states in an NMR quadrupolar system

<sup>1\*</sup>Ruben Auccaise Estrada, <sup>2</sup>Arthur Gustavo de Araújo Ferreira, <sup>2</sup>Eduardo Ribeiro de Azevêdo, <sup>3</sup>Eduardo Inácio Duzzioni, <sup>2</sup>Tito José Bonagamba, <sup>2</sup>Miled Hassan Youssef Moussa, <sup>4</sup>Roberto Silva Sarthour Júnior, <sup>4</sup>Ivan dos Santos Oliveira, <sup>4</sup>Itzhak Roditi

<sup>1</sup>Empresa Brasileira de Pesquisa Agropecuária, Rio de Janeiro, Brazil., <sup>2</sup>Instituto de Física de São Carlos, Universidade de São Paulo, São Carlos, Brazil., <sup>3</sup>Departamento de Física, Universidade Federal de Santa Catarina, Florianópolis, Brazil., <sup>4</sup>Centro Brasileiro de Pesquisas Físicas, Rio de Janeiro, Brazil.

The concepts of coherent and squeezed states are well established in the context of light and atoms[1]. In quantum mechanics, the importance of coherent state lies in the fact to minimize the Heisenberg's uncertainty principle. Coherent states describe, accordingly to quantum mechanical laws, the collective behavior of particle systems as take place, for example, in a Bose-Einstein condensate[2]. Squeezed states are generated from a coherent state by unitary transformations, in which the Hamiltonian has a nonlinear dependence about second quantization operators, angular momentum operators, or so on. This concept was extended to spin scenario, preserving commutation rules of angular momentum operators, and physical properties as occurs for light and in atoms[3].

The purpose of the present work is to show the possibility of extending this main concept to an NMR quadrupolar system. In order to achieve this objective NMR radiofrequency pulse techniques and deviation density matrix reconstruction procedures were employed. For implementing the proposed NMR experiments, <sup>23</sup>Na and <sup>133</sup>Cs quadrupole nuclei located in different lyotropic liquid crystals samples were used[4,5].

#### References:

- [1] M. O. Scully and M. S. Zubairy, Quantum Optics, Cambridge University Press 1997.
- [2] G. J. Milburn et al., Phys. Rev. A, 55, 4318–4324, (1997).
- [3] M. Kitagawa and M. Ueda, Phys. Rev. A, 47, 5138–5143, (1993).
- [4] R. Auccaise et al., arXiv 1301.2862 (2013).
- [5] A. G. Araújo-Ferreira et al., arXiv 1301.5554 (2013).

ACKNOWLEDGEMENTS: CAPES, CNPq, FAPESP, FAPERJ, Brazilian National Institute of Science and Technology for Quantum Information (INCT-IQ).

#### TU281: Theoretical Calculations of Chemical Shifts ( $\delta$ ) of Two Synthetic Intermediates for Guaianes and nor-Guaianes: A Comparison Between GIAO and CSGT Methods

<sup>1</sup>Christiane Feijó de Castro Porto, <sup>1</sup>Layla Rosário Barbosa, <sup>2</sup>Ygor W. Vieira, <sup>1\*</sup>Valdemar Lacerda Júnior, <sup>2</sup>Kleber Thiago de Oliveira, <sup>1</sup>Reginaldo Bezerra dos Santos, <sup>1</sup>Sandro José Greco, <sup>1</sup>Alvaro Cunha Neto, <sup>2</sup>Timothy John Brocksom, <sup>1</sup>Eustáquio Vinícius Ribeiro de Castro

<sup>1</sup>Federal University of Espírito Santo, <sup>2</sup>Federal University of São Carlos

Fused five- and seven-membered ring systems show peculiar structural features and these building blocks can be considered as advanced intermediates for the synthesis of a large number of biologically active compounds (sesquiterpenes, diterpenes, sesterterpenes).

The wide spectrum of biological activities allied with structural complexity make these compounds interesting targets for the synthetic and NMR studies.

Recently, structural assignments using NMR analysis, and supported by sophisticated theoretical calculations, have become important for providing a good correlation between experimental and theoretical results.

In previous studies, the NMR signals of two synthetical intermediates of guaianes and nor-guaianes were assigned, correlating the experimental and theoretical data.

The results of the theoretical calculations are directly linked to the method chosen. Therefore, this study aims at verifying which method (GIAO or CSGT) provides the best correlation with the experimental data of chemical shifts ( $\delta$ ) of  $^1\text{H}$  and  $^{13}\text{C}$  NMR for two synthetic Intermediates of guaianes and nor-guaianes.

The structures of compounds were drawn with the GaussView4.1 program and a conformational search was performed. The structures were optimized using Gaussian03 program at B3LYP/cc-pVDZ model. The calculations of  $\delta$  were performed at the B3LYP/cc-pVTZ, using GIAO and CSGT methods. The solvent effect (chloroform) was included. The study verified that for  $^{13}\text{C}$  the best results were achieved for calculations without solvent effect.

The structures of compounds were drawn with the GaussView4.1 program and a conformational search was performed. The structures were optimized using Gaussian03 program at B3LYP/cc-pVDZ model. The calculations of  $\delta$  were performed at the B3LYP/cc-pVTZ, using GIAO and CSGT methods. The solvent effect (chloroform) was included.

The study verified that for  $^{13}\text{C}$  the best results were achieved for calculations without solvent effect. For  $^1\text{H}$ , the best results were achieved when solvent effect was taken into account. Taken these values as reference, the study compared the GIAO and CSGT methods.

#### TH282: Transversal Relaxation Time Distribution from Central Nervous System MRI Data: an Ill-Conditioned Inverse Problem Analysis

**Bárbara Darós de Lelis Ferreira**, João Pedro Braga, \*Rita de Cássia Oliveira Sebastião

UFMG - Universidade Federal de Minas Gerais

The central nervous system (CNS), composed essentially of white and gray matter, is responsible to control the body functions and the CNS functioning is very important for person monitoring. The common technique used for this purpose is magnetic resonance imaging, MRI, with physical characteristics weighted images, for example, transversal relaxation time,  $T_2$  - weighted images. These properties are influenced by chemical environment which perturb the resolution and contrast of images, making difficult the tissue differentiation. This work intends to obtain the  $T_2$  distribution from CNS simulated MRI data. The process of obtaining the microscopic property of proton relaxation time distribution,  $T_2$ , from the macroscopic spin echo MRI experiments is a problem classified as an ill-conditioned inverse problem. These problems arise by not satisfying one of the three conditions: existence, uniqueness and continuity of solution. Since the model function is represented by a Fredholm integral equation, these three criteria do not work and robust techniques are required to solve this kind of problem. The Hopfield neural network was chosen to recover  $T_2$  distribution function and it was also analyzed considering errors in the simulated data together with errors in the neurons initial condition. It is believed considering  $T_2$  distribution function instead an average parameter, *i.e.* considering the magnetic field heterogeneities in each voxel, better contrast in the image and consequently improved diagnostic information can be achieved. The neural network approach was numerically stable and robust with noises in the MRI simulated data and deviations

in neurons initial conditions. These obtained results stated this methodology as a promising tool in MRI studies.

ACKNOWLEDGEMENTS: CNPq and FAPEMIG

#### HR-MAS

#### MO283: Analysis of magnetic nanoparticle functionalized with oleic acid by $^1\text{H}$ HR-MAS NMR

**<sup>1</sup>Rodrigo Alexandre Ferreira**, <sup>1</sup>Mábio João Santana, <sup>1</sup>Luiz Henrique Keng, <sup>1</sup>Luiz Henrique Keng Queiroz Júnior, <sup>2</sup>Dhiogo Mendes da Silva, <sup>2</sup>Emília Celma de Oliveira Lima, <sup>1\*</sup>Luciano Morais Lião

<sup>1</sup>*IQ-UFG, Laboratório de RMN*, <sup>2</sup>*IQ-UFG, Laboratório de Materiais*

The analysis of paramagnetic compounds by Nuclear Magnetic Resonance (NMR) is commonly unfeasible due to the extremely broad signals observed. On the other hand this analysis through High Resolution Magic Angle Spinning (HR-MAS) has proven to be an efficient strategy to study this kind of materials. HR-MAS NMR was applied to the study of iron oxide nanoparticles ( $\text{Fe}_2\text{O}_3$ ) functionalized with oleic acid providing spectra with excellent resolution. In these spectra multiplicity and coupling constant of olefin hydrogens could be perfectly observed. The spectra were performed in a Bruker Avance III 500 NMR spectrometer, operating at 11.75 Tesla, equipped with a 4-mm HRMAS probehead. The experiments were carried out in five concentrations ( $6.25 \times 10^{-5}$ ,  $6.25 \times 10^{-4}$ ,  $6.25 \times 10^{-3}$ ,  $9.38 \times 10^{-3}$ , and  $1.25 \times 10^{-2}$  mol.L $^{-1}$ ) and four spinning rates (1, 3, 5 and 8 kHz) to evaluate the importance of these parameters on the intensity and resolution of the NMR signals. The best result was observed at  $9.38 \times 10^{-3}$  mol L $^{-1}$  spinning at 8 kHz. The purification process monitored by  $^1\text{H}$  NMR shows that five cycles of dispersion in *n*-hexane and precipitation with ethanol is more efficient for remove 1-octadecene associated to the nanoparticles than five cycles of extraction with pure ethanol or butanol. We conclude the HR-MAS NMR technique is effective for improving the low resolution  $^1\text{H}$  NMR spectrum of paramagnetic samples, showing better results in comparison with experiments in liquid phase. This improvement comes from the minimization of the effects of viscosity and paramagnetic disturbances through the magic angle spinning, thus increasing both the resolution and the signal/noise ratio.

Acknowledgements: CNPq, CAPES, FINEP and UFG.

#### TU284: High Resolution Magic Angle NMR Profiling of Healthy and Pancreatic Ductal Adenocarcinoma Tissues

**<sup>1\*</sup>Tatiana Onofre de Lira**, <sup>2</sup>Rafael Kemp, <sup>1</sup>Tiago Venancio, <sup>2</sup>José Sebastião dos Santos, <sup>1</sup>Antonio Gilberto Ferreira

<sup>1</sup>*Departamento de Química de São Carlos, Universidade Federal de São Carlos*, <sup>2</sup>*Divisão de Cirurgia Digestiva, Departamento de Cirurgia e Anatomia, Faculdade de Medicina de Ribeirão Preto, Universidade de São Paulo*

Pancreatic cancer represents a challenge on diagnostic and therapy in modern medical science. The complex accessibility due to pancreas localization into abdominal cavity and specific clinical symptoms developing time, lead a diagnostic delay compromising prognosis for patients. Thus, medicine has been seeking alternatives that can help with accuracy, specificity and early diagnosis of pancreatic cancer. Various "omics" methodologies (genomics, transcriptomics and proteomics) have been employed with this purpose.

In this work, a case of study was introduced to evaluate the presence of different metabolites in healthy and pancreatic ductal adenocarcinoma cancer (PDA) tissues with the aim to investigate cellular physiology alterations. All biopsy tissues samples were furnished by Digestive Surgical Division at

Hospital das Clínicas from University of São Paulo (Ribeirão Preto-SP). 1D and 2D HRMAS were carried out on Bruker Avance-III 400 spectrometer equipped with 9.4 T Oxford narrow bore magnet and 4 mm with Z gradient HRMAS probehead. All the experiments were conducted at 6°C and the samples were spun at 4000Hz of spinning speed.

As result several compounds could be characterized among sugars, amino acids, lipids and organic acids through J-Resolved, COSY  $^1\text{H}$ - $^1\text{H}$ , HSQC  $^1\text{H}$ - $^{13}\text{C}$ . Particularly, in PDA tissues L-lactate appeared and  $\beta$ -glucose significantly decreases revealing preference in aerobic glycolysis, compromising the normal cellular energy process. In addition, huge decreases of PUFA, MUFA and phospholipids levels were observed. These alterations affect signaling functions, intra and extracellular substrate transport, osmolises, synthesis and degradation of lipids resulting in a failure of amino acids storage as phospholipids such as glycerophosphocholine. At last, differences on amino acids levels such as choline, taurine, alanine and betaine could also be observed in PDA tissues. As conclusion, this case of study could demonstrate the potential of HRMAS analysis for tissue physiology comprehension and clinical diagnosis.

Acknowledgments: CAPES, FAPESP, CNPQ, CBIP

## Posters Upgraded to Oral Presentation

**TH285: Metallobiology of neurodegenerative diseases: Structural and mechanistic basis behind the acceleration of amyloid protein assembly**

<sup>1,2</sup>M.C. Miotto, <sup>1,2</sup>A.A. Valiente Gabioud, <sup>3</sup>Andres Binolfi, <sup>4</sup>L. Quintanar, <sup>5</sup>Christian Griesinger, <sup>1,2\*</sup>Claudio O. Fernández

<sup>1</sup>*Instituto de Biología Molecular y Celular de Rosario (IBR-CONICET), Universidad Nacional de Rosario,* <sup>2</sup>*Max Planck Laboratory of Structural Biology, Chemistry and Molecular Biophysics of Rosario (MPLPbioR),* <sup>3</sup>*Department of NMR-assisted Structural Biology, In-cell NMR, Leibniz Institute of Molecular Pharmacology,* <sup>4</sup>*Centro de Investigación y de Estudios Avanzados (Cinvestav),* <sup>5</sup>*Department of NMR-based Structural Biology, Max Planck Institute for Biophysical Chemistry*

Alpha-synuclein (AS) aggregation is associated to neurodegeneration in Parkinson's disease (PD). At the same time, alterations in metal ion homeostasis may play a pivotal role in the progression of AS amyloid assembly and the onset of PD. Elucidation of the structural basis directing AS-metal interactions and their effect on AS aggregation constitutes a key step towards understanding the role of metal ions in AS amyloid formation and neurodegeneration. The structural properties of the AS-metal complexes were determined by the combined application of nuclear magnetic resonance (NMR) and electron paramagnetic resonance (EPR), circular dichroism (CD) spectroscopy, and matrix-assisted laser desorption ionization mass spectrometry (MALDI MS). This work provides a comprehensive view of recent advances attained in the metallobiology of AS amyloid diseases. A hierarchy in AS-metal ion interactions has been established: while divalent metal ions interact at a non-specific, low-affinity binding interface at the C-terminus of AS, copper binds with high affinity at the N-terminal region and it is the most effective metal ion in accelerating AS filament assembly.[1-4] The strong link between metal binding specificity and its impact on aggregation is discussed here on a mechanistic basis. A detailed description of the structural features and coordination environments of copper to AS is presented and discussed in the context of oxidative cellular events that might lead to the development of PD. These new findings of the structural and metallobiology of PD are discussed via a comparative analysis with the binding and affinity features of metal ions to the beta amyloid peptide of Alzheimer's disease.[5] Overall, the research findings presented here support the notion that perturbations in the metabolism of metal ions may be a common upstream event in the pathogenesis of neurodegenerative processes.[6]

## References

- [1] Rasia et al, Proc. Natl. Acad. Sci. U S A, 2005, 102, 4294-4299.
- [2] Bertoncini et al, Proc Natl Acad Sci U S A, 2005, 102: 1430-1435.
- [3] Binolfi et al, J. Am. Chem. Soc., 2008, 130, 11801-11812.
- [4] Binolfi et al, J. Am. Chem. Soc., 2011, 133, 194-196.
- [5] Valiente-Gabioud et al, J. Inorg Biochem., 2012, 117:334-341.
- [6] Binolfi et al, Coord. Chem Rev., 2012, 256:2188-2201.

## Acknowledgements

Financial support from ANPCyT, CONICET, Laboratorios Pförtner, Fundación Bunge y Born, Max Planck Society and Alexander von Humboldt Foundation is acknowledged.

**MO286: Structural Basis for the Interaction of Human  $\beta$ -Defensins 1 and 6 and Its Putative Chemokine Receptor CCR2 and Breast Cancer Microvesicles**

**\*Viviane Silva de Paula**, Robson Q. Monteiro, Fabio C. L. Almeida, Ana Paula Valente

*Universidade Federal do Rio de Janeiro*

Human  $\beta$ -defensins (hBD) are believed to function as alarm molecules that stimulate the adaptive immune system when a threat is present. In addition to its antimicrobial activity, defensins present other activities such as chemoattraction of a range of different cell types to the sites of inflammation. We have solved the structure of the human  $\beta$ -defensins 6 (hBD6) by NMR spectroscopy that contains a conserved  $\beta$ -defensin domain followed by an extended C-terminus. We also investigated the interaction of  $\beta$ -defensin 1 and 6 with microvesicles shed by breast cancer cell lines using NMR. Chemical shift mapping of the interaction showed that both defensins interact with microvesicles but in slightly different way, suggesting an inverse correlation with the aggressiveness potential of the cell. Furthermore, molecular docking using restraints derived from the NMR chemical shift data produced a model of the complex between hBD6 and a peptide derived from the extracellular domain of CC chemokine receptor 2 (Nt-CCR2) that reveals a contiguous binding surface on hBD6, which comprises amino acid residues of the  $\alpha$ -helix, loop between  $\beta$ 2- $\beta$ 3 and C-terminal. The microvesicles binding surface partially overlaps with the chemokine receptor interface. These data offer new insights into the structure-function relation of the hBD6-CCR2 interaction and may be helpful for the design of novel anti-cancer agents.

ACKNOWLEDGEMENTS: FAPERJ, CAPES, CNPq

**TU287: NMR Mapping of PCNA Interaction with Translesion Synthesis DNA Polymerase Rev1 Mediated by Rev1-BRCT Domain**

Yulia Pustovalova, Mark W. Maciejewski, **\*Dmitry M. Korzhnev**

*University of Connecticut Health Center*

Rev1 is a Y-family translesion synthesis (TLS) DNA polymerase involved in bypass replication across sites of DNA damage and postreplicational gap filling. In the process of TLS high-fidelity replicative DNA polymerases stalled by DNA damage are replaced by error-prone TLS enzymes responsible for the majority of mutagenesis in eukaryotic cells. The polymerase exchange that gains low-fidelity TLS polymerases an access to DNA is mediated by their interactions with proliferating cell nuclear antigen (PCNA). Rev1 stands alone from other Y-family TLS enzymes since it lacks the consensus PCNA-interacting protein box (PIP-box) motif, instead utilizing other modular domains for PCNA binding. Here we report solution NMR structure of an 11 kDa BRCA1 C-terminus (BRCT) domain from *S. cerevisiae* Rev1, and demonstrate with the use of TROSY NMR methods that Rev1-BRCT domain directly interacts with an 87 kDa PCNA in solution. The domain adopts  $\alpha/\beta$  fold ( $\beta$ 1- $\alpha$ 1- $\beta$ 2- $\beta$ 3- $\alpha$ 2- $\beta$ 4- $\alpha$ 3- $\alpha$ 4) typical for BRCT domain superfamily. PCNA-binding interface of the Rev1-BRCT domain comprises conserved residues of the outer surface of the  $\alpha$ 1 helix,  $\alpha$ 1- $\beta$ 1,  $\beta$ 2- $\beta$ 3 and  $\beta$ 3- $\alpha$ 2 loops. On the other hand, Rev1-BRCT binds to the inter-domain region of PCNA that overlaps with the binding site for the PIP-box motif. Furthermore, Rev1-BRCT domain bound to PCNA can be displaced by increasing amounts of the PIP-box peptide from TLS DNA polymerase pol $\eta$ , suggesting that Rev1-BRCT and pol $\eta$  PIP-box interactions with a given PCNA subunit are mutually exclusive. These results provide structural insights into PCNA recognition by TLS DNA polymerases that help better understand TLS regulation in eukaryotes.

**TH288: Detection of light induced intermediates of photoreceptor membrane proteins by in-situ photo-irradiated solid-state NMR**

<sup>1\*</sup>Akira Naito, <sup>1</sup>Yuya Tomonaga, <sup>1</sup>Tetsuro Hidaka, <sup>1</sup>Hiroki Yomoda, <sup>1</sup>Teruki Makino, <sup>1</sup>Izuru Kawamura, <sup>2</sup>Yuki Sudo, <sup>3</sup>Akimori Wada, <sup>3</sup>Takashi Okitsu, <sup>4</sup>Naoki Kamo

<sup>1</sup>Yokohama National University, <sup>2</sup>Nagoya University, <sup>3</sup>Kobe Pharmaceutical University, <sup>4</sup>Matsuyama University

Photoreceptor retinal proteins usually absorb photon to generate photo-isomerization, and consequently change the structure and dynamics of proteins. To generate retinal isomerization, we have developed the photo-irradiation system equipped to the solid-state NMR spectrometer [1].

Pharaonis phoborhodopsin (ppR or sensory rhodopsin II) is a negative phototaxis receptor of *Natronomonas pharaonis* and forms a 2:2 complex with the cognate transducer (pHtrII), which transmits the photosignal into cytoplasm. Light absorption of ppR initiates *trans-cis* photo-isomerization of the retinal chromophore followed by cyclic chemical reaction consisting of several intermediates (K, L, M and O). The M intermediate is thought to be an active state for signal transduction.

We have successfully trapped and observed the M intermediate by using newly developed photo-irradiated solid-state NMR system. <sup>13</sup>C NMR signal from [20-<sup>13</sup>C] retinal-ppR and ppR/pHtrII revealed that multiple M-intermediates (M1, M2 and M3) with 13-*cis*, 15-*anti* retinal configurations coexisted under the continuously photo-irradiated condition [1]. Further, since the life time of M1 state was much longer than those of the other M states, this M1 state could be distinguished from the other M states and assigned as N intermediate.

SrSRI (Salinibacter ruber sensory rhodopsin I) is a eubacterium rhodopsin and acting multiple function as attractant and repellent phototaxis. In the photocycle of SrSRI, M intermediate functions as attractant and P intermediate by absorbing second blue light as a double photon process shows as repellent. <sup>13</sup>C NMR signal of M intermediate in SrSRI was successfully trapped by illuminating 520 nm light, and the configuration of retinal was revealed to be 13-*cis*, 15-*anti*. P intermediate was trapped by illuminating second 365 nm light as a double photon process.

Photo-intermediate in photo-receptor membrane proteins is now possible to trap by using in-situ photo-irradiated solid-state NMR.

[1] Y. Tomonaga et al. Biophys. J. 2011, 101, L50-L52.

#### MO289: NMR Crystallography, from “Pas de deux” to Spin Choreography. Nanoporous Crystal Structures of Powders : Methods and Hardware.

<sup>1\*</sup>Francis Taulelle, <sup>2</sup>Frank Engelke, <sup>2</sup>Frank Decker, <sup>1</sup>Boris Bouchevreau, <sup>1</sup>Charlotte Matineau

<sup>1</sup>University of Versailles, <sup>2</sup>Bruker-Biopspin GmbH

Inorganic-organic hybrid nanoporous solids exhibits many challenges for their structure determination. They contain a framework, that is usually periodic or at least topologically periodic. However, these materials are hard to form single crystals, most of the time one has to resolve their crystal structure from powder. Additionally, they contain either additional templating agents, of the same nature than the organic linkers, making the activation (emptying the nanopores) of the materials difficult, if not impossible, and by and large, partial. Therefore, at synthesis or later when exchanged with gases or molecules, these exchanged crystals exhibit a periodic network and a non-periodic sub-lattice.

It will be shown on an alumina-phosphate lamellar nanoporous crystal [1] that X-ray diffraction has intrinsic limits for structure computability from a powder and this limit can be overcome by using NMR data. With this combined usage of XRD and NMR the average periodic structure can be determined. At a second level of structure determination NMR can resolve the structural non-periodic part of the crystal.

In a second part, it will be shown that the large number of NMR experiments that must be acquired to solve structures can be accelerated by using multiple channels probe (4 and 5

channels) [2] with multiple receivers acquisition. Multi-decoupling enhances the resolution that reaches about five times higher resolution power than the best synchrotron resolution power.

NMR Crystallography encompasses usage of prior data from XRD as cost function for the average structure determination as well as using new NMR hardware and software [3,4] with additional pulse sequences [5] to solve all the structure features of nanoporous crystals.

With this instrumental developments, one can devise for each structure resolution an original combination of pulse sequence manipulating the resonances between spins in a complex choreography of spins, grouped in a variety of motives that would progressively address all the aspects of the crystal complexity.

#### References

- [1] B. Bouchevreau, C. Martineau, C. Mellot-Draznieks, A. Tuel, M. R. Suchomel, O. Lafon, J. Trébosc, J. P. Amoureux, F.; Taulelle, Chem. Eur. J. in press.
- [2] C. Martineau, F. Engelke, F. Taulelle, J. Magn. Reson. 212 (2011) 311-319.
- [3] E. Kupce, R. Freeman, J. Magn. Reson. 206 (2010) 147-153, J. Magn. Reson. 213 (2011) 1-13.
- [4] E. Kupce, L. E. Kay, J. Biomol. NMR 54 (2012) 1-7.
- [5] Herbst, C.; Riedel, K.; Ihle, Y.; Leppert, J.; Ohlen-schläger, O.; Görlach, M.; Ramachandran, R. MAS solid state NMR of RNAs with multiple receivers. J Biomol NMR 2008, 41, 121–125.
- [6] C. Martineau, F. Engelke, F. Decker, F. Taulelle. J. Magn. Reson. Submitted.
- [7] V. Munch, F. Taulelle, T. Loiseau, G. Férey, A. Cheetham, S. Weigel, G.D. Stucky, Magn. Reson. Chem. 1999, 37, S100-S107.

#### TU290: Optimizing Ionic Liquids for CO<sub>2</sub> Capture: an NMR Approach

<sup>1</sup>Marta Corvo, <sup>1</sup>João Sardinha, <sup>2</sup>Sonia Maria Cabral de Menezes, <sup>3</sup>Jairton Dupont, <sup>3</sup>Graciane Marin, <sup>4</sup>Sandra Einloft, <sup>4</sup>Marcus Seferin, <sup>1</sup>Teresa Casimiro, <sup>1\*</sup>Eurico J. Cabrita

<sup>1</sup>REQUIMTE/CQFB, Dept. Química, Fac. Ciências e Tecnologia, Univ. Nova Lisboa, Portugal, <sup>2</sup>PETROBRAS/CENPES, RJ Brazil, <sup>3</sup>Dept. Química Orgânica, Inst. Química, Univ. Federal do Rio Grande do Sul, Brazil, <sup>4</sup>Fac. Química Pontifícia Univ. Católica Rio Grande do Sul, Brazil

Global warming has prompted the scientific community to look for new strategies for CO<sub>2</sub> capture and storage. Recent studies suggest that ionic liquids (ILs) can be alternative materials for CO<sub>2</sub> capture due to their high selectivity for CO<sub>2</sub> absorption. ILs physical and chemical properties can be enhanced and modified by both their cationic and anionic moieties and this is the reason for their broad range of applications. Considering that ILs properties can be designed to satisfy specific application requirements, the optimization of ILs for CO<sub>2</sub> capture is a matter of great interest.[1-3]

Herein we present a detailed NMR study focused on the evaluation of the interactions between ILs and CO<sub>2</sub>. Through careful structural modifications we were able to identify CO<sub>2</sub>-philic features by the analysis of CO<sub>2</sub> solvation in imidazolium ILs. Our High Pressure NMR (HPNMR) methodology allows a direct measurement of CO<sub>2</sub> solubility in ILs and an in-situ assessment of the relationship of all the species involved in the solvation process - cation/anion/CO<sub>2</sub>. HP-NMR experiments based on NOE and multinuclear diffusion NMR experiments using the PGSE technique combined with molecular dynamics simulations enabled a molecular based interpretation for the solvation mechanism. This systematic

study allowed the identification of promising candidates for CO<sub>2</sub> capture.

[1] X Zhang, X Zhang, H Dong, Z Zhao, S Zhang and Y Huang *Energy Environ. Sci.*, 2012, 5, 6668- 6681.

[2] M Ramdin, TW Loos and TJH Vlucht *Energy Environ. Sci.*, 2012, 5, 8149-8177.

[3] JL Anderson, JK Dixon and JF Brennecke *Acc. Chem. Res.* 2007, 40, 1208-1216.

*The authors would like to thank Petróleo Brasileiro SA – PETROBRAS, Fundação para a Ciência e Tecnologia (FCT) and Ministério da Educação (CQFB Strategic Project PEst-C/EQB/LA0006/2011 and Project PTDC/QUI-QUI/098892/2008) for financial support. The NMR spectrometers are part of the National NMR Network (RNRMN) and are funded by FCT.*

#### TH291: Determining supramolecular organisation of ion channels by solid-state NMR and computational methods

<sup>1</sup>\*Markus Weingarth, <sup>1</sup>Elwin van der Cruisen, <sup>1,2</sup>Alexander Prokofyev, <sup>1</sup>Eline Koers, <sup>1</sup>Alexandre M. J. J. Bonvin, <sup>2</sup>Olaf Pongs, <sup>1</sup>Marc Baldus

<sup>1</sup>Utrecht University, Bijvoet Center for Biomolecular Research, Utrecht, The Netherlands, <sup>2</sup>Saarland University, Faculty of Medicine, Department of Physiology, Homburg, Germany

Protein supramolecular structure invokes the conformation beyond a single protein. While the protein is held together by intramolecular forces comprising strong interactions like covalent bonds, supramolecular structures are often composed of weaker intermolecular contacts. The latter ones confer great diversity and sensitivity to their environment upon these multi-molecular arrangements.

Membrane protein are exposed to a particularly complex habitat which crucially modulates protein structure and functions, however, the molecular basis of such modulations is hitherto poorly understood. What is more, its transient character renders the study of membrane protein supramolecular organization experimentally very challenging.

Using the potassium channels KcsA and KcsA-Kv1.3 as examples, we demonstrate how the combination of solid-state NMR and computational approaches, assisted by electrophysiological measurements, allows dissecting various aspects of membrane protein supramolecular structure, including, *inter alia*, annular and non-annular protein – lipid binding, the influence of structural water or protein – protein interactions in membranes.

#### MO292: Atomistic Descriptions of Protein Dynamics on Multiple Timescales From NMR Chemical Shifts

\*Paul Robustelli

Columbia University

NMR chemical shifts are highly sensitive probes of molecular structure. This work illustrates two approaches for utilizing the structural information contained in chemical shifts to obtain atomistic descriptions of the structural fluctuations of proteins on the ns- $\mu$ s and millisecond timescales.

In the first approach, semi-empirical NMR chemical shift prediction methods are used to evaluate the dynamically averaged values of backbone chemical shifts obtained from unbiased molecular dynamics (MD) simulations of proteins on the ns- $\mu$ s timescale [1]. MD-averaged chemical shift predictions generally improve agreement with experimental values when compared to predictions made from static X-ray structures and a detailed analysis of the structural dynamics and conformational changes associated with the improvements provide support for specific motional processes in proteins. Chemical shifts are sensitive reporters of fluctuations in backbone and side chain torsional angles, aromatic ring positions, and the

geometries of hydrogen bonds. Improved chemical shift predictions result from population-weighted sampling of multiple conformational states and from sampling smaller fluctuations within conformational basins.

In the second approach, chemical shifts and anisotropic restraints obtained from relaxation dispersion experiments are used to determine the structure of a sparsely-populated, on-pathway folding intermediate that folds on the millisecond timescale [2]. CPMG measurements are used to measure backbone chemical shifts, RDCs, and RCSAs of the 2% populated folding intermediate of the A39V/N53P/V55L Fyn SH3 domain and the structure of the intermediate is calculated using a recently developed chemical shift restrained molecular dynamics structure calculation protocol [3]. The structure provides a detailed characterization of the non-native interactions stabilizing an aggregation-prone intermediate under native conditions and insight into how such an intermediate can derail the folding pathway and initiate fibrillation.

These results illustrate that NMR chemical shifts can be used to provide atomistic descriptions of protein motions on multiple timescales.

[1] P Robustelli, KA Stafford, AG Palmer III, *JACS*, 134, 6365-6374 (2012)

[2] P Nuedecker, P Robustelli, A Cavalli, P Walsh, P Lundstrom, A Zarrine-Afsar, S Sharpe, M Vendruscolo, *LE Kay, Science*, 336, 362-366 (2012)

[3] P Robustelli, KJ Kohlhoff, A Cavalli, M Vendruscolo, *Structure*, 18, 1-11 (2010)

#### TU293: High Resolution Para-Hydrogen Induced Polarization (PHIP) in Inhomogeneous Magnetic Fields

<sup>1,2</sup>\*Lisandro Buljubasich, <sup>1,2</sup>Ignacio Prina, <sup>3</sup>María Belén Franzoni, <sup>3</sup>Kerstin Münnemann, <sup>3</sup>Hans Wolfgang Spiess, <sup>1,2</sup>Rodolfo Héctor Acosta

<sup>1</sup>FAMAF – Universidad Nacional de Córdoba, <sup>2</sup>IFEG – CONICET, <sup>3</sup>Max Plank Institut für Polymerforschung

The application of parahydrogen for the generation of hyperpolarization has increased continuously during the last years. When the chemical reaction that deposits the parahydrogen atoms into the target molecule is carried out at the same field as the NMR experiment (PASADENA protocol [1]) an anti-phase signal is obtained, with a separation of the resonance lines of only a few Hz. This imposes a stringent limit to the required homogeneity of the magnetic field in order to avoid signal cancellation. In this work we show that the spectrum of the PHIP signal acquired with a Carr-Purcell-Meiboom-Gil (CPMG) sequence, referred to as *J*-Spectroscopy [2-4], not only presents an enhanced spectral resolution compared to standard the NMR-spectrum, but also avoids partial peak cancellation.

Experimental and numerical simulations concerning the hydrogenation of Hexene with parahydrogen in PASADENA conditions are presented. Acquisition with a digital filter is used to select a desired multiplet, namely a partial *J*-Spectrum acquisition [3]. The performance of the method is tested on a thermally polarized sample, showing that the corresponding partial *J*-Spectra are unaffected by large inhomogeneities in the polarizing magnetic field. Finally, limitations and applicability of the method to obtain either spectral information of the sample or to monitor chemical reactions of very diluted samples will be discussed.

#### References

[1] Russell, C. and Weitekamp, D. P., *J. Am. Chem. Soc.* 109, 5541-5542 (1987)

[2] Allerhand, A, *J. of Chem. Phys.* 44 (1966)

[3] Freeman, R. and Hill H. D. W., *J. Chem. Phys.* 54 (1971)

[4] Vold, R. L. and Vold, R. R., J. Magn. Res. 13, 38-44 (1974)

**TH294: Human Macrophage Lectin (CLEC10A) recognition of monosaccharides related to tumor marker Tn-antigen studied by  $^1\text{H}$  and  $^{19}\text{F}$  NMR.**

<sup>1</sup>\*Francisco Javier Cañada, <sup>1</sup>Anneloes Oude Vrielink, <sup>1,2</sup>Filipa Marcelo, <sup>1</sup>Ana Manzano, <sup>1</sup>Pilar Blasco, <sup>1</sup>Jesús Jiménez-Barbero, <sup>3</sup>Sabine Andre, <sup>3</sup>Hans-Joachim Gabius

<sup>1</sup>Centro de Investigaciones Biológicas, CIB-CSIC Chemical and Physical Biology Department. Ramiro de, <sup>2</sup>REQUIMTE, CQFB, DQ, FCT-UNL, 2829-516 Caparica, Portugal, <sup>3</sup>Institute of Physiological Chemistry, Faculty of Veterinary Medicine, Ludwig-Maximilians-University,

In pathological tissues mucins, heavily O-glycosylated proteins of cellular surfaces, present perturbed glycosylation patterns that are being considered as tumor markers and are attracting a growing interest for the design and developing of antitumor vaccines. Interestingly, some of these carbohydrate related tumor markers are known carbohydrate antigens recognized by C-type (calcium dependent) lectins expressed in cells of the immune system envisioning an important role for these interactions in both innate and adaptive immune responses[1]. Human macrophages express in their surface the so call Human Macrophage Lectin (HML-2, c-type lectin from family 10, CLec10A) that recognizes carbohydrates related to Tn antigen, (O-glycosides of N-Acetyl-Galactosamine with serine or threonine). In the presented work the binding mode of Galactose and Galactosamine and fluorogalactoses monosaccharides will be shown as it has been characterized by means of  $^1\text{H}$  and  $^{19}\text{F}$  NMR studies applying saturation transfer difference (STD) and  $T_2$  perturbation strategies complemented by molecular modeling and docking studies[2]. The importance of all hydroxyl groups of the galactose-derived monosaccharide ligands and the dependency of calcium for carbohydrate recognition by this c-type lectin has been deduced from those studies.

[1] "Sweet preferences of MGL: carbohydrate specificity and function", van Vliet SJ, Saeland E, van Kooyk Y. Trends Immunol. 2008 29(2):83-90.

[2] "Carbohydrate-protein interactions: a 3D view by NMR", Roldós V, Cañada FJ, Jiménez-Barbero J., Chembiochem. 2011 12(7):990-1005.

Acknowledgments: *This work has been carried out with financial aid of the MINECO, Spain (Project number CTQ2009-08536)*

**MO295: High resolution conformational description of Alpha-synuclein inside neurons using mammalian In-cell NMR**

Andres Binolfi, Beata Bekei, Francois-Xavier Theillet, Honor M. Rose, \*Philipp Selenko

Leibniz Institut für Molekulare Pharmakologie (FMP-Berlin)

The intrinsically disordered protein alpha-synuclein (AS) has been involved in the onset of Parkinson's disease (PD) through the conversion of its native monomeric state into beta-sheet rich amyloid fibrils in dopaminergic neurons [1]. So far, most of the structural studies aimed to understand this conversion were conducted on isolated protein samples, under conditions that differ substantially from the crowded *in vivo* environments of intact cells. The question remains whether the features observed for AS *in vitro* correlate with its cellular behaviour. Until recently, there were no means of looking into live cells with high enough resolution to address such important unresolved issues. The development of In-cell NMR spectroscopy techniques changed this notion [2]. Here, we present high-resolution In-cell NMR data on the structural and dynamic properties of AS in five different mammalian cell lines that also include dopaminergic neurons of the *Substantia nigra*. By using a novel approach to efficiently deliver isotopically enriched protein samples into the cytosol of cultured

mammalian cells we were able to record highly reproducible In-cell heteronuclear NMR spectra. Moreover, residue specific dynamic information from relaxation experiments was obtained. By directly comparing these in-cell NMR results with AS data from different *in vitro* environments mimicking intracellular viscosity and macromolecular crowding, we are in the process of delineating physical and biological contributions to AS's different *in vivo* behaviours. Results emerging from this work contribute to the understanding of the native conformations of AS and lays the ground to further perform high-resolution *in situ* investigations under conditions that lead to intracellular aggregation and neurodegeneration as observed in Parkinson's disease.

[1] Lashuel, H. A. et al (2012) Nat. Rev. Neurosci. 14, 38-48

[2] Ito, Y., and Selenko, P. (2010) Curr. Opin. Struct. Biol. 20, 640-648.

**TU296: Defining the Flexible and Fixed Sides of a Protein Channel by EPR**

\*Betty J. Gaffney

Florida State University

Lipoxygenases are ubiquitous proteins that oxidize polyunsaturated chains at different positions, but do so with a highly conserved structural motif of 20 helices. Because mechanistic details have been difficult to obtain by crystallography, EPR spectroscopy approaches have been implemented. Lipoxygenases are naturally paramagnetic due to an iron involved in catalysis. We have made them additionally paramagnetic by adding site-directed spin labels at selected sites. Using several EPR approaches, we have found the entrance to the active site and have examined an  $\alpha$ -helix that must move to allow substrate to enter the deep cavity. The non-heme iron is bound to five protein side chains and water and is located centrally in the structure, 25-35 Å from the surfaces. The polar end of a lipid substrate analog was found on the surface at one end of the internal cavity in a lipoxygenase with pH-gating of substrate access (Biophys J 103: 2134 (2012)). A new bacterial lipoxygenase structure, with a lipid bound also seems to have a helical "lid" protecting a similar entrance to the active site. To examine how lipid binding "opens" the way to catalytic iron, we have scanned the gating helix with spin labels and examined, by power saturation, relaxation of the spin at many helix residues when a lysolipid is present. In comparison to substrate insensitive positions, measured in the reference above, the gating helix distances to iron increase in the presence of substrate analog, indicating a shift of the helix backbone. The EPR spectra of ferric lipoxygenases with and without lipids in the active site also confirm remarkable conservation of active site structure in lipoxygenases from bacteria and eukaryotes.

**TH297: Comparison of Structure of Cyanobacteria and Spinach PSII Studied by PELDOR**

<sup>1</sup>\*Asako Kawamori, <sup>2</sup>Jiang-Ren Shen, <sup>3</sup>Hiroyuki Mino

<sup>1</sup>AGAPE-Kabutoyama Institute of Medicine, <sup>2</sup>Department of Biology, Okayama University, <sup>3</sup>Department of Physics, Nagoya University

The Structure of Cyanobacterium has been determined recently with resolution of 1.9 Å (Umena et al. NATURE (2011) 473 55) We have determined the distances between electron transfer components of PSII in Spinach with PELDOR (Pulsed Electron Double Resonance) with accuracy of 1 Å, 27 Å for  $Y_D$ - $Y_Z$ ,  $Y_D$ - $Mn_4$  cluster by measurement of dipolar interactions between radicals. Usually Electron Spin is not localized and hyperfine constants reflecting spin distribution are observed. Point dipolar approximation is not correct to determine radical distances. In this report we present the distance estimation by taking account of spin distribution. Typically distances of chlorophylls and carotenoid from  $Y_D$  are reported based on spin distributions, which were de-

rived hyperfine constants of each radical, and crystal structure data.

In a cyanobacterium the distances obtained by PELDOR are not coincident with those in spinach but different values are obtained. Several radical pairs produced by light illumination will be compared for cyanobacteria and spinach.

#### MO298: Sensitivity enhancement in solution NMR through dynamic nuclear polarization of encapsulated proteins

<sup>1</sup>Kathleen G. Valentine, <sup>2</sup>Guinevere Mathies, <sup>1</sup>Nathaniel V. Nucci, <sup>1</sup>Igor Dodevski, <sup>1</sup>Sabrina Bédard, <sup>1</sup>Matthew Stetz, <sup>2</sup>Thach V. Can, <sup>2</sup>Robert G. Griffin, <sup>1\*</sup>A. Joshua Wand

<sup>1</sup>University of Pennsylvania, <sup>2</sup>Massachusetts Institute of Technology

Solution NMR has contributed significantly to studies of the structural and dynamic aspects of proteins and the information inherent in NMR phenomena offers much more. Yet, despite tremendous advances in technology, experimental design and analytical strategies, solution NMR remains fundamentally restricted due to its inherent insensitivity. Thus, it seems important to improve the sensitivity of the solution NMR experiment in order to reduce experiment time, lower the absolute quantities of sample required and open a lower concentration regime where proteins of limited solubility can be accessed. With this in mind there has been a revival of dynamic nuclear polarization (DNP). In solution, it is thought that such DNP transfer will occur primarily through the Overhauser effect. The basic strategy is to saturate the electronic transition of a stable free radical and transfer this non-equilibrium polarization to the hydrogen spins of water, which will in turn transfer polarization to the hydrogens of the dissolved macromolecule. Unfortunately, technical aspects of this approach seem to prove fatal to the idea in its current form. The primary reason is that the frequency of the electron transition of suitable radicals lies in the sub-THz spectrum where water absorbs strongly and results in catastrophic heating of the sample. In addition, the residence time of water on the surface of the protein is too short for efficient transfer of polarization. Here we take advantage of the properties of solutions of encapsulated proteins dissolved in low viscosity solvents. Such samples are largely transparent to the subTHz frequencies required and thereby avoid significant heating during saturation of the electronic transition. Nitroxide radical is introduced into the reverse micelle system in three ways: covalently attached to the protein; covalently attached to a surfactant embedded in the reverse micelle shell; and free in the aqueous core. DNP experiments at the X-band EPR frequency have yielded initial enhancements from the nitroxide embedded in the surfactant to the water on the order of -35. In addition, we find that the hydration properties of encapsulated proteins allow for efficient polarization transfer from water to the amide hydrogens in a protein. Thus the merging of the reverse micelle technology with DNP demonstrates the potential to provide a significant increase in the sensitivity of solution NMR spectroscopy of proteins and other bio-macromolecules. Supported by the NIH and the NSF.

#### TU299: DNP Surface Enhanced NMR (SENS): a Tool for Structural Investigation of Supported Catalysis

<sup>1\*</sup>Moreno Lelli, <sup>1</sup>Alexandre Zagdoun, <sup>1</sup>David Gajan, <sup>1</sup>Aaron J. Rossini, <sup>4</sup>Olivier Ouari, <sup>4</sup>Paul Tordo, <sup>3</sup>Chloé Thieuleux, <sup>2</sup>Christophe Copéret, <sup>1</sup>Anne Lesage, <sup>1</sup>Lyndon Emsley

<sup>1</sup>Centre de RMN à Très Hauts Champs, Université de Lyon (CNRS/ENS Lyon/UCB Lyon 1), <sup>2</sup>Department of Chemistry, ETH Zürich, Switzerland, <sup>3</sup>Institut de Chimie de Lyon, Université de Lyon (CNRS-Université Lyon 1-ESCE Lyon), <sup>4</sup>Aix-Marseille Université, CNRS, Institut de Chimie Radicale (ICR), Marseille

In recent years, our group has demonstrated that high-field DNP in MAS solid-state NMR at low temperature (100 K) can be applied to investigate the structure of surfaces of materials. In this approach, which we dubbed DNP surface enhanced NMR spectroscopy (SENS), the polarizing agent (for example an organic di-nitroxide radicals such as bCTbK, etc.) is introduced into the sample by incipient wetting impregnation with a radical solution. Upon irradiation with microwaves the DNP effect enhances polarization of the <sup>1</sup>H nuclei of the solvent and the surface, and this enhanced <sup>1</sup>H polarization can then be transferred to the surface hetero-nuclei (<sup>13</sup>C, <sup>15</sup>N, <sup>29</sup>Si or <sup>27</sup>Al) by cross-polarization (CP).[1,2] The SENS method can be extended to a large set of solvents, thus extending the nature of the accessible systems to include many modern materials, such as nanoparticulate silica, metal-organic-frameworks (MOF), catalyst precursors or organometallic systems,... Here we will present the most recent developments in DNP SENS, and in particular show how this allows the acquisition of multidimensional <sup>1</sup>H-<sup>29</sup>Si and/or <sup>1</sup>H-<sup>13</sup>C correlation spectra of active surface species. The multi-dimensional spectra yield detailed three-dimensional structural information of tethered surface species.[3] The structural information obtained by DNP SENS opens the way to a more rational design of supported catalysis.

[1] A. Lesage, M. Lelli, D. Gajan, M. A. Caporini, V. Vitzthum, P. Mieville, J. Alauzun, A. Roussey, C. Thieuleux, A. Mehdi, G. Bodenhausen, C. Copéret, L. Emsley, J. Am. Chem. Soc. 2010, 132, 15459-15461;

[2] M. Lelli, D. Gajan, A. Lesage, M. A. Caporini, V. Vitzthum, P. Mieville, F. Heroguel, F. Rascon, A. Roussey, C. Thieuleux, M. Boualleg, L. Veyre, G. Bodenhausen, C. Copéret, L. Emsley, J. Am. Chem. Soc. 2011, 133, 2104-2107;

[3] M. Samantaray, J. Alauzun, D. Gajan, S. Kavita, A. Mehdi, L. Veyre, M. Lelli, A. Lesage, L. Emsley, C. Copéret, C. Thieuleux J. Am. Chem. Soc. 2013 in press

#### TH300: In situ MR: Pore condensation at elevated temperature and pressure

<sup>1\*</sup>Matthew P. Renshaw, <sup>1</sup>S. Tegan Roberts, <sup>2</sup>Belinda S. Akpa, <sup>1</sup>Mick D. Mantle, <sup>1</sup>Andrew J. Sederman, <sup>1</sup>Lynn F. Gladden

<sup>1</sup>University of Cambridge, <sup>2</sup>University of Illinois at Chicago

Magnetic Resonance (MR) methods, being non-invasive and non-destructive, are ideal for probing heterogeneous catalytic systems under realistic operating conditions [1,2]. However, until recently, the processes studied using MR have been performed under mild conditions (typically < 5 atm and < 200 °C). We have recently commissioned a fixed-bed reactor, compatible with operation inside a superconducting magnet, which can be operated up to a temperature of 350 °C and a pressure of 31 atm while simultaneously performing MR experiments.

To demonstrate its capability we have studied the effect of confinement in mesopores on the vapour-liquid phase change of cyclohexane to elucidate pore filling and emptying mechanisms. The understanding of confinement effects, particularly at realistic reaction conditions, is an important consideration in heterogeneous catalysis.

Isothermal (150 °C and 188 °C) vapour-liquid phase change cycles of cyclohexane in a bed of titania pellets were conducted. <sup>1</sup>H spin density images reveal changes in pore saturation of the pellets as the phase boundary is crossed. Pore confinement effects are exhibited, as liquid remains within the pores after bulk liquid has vaporised. Pore saturation during the evaporation-condensation cycles exhibits hysteresis, demonstrating the differences between the filling and emptying mechanisms in these systems. The data are analogous to N<sub>2</sub> adsorption isotherms that characterise pore diameter



and surface area, but are conducted for a relevant species at realistic conditions.

Data from these MR images, in conjunction with  $^1\text{H}$   $T_1$  and  $T_2$  relaxation time measurements and pulsed field gradient diffusion measurements, are used to assess the mechanism of pore filling and emptying in addition to revealing information about the formation of liquid films.

The use of the in situ MR reactor is currently being extended to study heterogeneous catalytic reactions.

[1] Gladden et al., *Catalysis Today*, 155 (2010) 157-163.

[2] Lysova and Koptug, *Chemical Society Reviews*, 39 (2010) 4585-4601.

#### **MO301: Pore Sizes Distribution of Unconsolidated Geomaterials**

<sup>2,3\*</sup>Marcos Montoro, <sup>1,3</sup>Lucas C. Cerioni, <sup>3</sup>Daniel José Pusiol

<sup>1</sup>*Spinlock SRL*, <sup>2</sup>*Universidad Nacional de Córdoba*, <sup>3</sup>*CONICET*

Pore size and pore sizes distribution of soils and rocks control

many hydraulic and mechanical properties of natural geomaterials such as hydraulic conductivity and shear resistance. Pore size and sizes distribution of rocks depend on their mineral composition and the geological processes involved in their formation, while for unconsolidated materials such as soils, depend on grain sizes, grain sizes distribution and overburden pressure. The aim of this project is to correlate transversal relaxation time ( $T_2$ ) with grain size of loose sandy soils in systems of single and double porosity. In this research we applied Time Domain Nuclear Magnetic Resonance (TD-NMR) to measure the magnetization decaying curve of samples composed of selected sizes of sand grains, poor graded sands, silty sands, silt and clay. This was performed by a CPMG pulse sequence using a low field (12 MHz) spectrometer (SLK-100). Obtained results show that transversal relaxation time and its distribution are strongly correlated with grain sizes and their distribution. These results allow improving the knowledge about pore sizes distribution when needed for modeling porous materials using numerical techniques such as pore networks.

ACKNOWLEDGEMENTS: CONICET, SECyT-UNC, FONTAR, FONCYT

## Index of Authors

- Aakagi**, Kenichi TU203  
**Abboud**, Khalil A. TU254  
**Abiko**, Layara A. MO046  
**Abreu**, Valéria TU194  
**Abriata**, Luciano A. TU008, OP075, TH216, MO217  
**Achilles**, Anja OP057  
**Ackerbauer**, Daniela TU047  
**Acosta**, Rodolfo Héctor UP146, TH207, TU239, TH267, TU293  
**Adesso**, Gerardo TU146  
**Afonso**, Luciana Caminha TH180, MO208  
**Agarval**, Vipin UP135  
**Aguiar**, Daniel Lima Marques de TH084, TH090  
**Aguiar**, Paula Fernandes de MO115  
**Aguiar**, Ramon Pinheiro TH033  
**Ahn**, Jinwoo TU038  
**Ahn**, Sangdoo TU212  
**Ahola**, Susanna UP098  
**Akoury**, Elias TU005  
**Akpa**, Belinda S. UP154, TH300  
**Al-Hashimi**, Hashim M. PL045  
**Alajarín**, Mateo MO127  
**Albernaz**, Fabiana Pestana MO025  
**Alborghetti**, Marcos Rodrigo TU197  
**Alcantara**, Glaucia Braz MO097, TU188, TH189  
**Alencastro**, Ricardo Bicca de TH084, TH090  
**Alkorta**, Ibon MO064  
**Allix**, Mathieu OP038  
**Almeida**, Fabio C. L. MO004, TH015, UP162, MO025, TU026, TH030, TH033, MO034, MO037, TU041, TH042, TU047, MO049, TH108, TH114, OP005, MO190, TU194, MO286  
**Almeida**, Queli Aparecida Rodrigues de TU155  
**Almeida**, Vinícius Mansur Dose Lage de TU266  
**Alphonse**, Sébastien TH096  
**Alvares**, Rohan TH135  
**Alvarez-Martinez**, Cristina OP148  
**Alves**, Nathalia S. TH048  
**Amata**, Irene TU017, UP054  
**Ambrosio**, Andre Luis Berteli TH054, TU056  
**Amit**, Eran MO073  
**Amo**, Juan-Miguel Lopez del OP070  
**Amonette**, James E. TU245  
**Amorim**, Gisele Cardoso de TH033, MO034  
**Amorim**, Mauro B. de TU176  
**Amoureux**, Jean Paul UP036, MO139, TU140, TH141, TU143  
**Anderson**, Jason OP124  
**Andrade**, Fabiana Diuk TU092  
**Andrade**, Flavia Guedes TH063  
**Andrade**, R. H. S. MO187  
**Andre**, Sabine UP017, TH294  
**Andreetta**, Mariane Barsi MO244  
**Andrews**, A. Ballard MO109  
**André**, Sabine MO001  
**Angeli**, Renata MO190  
**Angelis**, Martin Hrabě de TH180, MO208  
**Anglister**, Jacob TU002  
**AnoBom**, Cristiane D. TH048  
**Antzutkin**, Oleg N. OP073  
**Apparecido**, Rafael do Prado TU188  
**Arachchige**, Rajith J. OP134  
**Arake**, Luisa Mayumi Ribeiro TU032  
**Araki**, Koiti MO211  
**Arantes**, Guilherme Menegon TH039  
**Araújo**, Ana P.U. OP025  
**Araújo**, Renata Mendonça TU173  
**Arcos**, Daniel MO151  
**Ardavan**, A. TH222, MO223  
**Ardá**, Ana MO001  
**Aronson**, Matthew T. OP009  
**Arshava**, Boris TU002  
**Arthanari**, Haribabu TH036  
**Arthur**, Michel UP126  
**Asam**, Claudia TH108  
**Asami**, Sam MO139, OP070  
**Ascona**, Christian Rivera TH087  
**Ashbrook**, Sharon E. OP035  
**Assunção**, Bruno A. de TH024  
**Atala**, Daniel I.P. TU164  
**Atanasov**, Mihail OP020  
**Atchison**, David A. MO205  
**Atkinson**, Kevin D. OP159  
**Auccaise**, Ruben TU146  
**Auger**, Michele TU062  
**Azambuja**, Ana Paula TU116  
**Azeredo**, Rodrigo Bagueira de Vasconcellos MO247, TU263, MO277, TH279  
**Azeredo**, Sirlene O. F. TH153, MO154  
**Azevedo**, Eduardo N. de UP063  
**Azevedo**, Mariangela B. M. de MO076  
**Azevêdo**, Eduardo Ribeiro de TU092, TH093, OP057, TU146, TH276, MO280  
**Baaden**, Marc UP027  
**Baaske**, Philipp TU023  
**Bacchi**, Pedro TU191, TH195  
**Bagryanskaya**, Elena TU218, TH219, OP019  
**Bajaj**, Vikram S. OP068  
**Baker**, David OP133  
**Balbach**, Jochen MO199  
**Balcom**, Bruce J. OP097  
**Baldus**, Marc UP136, TU119, TH291  
**Balieiro**, Fabiano de Carvalho MO265, MO274  
**Ballesteros**, Rafael R. TU242  
**Baltisberger**, Jay H. OP034  
**Ban**, David OP086  
**Banères**, Jean-Louis UP027  
**Barberis**, Gaston TH225  
**Barbero**, Jesús Jiménez TH009  
**Barbet-Massin**, Emeline TH060  
**Barbosa**, Layla Rosário TU281  
**Barbosa**, Lúcio Leonel TU266, MO268, TU269  
**Barcellos Jr.**, Ewerton de MO085  
**Barreto**, Jéssica Resende TU035  
**Barros Jr.**, Wilson UP063  
**Barros**, Carlos Jonnatan Pimentel TH192, MO193  
**Barsottini**, Mario Ramos de Oliveira TU056  
**Basso**, Luis Guilherme M. TH051  
**Bastow**, T. TU068  
**Batista**, Aline TH108  
**Baud**, Matthias TU152  
**Bax**, Ad OP132  
**Bazin**, Laurent Terradot Alexandre OP137  
**Bechinger**, Burkhard TU050  
**Becker**, Stefan OP086, MO019, TU074, TH102, OP133  
**Beedle**, Christopher C. TU254  
**Bekei**, Beata UP089, MO295  
**Benavente**, E. MO229, TU230  
**Benedetti**, Celso E. TU053, TH054  
**Benoit**, Matthieu MO100  
**Bento**, Edson de Souza TH081, TH168  
**Bermel**, Wolfgang OP118  
**Bermudez**, Kalah TH018  
**Bernadó**, Pau TU017  
**Bernal**, Andrés TH165  
**Bernard**, Guy MO067  
**Bernardinelli**, Oigres Daniel TU092, TH093  
**Bernardo**, Camilla do Nascimento MO115  
**Berná**, José MO127  
**Berry**, Andrew J. OP035

- Berry**, Robert E. UP076  
**Berto**, Maria I. TU164  
**Bertoncini**, C. W. MO013  
**Beszonova**, Irina TH015  
**Beuerman**, Roger W. TH162  
**Bhuniya**, Sankarprasad TH213  
**Bianconi**, M. Lucia TH048  
**Bickelhaupt**, F. M. MO052  
**Bieschke**, Jan OP070  
**Billeter**, Martin MO004  
**Binolfi**, Andres UP072, UP089, TH285, MO295  
**Bjerring**, Morten OP073, UP059, TH201  
**Blackburn**, Mandy E. OP074  
**Blasco**, Pilar MO001, UP017, TH294  
**Bloch Jr.**, Carlos TU032  
**Bloise**, Antonio C. TU191, TH195  
**Blundell**, S. J. MO223  
**Blümich**, Bernhard TH207, OP155, MO259, TU260, MO262  
**Bode**, Bela OP127  
**Bodenhausen**, Geoffrey OP108, UP125, UP036  
**Boelens**, Rolf UP031  
**Boisbouvier**, Jerome MO100  
**Bok**, Robert OP040  
**Bolton**, David OP127  
**Bonagamba**, Tito J. PL066  
**Bonagamba**, Tito José TH087, TU146, TH147, TH210, TH237, TH243, MO244, TU248, MO265, MO274, MO280  
**Bonfim**, Rodrigo de Paiva Floro TH117  
**Bonvin**, Alexandre M. J. J. UP130, UP136, TU119, TH291  
**Boralle**, Nivaldo MO175  
**Borré**, Leandro B. MO091, MO094  
**Bouchard**, Louis OP067  
**Bouchevreau**, Boris UP012, MO289  
**Bougault**, Catherine UP126  
**Boyd**, Austin TH210, MO247, TU248  
**Braga**, Carolina Alvares TH063  
**Braga**, João Pedro TH282  
**Braga**, Vanessa L. Azevedo MO025  
**Bragatto**, Juliano TH093  
**Braide**, Otonye TU227  
**Braz Filho**, Raimundo TU173  
**Braz**, Daniel César TH087  
**Breiteneder**, Heimo TU047  
**Brey**, William W.  
**Brindle**, Kevin M. TH099, OP065  
**Brito**, Luciana M. TU278  
**Brito**, Rui M. TU023  
**Britt**, R. David OP008  
**Britto**, Manuel OP074  
**Brocksom**, Timothy John TU281  
**Brouwer**, Darren H. OP009  
**Brown**, Leonid MO118  
**Brown**, Steven P. MO079, OP056  
**Bruix**, Marta MO001, TH009  
**Bruschweiler-Li**, Lei MO046, OP129  
**Brutscher**, Bernhard OP055  
**Brüschweiler**, Rafael MO046, OP129  
**Bublin**, Merima TU047  
**Budker**, Dmitry OP010  
**Buldain**, Graciela Yolanda TU158  
**Buljubasich**, Lisandro TH066, UP146, TU293  
**Bunce**, Chris OP091, TU182  
**Burdisso**, Paula MO100  
**Buriol**, Lilian MO127  
**Burz**, David TH198, UP053  
**Bustos**, Silvina O. TU191, TH195  
**Byeon**, Chang-Hyeock TU038  
**Byeon**, In-Ja L. TU038  
**Bédard**, Sabrina UP111, MO298  
**Böckmann**, Anja UP135, OP137  
**Cabeça**, Luis Fernando OP153, TH270, TH273  
**Cabrita**, Eurico J. UP121, TU290  
**Cadars**, Sylvian OP009, OP038  
**Cai**, Shuhui TU137, TH138, MO202  
**Caldarelli**, Stefano OP161, TU242  
**Calderon Filho**, Cesar José TH225  
**Calvini**, Ítalo A. OP025  
**Camargo Jr.**, Sérgio S. MO094  
**Camargo**, A. S. S. de MO082  
**Cambui**, Erika Verena Figueiredo TH168  
**Camilloni**, Carlo UP131, TH129, MO130  
**Campos**, E. C. Menchaca TH255  
**Can**, Thach V. UP111, MO298  
**Canales**, Ángeles TH009  
**Canalis**, M.S. Blanco TH267  
**Canaviri**, Marcelo Torrez TH249  
**Candido**, Anne Caroline MO034  
**Canevarolo**, Rafael Renatino TU116, MO196, TH204  
**Cantrelle**, François-Xavier UP016  
**Caporini**, Marc UP036  
**Cappellaro**, Paola OP143  
**Cara**, Andrés Espinoza MO217  
**Carlier**, Marie-France UP016  
**Carlos**, Eduardo Fermino TU188, TH189  
**Carneiro**, Giovanna F. TH246, MO247  
**Carnevale**, Diego UP036  
**Carosio**, Maria Gabriela Aparecida TU272, TH273  
**Carpinella**, M. TH267  
**Carrara**, Caroline TU242  
**Carrigan**, John TU182  
**Carvalho**, Alexandre Plastino de MO277  
**Carvalho**, André de Souza OP153, TH261, TH273  
**Carvalho**, Erika Martins de MO088, TU089, TU110  
**Carvalho**, João Teles de TH087  
**Carvalho**, Mário Geraldo de TH159, MO160  
**Casano**, Gilles TH234  
**Casanova**, Federico TH207  
**Case**, David A. TU020  
**Casimiro**, María MO103  
**Casimiro**, Teresa UP121, TU290  
**Cassus**, Eduardo P. MO256  
**Castanheira**, Pedro TU023  
**Castañeda-Valencia**, Gloria MO169  
**Castellen**, Patricia MO055  
**Castilla**, Aracelys López MO031  
**Castillo**, Andrés M. TH165  
**Castro**, Cecilia MO184  
**Castro**, Eustáquio Vinícius Ribeiro de TU125, TU266, MO268, TU269, TU281  
**Catoire**, Laurent UP027  
**Cavalcante**, Gustavo Prione MO172  
**Cavalli**, Andrea UP131, MO130  
**Cavini**, Ítalo Augusto TH111  
**Cañada**, Francisco Javier MO001, UP017, TH294  
**Cerioni**, Lucas C. UP080, OP152, MO301  
**Cerioni**, Lucas Matías MO148, MO241, TH258  
**Cervantes**, Hernán Joel MO211  
**Chammas**, Roger TU191, TH195  
**Chang**, Kiyuk MO214  
**Chapman**, Bogdan E. TH144  
**Charlton**, Lisa M. TU038  
**Chary**, K. V. R. TU200  
**Chattah**, Ana Karina TH066, TH069, TU158, TH252  
**Chavarín**, Jorge Uruchurtu TH255  
**Chen**, Chunying MO178  
**Chen**, Dan UP007  
**Chen**, Der-Yow OP043  
**Chen**, Hao TU137  
**Chen**, Hsueh-Ying OP109  
**Chen**, Qun MO139, TU140  
**Chen**, Shizhen MO133  
**Chen**, Zhong TU137, TH138, MO202

- Cheong**, Cheajoon TU212  
**Chiario**, S.S.X. MO091  
**Chikayama**, Eisuke MO181  
**Chimon-Peszek**, Sandra TH018  
**Chinelatto Júnior**, L. S. MO091  
**Chmelka**, Bradley F. OP009  
**Cho**, Janggeun TU212  
**Cho**, Jee-Hyun TU212  
**Cho**, Min-Kyu TH102  
**Christou**, George TU254  
**Cilli**, Eduardo Maffud TH051  
**Cilli**, Eduardo Maffut TU113  
**Cipriano**, Daniel F. TU086  
**Ciulli**, Alessio TU023, TU152  
**Claramunt**, Rosa M. MO064  
**Clausen**, Katherine TH018  
**Claytor**, Kevin UP041  
**Clendinen**, Chaevien  
**Cobas**, Carlos TH132  
**Cobo**, Marcio F. OP057  
**Cobra**, Paulo Falco MO112, OP153  
**Coelho**, Felipe B. TU209  
**Coen**, Donald M. TH036  
**Coey**, Aaron UP116  
**Cohen**, Tal TU275  
**Cole**, Jonathan TU149  
**Coletta Filho**, Helvecio Della TH186  
**Colnago**, Luiz Alberto TU077, MO106, MO112, TU134, OP153, TH261, TH264, TH270, MO271, TU272, TH273  
**Comellas**, Gemma OP117  
**Conesa**, Pablo TH183  
**Conibear**, Anne OP160  
**Conradi**, Mark OP102  
**Constable**, R. Todd OP061  
**Copéret**, Christophe TH234, UP110, TU299  
**Cordeiro**, Tiago OP029  
**Cordeiro**, Yraima MO007, TH126  
**Correa**, Daniel H A TH063  
**Correa**, Maria Elvira Pizzigatti TU197  
**Correia**, Vinícius Soares da Paixão TU131  
**Corvo**, Marta UP121, TU290  
**Costa-Filho**, Antonio José OP025, TH051, TU113, TH231  
**Costa**, João M. MO256  
**Coutinho**, Bernardo TH246  
**Craik**, David J OP160  
**Cruickshank**, Paul OP127  
**Cruijssen**, Elwin A. W. van der TU119  
**Cruijssen**, Elwin van der UP136, TH291  
**Crusca Júnior**, Edson TH051  
**Crusca**, Edson TU113, TH231  
**Cruz**, Joao Felipe Alves da TU134  
**Cunha**, Alfredo G. MO085  
**Cvitanic**, Tonci MO073  
**D'Andréa**, Everton Dias TU029  
**D'Eurydice**, Marcel N. TH237, TU248  
**D'Eurydice**, Marcel Nogueira MO244  
**Danieli**, Ernesto TH207, TU260, MO262  
**Daraku**, T. MO052  
**Darbello**, Daniel de Menezes TH057, MO058  
**Dasari**, Muralidhar OP070  
**Davalos**, Angie Lizeth MO043  
**Davis**, Ryan M. UP041  
**Decker**, Frank UP012, MO289  
**Demers**, Jean-Philippe OP133  
**Deng**, Feng MO070, TU140, TH141  
**Denkert**, Carsten MO184  
**Dente**, Axel D. TH066  
**Denysenkov**, Vasyl PL003  
**Deschamps**, Michael OP038  
**Deshpande**, Rashmi UP104  
**Déville**, Célia UP016  
**Dias**, David M. TU023, TU152  
**Dias**, Sandra Martha Gomes TU056, TH204  
**Didry**, Dominique UP016  
**Diehl**, Annette TH063  
**Diercks**, Tammo OP114  
**Dietz**, Carsten OP077  
**Ding**, Fa-Xiang TU002  
**Diuk**, Fabiana TH276  
**Dlubac**, Katherine OP096  
**Doan**, Peter E. TU233  
**Dodd**, Stephen OP043  
**Dodevski**, Igor UP111, MO298  
**Dolde**, Florian OP157  
**Domingues**, Mariane N. TU053, TH054  
**Donoso**, J. P. MO229, TU230  
**Donovan**, Kevin J. MO016  
**Doty**, F David MO151  
**Driehuys**, Bastiaan OP039  
**Drozdyuk**, Irina OP019  
**Duckett**, Simon B OP159  
**Dugar**, Sneha TH072  
**Dupont**, Jairton UP121, TU290  
**Duzzioni**, Eduardo Inácio MO280  
**Dyszy**, Fábio H. OP025  
**Eckert**, Hellmut UP104, MO082, UP037  
**Edison**, Arthur S.  
**Edwards**, John C. MO109, TU275  
**Eiden**, Michael MO184  
**Einloft**, Sandra UP121, TU290  
**Elguero**, José MO064  
**Ellis**, Paul MO151  
**Emami**, Sanaz MO118  
**Emmerich**, Francisco G. MO085  
**Emsley**, Lyndon TH060, TH234, UP110, TU299  
**Emwas**, Abdul-Hamid TH078  
**Endeward**, Burkhard PL003  
**Engelke**, Frank UP012, MO289  
**Engelsberg**, Mario UP063  
**Entzminger**, George MO151  
**Eon**, Jean Guillaume TH117  
**Erlach**, Markus Beck TH045  
**Ernst**, Matthias UP135  
**Escobar**, Melissa Quintero TH204  
**Espindola**, Ana Paula TH186  
**Espinoza-Cara**, Andrés OP075  
**Estrada**, Ruben Aucaise TH147, MO265, MO274, MO280  
**Falson**, Pierre OP137  
**Fam**, Maged OP078  
**Fan**, Ying MO118  
**Fanucci**, Gail E OP074, TU227  
**Farah**, Chuck OP148  
**Farah**, Chuck S. MO043  
**Faria**, Gregório C. OP057  
**Faria**, Roberto de Barros TU155  
**Faria**, Tiago TU023  
**Farias**, Fábio L. L. MO256  
**Fattori**, Juliana MO076  
**Favaro**, Denize C. MO046, OP148  
**Favaro**, Denize Cristina MO043  
**Fayon**, Franck OP038  
**Fedin**, Matvey TU218, TH219, OP019  
**Fekete**, Marianna OP159  
**Felli**, Isabella C. OP051  
**Feng**, Yesu UP041  
**Fenwick**, R. Bryn OP086  
**Ferella**, Lucio TU020  
**Ferguson**, Stuart J. OP004  
**Fernandes**, R. G. MO082  
**Fernandes**, Tácio Vinício Amorim TH051  
**Fernández**, Claudio O. OP052, MO013, UP072, TH285  
**Fernández**, Ignacio MO103  
**Ferreira Júnior**, Eli da Silva TU098  
**Ferreira**, Antonio Gilberto MO136, OP092, TU284  
**Ferreira**, Arthur Gustavo de Araujo MO244  
**Ferreira**, Arthur Gustavo de Araújo TH147, MO280  
**Ferreira**, Bárbara Darós de Lelis TH282  
**Ferreira**, Daniel R. TU245  
**Ferreira**, Fatima TU047, TH108

- Ferreira, Marcos Davi** MO271
- Ferreira, Rafaela Oliveira** TH159
- Ferreira, Rodrigo Alexandre** MO283
- Ferreira, Vinicius Sousa** TU080, TU104
- Ferretti, Giulia D. S.** TH126
- Ferrone, Marcus** OP040
- Feuerstein, Sophie** OP055
- Fiat, Daniel** TU206, UP141
- Fidalgo, Tatiana Kelly S.** TU026, MO190, TU194
- Fiehn, Oliver** MO184
- Figueira, Elza C.S.** TU257
- Figueiredo, Luis de** MO163
- Figueredo, Irineu** MO250, TH279
- Figueroa-Villar, José Daniel** OP015, TH153, MO154, TU170
- Filho, Elenilson G. A.** TH276
- Filippov, Andrei** OP073
- Fillion, Matthieu** TU062
- Fink, Brian** UP158
- Fink, Uwe** OP070
- Finkelstein-Shapiro, Daniel** TH228
- Firmino, Paulo Renato Alves** TH192, MO193
- Flores, Douglas William Menezes** MO271
- Florian, Pierre** OP038
- Fogeron, Marie-Laure** UP135
- Foguel, Débora** MO007, TH063
- Foley, David A.** TU275
- Fontes, Adriana Da Silva** TU221
- Fontes, Sérgio Rodrigues** TH243
- Forato, Lucimara Aparecida** TU077
- Forse, Alex** OP101
- Fortulan, Carlos Alberto** TH243
- Foster, Mark P.** MO010, TU128
- Fraga, Luciana Elena M. S.** TH030
- Franzoni, María Belén** UP146, TU293
- França, José Adonias Alves de** MO142, MO166
- Fredriksson, Jonas** MO004
- Freed, Jack H.** OP128
- Freeman, Ray** MO016, OP119
- Freire, Guilherme M.** TU209
- Freitas-Fernandes, Liana B.** TU026, MO190, TU194
- Freitas, Deisy dos Santos** TH189
- Freitas, Jair C. C.** MO085, TU086
- Freitas, Monica Santos de** TH063
- Fries, Pascal H.** UP084
- Fritzingier, Bernd** MO238
- Fritzsching, Keith J.** OP124
- Frizzo, Clarissa Piccinin** MO127
- Frost, Stefan** TH012
- Frydman, Lucio** MO016, OP122, PL001
- Fu, Riqiang** TH072
- Fuchs, Helmut** TH180, MO208
- Funk, Alexander M.** UP084
- Fursova, Elena** TH219
- Furtado, Joana** TU023
- Furuita, K.** MO052
- Fändrich, Marcus** OP070
- G.N, Manjunatha Reddy** TU242
- Gabioud, A.A. Valiente** UP072, TH285
- Gabius, Hans-Joachim** MO001, UP017, TH294
- Gabrienko, Anton** TU218
- Gaffney, Betty J.** UP026, TU296
- Gailus-Durner, Valérie** TH180, MO208
- Gajan, David** UP110, TU299
- Galdeano, Carles** TU152
- Galiana, Gigi** OP061
- Gambarra-Neto, Francisco F.** TH105, TU107
- Gao, Min** OP134
- Garaga, Mounesha N.** OP009
- Garbacz, Piotr** MO067
- García-Mayoral, María Flor** TH009
- García, Jesús** OP029
- García, Julia Inés** TH258
- Gardiennet, Carole** OP137
- Garnero, Claudia** TH069
- Garratt, Richard Charles** TH111, TH231
- Garwood, Michael** OP139
- Gataullin, Eduard M.** TU224, UP022
- Gauvin, Régis** TH141
- Gava, Lisandra Marques** TH063
- Gehring, Kalle** MO022
- Geldereren, Peter van** OP142
- Gelves, Luis G. V.** MO094
- Gennis, Robert B.** OP117
- Gentner, M.** OP033
- George, Julia M.** OP117
- Geraldes, Carlos F. G. C.** TU023, TU152
- Geraldes, Carlos F.G.C.** OP062
- Ghose, Ranajeet** TH096
- Giachetti, Andrea** TU020
- Giammatteo, Paul J.** TU275
- Gil, Roberto R.** OP085
- Gil, Rosane Aguiar da Silva** San TH084, MO088, TU089, TH090, MO091, MO094
- Giller, Karin** TH102, OP133
- Giotto, Marcus V.** TU245
- Giraudeau, Patrick** MO136
- Girolami, Davide** TU146
- Giusti-Paiva, Alexandre** MO172
- Gladden, Lynn F.** OP079, UP154, TH300
- Gnida, Manuel** UP031
- Goddard, Alan D.** OP004
- Goddard, P.A.** TH222
- Godoy, Michele Maria Gonçalves de** TH192, MO193
- Goldfarb, Daniella** OP087
- Gollnick, Paul** MO010
- Golotvin, Sergey** TU161
- Gomes, Andre M. O.** TH048
- Gomes, Bruna Ferreira** OP153, TH270
- Gomez, C.G.** TU239
- Gomez, Leonardo D.** TH093
- Gonsalves, Elicardo** MO190
- Gonzalez, G.** MO229, TU230
- Gonzalez, Mariano M.** TU008
- González-Beltrán, Alejandra** TH183
- González-Pérez, Martha** TU098
- Gonçalves, Eduardo Corrêa** MO277
- Gonçalves, Gustavo R.** MO085, TU086
- Gonçalves, Kaliandra** TH204
- Good, Jeremy A.** TU149
- Gossert, Alvar** TH003
- Goulart, Henrique Fonseca** TH081
- Grandinetti, Philip J.** OP034
- Grangeasse, Christophe** TH096
- Greco, Sandro José** TU281
- Green, Gary G. R.** OP159
- Green, Richard A.** OP159
- Green, Steven J.** TU149
- Grey, Clare. P.** OP101
- Griesinger, Christian** OP086, MO013, UP072, TU074, TU122, OP133, TH285
- Griffin, John** OP101
- Griffin, John M.** OP035
- Griffin, Jules** TH183, MO184
- Griffin, Robert G.** UP111, OP013, MO298
- Grigorjev, Igor** TH219
- Grombacher, Denys** OP096
- Gromilov, Sergey** TU218
- Gronenborn, Angela M.** TU038, PL165
- Groot, Berend L. de** OP086
- Grunewald, Elliot** OP096
- Grzesiek, S.** OP033
- Gu, Yina** OP129
- Gueiros-Filho, Frederico José** MO055
- Guerreiro Filho, Oliveira** TH057, MO058
- Guimarães, Maria José C. O.** TU101
- Guimarães, Vinícius Ferreira** MO172

- Guittet**, Eric UP027, UP016
- Guo**, Qianni MO133
- Gupta**, Rashmi OP133
- Gupta**, Shaan TH135
- Gustavsson**, Martin MO061
- Günther**, Ulrich L. OP091, TU182, TU236
- Hagens**, Tona von OP077
- Hagn**, Franz TH120
- Hails**, Guillermo MO100
- Hallwass**, Fernando MO142, MO166, MO187
- Han**, Oc Hee UP103
- Han**, Songi OP046
- Han**, Yi OP138
- Hanna**, John V. TH075, MO079
- Hansen**, Michael Ryan UP011
- Harada**, Yoshie TH150
- Harvey**, Peter UP084
- Harzstark**, Andrea OP040
- Haug**, Kenneth TH183
- Hauk**, Priscila MO046
- Hausnerova**, Berenika MO259
- Hawkes**, Geoffrey Ernest TH081, TH168
- Hayes**, Sophia E. MO145, OP102
- He**, Yao TU014
- Hediger**, Sabine UP126
- Heijenoort**, Carine van UP016
- Henriques**, Sonia T OP160
- Hercík**, Kamil TU038
- Heredia**, Gabriela Pinheiro TU029
- Herlein**, Judith UP158
- Hidaka**, Tetsuro UP088, TH288
- Highton**, Louise A. R. OP159
- Hill**, Stephen TU254
- Hilty**, Christian OP109
- Hinderberger**, Dariush OP023
- Ho**, Oanh TH012
- Hoffman**, Brian M. TU233
- Hogle**, James M. TH036
- Holland**, D. J. OP079
- Holte**, Laura MO151
- Hong**, Kwan Soo TU212, TH213, MO214, TU215
- Hong**, Mei PL069, OP124
- Honorato**, Hercílio D. A. TU086
- Hooker**, Jerris W.
- Hooper**, Alex J. J. OP159
- Horev**, Judith UP140
- Horjales**, Eduardo TU044
- Hosztafi**, Sándor MO028
- Hou**, Guangjin MO139
- Hoyt**, David W. UP099
- Hritz**, Jozef TU038
- Hsieh**, Ming-Feng OP009
- Hsu**, Chaohsiung UP064
- Hu**, Bingwen MO139, TU140
- Hu**, De-en OP065
- Hu**, Hong-Yu TU011
- Hu**, Jian Z. UP099
- Huang**, J.-r. OP033
- Huang**, Jing TU179
- Huang**, Susie Y. UP042
- Huang**, Xi OP074
- Huber**, Matthias UP135
- Huber**, Roland MO121
- Hunkeler**, Andreas OP137
- Hunter**, Robert OP127
- Hurlimann**, Martin D. TU248
- Husson**, Clotilde UP016
- Hwang**, Lian-Pin UP064
- Hård**, Torleif OP073
- Hürlimann**, Martin D. OP100
- III**, Arthur G. Palmer MO124
- III**, George Cutsail TU233
- Igarashi**, Ruji TH150
- Igea**, Ana TU017, UP054
- Ihms**, Elihu MO010
- Inomata**, Kohsuke TU203
- Iqbal**, Anwar MO049
- Ivanshin**, Vladimir A. TU224, UP022
- Izadi-Pruneyre**, Nadia UP048
- Jackowski**, Karol UP120
- Jain**, Sheetal Kumar UP059
- Jaremko**, Lukasz MO019, TH102
- Jaremko**, Mariusz MO019, TH102
- Jaroniec**, Christopher P. OP134
- Jaudzems**, Kristaps TH060
- Jault**, Jean-Michel OP137
- Javkhlantugs**, Namsrai TU059
- Jayaseelan**, Kalai Vanii MO163
- Jerschow**, Alexej UP145
- Jeschke**, Gunnar OP077, TH234
- Jeziorna**, Agata TU083
- Jiang**, Peng MO232
- Jiang**, Weiping MO133
- Jiménez-Barbero**, Jesús MO001, UP017, TH294
- Johnson**, Robert L. OP124
- Jones**, Catherine E. MO205
- Jones**, Oliver A.H. UP094
- Jung**, Ji-Ho OP018
- Junior**, Luiz S. C. MO256
- Junker**, Jochen MO115, TU155, TH171
- Júnior**, Antônio M. TU164
- Kabengi**, Nadine J. TU245
- Kalbitzer**, Hans Robert OP025, TH045, TH111
- Kaminski**, D. TH222, MO223
- Kamo**, Naoki UP088, TH288
- Kang**, Jongeun MO214
- Kannan**, Arvind MO130
- Kaptein**, Robert UP031
- Karabanov**, Alexander OP112
- Kasthurirangan**, Sanjeev MO205
- Katahira**, R. MO052
- Kawamori**, Asako UP150, TH297
- Kawamura**, Izuru UP088, TU059, MO118, TH288
- Kay**, Lewis E. MO016, OP070
- Kear**, Jamie L. OP074
- Keeble**, David OP127
- Keeler**, Eric OP034
- Kemp**, Rafael TU284
- Keng**, Luiz Henrique MO283
- Kennedy**, Brett W.C. OP065
- Kenwright**, Alan M. UP084
- Keren**, Amit MO073
- Kessler**, Naama TU002
- Kettunen**, Mikko I. OP065
- Khanim**, Farhat OP091, TU182
- Khetrapal**, C.L. TH177
- Khitrin**, Anatoly UP145
- Khramtsov**, Valery V. UP021
- Khrumkacheva**, Olesya TH219
- Kikuchi**, Jun UP093, MO181
- Killner**, Mario Henrique Montazzolli TU260, MO262
- Kim**, Hai-Young TH102
- Kim**, Hyun Min TU215
- Kim**, Ji-Sun OP018
- Kim**, Jong Seung TH213
- Kim**, Yongae OP018
- King**, Scott P. MO079
- Kira**, Atsushi TU059
- Kirilyuk**, Igor TH219
- Kleckner**, Ian R. MO010, TU128
- Knight**, Michael J. TH060
- Knight**, Rosemary OP096
- Kock**, Flávio Vinicius Crizóstomo TU266, MO268
- Koczula**, Katarzyna OP091
- Koehler**, Joerg TH045
- Koers**, Eline UP136, TH291
- Kojima**, C. MO052
- Kolbe**, Michael OP133
- Kolokolov**, Daniil TU218
- Kondo**, Y. MO052
- Koretsky**, Alan P. OP043
- Korzhnev**, Dmitry M. TH015, UP049, MO037, TU287
- Kostadinova**, Maria TU047
- Kovacs**, Helena TH003
- Kozlov**, Guennadi MO022
- Krebs**, Manuel TH210
- Kremer**, Werner TH045
- Kreutz**, Christoph MO121, TH123
- Kritsiligkou**, Paraskevi OP004
- Kryukov**, Eugeny TU149
- Krzystek**, J. MO232
- Kuchel**, Philip W. OP095, TH144
- Kukic**, Predrag TH129
- Kuktaite**, Ramune TU092

- Kulminskaya**, Natalia TH201
- Kumagaia**, Patricia S. TH231
- Kunert**, Britta OP137
- Kupče**, Ēriks MO016, OP119
- Kurbatska**, Victoria TU002
- Kurhanewicz**, John OP040
- Kurizki**, Gershon OP122
- Kuster**, Ricardo M MO034
- Kwiatkowski**, Grzegorz OP112
- Köckenberger**, Walter OP112
- Kędziorek**, Mariusz MO067
- Labate**, Carlos Alberto TH093
- Lacerda Júnior**, Valdemar TU125, TU266, MO268, TU269, TU281
- Lacour**, Jérôme TU242
- Ladizhansky**, Vladimir MO118, OP149
- Lafon**, Olivier UP036, MO139, TU140, TH141
- Lamberto**, G. R. MO013
- Lanfredi**, Alexandre J. C. MO226
- Lange**, Adam TU074, OP133
- Laraoui**, Abdelghani OP157
- Larion**, Mioara OP129
- Larkin**, Timothy J. TH099
- Lavayen**, V. TU230
- Lavorente**, Gabriela Bassetti TH093
- Leal**, Ana Paula F. TU110
- Leal**, Katia Z. TH090
- Lecoq**, Lauriane UP126
- Lee**, Brittany
- Lee**, Chulhyun TU212
- Lee**, Donghan OP086
- Lee**, Hyunseung TH213, TU215
- Lee**, Jae-Seung UP145
- Lee**, Sumin TH213
- Lee**, Youngbok OP109
- Leftin**, Avi PL001
- Lehmann-Horn**, J. A. TU068
- Lehtivarjo**, Juuso MO130
- Leigh**, Kendra TH036
- Leite**, Érika de Almeida MO193
- Leitão**, Alexandre Amaral TH084, TH090
- Lelli**, Moreno UP110, TU299
- Lendel**, Christofer OP073
- Leonciks**, Ainars TU002
- Leonov**, Andrei TU122
- Lesage**, Anne TH060, TH234, UP110, TU299
- Leskes**, Michal OP101
- Levin**, Judith G. TU038
- Levitt**, Malcolm H. PL044
- Levstein**, Patricia R. TH066, OP144
- León**, A.E. TH267
- Li**, Dawei OP129
- Li**, Dong
- Li**, Haidong MO133
- Li**, Yixuan TU140
- Li**, Zhao MO133, UP042, UP064
- Liedl**, Klaus MO121
- Lim**, Sing Mei UP007
- Lim**, Yong Taik TU215
- Lima**, Emília Celma de Oliveira MO283
- Lima**, J. F. MO229, TU230
- Lima**, Jerson MO025
- Lima**, José Fernando de TH051
- Lima**, Maria E. de TH024
- Lima**, Marisa Aparecida TH093, TH237
- Lima**, Nerilson Marques MO175
- Lin**, Yanqin MO202
- Lin**, Yulan TH138
- Lin**, Yung-Ya UP042, UP064
- Lin**, Zhongjie TH075
- Linck**, Yamila Garro TU260
- Lindahl**, Martin TH201
- Linden**, Elisabeth G. van der MO094
- Linser**, Rasmus TH120
- Lira**, Tatiana Onofre de TU284
- Liu**, J. TH222
- Lião**, Luciano Morais TU080, TU104, TH105, TU107, TU188, MO283
- Llases**, M. E. MO013
- Lloyd**, Lyrelle S. OP159
- LoSan**, Talita TH114
- Login**, Frederic TH012
- Loibl**, Sibylle MO184
- Loiola**, Rodrigo Azevedo MO211
- Long**, Dong OP129
- Long**, Joanna TU227
- Longhi**, Marcela TH069
- Lopes**, Edmundo Pessoa de Almeida TH192, MO193
- Lopes**, Thiago I. B. TU164
- Lopes**, Thierry R. MO085
- Lopez**, Claire TU242
- Loquet**, Antoine OP133
- Lorin**, Aurelien TU062
- Loring**, John S. UP099
- Loth**, Karine UP031
- Lourenço**, Gustavo V. TU209
- Luchinat**, Claudio OP156
- Ludwig**, Christian OP091, TU182, TU236
- Luján**, Juan Fernando Collados TU185
- Lungwitz**, Bernhard TH210
- Luo**, Qing MO133
- Luy**, Burkhard OP082
- Lye**, Ming TH036
- López-Prados**, Javier TH009
- López**, Concepción MO064
- López**, Jesús García TU185
- Macdonald**, Peter M. TH135
- Machado**, Luciana Elena S. F. TH015, MO037, MO049
- Machado**, Sérgio de Paula TU155
- Machado**, Vinicius de França MO247, MO250, TH279
- Maciejewski**, Mark W. UP049, TU287
- Madhu**, P. K. OP071
- Maffei**, Mariano TU017, UP054
- Mafra**, Luís MO064, OP060, TH156
- Magalhães**, Mariana T. Q. MO037
- Magon**, Cláudio José TU071, TU134, MO229, TU230
- Maguire**, Eamonn TH183
- Mahendraker**, Tejasvi TH183
- Mainz**, Andi OP070
- Makino**, Teruki UP088, TH288
- Maldonado**, Andres TH198
- Maltsev**, Alex OP132
- Manson**, J. L. TH222
- Mantle**, Mick D. OP079, UP154, TH300
- Mantsyzov**, Alexey OP132
- Manzano**, Ana UP017, TH294
- Marana**, Sandro Roberto TH039
- Marassi**, Francesca M. OP024
- Marcelo**, Filipa UP017, TH294
- Marco-Rius**, Irene TH099
- Marconcini**, Lucinéia Vizzotto MO271
- Marin**, Graciane UP121, TU290
- Marques**, Mayra de A. MO007
- Marquez**, Brian L. TU275
- Marsaioli**, Anita J. TU164
- Martin**, Gary E OP118
- Martins**, Carla TU194
- Martins**, Felipe Terra TU080, TU104
- Martins**, Gabriel R. TU176
- Martins**, Marcos A. P. MO127
- Martins**, Mateus TU209
- Martínez**, Juan Manuel Lázaro TU158, TH252
- Maryunina**, Ksenia OP019
- Mascarenhas**, Artur José Santos TH081
- Maso**, Lianna Di TH018
- Massiot**, Dominique OP038
- Mateo**, Carlos TU251
- Mathies**, Guinevere UP111, MO298
- Matineau**, Charlotte UP012, MO289
- Matsuoka**, Hideto OP019
- Mattea**, Carlos TH240
- Mauro**, Eduardo Di MO220, TU221
- Mavridou**, Despoina A.I. OP004

- McDonough**, Kathleen UP053
- McElroy**, Craig A. MO010
- McInnes**, E. J. L. MO223
- McQueen-Mason**, Simon J. TH093
- Meier**, Beat H. UP135, OP137
- Meira**, Douglas Adamoski TU056
- Melo**, Carolina Pereira de Souza MO196
- Melquiond**, Adrien UP130
- Mendes**, Ygara S. TH048
- Menegola**, Julia TU116
- Menezes**, Rachel Santos de MO040
- Menezes**, Sonia Maria Cabral de MO091, UP121, TU125, MO256, TU290
- Meriles**, Carlos A. OP157
- Merkle**, Hellmut OP142
- Messinger**, Robert J. OP009, OP038
- Mewis**, Ryan E. OP159
- Meyer**, Jacques TU233
- Miljak**, D. G. TU068
- Miller**, Brian OP129
- Millet**, Oscar OP029, OP114
- Min**, Hlaing OP109
- Mino**, Hiroyuki UP150, TH297
- Miotto**, M.C. UP072, TH285
- Miranda Filho**, Fernando Luis TU095
- Miranda**, Fabio da Silva TU263
- Miranda**, Manoel Messias P. TU077
- Mirzahosseini**, Arash MO028
- Mitchell**, J. OP079
- Mitra**, Mithun TU038
- Miyamoto**, Catarina A. MO049
- Mkami**, Hassane El OP127
- Moeginger**, Bernhard MO259
- Mohorič**, Aleš MO238, TU251
- Molle**, Inge Van TU152
- Monteiro**, Marcos Roberto TH105, TU107, TH276
- Monteiro**, Mavis L. MO076
- Monteiro**, Paulo TH078
- Monteiro**, Robson Q. UP162, MO286
- Monti**, Gustavo Alberto TU158, TU239, TH252
- Montoro**, Marcos MO241, UP080, MO301
- Montrazi**, Elton Tadeu TH243
- Moon**, Hyeyoung TH213, MO214
- Moore**, Eric PL002
- Moore**, Jeremy OP102
- Moraes**, Adolfo G. TH108
- Moraes**, Adolfo H. MO037, TH042, TU047
- Moraes**, Tiago Bueno de MO106, TU134
- Moreira**, Raphaell MO082
- Moreno**, M. MO229
- Moreth**, Kristin MO208
- Morgada**, Marcos N. OP075, TH216
- Morgan**, Vinícius Gomes TU269
- Morin**, S. OP033
- Morozov**, Denis TH219
- Moré**, Cristian Sebastián TH258
- Moura**, Luiza Cristina de TH117
- Moussa**, Miled Hassan Youssef MO280
- Mozley**, Erin C. OP004
- Muhammad**, Asif TU263, TH279
- Mujica**, Vladimiro TH228
- Mullen**, Dan MO061
- Munhoz**, Victor H. O. TU050
- Muniz**, Adriane M. S. MO190
- Munro**, Rachel MO118
- Munte**, Claudia Elisabeth OP025, TU044, TH045, TH051, TH111, TU113, TH231
- Murakami**, Mario T. TH054
- Murayama**, Syuhei TU203
- Murphy-Boesch**, Joseph OP043
- Muthu**, Dhanasekaran UP076
- Muñoz**, Roberto Rodriguez TH255
- Münnemann**, Kerstin UP146, TU293
- N.Garaga**, Mounesha OP038
- Nadal**, Jurandir MO190
- Nadaud**, Philippe S. OP134
- Naider**, Fred TU002
- Naito**, Akira UP088, TU059, TH288
- Nand**, Deepak TU119
- Nantes**, Iseli L. MO226
- Nardini**, Viviani TH174
- Nascimento**, Claudia Jorge do TU170
- Nascimento**, L. S. MO187
- Nascimento**, Otaciro R. MO226, MO229
- Nascimento**, Patrícia Coelho TU131
- Nast**, Robert E.
- Naughton**, Shannon TH018
- Naumann**, Christoph TH144
- Navas**, D. TU230
- Navon**, Gil UP140
- Nebreda**, Angel R. TU017, UP054
- Neese**, Frank OP020
- Nelson**, Sarah OP040
- Neschen**, S TH180
- Neto**, Alvaro Cunha TU125, TU281
- Neto**, Denise Cristian Ferreira TH153
- Neto**, Francisco Gomes TH030
- Neto**, Roberto P. Cucinelli MO094
- Netto**, Antonio Marchi MO259
- Neugebauer**, Petr PL003
- Nicholson**, Jeremy K. PL106
- Nielsen**, Jakob TH201
- Nielsen**, Niels Christian OP073, UP059, OP123, TH201
- Nieto**, Pedro N. TH009
- Nieuwkoop**, Andrew J. OP117
- Nishchenko**, Alena TU218
- Nishimura**, Katsuyuki TU059
- Nisius**, L. OP033
- Noel**, Mathieu TU062
- Nogueira**, Marcela Christina Oliveira TU155, TH171
- Noh**, Young-Woock TU215
- Nordlund**, Pär UP007
- Norman**, David OP127
- Noszál**, Béla TH027, MO028
- Nour**, Zalfa OP009
- Nourikyan**, Julian TH096
- Novotny**, Etelvino Henrique MO265, MO274
- Nucci**, Nathaniel V. UP111, MO298
- Nunes**, Luiza Maria da Silva OP153, TH270
- Nunes**, Wilian da Silva MO097
- Nyman**, Tomas UP007
- Ohashi**, William TH186
- Ohno**, Ayako TU203
- Okitsu**, Takashi UP088, TH288
- Oliveira Junior**, Marcos de TU071
- Oliveira Júnior**, Ivan dos Santos TH147
- Oliveira-Silva**, Rodrigo de TH237, MO274
- Oliveira**, Andre Marco de MO025
- Oliveira**, Andrea Cheble de MO025, TH048
- Oliveira**, Caroline Silva de TU188
- Oliveira**, Eduardo Barreto TH249
- Oliveira**, Emanuele Catarina da Silva TU125
- Oliveira**, Everton Lucas de MO244
- Oliveira**, Guilherme A. P. de MO007, TH126
- Oliveira**, Ivan dos Santos TU146, MO280
- Oliveira**, Jessica TU041
- Oliveira**, Juliana Ferreira de TU056
- Oliveira**, Kleber Thiago de MO136, TU281
- Oliveira**, Livia Roberta P. de TU194
- Oliveira**, Luciana Coutinho de MO043, MO046, OP148
- Oliveira**, Paulo Sérgio Lopes de TU056
- Oliveira**, Thais MO034
- Ono**, A. MO052
- Opella**, Stanley OP151
- Orcellet**, M. L. MO013
- Oresic**, Matej MO184



- Orgován**, Gábor TH027, MO028
- Ortega**, Gabriel OP114
- Ortiz**, Fernando López MO103, TU185
- Oschkinat**, Hartmut TH063, OP028
- Ota**, Shoko TU098
- Ott**, Maria UP058
- Ouari**, Olivier TH234, UP110, TU299
- Ovcharenko**, Victor OP019
- Ozarowski**, Andrew MO232
- Pagès**, Guilhem OP095
- Paim**, A. P. S. MO187
- Paiva**, Fernando Fernandes TH210
- Paluch**, Piotr TU083, TU143
- Parella**, Teodor OP083
- Park**, Hyo Eun MO214
- Park**, Junwon TH213
- Parker**, David UP084
- Pascutti**, Pedro Geraldo TH051
- Pastawski**, Horacio M. TH066, OP144
- Patiny**, Luc TH165
- Paula**, Viviane Silva de MO004, TH015, UP162, TU041, MO286
- Paulsen**, Harald OP077
- Pawlak**, Tomasz TU083, TU143
- Paëpe**, Gaël De UP126
- Pelc**, Damjan MO253
- Pell**, Andrew J. TH060
- Pellecchia**, Maurizio OP014
- Penzel**, Susanne UP135, OP137
- Peobody**, David MO025
- Pepin**, Alexandre TH210
- Pereira**, Carla Karine Barbosa TH168
- Pereira**, Elen G. TH126
- Pereira**, Fabiola Manhas Verbi TH264
- Pereira**, G. E. MO187
- Pereira**, Gonçalves Amarante Guimarães TU056
- Pereira**, Luciana TU194
- Pereira**, Natália Corrêa TH030
- Pereira**, Wagner Luiz TU170
- Peres**, Augusto C. C. MO256
- Perez**, Javier UP016
- Perez**, Yolanda TU017
- Perlo**, Josefina TH207
- Pervushin**, Konstantin UP007, TH162
- Peters**, Dana C. OP061
- Petronilho**, Elaine da C. TH153
- Piló-Veloso**, Dorila TH024, TU050
- Pimentel**, H.R.X. MO091
- Pinheiro**, Natália G. S TH024
- Pintacuda**, Guido TH060
- Pinto**, Andressa P. A. OP025
- Pinto**, Diogo O. Soares TH087, TU146
- Pinto**, Thiago Rodrigues MO025
- Pinto**, Vinícius S. TH105, TU107
- Pires**, Diego Arantes Teixeira TU032, TU170
- Pires**, José Ricardo Murari TU029, MO031, MO040
- Pizetta**, Daniel C. TU209
- Placial**, Jean-Pierre UP016
- Plevin**, Michael OP055
- Plivelic**, Tomás S. TU092
- Pol**, Rostislav TU161
- Polenova**, Tatyana MO139
- Polienko**, Yulija TH219
- Polikarpov**, Igor TH093, TH237
- Polli**, Roberson Saraiva TH087, TH210, TH243
- Polyhach**, Yevhen OP077
- Pomarico**, Luciana TU194
- Pomin**, Vitor Hugo TU041
- Pongs**, Olaf UP136, TU119, TH291
- Pons**, Miquel OP029, TU017, UP054
- Ponte**, Santiago L. TH132
- Poole**, Katie M. TU254
- Pope**, James M. MO205
- Popot**, Jean-Luc UP027
- Porto**, Christiane Feijó de Castro TU281
- Postigo**, Matheus Pereira MO112
- Potapov**, Alexey PL002
- Potrzebowski**, Marek J. TU083, TU143
- Pourpoint**, Frédérique TH141
- Požek**, Miroslav MO073, MO253
- Prado**, Paula Favoretti Vital do TU056
- Prates**, Maura Viana TU032
- Prina**, Ignacio UP146, TU293
- Prisner**, Thomas F. PL003
- Prokofyev**, Alexander UP136, TU119, TH291
- Prosser**, Scott TH135
- Provencher**, Marie-Eve TU062
- Puckeridge**, Max OP095, TH144
- Puglisi**, Joseph D. UP116
- Purusottam**, Rudra Narayan UP125
- Pusiol**, Daniel José MO148, MO241, UP080, TH258, OP152, MO301
- Pustovalova**, Yulia TH015, UP049, TU287
- Pérez-Aparicio**, Roberto UP058
- Qian**, Chunqi OP043
- Queiroz Júnior**, Luiz Henrique Keng TU080, TU104, MO136, MO283
- Quintanar**, L. UP072, TH285
- Rabbani**, Said R. TU191, TH195, MO211
- Ragavan**, Mukundan OP109
- Ramaswamy**, Vijaykumar
- Ramos**, Bruna M. C. TH054
- Ramos**, Carlos Henrique TH063
- Ramos**, Ingrid Graça TH081
- Rangel**, Luciana Pereira MO025
- Raschle**, Thomas TH120
- Rasia**, Rodolfo Maximiliano MO100
- Ravotti**, Francesco UP135
- Redfield**, Christina OP004
- Reibarkh**, Mikhail OP118
- Reich**, Daniel OP142
- Reichert**, Detlef OP057
- Reif**, Bernd MO139, OP070
- Reinhard**, Friedemann OP157
- Religa**, Tomasz OP070
- Ren**, Jinjun MO082, UP037
- Ren**, Pingping TU179
- Renault**, Louis UP016
- Renshaw**, Matthew P. UP154, TH300
- Resende**, Jackson A. L. C. TH090
- Resende**, Jarbas M. TH024, TU050
- Reverdatto**, Sergey TH198, UP053
- Rezende**, Camila Alves TH093, TH237
- Rezende**, Carlos A. TH090
- Ribeiro**, Tatiana Santana TU077
- Ribotta**, P.D. TH267
- Riedel**, Dietmar OP133
- Rienstra**, Chad M. OP117
- Rio**, Edmilson TH246
- Rios**, Edmilson Helton MO247, MO250, MO256, TH279
- Rivlin**, Michal UP140
- Roberts**, S. Tegan UP154, TH300
- Robertson**, Duncan OP127
- Robles**, Ivan Erick Castañeda TH255
- Robustelli**, Paul UP115, MO124, MO292
- Rocca-Serra**, Philippe TH183
- Rocha**, Cristiane B. MO007
- Rocha**, João TH156
- Rochaa**, Cláudia Quintino da MO172
- Roditi**, Itzhak TH147, MO280
- Rodrigues Filho**, Ubirajara P. TU071
- Rodrigues**, Diego Alves TU080, TU104
- Rodrigues**, Letícia V. MO127
- Rodrigues**, Raquel Pantoja Barreiros MO115, TU155
- Rodrigues**, Stephen Fernandes de Paula MO211
- Rodrigues**, Tiago B. OP065

- Rohwedder**, Jarbas José Rodrigues TU260, MO262
- Rojas**, Leonardo MO076
- Romanuka**, Julija UP031
- Romeiro**, Luiz Antônio Soares TU131
- Roos**, Annette UP007
- Rosato**, Antonio TU020, TH021
- Rose**, Honor M. UP089, MO295
- Rosengren**, K Johan OP160
- Rossini**, Aaron J. TH234, UP110, TU299
- Rosso**, Kevin M. UP099
- Ruiz**, Naira Machado da Silva MO256
- Rö melt**, Michael OP020
- SZE**, Kong Hung TU011
- Saalwächter**, Kay UP058, OP057
- Sabo**, Michael OP086
- Sagdeev**, Renad OP019
- Saha**, Dipta MO145
- Sahakyan**, Aleksandr MO130
- Salager**, Elodie OP101
- Salek**, Reza TH183, MO184
- Salinas**, Roberto Kopke TH039, MO043, MO046
- Salinas**, Roberto OP129, OP148
- Salvatella**, Xavier OP086
- Sam**, My D. TH036
- Samoson**, Ago UP135
- Samouilov**, Alexandre MO235
- Sanders**, Kevin OP034
- Sano**, Walter TU221
- Sansone**, Susanna-Assunta TH183
- Sant’Ana**, Antônio Euzébio Goulart TH081, TH168
- Sant’Anna**, Quézia da Silva TH171
- Santana**, Juliana Santos TH063
- Santana**, Mábio João MO283
- Santos Jr.**, Emanuel MO094
- Santos-Filho**, Osvaldo Andrade MO088
- Santos**, Bernardo Coutinho Camilo dos MO247, MO250
- Santos**, Carlos Henrique Corrêa dos MO160
- Santos**, Carolina G. dos MO226
- Santos**, Daniel M. TH024
- Santos**, Fabiane Aparecida Batalha dos MO136
- Santos**, José Sebastião dos TU284
- Santos**, Marcelo Henrique dos MO172
- Santos**, Raquel MO190
- Santos**, Reginaldo Bezerra dos TU281
- Santos**, Sérgio M. MO064, OP060, TH156
- Santos**, Tereza Cristina dos TU089
- Sant’Anna**, Raphaela Teresa TU155
- Sant’Anna**, Ricardo Oliveira TH063
- Sardinha**, João UP121, TU290
- Sardo**, Mariana MO064
- Saridakis**, Emmanuel OP004
- Sarthour Júnior**, Roberto Silva TU146, TH147, MO280
- Sarzedas**, Carolina Galvão TU035
- Sass**, H.-J. OP033
- Sati**, Pascal OP142
- Sattler**, Michael OP090
- Sayegh**, Raphael Santa Rosa TH039
- Scheler**, Ulrich MO238
- Scherf**, Tali TU002
- Schettino Jr.**, Miguel A. MO085, TU086
- Schiemann**, Olav OP127
- Schmidt-Rohr**, Klaus OP124
- Schmidt**, Rita PL001
- Schneider**, Horst UP058
- Schneider**, José Fabian TU065, UP104, TU071
- Schnur**, Einat TU002
- Schomburg**, Benjamin TU074
- Schreier**, Shirley TH114
- Schubert**, Volker MO001
- Schug**, Alexander UP006
- Schulthes**, Cristian P. TU245
- Schwalbe**, Harald UP032
- Schwarten**, Melanie OP055
- Schwartz**, Lawrence TH246
- Schwiegg**, Claudia OP086
- Schwieters**, Charles D. TH102, OP134
- Schütz**, Anne OP137
- Scramin**, Juliana TU077
- Sears**, Jesse A. UP099
- Sebastião**, Pedro José TU278
- Sebastião**, Rita de Cássia Oliveira TH282
- Sederman**, Andrew J. OP079, UP154, TH300
- Seferin**, Marcus UP121, TU290
- Seidl**, Peter R. TU101
- Selenko**, Philipp UP089, MO295
- Semaan**, Felipe Silva TU263
- Sengupta**, Ishita OP134
- Separovic**, Frances OP163
- Serial**, M.R. TH267
- Serrao**, Eva M. OP065
- Sesti**, Erika MO145
- Seyedlar**, Amin Ordikhani TH240
- Sforça**, Mauricio Luis TU053, TH054, MO055, TU056, TU197
- Sgourakis**, Nikolaos OP133
- Shanks**, Brent OP124
- Sharma**, Mayuri TH036
- Shekhtman**, Alexander TH198, UP053
- Shemesh**, Noam OP122
- Shen**, Jiang-Ren UP150, TH297
- Shen**, Yang OP132
- Shevelkov**, Veniamin OP133
- Shi**, Chaowei
- Shi**, Lichi MO118
- Shi**, Pan
- Shi**, Yunyu OP050
- Shirakawa**, Masahiro TH150, TU203
- Shundrina**, Inna TU218
- Siepel**, Florian TU122
- Silletta**, Emilia V. TH207, TU239
- Silva Filho**, Eloi Alves da MO268
- Silva**, Afonso OP142
- Silva**, André L. MO226
- Silva**, Antonio Jorge Ribeiro da TU176
- Silva**, Daniel F. OP025
- Silva**, Daniel Varón MO001
- Silva**, Danilo M.D. Delfino da TU209
- Silva**, Dhiogo Mendes da MO283
- Silva**, Dulce Helena Siqueira MO175
- Silva**, Emerson Oliveira Da TU095
- Silva**, Fernanda B. da TU101
- Silva**, Gil V. J. da TH174
- Silva**, Glauciane R.D. TU164
- Silva**, Hana Karina Pereira da TH093
- Silva**, I. D. A. MO229
- Silva**, Isabela Almeida TU146
- Silva**, Jerson L. MO007, TH048, TH126
- Silva**, Lorena M. A. TH276
- Silva**, Milton Neto da TU110, TU257
- Silva**, Pablo Nascimento da MO277
- Silva**, Ricardo Oliveira da TH192, MO193
- Silva**, Rodrigo de Oliveira TH087, MO265
- Silva**, Romeu Ricardo da TU194
- Silva**, Ronaldo Dionísio da TH192
- Silva**, Simone P. MO094
- Silva**, Tania Maria S. da TH159
- Silva**, Virginia Cláudia da MO160
- Silveira**, Camila P. MO076, TU101
- Silveira**, Edilberto Rocha TU131, TU173
- Silveira**, Ivna A. F. B. TU110
- Simorre**, Jean-Pierre UP126
- Simões**, Clara MO154
- Singh**, Himanshu TU200
- Sivalingam**, Kantharuban OP020
- Sivitz**, William UP158
- Skora**, L. OP033

- Smith**, Colin OP086  
**Smith**, Graham OP127  
**Smith**, Pieter ES OP122  
**Soares**, Vera L. P. MO094  
**Solomon**, Eddy PL001  
**Solyom**, Zsolia OP055  
**Song**, Yi-Qiao OP081, TH246  
**Soprano**, Adriana S. TU053  
**Sorenson**, Martha M. MO007  
**Sotoma**, Shingo TH150  
**Sotta**, Paul UP058  
**Sousa Júnior**, Paulo Teixeira de MO160  
**Sousa**, Eduardo Gomes Rodrigues de MO088, TU089  
**Souza**, Andre TH210, MO247, TU248  
**Souza**, André Alves de TH279  
**Souza**, Claudia M. G. de TU191, TH195  
**Souza**, Diorge Paulo de MO043  
**Souza**, Diorge OP148  
**Souza**, Eugênio Furtado de TH084  
**Souza**, Isis Torres TH168  
**Souza**, Ivete P. R. de MO190, TU194  
**Souza**, Ivete R. P. de TU026  
**Souza**, Tatiana A.C.B. TU053  
**Souza**, Theo L. F. MO025, TH048  
**Souza**, Tiago A. TU053  
**Sperling**, Lindsay J. OP117  
**Spielberg**, E. T. MO223  
**Spiess**, Hans Wolfgang UP146, TU293  
**Spindler**, Phillip PL003  
**Spitzer**, Romana MO121  
**Spitzmesser**, JB MO151  
**Staab**, John MO151  
**Stanton**, Christopher J. MO145  
**Stapf**, Siegfried TH240, TU251  
**Staudacher**, Tobias OP157  
**Steinbeck**, Christoph MO163, TH183  
**Steinhaus**, Johannes MO259  
**Stelzl**, Lukas OP004  
**Stepanov**, Alexander TU218  
**Stepišnik**, Janez MO238, TU251  
**Stetz**, Matthew UP111, MO298  
**Stevens**, Julie M. OP004  
**Strizhakov**, Rodion TH219  
**Strumia**, M.C. TU239  
**Stupp**, Gregory S.  
**Suarez**, Irina Paula MO100  
**Suarez**, Marisa C. MO007  
**Subramanian**, M. A. MO232  
**Sudo**, Yuki UP088, TH288  
**Surface**, J. Andrew OP102  
**Suter**, Dieter OP147  
**Sychrovsky**, Vladimir MO052  
**Takahashi**, Hiroki UP126  
**Takegoshi**, K. PL107  
**Tam**, Leo OP061  
**Tamaki**, Fabio Kendi TH039  
**Tanaka**, Yoshiyuki MO052  
**Tang**, Huiru MO157, MO178, TU179  
**Tang**, Joel A. TH072  
**Tang**, Ming OP117  
**Tannús**, Alberto TU209, TH210  
**Tars**, Kaspars TH060  
**Tasic**, Ljubica MO076, TU101, TH186  
**Taulelle**, Francis UP012, MO289  
**Tavares**, Maria Inês Bruno MO094, TU278  
**Tayler**, A. B. OP079  
**Tayler**, Michael C. D. TH099  
**Taylor**, Rae TH078  
**Teixeira**, Francesco Brugnera TU044  
**Teixeira**, Paulo José Pereira Lima TU056  
**Teixeira**, Róbson Ricardo TU170  
**Tekely**, Piotr UP125  
**Teles**, Rubens Rodrigues MO142, MO166  
**Telkki**, Ville-Veikko UP098  
**Telser**, Joshua MO232, TU233  
**Temel**, Deniz B. TH096  
**Teo**, Hsiangling UP007  
**Terskikh**, Victor MO067  
**Theillet**, Francois-Xavier UP089, MO295  
**Theis**, Thomas OP138, UP041  
**Thiemann**, Otavio Henrique MO112  
**Thieuleux**, Chloé UP110, TU299  
**Thompson**, Karen TH201  
**Thurber**, Kent PL002  
**Tian**, Changlin TU014,  
**Tiezzi**, Henrique Oliveira TU056  
**Timco**, G. A. MO223  
**Tinoco**, Luzineide Wanderley TU035, MO169  
**Tischer**, I. TU167  
**Tiziano**, Grazielle. V. MO256  
**Tochio**, Hidehito TH150, TU203  
**Toma**, Sergio Hiroshi MO211  
**Tomatis**, Pablo E. TU008  
**Tomonaga**, Yuya UP088, TH288  
**Toms**, Harold TH081  
**Tordo**, Paul TH234, UP110, TU299  
**Tozoni**, José Roberto TH087  
**Traaseth**, Nathaniel J MO061  
**Trbovic**, Nikola MO124  
**Trease**, Nicole M. OP101  
**Trebosc**, Julien TU140, TH141  
**Trellet**, Mikael UP130  
**Tretyakov**, Evgeny TH219, OP019  
**Trevizan**, Willian Andrighetto TH246, MO247, MO250  
**Trzeciak-Karlikowska**, Katarzyna TU083  
**Trébosc**, Julien UP036, MO139  
**Trésaugues**, Lionel UP007  
**Tse**, Ho Sum TU011  
**Tsimanis**, Alexander TU002  
**Tsuchida**, Jefferson Esquina TU065, TH237  
**Tsuchida**, Jefferson UP104  
**Tsutsumi**, Atsushi TU059  
**Tugarinov**, Vitali OP129  
**Tuna**, F. MO223  
**Turcu**, Flaviu R.V. UP099  
**Tuttle**, Marcus D. OP117  
**Tycko**, Robert PL002  
**Tzarfaty**, Galia UP140  
**Tzarfaty**, Ilan UP140  
**Täubert**, Sebastian TU122  
**Uchiyama**, Mayara Klimuk MO211  
**Ueda**, Kazuyoshi TU059  
**Ugurbil**, Kamil PL164  
**Ulzega**, Simone UP036  
**Umeyama**, Masako TU059  
**Unden**, Gottfried TU074  
**Unverzagt**, Carlo MO001  
**Vaiss**, Viviane da Silva TH084, TH090  
**Vajpai**, N. OP033  
**Vaknin**, David TH225  
**Valdés-Solis**, Maria José Iglesias TU185  
**Valente**, Ana Paula MO004, TH015, UP162, OP047, TU026, TH030, TH033, MO037, TU041, TH042, TU047, TH048, MO049, TH108, TH114, TH126, MO190, TU194, MO286  
**Valentine**, Kathleen G. UP111, MO298  
**Valezi**, Daniel Farinha MO220  
**Varani**, Luca TH042  
**Vargas**, Geovana TH042  
**Veber**, Sergey OP019  
**Vega**, Daniel TU158  
**Veglia**, Gianluigi OP030, MO061  
**Velez-Jurado**, A.K. TU167  
**Veloro**, Angelo M. OP074  
**Venancio**, Tiago TU284  
**Vendruscolo**, Michele UP131, TH129, MO130  
**Venâncio**, Tiago TH276  
**Vera**, I.M.S. de OP074  
**Verardi**, Raffaello MO061  
**Verly**, Rodrigo M. TH024, TU050  
**Verma**, Abhinav UP006  
**Viani**, Elisabetta UP116  
**Vicente**, Eduardo Festozo TH051, TU113  
**Vicentin**, Bruno Luiz Santana TU221

- Vidal**, Thaís Jerônimo TU035
- Vidoto**, Edson Luiz Gea TU209, TH210, TH243
- Vieira**, Fernando Henrique TH261
- Vieira**, Ygor W. TU281
- Vigneron**, Daniel B. OP040
- Vila**, Alejandro J. TU008, OP075, TH216, MO217
- Vilegas**, Wagner MO172
- Vilela**, Fabiana Cardoso MO172, MO172
- Vinaik**, Roohi MO022
- Vizthum**, Veronika UP036
- Voyer**, Normand TU062
- Vrielink**, Anneloes Oude UP017, TH294
- Véron**, Emmanuel OP038
- Wada**, Akimori UP088, TH288
- Wagner**, Gerhard TH036, TH120, OP113
- Walbrecker**, Jan O. OP096
- Walker**, F. Ann UP076
- Wallner**, Michael TH108
- Walls**, Jamie D. UP042
- Walsh**, David OP096
- Walter**, Eric D. TU245
- Walter**, Glenn A.
- Walter**, Korvin F. A. OP086
- Wand**, A. Joshua UP111, MO298
- Wang**, Conan OP160
- Wang**, Hao OP101
- Wang**, Qiang TU140, TH141
- Wang**, Qiu UP041
- Wang**, Shenlin MO118
- Wang**, Yulan MO157, MO178
- Wanker**, Erich E. OP070
- Warren**, Warren S. OP138, UP041
- Washington**, Jacqueline UP053
- Wasielewski**, Emeric TU023
- Wasylishen**, Roderick E. MO067
- Webber**, A. L. TH222, MO223
- Weber**, David J. TH006
- Wedge**, C. J. MO223
- Weingarth**, Markus UP136, TU119, TH291
- Weise**, Christoph TH012
- Wheeler**, Dustin MO145
- Wheeler**, Patrick TU161
- Whittaker**, Sara B-M. TH054
- Wiktor**, M. OP033
- Willbold**, Dieter OP055
- Williams**, Mark TH183
- Williamson**, R. Thomas OP118
- Wimperis**, Stephen OP035
- Winpenny**, R. E. P. MO223
- Wist**, Julien TH165, TU167
- Withers**, Richard S.
- Wolf-Watz**, Hans TH012
- Wolf-Watz**, Magnus UP006, TH012
- Wrachtrup**, Jörg OP157, OP105
- Wu**, Fangming TU014,
- Wunderlich**, Christoph MO121, TH123
- Wylde**, Richard OP127
- Xu**, Jun TU140
- Yamanaka**, D. MO052
- Yamauchi**, Seigo OP019
- Yan**, Si MO139
- Yang**, Bai TH162
- Yang**, Yong TH072
- Yau**, Wai-Ming PL002
- Ye**, Chaohui MO133
- Ying**, Jinfa OP132
- Yokota**, Hiroaki TH150
- Yomoda**, Hiroki UP088, TH288
- Yoshinari**, Yosuke TH150
- Yu**, Liping UP158
- Yu**, Xin OP043
- Yulikov**, Maxim TH234
- Yunes**, José Andrés MO196
- Zaballa**, María-Eugenia OP075
- Zagdoun**, Alexandre TH234, UP110, TU299
- Zanotto**, Edgar Dutra TU065
- Zell**, Mark T. TU275
- Zeng**, Haifeng OP109
- Zeri**, Ana Carolina de Mattos TU053, TH054, MO055, TU056, MO058, TU116, MO196, TU197, TH204
- Zeri**, Carolina de Mattos TH057
- Zhang**, Chenwei TU014
- Zhang**, Hongjun UP076
- Zhang**, Ji MO133
- Zhang**, Limin MO178, TU179
- Zhang**, Zhiyong TU137, TH138
- Zhong**, Guiming TH072
- Zhou**, Lina OP101
- Zhou**, Pei UP041
- Zhou**, Xin MO133
- Zhou**, Zijian OP138
- Zwart**, Jacco de OP142
- Zweckstetter**, Markus TU005, MO019, TH102
- Álvarez**, Gonzalo A OP122
- Åden**, Jörgen UP006
- šebera**, J. MO052

## Directory of Participants

**Afonso de Andre, Carlos**  
SPWLA  
MACAE, Brazil  
deandre@petrobras.com.br

**Abbotts, Frances T**  
BG E&P Brasil Ltda  
Rio de Janeiro, Brazil  
frances.abbotts@bg-group.com

**Abiko, Layara Akemi**  
University of São Paulo  
São Paulo, Brazil  
layara@usp.br

**Abrantes, Luiza T**  
Petroleo Brasileiro S.A  
Rio de Janeiro, Brazil  
luiza.abrantes@petrobras.com.br

**Acosta, Rodolfo H.**  
FAMAF-Universidad Nacional de  
Cordoba  
CORDOBA, Argentina  
racosta@famaf.unc.edu.ar

**Afonso, Luciana Caminha**  
Helmholtz Center Munich  
Neuherberg, Germany  
luciana.afonso@helmholtz-  
muenchen.de

**Aguiar, Daniel L.M.**  
Universidade Federal do Rio de  
Janeiro  
Rio de Janeiro, Brazil  
aguiardlm@iq.ufrj.br

**Ahola, Susanna**  
NMR Research Group, University of  
Oulu  
Oulu, Finland  
susanna.ahola@oulu.fi

**Ailion, David C**  
University of Utah  
Salt Lake City, United States  
dailion@physics.utah.edu

**Akoury, Elias**  
Max-Planck-Institute for Biophysical  
Chemistry  
Göttingen, Germany  
elak@nmr.mpiibpc.mpg.de

**AL, Susmitha**  
Tata Institute of Fundamental Re-  
search  
Mumbai, India  
susmitha.pmk@gmail.com

**Al-Hashimi, Hashim**  
University of Michigan  
Ann Arbor, Brazil  
hashimi@umich.edu

**Albernaz, Fabiana P.**  
Universidade Federal do Rio de  
Janeiro  
Rio de Janeiro, Brazil  
fabianalbernaz@gmail.com

**Alborghetti, Marcos R**  
Brazilian Biosciences National Labo-  
ratory - LNBio/CNPEM  
Campinas, Brazil  
marcos.alborghetti@lnbio.cnpem.br

**Alcantara, Glaucia B.**  
Universidade Federal de Mato Grosso  
do Sul  
Campo Grande, Brazil  
glabraz@yahoo.com.br

**Almeida, Fabio C.L.**  
Federal University of Rio de Janeiro  
Rio de Janeiro, Brazil  
fabioceneviva@gmail.com

**Alvares, Rohan**  
University of Toronto  
Mississauga, Canada  
rohan.alvares@mail.utoronto.ca

**Alves, Nathalia S**  
Universidade Federal do Rio de  
Janeiro  
Rio de Janeiro, Brazil  
nsalves@bioqmed.ufrj.br

**Alves da Cruz, Joao Felipe**  
Universidade Federal de São Carlos  
São Carlos, Brazil  
alves.joaof@gmail.com

**Alves Rodrigues, Diego A. R.**  
Universidade Federal de Goiás  
APARECIDA DE GOIÂNIA, Brazil  
rodrigues.quimica.rmn@hotmail.com

**Amata, Irene**  
Insitute for Research in Biomedicine  
(IRB) of Barcelona, and University  
of Barcelona  
Barcelona , Spain  
irene.amata@irbbarcelona.org

**Amorim, Gisele C**  
Centro Nacional de Ressonância  
Magnética Nuclear - Universidade  
Federal do Rio de Janeiro  
Rio de Janeiro, Brazil  
gamorim@cnrmn.bioqmed.ufrj.br

**Amoureux, Jean Paul**  
Lille University  
Villeneuve d'Ascq, France  
jean-paul.amoureux@univ-lille1.fr

**Andrade, Fabiana D**  
Institute of Physics of São Car-  
los/USP  
São Carlos , Brazil  
fabianadiuk@yahoo.com.br

**Andrade, Raphael H.S.**  
Universidade Federal de Pernambuco  
/ Instituto Federal de Educação,  
Ciência e Tecnologia de Perna  
Recife, Brazil  
profraphaelsoares@gmail.com

**Anglistter, Jacob**  
Weizmann Institute  
Rehovot, Israel  
Jacob.Anglistter@Weizmann.ac.il

**Arake, Luisa M**  
Embrapa Cenargen  
Brasilia, Brazil  
luisa.mayumi@gmail.com

**Araujo, Renata Mendonça**  
Universidade Federal do Ceará  
Natal, Brazil  
renat.onca@gmail.com

**Ardá, Ana**  
Centro de Investigaciones Biológicas-  
CSIC  
Madrid, Spain  
aarda@cib.csic.es

**Arthanari, Haribabu**  
Harvard Medical School  
Boston, United States  
hari@hms.harvard.edu

**Ascona, Christian Rivera**  
Instituto de Física de São Carlos -  
Universidade de São Paulo  
São Carlos, Brazil  
crivera@ursa.ifsc.usp.br

**Ashbrook, Sharon**  
University of St Andrews  
St Andrews, United Kingdom  
sema@st-andrews.ac.uk

**Auccaise, Ruben**  
Empresa Brasileira de Pesquisa  
Agropecuária  
Rio de Janeiro, Brazil  
rauccais@cbpf.br

**Auger, Michele**  
Universite Laval  
Quebec, Canada  
michele.auger@chm.ulaval.ca

**Azeredo, Rodrigo**  
Universidade Federal Fluminense  
Niteroi, Brazil  
rbagueira@vm.uff.br

**Azevedo, Clerio F**  
D'Or Institute for Research and Ed-  
ucation (IDOR)  
Rio de Janeiro, Brazil  
clerio.azevedo@gmail.com

**Azevedo, Graziella V T**  
Petróleo Brasileiro S.A  
rio de Janeiro, Brazil  
grazi@petrobras.com.br

**Bagryanskaya, Elena G.**  
Novosibirsk Institute of Organic  
Chemistry SB RAS  
Novosibirsk, Russia 166 Rwanda  
egbagryanskaya@nioch.nsc.ru

**Bai, Yang**

Nanyang Technological University,  
School of Biological Sciences  
singapore, Singapore  
yangbai80@gmail.com

**Baines, Victoria**

Schlumberger  
Rio de Janeiro, Brazil  
vbaines@slb.com

**Bajaj, Vikram**

University of California, Berkeley  
and Lawrence Berkeley National  
Laboratory  
Berkeley, United States  
vikbajaj@gmail.com

**Balbach, Jochen**

University of Halle  
Halle, Germany  
jochen.balbach@physik.uni-halle.de

**Balcom, Bruce J**

University of New Brunswick  
Fredericton, Canada  
bjb@unb.ca

**Barberis, Gaston E**

Instituto de Física UNICAMP  
Campinas, Brazil  
barberis@ifi.unicamp.br

**Barbet-Massin, Emeline**

Centre de RMN à Très Hauts  
Champs  
Villeurbanne, France  
emeline.barbetmassin@ens-lyon.fr

**Barbosa, Lúcio Leonel**

Federal University of Espírito Santo  
Vitória, Brazil  
luciolbar@gmail.com

**Barison, Andersson**

Paraná Federal University  
Curitiba, Brazil  
anderbarison@gmail.com

**Barros, Carlos J. P.**

Universidade Federal de Pernambuco  
Recife, Brazil  
carlos.pbarros@ufpe.br

**Barros Junior, Wilson**

Federal University of Pernambuco  
Recife, Brazil  
wilson@df.ufpe.br

**Basso, Luis GM**

University of Sao Paulo  
Sao Carlos, Brazil  
guilhermemansor@ursa.ifsc.usp.br

**Batista, Aline L.**

Universidade Federal do Rio de  
Janeiro  
Rio de Janeiro, Brazil  
aline\_alb12@yahoo.com.br

**Bax, Ad**

NIDDK, National Institutes of  
Health  
Bethesda, United States  
bax@nih.gov

**Belisle, Katherine**

Cambridge Isotope Laboratories,  
Inc.  
Andover, United States  
katherineb@isotope.com

**Bento, Edson de Souza**

Universidade Federal de Alagoas  
Maceio, Brazil  
edson.iqb@gmail.com

**Bernardinelli, Oigres Daniel**

USP IFSC  
São Carlos, Brazil  
oigres.daniel@gmail.com

**Bernardo, Camilla Nascimento**

Fundação e Instituto Oswaldo Cruz  
Rio de Janeiro, Brazil  
camilla\_nb@yahoo.com.br

**Billeter, Martin**

University of Gothenburg  
Gothenburg, Sweden  
martin.billeter@chem.gu.se

**Binolfi, Andres**

Leibniz-Institut für Molekulare  
Pharmakologie (FMP)  
Berlin, Germany  
binolfi@fmp-berlin.de

**Bize-Forest, Nadege**

Schlumberger  
Rio de Janeiro, Brazil  
NBize-forest@slb.com

**Blümich, Bernhard**

RWTH Aachen University  
Aachen, Germany  
bluemich@itmc.rwth-aachen.de

**Böckmann, Anja**

Institut de Biologie et Chimie des  
Protéines, CNRS-Université de Lyon  
Lyon, France  
a.boeckmann@ibcp.fr

**Bodenhausen, Geoffrey**

EPFL SB ISIC LRMB  
LAUSANNE, Switzerland  
geoffrey.bodenhausen@epfl.ch

**Boelens, Rolf**

Utrecht University  
Utrecht, Netherlands  
r.boelens@uu.nl

**Bonagamba, Tito José**

Instituto de Física de São Carlos -  
USP  
São Carlos, Brazil  
tito@ifsc.usp.br

**Bonfim, Rodrigo P F**

UFRJ  
Rio de Janeiro, Brazil  
rodrigobonfim@iq.ufrj.br

**Bonvin, Alexandre M.J.J.**

Utrecht University, Faculty of Sci-  
ence, Bijvoet Center  
Utrecht, Netherlands  
a.m.j.j.bonvin@uu.nl

**Borovskaya, Irina**

Schlumberger  
Rio de Janeiro, Brazil  
iborovskaya@slb.com

**Bouchard, Louis-Serge**

University of California, Los Angeles  
Los Angeles, United States  
louis.bouchard@gmail.com

**Boyd, Austin**

Schlumberger  
Rio de Janeiro, Brazil  
boyd2@exchange.slb.com

**Braide, Otonye**

University of Florida  
Gainesville, United States  
otonyebraide@gmail.com

**Brito, Luciana M.**

IMA-UFRJ  
Rio de Janeiro, Brazil  
lucianabrito@ima.ufrj.br

**Britt, R David**

University of California, Davis  
Davis, United States  
rdbritt@ucdavis.edu

**Brown, Steven P.**

University of Warwick  
Coventry, United Kingdom  
S.P.Brown@warwick.ac.uk

**Bruix, Marta**

IQFR-CSIC  
Madrid, Spain  
mbruix@iqfr.csic.es

**Bruschweiler, Rafael**

Florida State University and  
NHMFL  
Tallahassee, United States  
bruschweiler@magnet.fsu.edu

**Brutscher, Bernhard**

Institut de Biologie Structurale  
Grenoble, France  
bernhard.brutscher@ibs.fr

**Buarque Muller, Camilla Djenne**

Pontificia Universidade Católica do  
Rio de Janeiro  
Rio de Janeiro, Brazil  
camilla-buarque@puc-rio.br

**Budker, Dmitry**

University of California at Berkeley  
Berkeley, United States  
budker@berkeley.edu

**Buljubasich, Lisandro**

Fa.M.A.F.-IFEG, Córdoba-  
Argentina  
Córdoba, Argentina  
lbuljubasich@gmail.com

**Burai, Laszlo**

Servier Research Institute of Medicinal Chemistry  
Budapest, Hungary  
laszlo.burai@hu.netgrs.com

**Burdisso, Paula**

Instituto de Biología Molecular y Celular de Rosario  
Rosario, Argentina  
burdisso@ibr-conicet.gov.ar

**Byeon, Chang-Hyeock**

University of Pittsburgh  
Pittsburgh, United States  
chb49@pitt.edu

**Byeon, In-Ja L**

University of Pittsburgh  
Pittsburgh, United States  
ilb6@pitt.edu

**Cabrita, Eurico J**

REQUIMTE, Faculdade de Ciências e Tecnologia - UNL  
Caparica, Portugal  
ejc@fct.unl.pt

**Caldarelli, Stefano**

ICSN CNRS UPR 2301  
PALAISEAU, France  
s.caldarelli@univ-amu.fr

**Calderon, Cesar J**

UNICAMP  
Campinas, Brazil  
cesinhacalderon@gmail.com

**Camilloni, Carlo**

University of Cambridge  
Cambridge, United Kingdom  
cc536@cam.ac.uk

**Cañada, Francisco Javier**

Centro Investigaciones Biológicas, CIB CSIC  
Madrid, Spain  
jcanada@cib.csic.es

**Canevarolo, Rafael R**

Laboratório Nacional de Biociências  
Campinas, Brazil  
rafaelcanevarolo@gmail.com

**Cappellaro, Paola**

Massachusetts Institute of Technology  
Cambridge, United States  
pcappell@mit.edu

**Carneiro, Giovanna**

Schlumberger  
Rio de Janeiro, Brazil  
gcarneiro2@slb.com

**Carneiro, Sandra R R**

Petrobras  
Rio de Janeiro, Brazil  
sandra\_carneiro@petrobras.com.br

**Carosio, Maria G. A.**

Institute of Chemistry of São Carlos  
São Carlos, Brazil  
m.gabbiini@gmail.com

**Carpinella, Mariela**

FaMAF CONICET - Universidad Nacional de Córdoba, Argentina  
Córdoba, Argentina  
mariela.carpinella@gmail.com

**Carvalho, André S**

Universidade Federal de São Carlos  
São Carlos, Brazil  
scarvalho.andre@gmail.com

**Cassús, Eduardo P**

Petróleo Brasileiro S.A.  
Rio de Janeiro, Brazil  
edu.cassus@gmail.com

**Castañeda, Ivan Erick Ivan E.**

Universidad Autónoma del Estado de Morelos  
Cuernavaca, Mexico  
ivanecr@gmail.com

**Castañeda Valencia, Gloria Maria**

Iris Valencia Rivera  
Rio de Janeiro, Brazil  
lubili6@hotmail.com

**Castellen, Patricia**

LN Bio  
Campinas, Brazil  
patricia.castellen@lnbio.cnpem.br

**Catoire, Laurent J**

CNRS - IBPC  
Paris, France  
laurent.catoire@ibpc.fr

**Cavini, Ítalo A**

Instituto de Física de São Carlos - USP  
São Carlos, Brazil  
italo.cavini@usp.br

**Cerioni, Lucas M C**

Spinlock SRL - CONICET  
Cordoba, Argentina  
lcerioni@nmr-spectrometers.com

**Chattah, Ana K**

FaMAF and CONICET, Cordoba, Argentina  
Córdoba, Argentina  
kchattah@gmail.com

**Chaykovsky, Mark**

Bruker do Brasil  
Atibaia, Brazil  
Mark.Chaykovsky@bruker-biospin.com

**Chinelatto-Júnior, Luiz S**

Petróleo Brasileiro S.A.  
Rio de Janeiro, Brazil  
lsilvino@petrobras.com.br

**Chira, Pedro O**

Halliburton  
Rio de Janeiro, Brazil  
pedro.chira@halliburton.com

**Chmelka, Bradley F**

University of California, Santa Barbara  
Santa Barbara, United States  
bradc@engineering.ucsb.edu

**Cho, Jee-Hyun**

Korea Basic Science Institute  
Ochang-eup, South Korea  
jhcho@kbsi.re.kr

**Cobas Gomez, Carlos**

MESTRELAB RESEARCH, S.L.  
Santiago de Compostela, Spain  
carlos@mestrelab.com

**Cole, Jonathan**

Cryogenic Ltd.  
London, United Kingdom  
jonathan04.cole@gmail.com

**Colnago, Luiz Alberto**

Embrapa  
São Carlos, Brazil  
colnago@cnpdia.embrapa.br

**Correia, Maury D**

Petrobras  
Rio de Janeiro, Brazil  
maury.duarte@petrobras.com.br

**Corvo, Marta**

REQUIMTE, CQFB  
Caparica, Portugal  
marta.corvo@fct.unl.pt

**Costa-Filho, Antonio J**

University of São Paulo  
Ribeirão Preto, Brazil  
ajcosta@ffclrp.usp.br

**Cowsik, Sudha M**

Jawaharlal Nehru University, New Delhi  
New Delhi, India  
scowsik@gmail.com

**Coy, Andrew**

Magritek  
Wellington, New Zealand  
andrew@magritek.com

**Craik, David J**

The University of Queensland  
Brisbane, Australia  
d.craik@imb.uq.edu.au

**Crossley, Nigel**

Oxford Instruments  
Abingdon, United Kingdom  
nigel.crossley@oxinst.com

**Crusca, Edson**

University of São Paulo  
São Carlos, Brazil  
ecrusca@gmail.com

**Cvitanic, Tonci**

University of Zagreb  
Zagreb, Croatia  
tcvitanic@phy.hr

**D'Andréa, Éverton Dias**  
Universidade Federal do Rio de Janeiro  
Rio de Janeiro, Brazil  
evertondandrea@gmail.com

**da Silva, Gil V. J.**  
FFCLRP / University of São Paulo  
Ribeirão Preto, Brazil  
gvjdsilv@usp.br

**da Silva, Milton N.**  
Instituto de Tecnologia em Imunobiológicos  
RIO DE JANEIRO, Brazil  
milton@bio.fiocruz.br

**Darbello, Daniel de Menezes**  
Laboratório Nacional de Biociências  
Campinas, Brazil  
ddarbello@yahoo.com.br

**de Araujo Ferreira, Arthur G**  
Instituto de Física de São Carlos  
São Carlos, Brazil  
arthurferreira@gmail.com

**de Azevedo, Eduardo R**  
Universidade de São Paulo  
São Carlos - SP, Brazil  
azevedo@ifsc.usp.br

**de Carvalho, Erika Martins**  
Instituto de Tecnologia em Farmacos  
Rio de Janeiro, Brazil  
erikamc@far.fiocruz.br

**de Carvalho, Mário Geraldo**  
Universidade Federal Rural do Rio de Janeiro  
Seropédica, Brazil  
mgeraldo@ufrj.br

**De Goitia, Adriana Mendes**  
PUC-RIO  
Rio De Janeiro, Brazil  
asmendes.puc@petrobras.com.br

**de Oliveira, Guilherme A. P.**  
Federal University of Rio de Janeiro  
Rio de Janeiro, Brazil  
mrguiba@superig.com.br

**de Oliveira, Livia R. P.**  
Universidade Federal do Rio de Janeiro - Faculdade de Odontologia  
Rio de Janeiro, Brazil  
liviarioberta@yahoo.com.br

**de Paula, Viviane S**  
Universidade Federal do Rio de Janeiro  
Rio de Janeiro, Brazil  
vpaula@cnrmn.bioqmed.ufrj.br

**de Souza, João Carlos**  
Agilent Technologies  
Barueri, Brazil  
joao.souza@agilent.com

**de Souza Filho, Jose D**  
Universidade Federal de Minas Gerais  
Belo Horizonte, Brazil  
peixe@ufmg.br

**Della Vecchia, Miguel A**  
Instituto Nacional de Tecnología Industrial  
San Martín, Argentina  
miguel.della.vecchia@gmail.com

**Deng, Feng**  
Wuhan Institute of Physics and Mathematics, Chinese Academy of Sciences  
Wuhan, People's Republic of China  
dengf@wipm.ac.cn

**Deslauriers, Roxanne**  
iRDs  
Headingley, Canada  
Roxanne.Deslauriers@gmail.com

**Di Mauro, Eduardo**  
Universidade Estadual de Londrina  
LONDRINA, Brazil  
dimauro@uel.br

**Dias, David M**  
University of Cambridge  
Cambridge, United Kingdom  
dmgfd2@cam.ac.uk

**Dinse, Klaus-Peter**  
Physics Dept. FU Berlin Germany  
Berlin, Germany  
dinse@physik.fu-berlin.de

**Doty, Francis David**  
Doty Scientific, Inc.  
Columbia, United States  
david@dotynmr.com

**Doty, Judy**  
Doty Scientific, Inc.  
Columbia, United States  
judy@dotynmr.com

**Driehuys, Bastiaan**  
Duke University  
Durham, United States  
bastiaan.driehuys@duke.edu

**Duckett, Simon B**  
University of York  
York, United Kingdom  
simon.duckett@york.ac.uk

**Duyn, Jeff H**  
National Institutes of Health, USA  
Bethesda, United States  
jhd@helix.nih.gov

**Eckert, Hellmut**  
IFSC, University of São Paulo  
São Carlos, Brazil  
eckert@ifsc.usp.br

**Edwards, John C**  
Process NMR Associates  
Danbury, United States  
john@process-nmr.com

**El-Bacha, Tatiana**  
Universidade Federal do Rio de Janeiro  
Rio de Janeiro, Brazil  
elbachat@gmail.com

**Emwas, Abdul-Hamid M**  
King Abdullah University of Science and Technology  
Thuwal, Saudi Arabia  
abdelhamid.emwas@kaust.edu.sa

**Engelsberg, Mario**  
Universidade Federal de Pernambuco  
Recife, Brazil  
mario@df.ufpe.br

**Escobar, Rodolfo**  
Halliburton  
Rio de Janeiro, Brazil  
rodolfo.escobar@halliburton.com

**Espindola, Ana Paula**  
Ana Paula Espindola  
Barueri, Brazil  
ana-paula.espindola@agilent.com

**Espinoza Cara, Andrés**  
Instituto de Biología Molecular y Celular de Rosario  
Rosario, Argentina  
espinoza@ibr-conicet.gov.ar

**Falco Cobra, Paulo**  
Instituto de Química de São Carlos, Universidade de São Paulo  
São Carlos, Brazil  
paulofcobra@gmail.com

**Fam, Maged**  
Halliburton  
Bogota, Colombia  
maged.fam@halliburton.com

**Fanucci, Gail E**  
University of Florida  
Gainesville, United States  
fanucci@chem.ufl.edu

**Farias, Fábio LL**  
Petróleo Brasileiro SA  
Rio De Janeiro, Brazil  
pardal\_fabio@yahoo.com.br

**Favaro, Denize C.**  
University of São Paulo  
São Paulo, Brazil  
favarodenize@gmail.com

**Fedin, Matvey V.**  
International Tomography Center SB RAS  
Novosibirsk, Russia 166  
mfedin@tomo.nsc.ru

**Felli, Isabella C.**  
CERM, University of Florence, Italy  
Sesto Fiorentino (Florence), Italy  
felli@cerm.unifi.it

**Feng, Yesu**  
Duke University  
Durham, United States  
yesu.feng@duke.edu



**Fernandez, Cesar**  
Novartis Pharma AG  
Basel, Switzerland  
cesar.fernandez@novartis.com

**Fernandez, Claudio Oscar**  
Universidad Nacional de Rosario, Instituto de Biología Molecular y Celular de Rosario  
Rosario, Argentina  
fernandez@ibr.gov.ar

**Ferraris, Paolo**  
Schlumberger  
Rio de Janeiro, Brazil  
ferraris@slb.com

**Ferraz, Erica K P**  
Petrobras S.A.  
Macaé, Brazil  
erica.kato@petrobras.com.br

**Ferreira, Antonio Gilberto**  
Federal University of São Carlos  
São Carlos, Brazil  
GIBA\_04@YAHOO.COM.BR

**Ferreira, Bárbara D**  
UFMG - Universidade Federal de Minas Gerais  
Belo Horizonte, Brazil  
barbaralelis@hotmail.com

**Ferreira, Fernanda G Meireles**  
Centro Nacional de Bioimagem  
Rio de Janeiro, Brazil  
nandagmferreira@gmail.com

**Ferreira, Matheus E**  
Instituto Nacional de Ciência e Tecnologia de Biologia Estrutural e Bioimagem  
Rio de Janeiro, Brazil  
matheustec92@gmail.com

**Ferreira, Rodrigo Alexandre**  
**Ferreira Alexandre**  
Universidade Federal de Goiás  
Goiânia, Brazil  
rodrigoufgaf@gmail.com

**Ferreira Neto, Denise C.**  
Instituto Militar de Engenharia  
Rio de Janeiro, Brazil  
denisecristian@gmail.com

**Fiat, Daniel**  
University of Illinois at Chicago  
Chicago, United States  
d6336f@gmail.com

**Fidalgo, Tatiana KS**  
Federal University of Rio de Janeiro  
Niterói, Brazil  
tatianaksfidalgo@gmail.com

**Figueira, Elza Cristina S**  
Instituto de Tecnologia em Imunobiológicos  
Rio de Janeiro, Brazil  
marcela.soares@bio.fiocruz.br

**Figuerola-Villar, José D**  
Military Institute of Engineering  
Rio de Janeiro, Brazil  
jdfv2009@gmail.com

**Finkelstein-Shapiro, Daniel**  
Arizona State University  
Evanston, United States  
d-finkelstein-shapiro@northwestern.edu

**Florian, Pierre**  
CEMHTI-CNRS  
Orléans, France  
pierre.florian@cnrs-orleans.fr

**Foster, Mark P**  
The Ohio State University  
Columbus, United States  
foster.281@osu.edu

**França, Camila**  
BG Group  
Rio de Janeiro, Brazil  
camila.franca@bg-group.com

**França, José Adonias**  
Universidade Federal de Pernambuco  
Recife, Brazil  
adonias.jf@gmail.com

**Fredriksson, Jonas MB**  
Gothenburg University Sweden  
Gothenburg, Sweden  
jonas.mb@gmail.com

**Freed, Jack H**  
Cornell University  
Ithaca, United States  
jhf3@cornell.edu

**Freire, Ronaldo C**  
Petrobras  
Rio de Janeiro, Brazil  
ronaldocfreire@petrobras.com.br

**Freitas, Daniel**  
Merck Millipore  
Rio de Janeiro, Brazil  
daniel.freitas@merckgroup.com

**Freitas, Deisy S.**  
Universidade Federal de Mato Grosso do Sul  
Campo Grande, Brazil  
deisysantos89@yahoo.com.br

**Freitas, Jair C C**  
Department of Physics, Federal University of Espírito Santo (UFES)  
Vitória, Brazil  
jairecfreitas@yahoo.com.br

**Freitas, Mônica Santos de**  
Universidade Federal do Rio De Janeiro  
Rio de Janeiro, Brazil  
msfreitas@bioqmed.ufrj.br

**Freitas-Fernandes, Liana B**  
Federal University of Rio de Janeiro  
Rio de Janeiro, Brazil  
liana.fernandes@clinicaeso.com.br

**Frey, Michael**  
JEOL USA, Inc  
Peabody, United States  
frey@jeol.com

**Frizzo, Clarissa P.**  
Universidade Federal de Santa Maria  
Santa Maria, Brazil  
clarissa.frizzo@yahoo.com.br

**Frydman, Lucio**  
Weizmann Institute  
Rehovot, Israel  
lucio.frydman@weizmann.ac.il

**Fu, Riqiang**  
Nat'l High Magnetic Field Lab  
Tallahassee, United States  
rfu@magnet.fsu.edu

**Funk, Alexander M**  
Durham University  
Durham, United Kingdom  
a.m.funk@durham.ac.uk

**Gaffney, Betty J.**  
Florida State University  
Tallahassee, United States  
gaffney@bio.fsu.edu

**Galiana, Gigi**  
Yale University  
New Haven, United States  
gigi.galiana@yale.edu

**Gambarra-Neto, Francisco F.**  
Universidade Federal de Goiás  
Goiânia, Brazil  
chicogambarra@gmail.com

**Garbacz, Piotr**  
University of Warsaw  
Warsaw, Poland  
pgarbacz@chem.uw.edu.pl

**García Mayoral, María Flor**  
Instituto de Química Física Rocasolano, Consejo Superior de Investigaciones Científicas  
Madrid, Spain  
mgarcia@iqfr.csic.es

**Garro Linck, Yamila**  
RWTH Aachen University  
Aachen, Germany  
yamigarro@gmail.com

**Garwood, Michael**  
University of Minnesota  
Minneapolis, United States  
gar@cmrr.umn.edu

**Gataullin, Eduard M.**  
Kazan (Volga Region) Federal University  
Kazan, Russia 166 Rwanda  
edikgat@gmail.com

**Geraldes, Carlos F.**  
University of Coimbra  
Coimbra, Portugal  
geraldes@ci.uc.pt

**Ghiviriga, Ion**

University of Florida  
Gainesville, United States  
ion@chem.ufl.edu

**Ghose, Ranajeet**

City University of New York  
New York, United States  
rghose@ghoselab.org

**Gil, Ana M**

University of Aveiro  
Aveiro, Portugal  
agil@ua.pt

**Gil, Roberto R.**

Carnegie Mellon University  
Pittsburgh, United States  
rgil@andrew.cmu.edu

**Gimbaud, Sylvain**

Bruker do Brasil  
Atibaia, Brazil  
Sylvain.Guimbaud@bruker.de

**Giotto, Marcus**

University of Connecticut  
STORRS, United States  
mgiotto@ims.uconn.edu

**Gladden, Lynn F**

University of Cambridge  
Cambridge, United Kingdom  
lfg1@cam.ac.uk

**Goldfarb, Daniella**

Weizmann Institute of Science  
Rehovot, Israel  
daniella.goldfarb@weizmann.ac.il

**Gomes, Bruna F**

Universidade de São Paulo  
SÃO CARLOS, Brazil  
brunalusp@gmail.com

**Gomes, Rosana Garrido**

Pontifícia Universidade Católica do  
Rio de Janeiro  
Rio de Janeiro, Brazil  
rosanagg@puc-rio.br

**Goncalves, Eduardo Correa**

Universidade Federal Fluminense  
Niteroi, Brazil  
ecgrj@ig.com.br

**González, Carlos**

Instituto de Química Física Rocasolano - CSIC  
Madrid, Spain  
cgonzalez@iqfr.csic.es

**Gonzalez, Mariano M.**

IBR - CONICET  
Rosario, Argentina  
mgonzalez@ibr-conicet.gov.ar

**González-Pérez, Martha**

Instituto de Pesquisas Tecnológicas  
São Paulo, Brazil  
marthagperez22@gmail.com

**Gore, John C**

Vanderbilt University  
Nashville, United States  
john.gore@vanderbilt.edu

**Grandinetti, Philip**

Ohio State University  
Columbus, United States  
grandinetti.1@osu.edu

**Graterol Parodi, Jussell J**

Rio de Janeiro, Brazil  
jussellg@hotmail.com

**Green, Derrick**

Green Imaging Technologies  
Fredericton, Canada  
Derrick.Green@GreenImaging.com

**Grey, Clare P**

University of Cambridge  
Cambridge, United Kingdom  
cpg27@cam.ac.uk

**Griesinger, Christian**

Max-Planck-Institute for Biophysical  
Chemistry  
Goettingen, Germany  
sekr@nmr.mpibpc.mpg.de

**Griffin, Robert G.**

Massachusetts Institute of Technology  
Cambridge, United States  
rgg@mit.edu

**Gromov, Igor**

Bruker do Brasil  
Atibaia, Brazil  
igor.gromov@bruker-biospin.de

**Gronenborn, Angela M.**

University of Pittsburgh School of  
Medicine  
Pittsburgh, United States  
amg100@pitt.edu

**Grunewald, Elliot**

Vista Clara, Inc.  
Mukilteo, United States  
elliott@vista-clara.com

**Grunin, Leonid**

CEO of Resonance Systems Ltd.  
Yoshkar-Ola, Russia 166 Rwanda  
mobilenmr@hotmail.com

**Grzesiek, Stephan**

University of Basel  
Basel, Switzerland  
stephan.grzesiek@unibas.ch

**Guenther, Ulrich L**

University of Birmingham  
Birmingham, United Kingdom  
u.l.gunther@bham.ac.uk

**Guittet, Eric**

CNRS-ICSN  
Gif sur Yvette, France  
guittet@icsn.cnrs-gif.fr

**Gusmao, Karla A G**

Universidade Federal de Minas  
Gerais  
Belo Horizonte, Brazil  
karlaagg@hotmail.com

**Hallwass, Fernando**

Universidade Federal de Pernambuco  
Recife, Brazil  
hallwass@ufpe.br

**Han, Oc Hee**

Korea Basic Science Institute  
Daegu, South Korea  
ohhan@kbsi.re.kr

**Han, Songi**

Department of Chemistry and Biochemistry, University of California  
Santa Barbara  
Santa Barbara, United States  
songi@chem.ucsb.edu

**Hansen, Michael Ryan**

Max-Planck-Institute for Polymer  
Research  
Mainz, Germany  
mrh@mpip-mainz.mpg.de

**Hård, Torleif**

Swedish University of Agricultural  
Sciences  
Uppsala, Sweden  
torleif.hard@slu.se

**Hayes, Sophia E**

Washington University  
Saint Louis, United States  
hayes@wustl.edu

**He, Yao**

University of Science and Technology  
of China  
Hefei, People's Republic of China  
heyao@mail.ustc.edu.cn

**Herrera, Ricardo**

Halliburton  
Rio de Janeiro, Brazil  
ricardo.herrera@halliburton.com

**Hilty, Christian**

Texas A&M University  
College Station, United States  
chilty@chem.tamu.edu

**Hinderberger, Dariush**

Max Planck Institute for Polymer  
Research  
Mainz, Germany  
dariush.hinderberger@mpip-mainz.mpg.de

**HONG, Kwan Soo**

Korea Basic Science Institute  
Cheongwon, South Korea  
kshong@kbsi.re.kr

**Hong, Mei**

Iowa State University  
Ames, United States  
mhong@iastate.edu

**Honorato, Hercilio D. A.**

Petrobras  
Rio de Janeiro, Brazil  
herciliodeangeli@yahoo.com.br

**Hosur, Ramakrishna V**

Tata Institute of Fundamental Research  
Mumbai, India  
hosur@tifr.res.in

**Hurlimann, Martin**

Schlumberger - Doll Research  
Cambridge, United States  
hurlimann@slb.com

**Iglesias, Marfa José**

Universidad de Almería  
Almería, Spain  
mjigle@ual.es

**Iqbal, Anwar**

Federal University of Rio de Janeiro  
Rio de Janeiro, Brazil  
anwar@cnrmn.bioqmed.ufrj.br

**Iulianelli, Gisele Cristina Valle**

Universidade Federal do Rio de Janeiro  
Rio de Janeiro, Brazil  
gisele@ima.ufrj.br

**Ivanshin, Vladimir A.**

Kazan (Volga Region) Federal University  
Kazan, Russia 166 Rwanda  
Vladimir.Ivanshin@ksu.ru

**Izadi-Pruneyre, Nadia**

Institut Pasteur  
Paris, France  
nadia.izadi-pruneyre@pasteur.fr

**Jackowski, Karol**

Faculty of Chemistry, University of Warsaw, Poland  
Warszawa, Poland  
kjack@chem.uw.edu.pl

**Jaen, Damaris Quesada**

Bruker do Brasil  
Atibaia, Brazil  
damaris.jaen@bruker.com.br

**Jain, Sheetal Kumar**

Aarhus University  
Aarhus, Denmark  
sheetaliiser@gmail.com

**Jaremko, Lukasz**

Max Planck Institute for Biophysical Chemistry  
Goettingen, Germany  
jaremko@gmail.com

**Jaremko, Mariusz**

Max Planck Institute for Biophysical Chemistry  
Goettingen, Germany  
antypater@gmail.com

**Jaroniec, Christopher P**

Ohio State University  
Columbus, United States  
jaroniec.1@osu.edu

**Jayaseelan, Kalai**

EMBL-EBI  
Cambridge, United Kingdom  
kalai@ebi.ac.uk

**Jegade, Olamide M**

BG E&P Brasil Ltda  
Rio de Janeiro, Brazil  
olamide.jegade@bg-group.com

**Jerschow, Alexej**

New York University  
New York, United States  
alexej.jerschow@nyu.edu

**Jeschke, Gunnar**

ETH Zurich  
Zurich, Switzerland  
gjeschke@ethz.ch

**Jimenez-Barbero, Jesus**

Centro de Investigaciones Biológicas, CSIC  
MADRID, Spain  
jjbarbero@cib.csic.es

**Jonaitis, Ivan**

Agilent Technologies  
Barueri, Brazil  
ivan\_jonaitis@agilent.com

**Jones, Oliver A.H.**

RMIT University  
Melbourne, Australia  
oliver.jones@rmit.edu.au

**Júnior, Gilson S**

Petrobras  
Rio de Janeiro, Brazil  
gilsonjunior@outlook.com

**Junker, Jochen**

Fundação Oswaldo Cruz  
Rio de Janeiro, Brazil  
junker@cdts.fiocruz.br

**Kaminski, Danielle**

University of Oxford  
Oxford, United Kingdom  
danielle.kaminski@physics.ox.ac.uk

**Kannan, Arvind**

Cambridge University  
Cambridge, United Kingdom  
ak782@cam.ac.uk

**Kaptein, Robert**

Utrecht University  
Culemborg, Netherlands  
r.kaptein@uu.nl

**Karipidis, Taisiya K**

OAO Gazprom do Brasil  
Rio de Janeiro, Brazil  
taisiya.karipidis@gmail.com

**Kawamori, Asako**

AGAPE-Kabutoyama Institute of Medicine  
Nishinomiya, Japan  
agape-kawa@nifty.com

**Kerssebaum, Rainer**

Bruker do Brasil  
Atibaia, Brazil  
Rainer.Kerssebaum@bruker-biospin.de

**Khetrapal, C L**

Centre of Biomedical Magnetic Resonance  
Lucknow, India  
clkhetrapal@hotmail.com

**Khrantsov, Valery V**

The Ohio State University  
Columbus, United States  
valery.khrantsov@osumc.edu

**Kikuchi, Jun**

RIKEN  
Yokohama, Japan  
kikuchi@psc.riken.jp

**Kikuchi, Marcelo M**

Petrobras  
Santos, Brazil  
massaru@petrobras.com.br

**Killner, Mario H. M.**

Instituto de Química Unicamp  
Campinas, Brazil  
killner.mario@gmail.com

**Kim, Hyun Min**

Korea Basic Science Institute  
Cheongwon-Gun, Chungbook, South Korea  
khm84@kbsi.re.kr

**Kim, Yongae**

Hankuk University of Foreign Studies  
Yong-In, South Korea  
yakim@hufs.ac.kr

**King, Scott P**

University of Warwick  
Coventry, United Kingdom  
scott.king@warwick.ac.uk

**Kock, Flávio Vinicius Crizóstomo**

Universidade Federal do Espírito Santo  
Conceição da Barra, Brazil  
kock.flavio@gmail.com

**Kockenberger, Walter**

University of Nottingham  
Nottingham, United Kingdom  
walter.kockenberger@nottingham.ac.uk

**Koretsky, Alan P.**

NIH, NINDS, LFMI  
Bethesda, United States  
paza@mail.nih.gov

**Korzhnev, Dmitry M.**  
University of Connecticut Health  
Center  
Farmington, United States  
korzhniev@uchc.edu

**Kovacs, Helena**  
Bruker BioSpin  
Fällanden, Switzerland  
helena.kovacs@bruker.ch

**Kozlov, Guennadi**  
McGill University  
Montreal, Canada  
guennadi.kozlov@mcgill.ca

**Kuchel, Philip W**  
University of Sydney  
Sydney, Australia  
philip.kuchel@sydney.edu.au

**Kukic, Predrag**  
University of Cambridge, UK  
Cambridge, United Kingdom  
pk397@cam.ac.uk

**Kulminkaya, Natalia V**  
Aarhus University  
Aarhus, Denmark  
nk@chem.au.dk

**Kupce, Eriks**  
Bruker Ltd.  
Coventry, United Kingdom  
eriks.kupce@bruker.co.uk

**Lacerda Jr., Valdemar**  
Departamento de Química, Centro  
de Ciências Exatas, Universidade  
Federal do Espírito Santo  
Vitória, Brazil  
vljuniorqui@gmail.com

**Ladizhansky, Vlad**  
University of Guelph  
Guelph, Canada  
vladizha@uoguelph.ca

**Laker, Timothy J**  
Sigma-Aldrich  
Miamisburg, United States  
timothy.laker@sial.com

**Lange, Adam**  
Max Planck Institute for Biophysical  
Chemistry, Goettingen  
Goettingen, Germany  
adla@nmr.mpiibpc.mpg.de

**Latorre, Leandro**  
Advanced Chemistry Development,  
Inc. (ACD/Labs)  
Toronto, Canada  
leandro.latorre@acdlabs.com

**Lázaro Martínez, Juan M.**  
CONICET & Universidad de Buenos  
Aires  
Ciudad Autónoma de Buenos Aires,  
Argentina  
jmlazaromartinez@gmail.com

**Lee, Hyunseung**  
Korea Basic Science Institute  
Chungcheungbuk-Do, South Korea  
hsys0307@kbsi.re.kr

**Lehmann-Horn, Jochen A**  
CSIRO  
Lucas Heights, Australia  
jochen.lehmann-horn@csiro.au

**Lelli, Moreno**  
CNRS/ENS Lyon/UNiversité Lyon-1  
Villeurbanne, France  
Moreno.Lelli@ens-lyon.fr

**Levitt, Malcolm H**  
University of Southampton, UK  
Southampton, United Kingdom  
mhl@soton.ac.uk

**Li, Zhao**  
University of California, Los Angeles  
Los Angeles, United States  
zhaoli@chem.ucla.edu

**Liao, Luciano M**  
Universidade Federal de Goiás  
Goiânia, Brazil  
luciano@quimica.ufg.br

**Lima, Nerilson Marques**  
Núcleo de Bioensaios, Biossintese e  
Ecofisiologia de Produtos Naturais -  
Instituto de Química  
Araraquara, Brazil  
nerilsonmarques@gmail.com

**Lin, Yung-Ya**  
University of California, Los Angeles  
Los Angeles, United States  
yylin@chem.ucla.edu

**Lin, Zhongjie**  
University of Warwick  
Coventry, United Kingdom  
Z-J.Lin@warwick.ac.uk

**Lins, Fernando**  
SIGMA-ALDRICH  
Sao Paulo, Brazil  
fernando.lins@sial.com

**Linser, Rasmus J**  
UNSW Sydney & Harvard Medical  
School Boston  
Sydney, Australia  
rasmus\_linser@hms.harvard.edu

**Llases, Marfa Eugenia**  
Institute of Molecular and Cell Biol-  
ogy of Rosario; Max-Planck Labora-  
tory of Rosario  
Rosario, Argentina  
llases@ibr-conicet.gov.ar

**Lopes, Thiago I.B**  
Universidade Estadual de Campinas  
Campinas, Brazil  
inacio\_thiago@hotmail.com

**Lopes, Thierry R**  
Universidade Federal do Espírito  
Santo  
Serra, Brazil  
thierryrl@gmail.com

**López Castilla, Aracelys**  
Universidade Federal do Rio de  
Janeiro  
Rio de Janeiro, Brazil  
aracelyslopez@gmail.com

**López Ortiz, Fernando**  
Universidad de Almería  
Almería, Spain  
flortiz@ual.es

**Luchinat, Claudio**  
CERM University of Florence - Italy  
Sesto Fiorentino, Italy  
luchinat@cern.unifi.it

**Luy, Burkhard**  
Karlsruhe Institute of Technology  
(KIT)  
Karlsruhe, Germany  
Burkhard.Luy@kit.edu

**Machado, Luciana ESF**  
Universidade Federal do Rio de  
Janeiro  
Rio de Janeiro, Brazil  
lmachado@cnrmn.bioqmed.ufrj.br

**Machado, Vinicius**  
Petrobras S.A.  
Rio de Janeiro, Brazil  
viniciusfm@petrobras.com.br

**Madhu, Perunthiruthy**  
TIFR, Mumbai, India  
Colaba, Mumbai, India  
madhu@tifr.res.in

**Mafra, Luís**  
University of Aveiro (CICECO labo-  
ratory)  
Aveiro, Portugal  
lmafra@ua.pt

**Magalhaes, Mariana T.Q.**  
Universidade Federal do Rio de  
Janeiro  
Rio de Janeiro, Brazil  
mariana.quezado@gmail.com

**Magon, Claudio J**  
Instituto de Física de São Carlos -  
Universidade de São Paulo  
São Carlos, Brazil  
magon@ifsc.usp.br

**Manrao, Suraj P**  
Isotec Stable Isotope Group  
Old Bridge, United States  
surajmanra@aol.com

**Marassi, Francesca M**  
Sanford-Burnham Medical Research  
Institute  
La Jolla, United States  
fmarassi@sbmri.org

**Marathias , Bill**

Agilent Technologies  
Barueri , Brazil  
bill.marathias@agilent.com

**Marchi Netto, Antonio**

Rheinisch-Westfaelische Technische  
Hochschule Aachen  
Aachen, Germany  
nettomarchi@gmail.com

**Marco-Rius, Irene**

University of Cambridge and Cancer  
Research UK  
Cambridge, United Kingdom  
im351@cam.ac.uk

**Marsaioli, Anita J**

Chemistry Institute - University of  
Campinas  
Campinas, Brazil  
anita@iqm.unicamp.br

**Martin, Gary E.**

Merck Research Laboratories  
Summit, United States  
lighthousephoto@gmail.com

**Martins, Gabriel R**

Universidade Federal Rio de Janeiro  
Rio de Janeiro, Brazil  
gabrielmartins@gmail.com

**Medeiros, Murilo T**

BG E&P Brasil Ltda  
Rio de Janeiro, Brazil  
murilo.medeiros@bg-group.com

**Meguellatni, Sylvain**

Bruker do Brasil  
Atibaia, Brazil  
Sylvain.Meguellatni@bruker-biospin.de

**Meier, Beat**

ETH Zurich  
Zurich, Switzerland  
beme@ethz.ch

**Menezes, Rachel S**

Universidade Federal do Rio de  
Janeiro  
Rio de Janeiro, Brazil  
kelmenezes@hotmail.com

**Menezes, Sonia Cabral de**

Petrobras S.A.  
Rio de Janeiro, Brazil  
soniac@petrobras.com.br

**Meriles, Carlos A**

City College of New York - CUNY  
New York, United States  
cmeriles@sci.cuny.cuny.edu

**Millet, Oscar**

CIC bioGUNE  
Derio, Spain  
omillet@cicbiogune.es

**Millis, Kevin**

Cambridge Isotope Laboratories,  
Inc.  
Andover, United States  
kevinm@isotope.com

**Miotto, Marco C**

Institute of Molecular and Cell Biol-  
ogy of Rosario; Max-Planck Labora-  
tory of Rosario  
Rosario, Argentina  
miotto@ibr-conicet.gov.ar

**Miranda Filho, Fernando Luis**

Instituto de Macromoléculas Profes-  
sora Eloisa Mano  
Rio de Janeiro, Brazil  
fernandoluis\_ital@hotmail.com

**Moll, Jorge**

D'Or Institute for Research and Ed-  
ucation (IDOR)  
Rio de Janeiro, Brazil  
Jorge.Moll@idor.org

**Montenegro, André**

Sigma-Aldrich  
São Paulo, Brazil  
andre.montenegro@sial.com

**Monti, Gustavo A**

FaMAF-UNC and IFEG-CONICET  
Cordoba, Argentina  
monti@famaf.unc.edu.ar

**Montoro, Marcos A**

Spinlock SRL - CONICET - Univer-  
sidad Nacional de Córdoba  
Córdoba, Argentina  
mmontoro@efn.uncor.edu

**Montrazi, Elton T**

São Carlos Institute of Physics - Uni-  
versity of São Paulo  
Piracicaba, Brazil  
elton.montrazi@gmail.com

**Moraes, Adolfo H**

Universidade Federal do Rio de  
Janeiro  
Rio de Janeiro, Brazil  
adolfofisica@gmail.com

**Moraes, Tiago Bueno**

University of São Paulo  
São Carlos, Brazil  
tiagobuomoraes@gmail.com

**Morcomber , Corey**

Agilent Technologies  
Barueri , Brazil  
corey.morcombe@agilent.com

**Moreira Silva, Raphael Junnio**

São Carlos Institute of Physics  
São Carlos, Brazil  
moreira@ursa.ifsc.usp.br

**Morgada, Marcos N**

Instituto de Biología Molecular y  
Celular de Rosario  
Rosario, Argentina  
morgada@ibr-conicet.gov.ar

**Morgan, Vinícius G.**

Universidade Federal do Espírito  
Santo  
Serra, Brazil  
viniciusmorgan2@gmail.com

**Mossinger, Alan**

Petrobras  
Rio de Janeiro, Brazil  
alan.mossinger@petrobras.com.br

**Muhammad, Asif**

Universidade Federal Fluminense  
Niterói , Brazil  
amchemist79@gmail.com

**Munhoz, Victor H. O.**

Universidade Federal de Minas  
Gerais  
Belo Horizonte, Brazil  
victor.munhoz@gmail.com

**Munte, Claudia E**

Instituto de Física de São Carlos  
São Carlos, Brazil  
claudia.munte@ifsc.usp.br

**Naidés, Claudio H**

Petrobras S.A.  
Rio de Janeiro, Brazil  
claudio.naides@petrobras.com.br

**Naito, Akira**

Yokohama National University  
Yokohama, Japan  
naito@ynu.ac.jp

**Nantes, Iseli L.**

Universidade Federal do ABC  
Santo André, Brazil  
ilnantes@gmail.com

**Nascimento, Claudia J**

Universidade Federal do Estado  
do Rio de Janeiro/Universidade de  
Brasília  
Rio de Janeiro, Brazil  
claudia.j.nascimento@gmail.com

**Nascimento, Karina RPR**

Petróleo Brasileiro S.A  
Rio de Janeiro, Brazil  
karinarprn@petrobras.com.br

**Nascimento, Marco Antonio  
Chaer**

Universidade Federal do Rio de  
Janeiro  
Rio de Janeiro, Brazil  
chaer01@gmail.com

**Navon, Gil**

Tel Aviv University  
Tel Aviv, Israel  
navon@post.tau.ac.il

**Neese, Frank**

Max Planck Institute for Chemical  
Energy Conversion  
Muelheim an der Ruhr, Germany  
frank.neese@cec.mpg.de

**Netto, Paulo**  
Petrobras  
Rio de Janeiro, Brazil  
pnetto@petrobras.com.br

**Nicholson, Jeremy K**  
Imperial College London  
London, United Kingdom  
j.nicholson@imperial.ac.uk

**Nicot, Benjamin**  
Schlumberger  
Rio de Janeiro, Brazil  
bnicot@slb.com

**Nielsen, Niels Chr.**  
Aarhus University, Denmark  
Aarhus, Denmark  
ncn@inano.au.dk

**Noszál, Béla**  
Simmelweis University  
Budapest, Hungary  
noszal.bela@pharma.simmelweis-univ.hu

**Nunes, Wilian S**  
Mato Grosso do Sul University  
Campo Grande, Brazil  
willnunesquimica@gmail.com

**Oliveira, Aline L**  
Universidade de Brasília  
Brasília, Brazil  
aline.alo@gmail.com

**Oliveira, Caroline S**  
Universidade Federal de Mato Grosso do Sul  
Londrina, Brazil  
karolsilvaoliveira@yahoo.com.br

**Oliveira, Eduardo B**  
Petrobras  
Rio de Janeiro, Brazil  
eduardo.oliveira@petrobras.com.br

**Oliveira, Emanuele Silva**  
Universidade Federal do Espírito Santo  
Serra, Brazil  
emanuele\_cso@hotmail.com

**Oliveira, Everton L**  
São Carlos Institute of Physics - University of São Paulo  
Araraquara, Brazil  
everton.lucas.oliveira@usp.br

**Oliveira, Jessica M**  
Universidade Federal do Rio de Janeiro  
Rio de Janeiro, Brazil  
jessica003oliveira@gmail.com

**Oliveira, Juliana**  
Faculdades católicas  
Rio de Janeiro, Brazil  
juli\_oliveira3@yahoo.com.br

**Oliveira, Juliana F.**  
Laboratório Nacional de Biociências/LNBio  
Campinas, Brazil  
juliana.oliveira@lnbio.cnpem.br

**Oliveira, Luciana C**  
Instituto de Química- Universidade de São Paulo  
São Paulo, Brazil  
luciana@iq.usp.br

**Oliveira, Rodolfo**  
Schlumberger  
Rio de Janeiro, Brazil  
roliveira4@slb.com

**Oliveira Junior, Marcos**  
Universidade de São Paulo  
São Carlos, Brazil  
mjuni@ursa.ifsc.usp.br

**Onofre de Lira, Tatiana**  
Universidade Federal de São Carlos  
São Carlos, Brazil  
liraot@yahoo.com.br

**Opella, Stanley**  
University of California, San Diego  
La Jolla, United States  
sopella@ucsd.edu

**Orlandi, Aristides N**  
Schlumberger  
Rio de Janeiro, Brazil  
aorlandi2@slb.com

**Oschkinat, Hartmut**  
Leibniz-Institut für Molekulare Pharmakologie  
Berlin, Germany  
oschkinat@fmp-berlin.de

**Ott, Maria**  
Martin-Luther University Halle-Wittenberg  
Halle, Germany  
maria.ott@physik.uni-halle.de

**Ozaki, Elisa**  
Sigma-Aldrich  
São Paulo, Brazil  
elisa.ozaki@sial.com

**Paluch, Piotr**  
Center of Molecular and Macromolecular Study Polish Academy of Science  
Lodz, Poland  
ppaluch@cbmm.lodz.pl

**Parella, Teodor**  
Universitat Autònoma de Barcelona  
Bellaterra, Spain  
teodor.parella@uab.cat

**Pastawski, Horacio M.**  
Instituto de Física Enrique Gaviola- Universidad Nacional de Córdoba  
Córdoba, Argentina  
horacio@famaf.unc.edu.ar

**Pawlak, Tomasz**  
Centre of Molecular and Macromolecular Studies Polish Academy of Science  
90363, Poland  
tpawlak@cbmm.lodz.pl

**Pelc, Damjan**  
University of Zagreb, Faculty of Science  
Zagreb, Croatia  
dpelc@phy.hr

**Pellecchia, Maurizio**  
Sanford-Burnham Medical Research Institute  
La Jolla, United States  
mpellecchia@sanfordburnham.org

**Pereira, Fabíola M. V.**  
Embrapa Instrumentação  
São Carlos, Brazil  
fmverbi@uol.com.br

**Pereira, Natália C.**  
Universidade Federal do Rio de Janeiro  
Rio de Janeiro, Brazil  
naty\_pereira25@hotmail.com

**Pereira, Rosana C. L.**  
Petrobras/CENPES  
Rio de Janeiro, Brazil  
rosanacardoso@petrobras.com.br

**Perona Jiménez, Ricardo**  
Repsol Sinopec  
Rio de Janeiro, Brazil  
rperonaj@repsolsinopec.com

**Pervushin, Konstantin**  
Nanyang Technological University  
Singapore, Singapore  
kpervushin@ntu.edu.sg

**Pilo-Veloso, Dorila**  
Universidade Federal de Minas Gerais  
Belo Horizonte, Brazil  
dorila@zeus.qui.ufmg.br

**Pinheiro-Aguiar, Ramon**  
Federal University of Rio de Janeiro  
Rio de Janeiro, Brazil  
paguiarramon@gmail.com

**Piovani, Mônica R**  
Shimadzu do Brasil Comercio LTDA  
São Paulo, Brazil  
monica.piovani@shimadzu.com.br

**Pires, Diego A. T.**  
Universidade de Brasília  
Brasília, Brazil  
diego.pires.88@gmail.com

**Pires, Jose R**  
Universidade Federal do Rio de Janeiro  
Rio de Janeiro, Brazil  
jrmpires@cnrmn.bioqmed.ufrj.br

**Pizetta, Daniel C**

Instituto de Física de São Carlos - USP  
sao carlos, Brazil  
daniel.pizetta@usp.br

**Polinski, Ralf**

Schlumberger  
Rio de Janeiro, Brazil  
ralf.polinski@slb.com

**Polli, Roberson S**

Universidade de São Paulo - Instituto de Física de São Carlos  
São Carlos, Brazil  
roberson@ursa.ifsc.usp.br

**Pons, Miquel**

University of Barcelona  
Barcelona, Spain  
mpons@ub.edu

**Poole, Katherine M**

University of Florida  
Gainesville, United States  
poole@chem.ufl.edu

**Pope, James M**

Queensland University of Technology, Brisbane, Australia  
Brisbane, Australia  
j.pope@qut.edu.au

**Porto, Christiane F. C.**

Universidade Federal do Espírito Santo  
vitoria, Brazil  
chris\_feijo@hotmail.com

**Prisner, Thomas Ferdinand**

J. W. Goethe University  
Frankfurt, Germany  
prisner@chemie.uni-frankfurt.de

**Puglisi, Joseph D**

Stanford University  
Stanford, United States  
puglisi@stanford.edu

**Pusiol, Daniel**

IFEG-CONICET-SPINLOCK  
Córdoba, Argentina  
daniel.pusiol@gmail.com

**Queiroz, Ricardo**

BG E&P Brasil Ltda  
Rio de Janeiro, Brazil  
ricardo.queiroz@bg-group.com

**Queiroz Junior, Luiz H K**

Universidade Federal de Goiás  
Goiânia, Brazil  
professorkeng@gmail.com

**Quintero Escobar, Melissa**

LN BIO  
campinas, Brazil  
quinteromelissa@hotmail.com

**Rabbani, Said R.**

São Paulo University  
São Paulo, Brazil  
srabbani@if.usp.br

**Ramos, Bruna MC**

Laboratório Nacional de Biociências  
Campinas, Brazil  
bruna.campos@lnbio.cnpem.br

**Ramos, Paulo Frederico de Oliveira**

Baker Hughes Incorporated  
Rio de Janeiro, Brazil  
ramospfred@yahoo.com.br

**Rasia, Rodolfo M.**

Instituto de Biología Molecular y Celular de Rosario, Argentina  
Rosario, Argentina  
rasia@ibr.gov.ar

**Redfield, Christina**

University of Oxford  
Oxford, United Kingdom  
christina.redfield@bioch.ox.ac.uk

**Reif, Bernd**

TU Muenchen  
Garching, Germany  
reif@tum.de

**Reis, Alvaro Campassi**

Petrobras  
Natal, Brazil  
campassi@petrobras.com.br

**Renshaw, Matthew P**

University of Cambridge  
Cambridge, United Kingdom  
mpr34@cam.ac.uk

**Resende, Jarbas M**

Universidade Federal de Minas Gerais  
Belo Horizonte, Brazil  
jarbas@netuno.lcc.ufmg.br

**Rey, Nicolás A.**

Pontifícia Universidade Católica do Rio de Janeiro  
Rio de Janeiro, Brazil  
nicoarey@puc-rio.br

**Rezende, Carlos A**

Universidade Federal Fluminense  
Rio de Janeiro, Brazil  
carlosasrezende@yahoo.com.br

**Ribeiro, Tatiana Santana**

Universidade Federal de São Carlos  
São Carlos, Brazil  
tatiana@cca.ufscar.br

**Rienstra, Chad M**

University of Illinois at Urbana-Champaign  
Urbana, United States  
rienstra@illinois.edu

**Rigotti, Italo**

Petrobras S.A.  
Rio de Janeiro, Brazil  
irigotti@petrobras.com.br

**Riley, Scott A**

Tecmag, Inc.  
Houston, United States  
sriley@tecmag.com

**Rios, Edmilson H**

National Observatory  
Niterói, Brazil  
edmilsonheltonrios@yahoo.com.br

**Robustelli, Paul**

Columbia University  
New York, United States  
pr2143@columbia.edu

**Rocha, Cláudia Q.**

Instituto de Química-Unesp- Araraquara  
Araraquara, Brazil  
claudiarocha3@yahoo.com.br

**Rodrigues, Tiago Brandão**

Cancer Reserch UK Cambridge Institute  
Cambridge, United Kingdom  
tiago.rodrigues@cruk.cam.ac.uk

**Romero, Pedro A.**

Halliburton  
Rio de Janeiro, Brazil  
pedro.romero@halliburton.com

**Rosato, Antonio**

University of Florence  
Sesto Fiorentino, Italy  
rosato@cerm.unifi.it

**Ruiz, Naira M.S.**

PUC-Rio  
Rio de Janeiro, Brazil  
nairaruiz.puc@petrobras.com.br

**Salek, Reza**

EMBL-EBI  
Cambridge, United Kingdom  
reza.salek@ebi.ac.uk

**Sales, Caroline R**

Petrobras  
Rio de Janeiro, Brazil  
carolinesales@petrobras.com.br

**Sales, Edijane Matos**

Instituto Militar de Engenharia  
Rio de Janeiro, Brazil  
edijane\_matos@hotmail.com

**Salinas, Roberto K.**

Universidade de São Paulo  
Sao Paulo, Brazil  
roberto@iq.usp.br

**Salomoni, Roberto R**

Petrobras  
Rio de Janeiro, Brazil  
robertosalomoni@petrobras.com.br

**Samouilov, Alexandre V.**

The Ohio State University Wexner Medical Center  
Columbus, United States  
Alex.Samouilov@osumc.edu

**San Gil, Rosane A.S.**

Universidade Federal do Rio de Janeiro, Instituto de Química  
Rio de Janeiro, Brazil  
rsangil@iq.ufrj.br

**Sanderson, Mark R**  
King's College London  
London, United Kingdom  
mark.sanderson@kcl.ac.uk

**Sant'Anna, Quézia**  
Fundação Oswaldo Cruz  
Rio de Janeiro, Brazil  
quezasantanna@yahoo.com.br

**Santana, Juliana S**  
Instituto de Bioquímica Médica  
Cidade Universitária - Rio de Janeiro, Brazil  
jujubasster@gmail.com

**Santos, Bernardo C C**  
Petrobras  
Rio de Janeiro, Brazil  
bernardo.coutinho@petrobras.com.br

**Santos, Daniel**  
Merck Millipore  
Rio de Janeiro, Brazil  
daniel.santos@merckgroup.com

**Santos, Daniel Ribas**  
Bruker do Brasil  
Atibaia, Brazil  
daniel.santos@bruker.com.br

**Santos, Talita**  
UFRJ (CNRMN)  
Rio de Janeiro, Brazil  
tsantos@cnrmn.bioqmed.ufrj.br

**Sarzedas, Carolina G**  
Universidade Federal do Rio de Janeiro  
Rio de Janeiro, Brazil  
carolsarzedas@yahoo.com.br

**Sattler, Michael**  
Helmholtz Zentrum München & Technische Universität München  
Neuherberg, Germany  
sattler@helmholtz-muenchen.de

**Sayegh, Raphael S R**  
University of São Paulo  
São Paulo, Brazil  
rrsayegh@yahoo.com.br

**Schefer, Alexandre Bezerra**  
Bruker do Brasil  
Atibaia, Brazil  
alexandre.schefer@bruker.com.br

**Schmidt-Rohr, Klaus**  
Iowa State University  
Ames, United States  
srohr@iastate.edu

**Schneider, Jose F.**  
Universidade de São Paulo  
São Carlos, Brazil  
schnei@ifsc.usp.br

**Schomburg, Benjamin**  
Max-Planck-Institute for Biophysical Chemistry  
Goettingen, Germany  
besc@nmr.mpibpc.mpg.de

**Schwalbe, Harald**  
Goethe-University Frankfurt  
Frankfurt, Germany  
schwalbe@nmr.uni-frankfurt.de

**Separovic, Frances**  
University of Melbourne  
Melbourne, Australia  
fs@unimelb.edu.au

**Serra, Anna Carolina**  
Tedia Brazil  
Rio de Janeiro, Brazil  
carol.serra@tediabrasil.com.br

**Sforça, Maurício L**  
Centro Nacional de Pesquisa em Energia e Materiais  
Campinas, Brazil  
mauricio.sforca@lnbio.cnpem.br

**Shekhtman, Alexander**  
State University of New York at Albany  
Albany, United States  
ashekhtman@albany.edu

**Shi, Yunyu**  
University of science and technology of China  
Hefei, People's Republic of China  
yyshi@ustc.edu.cn

**Shimada, Ichio**  
The University of Tokyo  
Tokyo, Japan  
shimada@iw-nmr.f.u-tokyo.ac.jp

**Silletta, Emilia V.**  
FAMAF – Universidad Nacional de Córdoba, IFEG – CONICET  
Córdoba, Argentina  
emiliasilletta@gmail.com

**Silva, Afonso C.**  
National Institutes of Health  
Bethesda, United States  
SilvaA@ninds.nih.gov

**Silva, Geovana Vargas**  
Universidade Federal do Rio de Janeiro  
Rio de Janeiro, Brazil  
geovanaavargas@gmail.com

**Silva, Isabela A**  
Universidade de São Paulo - Instituto de Física de São Carlos  
São Carlos - SP, Brazil  
isa.almeidasilva@gmail.com

**Silva, Marcio S.**  
University of São Paulo  
São Paulo, Brazil  
marciosasi@usp.br

**Silva, Maria Isabel Pais da**  
Faculdades Católicas  
Rio de Janeiro, Brazil  
isapais@puc-rio.br

**Silva, Monica T**  
Petrobras  
RIO DE JANEIRO, Brazil  
monicats@petrobras.com.br

**Silva, Rodrigo de Oliveira**  
São Carlos Institute of Physics - University of São Paulo  
São Carlos, Brazil  
rsilv@ursa.ifsc.usp.br

**Silva Pinto, Vinicius**  
Universidade Federal de Goiás  
Goiânia, Brazil  
vspufg@gmail.com

**Silveira, Camila P**  
UFRJ - UNICAMP  
Valinhos, Brazil  
cami.silveira@gmail.com

**Silveira, Edilberto R.**  
Universidade Federal do Ceará  
Fortaleza, Brazil  
edil@ufc.br

**Simões, Clara**  
Instituto Militar de Engenharia  
Rio de Janeiro, Brazil  
clarinha@irmaos.com

**Simões, Marcelo Luiz**  
EMPRESA BRASILEIRA DE PESQUISA AGROPECUÁRIA  
São Carlos, Brazil  
marcelo@cnpdia.embrapa.br

**Simões, Vanessa S**  
Schlumberger  
Rio de Janeiro, Brazil  
vanessasimoes@gmail.com

**Simorre, Jean-Pierre**  
CNRS  
GRENOBLE, France  
jean-pierre.simorre@ibs.fr

**Smith, Graham M**  
University of St Andrews  
St Andrews, United Kingdom  
gms@st-and.ac.uk

**Soares, Viviane Faria**  
Empresa Brasileira de Pesquisa Agropecuária  
São Carlos, Brazil  
viviane@cnpdia.embrapa.br

**Soeiro, Paulo Antero Sure**  
Petrobras  
Rio de Janeiro, Brazil  
soeiro@petrobras.com.br

**Song, Yiqiao**  
Schlumberger  
Cambridge, United States  
ysong@slb.com

**Sotoma, Shingo**  
Kyoto university  
kyoto, Japan  
sotoma.shingo.75w@st.kyoto-u.ac.jp



**Sousa, Eduardo G. R. de**  
Farmanguinhos/FIOCRUZ  
Rio de Janeiro, Brazil  
esousa@far.fiocruz.br

**Sousa Ferreira, Vinicius**  
Universidade Federal de Goiás  
Goiânia, Brazil  
viniciusquimica.12@gmail.com

**Souza, Andre A.**  
Schlumberger Brazil Research and  
Geoengineering Center  
Rio de Janeiro, Brazil  
asouza19@slb.com

**Souza, Anelise L**  
Petrobras  
Rio de Janeiro, Brazil  
ANELISE.LIMA@PETROBRAS.COM.BR

**Souza, Claudia M G de**  
Instituto de Pesquisas Tecnológicas  
do Estado de SP  
São Paulo, Brazil  
claupt@gmail.com

**Souza, Isis T**  
Universidade Federal de Alagoas  
Maceió, Brazil  
isinhasouza@gmail.com

**Spiess, Hans Wolfgang**  
Max-Planck-Institute Polymer Re-  
search Mainz  
Mainz, Germany  
spiess@mpip-mainz. mpg.de

**Spitzer, Romana**  
University of Innsbruck  
Innsbruck, Brazil  
Romana.Spitzer@uibk.ac.at

**Stael, Giovanni C**  
Observatório Nacional  
Rio de Janeiro, Brazil  
stael@on.br

**Steinbeck, Christoph**  
EMBL-EBI  
Cambridge, United Kingdom  
steinbeck@ebi.ac.uk

**Stepišnik, Janez**  
University of Ljubljana, FMF and In-  
stitute "Jozef Stefan"  
Ljubljana, Slovenia  
Janez.Stepisnik@fmf.uni-lj.si

**Suter, Dieter**  
TU Dortmund  
Dortmund, Germany  
Dieter.Suter@tu-dortmund.de

**Sychrovsky, Vladimir**  
Institute of Organic Chemistry and  
Biochemistry, Academy of Sciences  
of the Czech Republic  
Prague, Czech Republic  
vladimir.sychrovsky@uochb.cas.cz

**Sze, Kong Hung**  
University of Hong Kong  
Hong Kong SAR, People's Republic  
of China  
khsze@hku.hk

**Takegoshi, Kiyonori**  
Kyoto University  
Kyoto, Japan  
takeyan@kuchem.kyoto-u.ac.jp

**Tang, Huiur**  
Wuhan Institute of Physics and  
Mathematics  
Wuhan, People's Republic of China  
huiur.tang@wipm.ac.cn

**Tasic, Ljubica**  
University of Campinas  
Campinas, Brazil  
ljubica@iqm.unicamp.br

**Täubert, Sebastian**  
Max-Planck-Institute for Biophysical  
Chemistry  
Göttingen, Germany  
seta@nmr.mpibpc.mpg.de

**Taulelle, Francis**  
University of Versailles Saint  
Quentin en Yvelines  
Versailles, France  
francis.taulelle@uvsq.fr

**Tavares, Maria Ines Bruno**  
IMA-UFRJ  
Rio de Janeiro, Brazil  
mibt@ima.ufrj.br

**Teixeira, Francesco B.**  
Instituto de Física de São Carlos -  
USP  
São Carlos, Brazil  
francesco.teixeira@usp.br

**Tekely, Piotr**  
Ecole Normale Supérieure/CNRS  
Paris, France  
Piotr.Tekely@ens.fr

**Teles, Rubens Rodrigues**  
Universidade Federal de Pernambuco  
Recife, Brazil  
Rubensteles2000@yahoo.com.br

**Telser, Joshua**  
Roosevelt University  
Chicago, United States  
jtelsr@roosevelt.edu

**Tochio, Hidehito**  
Kyoto University  
Kyoto, Japan  
tochio@moleng.kyoto-u.ac.jp

**Tovar-Moll, Fernanda Freire**  
IDOR/UFRJ  
Rio de Janeiro, Brazil  
fernanda.tovarmoll@idor.org

**Trail, John**  
Magritek  
Wellington, New Zealand  
exhibit@magritek.com

**Trébosc, Julien**  
Unité de Catalyse et Chimie du  
Solide - Université de Lille 1  
Villeneuve d'Ascq, France  
julien.trebosc@univ-lille1.fr

**Trevizan, Willian A**  
Petrobras  
Rio de Janeiro, Brazil  
williantrevizan@petrobras.com.br

**Tsuchida, Jefferson E**  
Universidade de São  
Paulo/Universidade Federal de  
São Carlos  
São Carlos, Brazil  
jetsuchida@gmail.com

**Turcu, Flaviu**  
"Babes-Bolyai" University  
Cluj-Napoca, Romania  
fturcu@phys.ubbcluj.ro

**Tycko, Robert**  
National Institutes of Health  
Bethesda, United States  
robertty@mail.nih.gov

**Ugurbil, Kamil**  
University of Minnesota  
Minneapolis, United States  
kamil@cmrr.umn.edu

**Valente, Ana Paula**  
Federal University of Rio de Janeiro  
Rio de Janeiro, Brazil  
valente@cnrmn.bioqmed.ufrj.br

**Valezi, Daniel F**  
Universidade Estadual de Londrina  
Londrina, Brazil  
danieltds@hotmail.com

**Veglia, Gianluigi**  
University of Minnesota  
Minneapolis, United States  
vegli001@umn.edu

**Velez Jurado, Ana K**  
Universidad del Valle  
Cali, Colombia  
ana.velez@correounivalle.edu.co

**Venâncio, Tiago**  
Universidade Federal de São Carlos  
São Carlos, Brazil  
t\_venancio@yahoo.com

**Viani Puglisi, Elisabetta**  
Stanford University  
Stanford, United States  
epuglisi@stanford.edu

**Vicentin, Bruno L S**  
Universidade Estadual de Londrina  
Londrina, Brazil  
bsvicentin@gmail.com

**Vieira de Luca, Pedro H**  
Repsol Sinopec  
Rio de Janeiro, Brazil  
ph.vieira@repsolsinopec.com

**Vigneron, Daniel**

University of California San Francisco  
San Francisco, United States  
dan.vigneron@ucsf.edu

**Vila, Alejandro J**

Instituto de Biología Molecular y Celular de Rosario  
Rosario, Argentina  
vila@ibr-conicet.gov.ar

**Vilcachagua, Janaina D**

Instituto de Química - Universidade de São Paulo - USP/SP  
Sao Paulo, Brazil  
janadv@gmail.com

**Vivero, Santiago Domingez**

MESTRELAB RESEARCH, S.L.  
Santiago de Compostela, Spain  
santi@mestrelab.com

**Wagner, Gerhard**

Harvard Medical School  
Boston, United States  
gerhard\_wagner@hms.harvard.edu

**Walker, Frances Ann**

University of Arizona  
Tucson, United States  
awalker@email.arizona.edu

**Wand, Joshua**

University of Pennsylvania  
Philadelphia, United States  
wand@mail.med.upenn.edu

**Wang, Yulan**

Wuhan Institute of Physics and Mathematics  
Wuhan, People's Republic of China  
yulan.wang@wipm.ac.cn

**Warren, Warren S**

Duke University  
Durham, United States  
warren.warren@duke.edu

**Weber, David J.**

University of Maryland School of Medicine  
Baltimore, United States  
dweber@som.umaryland.edu

**Wegner, Sebastian**

Bruker do Brasil  
Atibaia, Brazil  
sebastian.wegner@bruker-biospin.de

**Weingarth, Markus**

Utrecht University  
De Bilt, Netherlands  
m.h.weingarth@uu.nl

**Werdan, Ciro Cordeiro**

Tedia Brazil  
Rio de Janeiro, Brazil  
ciro.werdan@tediabrazil.com.br

**Wheeler, Patrick**

Advanced Chemistry Development, Inc. (ACD/Labs)  
Toronto, Canada  
patrick.wheeler@acdlabs.com

**Whittaker, Sara**

The Henry Wellcome Building for Biomolecular NMR Spectroscopy, University of Birmingham, UK  
Birmingham, United Kingdom  
s.b.whittaker@bham.ac.uk

**Wist, Julien**

NMR Lab, Universidad del Valle  
Cali, Colombia  
julien.wist@correounivalle.edu.co

**Wolf-Watz, Magnus**

Umeå University  
Umeå, Sweden  
magnus.wolf-watz@chem.umu.se

**Wrachtrup, Joerg**

3rd Physical Institute, University of Stuttgart  
Stuttgart, Germany  
wrachtrup@physik.uni-stuttgart.de

**Wunderlich, Christoph H**

Universität Innsbruck  
Innsbruck, Austria  
christoph.wunderlich@student.uibk.ac.at

**Yu, Liping**

University of Iowa  
Iowa City, United States  
Liping-Yu@uiowa.edu

**Zagdoun, Alexandre**

CRMN ENS Lyon  
Villeurbanne, France  
alexandre.zagdoun@ens-lyon.fr

**Zeri, Ana Carolina M**

Brazilian Biosciences National Laboratory  
campinas, Brazil  
ana.zeri@lnbio.cnpem.br

**Zhou, Xin**

Wuhan Institute of Physics and Mathematics  
Wuhan, People's Republic of China  
xinzhou@wipm.ac.cn

**Zinn, Fabiano Kauer**

Shimadzu do Brasil Comercio LTDA  
São Paulo, Brazil  
kauer@shimadzu.com.br

## Late Participants

**Apparecido, Rafael do P**

UFMS  
Campo Grande, Brazil  
apparecido.prado@yahoo.com.br

**Barbosa, Rodrigo Jorge V**

Universidade Federal do Rio de Janeiro  
Rio de Janeiro, Brazil  
rodrigovjb@hotmail.com

**Bharatam, Jagadeesh**

Indian Institute of Chemical Technology, Hyderabad  
Hyderabad, India  
bj@iict.res.in

**Bramati, Ivanei**

D'OR Institute for Research and Education  
Rio de Janeiro, Brazil  
ibramati@gmail.com

**Buckley, Michael Dean**

Cryogenic - Insight Técnica  
São Paulo, Brazil  
michael@insighttecnica.com

**Corbett, Patrick WM**

Heriot-Watt University  
Edinburgh, United Kingdom  
patrick.corbett@pet.hw.ac.uk

**de Moraes, Fernanda H P**

UFRJ / IDOR  
Rio de Janeiro, Brazil  
fernandahmoraes@gmail.com

**de Souza, Andrea S**

IDOR / UFRJ / REDE D'OR  
Rio de Janeiro, Brazil  
andrea.silveiradesouza@gmail.com

**Gauthier, Alan**

BRUKER  
ATIBAIA, Brazil  
Al.Gauthier@bruker-biospin.com

**Gelev, vladimir**

FB Reagents DBA  
cambridge, United States  
doktor.gelev@gmail.com

**Goncalves, Eleno Paes**

SUPERLAB Instrumentação  
Analítica LTDA  
São Paulo, Brazil  
eleno@autoanalitica.com.br

**Hawkins, Elizabeth**

Springer-Verlag GmbH  
Heidelberg, Germany  
elizabeth.hawkins@springer.com

**Holmes, Elaine**

Imperial College  
London, United Kingdom  
elaine.holmes@imperial.ac.uk

**Ivanshin, Vladimir A.**

Kazan Federal (Volga region) University  
Kazan, Russia 166 Rwanda  
Vladimir.Ivanshin@kpfu.ru

**Martel, Laura B.C.**

Halliburton  
Rio de Janeiro, Brazil  
laura.martel@halliburton.com

**Paiva, Fernando F**

Universidade de São Paulo  
São Carlos, Brazil  
paiva@ifsc.usp.br

**Pestana, Fernanda**

UFRJ  
Rio de Janeiro, Brazil  
pestanaufrj@gmail.com

**Quinting, Gregory R**

Anasazi Instruments  
Indianapolis, United States  
greg.quinting@aiinmr.com

**Ribeiro, Abel**

dpUNION  
São Paulo, Brazil  
pmagalhaes@dpunion.com.br

**Salazar , Jesus P**

Baker Hughes do Brasil  
Rio de Janeiro, Brazil  
jesus.salazar3@bakerhughes.com

**Teixeira, Camila**

CENABIO-UFRJ  
Rio de Janeiro, Brazil  
teixeiras.camila@gmail.com

**van Daalen, Rob**

Elsevier  
Amsterdam, Netherlands  
g.daalen@elsevier.com

**Vezin, Hervé**

CNRS LASIR UMR 8516 Université  
Lille 1  
Villeneuve d'Ascq, France  
herve.vezin@univ-lille1.fr